



Wind Energy Engineering



A Handbook for Onshore and
Offshore Wind Turbines

Edited by

Trevor M. Letcher



Wind Energy Engineering

This page intentionally left blank

Wind Energy Engineering

A Handbook for Onshore
and Offshore Wind Turbines

Edited by

Trevor M. Letcher



ACADEMIC PRESS

An imprint of Elsevier
elsevier.com

Academic Press is an imprint of Elsevier
125 London Wall, London EC2Y 5AS, United Kingdom
525 B Street, Suite 1800, San Diego, CA 92101-4495, United States
50 Hampshire Street, 5th Floor, Cambridge, MA 02139, United States
The Boulevard, Langford Lane, Kidlington, Oxford OX5 1GB, United Kingdom

Copyright © 2017 Elsevier Inc. All rights reserved.

No part of this publication may be reproduced or transmitted in any form or by any means, electronic or mechanical, including photocopying, recording, or any information storage and retrieval system, without permission in writing from the publisher. Details on how to seek permission, further information about the Publisher's permissions policies and our arrangements with organizations such as the Copyright Clearance Center and the Copyright Licensing Agency, can be found at our website: www.elsevier.com/permissions.

This book and the individual contributions contained in it are protected under copyright by the Publisher (other than as may be noted herein).

Notices

Knowledge and best practice in this field are constantly changing. As new research and experience broaden our understanding, changes in research methods, professional practices, or medical treatment may become necessary.

Practitioners and researchers must always rely on their own experience and knowledge in evaluating and using any information, methods, compounds, or experiments described herein. In using such information or methods they should be mindful of their own safety and the safety of others, including parties for whom they have a professional responsibility.

To the fullest extent of the law, neither the Publisher nor the authors, contributors, or editors, assume any liability for any injury and/or damage to persons or property as a matter of products liability, negligence or otherwise, or from any use or operation of any methods, products, instructions, or ideas contained in the material herein.

Library of Congress Cataloging-in-Publication Data

A catalog record for this book is available from the Library of Congress

British Library Cataloguing-in-Publication Data

A catalogue record for this book is available from the British Library

ISBN: 978-0-12-809451-8

For Information on all Academic Press publications
visit our website at <https://www.elsevier.com/books-and-journals>



Working together
to grow libraries in
developing countries

www.elsevier.com • www.bookaid.org

Publisher: Joe Hayton

Acquisition Editor: Lisa Reading

Editorial Project Manager: Ashlie Jackman

Production Project Manager: Anusha Sambamoorthy

Cover Designer: Matthew Limbert

Typeset by MPS Limited, Chennai, India

Contents

List of Contributors	xvii
Preface	xix

Part I **Introduction**

1. Why Wind Energy?

Trevor M. Letcher

1.1 Introduction	3
1.2 Climate Change	3
1.3 Background	5
1.4 Advantages of Wind Energy	8
1.5 Challenges Facing the Wind Turbine Industry	10
1.6 The Potential of Wind Energy Worldwide	13
References	13

Part II **Wind Resource and Wind Energy Worldwide**

2. Wind Power Fundamentals

Alexander Kalmikov

2.1 Wind Physics Basics: What Is Wind and How Wind Is Generated	17
2.2 Wind Types: Brief Overview of Wind Power Meteorology	18
2.3 Fundamental Equation of Wind Power: Kinetic Energy Flux and Wind Power Density	19
2.4 Wind Power Capture: Efficiency in Extracting Wind Power	21
2.5 Conclusion	23
References	23

3. Estimation of Wind Energy Potential and Prediction of Wind Power

Jing Shi and Ergin Erdem

3.1	Introduction	25
3.2	Principles for Successful Development for a Wind Assessment Program	26
3.3	Main Aspects of a Wind Assessment Program	28
3.4	Estimating Wind Power Based on Wind Speed Measurements	33
3.5	Wind Resource Estimation Project: Scope and Methods	34
3.6	Further Considerations for Wind Speed Assessment	38
3.7	Wind Speed and Power Forecasting	39
3.8	Conclusions	44
	References	44

4. Global Potential for Wind-Generated Electricity

Xi Lu and Michael B. McElroy

4.1	Introduction	51
4.2	Methodology	54
4.3	Results	58
4.3.1	Global Perspective	58
4.3.2	US Perspective	61
4.3.3	China Perspective	65
4.4	Concluding Remarks	68
	Acknowledgments	71
	References	71

5. The Future of Wind Energy Development in China

Pei-yang Guo, Dan-yang Zhu, Jacqueline Lam, and Victor O.K. Li

5.1	Introduction	75
5.2	Wind Energy Development in China	76
5.2.1	Overview	76
5.2.2	Electricity Market and Wind Energy Market in China	76
5.3	Wind Energy Development in China: Barriers and Drivers	80
5.3.1	Barriers to Wind Energy Development in China	81
5.3.2	Drivers of Wind Energy Development in China	86
5.4	The Future of Wind Energy Development in China	89
5.4.1	Distributed Generation Deployment and Proactive Transmission Planning	89
5.4.2	Offshore Wind Power Planning	89
5.4.3	Smart Grid	90
5.4.4	Merit-Order-Based Dispatch	90
5.4.5	Pricing Improvement	91

5.5 Conclusion	91
Acknowledgment	92
References	92
6. Wind Power in the German System—Research and Development for the Transition Toward a Sustainable Energy Future	
<i>Matthias Luther, Kurt Rohrig, and Wilhelm Winter</i>	
6.1 Integration of Renewables in Germany and Europe	95
6.2 Onshore and Offshore Wind Development	99
6.3 Network Operation and Grid Development	102
6.3.1 Innovative Methods to Plan and Operate the Power System	105
6.3.2 The System Operation Network Codes	108
6.3.3 The Market-Related Network Codes	108
6.3.4 The Connection-Related Network Codes	109
6.4 Further Research and Development for Wind Power Integration	110
6.4.1 New Control Concepts for PE-Dominated Power Systems	111
6.4.2 Wind Power Forecasts	112
6.4.3 Wind Farm Clusters	114
6.4.4 Virtual Power Plants	117
6.4.5 Sector Coupling Concepts	118
6.4.6 European Wind Integration Projects and Studies	119
6.5 Summary	121
References	122

Part III

Wind Turbine Technology

7. History of Harnessing Wind Power

Magdi Ragheb

7.1 Introduction	127
7.2 Wind Machines in Antiquity	129
7.3 Islamic Civilization Windmills	130
7.4 Medieval European Windmills	132
7.5 Aegean and Mediterranean Windmills	133
7.6 Dutch and European Windmills	135
7.7 The American Windmill	138
7.8 Historical Developments	139
7.9 Windmills Applications	141
7.10 Discussion	141
References	142

8. Wind Turbine Technologies

Anca D. Hansen

8.1 Introduction	145
8.2 Overview of Wind Turbine Components	145
8.2.1 Aerodynamic Rotor	146
8.2.2 Transmission System	146
8.2.3 Generator	147
8.2.4 Power Electronic Interface	151
8.2.5 Control System and Wind Turbine Control Capabilities	152
8.3 Contemporary Wind Turbine Technologies	155
8.3.1 Fixed-Speed Wind Turbines (Type 1)	155
8.3.2 Limited Variable-Speed Wind Turbines (Type 2)	156
8.3.3 Variable-Speed Wind Turbines With Partial-Scale Power Converter (Type 3)	157
8.3.4 Variable-Speed Wind Turbines With Full-Scale Power Converter (Type 4)	158
8.4 Conclusions	159
References	159

9. Aerodynamics and Design of Horizontal-Axis Wind Turbines

Martin O.L. Hansen

9.1 Introduction	161
9.2 A Short Description on How a Wind Turbine Works	162
9.3 1D Momentum Equations	163
9.4 Blade Element Momentum Method	167
9.4.1 The Blade Element Momentum Method	172
9.5 Use of Steady Blade Element Momentum Method	172
9.6 Aerodynamic Blade Design	178
9.7 Unsteady Loads and Fatigue	181
9.8 Brief Description of Design Process	183
References	183

10. Vertical Axis Wind Turbines: Farm and Turbine Design

Robert Whittlesey

10.1 Vertical Axis Wind Turbines History	185
10.2 Vertical Axis Wind Farms	186
10.2.1 Initial Research on VAWT Farms	186
10.2.2 Power Density	187
10.3 Design Guidelines	188
10.3.1 Power Coefficient	189

10.3.2	Lift Versus Drag-Based VAWT	189
10.3.3	Starting	193
10.3.4	Blade Airfoil Choice	194
10.3.5	Blade-Tip Vortices	197
10.3.6	Blade Reynolds Number	198
10.3.7	Turbine Mass	198
10.3.8	Turbine Diameter	198
10.3.9	Number of Blades	199
10.3.10	Struts	199
10.4	Summary	200
	References	200

11. Multielement Airfoils for Wind Turbines

Adam M. Ragheb and Michael S. Selig

11.1	Introduction	203
11.2	Transportation Benefits	204
11.3	Structural Benefits	205
11.4	Multielement Wind Turbine Blades	206
11.5	Other Multielement Wind Turbine Research	215
11.6	Discussion	216
	Acknowledgments	217
	References	218

12. Civil Engineering Aspects of a Wind Farm and Wind Turbine Structures

Subhamoy Bhattacharya

12.1	Energy Challenge	221
12.2	Wind Farm and Fukushima Nuclear disaster	221
12.2.1	Case Study: Performance of Near Shore Wind Farm During 2012 Tohoku Earthquake	221
12.3	Wind Farm Site Selection	224
12.3.1	Case Studies: Burbo Wind Farm (see Fig. 12.6 for location)	226
12.3.2	ASIDE on the Economics	227
12.4	General Arrangement of a Wind Farm	228
12.5	Choice of Foundations for a Site	228
12.6	Foundation Types	228
12.6.1	Gravity-Based Foundation System	233
12.6.2	Suction Buckets or Caissons	233
12.6.3	Pile Foundations	234
12.6.4	Seabed Frame or Jacket Supporting Supported on Pile or Caissons	235
12.6.5	Floating Turbine System	237

12.7 Site Layout, Spacing of Turbines, and Geology of the Site	239
12.7.1 Case Study: Westermost Rough	240
12.7.2 Economy of Scales for Foundation	241
References	242
13. Civil Engineering Challenges Associated With Design of Offshore Wind Turbines With Special Reference to China	
<i>Subhamoy Bhattacharya, Lizhong Wang, Junwei Liu, and Yi Hong</i>	
13.1 Offshore Wind Potential in China	243
13.2 Dynamic Sensitivity of OWT Structures	245
13.3 Dynamic Issues in Support Structure Design	247
13.3.1 Importance of Foundation Design	252
13.4 Types and Nature of the Loads Acting on the Foundations	254
13.4.1 Loads Acting on the Foundations	254
13.4.2 Extreme Wind and Wave Loading Condition in Chinese Waters	257
13.5 Ground Conditions in Chinese Waters	260
13.5.1 Bohai Sea	261
13.5.2 Seismic Effects	264
13.6 A Note on SLS Design Criteria	265
13.7 Challenges in Analysis of Dynamic Soil–Structure Interaction	266
13.8 Foundation Design	269
13.8.1 Challenges in Monopile Foundation Design and Installation	270
13.8.2 Jacket on Flexible Piles	271
13.9 Concluding Remarks	271
References	272
14. Numerical Methods for SSI Analysis of Offshore Wind Turbine Foundations	
<i>Susana Lopez-Querol, Liang Cui, and Subhamoy Bhattacharya</i>	
14.1 Introduction	275
14.1.1 Need for Numerical Analysis for Carrying out the Design	281
14.2 Types of Numerical Analysis	281
14.2.1 Standard Method Based on Beam on Nonlinear Winkler Spring	281
14.2.2 Advanced Analysis (Finite Element Analysis and Discrete Element Modeling) to Study Foundation–Soil Interaction	283

14.3 Example Application of Numerical Analysis to Study SSI of Monopile	285
14.3.1 Monopile Analysis Using DEM	286
14.3.2 Monopile Analysis Using FEM Using ANSYS Software	290
References	295
15. Reliability of Wind Turbines	
<i>Shuangwen Sheng and Ryan O'Connor</i>	
15.1 Introduction	299
15.2 Fundamentals	301
15.2.1 Terminology	301
15.2.2 Taxonomy	303
15.2.3 Failure Types	304
15.3 Current Status	305
15.4 Reliability Engineering	312
15.4.1 Data Collection	312
15.4.2 Model Development	315
15.4.3 Forecasting	319
15.5 Case Studies	320
15.5.1 Gearbox Spares Planning	320
15.5.2 Pitch Bearing Maintenance Scheduling	321
15.6 Conclusions	325
Acknowledgments	325
References	325
16. Practical Method to Estimate Foundation Stiffness for Design of Offshore Wind Turbines	
<i>Saleh Jalbi, Masoud Shadlou, and Subhamoy Bhattacharya</i>	
16.1 Introduction	329
16.2 Methods to Estimate Foundation Stiffness	332
16.2.1 Simplified Method (Closed-Form Solutions)	334
16.2.2 Standard Method	336
16.2.3 Advanced Method	336
16.3 Obtaining Foundation Stiffness From Standard and Advanced Method	337
16.3.1 Example Problem (Monopile for Horns Rev 1)	340
16.4 Discussion and Application of Foundation Stiffness	345
16.4.1 Pile Head Deflections and Rotations	345
16.4.2 Prediction of the Natural Frequency	346
16.4.3 Comparison With SAP 2000 Analysis	349
Nomenclature	350
References	351

17. Physical Modeling of Offshore Wind Turbine Model for Prediction of Prototype Response

Domenico Lombardi, Subhamoy Bhattacharya, and George Nikitas

17.1	Introduction	353
17.1.1	Complexity of External Loading Conditions	353
17.1.2	Design Challenges	355
17.1.3	Technical Review/Appraisal of New Types of Foundations	358
17.1.4	Physical Modeling for Prediction of Prototype Response	358
17.2	Physical Modeling of OWTs	359
17.2.1	Dimensional Analysis	360
17.2.2	Definition of Scaling Laws for Investigating OWTs	360
17.3	Scaling Laws for OWTs Supported on Monopiles	361
17.3.1	Monopile Foundation	361
17.3.2	Strain Field in the Soil Around the Laterally Loaded Pile	361
17.3.3	CSR in the Soil in the Shear Zone	363
17.3.4	Rate of Soil Loading	364
17.3.5	System Dynamics	364
17.3.6	Bending Strain in the Monopile	365
17.3.7	Fatigue in the Monopile	365
17.3.8	Example of Experimental Investigation for Studying Long-Term Response of 1–100 Scale OWT	366
17.4	Scaling Laws for OWTs Supported on Multipod Foundations	368
17.4.1	Typical Experimental Setups and Results	372
17.5	Conclusions	373
	References	373

Part IV Generation of Electricity

18. Energy and Carbon Intensities of Stored Wind Energy

Charles J. Barnhart

18.1	The Need for Storage	377
18.2	Key Characteristics for Storage	378
18.3	Net Energy Analysis of Storing and Curtailing Wind Resources	380
18.4	The Carbon Footprint of Storing Wind Energy	383
18.5	Conclusions	385
	References	386

19. Small-Scale Wind Turbines*Patrick A.B. James and AbuBakr S. Bahaj*

19.1	Introduction	389
19.2	The Fundamental Concern for Micro-Wind: The Wind Resource	395
19.3	Building Mounted Turbines	401
19.3.1	Rural Building Mounted Turbine	405
19.3.2	Suburban Building Mounted Turbine	407
19.3.3	Urban Building Mounted Turbine	408
19.3.4	Summary Findings: Building Mounted Turbines	409
19.3.5	Field Trial Observations: Pole Mounted Turbines	411
19.4	The Future for Micro-Wind	414
19.5	Conclusions	415
Acknowledgments		416
References		416

20. Integration Into National Grids*Jurgen Weiss and T. Bruce Tsuchida*

20.1	Wind Integration: What it Means and Why We Need it	419
20.2	Current/Standard Measures for Wind Integration	421
20.3	The Future of Wind Integration	429
20.4	Conclusions	434
References		435

Part V**Environmental Impacts of Wind Energy****21. Life Cycle Assessment: Meta-analysis of Cumulative Energy Demand for Wind Energy Technologies***Michael Carbajales-Dale*

21.1	Introduction	439
21.2	Wind Energy Technologies	440
21.2.1	Rotor	442
21.2.2	Nacelle	442
21.2.3	Tower	443
21.2.4	Foundation	443
21.2.5	Balance of Systems	443
21.3	Life-Cycle Assessment	444
21.3.1	Cumulative Energy Demand	444
21.3.2	Energy Payback Time	444
21.3.3	Fractional Reinvestment	445
21.4	Meta-analysis	445
21.4.1	Literature Search	445

21.4.2	Literature Screening	446
21.4.3	Harmonization of Study Boundaries and Data	446
21.5	Results and Discussion	446
21.5.1	Capital Energetic Costs (CEC)	446
21.5.2	Life-Cycle Energy Costs (LCEC)	447
21.5.3	Harmonization	447
21.5.4	Components	449
21.5.5	Trends in Parameters	450
21.5.6	Net Energy Trajectory of the Global Wind Industry	450
21.6	Conclusions	452
Acknowledgments		453
References		453
Appendix A		457
Appendix B		473
22.	Environmental and Structural Safety Issues Related to Wind Energy	
<i>Kaoshan Dai, Kewei Gao, and Zhenhua Huang</i>		
22.1	Introduction	475
22.2	Wind-Energy-Induced Environmental Issues and Countermeasures	475
22.2.1	Effects on Animals and Mitigation Strategies	476
22.2.2	Noise Problems and Possible Solutions	478
22.2.3	Visual Impacts and Mitigation	479
22.2.4	Climate Change and Considerations	480
22.3	Structural Safety Studies for Wind Turbine Towers	481
22.3.1	Wind Turbine Tower Structural Performances Under Wind and Seismic Loads	481
22.3.2	Health Monitoring and Vibration Control of Wind Turbine Towers	483
22.4	Summary	485
Acknowledgments		486
References		486
23.	Wind Turbines and Landscape	
<i>Marc van Grieken and Beatrice Dower</i>		
23.1	A Passion for Landscape	493
23.2	What Is Landscape?	493
23.3	Changing Landscape	495
23.3.1	People's Opinions	495
23.4	Technological Advancement	498
23.5	The Perception of Wind Farms	502
23.5.1	Height and Size	502

23.5.2	Composition	504
23.5.3	Movement	504
23.6	Landscapes With Power Generation Objects	506
23.7	What Are the Effects of Wind Farms on Our Landscape?	508
23.7.1	Landscape Effects	509
23.7.2	Visual Effects	511
23.7.3	Landscape and Visual Effects	512
23.8	Mitigation	512
23.8.1	Strategic Approach	513
23.9	Conclusion	514
	References	515
24.	Global Rare Earth Supply, Life Cycle Assessment, and Wind Energy	
	<i>Zhehan Weng and Gavin M. Mudd</i>	
24.1	Background of Rare Earth Elements	517
24.2	Global REE Supply	519
24.3	REE Permanent Magnets	520
24.4	Life Cycle Assessment of the Use of REE Magnets in Wind Turbines	522
24.5	Global Wind Energy Projections	526
24.6	Implications for Future REE Supply	529
24.7	Conclusion	531
	References	532

Part VI

Financial Modeling/Wind Economics

25. Economics of Wind Power Generation

Magdi Ragheb

25.1	Introduction	537
25.2	Economic Considerations	537
25.3	Wind Energy Cost Analysis	539
25.4	Levelized Cost of Electricity	539
25.5	Net Present Value	540
25.6	Straight Line Depreciation	541
25.7	Price and Cost Concepts	542
25.8	Wind Turbines Prices	542
25.9	Intermittence Factor	542
25.10	Land Rents, Royalties, and Project Profitability	543
25.11	Project Lifetime	543
25.12	Benchmark Wind Turbine Present Value Cost Analysis	544
25.12.1	Investment	544
25.12.2	Payments	544
25.12.3	Current Income and Expenditures per Year	544

25.13 Incentives and Subsidies	546
25.13.1 Production Tax Credit (PTC)	546
25.13.2 Investment Tax Credit (ITC)	546
25.13.3 Renewable Energy Production Incentive (REPI)	547
25.14 Wind Turbine Present Value Cost Analysis Accounting for the PTC	548
25.14.1 Payments	548
25.14.2 Current Income and Expenditures per Year	548
25.15 Accounting for the PTC as Well as Depreciation and Taxes	550
25.16 Transmission and Grid Issues	553
25.17 Discussion	554
References	554

Part VII **Investment, Growth Trends, and the Future of Wind Energy**

26. Growth Trends and the Future of Wind Energy

Lauha Fried, Shruti Shukla, and Steve Sawyer

26.1 Introduction: Global Status of Wind Power (On- and Offshore) in 2015	559
26.1.1 Asia: Remarkable Year for China	560
26.1.2 North America: Resurgence in the United States	562
26.1.3 Europe: Unparalleled Year for Germany	563
26.1.4 Latin America and the Caribbean: Brazil Continues to Lead	564
26.1.5 Pacific	565
26.1.6 Africa and the Middle East	566
26.1.7 2015: Extraordinary Year Fueled by China's FIT Reduction Plan	566
26.2 Offshore Wind Energy	567
26.2.1 Europe Passes 11 GW Mark	570
26.2.2 UK Remains Largest Global Market	573
26.2.3 Germany Had an Exceptional Year	573
26.2.4 Netherlands: Fourth Largest Market Globally	574
26.2.5 France Gearing up to Deliver	575
26.2.6 China Passes the 1 GW Milestone	575
26.2.7 Domestic Industry Moves Japan Forward	576
26.2.8 Upcoming Markets	578
26.3 The Future: Market Forecast (On- and Offshore) to 2020	580
References	586

Index	587
--------------	-----

List of Contributors

AbuBakr S. Bahaj University of Southampton, Southampton, United Kingdom

Charles J. Barnhart Western Washington University, Bellingham, WA, United States

Subhamoy Bhattacharya University of Surrey, Guildford, United Kingdom

Michael Carbajales-Dale Clemson University, Anderson, SC, United States

Liang Cui University of Surrey, Guildford, United Kingdom

Kaoshan Dai Tongji University, Shanghai, China

Beatrice Dower MVGLA, Perthshire, United Kingdom

Ergin Erdem Robert Morris University, Moon Township, PA, United States

Lauha Fried Global Wind Energy Council, Brussels, Belgium

Kewei Gao Tongji University, Shanghai, China

Pei-yang Guo The University of Hong Kong, Hong Kong, China

Anca D. Hansen Technical University of Denmark, Roskilde, Denmark

Martin O.L. Hansen Technical University of Denmark, Lyngby, Denmark

Yi Hong Zhejiang University, Zhejiang Sheng, China

Zhenhua Huang University of North Texas, Denton, TX, United States

Saleh Jalbi University of Surrey, Guildford, United Kingdom

Patrick A.B. James University of Southampton, Southampton, United Kingdom

Alexander Kalmikov Massachusetts Institute of Technology, Cambridge, MA, United States

Jacqueline Lam The University of Hong Kong, Hong Kong, China; The University of Cambridge, Cambridge, United Kingdom

Trevor M. Letcher University of KwaZulu-Natal, Durban, South Africa

Victor O.K. Li The University of Hong Kong, Hong Kong, China; The University of Cambridge, Cambridge, United Kingdom

Junwei Liu Qingdao University of Technology, Qingdao Shi, China

Domenico Lombardi The University of Manchester, Manchester, United Kingdom

Susana Lopez-Querol University College London, London, United Kingdom

Xi Lu Tsinghua University, Beijing, China

- Matthias Luther** Friedrich-Alexander-University of Erlangen-Nuremberg, Erlangen, Germany
- Michael B. McElroy** Harvard University, Cambridge, MA, United States
- Gavin M. Mudd** Monash University, Clayton, VIC, Australia
- George Nikitas** University of Surrey, Guildford, United Kingdom
- Ryan O'Connor** eDF Renewable Energy, Denver, CO, United States
- Adam M. Ragheb** University of Illinois at Urbana-Champaign, Urbana, IL, United States
- Magdi Ragheb** University of Illinois at Urbana-Champaign, Urbana, IL, United States
- Kurt Rohrig** Fraunhofer-Institut für Windenergie und Energiesystemtechnik IWES, Kassel, Germany
- Steve Sawyer** Global Wind Energy Council, Brussels, Belgium
- Michael S. Selig** University of Illinois at Urbana-Champaign, Urbana, IL, United States
- Masoud Shadlou** University of Surrey, Guildford, United Kingdom
- Shuangwen Sheng** National Renewable Energy Laboratory, Golden, CO, United States
- Jing Shi** University of Cincinnati, Cincinnati, OH, United States
- Shruti Shukla** Global Wind Energy Council, Brussels, Belgium
- T. Bruce Tsuchida** The Brattle Group, Cambridge, MA, United States
- Marc van Grieken** MVGLA, Perthshire, United Kingdom
- Lizhong Wang** Zhejiang University, Zhejiang Sheng, China
- Jurgen Weiss** The Brattle Group, Cambridge, MA, United States
- Zhehan Weng** Monash University, Clayton, VIC, Australia; Ghent University, Ghent, Belgium
- Robert Whittlesey** Exponent, Los Angeles, CA, United States
- Wilhelm Winter** Tennet TSO GmbH, Bayreuth, Germany
- Dan-yang Zhu** The University of Hong Kong, Hong Kong, China

Preface

Wind Energy Engineering is an outcome of our earlier book, *Future Energy, improved, sustainable and clean options for our planet, 2nd edition* (Elsevier 2014). It was felt that the wind turbine industry was developing so rapidly that it was now necessary to compile a collection of wind energy related topics into one volume.

The use of renewable energy sources such as wind and sun for electricity generation is becoming commonplace in our society as we move away from fossil fuels to more sustainable forms of energy, free from carbon dioxide production. The move cannot come quickly enough as each month we hear that the previous month was the hottest month since records began and that CO₂ levels are increasing every year and have now passed the 400 ppm level.

Our book gives an all-round view of wind energy with a special focus on technical issues surrounding wind turbines. The 26 chapters are divided into the following seven sections: Introduction; Wind Resource and Wind Energy Worldwide; Wind Turbine Technology; Generation of Electricity; Environmental Impacts of Wind Energy; Financial Modeling/Wind Economics; Investment, Growth Trends, and the Future of Wind Energy. In more detail the book includes chapters on the following areas:

- Scientific aspects (basic theory of wind energy, global potential for producing electricity from wind);
- Wind energy in China and in Germany to give a flavor of developments in two leading wind energy countries;
- The history of wind power;
- Engineering aspects that include the design of different types of wind turbines, basic technologies and problems, and reliability of wind turbines;
- Electricity generation including integration into national grids, small-scale turbines, and the storing of excess electricity;
- Environmental aspects including life cycle investigation, landscape, and safety issues;
- Economics of wind power generation;
- Growth trends and the projected future of wind power.

It is hoped that the book will act as a springboard for new developments and perhaps lead to synergistic advances by linking ideas from different

chapters. Another way that this book can help in expanding and developing the wind industry is through contact between readers and authors and to this effect email addresses of the authors have been included.

This volume is unique in the genre of books of related interests in that each chapter of *Wind Energy Engineering* has been written by an expert scientist or engineer, working in the field. Authors have been chosen for their expertise in their respective fields and come from 12 countries: Australia, Belgium, China, Denmark, Germany, Hong Kong, Finland, India, Russia, South Africa, United Kingdom, and the United States. Most of the authors come from developed countries as most of the research and development in this relatively new field, is based in these countries. However, we look forward to the future when new approaches to wind energy, focusing on local conditions in emerging countries, are developed by scientists and engineers working in those countries. Perhaps this new book will aid in this endeavor.

The chapters in this book can be considered as snapshots, taken in 2016, of the state of this rapidly developing industry. Like *Future Energy*, one can expect an updated version of *Wind Energy Engineering* in a few years' time. *Wind Energy Engineering* goes hand in hand with two other books we have recently published: *Climate Change: Observed Impacts on Planet Earth, 2nd edition*, (Elsevier 2015); and *Storing Energy: with Special Reference to Renewable Energy Sources*, (Elsevier, 2016).

For consistency and to appeal to an international audience, the International System of Units and Quantities is reflected in the book with the use of the Système International d'Unités (SI) throughout. Other units such as Imperial units are written in parenthesis. The index notation is used to remove any ambiguities; e.g., billion and trillion are written as 10^9 and 10^{12} , respectively. To avoid further ambiguities the concept of the quantity calculus is used. It is based on the equation: physical quantity = number \times unit. To give an example: power = 200 W and hence: 200 = power/W. This is of particular importance in the headings of tables and the labeling of graph axes.

A vital concern related to the development and use of renewable and sustainable forms of energy, such as wind, is the question of what can be done when it appears that politicians misunderstand or ignore, and corporations overlook the realities of climate change and the importance of renewable energy sources. The solution lies in sound scientific data and education. As educators we believe that only a sustained grassroots movement to educate citizens, politicians, and corporate leaders of the world has any hope of success. Our book is part of this aim. It gives an insight into the subject, which we hope readers will consider and discuss. The book is written, not only for students, teachers, professors, and researchers into renewable energy, but politicians, government decision-makers, captains of industry, corporate leaders, journalists, editors, and all other interested people.

I wish to thank all 47 authors and coauthors for their cooperation, help, and especially, for writing their chapters. It has been a pleasure working with each and every one of the authors. I thank my wife, Valerie for all the help she has given me over these long months of putting the book together. I also wish to thank Elsevier for their professionalism and help in producing this well-presented volume. Finally I wish to thank Professor Ron Weir of IUPACs Interdivisional Committee for Terminology, Nomenclature, and Symbols for his help and advice.

Trevor M. Letcher
Stratton on the Fosse
Somerset
December 2016

This page intentionally left blank

Part I

Introduction

This page intentionally left blank

Chapter 1

Why Wind Energy?

Trevor M. Letcher

University of KwaZulu-Natal, Durban, South Africa

Email: trevor@letcher.eclipse.co.uk

1.1 INTRODUCTION

Wind Energy Engineering: A Handbook for Onshore and Offshore Wind Turbines is aimed at giving an overview and an insight into most aspects of wind energy. The industry is rapidly reaching a mature stage and it was felt that the time had come to take stock of the wide-ranging topics linked to the generation of electricity from wind. These topics include: an historical background; the reasons for the interest in wind energy; the fundamental science behind the industry; engineering aspects of building wind turbines, generating electricity, and coupling to the grid, environmental issues; economics; and the future prospects of the industry. Having all these disparate topics in one volume of 26 chapters gives the reader a chance to get know the subject and for the specialist to delve deeper. The latter will be rewarded with copious references to the latest work for further study. This book is an outcome of an earlier book we published, entitled *Future Energy: Improved, Sustainable and Clean Options for Our Planet, 2nd edition* (Elsevier, 2014), where only one out of thirty one chapters was devoted to wind energy.

1.2 CLIMATE CHANGE

Today with the specter of global warming and climate change looming over us, there is a need for the energy industry to find energy sources free of carbon dioxide pollution. Energy-related carbon dioxide (CO₂) emissions contribute the majority of global greenhouse gas (GHG) emissions (66%) [1]; these include: electricity production, transport in all its forms, cement making and industry, to mention a few. The fight against climate change must become an important feature in energy policy-making, but the implications are daunting. The emission goals pledged by countries under the United Nations Framework Convention on Climate Change (UNFCCC) are laudable but it is still not enough to reach the level of keeping global

warming to just 2°C above the preindustrial level by 2035. This temperature rise was first mooted in 1996 by the environment ministers of the European Council who declared that “global average temperatures should not exceed 2 degrees above the pre-industrial level.” It took until 2010, when the Cancun Agreement was signed, before the 2°C was enshrined in an international climate policy agreement to “hold the increase in global average temperature below 2°C above preindustrial levels.”

The spotlight is on the renewable energy industry to find energy sources free of carbon dioxide pollution. The other options are to reduce our consumption of energy and consequently our standard of living or to capture CO₂ and bury it in caverns or under the sea (capture and storage, CCS). For many reasons, including our natural reticence toward lowering our standard of living, the cost of CCS, the increasing rise in the population of the world, the aspirations of all to a life with available electricity, it is unlikely that these two options will prevail. To put the problem in perspective, the world energy production (this includes: transport, electricity, heating, and industrial) reached 570 EJ (13,800 million tonnes of oil equivalent (Mtoe)) in 2014, up 1.5% from 2013 [2,3]. In spite of dire warnings there seems to be little international governmental control in reducing this. Fossil fuels still account for 81% of this production—0.4% lower than in 2013—in spite of rising oil (+2.1%), coal (+0.8%) and natural gas production (+0.6%). A small positive sign on the horizon was the fact that during 2014, the energy production by renewable forms of energy did grow significantly, albeit from a low base. For example, hydroelectricity production was up 2.5% and accounted for 2.4% of global energy production, while wind and solar photovoltaics continued their rapid growth (+11% and +35%, respectively), but accounted for around only 1% of global energy production. In 2014 nonfossil sources, biofuels, and waste accounted for 10.2% of world energy production. Nuclear energy contributed 4.7% to the global energy production [3].

In this book we will focus our attention on electricity generation from wind energy. In *Future Energy* [1] we reported that the production of electricity worldwide was responsible for 26% of the global GHGs (mainly CO₂ and CH₄). Fossil fuel was responsible for producing 65% of global electricity (coal 38%, gas 22%, and oil 5%) (see Table 1.1) [4]. Wind and solar energy are at the forefront of the drive to significantly reduce the GHGs to meet the 2°C limit. This is largely because we know that if we can replace fossil fuel with wind and solar energy for generated electricity, we can significantly reduce CO₂ emissions. At the moment wind turbines (433 GW in 2015) [5] have a greater installed capacity, worldwide, than do solar photovoltaics (242 GW in 2016) [6], but this is still a mere drop in the ocean. Wind and solar energy produce only 4% of the global supply of electricity [4]. There is much work to be done. Unfortunately, coal, the worst of the fossil fuel polluters, is still the main energy source for generating electricity. The chief culprits are China, the United States, and Australia; coal produces 72% of

TABLE 1.1 Total World Electricity Production in 2014 [4]

Energy Source	World/%	Euro 27/%	North America/%	Asia/%
Coal	38	26	33	59
Natural gas	22	15	28	13
Hydroelectric	17	11	13	15
Nuclear	11	27	17	4
Oil	5	2	2	4
Biomass, solar, tides	4	9	2	3
Wind	4	9	4	2
Total energy/TW h	22,433	3062	5211	9372
Average power/GW	2559	350	594	1069

China's electricity (total electricity is 5145 TW h) and 38% of the USA's electricity (total electricity is 4255 TW h). Australia is the largest exporter of coal (metallurgical and thermal) in the world (35%) and in 2010–11 exported 283 Mt of coal with more than half going to Japan and China. It was forecast that this figure would increase by over 70% to 486 Mt in 2016–17 [7]. This does fly in the face of the Australian Federal Government's renewable energy target of producing 33 TW h of electricity from renewable sources by 2020 [8,9].

With well-developed wind and other renewable energy industries, we will not need to consider fracking, exploiting tar sands for oil and gas, or any other environmentally unfriendly fossil fuel mining; we should be working toward a situation where our huge fossil fuel reserves in all its forms are left in the ground. In reality, this will only come about when wind energy and other renewable forms of energy become cheaper and more convenient to use than fossil fuel. With mass production and bigger and more efficient wind turbines, this might well come about in the next decade.

1.3 BACKGROUND

The extraction of kinetic energy from wind and its conversion to useful types of energy is a process which has been used for centuries. It is believed that the first windmills were invented 2000 years ago by the Persians and also by the Chinese and were used to grind corn and also to lift water (see [Chapter 8: Wind Turbine Technologies](#)). Later the Dutch would develop windmills to drain their land in the 14th century and, by the 19th century, millions of small windmills were installed in the United States

and throughout the world for pumping water (from boreholes) and for stock and farm home water needs. The 19th century also saw the development of small wind machines (0.2–3 kW producing 32 V direct current) in rural areas in America to operate appliances. These early developments came to an end when the 1936 Rural Electrification Administration was created and grid electricity was supplied to most rural communities. The generation of grid electricity, using wind turbines, has its origins in the United States in the 1970s. Its development was initiated by the need to replace energy derived from fossil fuels with renewable forms of energy. Of all the renewable forms of energy (wind, solar, geothermal, and hydroelectric), wind and solar have shown very positive growth. Over the past 11 years wind energy capacity has increased from 48 to 433 GW; solar PV from 2.6 to 242 GW; hydro from 715 to 1000 GW; and geothermal from 8.9 to 12 GW [10,11]. These figures reflect the maximum possible power available and not what was actually delivered. For example, the electricity obtained from hydroplants in 2014 was 3769 TW h which, when averaged over a year, is equivalent to 430 GW power.

Wind energy is really a secondary level form of energy, reliant on the Sun's uneven heating of the Earth's surface, thus creating temperature differentials which create density and pressure differences in the air. The disparity in heating is often a result of the different heat capacities of the material (e.g., soil, water) being heated by the Sun. This is seen in the daily land and sea breezes in every coastal region. The different reflective nature of the rocks, soil and vegetation, snow, and water also plays a part. The direction of the wind is partly determined by the rotation of the Earth (trade winds) and the topography of the land with winds channeled between mountains and hills with valleys acting as conduits. Taking these issues into account, the tops of hills and mountains, gaps in mountain ranges and coastal areas are often the best places to harness onshore wind power (see [Chapter 2: Wind Power Fundamentals](#) and [Chapter 3: Estimation of Wind Energy Potential and Prediction of Wind Power](#)).

The extraction of wind energy by turbine blades is based on the same principle that gives aeroplane wings their lift. The wind causes a pocket of low-pressure air on the downside of the blade. This causes the blade to move toward the low pressure causing the rotor to turn. This is known as the *lift*. The force of this lift is much stronger than the force of the wind against the frontside of the blade. This is called the *drag*. A combination of the lift and drag causes the rotor to spin. This turns the generator and makes electricity. The power generated by a wind turbine is proportional to the cube of the wind velocity ($P = av^3$, where P is power; a is a constant; and v is the wind velocity). Also the power generated is proportional to the area swept out by the blades making the power a function of the square of blade length ($P = br^2$, where b is a constant and r is the length of the blade); so the bigger

the blade the more power can be extracted—hence the drive to make larger and larger wind turbines (see [Chapters 2, 3](#) and [Chapters 8–11](#)). Another issue with the placing of wind farms is that the wind offshore is stronger and more constant (daily with land and sea breezes) than it is onshore. Furthermore, most cities are situated in coastal regions and this could mean a reduction in electricity transmission costs if wind farms are situated offshore and near the customer base. These issues make it very likely that the future of wind energy lies in offshore wind farms, in spite of the fact that offshore wind farms cost more to establish than do onshore wind farms.

The rapid development of wind turbine technology has been due to the ingenuity of skillful engineers and material scientists. The first serious wind turbines developed for electricity production in the 1970s were rated at about 500 kW; today 8 and 10 MW turbines are being erected with plans to design 20 MW turbines. A typical, modern 3 MW wind turbine can produce enough electricity to power 1000 American homes. The largest wind turbine today is the American designed *SeaTitan* rated at 10 MW with a rotor diameter of 190 m. One of the reasons for the high structure is that the winds are more stable and faster the higher the turbine is from the ground or the sea. The offshore turbines tend to be larger than the onshore turbines. The limit to the size of wind turbines being manufactured and commissioned is at present determined by the problems in transporting the large blades and pillar components, the mechanic strength of the glass fiber blades, and the size of the cranes required to erect the turbines and cost. A solution to some of these problems is to build the blades and pillars offshore (see [Chapters 8–16](#)). A similar situation exists for oil rigs.

In spite of wind energy producing only 4% to the world's electricity, some countries have embraced this technology more than others. In the European Union wind energy contributes 9% of the electricity production, while in the North America this figure is only 4% (see [Table 1.1](#)). The application of wind energy in producing electricity is fast becoming a major contribution to the energy mix of many countries in Europe. In Denmark, e.g., wind turbines contribute 40% of all electrical production from its 5 GW installed turbine capacity [12]. It was reported that in Portugal, for 4 days in 2016, all the electricity used was from renewable sources and of this 22% came from wind energy [13] (see [Chapter 26: Growth Trends and the Future of Wind Energy](#)).

The global capacity of wind energy is about 700 TW h or 433 GW. The leaders in the world are the United States 182 TW h, China 148 TW h, and Germany 58 TW h [4] (see [Chapter 5: The Future of Wind Energy Development in China](#) and [Chapter 6: Wind Power in the German System-Research and Development for the Transition Toward a Sustainable Energy Future](#)). If the current rate of growth continues, wind energy could supply a third of all global energy by 2050.

1.4 ADVANTAGES OF WIND ENERGY

There are many advantages to using wind turbines to generate electricity and these advantages have been the driving force behind their rapid development.

- *Provision for a clean source of energy.* The almost pollution free nature of wind energy is one of the compelling reasons for its development. It delivers electricity without producing carbon dioxide. The relatively small amount of GHG emissions associated with wind turbines is produced in the manufacture and transport of the turbines and blades. It is also free of particulates which are a major problem with coal-fired power stations. Particulates have been blamed for the rise of asthma and possibly Alzheimer's disease in our society, so any reduction in these fine particles floating in the atmosphere is a major health advantage. Another atmospheric pollutant that comes with coal- or oil-fired power stations is sulfur dioxide, formed from the burning of sulfur impurities. It is this SO₂ that is largely responsible for acid rain and also climate change; replacing fossil fuel power stations with wind energy and other renewable energy can rid the planet of this dangerous pollutant.

It is estimated that a 1 MW wind turbine offsets 2360 t (2600 US tonnes) of CO₂ [14].

- *Sustainability.* Whenever the Sun shines and the wind blows, energy can be harnessed and sent to the grid. This makes wind a sustainable source of energy and another good reason to invest in wind farms. Furthermore with the advent of climate change and global warming (the air molecules are moving faster), there is more energy in the atmosphere and we can expect stronger winds in the future.
- *Location.* Wind turbines can be erected almost anywhere, e.g., on existing farms. Very often good windy sites are not in competition with urban development or other land usage; such areas include the tops of mountains or in gullies between hills (see [Chapter 4: Global Potential for Wind Generated Electricity](#) and [Chapter 23: Wind turbines and Landscape](#)).
- *Compatibility with other land uses.* Wind turbines can be erected on pastureland with little disturbance to the animals and the general farming activities. Other areas such as near landfills sites, the sides of motorways and major roads, where urban development is unlikely to take place, are ideal locations to consider for wind farms.
- *Reduction of costly transport costs of electricity from far-away power stations.* Transporting alternating current electricity great distances is expensive because of the cost of the cables and pylons and also because of the loss of power due to the electrical resistance of the cables.
- *National security.* The wind is a free source of energy. Being independent of foreign sources of fuel (e.g., fossil fuel and indeed of electricity) is a great advantage. It means no price hikes over which we have no control and no embargoes on importing fuel or even electricity from foreign countries.

- *Conservation of water.* Traditional power stations using coal, oil, gas, or nuclear fuel all use large volumes of water [15]. Wind farms use no water. In September 2012 Civil Society Institute of the United States published a report, “The Hidden Costs of Electricity: Comparing the Hidden Costs of Power Generation Fuels.” Their conclusions were that: nuclear uses $2660\text{--}4180 \text{ L} (\text{MW h})^{-1}$ ($700\text{--}1100 \text{ gal} (\text{MW h})^{-1}$) in closed-loop systems; coal uses $1750\text{--}2280 \text{ L} (\text{MW h})^{-1}$ ($500\text{--}600 \text{ gal} (\text{MW h})^{-1}$) in closed loop; biomass uses $152,000\text{--}380,000 \text{ L} (\text{MW h})^{-1}$ ($40,000\text{--}100,000 \text{ gal} (\text{MW h})^{-1}$) for irrigating crops to burn; solar uses $855\text{--}1976 \text{ L} (\text{MW h})^{-1}$ ($225\text{--}520 \text{ gal} (\text{MW h})^{-1}$) (washing photovoltaic panels); and wind uses $170\text{--}320 \text{ L} (\text{MW h})^{-1}$ ($45\text{--}85 \text{ gal} (\text{MW h})^{-1}$).
- *Reduction of destructive mining.* The pumping of oil and gas (especially from ocean beds) and the mining of coal or uranium all have serious environmental impacts on the sea or land. Wind farms are relatively benign in this respect and farming and other activities can take place around the turbines as the real action is over a hundred meters above the ground or sea. See Ref. [16] for the environmental issues with coal mining in Australia.
- *Short commissioning time.* Wind farms can be commissioned over a relatively short time, and 2 or 3 years from conception to electricity production is not impossible. This can be compared to the many decades it takes to design, build, and commission a nuclear power station [16]. The fast rate of growth of the wind energy industry over the past 40 years could well be due to the speed at which wind farms can be commissioned.
- *Cost effectiveness.* Over the past decade, the cost of turbines has decreased significantly as a result of improved designs and mass production, so that today the cost of producing electricity from wind farms is now very competitive with fossil fuel-derived electricity [17]. Together, with the drop in investment costs, there has been a significant increase in the efficiency of turbines through increased hub height and larger rotor blade diameter. The overall cost of wind energy is linked to the energy used in turbine manufacture. Wind energy is capital intensive with 75% of the total cost of energy related to the upfront costs of manufacturing the turbines foundations, electrical equipment, and grid connections [18]. It has been estimated that the energy used in the production of a turbine is recouped in the 7 months of operation and when one considers that the lifespan of a turbine is over 30 years the energy and financial gain is significant (see Chapter 21: Life Cycle Assessment: Metaanalysis of Cumulative Energy Demand for Wind Energy Technologies) [19].
- *Creation of jobs and local resources.* The wind turbine industry is a rapidly growing industry and employs thousands of workers in the manufacture processes, transport of turbines, erection of turbines, and in servicing working turbines. Wind Energy projects can be of great help in developing local resources, labor, capital, and even materials. In 2016 the US Energy Department analyzed the future of wind energy and quantified

the environmental, social, and economic benefits coming from the wind industry. The industry in the United States currently supports more than 50,000 jobs in services such as manufacturing, installation, and maintenance. Wind energy has become part of the country's clean energy mix. It suggested that by 2050, more than 600,000 wind-related jobs could be supported by the industry [20].

- *Source of income for farmers, ranchers and foresters and grid operators.* Land for onshore wind farms is leased to electricity supply companies, making a tidy profit for the landowners who can carry on the normal activity on the land with little interference from the turbines. Lease times between 25 and 50 years are common. The UK Government has suggested that for a 2.5 MW turbine, costing $\text{£}3.3 \times 10^6$, the payback time was between 1 and 5 years, allowing plenty of time for a good return on the investment [21,22].
- *Rapid instigation of power.* National grids supply a steady level of electricity (the base load) to meet the needs of a country. If for some reason the supply of electricity needs to be suddenly increased that is not always possible as it can take days to start up a new power station. If the wind is blowing or if the wind energy has been stored then the supply can take just minutes to feed into the national grid.
- *Diversification of power supply.* With our total reliance on electricity it is well worth diversifying our energy sources so that we are not reliant on one type of energy, be it fossil fuel (which is at the mercy of foreign governments which can raise prices suddenly as was done in the 1970s), nuclear (again we are at the mercy of countries supplying uranium), or solar (the Sun does not always shine).
- *Stability of cost of electricity.* Once the wind farm is in place the cost of the electricity to customers should be stable. It is not a function of the price of imported fuels [22].
- *International cooperation.* It has been found that in many instances there is a clear relationship between a manufacturer's success in its home country market and its eventual success in the global wind power market. Lewis and Wiser recently wrote, "Government policies that support a sizable, stable market for wind power, in conjunction with policies that specifically provide incentives for wind power technology to be manufactured locally, are most likely to result in the establishment of an internationally competitive wind industry" [23]. This comment written 10 years ago could well have been written today, and illustrates the importance and success of international cooperation.

1.5 CHALLENGES FACING THE WIND TURBINE INDUSTRY

There are of course a number of challenges associated with harnessing the power of the wind.

- *The intermittency of wind.* Wind is unpredictable and this is perhaps the most important of all the problems associated with electricity production from wind farms. The wind may not be blowing when the electricity from a wind farm is required. Furthermore, when the wind is blowing and electricity is being produced, it is possible that the energy is not required. The solution is to store the electricity when it is not required and using the stored electricity in times of need. This can be done in a number of ways: batteries, pumped water storage, pumped air or methane into caverns, and even driving trains up hills (see [Chapter 4: Global Potential for Wind Generated Electricity](#) and [Chapter 18: Energy and Carbon Intensities of Stored Wind Energy](#)) [24].
- *Good sites are often in remote locations.* The best windy sites are often in hilly, mountainous regions away from urban areas. This does mean that the electricity produced onshore has to be transported along expensive high-voltage cables to reach customers.
- *Noise pollution.* The noise from a rotating wind turbine falls off exponentially with distance from the tower, and at 500 m the sound level is less than 35 dB which is not very much when normal conversation is rated at 60 dB (see [Chapter 23: Wind Turbines and Landscape](#)) [25].
- *Aesthetics.* While some people deplore the sight of wind turbines, others look upon them as pleasing and useful structures. We have over the past century got use to massive pylons marching across our countryside, carrying high-voltage lines. Surely wind turbines are better looking than that! There have been thoughts of painting wind turbines to fit in with the landscape (see [Chapter 23: Wind Turbines and Landscape](#)).
- *Turbine blades can damage wildlife.* There is much evidence that birds and bats are being killed by the turning blades of wind turbines. However the impact on these populations is negligible compared to the large number of bird deaths caused by household cats, car windscreens, sparrow hawks, etc.; it is reported that collisions with turbine blades results in 33,000 bird deaths, while cats are responsible for 100–200 million each year in the United States. It has been reported that the modern very large bladed slow-turning turbines are responsible for far fewer bird deaths than the faster turning turbines (see [Chapter 23: Wind Turbines and Landscape](#)) [26,27].
- *Safety.* The major safety hazard associated with turbines, once they are in place, is the possibility of a blade coming adrift, which could cause serious harm to people or animals nearby. Furthermore a buckled blade could cause a collapse of the tower and that too could cause a serious damage. Wind turbines should be erected away from human habitation (see [Chapter 22: Environmental and Structural Safety Issues Related to Wind Energy](#)).
- *Frequency of light and shadows.* It has been reported that the frequency and strobe effect of turning blades could have an effect on the

human brain. Wind turbines produce a shadow flicker by the interruption of sunlight by the turbine blades. Research work has shown that this flicker can cause epilepsy in certain patients [28]. It was found that the proportion of patients affected by viewing wind turbines, expressed as distance in multiples of the hub height of the turbine, showed that seizure risk does not decrease significantly until the distance exceeds 100 times the hub height. The results show that the flash frequency is the critical factor and should be kept to a maximum of 3 per second, i.e., 60 revolutions per minute for a three-bladed turbine. Furthermore, on wind farms the shadows cast by one turbine on another should not be viewable by the public if the cumulative flash rate exceeds 3 per second. If possible, turbine blades should not be reflective [28]. Wind turbines are designed to operate over a given range of wind speeds and this is usually between 4 and 15 m s^{-1} (between 10 and 40 miles per hour). The speed of the rotating blade can be controlled and slow-rotating turbines could make turbines less of a problem for epilepsy sufferers and for other problems such as the danger to birds and bats.

- *New and unfamiliar technology.* Wind turbines and their accompanying generators can be considered as new technology and are often unfamiliar to most general engineers. This can be a problem if a turbine malfunctions in a rural area. The infrastructure and training of staff to support and maintain turbines must accompany commissioning of new turbines. However, it is reported that wind turbines require less maintenance than do many other electricity producing equipment [29].
- *Shortage of the rare earth element, neodymium, needed to manufacture turbine magnets.* Modern turbines require special permanent magnets and these are made from an alloy that contains the rare earth element neodymium (Nd). A 3 MW turbine needs a 2.7 kg magnet made from neodymium, iron, and boron (NdFeB). These are permanent magnets and are very much stronger than iron magnets. It is necessary to have such strong magnets in order to generate electricity at the slow speeds that wind turbines operate at. It is a case of “the stronger the magnet the more the electrons move.” The supply of neodymium and other rare earths has been dominated by China but this is slowly changing with the reopening mines in the United States (see [Chapter 24: Global Rare Earth Supply, Life Cycle Assessment, and Wind Energy](#)).
- *Initial cost.* The initial cost of setting up a wind farm is perhaps the most serious drawback. It is for this reason that many governments throughout the world still offer subsidies. This is however outweighed by the rewards over the lifetime of the turbine, both financial and environmental (see [Chapter 25: Economics of Wind Power Generation](#)) [30].

In the United States, most of the commercial-scale turbines installed today are 2 MW in size and cost roughly \$3–4 million [31].

1.6 THE POTENTIAL OF WIND ENERGY WORLDWIDE

The potential for wind energy is enormous, especially in developing countries. This is particularly true in rural communities which are not yet linked to grid electricity. For these regions it is an economically viable alternative to diesel engines and even coal-fired power stations [32]. Developing countries with their often obsolete energy supply structures should be investing in this new and proven energy industry, which is fast reaching market maturity. In many cases it would save on buying fuel from other countries and instead that could enjoy the luxury of free fuel in the form of wind (see [Chapter 4](#): Global Potential for Wind Generated Electricity). One issue we must not overlook and that is the linking of wind turbine farms and national grids. This has been part of the success story of the wind industry (see [Chapter 17](#): Physical Modeling of Offshore Wind Turbine Model for Prediction of Prototype Response and [Chapter 19](#): Small Scale Wind Turbines). The next major advancement could well be more effective energy storage for times when the wind is blowing and electricity is not required (see [Chapter 18](#): Energy and Carbon Intensities of Stored Wind Energy).

Even in developed and industrialized countries wind is becoming a major player (see [Chapter 5](#): The Future of Wind Energy Development in China, [Chapter 6](#): Wind Power in the German System-Research and Development for the Transition Toward a Sustainable Energy Future, and [Chapter 26](#): Growth Trends and the Future of Wind Energy). To put it in perspective, on Sunday about 2 p.m. on 15 May over 95% of Germany's electricity was supplied by renewable energy (36% by wind, 45.2% by solar energy, and the rest by hydro and biomass) [33]. That could not have been envisaged 40 years ago. A Norwegian island is showing the way for rural communities. It has a population of 4000 and is totally dependent on wind energy for all its electricity. The 21 wind turbines, most of which are part-owned by the islanders, supply the island with almost 30×10^6 kW h of energy and on top of that 80×10^6 kW h is sold to the national grid. In Denmark 39% of the electricity produced is from wind power. This stems from a decision in 1985 to abandon nuclear power and invest in renewable energy. This initiated the beginning of the Danish domination of turbine manufacturing in Europe [34]. For many developed countries, the incentive to invest heavily in wind energy has been dictated by the need to reduce CO₂ emissions. However, today, with the competitive price of wind energy [17] (see [Chapter 25](#): Economics of Wind Power Generation) and the rising cost of fossil fuel exploration and the political drive to close coal-fired power stations, the future looks very bright for the wind turbine industry.

REFERENCES

- [1] Letcher TM. Future energy: improved, sustainable and clean options for our planet. 2nd ed. London: Elsevier; 2014.

14 PART | I Introduction

- [2] <https://www.iea.org/publications/freepublications/publication/KeyWorld_Statistics_2015.pdf>.
- [3] <<https://yearbook.enerdata.net/>>.
- [4] <www.tsp-data-portal.org/breakdown-of-electricity-generation-by-energy-source#tspQvchart>.
- [5] <www.gwec.net/global-figures/wind-in-numbers/>.
- [6] <<https://www.ise.fraunhofer.de/de/downloads/pdf-files/aktuelles/photovoltaics-report-in-englisher-sprache.pdf>>.
- [7] <<http://www.minerals.org.au/resources/coal/exports>>.
- [8] <<https://www.cleanenergycouncil.org.au/policy-advocacy/renewable-energy-target.html>>.
- [9] <<http://www.industry.gov.au/resource/Mining/AustralianMineralCommodities/Pages/Coal.aspx>>.
- [10] <http://www.ren21.net/Portals/0/documents/activities/Topical%20Reports/REN21_10yr.pdf>.
- [11] <<http://www.ren21.net/status-of-renewables/global-status-report/>>.
- [12] <<http://denmark.dk/en/green-living/wind-energy/>>.
- [13] <<https://www.theguardian.com/environment/2016/may/18/portugal-runs-for-four-days-straight-on-renewable-energy-alone>>.
- [14] <http://apps2.eere.energy.gov/wind/windexchange/pdfs/economic_development/2009/ma_wind_benefits_factsheet.pdf>.
- [15] <http://www.synapse-energy.com/sites/default/files/SynapseReport.2012-09.CSI_Hidden-Costs.12-013.pdf>.
- [16] <<http://www.ewea.org/wind-energy-basics/faq>>.
- [17] <http://www.eia.gov/forecasts/aoe/assumptions/pdf/table_8.2.pdf>.
- [18] <http://pineenergy.com/files/pdf/Economics_of_Wind_Main_Report_FINAL_lr.pdf>.
- [19] Duggy A, Rogers M, Ayompe L. Renewable energy and energy efficiency: assessment of projects and policies. Chichester: Wiley Blackwell; 2015.
- [20] <<http://energy.gov/eere/articles/wind-energy-supporting-600000-jobs-2050>>.
- [21] <<https://www.wind-watch.org/documents/five-questions-to-ask-before-signing-a-wind-energy-lease>>.
- [22] <http://www.local.gov.uk/home/-/journal_content/56/10180/3510194/ARTICLE>.
- [23] Lewis JI, Wise RH. Fostering a renewable energy technology industry. Energy Policy 2007;35(3):1844–2857.
- [24] Letcher TM, editor. Storing energy: with special reference to renewable energy sources. New York, NY: Elsevier; 2016 [25 chapters], 565 pp., ISBN: 978-0-128-03440-8.
- [25] <<http://ramblingsdc.net/wtnoise.html>>.
- [26] <https://www1.eere.energy.gov/wind/pdfs/birds_and_bats_fact_sheet.pdf>.
- [27] <<http://savetheeaglesinternational.org/new/us-windfarms-kill-10-20-times-more-than-previously-thought.html>>.
- [28] Harding G, Harding P, Wilkins A. Wind turbines, flicker, photosensitive epilepsy. Epilepsia 2008;49:1095–8.
- [29] <<http://www.windmeasurementinternational.com/wind-turbines/om-turbines.php>>.
- [30] <<https://www.renewablesfirst.co.uk/windpower/windpower-learning-centre/how-much-does-a-farm-wind-turbine-small-wind-farm-turbine-cost/>>.
- [31] <http://www.windindustry.org/how_much_do_wind_turbines_cost>.
- [32] <<http://www.altenergy.org/Glossary/intro.html>>.
- [33] <<http://www.sciencealert.com/last-sunday-95-percent-of-germany-s-energy-was-provided>> provided by renewables.
- [34] <<http://www.ieawind.org/countries/denmark.html>>.

Part II

Wind Resource and Wind Energy Worldwide

This page intentionally left blank

Chapter 2

Wind Power Fundamentals

Alexander Kalmikov

Massachusetts Institute of Technology, Cambridge, MA, United States

Email: kalex@mit.edu

2.1 WIND PHYSICS BASICS: WHAT IS WIND AND HOW WIND IS GENERATED

Wind is atmospheric air in motion. It is ubiquitous and one of the basic physical elements of our environment. Depending on the speed of the moving air, wind might feel light and ethereal, being silent and invisible to the naked eye. Or, it can be a strong and destructive force, loud, and visible as a result of the heavy debris it carries along. The velocity of the air motion defines the strength of wind and is directly related to the amount of energy in the wind, i.e., its *kinetic energy*. The source of this energy, however, is *solar radiation*. The electromagnetic radiation from the Sun unevenly heats the Earth surface, stronger in the tropics and weaker in the high latitudes. Also, as a result of a differential absorption of sunlight by soil, rock, water, and vegetation, air in different regions warms up at different rate. This uneven heating is converted through convective processes to air motion, which is adjusted by the rotation of the Earth. The convective processes are disturbance of the hydrostatic balance whereby otherwise stagnant air masses are displaced and move in reaction to forces induced by changes in air density and buoyancy due to temperature differences. Air is pushed from high- to low-pressure regions, balancing friction and inertial forces due to the rotation of the Earth.

The patterns of differential Earth surface heating as well as other thermal processes such as evaporation, precipitation, clouds, shade, and variations of surface radiation absorption appear on different space and time scales. These are coupled with dynamical forces due to Earth rotation and flow momentum redistribution to drive a variety of wind generation processes, leading to the existence of a large variety of wind phenomena. These winds can be categorized based on their spatial scale and physical generation mechanisms.

2.2 WIND TYPES: BRIEF OVERVIEW OF WIND POWER METEOROLOGY

Wind systems span a wide range of spatial scales, from global circulation on the planetary scale, through synoptic scale weather systems, to mesoscale regional and microscale local winds. Table 2.1 lists the spatial scales of these broad wind type categories. Examples of planetary circulations are sustained zonal flows such as the jet stream, trade winds, and polar jets. Mesoscale winds include orographic and thermally induced circulations [1]. On the microscale wind systems include flow channeling by urban topography [2] as well as submesoscale convective wind storm phenomena as an example.

A long list of various wind types can be assembled from scientific and colloquial names of different winds around the world. The associated physical phenomena enable a finer classification across the spatial scales. Generating physical mechanisms define geostrophic winds, thermal winds, and gradient winds. Katabatic and anabatic winds are local topographic winds generated by cooling and heating of mountain slopes. Bora, Foehn, and Chinook are locale specific names for strong downslope wind storms [3]. In Greenland, Piteraq is a downslope storm as strong as a hurricane, with sustained wind speeds of 70 m s^{-1} (160 miles per hour). In coastal areas sea breeze and land breeze circulations are regular daily occurrences. Convective storms generate strong transient winds, with downdrafts which can be particularly dangerous (and not very useful for wind power harvesting). Disastrous hurricanes and typhoons, as well as smaller scale tornadoes, are examples of very energetic and destructive wind systems. A microscale version of these winds is gusts, dust devils, and microbursts. Nocturnal jets appear in regular cycles in regions with specific vertical atmospheric structure. Atmospheric waves driven by gravity and modulated by topography are common in many places. Locale specific regional wind names include Santa Anas, nor'easters, and etesian winds, to mention just few.

TABLE 2.1 Spatial Scales of Wind Systems and a Sample of Associated Wind Types

Spatial Scales	Wind Types	Length Scale
Planetary scale	Global circulation	10,000 km
Synoptic scale	Weather systems	1000 km
Mesoscale	Regional orographic or thermally induced circulations	10–100 km
Microscale	Local flow modulation, boundary layer turbulent gusts	100–1000 m

Meteorology is the scientific field involved in the study and explanation of all these wind phenomena. It enables both a theoretical understanding and the practical forecasting capabilities of wind capabilities. Statistics of observed wind occurrences define wind climates in different regions. Mathematical and computer models are used for theoretical simulation, exploratory resource assessment, and operational forecasting of winds. Meteorology literature focusing on wind power is available in the form of introductory texts and reviews [4–7].

2.3 FUNDAMENTAL EQUATION OF WIND POWER: KINETIC ENERGY FLUX AND WIND POWER DENSITY

The fundamental equation of wind power answers the most basic quantitative question—*how much energy is in the wind*. First we distinguish between concepts of *power* and *energy*. Power is the time-rate of energy. For example, we will need to know how much energy can be generated by a wind turbine per unit time. On a more homely front, the power of the wind is the rate of wind energy flow through an open window.

Wind energy depends on:

- amount of air (the volume of air in consideration),
- speed of air (the magnitude of its velocity),
- mass of air (related to its volume via density).

Wind power quantifies the amount of wind energy flowing through an area of interest per unit time. In other words, wind power is the flux of wind energy through an area of interest. *Flux* is a fundamental concept in fluid mechanics, measuring the rate of flow of any quantity carried with the moving fluid, by definition normalized per unit area. For example, *mass flux* is the rate of mass flow through an area of interest divided by this area. *Volume flux* is the volume flowing through area of interest per unit time and per unit area. Consider an area element A (Fig. 2.1) and flow of magnitude U through this area. (Here we restrict the discussion to flow perpendicular to the area of interest. In general, flow is a vector quantify that can be oriented in any direction and only its component perpendicular to the area element is considered when quantifying the flux through that area.) The volume of air flowing through this area during unit time dt is given by the volume of the

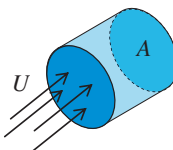


FIGURE 2.1 Schematics of air flow at velocity U through area A . The cylinder depicts the volume flowing in unit time dt through area A .

cylinder with cross section area A and length $U \cdot dt$, i.e., the volume $A \cdot U \cdot dt$. Therefore volume flow rate is $A \cdot U$, the volume flux is U . The mass flow rate is derived by multiplying the volume flow rate by the density of the flow ρ and is equal to the mass of that cylinder divided by unit time

$$\frac{dm}{dt} = \rho \cdot A \cdot U \quad (2.1)$$

Wind energy by definition is the energy content of air flow due to its motion. This type of energy is called the *kinetic energy* and is a function of fluid's mass and velocity, given by

$$KE = \frac{1}{2} \cdot m \cdot U^2 \quad (2.2)$$

Wind power is the rate of kinetic energy flow. In derivation similar to the other flow rate quantities discussed earlier, the amount of kinetic energy flowing per unit time through a given area is equal to the kinetic energy content of the cylinder in Fig. 2.1.

$$P = \frac{1}{2} \cdot \frac{dm}{dt} \cdot U^2 \quad (2.3)$$

Here mass flow rate (2.1) was substituted for air mass in Eq. (2.2). The resultant equation for wind power is

$$P = \frac{1}{2} \cdot \rho \cdot A \cdot U^3 \quad (2.4)$$

This is a fundamental equation in wind power analysis. It exhibits a highly nonlinear cubic dependence on wind speed. Whereby doubling the wind speed leads to eightfold increase in its available power. This explains why ambient wind speed is the major factor in considering wind energy. In Eq. (2.4), the power of the wind is a linear function of air density and as a result of the limited range of air density fluctuations, the density is of secondary importance. The power dependence on the area implies a nonlinear quadratic dependence on the radius of a wind turbine swept area, highlighting the advantages of longer wind turbine blades.

It is customary to normalize ambient wind power dividing by the area of interest; i.e., in terms of specific power flow. This leads to the definition of kinetic wind energy flux, known as the *wind power density (WPD)*. Similarly to the definitions of flux and flow rate above, wind energy flux is wind energy flow rate per unit area is given by:

$$WPD \equiv \frac{P}{A} = \frac{1}{2} \cdot \rho \cdot U^3 \quad (2.5)$$

WPD is used to compare wind resources independent of wind turbine size and is the quantitative basis for the standard classification [8] of wind

TABLE 2.2 Wind Power Classes Measured at 50 m Above Ground According to NREL Wind Power Density-Based Classification

Wind Power Classification			
Wind Power Class	Resource Potential	Wind Power Density/W m ⁻²	Wind Speed/m s ⁻¹
1	Poor	0–200	0.0–5.9
2	Marginal	200–300	5.9–6.7
3	Fair	300–400	6.7–7.4
4	Good	500–600	7.4–7.9
5	Excellent	500–600	7.9–8.4
6	Outstanding	600–800	8.4–9.3
7	Superb	>800	>9.3

Wind speed corresponding to each class is the mean wind speed based on Rayleigh probability distribution of equivalent mean wind power density at 1500 m elevation above sea level. Source: Data adopted from http://www.nrel.gov/gis/data/GIS_Data_Technology_Specific/United_States/Wind/50m/Colorado_Wind_50m.zip [11].

resource at the National Renewable Energy Laboratory (NREL) of the United States. Mean WPD has advantages over mean wind speed for comparing sites with different probability distribution skewness, because of the cubic nonlinear dependence of wind power on wind speed (see Fig. 11 in Ref. [9] and discussion therein). Further technical details of this classification system were originally introduced in Ref. [10]. Typical values of wind power classes with the corresponding power densities and mean wind speeds are presented in Table 2.2.

2.4 WIND POWER CAPTURE: EFFICIENCY IN EXTRACTING WIND POWER

In Section 2.3 we considered the total wind power content of ambient air flow. Fundamentally, not all this power is available for utilization. The efficiency in wind power extraction is quantified by the *Power Coefficient* (C_p), which is the ratio of power extracted by the turbine to the total power of the wind resource $C_p = P_T/P_{\text{wind}}$.

Turbine power capture therefore is given by

$$P_T = \frac{1}{2} \cdot \rho \cdot A \cdot U^3 \cdot C_p \quad (2.6)$$

which is always smaller than P_{wind} . In fact, there exists a theoretical upper limit on the maximum extractable power fraction—known as the *Betz Limit*.

According to Betz theory [12] the maximum possible power coefficient is $C_p = 16/27$, i.e. 59% efficiency is the best a conventional wind turbine can do in extracting power from the wind. The reason why higher, e.g., 100%, efficiency is not possible is due to the fluid mechanical nature of wind power, dependent on the continuous flow of air in motion. If, hypothetically speaking, 100% of kinetic energy was extracted then the flow of air would be reduced to a complete stop and no velocity would remain available to sustain the flow through the extraction mechanism, irrespective of the specific wind turbine technology used. The maximum extraction efficiency is achieved at the optimum balance of the largest wind slowdown that still maintains sufficiently fast flow past the turbine. (See Refs. [13,14] for further technical details and an historic account of Betz limit derivations by contemporary researchers.)

Another key metric of wind power efficiency is the *Capacity Factor* (*CF*) quantifying the fraction of the installed generating capacity that actually generates power.

$$CF = \frac{E_{\text{actual}}}{E_{\text{ideal}}} = \frac{\text{Time} \cdot \bar{P}}{\text{Time} \cdot P_N} = \frac{\bar{P}}{P_N} \quad (2.7)$$

The *CF* is the ratio of the actual generated energy to the energy which could potentially be generated by the system in consideration under ideal environmental conditions. Considering that energy is the product of its time-rate, i.e., the power with the elapsed time, this energy ratio is equal the ratio of average power \bar{P} to the nominal power of the system P_N . For a single wind turbine this nominal power is equal to its nameplate capacity, typically the maximum power it can generate under favorable wind conditions. Considering a typical power curve for a turbine (Fig. 2.2) this is the flat region for strong wind just below the cut-out wind speed.

Equivalently, *CF* can be regarded as the fraction of the year the turbine generator is operating at rated power (nominal capacity), i.e., the fraction of the effective time relative to the total time

$$CF = \frac{E_{\text{actual}}}{E_{\text{ideal}}} = \frac{E_{\text{actual}}}{\text{Time} \cdot P_N} = \frac{E_{\text{actual}}/P_N}{\text{Time}} = \frac{\text{Time}_{\text{effective}}}{\text{Time}} \quad (2.8)$$

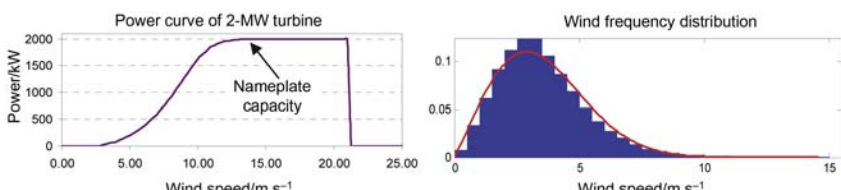


FIGURE 2.2 Typical wind turbine power curve (left panel) and the statistics of wind variability (right panel) given by a histogram and Weibull probability density fit.

Therefore total annual energy generation can be calculated by multiplying turbine (or wind plant) rated power P_N by time length of 1 year and by CF .

$$E_{\text{actual}} = P_N \cdot \text{Time}_{\text{effective}} = P_N \cdot \text{Time} \cdot CF \quad (2.9)$$

A typical value of CF for an economically viable project is 30%, reaching about 50% in regions with a very good wind resource. The CF is based on both the characteristics of the turbine and the site—integrating the power curve with the wind resource variability (Fig. 2.2) produces the actual generation or the average power. This highlights the dependence of power production on wind variability and the importance of wind meteorology and climatology for wind power forecasting and resource assessment.

2.5 CONCLUSION

Wind power is concerned with the utilization of kinetic wind energy. This is the energy contained in air motion itself. Since this is a form of mechanical energy of a moving fluid, its quantification requires elements of fluid mechanics. We reviewed the concepts of kinetic energy flux and derived the fundamental equation of wind power—quantifying the rate of wind energy flow. Standard metrics of wind power resource and utilization efficiency were introduced. The nature of wind was discussed with a brief overview of wind power meteorology.

REFERENCES

- [1] Pielke Sr RA. Mesoscale meteorological modeling, vol. 98. New York, NY: Academic Press; 2013.
- [2] Kalmikov A. Uncovering MIT wind myths through micro-climatological CFD analysis. arXiv 2013;1310:3538.
- [3] Durran DR. Downslope winds. Encyclopedia of atmospheric sciences. Amsterdam: Academic Press; 2003.
- [4] Emeis S. Wind energy meteorology. Berlin, Heidelberg: Springer Berlin Heidelberg; 2013.
- [5] Petersen EL, Mortensen NG, Landberg L, Højstrup J, Frank HP. Wind power meteorology. Part I: climate and turbulence. Wind Energy 1998;1:25–45.
- [6] Petersen EL, Mortensen NG, Landberg L, Højstrup J, Frank HP. Wind power meteorology. Part II: siting and models. Wind Energy 1998;1:55–72.
- [7] Banta RM, Pichugina YL, Kelley ND, Hardesty RM, Brewer WA. Wind energy meteorology: Insight into wind properties in the turbine-rotor layer of the atmosphere from high-resolution doppler lidar. Bull Am Meteorol Soc 2013;94:883–902.
- [8] <http://rredc.nrel.gov/wind/pubs/atlas/appendix_A.html>; <http://www.nrel.gov/gis/wind_detail.html>.
- [9] Elliott DL, et al. Wind energy resource assessment of the Caribbean and Central America. Richland, WA: No. PNL-6234. Pacific Northwest National Laboratory (PNNL); 1987. Available from: <http://dx.doi.org/10.2172/971424>.

24 PART | II Wind Resource and Wind Energy Worldwide

- [10] Elliott DL, Barchet WR. Wind energy resources atlas. Volume 1. Northwest region. United States: N. p.; 1980. <http://dx.doi.org/10.2172/5319588>.
- [11] <http://www.nrel.gov/gis/data/GIS_Data_Technology_Specific/United_States/Wind/50m/Colorado_Wind_50m.zip>.
- [12] Betz A. The maximum of the theoretically possible exploitation of wind by means of a wind motor. *Wind Eng* 2013;37(4):441–6. Translation of: Das Maximum der theoretisch möglichen Ausnützung des Windes durch Windmotoren, *Zeitschrift für das gesamte Turbinenwesen*, Heft 26, 1920.
- [13] van Kuik GAM. The Betz-Joukovsky limit: on the contributions to rotor aerodynamics by the British, German and Russian scientific schools. *Wind Energy* 2012;15:335–44.
- [14] van Kuik GAM. The Lanchester-Betz-Joukovsky limit. *Wind Energy* 2007;10:289–91.

Chapter 3

Estimation of Wind Energy Potential and Prediction of Wind Power

Jing Shi¹ and Ergin Erdem²

¹*University of Cincinnati, Cincinnati, OH, United States*, ²*Robert Morris University,*

Moon Township, PA, United States

Email: Shij3@ucmail.uc.edu, erdem@rmu.edu

3.1 INTRODUCTION

Wind is one of the prominent renewable energy resources. The percentage of wind energy-based resources for electricity generation has been steadily growing. Currently Denmark is producing over 40% of its electricity from wind-based resources [1]. There is a strong growth pattern in terms of the installed wind capacity. To cite an instance, the installed worldwide wind capacity reached 432 419 MW at the end of 2015. When compared with the figures of 2014, this represents an increase of nearly 17% (i.e., this figure was 369 695 MW at the end of 2014) [2]. The adoption rates of utilizing wind-based resources for generating wind energy, as expected, are different throughout various regions in the world. In the United States, 4% of the total electricity is obtained from wind-based resources, while the State of Iowa produces 31% of the electricity from wind-based resources [3].

To assess the wind energy feasibility at a particular site, it is imperative to conduct a successful wind resource assessment and measuring program. To embark on such a study, it is important to develop a sound quality assurance plan and framework associated with each wind potential program. The measurement, equipment, and apparatus selection that have acceptable standards, data collection, and analysis schemes are important aspects to consider.

Usually, wind potential assessment programs consist of several important steps. These can be listed as preliminary area identification, area wind resource evaluation, and micrositing (i.e., choosing the best location for wind turbines within the wind potential assessment site) [4]. Those aspects are discussed in more detail in the following sections.

The first wind resource assessment program starts with wind atlases (i.e., wind resource maps) depicting the wind potential. The data obtained from satellites is now being used extensively along with the data obtained from ground resources. To cite an instance, Solar and Wind Energy Resource Assessment (SWERA) project for the United Nations Environment Programme is one of the extensive initiatives that have been formed for this purpose [5].

During the recent decades, considerable effort has been spent on improving the accuracy and detailing level of wind atlases. To improve the accuracy, extensive network of ground measurement units must be deployed. With the inclusion of the satellite and remotely obtained data, the accuracy and resolution of the atlases should significantly improve. As such, there is an ongoing effort initiated by the International Renewable Energy Agency to combine the publicly available Geographic Information System (GIS) data to obtain a comprehensive picture of the available wind resources. For this purpose the *Energy Sector Management Assistance Program* (ESMAP) has allocated US\$22.5 million for supporting the projects conducted over 12 different countries until 2018 [6]. However, it should be also kept in mind that there is a need for actual field work no matter how detailed and accurate the wind atlases are. The data should be validated for short-, medium-, and long-term time periods for tapping the whole potential of a wind site.

The outline of the chapter is as follows. In [Section 3.2](#), we discuss the main principles associated with developing a successful wind assessment program. In [Section 3.3](#), we outline the main aspects of a wind potential assessment program which involves instrumentation, data handling, preliminary analysis, and hind-sight analysis such as *Measure-Correlate-Predict* (i.e., MCP). In [Section 3.4](#), the methods for obtaining the average wind power based on wind speed measurements are described. In [Section 3.5](#), we discuss the aspects associated with the wind assessment such as the scale of analysis (i.e., microscale, mesoscale, and macroscale), the analytical models and software that might be utilized for the siting purposes, (e.g., *Wind Atlas Analysis and Application Program* (WAsP), *Computational Fluid Dynamics* (CFD)-based approaches, and the spatial exploration models. In [Section 3.6](#), we provide additional considerations associated with wind resource assessment such as extreme wind speed analysis, rugged terrain analysis, wake of turbines, uncertainty analysis, and estimation of losses associated with electricity production. In [Section 3.7](#), we summarize the analytical approaches associated with the forecasting of wind speed and wind power. In [Section 3.8](#), we provide overall conclusive remarks.

3.2 PRINCIPLES FOR SUCCESSFUL DEVELOPMENT FOR A WIND ASSESSMENT PROGRAM

A successful wind assessment program includes: site identification, preliminary resource assessment, and micrositing according to New York State Energy Research and Development Authority [8], with wind atlases serving as

a valuable tool for preliminary analysis. Apart from using wind atlases, there are additional steps that should be performed. These are identified as: (1) instantaneous wind speed measurement to estimate the wind potential; (2) interviewing stakeholders regarding the environmental impact of the wind turbines; (3) studying the meteorological information regarding the wind speed and wind direction; (4) availability of land; and (5) terrain features, i.e., surveying the obstructions that might impede the wind flow [7].

In general, a preliminary resource assessment includes defined measurement plans where the key decisions on the tower placement, height, and instrumentation are given. Besides those decisions, the determination of whether adequate wind resources exist within the specified area, a comparison of different areas for distinguishing relative development potential, obtaining representative data for the estimation of economic viability and performance of wind turbines, and the screening of the potential of wind turbine installation sites are also important considerations [4].

Regarding micrositing, the main aspects of decision-making involve conducting additional measurements for validating the data, conducting the necessary adjustments for the wind shear and the long-term wind climate, numerical flow modeling, and the corresponding uncertainty estimation. Moreover, in the micrositing phase, small-scale variability of the wind resource over the terrain of interest is quantified to position one or more wind turbines to maximize overall energy output [8].

Wind atlases are the starting point for a preliminary site selection. However, it should be kept in mind that these maps give only a rough estimate and might differ from the actual wind speeds by $\pm 10\%-15\%$. Since wind power is a function of the cube of the wind speed, the deviation between actual and estimated wind output could be further compounded; this might lead to the differences of up to $\pm 20\%$ [9].

Usually, the classification of wind sites with respect to wind potential is on a five-scale rating. According to this classification, class-5 is considered as extremely suitable for a wind farm, whereas class-1 is deemed as unfeasible. In that regard, Bennui et al. [10] use GIS and employ a multiple decision criteria-based method to classify wind sites. The decision criteria are: wind speed information, elevation, slope, highways and railways, built-up area, forest zone, and scenic area.

Researchers have developed comprehensive methods for assessing wind potential. To cite an instance, Lawan et al. [11] conduct a structured analysis and review the steps for conducting the wind resource assessment program for Malaysia. They also discuss the prospects and challenges of using wind energy both in the developing and developed countries. It is believed that the developing countries especially in Asia have untapped potential for wind energy and suggested that the government and private entities should work together, especially for harvesting wind energy in remote and rural areas. It is also pointed out that wind speed distribution, energy potential modeling, determining cut-in, cut-out and rated wind turbine velocities, wind speed

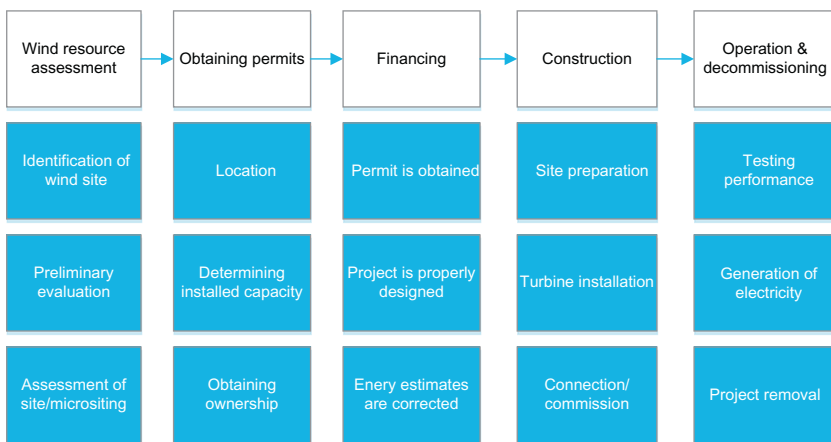


FIGURE 3.1 Stages of the wind energy project lifecycle [14].

profiling, and proper software selection are important aspects once the wind potential is properly assessed.

In a similar fashion, there are some analytical methods used for comparing wind potentials at different sites. Corbett et al. [12] develop a methodology based on the CFD approach for comparing 13 wind farm sites involving 74 mast pairs. The CFD-based approach should be fine-tuned with respect to the flow characteristics of the wind, using care, expertise, and engineering judgment especially for complex terrain conditions. Additionally, wind assessment programs could play a pivotal role in shaping the decisions. For instance, Wang et al. [13] emphasize the importance of holistic approaches that would necessitate the integration challenges associated with the Chinese wind energy policies. To obtain full potential of wind-based resources, it is vital to determine the predictability with successful forecasting models, and improve energy markets with the objectives of long-term development and pricing reforms. To enhance predictability and creating effective markets, research and development on wind resource assessment programs are of paramount interest and these activities should be conducted in a transparent manner. The steps that should be conducted for realizing a successful wind energy system is given in Fig. 3.1.

3.3 MAIN ASPECTS OF A WIND ASSESSMENT PROGRAM

One of the most important parameters in determining the electric power obtained from the wind-based resources is wind speed. The general equation relating wind power to swept area, wind speed, and density of air is [7]:

$$P_w = \frac{1}{2} \rho A v^3 \quad (3.1)$$

where P_w is the wind power, ρ is the density of the air, and v is the wind speed. This represents the total energy obtained from the wind flow. In terms of generating electric energy, only a certain proportion of the kinetic energy of the wind can be converted. This relation can be expressed as,

$$P_e = \eta_e \eta_m C_p P_w \quad (3.2)$$

where P_e is the amount of electric power generated, η_e is the electric conversion efficiency of the wind turbine, η_m is the mechanical efficiency, and C_p is the power coefficient. The upper limit for the power coefficient (i.e., the proportion of the amount that can be extracted from the kinetic energy of the wind) is 59.3% regardless of the geometry of the wind turbine. Usually the power coefficient of the modern wind turbines is between 45% and 50% [15]. Fig. 3.2 is a typical power curve of a wind turbine that shows the relation between the generated wind power and the wind speed.

As illustrated in Fig. 3.2, at low wind speeds, there is not enough torque applied by the wind to generate electricity. The minimum wind speed at which electricity can be generated is called the cut-in speed, namely, the speed at which the rotor of the wind turbine begins turning. As described in Eqs. (3.1) and (3.2), the generated wind power increases with the cube power of the wind speed, up to a certain value which is called rated power. The rated output is usually obtained at the maximum speed that the rotor is allowed to turn. Usually, the wind turbine manufacturers place an upper limit on the speed that the blades are allowed to turn to increase the longevity of the blades by preventing and minimizing bird impacts, rain, erosion, etc. [16]. Typically, the tip of the blade of the rotor turns at a maximum speed of 120 m s^{-1} . Turning the blades faster could lead to problems. Beyond a certain speed, in order to prevent structural damages, the rotor is brought to a

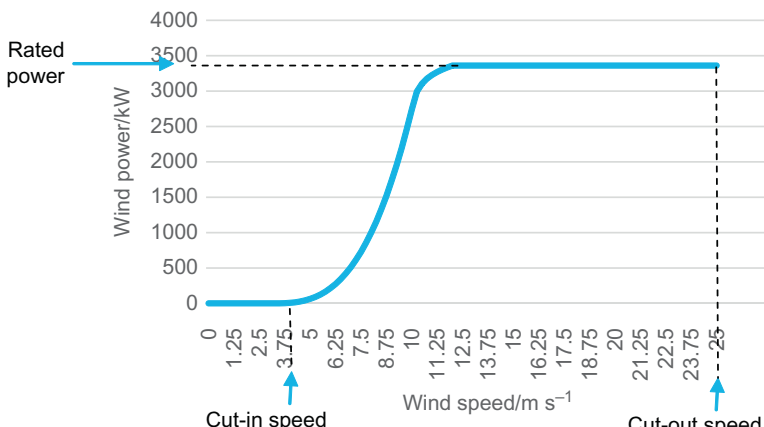


FIGURE 3.2 Power curve of a typical wind turbine.

standstill by a brake. This particular wind speed is called the cut-out wind speed.

To determine the potential of a wind-based resource to the fullest extent, identification and survey of the site are the most vital concern. For this purpose, proper instrumentation plays a crucial role. Wind power maps give only a crude information regarding the specific information sites. To characterize the wind-related properties, and collect associated data, a sound data acquisition program with the following aspects should be taken into consideration [8]:

- Equipment procurement tailored according to program specifications;
- Equipment calibration, frequency, method, and reporting requirements;
- Monitoring station installation, verification, and checklists related with maintenance and operation;
- Data collection and screening;
- Data analysis guidelines that also includes corresponding calculations;
- Data validation methods and flagging criteria, the frequency of reporting, and associated format;
- Internal audits for various aspects such as site installation, operation and maintenance, and data handling.

Some consider placing remote sensing equipment for collecting the wind-related data. In a study conducted by Rodrigo et al. [17], the procedures for the testing and evaluation of the remote sensing equipment for the wind-related attributes were investigated. For this purpose, two terrains with different topologies (i.e., a flat and a complex terrain) are considered. An intercomparison between sound- and light-based equipment (i.e., SODAR—*Sound Detection and Ranging* system and LIDAR—*Light Detection and Ranging* system) that can remotely sense the wind is made. The researchers use a single-point regression, ensemble-averaged profile analysis, and a performance matrix in the evaluation steps and discuss the principles associated with the remote sensing equipment for a wide variety of terrain conditions. The analysis is helpful for extending the scope of the wind energy potential assessment campaigns and measuring the corresponding wind attributes at certain heights without the need for installing anemometers at specified distances. It is concluded that although the remote sensing technologies using the sound and light wave technologies show improvement, defining standards for testing and calibration is difficult for the complex terrain applications. It is also indicated that a multitude of prototype designs in terms of the uncertainty of the measurements with respect to various terrain conditions should be evaluated for remote sensing equipment in order to develop standards for generating bankable data.

For the wind turbines located offshore, other approaches are of interest. To cite an instance, Nicholls-Lee [18] discusses the possibility of

instrumentation platforms that have the mobility deployed for assessing of wind potential offshore. The feasibility of lightweight, floating platform for a repositionable meteorological measurement station is evaluated. Contrary to the traditional anemometers, LIDAR is adopted for capturing the wind speed and direction at the specified heights. Such a platform could be a viable alternative to deploying costly masts to capture the offshore wind potential. Other researchers discuss the potential for utilizing the data captured by satellites for conducting wind resource assessment [19,20].

Aside from the wind speed, one of the most important wind attributes is the ambient air temperature. The air temperature determines the air density. As indicated in Eq. (3.3), wind power increases with the air density. The relation between the air temperature and the air density for humid air can be approximated using the ideal gas formula;

$$\rho_{\text{humid air}} = \frac{p_d}{R_d T} + \frac{p_v}{R_v T} \quad (3.3)$$

where $\rho_{\text{humid air}}$ is the density of humid air (in kg m^{-3}), p_d is the partial pressure of the dry air (in Pascal), T is the temperature (in Kelvin), R_d is the specific gas constant for dry air (i.e., $287.058 \text{ J}(\text{kg K})^{-1}$), p_v is the partial pressure of the water vapor (in Pascal), and R_v is the specific gas constant for water vapor (i.e., $461.495 \text{ J}(\text{kg K})^{-1}$). The temperature readings should be conducted at several meters above the ground to minimize the effects of surface heating [7].

Another consideration is the determination of the distance between the measurement point and the potential location of the wind turbine. It should be kept in mind that as the terrain becomes more complex due to the variability associated with the local wind characteristics, the maximum distance between the point of measurement and the potential location should decrease. As a rule of thumb, that distance should be 5–8 km for a relatively simple terrain, and 1–3 km for the regions where complex terrain conditions are present (e.g., steep geometrically complex ridgelines, coastal sites with varying distance from the shore or heavily forested areas) [8]. This necessitates the placement of a larger number of measurement towers for wind farms as compared to stand-alone turbines. Intuitively, the number of towers should be increased to analyze the perturbation of the more complex terrain on the wind flow. In that regard, the tower placement should be representative of the turbine locations. Nevertheless, in order to obtain a comprehensive picture and analyze the wind flow over an area more accurately, some towers should also be placed at the coordinates where less than ideal conditions exist [21].

For deciding on the final location of turbines, a preliminary analysis needs to be conducted using software (e.g., WindPRO) based on the wind resource maps and terrain-based constraints. The siting of wind turbines at a

location involves grouping turbines into clusters based on distance. For relatively flat terrains, the rule of thumb is to place 10–12 turbines in one cluster, and for more complex terrains, place 5–7 wind turbines in one cluster. After forming the cluster, the median wind speed within the cluster is calculated based on the wind resource map, and the locations at which the median speed is observed are selected for the potential location for the measurement points and hence the construction of towers. Usually, two or three candidate locations are selected for a tower. Then, by visual examination, the final locations of those towers (one for each cluster) are selected in such a way that those towers are sufficiently spread out [22].

Furthermore, consideration should be given to the extrapolation of data obtained from different wind sites. The following simple equation might be used for this purpose [8]:

$$v_2 = v_1 \left(\frac{h_2}{h_1} \right)^\alpha \quad (3.4)$$

where v_1 is the known speed at measurement height h_1 , v_2 denotes the wind speed at the height h_2 where the wind speed is extrapolated, and α is the wind shear exponent. There are various factors that affect the wind shear exponent, including vegetation cover, terrain, general climate, and even the time of the day. In the literature, α values ranging between 0 and 0.4 are reported [8].

Not only the new measurement facilities, but also the existing measurement units might be used for wind resource assessment. For this purpose, existing towers, airport measurement units, and spatial extrapolation models might be used. Waewsak et al. use 120 m wind tower at the shoreline to analyze the monthly mean wind speeds and dominant wind directions. Using this data, they obtain a 20 m resolution microscale map, and estimate the annual energy productions, wake effects, and theoretical capacity factors [23]. In a similar fashion, Kim and Kim [24] use the AMOS (Aerodrome Meteorological Observation System) wind data measured at Yeosu Airport to develop a wind resource map. Based on this map and by employing three cases with different designs for the wind turbine, a comparative economic analysis is conducted.

Generally, MCP can be defined as the collection of methods that are used for the estimation of long-term wind resources based on short-term data. The idea is about using the short-term campaign and correlating it with an overlapping but climatologically representative time series (i.e., 5 years, preferably 10 years) [25]. The larger the wind project becomes (in terms of installed capacity, power rating, or similar performance measures), the more important the accurate prediction of the wind resources. For smaller projects (i.e., for wind farms with less than 100 MW output), the length

of time for recording measurements varies between 4 and 6 weeks [8]. However, for larger projects long-term measurements might be needed for capturing the differences due to the change of seasons, or factors associated with a complex terrain. The methods that have been used to extrapolate data for long-term performance began in the 1940s for single stations, and gradually evolved into more complex methods. Those early methods usually use linear, nonlinear, and probabilistic transfer functions and could be applied to a time series data as well as to frequency distributions of associated wind speeds [26].

3.4 ESTIMATING WIND POWER BASED ON WIND SPEED MEASUREMENTS

After the data acquisition and validation phase, the next step is to analyze the data for estimating the wind energy that would be produced over a certain period. As previously indicated, the wind speed varies over time and statistical distributions might be employed for this case. Weibull distributions are usually employed for modeling wind speed distributions [27]. Based on this assumption, the following model can be used to estimate the wind power output. Following Eq. (4.5), the average wind power can be calculated as [28]:

$$P_{ave} = \zeta P_E \quad (3.5)$$

where P_{ave} is the average wind factor, ζ is the capacity factor, and P_E is the electricity power generated. To find the ζ value, the following integral should be evaluated;

$$\zeta = \frac{1}{V_R^3} \int_{v_c}^{v_R} v^3 f(v) dv + \int_{v_R}^{V_F} f(v) dv \quad (3.6)$$

where V_R is the wind speed at which the rated power is reached, v_c is the cut-in speed, V_F is the cut-out speed, and $f(v)$ is the probability density function of the wind speed. Assuming that the Weibull distribution, which is one of the most widely used distribution for characterizing wind speed, is used, ζ can be calculated as:

$$\zeta = \left(\frac{v_c}{v_R} \right)^3 e^{-(v_c/c)^k} + 3 \frac{\Gamma(3/k)}{k} \left(\frac{v_R}{c} \right)^3 \left[\gamma \left(\left(\frac{v_R}{c} \right)^k, \frac{3}{k} \right) - \gamma \left(\left(\frac{v_c}{c} \right)^k, \frac{3}{k} \right) \right] - e^{(v_f/c)^k} \quad (3.7)$$

where (v_R/c) is the normalized rated speed, Γ is the gamma function, γ is the incomplete gamma function, c is the Weibull scale parameter, and k is the shape parameter.

The Weibull scale parameter can be estimated from the following equation:

$$k = \left(\frac{\sigma}{\bar{x}}\right)^{-1.086} \quad (3.8)$$

$$\frac{c}{\bar{x}} = \left(0.568 + \frac{0.433}{k}\right)^{\frac{1}{k}} \quad (3.9)$$

where σ is the standard deviation of the wind speed and \bar{x} is the average wind speed.

Various approaches have been used for determining the underlying distribution governing the wind speed equation. Zhou et al. [29] have compared various distributions for modeling the wind speed distribution, and conclude that the maximum entropy-based functions proved to be a versatile tool. The authors conduct a comprehensive study on five North Dakota Sites and indicate that no distribution outperforms any others but Rayleigh-based distributions in general are inferior when compared to other distributions (e.g., maximum entropy based, Weibull, Rayleigh, gamma, lognormal, and inverse Gaussian). Some researchers have used the bivariate distribution for modeling and characterizing wind attributes (i.e., direction and speed) simultaneously. Erdem et al. [30] provide a comparison for modeling the wind speed and direction using three different approaches (namely, angular-linear, Farlie–Gumbel–Morgenstern (FGM) and anisotropic lognormal approaches), in terms of the root mean square error and R^2 values. The FGM approach provides compatible results, while the anisotropic normal distribution lags behind. Fractional distributions can also be used for modeling the wind speed distributions, e.g., the fractional Weibull distributions [31]. Some researchers develop nontraditional methods for characterizing the wind speed distributions over a long period of time. Li and Shi [32] combine an averaging Bayesian model and Markov Chain Monte Carlo sampling methods, and conclude that the combined approach provided comparative reliability and robustness in describing the long-term wind speed distributions for the selected wind sites.

3.5 WIND RESOURCE ESTIMATION PROJECT: SCOPE AND METHODS

In terms of the scope, wind resource assessment can be conducted at different levels (i.e., microscale, mesoscale, and macroscale). As the name implies, microscale wind resource assessment campaigns usually entails assessing the wind power for a smaller region such as the local/site coverage; mesoscale entails the national coverage; and macroscale usually focuses on estimating the wind potential on a global scale. The resolution of the wind power assessment program differs widely with respect to scale. In general,

microscale entails a resolution of between 10 and 100 m; mesoscale entails the resolution of approximately 5 km; and macroscale incorporates a resolution of approximately 50–200 km [33].

The estimates for global wind power vary depending on the assumptions and associated constraints. Most researchers evaluate the potential of both onshore and offshore winds. The estimate for total wind potential varies considerably. Lu et al. [34] predict the global wind energy potential to be 840 000 TW h per year based on the Goddard Earth Observing System Data Assimilation System (GEOS-5 DAS) dataset. This dataset uses a weather/climate model incorporating inputs from a wide variety of observational sources (surface and sound measurements) and a suite of measurements and observations from a combination of airborne vehicles (i.e., aircraft, balloons, ships, and drones), sea units (ships and buoys), and satellites. This creates fairly accurate high-resolution wind potential maps. The authors indicate that 36% of the capacity factor is the breakeven point for satisfying the world demand for electricity power if those wind turbines are only located onshore. On the other hand, Hoogwijk and Graus [35] by employing a more constrained model, estimate that the global capacity for wind-based resources for generating electricity is 110 000 TW h per year. The authors indicate that the theoretical potential involves natural and climatic factors, while geographical potential involves examining land use and land cover limitations. It is also indicated that market potential involves demand for energy, competing technologies, and examining corresponding policies and measures.

As previously described, various models are employed for describing wind flow. These models, usually used for micrositing decisions, can be divided into four categories: conceptual, experimental, statistical, and numerical [8]. As the name implies, conceptual models refer to the basic concepts and discuss how wind flow is affected by the terrain. Some researchers employ the conceptual models to quantify the effects of offshore and coastal wind turbines on the ecology. To cite an instance, Wilson et al. [36] use those models to evaluate the impact of offshore wind turbines and the associated infrastructure (e.g., substations and subsea cables, etc.) on the sea life.

Experimental models usually involve creating physical models of the terrain, and experimentally studying the actual flow. Experimental models are traditionally employed for testing wind turbine designs or validating analytical wind flow models [37,38]. Usually those designs necessitate the use of wind tunnels or related equipment. Recently, other means have been developed. For example, Conan et al. [39] use sand erosion model to detect and evaluate high wind speed areas for wind power estimation. This model is low cost, easy to build, and repeatable, and it can be used to estimate the wind characteristics such as the amplification factor and the fractional speed-up ratio.

Statistical models aim at finding the relation between various terrain characteristics (e.g., surface roughness, elevation, and slope exposure) and the

wind power [8]. Shahab et al. [40] use parametric and nonparametric statistical approaches for determining the requirements associated with an energy storage system for providing the baseload for wind farms. Forest et al. [41] use the multiple kernel learning regression for assessing the wind performance over a complex terrain. Rather than the topographic indexes to obtain the regression equation, their method is based on the support vector regression method. One advantage of the approach is that the algorithm, based on the inclusion of additional data in a nonparametric fashion, actually learns.

Numerical models can be divided into four major groups. The first group is the mass-consistent models, which are formed by the group of equations based on the principle of mass conservation. Those models were developed in 1970s and 1980s and have been used with success as approximation techniques even for the complex terrain. The success is due to their simplicity and the applicability of the physical principles governing the equations [42]. The second generation of the models that are collectively known as Jackson–Hunt based approach incorporates the conservation of momentum as well as the conservation of mass by employing Navier–Stokes type of the equations [43]. Over the years, the basic theoretical construction has been developed which has led to some widely used software packages. Among them, WAsP is a popular choice for the micrositing decisions for wind turbines [44]. The MS3DJH/3R models are used in conjunction with the mass-consistent models to study boundary layer flow over analytical two-dimensional hills with varying slope [45]. Raptor Nonlinear (Raptor NL) software is used for modeling the wind flow over the steep terrain [46].

Among the Jackson–Hunt based approach, the WAsP software has been enjoying popularity especially in Europe. It was first developed by the Technical University of Denmark in 1987 and has been further enhanced over time to incorporate different models for the projection of horizontal and vertical extrapolation of data for application over different types of terrain [47]. Various modules for WAsP have also been developed, such as the functionality to estimate the effects of surface roughness changes and obstacles [8,48].

Recently, the third group of numerical models (i.e., CFD-based approaches) is also gaining popularity thanks to increasing computing power. These approaches are usually aimed at developing a steady-state independent solution for wind and turbulence fields, which can be used for wind power assessment for complex terrains [49]. CFD models make use of the equations based on Reynolds-averaged Navier–Stokes for motion [50]. The CFD-based models can also be used for regions where thermal instability exist [22]. CFD-based approaches on the real-life problems have a mixed success. While they have been verified in the experimental setting with 2D and 3D flow with the steep hills using wind tunnels researchers report mixed results for wind power estimation for real-life cases [8,51–53].

The fourth group of numerical methods incorporates the mesoscale numerical weather prediction (MNWP) models. Those models are usually

employed for weather forecasting, and can also incorporate energy and time. Such models can be used for modeling various atmospheric-related phenomena such as thermally driven mesoscale circulations, atmospheric stability, and buoyancy. Other wind-related characteristics such as pressure, humidity, and temperature can also be modeled. One of the shortcomings is that the computational resource requirements for these models are prohibitively large [14]. A general flowchart for the MNWP model is presented in Fig. 3.3.

Meanwhile, researchers have explored the feasibility of hybrid approaches. There are some applications which combine the MNWP models with the Jackson–Hunt based models or the mass-consistent models such as the AWS Truepower's MesoMap, Risoe National Laboratory's Karlsruhe Atmospheric Mesoscale Model-Wind Atlas Analysis and Application Program (KAMM-WAsP), and Environment Canada's AnemoScope system [55–57].

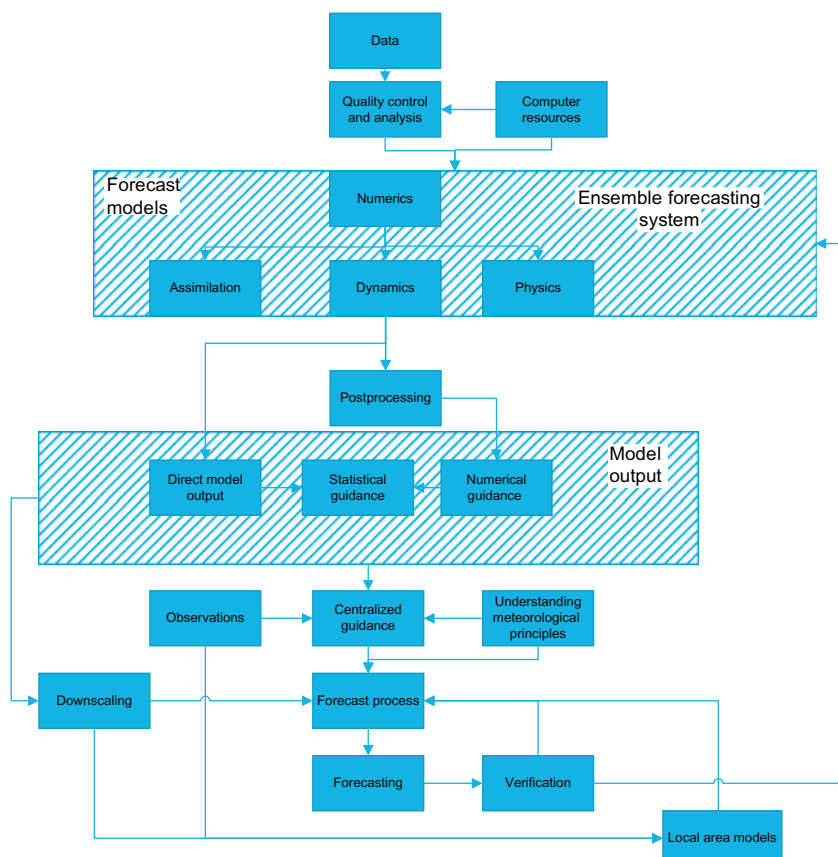


FIGURE 3.3 Components of the mesoscale numerical weather prediction systems [54].

In addition, spatial extrapolation models can be used for extrapolating the wind data obtained from one wind location to assess the potential at another wind site. Techniques based on statistics or artificial intelligence have been used for this purpose. To cite an instance, Garcia-Rojo [58] employs a procedure based on the calculation of the joint probability distribution of the wind at a local station and a meteorological mast, and compares it with the estimation of a MCP model. Some researchers employ the spatial extrapolation models for predicting the wind power in a vertical sense in such a way that the data obtained from a certain height is extrapolated to obtain an estimate for a different height. As an example, Durišić and Mikulović [59] use wind data obtained at three different locations to form a synthetic model using the method of least squares [59]. The proposed approach can also be used as a tool to refine the input for the WAsP model.

3.6 FURTHER CONSIDERATIONS FOR WIND SPEED ASSESSMENT

Wind turbines are designed to shut off to prevent damage beyond a threshold wind speed. In analyzing extreme winds, An and Pandey [60] compare four different approaches (i.e., Standard Gumbel, Modified Gumbel, Peaks-Over-Threshold (POT), and *Method of Independent Storms* (MIS)), and conclude that the MIS produced more reliable results as compared to other type of the methods, especially the POT method.

Terrain characteristics are also worth considering. Wind assessment becomes more difficult with increasing terrain complexity; traditional WAsP software works better for the flatter terrains. A ruggedness index can be analogously defined as the percentage of the terrain that has a slope greater than the threshold value. By calculating the index, it would be possible to develop correction procedures for the estimates obtained from the WAsP model for more complex terrains [61].

Various sources of uncertainties exist that might impede accurate assessment of wind potential at a particular site. These uncertainties can be classified as:

- Uncertainties due to the measurement accuracy;
- Uncertainties due to historical wind resources;
- Uncertainties due to the change in the climate over the long term in the future;
- Change of the wind shear;
- Wind flow modeling.

For a project with a life span of 10 years, the total compounded effect of uncertainties from different sources might vary between 4.1% and 7.5% [8].

The estimation of losses affects the wind potential assessment. As a rule of thumb, for the losses associated with a small wind turbine, the theoretical

output must be reduced for accommodating real-world operating conditions. This deratement factor might reach up to 15%–30%. Usually, the following factors are cited as the sources for losses [62]:

- *Density of air:* Density of air decreases with increasing temperature and elevation, and reduced air density leads to a decrease in wind power output.
- *Turbine availability:* Breakdowns, scheduled and unscheduled maintenance might decrease the availability of a wind turbine. Various researchers have conducted research on determining optimal preventive and scheduled maintenance strategy for maximizing turbine availability to minimize losses [63,64].
- *Site availability:* Due to factors associated with the grid (e.g., brownouts or blackouts), some losses might be encountered. As such, the temperature outside the operating range of the wind turbine might also contribute to the losses. The losses are usually higher when the electric power is transmitted at lower voltages.
- *Site losses:* Losses due to transmission of electric energy might be encountered.
- *Turbulence:* Due to the specific terrain factors, resulting turbulence might reduce the wind power by up to 4%.

The wake of the turbines is another factor. It is suggested in the literature that in order to reduce wake losses at wind farms, turbines should be spaced between 5 and 9 rotor diameters in the prevailing wind direction, and between 3 and 5 rotor diameters in the direction perpendicular to the prevailing wind [60].

3.7 WIND SPEED AND POWER FORECASTING

Since wind is an intermittent energy source, predicting a reliable supply of wind power is a challenging task that should be addressed accordingly. Accurate forecasting reduces the uncertainty and streamlines the planning activities associated with the grid. To forecast wind speed and power, numerous methods have been proposed in the literature. Depending on the time horizon associated with the forecasting period, wind forecasting can be divided into four distinct categories [65]:

- *Very short-term forecasting:* The time scale varies between a few seconds to 30 minutes, and forecasting is usually conducted for the electricity market for clearing and regulation action.
- *Short-term forecasting:* The time scale is between 30 minutes to 6 hours, and the forecasts are used for making economic load dispatching, and load increment/decrement decisions.

- *Medium-term forecasting*: The forecasting horizon varies between 6 hours and 1 day. These forecasts are generally employed for online and offline decisions associated with the generator and operational security in the day ahead markets.
- *Long-term forecasting*: Long-term forecasting entails time period between 1 day and 1 week or more. Usually this type of forecasts is used to assist the decision-making processes for reserve requirement decisions, and maintenance scheduling for minimizing operating cost.

There are various methods that can be employed in terms of forecasting wind speed. Fig. 3.4 provides an overview on the general classification in the literature. Persistence-based models assume the previous period value as the forecast for a future period. This method works well especially for very short-term and short-term forecasting [66]. Meanwhile, it is usually used for benchmarking purposes to test the forecasting quality of other methods.

Numerical weather prediction–based methods are usually used for forecasting the local weather and air related attributes. Various software packages for numerical weather prediction (NWP) methods have been developed, which include the *High Resolution Local Area Model* (HIRLAM), the hydrostatic ETA model (i.e., a hydrostatic model that employs the eta vertical coordinate), *Aire Limitée Adaptation dynamique Développement International* (ALADIN) model [68–70]. One striking difference between the NWP model and the other models is that various wind attributes other than wind speed can be forecasted (e.g., pressure, density, direction, temperature, and humidity) with the NWP model. However, the forecasts obtained by the NWP models depend heavily on the initial conditions; therefore providing an ensemble forecast increases the reliability of prediction. Unfortunately, the use of NWP-based methods does require a large amount of computing power, and even with the right set of the inputs, due to the chaotic behavior, forecasting the wind attributes beyond a couple of weeks ahead is usually not possible. Generally, this model performs well

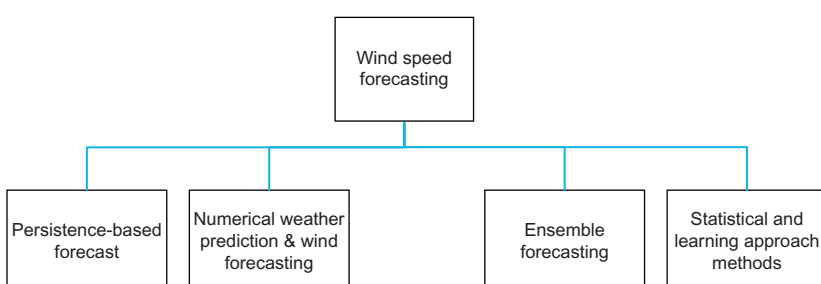


FIGURE 3.4 Classification of wind speed forecasting models [67].

for the long term, but short-term predictions are inferior compared to other methods. Moreover, the NWP models, due to the high cost of collecting the input set and the high computing costs, are only used once or twice daily [65]. Since the NWP method serves as a platform for forecasting the future weather state, the output might be further processed to obtain finer estimates with respect to the wind attributes. In that regard, Cassola and Burlando [71] apply the Kalman filtering method for improving the wind speed and wind power forecasts for the very short term. Some researchers also use neural networks for postprocessing model output forecasts obtained from the NWP models [72]. In a similar sense, the output of the NWP models might be further postprocessed for identifying certain deviating patterns. For instance, Bossavy et al. [73] use the derivative filtering approach for edge detection to characterize ramp events when the power production of the wind turbine significantly deviates from the usual electricity generation pattern.

Statistical and learning-based approaches incorporate various methods from statistics and artificial intelligence. Statistical-based approaches usually incorporate techniques applied on a time series data such as *Auto Regressive Integrated Moving Average* (ARIMA) based methods. There are various implementations of ARIMA-based models in the literature, such as fractional ARIMA-based models and joint *Auto Regressive Moving Average* (i.e., ARMA) models for predicting wind attributes simultaneously [74,75]. ARMA-based models are based on the previous period's wind speeds/power and past error terms. In general, the ARMA-based model can be expressed as [76]:

$$y_t = \delta + \sum_{i=1}^p \varphi_i y_{t-i} + \sum_{j=1}^q \phi_j e_{t-j} + e_t \quad (3.10)$$

where δ is the constant term associated with the stochastic process of the ARMA model, φ_i is the i th autoregressive coefficient, ϕ_j is the coefficient of j th moving average, e_t is the error term at time period t , and y_t represents the value of wind speed observed or forecasted at time period t .

In addition to the traditional static ARMA models, researchers have developed dynamic versions for capturing inherent nonstationary wind speeds. In that regard, Huang and Chalabi [77] use the smoothed integrated random walk processes to model the coefficients of model parameters. Recently, there is a growing interest in combining the traditional ARMA-based models with other approaches. In that vein, Liu et al. [78] develop two approaches where the ARMA model is linked with *artificial neural network* (ANN) and Kalman filter based methods, and Shi et al. [79] combine ARMA with ANN and support vector machines (SVMs) for the same purpose. It is concluded that those models perform well for the nonstationary wind speed prediction in wind power systems. The statistical-based methods are not only

limited to the ARMA-based models. For instance, Liu et al. [80] adopt the Modified Taylor Kriging model and compare the forecast quality to ARMA-based approaches.

Researchers have also explored the possibility of implementing Auto-Regressive Conditional Heteroskedasticity (ARCH) and Generalized Auto-Regressive Conditional Heteroskedasticity (GARCH) based models for modeling the variability of wind speed. Those variance equations can be incorporated in the mean regression equation and (-M) counterparts can be created in this fashion. Liu et al. compare 10 different ARMA-GARCH(-M) based approaches for modeling the volatility and conclude that no model outperforms the other, and indicate that as the height increases, the power of the model decreases [81]. Those studies are important for providing the interval forecast and calculating the operation probability of the wind turbines and conditional expected wind output [82,83].

On the other hand, ANN is a technique that has been used to map the random input vector(s) to outputs without prior assumptions of a fixed relationship. The neural network can learn based on the existing data, discover the hidden patterns, and use the past data to predict future ones. Successful implementations of ANNs for wind speed forecasting exist in the literature [84,85]. Li and Shi [86] compared three different ANNs, namely adaptive linear element (ADALINE), feed-forward back-propagation (FFBP) and radial basis function (RBF) for 1 hour ahead of wind speed predictions and came to the conclusion that no model outperformed any other, and that wind sites should be evaluated in terms of the performance of different ANNs on a case-by-case approach. Bilgili et al., using a logistic sigmoid transfer function, a linear transfer function as an activation function, and resilient propagation as a learning approach, developed a model for forecasting the wind speed based on the data obtained from neighboring locations [87]. Kani and Ardehali combined ANNs and the Markov chain models to develop a combined approach for very short-term forecasting of wind speed. Markov Chain based approach is employed for capturing long-term trends [88]. Fadare used 200 year data obtained from 28 ground stations and develop a three-layered, feed-forward, back-propagation network with different configurations to forecast the wind speed in Nigeria [89]. There are also other artificial intelligence methods developed for wind speed prediction purpose such as spatial correlation-based approaches, fuzzy logic-based approaches, wavelet transforms-based approaches, entropy-based training methods [90–92], and SVM approaches [93].

Ensemble forecasting usually involves a large set of runs to predict the wind speed. Those ensemble forecasts are used for examining the future forecasts and the similarities between those outcomes are examined to obtain an insight on the reliability of forecast. As previously indicated, these models are especially useful with NWP-based models [94]. Associated with ensemble forecasting, hybrid methods are also gaining popularity. Usually hybrid

methods fall into two categories. These categories can be expressed as follows [85]:

- Weighting-based approaches
- Other approaches that
 - combined approaches including data preprocessing techniques
 - combined approaches including parameter selection and optimization techniques
 - combined approaches including error processing techniques.

Weighting based algorithms involve the determination of the relative effectiveness of each model and assigning them a value indicating the special importance in the combined models [95]. Han and Liu [96] used the maximum entropy principle to obtain weight coefficients for six individual models (persistent, ARIMA, and four ANN-based models) for different prediction horizon times (i.e., between 1 and 6 hours). Recently reported research involved the combination of different regression algorithms by means of a so-called *Multiple Architecture System* (MAS). Bouzgou and Benoudjite [97] implemented the MAS to combine different regression models to forecast wind speed. Li et al. [98] developed a two-stage approach where the outputs of the forecasts from different neural networks were combined using Bayesian adaptive combination, and concluded that applying Bayesian combination on the top of the individual forecasts can significantly improved the accuracy as compared to forecasts obtained from stand-alone ANNs.

Combined approaches using the preprocessing techniques, involve decomposing the nonlinear wind speed data to stationary and regular subseries and applying filtering techniques for filtering out redundant parts [85]. Wavelet transformation-based methods are gaining popularity with these combined techniques. Lei and Ran combined a wavelet transformation with the ARMA model and indicate that the particular combined approach performs better as compared to the stand-alone ARMA-based approaches [99]. Also, it Zhang et al. combined a wavelet transformation with an ANN to obtain satisfactory results [100].

On the other hand, other approaches have taken a selection of explanatory variables and determined model parameters [85]. For example, Xingpei et al. [101] used a back-propagation neural network, where the initial weights and bias are optimized by employing genetic algorithms. It is indicated that the proposed approach performs better than only using ANNs. In a similar manner, other researchers have experimented with a simulated annealing based approach for finding the parameters of the SVMs [102].

Related research is also conducted based on the postprocessing of the error terms to identify the patterns of systematic underestimation and overestimation. As an example, Louka et al. [103] applied the Kalman filtering

method to reduce the error terms for two NWP models namely SKIRON which is named after the wind which blew from the Scironian rocks in Kineta, Greece and *Regional Atmospheric Modeling System (RAMS)* model. Wang et al. [104] adopted the ARMA models to provide a fit for the wind speed data where the error terms were modeled using the simulated GARCH (1,1)-based approach.

3.8 CONCLUSIONS

In this chapter, we discussed various aspects of wind power assessment and forecasting. The principles of developing a successful wind assessment programs are outlined. Various models that might be used for the micrositing decisions (i.e., mass-consistent based methods, Jackson–Hunt based models, methods based on CFD, spatial correlation–based methods) are discussed. Also, the important aspects of wind resource assessment analysis such as the spacing between wind turbines, uncertainty analysis, and loss estimation are discussed. In Section 3.7, we provide the classification on the types of methods used for the wind speed and wind power forecasting with the objective of reducing the uncertainty in electricity generated from wind-based resources.

It is worth mentioning that a successful wind power assessment program entails the implementation of many tasks such as preliminary wind analysis, selection of wind sites, micrositing, and accurate capture of existing wind flow profiles. Not only is the assessment of the wind power important, but also the accurate forecasts of wind speed and wind power are important considerations for tapping the full potential of wind-based resources.

REFERENCES

- [1] Euractiv.com. Denmark breaks its own world record in wind energy, <<http://www.euractiv.com/section/climate-environment/news/denmark-breaks-its-own-world-record-in-wind-energy/>>; May 2016.
- [2] Global Wind Energy Council. Global wind statistics, <http://www.gwec.net/wp-content/uploads/vip/GWEC-PRstats-2015_LR.pdf>; 2015.
- [3] American Wind Energy Association, US. Number One in the world in wind energy production, Wind supplied Iowa with over 31 percent of its electricity last year, <<http://www.awea.org/MediaCenter/pressrelease.aspx?ItemNumber=8463>>; May 2016.
- [4] Bailey BH, McDonald SL, Bernadett DW, Markus MJ, Elsholz KV. Wind resource assessment handbook. Subcontract No. TAT-5-15283-01; 1997. AWS Scientific, Inc. Albany, NY, USA.
- [5] Open Energy Information, <<http://en.openei.org/doe-opendata/dataset/cecf687d-28e3-4e27-b3a4-269a02acd8a0/resource/190c9a87-e89a-48ef-bf27-68fae2e77bb9/download/global2-windmaps.doc>>; May 2016.
- [6] ESMAP, Energy Sector Management Assistance Program. Renewable energy resource mapping initiative, <http://esmap.org/RE_mapping>; May 2016.

- [7] Prasad RD, Bansal RC. Technologies and methods used in wind resource assessment. *Handbook of Renewable Energy Technology*. Singapore: World Scientific Publishing; 2011. p. 69.
- [8] New York State Energy Research and Development Authority. Wind resource assessment handbook, Final Report 10-30, <<http://www.nyserda.ny.gov/-/media/Files/Publications/Research/Biomass-Solar-Wind/wind-resource-assessment-toolkit.pdf>>; October 2010.
- [9] Windustry. Wind resource assessment, <http://www.windustry.org/community_wind_-toolbox-4-wind-resource-assessment>; May 2016 [chapter 4].
- [10] Bennui A, Rattanamanee P, Puetpaiboon U, Phukpattaranont P, Chetpattananondh K. Site selection for large wind turbine using GIS. In: Proceedings of the PSU-UNS international conference on engineering and environment, Phuket, Thailand; 2007.
- [11] Lawan SM, Abidin WAWZ, Chai WY, Baharun A, Masri T. The status of wind resource assessment (WRA) techniques, wind energy potential and utilisation in Malaysia and other countries. *ARPN J Eng Appl Sci* 2013;8(12):1039–53.
- [12] Corbett J, Whiting R, Bleeg J, Woodcock J, Horn U, Landberg L, et al. CFD can consistently improve wind speed predictions and reduce uncertainty in complex terrain. In: Proceedings of European wind energy conference, Copenhagen, Denmark; 2012.
- [13] Wang Z, Qin H, Lewis JI. China's wind power industry: policy support, technological achievements, and emerging challenges. *Energy Policy* 2012;51:80–8.
- [14] Brower M. Wind resource assessment: a practical guide to developing a wind project. Hoboken, NJ: John Wiley & Sons; 2012.
- [15] Enercon. Calculated power curve, Enercon E141, EP4, <<http://www.enercon.de/en/products/ep-4/e-141-ep4/>>; May 2016.
- [16] Gurit.com. Wind turbine blade aerodynamics, <<http://www.gurit.com/files/documents/2aerodynamicspdf.pdf>>; May 2016.
- [17] Rodrigo JS, Guillén FB, Arranz PG, Courtney MS, Wagner R, Dupont E. Multi-site testing and evaluation of remote sensing instruments for wind energy applications. *Renewable Energy* 2013;53:200–10.
- [18] Nicholls-Lee R. A low motion floating platform for offshore wind resource assessment using lidars. Proceedings of ASME 2013 32nd international conference on ocean, offshore and arctic engineering. Nantes: American Society of Mechanical Engineers; 2013. p. V008T09A036.
- [19] Gadad S, Deka PC. Offshore wind power resource assessment using Oceansat-2 scatterometer data at a regional scale. *Appl Energy* 2016;176:157–70.
- [20] Soukissian T, Karathanasi F, Axaopoulos P. Satellite-based offshore wind resource assessment in the Mediterranean. *IEEE J Oceanic Eng* 2016;99:1–14 <http://dx.doi.org/10.1109/JOE.2016.2565018>.
- [21] AWS Truepower. Wind resource assessment practical guidance for developing a successful wind project, <<https://www.awstruepower.com/assets/Wind-Resource-Assessment-Practical-Guidance-for-Developing-a-Wind-Project-Brower-Dec2012.pdf>>; May 2016.
- [22] Asian Development Bank. Guidelines for wind resource assessment: best practices for countries initiating wind development, <<http://www.adb.org/sites/default/files/publication/42032/guidelines-wind-resource-assessment.pdf>>; May 2016.
- [23] Waewsak J, Chaichana T, Chancham C, Landry M, Gagnonc Y. Micro-siting wind resource assessment and near shore wind farm analysis in Pakpanang District, Nakhon Si Thammarat Province, Thailand. *Energy Procedia* 2014;52:204–15.
- [24] Kim H, Kim B. Wind resource assessment and comparative economic analysis using AMOS data on a 30 MW wind farm at Yulchon district in Korea. *Renewable Energy* 2016;85:96–103.

- [25] Landberg L, Myllerup L, Rathmann O, Petersen EL, Jørgensen BH, Badger J, et al. Wind resource estimation—an overview. *Wind Energy* 2003;6(3):261–71.
- [26] Carta JA, Velázquez S, Cabrera P. A review of measure-correlate-predict (MCP) methods used to estimate long-term wind characteristics at a target site. *Renewable Sustainable Energy Rev* 2013;27:362–400.
- [27] Torres JL, Garcia A, De Blas M, De Francisco A. Forecast of hourly average wind speed with ARMA models in Navarre (Spain). *Solar Energy* 2005;79(1):65–77.
- [28] Jangamshetti SH, Rau VG. Normalized power curves as a tool for identification of optimum wind turbine generator parameters. *IEEE Trans Energy Convers* 2001;16(3):283–8.
- [29] Zhou J, Erdem E, Li G, Shi J. Comprehensive evaluation of wind speed distribution models: a case study for North Dakota sites. *Energy Convers Manage* 2010;51(7):1449–58.
- [30] Erdem E, Shi J. Comparison of bivariate distribution construction approaches for analysing wind speed and direction data. *Wind Energy* 2011;14(1):27–41.
- [31] Yu Z, Tuzuner A. Fractional Weibull wind speed modeling for wind power production estimation. In: Proceedings of IEEE power & energy society general meeting, Calgary, Alberta, Canada; 2009.
- [32] Li G, Shi J. Application of Bayesian model averaging in modeling long-term wind speed distributions. *Renewable Energy* 2010;35(6):1192–202.
- [33] Badger J, Mortensen N, Hahmann A, Bingol A. Introduction to mesoscale and microscale wind resource mapping. In: Proceedings of mesoscale mapping of RE resources ESMAP knowledge exchange forum, Washington DC, USA; 2009.
- [34] Lu X, McElroy MB, Kiviluoma J. Global potential for wind-generated electricity. *Proc Natl Acad Sci* 2009;106(27):10933–8.
- [35] Hoogwijk M, Graus, W. Global potential of renewable energy sources: a literature assessment. Background report prepared by order of REN21. Ecofys, PECSNL072975; 2008.
- [36] Wilson JC, Elliott M, Cutts ND, Mander L, Mendão V, Perez-Dominguez R, et al. Coastal and offshore wind energy generation: is it environmentally benign? *Energies* 2010;3(7):1383–422.
- [37] Battisti L, Benini E, Brightenti A, Castelli MR, Dell'Anna S, Dossena V, et al. Wind tunnel testing of the DeepWind demonstrator in design and tilted operating conditions. *Energy* 2016;111:484–97.
- [38] Barranger N, Ternisien T, Kallos G. An intercomparison study between RAMS and CRES-Flow-NS models and evaluation with wind tunnel experimental data: Toward improving atmospheric modeling for wind resource assessment. *J Wind Eng Ind Aerodyn* 2015;142:272–88.
- [39] Conan B, van Beeck J, Aubrun S. Sand erosion technique applied to wind resource assessment. *J Wind Eng Ind Aerodyn* 2012;104:322–9.
- [40] Shahab S, Jozani MJ, Bibea E, Molinski M. A statistical algorithm for predicting the energy storage capacity for baseload wind power generation in the future electric grids. *Energy* 2015;89:793–802.
- [41] Foresti L, Tuia D, Kanevski M, Pozdnoukhov A. Learning wind fields with multiple kernels. *Stochastic Environ Res Risk Assess* 2011;25(1):51–66.
- [42] Ratto CF, Festa R, Romeo C, Frumento OA, Galluzzi M. Mass-consistent models for wind fields over complex terrain: the state of the art. *Environ Software* 1994;9(4):247–68.
- [43] Jackson PS, Hunt JCR. Turbulent wind flow over low hill. *Q J R Meteorol Soc* 1975;101:929–55.
- [44] Nouri A, Babram MA, Elwarraki E, Enzili M. Moroccan wind farm potential feasibility. Case study. *Energy Convers Manage* 2016;122:39–51.

- [45] Finardi S, Brusasca G, Morselli MG, Trombetti F, Tampieri F. Boundary-layer flow over analytical two-dimensional hills: a systematic comparison of different models with wind tunnel data. *Boundary-Layer Meteorol* 1993;63(3):259–91.
- [46] Ayotte KW. A nonlinear wind flow model for wind energy resource assessment in steep terrain. In: Proceedings of global windpower conference, Paris, France; 2002.
- [47] Petersen EL, Mortensen NG, Landberg L, Højstrup J, Frank HP. Wind power meteorology. Roskilde: Risø National Laboratory, Technical Document No. Risø-I-1206 (EN); 1997.
- [48] Miljødata EO. Case studies calculating wind farm production-main report. Denmark: Energi-og Miljødata; 2002.
- [49] Berge E, Gravdahl AR, Schelling J, Tallhaug L, Undheim O. Wind in complex terrain. A comparison of WAsP and two CFD-models. In: Proceedings from EWEC, vol. 27. Athens, Greece; 2006.
- [50] Toja-Silva F, Peralta C, Lopez-Garcia O, Navarro J, Cruz I. Roof region dependent wind potential assessment with different RANS turbulence models. *J Wind Eng Ind Aerodyn* 2015;142:258–71.
- [51] Bitsuamlak GT, Stathopoulos T, Bédard C. Numerical evaluation of wind flow over complex terrain: review. *J Aerosp Eng* 2004;17:135–45.
- [52] Murakami S, Mochida A, Kato S. Development of local area wind prediction system for selecting suitable site for windmill. *J Wind Energy Ind Aerodyn* 2003;91:1759–75.
- [53] Sumner J, Watters CS, Masson C. CFD in wind energy: the virtual, multiscale wind tunnel. *Energies* 2010;3:989–1013.
- [54] Comet Meted. NWP and ensemble model systems forecast, <http://www.meted.ucar.edu/nwp/model_fundamentals/navmenu.php>; May 2016 [accessed 31.05.16].
- [55] Brower M. Validation of the WindMap Program and development of MesoMap. In: Proceeding from AWEA's WindPower conference, Washington, DC, USA; 1999.
- [56] Frank HP, Rathmann O, Mortensen N, Landberg L. The numerical wind atlas, the KAMM/WAsP method. Riso-R-1252 report from the Risø National Laboratory, Roskilde, Denmark, 59; 2001.
- [57] Yu W, Benoit R, Girard C, Glazer A, Lemarquis D, Salmon JR, et al. Wind energy simulation toolkit (WEST): a wind mapping system for use by the wind-energy industry. *Wind Eng* 2006;30:15–33.
- [58] García-Rojo R. Algorithm for the estimation of the long-term wind climate at a meteorological mast using a joint probabilistic approach. *Wind Eng* 2004;28(2):213–23.
- [59] Đurišić Ž, Mikulović J. A model for vertical wind speed data extrapolation for improving wind resource assessment using WAsP. *Renewable Energy* 2012;41:407–11.
- [60] An Y, Pandey MD. A comparison of methods of extreme wind speed estimation. *J Wind Eng Ind Aerodyn* 2005;93(7):535–45.
- [61] Mortensen NG, Bowen AJ, Antoniou I. Improving WAsP predictions in (too) complex terrain. In: Proceedings of the European wind energy conference and exhibition, Athens, Greece; 2006.
- [62] Northern Power Systems, Engineering Bulletin, Energy Production Estimating. Estimating annual energy production from a Northern Power® NPS 100™ wind turbine, <<http://www.northernpower.com/wp-content/uploads/2014/10/NPS-White-Paper-Energy-Production-Estimating.pdf>>; May 2016.
- [63] Byon E, Ntiamo L, Ding Y. Optimal maintenance strategies for wind turbine systems under stochastic weather conditions. *IEEE Trans Reliab* 2010;59(2):393–404.
- [64] Andrawus J, Watson J, Kishk M. Wind turbine maintenance optimisation: principles of quantitative maintenance optimisation. *Wind Eng* 2007;31(2):101–10.

- [65] Soman SS, Zareipour H, Malik O, Mandal P. A review of wind power and wind speed forecasting methods with different time horizons. In: Proceedings of North American Power Symposium (NAPS), IEEE, Arlington, Texas, USA; 2010.
- [66] Lei M, Shiyan L, Chuanwen J, Hongling L, Yan Z. A review on the forecasting of wind speed and generated power. *Renewable Sustainable Energy Rev* 2009;13(4):915–20.
- [67] Foley AM, Leahy PG, Marvuglia A, McKeogh EJ. Current methods and advances in forecasting of wind power generation. *Renewable Energy* 2012;37(1):1–8.
- [68] Källén E. HIRLAM documentation manual, System 2.5, Technical report. S-60176 Norrköping, Sweden; 1996.
- [69] Lazić L, Pejanović G, Živković M. Wind forecasts for wind power generation using the Eta model. *Renewable Energy* 2010;35(6):1236–43.
- [70] Bubnova R, Hello G, Bénard P, Geleyn J-F. Integration of the fully-elastic equations cast in the hydrostatic pressure terrain-following coordinate in the framework of the ARPEGE/ALADIN NWP system. *Mon Weather Rev* 1995;123:515–35.
- [71] Cassola F, Burlando M. Wind speed and wind energy forecast through Kalman filtering of Numerical Weather Prediction model output. *Appl Energy* 2012;99:154–66.
- [72] De Giorgi MG, Ficarella A, Tarantino M. Assessment of the benefits of numerical weather predictions in wind power forecasting based on statistical methods. *Energy* 2011;36(7):3968–78.
- [73] Bossavy A, Girard R, Kariniotakis G. Forecasting ramps of wind power production with numerical weather prediction ensembles. *Wind Energy* 2013;16(1):51–63.
- [74] Kavasseri RG, Seetharaman K. Day-ahead wind speed forecasting using f-ARIMA models. *Renewable Energy* 2009;34(5):1388–93.
- [75] Erdem E, Shi J. ARMA based approaches for forecasting the tuple of wind speed and direction. *Appl Energy* 2011;88(4):1405–14.
- [76] Montgomery DC, Jennings CL, Kulahci M. Introduction to time series analysis and forecasting. Hoboken, NJ: John Wiley & Sons; 2015.
- [77] Huang Z, Chalabi ZS. Use of time-series analysis to model and forecast wind speed. *J Wind Eng Ind Aerodyn* 1995;56(2):311–22.
- [78] Liu H, Tian HQ, Li YF. Comparison of two new ARIMA-ANN and ARIMA-Kalman hybrid methods for wind speed prediction. *Appl Energy* 2012;98:415–24.
- [79] Shi J, Zeng S. Evaluation of hybrid forecasting approaches for wind speed and power generation time series. *Renewable Sustainable Energy Rev* 2012;16(5):3471–80.
- [80] Liu H, Shi J, Erdem E. Prediction of wind speed time series using modified Taylor Kriging method. *Energy* 2010;35(12):4870–9.
- [81] Liu H, Erdem E, Shi J. Comprehensive evaluation of ARMA–GARCH (-M) approaches for modeling the mean and volatility of wind speed. *Appl Energy* 2011;88(3):724–32.
- [82] Liu H, Shi J, Qu X. Empirical investigation on using wind speed volatility to estimate the operation probability and power output of wind turbines. *Energy Convers Manage* 2013;67:8–17.
- [83] Liu H, Shi J, Erdem E. An integrated wind power forecasting methodology: interval estimation of wind speed, operation probability of wind turbine, and conditional expected wind power output of a wind farm. *Int J Green Energy* 2013;10(2):151–76.
- [84] Salcedo-Sanz S, Perez-Bellido AM, Ortiz-García EG, Portilla-Figueras A, Prieto L, Paredes D. Hybridizing the fifth generation mesoscale model with artificial neural networks for short-term wind speed prediction. *Renewable Energy* 2009;34(6):1451–7.
- [85] Tascikaraoglu A, Uzunoglu M. A review of combined approaches for prediction of short-term wind speed and power. *Renewable Sustainable Energy Rev* 2014;34:243–54.
- [86] Li G, Shi J. On comparing three artificial neural networks for wind speed forecasting. *Appl Energy* 2010;87(7):2313–20.

- [87] Bilgili M, Sahin B, Yasar A. Application of artificial neural networks for the wind speed prediction of target station using reference stations data. *Renewable Energy* 2007;32(14):2350–60.
- [88] Kani SP, Ardehali MM. Very short-term wind speed prediction: a new artificial neural network—Markov chain model. *Energy Convers Manage* 2011;52(1):738–45.
- [89] Fadare DA. The application of artificial neural networks to mapping of wind speed profile for energy application in Nigeria. *Appl Energy* 2010;87(3):934–42.
- [90] Alexiadis MC, Dokopoulos PS, Sahsamanoglou HS. Wind speed and power forecasting based on spatial correlation models. *IEEE Trans Energy Convers* 1999;14(3):836–42.
- [91] Damousis IG, Dokopoulos P. A fuzzy expert system for the forecasting of wind speed and power generation in wind farms. In: Proceedings of power industry computer applications, 2001. PICA 2001. Innovative computing for power-electric energy meets the market. 22nd IEEE Power Engineering Society international conference on. Sydney: IEEE; 2001. p. 63–69.
- [92] Liu D, Niu D, Wang H, Fan L. Short-term wind speed forecasting using wavelet transform and support vector machines optimized by genetic algorithm. *Renewable Energy* 2014;62:592–7.
- [93] Zhou J, Shi J, Li G. Fine tuning support vector machines for short-term wind speed forecasting. *Energy Convers Manage* 2011;52(4):1990–8.
- [94] Giebel G, Badger J, Landberg L, Nielsen HA, Nielsen T, Madsen H, et al. Wind power prediction ensembles, Report 1527. Denmark: Risø National Laboratory; 2005.
- [95] Sánchez I. Short-term prediction of wind energy production. *Int J Forecast* 2006;22:43–56.
- [96] Han S, Liu Y. The study of wind power combination prediction. In: Proceedings of the Asia-Pacific power and energy engineering conference (APPEEC), Chengdu, China; 2010.
- [97] Bouzgou H, Benoudjitt N. Multiple architecture system for wind speed prediction. *Appl Energy* 2011;88:2463–71.
- [98] Li G, Shi J, Zhou J. Bayesian adaptive combination of short-term wind speed forecasts from neural network models. *Renewable Energy* 2011;36(1):352–9.
- [99] Lei C, Ran L. Short-term wind speed forecasting model for wind farm based on wavelet decomposition. In: Proceedings of the third international conference on electric utility deregulation and restructuring and power technologies (DRPT), Nanjing, China; 2008.
- [100] Zhang X, Chongchong C, Wang W, Dai Y, The intelligent methods used in prediction the wind speed and output power of wind farm. In: Proceedings of the Asia-Pacific power and energy engineering conference (APPEEC), Shanghai, China; 2012.
- [101] Xingpei L, Yibing L, Weidong X. Wind speed prediction based on genetic neural network. Proceedings of the 4th IEEE conference on industrial electronics and applications (ICIEA), Hangzhou, China; 2009.
- [102] Hui T, Dongxiao N. Combining simulate anneal algorithm with support vector regression to forecast wind speed. In: Proceedings of the second IITA international conference on geoscience and remote sensing (IITA-GRS), Qingdao, China; 2010.
- [103] Louka P, Galanis G, Siebert N, Kariniotakis G, Katsafados P, Pytharoulis I, et al. Improvements in wind speed forecasts for wind power prediction purposes using Kalman filtering. *J Wind Eng Ind Aerodyn* 2008;96(12):2348–62.
- [104] Wang MD, Qiu QR, Cui BW. Short-term wind speed forecasting combined time series method and arch model. In: Proceedings of the international conference on machine learning and cybernetics (ICMLC), Xian, China; 2012.

This page intentionally left blank

Chapter 4

Global Potential for Wind-Generated Electricity

Xi Lu¹ and Michael B. McElroy²

¹Tsinghua University, Beijing, China, ²Harvard University, Cambridge, MA, United States

Email: xilu@tsinghua.edu.cn, mbm@seas.harvard.edu

4.1 INTRODUCTION

Fossil fuels—coal, oil, and natural gas—currently account for close to 80% of total global primary consumption of energy and for the bulk of emissions of the key greenhouse gas CO₂. The nations of the world at the 21st meeting of the Conference of the Parties (COP 21) to the UN Framework Convention on Climate Change (UNFCCC) in Paris in December 2015 committed to restrict future greenhouse gas emissions to ensure that the consequent increase in global average surface temperature should be limited to 2°C or less referenced with respect to conditions that applied in the preindustrial era. Meeting this objective will require no less than a sea change in the manner in which the world sources future energy [1]. Physical prospects for growth in hydro and biomass are limited. Nuclear is expensive. Geothermal could play a role though major investments in relevant research and development will be required to realistically evaluate its potential. The best options, given current understanding, involve combinations of wind and solar. This chapter offers an assessment of the overall potential for wind.

The energy absorbed by the Earth from the Sun over the course of a year totals approximately 3.9×10^{24} J (3.7 million quads where 1 quad = 10^{15} BTU and 1 BTU = 1055.06 J). To place this number in context, the total energy consumed globally by humans amounted to 5.66×10^{20} J (536.9 quads) in 2014, a little more than 1 part in 10 000 of the total supplied by the Sun. The solar energy absorbed by the Earth is realized primarily initially as heat, manifest in the atmosphere as internal energy (IE) complemented by a source of potential energy supplied by evaporation of water (LE). A fraction of IE (~40%) is converted to potential energy (PE), energy the air includes by virtue of its elevation relative to the surface. The fraction of the energy of the atmosphere manifest in kinetic form (KE)—wind—is extremely small relative to either IE or PE.

It accounts for as little as 763.8×10^{18} J (724 quads), 0.06% of the total energy content of the atmosphere. It is replaced, however, on average every 6.9 days implying a global annual source of about 4.04×10^{22} J (38 300 quads), approximately 73 times the total global demand for commercial energy, 466 times global consumption of energy in the form of electricity.

There are two important sources for KE in the atmosphere: one results from work supplied by the force of gravity acting to change the elevation of specific air masses; the second relates to work performed by the force associated with spatial gradients of pressure driving air across isobars, causing it to move from regions of high to regions of low pressure. Dissipation by friction in the near surface environment, at altitudes below about 1 km, is responsible for approximately 50% of the net global sink for KE with the balance contributed by viscous dissipation of small-scale turbulent elements at higher altitudes [2]. Huang and McElroy [3] using a temperature–pressure–wind record based on reanalysis of meteorological data covering the period January 1979 to December 2010, concluded that work supplied by gravitational and pressure forces was responsible for a globally averaged net source of KE equal to 2.46 W m^{-2} over this time interval, slightly more in the southern hemisphere, less in the north (2.49 W m^{-2} as compared to 2.44 W m^{-2}) [3]. As indicated earlier, this source would be sufficient to supply a quantity of kinetic energy significantly greater than the energy implicated in current demand for electricity or even in the demand for energy in all forms. Only a fraction of this global supply could be harnessed of course under realistic circumstances to produce electricity.

The electricity generated from an individual turbine is determined ultimately by the kinetic energy intercepted by the blades of the turbine. This depends in turn on the area swept out by the blades, on the density of the air intercepted by the blades, and on the cube of the wind speed (a factor proportional to the square of the wind speed defining the kinetic energy contained in a given volume of air, an additional factor to specify the rate at which this energy may be delivered to the turbine). In general, the greater the elevation of the rotor and the greater the diameter of the blades, the greater is the potential yield of electricity. Wind speeds increase typically as a function of elevation accounting for the advantage of the first of these considerations. The area intercepted by the blades of the turbine varies in proportion to the square of the diameter of the rotor accounting for the advantage of the second. In practice, there is a range of wind speeds over which a typical turbine may be expected to operate economically. At low speeds, frictional losses would be sufficient to offset any potential production of electricity. If wind speeds are too high, operation of the turbine could be hazardous and the blades are typically feathered to avoid damage. The quantity of electricity produced as a function of wind speed for a particular turbine design is defined in terms of what is referred to as the power curve. Power curves for the two representative turbine designs considered, the GE 2.5 and 3.6 MW models, are displayed in Fig. 4.1.

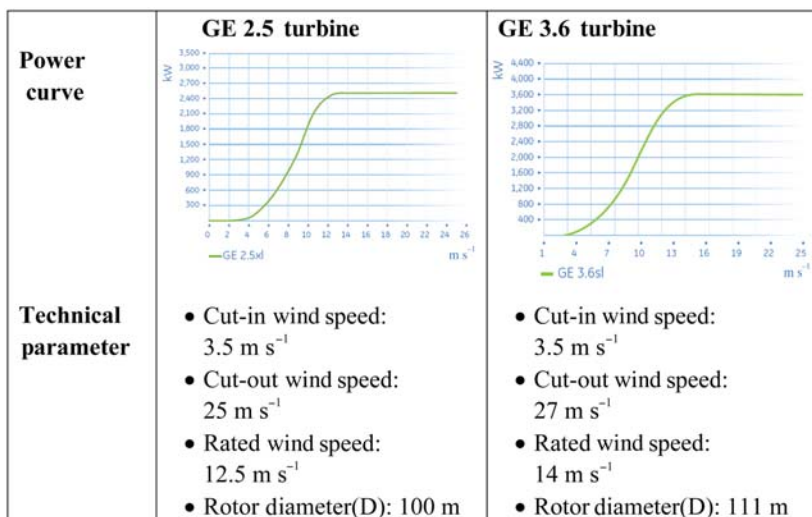


FIGURE 4.1 Power curves and representative technical parameters for the two GE turbines selected for purposes of the present investigation [4].

The yield of electricity anticipated from a particular wind farm depends on a number of factors, including the quality of the wind resource, the design of the turbines included in the facility and their spacing. The choice of spacing reflects a trade-off involving considerations of costs for individual turbines, costs for development of the site, and costs for laying power cables, in addition to costs anticipated for routine operation and maintenance of the facility. Turbines must be spaced to minimize interference in airflow due to interactions among individual turbines. This requires a compromise between the objective of maximizing the power generated per turbine and the competing incentive to maximize the number of turbines sited per unit area.

Two sources of data have been employed in the literature to evaluate the global potential for generation of electricity from wind. One is based on surface and/or sounding measurements of winds. The second makes use of what is referred to as assimilated meteorological data, with wind speeds derived from retrospective analysis of global meteorological data using a state-of-the-art weather/climate model incorporating inputs from a wide variety of observational sources [5] including not only surface and sounding measurements but also results from a diverse suite of measurements and observations taken from a combination of aircraft, balloons, ships, buoys, dropsondes and satellites—in short the gamut of all of the observational data employed to provide the world with the best possible meteorological forecasts, enhanced by application of these data in a retrospective analysis. The former approach was adopted by Archer and Jacobson in their pioneering early study of

potential global wind resources [6]. The latter was favored by Lu et al. and provides the basis for the bulk of the results discussed below [4].

The study by Archer and Jacobsen used data for 2000 incorporating inputs from 7753 individual surface meteorological stations complemented by results from 446 stations for which vertical soundings were available [6]. They restricted their attention to power that could be generated using a network of 1.5 MW turbines tapping wind resources from regions with annually averaged wind speeds in excess of 6.9 m s^{-1} (wind class 3 or better) at an elevation of 80 m. The meteorological stations employed in their analysis were concentrated to a significant extent in the United States, Europe, and Southeastern Asia. As a consequence, results inferred for other regions are subject to considerable uncertainty. To estimate the wind potential at a particular location, Archer and Jacobson used six empirical functions to develop a best least square fit to wind profiles observed at individual neighboring stations for which information was available from soundings [6]. They used an inverse square approach to average data from the five closest meteorological stations to select input for the wind profile adopted to calculate the power potential at a particular sample location. They argued that the estimates for wind power derived using this approach should be conservative on the low side for two reasons: first, the potential for bias introduced by use of the least square methodology should trend in that direction; and, second, the fact that the meteorological stations employed in the analysis were not selected optimally to capture most favorable wind conditions. They concluded that 20% of the total available global wind power potential could be tapped to provide as much as 123 PW h of electricity annually, seven times total global consumption, comparable to consumption of energy globally in all forms [6].

We outline in [Section 4.2](#) the procedures adopted by Lu et al. [4] in their study of global wind potential. Results are presented and discussed in [Section 4.3](#). [Section 4.4](#) addresses limitations in our ability to respond definitively to the challenges posed in the title to this chapter: to define the ultimate global potential for the generation of electric power using wind.

4.2 METHODOLOGY

The Lu et al. study took advantage of a simulation of global wind fields provided by Version 5 of the Goddard Earth Observing System Data Assimilation System (GEOS-5 DAS) [4]. The GEOS-5 analysis employs a terrain-following coordinate system defined by 72 vertical layers extending from the surface to a pressure level of 0.01 hPa (an altitude of approximately 78.2 km) [5]. Pressure levels are selected to resolve features of the atmosphere including both troposphere and stratosphere. Individual volume elements are defined in terms of their horizontal boundaries (latitude and longitude) and by the pressures at their top and bottom. The horizontal resolution of the simulation is 2/3-degree longitude by 1/2-degree latitude

(equivalent to approximately 67 km by 50 km at mid-latitudes). The model provides three-dimensional pressure fields at both layer centers and at layer edges, in addition to wind speeds (meridional and zonal) and temperatures at the midpoint of individual layers with a time resolution of 6 hours. The three lowest layers are centered at altitudes of approximately 71, 201, and 332 m. The 6 hour data for the three lowest layers were employed in the Lu et al. [4] analysis using an interpolation scheme described as follows to estimate temperatures, pressures, and wind speeds at 100 m, the hub height for the 2.5 and 3.6 MW turbines considered as representative and illustrative for purposes of the present discussion.

Knowing the values of pressures at the lower and upper edges of individual layers, together with temperatures and pressures at the midpoints of the layers, Lu et al. [4] calculated altitudes corresponding to the midpoints of the layers using an iterative application of the barometric law assuming a linear variation of temperature between the midpoints of the individual layers. The barometric law was applied also to calculate the pressure at 100 m. Wind speeds and temperatures at 100 m were computed using a cubic spline fit to the corresponding data at the midpoints of the three lowest layers.

The power curves reported by the General Electric Company for the turbine models considered here assume an air density of 1.225 kg m^{-3} under conditions corresponding to an air temperature of 15°C at a pressure of 1 atm [7]. To account for the differences in air density at the rotor elevations as compared to this standard, wind speeds in the published power/wind speed curves (Fig. 4.1) were adjusted according to the Eq. (4.1).

$$V_{\text{corrected}} = \left(\frac{P}{1.225 \cdot R \cdot T} \right)^{1/3} V_{\text{original}} \quad (4.1)$$

where P and T identify air pressures and temperatures at the hub height and R denotes the gas constant, $287.05 \text{ Nm} (\text{kg K})^{-1}$ for dry air.

In estimating the global potential for wind-generated electricity, it will be important to exclude locations for which it would be either impractical or uneconomic to install turbines. To this end, Lu et al. [4] elected to eliminate areas classified as forested, areas occupied by permanent snow or ice, and areas identified as either developed or urban. They were guided in their selection of locations for turbine deployment by data from the Moderate-Resolution Imaging Spectroradiometer (MODIS) instruments included in the payloads of NASA's Terra and Aqua satellites.

MODIS provides a record of the spatial distribution of different types of land cover observed over the Earth in 2001. Following a classification introduced by the International Geosphere-Biosphere Programme (IGBP), the record identifies 17 categories of land cover including 11 different classes of natural vegetation, 3 classes of developed areas, and 3 classes identifying areas occupied by permanent snow or ice (notably Greenland and

Antarctica). It singles out also regions classified as barren, areas with at most a sparse coverage of vegetation, and regions covered by water. It pinpoints regions identified as either urban or heavily developed. The horizontal resolution of the record is approximately 1 km by 1 km. Lu et al. [4] used the MODIS record to exclude from their analysis areas classified as forested, areas occupied by permanent snow or ice, areas covered by water and areas identified as either developed or urban. Environments identified by Lu et al. as inappropriate for wind resource development are indicated in Fig. 4.2.

Topographic relief data for both land and ocean areas were derived using the Global Digital Elevation Model (GTOPO30) of the Earth Resources Observation and Science (EROS) Data Center of the US Geological Survey (USGS). The spatial resolution of this data source for offshore environments (bottom topography) as applied here is approximately 1 km by 1 km [8]. A number of factors conspire to limit the development of offshore wind farms. Aesthetic considerations, e.g., have restricted development of wind resources in the near shore environment in the United States (the Cape Wind controversy as a case in point [9]) although objections to near shore installations in Europe appear to have been less influential. There is a need further to accommodate requirements for shipping, fishing, and for wildlife reserves, and to minimize potential interference with radio and radar installations. To account for these limitations, Musial and colleagues, in studies of the offshore wind power potential for the contiguous United States, chose to exclude placement of wind farms within 9.3 km (5 M where M refers to nautical mile) of shore and to limit development to 33% of the area between 9.3 and 37 km (5 and 20 M) offshore, while expanding potential development to 67% of the area between 37 and 92.6 km (20 and 50 M) [9–12].

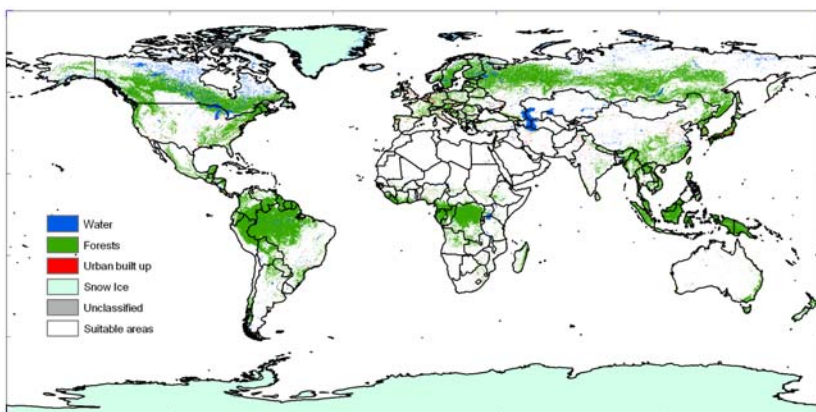


FIGURE 4.2 Global map of areas considered unsuitable for onshore wind turbine installation [4].

The expense of installing wind turbines offshore generally increases as a function of water depth and as a function of distance from shore. General Electric recommends that its turbines should be installed using state-of-the-art monopole structures fixed to the seabed for water depths less than 20 m. Water jacket tripod or quadrapod structures can support towers in waters up to 50 m [13,14]. For greater depths, it is necessary to resort to floating structures using technology developed by the oil and gas extraction industry [15]. Experience with the use of floating structures in the wind power business is relatively limited to date but its development is not expected to pose insuperable problems in the future, although it will certainly be more expensive.

Lu et al. [4], followed by Dvorak et al. [14], considered three possible regimes for offshore development of wind power defined by water depths of 0–20, 20–50, and 50–200 m. Somewhat arbitrarily, they limited potential deployment of wind farms to distances within 92.6 km (50 M) of the nearest shoreline, assuming that 100% of the area occupied by these waters could be available for development. A schematic summary of the approach they adopted in calculating wind power potential both onshore and offshore is presented in Fig. 4.3.

A further consideration in estimating the total global potential for wind-generated electricity concerns the criteria adopted to determine the spacing of turbines in particular wind farms. Restricting downstream interturbine wake power loss to less than 20% requires a downwind spacing of more than seven turbine rotor diameters with cross-wind spacing of at least four diameters [6,16]. Applying this constraint to the 2.5 MW GE turbines [17] (rotor diameter 100 m, radius 50 m) selected as representative for onshore wind deployment implies an interturbine spacing of 1 per 0.28 km^2 . Given the much

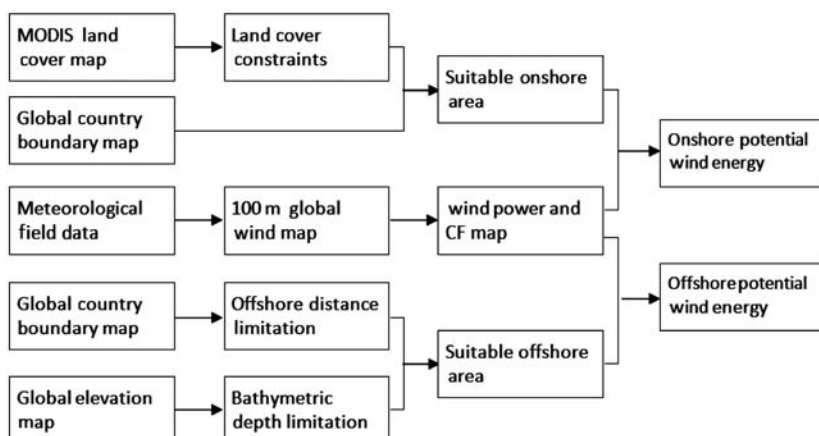


FIGURE 4.3 Schematic summary of the approach adopted to calculate potential wind energy both onshore and offshore [4].

higher expense for development of offshore wind farms, Lu et al. [4] elected to impose a greater relative spacing in this case in order to limit interturbine interference to less than 10%. This translates to a requirement for an interturbine spacing of 5×10 rotor diameters. Assuming deployment of GE 3.6 MW turbine [18] (rotor diameter 111 m, radius 55.5 m), positioning of turbines in this case should be restricted to 1 every 0.62 km^2 . The results presented in what follows reflect these assumptions.

4.3 RESULTS

4.3.1 Global Perspective

We restrict attention in what follows to locations in which wind conditions are projected to allow for the turbine choices considered here to function on an annual basis with capacity factors (CFs) of no less than 20%.

Results on a country-by-country basis are summarized in Fig. 4.4A and B for onshore and offshore environments, respectively. Placement of the turbines onshore and offshore was restricted as discussed earlier. Table 4.1 presents a summary of results for the 10 countries identified as the largest national emitters of CO₂ [19,20]. The data included here refers to national reporting of CO₂ emissions of 2012 and electricity consumption for these countries in 2011. Wind power potential for the world as a whole and for the contiguous United States is summarized in Table 4.2.

If the top 10 CO₂ emitting countries were ordered in terms of wind power potential, Russia would rank number one, followed by Canada with the United States in third position. There is an important difference to be emphasized, however, between wind power potential in the abstract and the fraction of the resource that is likely to be developed when subjected to realistic economic constraints. Much of the potential for wind power in Russia and Canada is located at large distances from population centers. Given the inevitably greater expense of establishing wind farms in remote locations and potential public opposition to such initiatives, it would appear unlikely that these resources will be developed in the near term. Despite these limitations, it is clear that wind power could make a significant contribution to the demand for electricity for the majority of the countries listed in Table 4.1, in particular for the four largest CO₂ emitters—China, the United States, India and Russia. It should be noted, however, the resource for Japan is largely confined to the offshore area, 82% of the national total. To fully exploit these global resources will require, inevitably, significant investment in transmission systems capable of delivering this power to regions of high load demand. Results for the contiguous United States and for China will be discussed in more detail in the following sections.

The electricity that could be generated potentially on a global basis using wind, displayed as a function of an assumed CF cutoff on installed turbines, is presented in Fig. 4.5A and B for onshore and offshore environments,

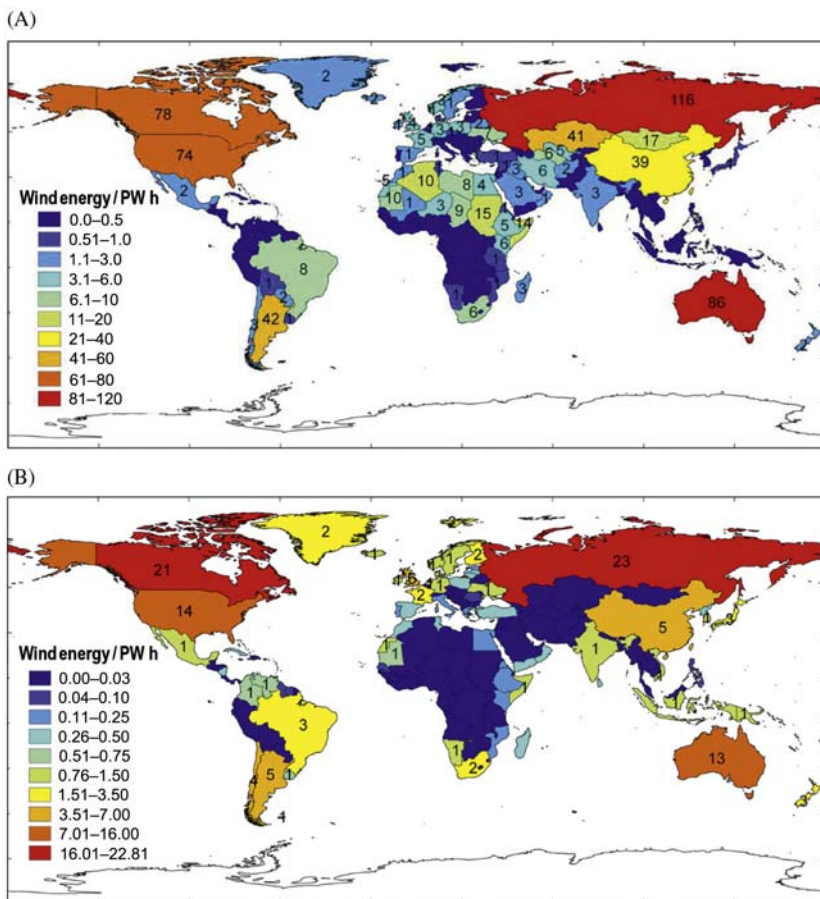


FIGURE 4.4 Annual wind energy potential country by country, restricted to installations with capacity factors greater than 20% with siting limited as discussed in the text: (A) onshore and (B) offshore [4].

respectively. The results in Fig. 4.5A suggest that total current global consumption of electricity could be supplied by wind, while restricting installation of land-based turbines to regions characterized by most favorable wind conditions, regions where the turbines might be expected to function with CFs greater than 53%. If the cutoff CF was lowered to 36%, the energy content of electricity generated using wind with land-based turbines globally would be equivalent to total current global consumption of energy in all forms. Cutoff CFs needed to accommodate similar objectives using offshore resources would need to be reduced as indicated in Fig. 4.5B. To place these considerations in context, we would note that CFs realized by turbines installed recently in the United States (in 2004 and 2005) have averaged close to 36% [21].

TABLE 4.1 Onshore and Offshore Wind Potential for the 10 Countries Identified as the Largest National Emitters of CO₂ [4]

No.	Country	CO ₂ Emission/ (10 ⁶ Metric Tonnes)	Electricity Consumption/ (TW h)	Potential Wind Energy/(TW h)		
				Onshore	Offshore	Total
1	China	8547.7	4207.7	39 000	4600	44 000
2	United States	5270.4	3882.6	74 000	14 000	89 000
3	India	1830.9	757.9	2900	1100	4000
4	Russia	1781.7	869.3	120 000	23 000	140 000
5	Japan	1259.1	983.1	570	2700	3200
6	Germany	788.3	537.9	3200	940	4100
7	South Korea	657.1	472.2	130	990	1100
8	Iran	603.6	185.8	5600	—	5600
9	Saudi Arabia	582.7	211.6	3000	—	3000
10	Canada	499.1	551.6	78 000	21 000	99 000

Note: CO₂ emission for 2012 and electricity consumption for 2011.

Source: Data from Boden TA, Andres RJ, Marland G. Preliminary 2011 and 2012 global & national estimates. In: Fossil-fuel CO₂ emissions. Oak Ridge, TN: Carbon Dioxide Information Analysis Center; 2013. p. 4 [19] and US EIA. International energy outlook. Washington, DC: U.S. Energy Information Administration; 2013. p. 312 [20].

TABLE 4.2 Annual Wind Energy Potential for Installations Onshore and Offshore for the World as a Whole and for the Contiguous United States

Areas		Worldwide		Contiguous United States	
		No CF Limitation	20% CF Limitation	No CF Limitation	20% CF Limitation
Energy (onshore areas)/(PW h)		1100	690	84	62
Energy (offshore areas)/(PW h)	0–20 m	47	42	1.9	1.2
	20–50 m	46	40	2.6	2.1
	50–200 m	87	75	2.4	2.2
Energy total/(PW h)		1300	840	91	68

Analysis assumes loss of 20% and 10% of potential power for onshore and offshore, respectively due to interturbine interference [4].

Note: All data assume offshore location distance within 92.6 km (50 M) of the nearest shoreline.

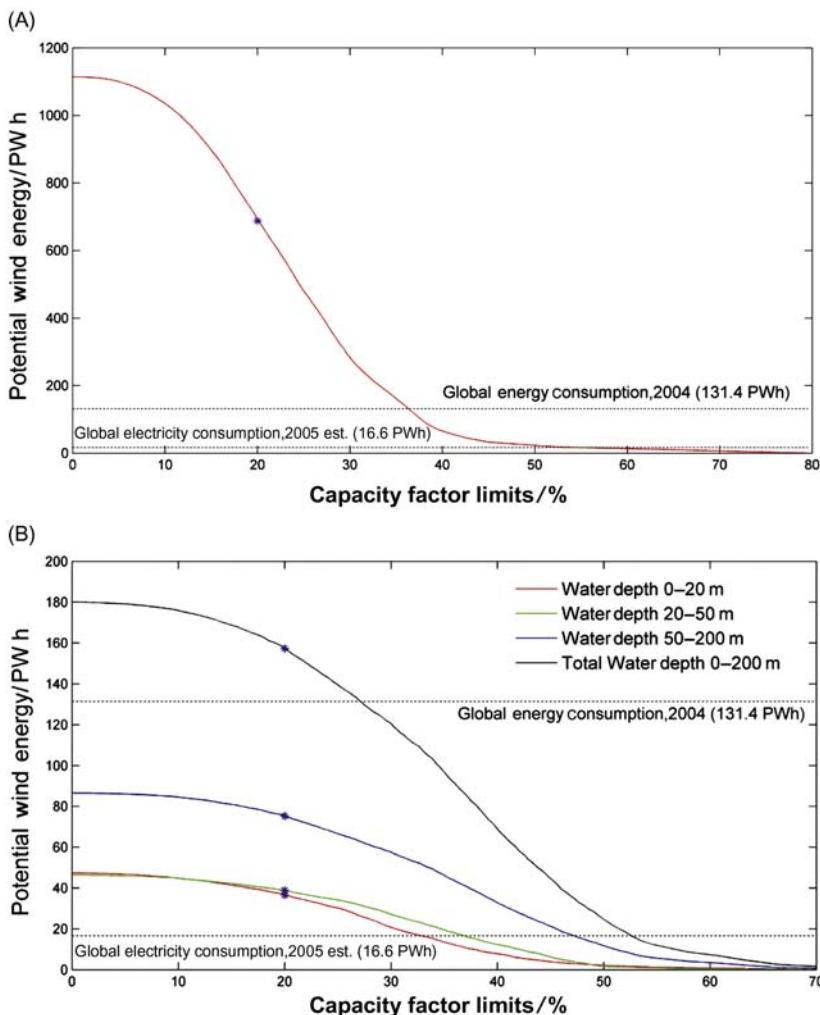


FIGURE 4.5 Annual wind energy potential as a function of assumed limits on capacity factors. Results corresponding to the capacity factor limit of 20% assumed in this study are indicated by *: (A) global onshore and (B) global offshore [4].

4.3.2 US Perspective

An estimate of the electricity that could be generated for the contiguous United States on a monthly basis (subject to the siting and capacity limitations noted earlier) is illustrated for both onshore and offshore environments in Fig. 4.6. Results presented here were computed using wind data for 2006. Not surprisingly, the wind power potential for both environments is greatest in Winter, peaking in January, lowest in Summer, with a minimum in

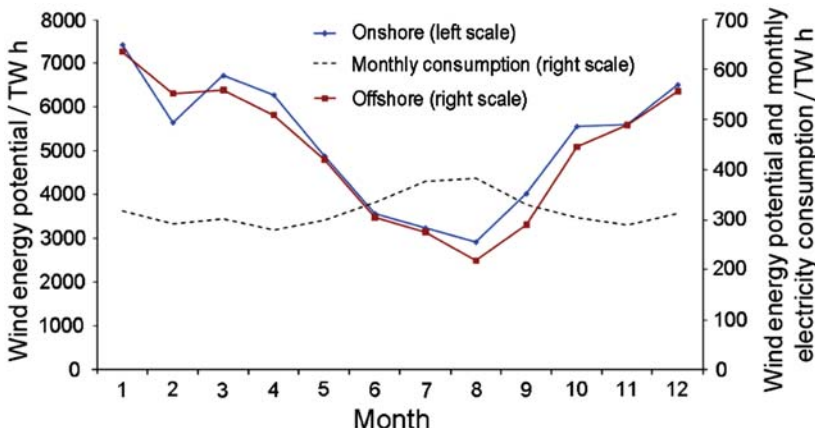


FIGURE 4.6 Monthly wind energy potential for the contiguous United States in 2006 with monthly electricity consumption for the entire United States [4].

August. Onshore potential for January, according to the results presented in Fig. 4.6, exceeds that for August by a factor of 2.5: the corresponding ratio computed for offshore locations is slightly larger, 2.9.

Fig. 4.6 includes also monthly data for consumption of electricity in the United States during 2006. Demand for electricity exhibits a bimodal variation over the course of a year with peaks in Summer and Winter, minima in Spring and Fall. Demand is greatest in Summer during the air-conditioning season. Summer demand exceeds the minimum in Spring/Fall demand typically between 25% and 35% on a US national basis depending on whether Summers are unusually warm or relatively mild. The correlation between the monthly averages of wind power production and electricity consumption is negative. Very large wind power penetration can produce excess electricity during large parts of the year. This situation could allow options for the conversion of electricity to other energy forms. Plug-in electric vehicles, e.g., could take advantage of short-term excesses in electricity system, while energy rich chemical species such as H₂ could provide a means for longer term storage.

Potential wind-generated electricity available from onshore facilities on an annually averaged state-by-state basis is presented in Fig. 4.7A. Note the high concentration of the resource in the central plains region extending northward from Texas to the Dakotas, westward to Montana and Wyoming, and eastward to Minnesota and Iowa. The resource in this region, as illustrated in Fig. 4.7B, is significantly greater than current local demand. Important exploitation of this resource will require, however, a significant extension of the existing power transmission grid. Expansion and upgrading of the grid will be required in any event to meet anticipated future growth in

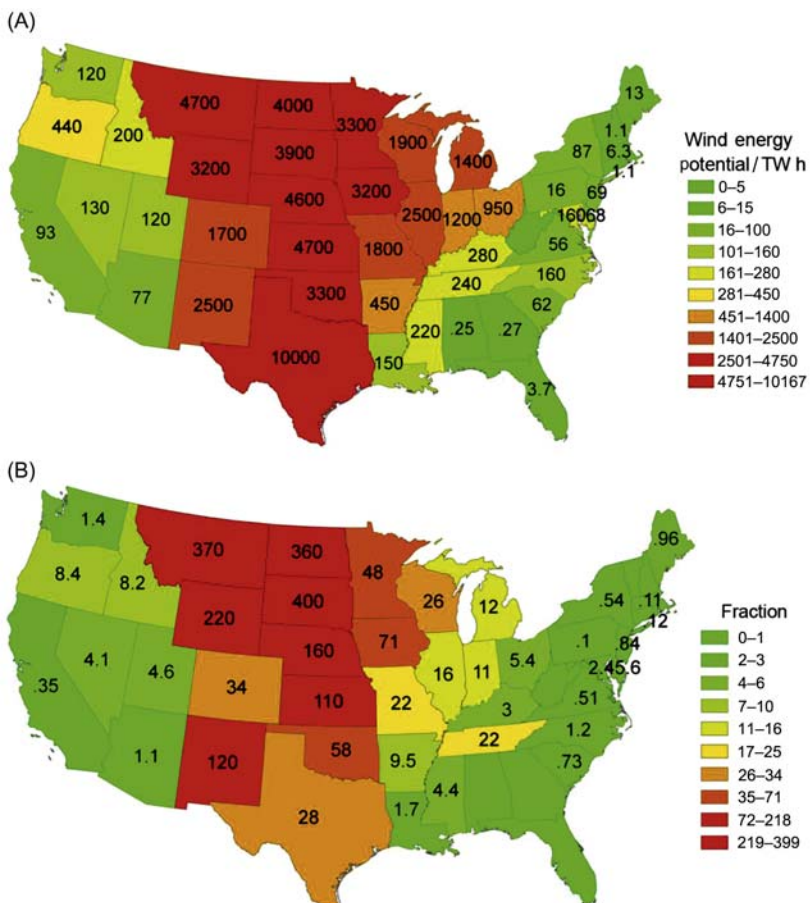


FIGURE 4.7 (A) Annual onshore wind energy potential on a state-by-state basis for the contiguous United States. (B) Same with (A), but expressed as fraction of total electricity retail sales in the states (2006) [4]. For example, the potential source for North Dakota exceeds current total electricity retail sales in that state by a factor of 360. *Data source for total electricity retail sales: <http://www.eia.doe.gov>.*

electricity demand. It will be important in planning for this expansion to recognize from the outset the need to accommodate contributions of power from regions rich in potential renewable resources, not only wind but also solar. The additional costs need not, however, be prohibitive [21]. ERCOT, the operator responsible for the bulk of electricity transmission in Texas, estimates the extra cost to transmit up to 4.6 GW of wind-generated electricity at about \$180 per kilowatt, approximately 10% of the capital cost for installation of the wind power-generating equipment [22].

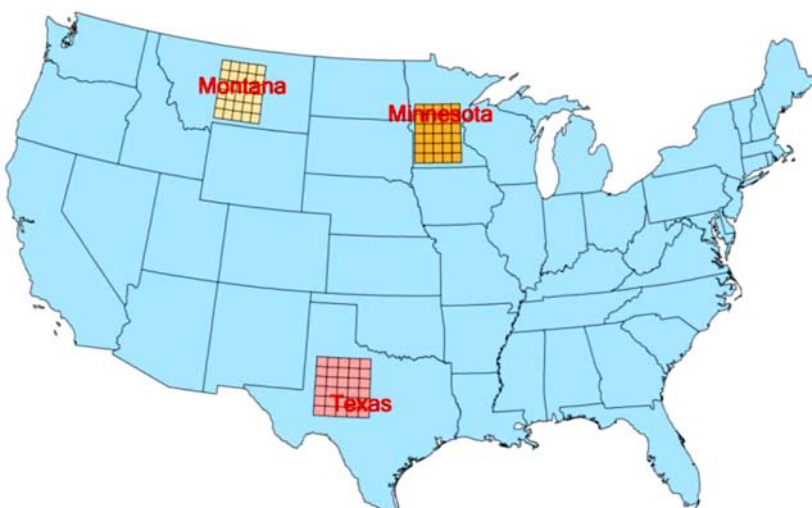


FIGURE 4.8 Locations of regions in Montana, Minnesota, and Texas selected to explore the spatial correlation of wind resources [4].

An important issue relating to the integration of electricity derived from wind into a grid incorporating contributions from a variety of sources relates to the challenge of matching supply with load demand incorporating a contribution from supply that is intrinsically variable both in time and space and subject to prediction errors. This challenge can be mitigated to some extent if the variations of wind sources contributing to an integrated transmission grid from different regions are largely uncorrelated. An anomalously high contribution from one region can be compensated in this case by an anomalously low contribution from another. To investigate the significance of this potential compensation, Lu et al. [4] examined the covariance of wind resources from three specific regions, one in Montana, the second in Minnesota, the third in Texas, as indicated in Fig. 4.8. Analysis of 6 hour averaged potential wind-generated supplies of electricity from the three regions over the four seasons, Winter, Spring, Summer, and Fall, yielded the results summarized in Table 4.3. Contributions from the three regions are essentially uncorrelated during the Winter months (October–March) with r values of less than 0.07. Correlation coefficients (r values), however, are relatively high in Summer (July–September) with values ranging from 0.28 (Montana vs Texas) to 0.37 (Montana vs Minnesota) with intermediate values in Spring. The analysis suggests that wind power could make a relatively reliable contribution to anticipated base load demand in Winter. It may be more difficult to incorporate wind power resources into projections of base load demand for other seasons, particularly for Summer.

TABLE 4.3 Correlations of Wind Power Potential Between Selected Regions of Montana (MT), Minnesota (MN), and Texas (TX) in Different Seasons for 2006 [4]

Correlation Coefficient (r)	January–March	April–June	July–September	October–December
MN–MT	0.027	0.11	0.37	−0.15
MN–TX	0.069	0.29	0.29	−0.060
MT–TX	0.065	0.26	0.28	−0.0024

4.3.3 China Perspective

McElroy et al. [23] applied the assimilated meteorology data resource as described earlier to assess also the potential for wind-generated electricity in China. The approach they followed in this case was generally similar to that adopted for the global and US applications described by Lu et al. [4]. In particular, they elected to exclude as possible sites for turbine deployment forested areas, areas occupied by permanent snow or ice, areas covered by water, and areas identified as either developed or urban. They excluded in the Chinese application also land areas with slopes larger than 20% [21]. Recognizing that turbine sizes installed in China are generally smaller than those favored in the United States, they chose to focus their study on deployment of a suite of 1.5 MW turbines, selecting for this purpose the GE 1.5 MW xle design [24]. The hub height for this model is at 80 m; the rotor diameter measures 82.5 m. The spacing between turbines in representative wind farms was selected similar to that adopted for wind farms installed in Inner Mongolia, 9 rotor diameters in the downwind direction, 5 rotor diameters in the direction perpendicular to the prevailing wind (9D × 5D), slightly larger than the spacing of 7D × 4D, adopted by Lu et al. [4]. Overall power loss due to turbine–turbine interactions with the spacing assumed in the China application is estimated at about 10% [25].

The spatial distribution of CFs evaluated for deployment of the 1.5 MW turbines considered here is illustrated in Fig. 4.9. CF defines the fraction of the rated power potential of a turbine that is actually realized over the course of a year given expected variations in wind speed. CF values for wind farms deployed in Inner Mongolia, as illustrated, e.g., in Fig. 4.9, are estimated to reach values as high as 40% indicating that 1.5 MW turbines installed in this region could potentially provide as much as 5.26 GW h of electricity over the course of a year. Wind conditions are notably favorable, and CF values are consequently large, over extensive regions of northern China (Inner Mongolia, Heilongjiang, Jilin, and Liaoning) and in parts of the west (Tibet,

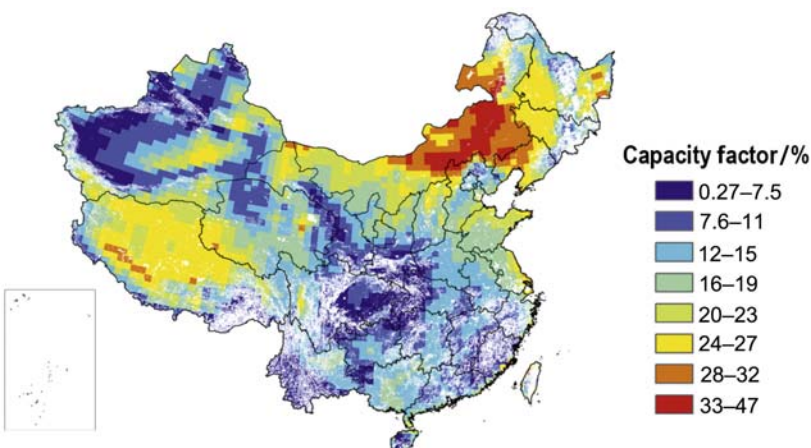


FIGURE 4.9 Spatial distribution of capacity factors evaluated for deployment of the 1.5 MW turbines [23].

Xinjiang, Qinghai, and Gansu). Wind farms deployed recently in the United States have achieved operational CFs as high as 48%, with an average of close to 35% [26]. By way of comparison, CFs for wind farms installed in China have been significantly lower than for the United States, close to 23% on average [27]. The relatively low operational performance for wind farms in China is attributed to a combination of factors: lower quality of the largely domestically produced turbines deployed in China as compared with turbines available on the international market; bottlenecks introduced by limitations imposed by the existing Chinese electricity grid; and suboptimal siting of wind farms due to inadequate prior screening of potentially available wind resources [28].

Electricity that could be generated from wind irrespective of price, restricted however to installations capable of operating with CFs greater than 20%, is illustrated for the existing seven electric grid areas of China in Fig. 4.10. The figure includes also results expressed as ratios with respect to the current production of electricity in these grid regions. The data displayed here suggests that a suite of 1.5 MW turbines deployed in onshore regions with favorable wind resources could provide potentially for as much as 24.7 PW h of electricity annually, more than seven times current national Chinese consumption.

Demand for electricity in China is spread more evenly throughout the year as compared to the United States where demand peaks in Summer. The pattern for China reflects the fact that the largest fraction of electricity in the country is used by industry (70%) as compared to only 29% for industry in the United States where demand for electricity is spread more evenly among residential, commercial, and industrial usage. Incorporating base load sources

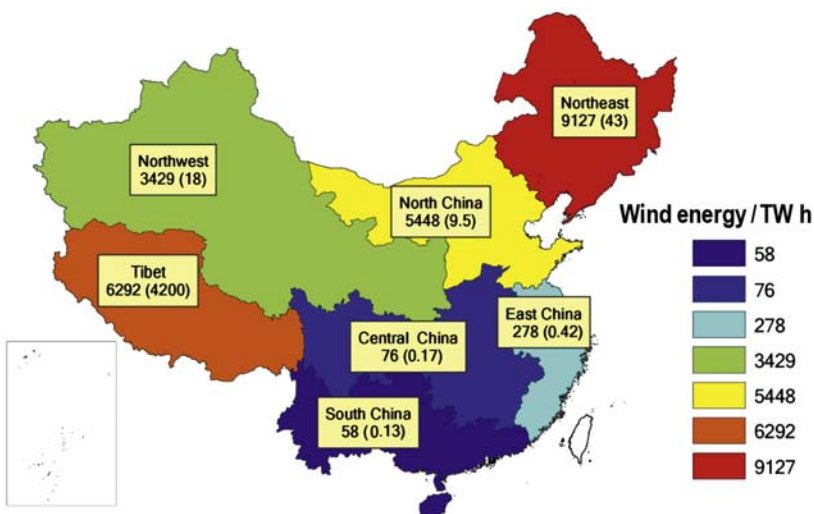


FIGURE 4.10 Potential electricity irrespective of price that could be generated over the seven electric grid areas of the Chinese mainland [23].

of electricity from coal-fired power plants poses relatively minor problems for grid managers charged with matching supplies of electricity with demand. Adjusting to an important, intrinsically variable, supply such as that from wind will require a more complex, and consequently more costly, grid management protocol.

Operators of an electric utility face a formidable and continuing challenge to ensure that production of electricity is targeted in real time to meet projected demand. In a typical power system, nuclear and coal-fired systems provide sources of what is referred to as base load power. That is to say, the assumption is that these systems will operate essentially continuously, with minimal opportunity to respond to either increases or decreases in demand. Typically, gas-fired systems, which can be turned on or off rapidly, provide the flexibility needed to react to changes in demand. Accommodating an input of power from an intrinsically variable source such as wind poses a particular problem for the orderly operation of a complex electric utility network.

Integration of wind energy into China's coal-heavy electricity system presents significant challenges owing to wind's variability and the grid's system-wide inflexibilities. As indicated in a recent study [28], China has greater capacity for wind installation compared to the United States (145.1 vs 75.0 GW) but generates less electricity from wind (186.3 vs 190.9 TW h). A study by Davidson et al. suggested a potential production of 2.6 PW h per year by 2030 [29]. Although this represents 26% of total projected electricity demand, it is only 10% of the total estimated physical potential of wind

resources in the country. Increasing the operational flexibility of China's coal fleet would allow wind to deliver nearly three-quarters of China's target of producing 20% of primary energy from nonfossil sources by 2030.

4.4 CONCLUDING REMARKS

The discussion to this point has sought to estimate the quantity of electricity that could be generated by selective placement of state-of-the-art wind turbines in regions judged suitable for their deployment. As indicated, the wind data employed in this analysis were derived from retrospective analysis of past meteorological conditions. In this sense, the present analysis may be interpreted as identifying the electricity that could have been produced from turbines installed at some point in the past when wind conditions may have been similar, and remained similar, to those identified in the database adopted here. The past is of course at best an imperfect prologue for the future. But, in planning for the future it may be the best option at our disposal.

Reservations that should be noted in addressing the charge indicated in the title of this chapter—to define the global potential for wind-generated electricity—include the following. Placement of a concentration of wind turbines at a particular location could have the potential to alter local and potentially even regional wind conditions. An extensive deployment of wind farms could have an impact on the budget of atmospheric kinetic energy leading to a potentially consequential change in the circulation of the global atmosphere. And responding to increasing concentrations of greenhouse gases, climate and wind conditions in the future may differ significantly from conditions that prevailed in the past. Quantitative projections for future wind power potential will be subject therefore to a level of inevitable unavoidable uncertainty.

The impact of wind farms on local meteorological conditions has been explored in a number of recent studies. Zhou et al. [30] used satellite data covering the period 2003–11 to analyze the response of regional surface temperature to the development of a wind farm in Texas. They found evidence for a significant upward trend in surface temperature, by as much as 0.72°C per decade, particularly at night and especially in the immediate neighborhood of the wind farms. Roy and Traiteur [31] found a similar pattern in their study of the response of temperatures to the development of a wind farm in San Gorgonio, California. They reported evidence for a statistically significant increase in temperature, by about 1°C , at an elevation of 5 m downwind of the wind farm at night. The increase persisted through the early morning, followed by modest cooling during the day. They suggested that the impacts of wind farms on local weather could be minimized by modifying the design of rotor systems, or by siting wind farms in regions defined by high levels of natural turbulence. They further identified the Midwest and

Great Plains regions of the United States as ideal for the placement of low-impact wind farms.

If the entire demand for electricity in the United States were to be accommodated by wind, the accompanying sink for kinetic energy would amount to approximately 6% of the sink contributed naturally by surface friction over the entire contiguous US land area, 11% for the sink identified with the area indicated in the foregoing as most favorable for wind farm development. The impact on the circulation of the atmosphere of potentially major commitments to wind power was explored in a number of recent studies, notably by Kirk-Davidoff and Keith [32] and Keith et al. [33]. They concluded that exploitation of wind resources at high levels of penetration might be expected to lead to significant changes in the circulation of the atmosphere, even in regions remote from the location of the involved turbines. They argued that the budget for the global inventory of atmospheric kinetic energy is regulated primarily by processes on the input side of the ledger rather than by the sink. An increase in friction resulting from the operation of large numbers of power-generating turbines could be compensated in this case, they argued, by a decrease in the dissipation of momentum by friction elsewhere. The global average surface temperature, they concluded, would not be expected to change significantly in the face of a large investment in wind-generated electricity. Temperatures at high latitude could decrease to a modest extent in response to an anticipated decrease in the efficiency of meridional heat transport. The impact could be viewed as positive in this case, an offset to some extent for the amplified warming projected to arise for this environment in response to the human-induced increase in the concentration of greenhouse gases.

The impact on the circulation of the atmosphere of a large-scale investment in wind farms was investigated also by Miller et al. [34] and by Marvel et al. [35]. Employing a simple parameterization approach to simulate the influence of turbine operations as a sink for atmospheric momentum, Miller et al. [34] concluded that turbines distributed uniformly over the Earth's surface could harvest kinetic energy sustainably at a rate ranging up to as much as 400 TW. If the turbines were deployed at an elevation of 100 m, the yield could be as great as 1800 TW. Using an alternate approach to parameterize the sink for momentum associated with the exploitation of wind resources, Jacobson and Archer [36] concluded that as the number of wind turbines increased over a large geographic region, extraction of power should first increase linearly, converging eventually to a limit, estimated as in excess of 250 TW for turbines sited at 100 m, rising to 380 TW for turbines deployed at an altitude of 10 km.

There is a notable discrepancy between these various estimates of wind potential. Adams and Keith [37] addressed the issue using a mesoscale model. They concluded that the generation of power from wind should be limited to an average of about 1 W m^{-2} for facilities distributed over an area

of approximately 100 km². They argued further that the results obtained using a mesoscale model should provide a useful guide to what might be expected on the basis of a more complete global model. The assertion, however, remains to be demonstrated.

Modern wind turbines are designed to operate effectively for life cycles ranging up to 25 years or even longer. Predictions of wind power for the next 25 years, including the need to anticipate the impact of intrinsic variability, will pose a challenge for prospective investors. Global and regional climate models have difficulty in accounting for historical trends in wind regimes. There is little reason to believe that they will be more successful in predicting the future. Pryor et al. [38], on the basis of existing research, argued that the changes in mean wind speeds and energy density anticipated for the future are unlikely to exceed the year-to-year variability ($\pm 15\%$) observed most recently over much of Europe and North America. Surface winds have declined in intensity in China, the Netherlands, the Czech Republic, the United States, and Australia over the past few decades [39–42]. The precise cause of this decline is uncertain. Vautard et al. [43] analyzed the extent and potential cause for the changes in surface wind speeds observed over northern mid-latitudes between 1979 and 2008, using data from 822 surface weather stations. They indicated that surface wind speeds declined by 5%–15% over almost all continental areas at northern mid-latitudes with the decrease greatest at higher wind speeds. In contrast, upper-air winds inferred from sea-level pressure gradients, and winds derived from weather reanalyses, exhibit no such trend. It has been suggested that an increase in surface roughness resulting from increases in biomass and related changes in land cover over Eurasia could account for as much as 25%–65% of the decrease in surface winds observed over this region.

Huang and McElroy [3], using assimilated meteorological data for the period January 1979–December 2010, investigated the origin of wind energy from both mechanical and thermodynamic perspectives. Their results indicate an upward trend in kinetic energy production over the past 32 years, suggesting that wind energy resources might increase in a warming climate. They highlighted further the fact that the total kinetic energy stock of the atmosphere displays significant interannual variability, responding notably to the changing phases of the El Niño–Southern Oscillation (ENSO) cycle. The potential for wind as a source of electricity at any particular location may be expected thus to vary not only on the long term but also interannually in response to natural fluctuations in the circulation of the atmosphere.

The overall conclusion from this chapter is that wind resources on a global scale could accommodate a large fraction of present and anticipated future demand for electricity. Concentration of facilities in specific regions might be expected to contribute to a change in prevailing local meteorological conditions. This change is unlikely, however, to be sufficiently disruptive as to offset the advantages that could be realized from the concentration in

the first place. Generation of electricity by capturing kinetic energy from the wind may be considered as an additional contribution to the surface friction that serves as the natural offset to the atmosphere's global production of kinetic energy. At high levels of penetration, wind facilities could have an appreciable influence on the budget of this important quantity: climate might be expected to adjust accordingly. Given foreseeable near term expansion of wind systems, however, this is unlikely to pose a serious problem. The most important limitation for future growth is likely to involve rather the challenge of responding to the intrinsic variability of the input from wind, compounded by the fact that this source may not be matched ideally to patterns of power demand.

ACKNOWLEDGMENTS

The work was supported by the State Environmental Protection Key Laboratory of Sources and Control of Air Pollution Complex, Collaborative Innovation Centre for Regional Environmental Quality, the National Key R&D Program “Formation mechanism and control technology of air pollution” (2016YFC0208900), and the Volvo Group in a research project of the Research Center for Green Economy and Sustainable Development, Tsinghua University. It was also supported by the Harvard Climate Change Solutions Fund and the Harvard Global Institute.

REFERENCES

- [1] McElroy MB. Energy and climate: vision for the future. Oxford: Oxford University Press; 2016.
- [2] Kung EC. Large-scale balance of kinetic energy in atmosphere. Mon Weather Rev 1966;4(11): 627–40.
- [3] Huang JL, McElroy MB. A 32-year perspective on the origin of wind energy in a warming climate. Renewable Energy 2015;77:482–92.
- [4] Lu X, McElroy MB, Kiviluoma J. Global potential for wind-generated electricity. Proc Natl Acad Sci USA 2009;106(27):10933–8.
- [5] Rienecker MM, et al. The GEOS-5 data assimilation system—documentation of versions 5.0.1, 5.1.0, and 5.2.0. In: Suarez MJ, editor. Technical report series on global modeling and data assimilation. Washington, DC: NASA; 2007. p. 118.
- [6] Archer CL, Jacobson MZ. Evaluation of global wind power. J Geophys Res 2005;110(D12):D12110.
- [7] IEC. In: Commission IE, editor. Wind turbines—Part 12-1: Power performance measurements of electricity producing wind turbines. Geneva: NYSE: IHS; 2005.
- [8] USGS Global Digital Elevation Model (GTOPO30). 30-Arc seconds. Sioux Falls, South Dakota: U. S. Geological Survey, Center for Earth Resources Observation and Science (EROS); 2006.
- [9] U.S. Department of Energy. Environmental impact statement for the proposed cape wind energy project. Washington, DC: U.S. Department of Energy; 2012.
- [10] Musial W, Butterfield S. Future for offshore wind energy in the United States. EnergyOcean 2004. Palm Beach, FL: National Renewable Energy Laboratory (NREL); 2004.

- [11] Musial W. Offshore wind energy potential for the United States. Wind Powering America -Annual State Summit. Colorado: Evergreen; 2005.
- [12] Musial W, Ram B. Large-scale offshore wind power in the United States: assessment of opportunities and barriers. Golden, CO: National Renewable Energy Laboratory; 2010.
- [13] Dvorak MJ, Archer CL, Jacobson MZ. California offshore wind energy potential. *Renewable Energy* 2010;35(6):1244–54.
- [14] Dvorak MJ, Stoutenburg ED, Archer CL, Kempton W, Jacobson MZ. Where is the ideal location for a US East Coast offshore grid? *Geophys Res Lett* 2012;39. Available from: <http://dx.doi.org/10.1029/2011GL050659>.
- [15] Sclavounos P, Tracy C, Lee S, ASME. Floating offshore wind turbines: responses in a seastate Pareto optimal designs and economic assessment. New York, NY: Amer Soc Mechanical Engineers; 2008.
- [16] Masters GM. Renewable and efficient electric power systems. Hoboken, NJ: John Wiley & Sons, Inc; 2004.
- [17] GE. 2.5 MW series wind turbine. Fairfield, CT: General Electric Energy; 2006.
- [18] GE. In: Energy G, editor. 3.6 MW Wind Turbine Technical Specifications. Fairfield, CT: General Electric Energy; 2006.
- [19] Boden TA, Andres RJ, Marland G. Preliminary 2011 and 2012 global & national estimates. *Fossil-fuel CO₂ emissions*. Oak Ridge, TN: Carbon Dioxide Information Analysis Center; 2013.
- [20] US EIA. International energy outlook. Washington, DC: U.S. Energy Information Administration; 2013.
- [21] US-DOE. 20% Wind energy by 2030, increasing wind energy's contribution to U.S. electricity supply. Washington, DC: U.S. Department of Energy; 2008.
- [22] ERCOT. Analysis of transmission alternatives for competitive renewable energy zones in Texas. Austin, TX: Energy Reliability Council of Texas (ERCOT); 2006.
- [23] McElroy MB, Lu X, Nielsen CP, Wang Y. Potential for wind-generated electricity in China. *Science* 2009;325(5946):1378–80.
- [24] GE. 1.5-MW series of wind turbines. Fairfield, CT: Energy GE; 2009.
- [25] Kempton W, Archer CL, Dhanju A, Garvine RW, Jacobson MZ. Large CO₂ reductions via offshore wind power matched to inherent storage in energy end-uses. *Geophys Res Lett* 2007;34(2):5.
- [26] Wiser R, Bolinger M. In: US-DOE, editor. Annual Report on U.S. Wind Power Installation, Cost and Performance Trends: 2007. Washington, DC: U.S. Department of Energy; 2008. p. 32.
- [27] Cyranoski D. Renewable energy: Beijing's windy bet. *Nature* 2009;457(7228):372–4.
- [28] Xi L, McElroy MB, Peng W, Liu S, Nielsen CP, Wang H. Challenges faced by China compared with the US in developing wind power. *Nat Energy* 2016;1(6):6.
- [29] Davidson MR, Zhang D, Xiong W, Zhang X, Karplus VJ. Modelling the potential for wind energy integration on China's coal-heavy electricity grid. *Nat Energy* July 2016;1:7.
- [30] Zhou LM, Tian YH, Roy SB, Thorncroft C, Bosart LF, Hu YL. Impacts of wind farms on land surface temperature. *Nat Clim Change* 2012;2(7):539–43.
- [31] Roy SB, Traiteur JJ. Impacts of wind farms on surface air temperatures. *Proc Natl Acad Sci USA* 2010;107(42):17899–904.
- [32] Kirk-Davidoff DB, Keith DW. On the climate impact of surface roughness anomalies. *J Atmos Sci* 2008;65(7):2215–34.

- [33] Keith DW, DeCarolis JF, Denkenberger DC, Lenschow DH, Malysherv SL, Pacala S, et al. The influence of large-scale wind power on global climate. *Proc Natl Acad Sci USA* 2004;101(46):16115–20.
- [34] Miller LM, Brunsell NA, Mechem DB, Gans F, Monaghan AJ, Vautard R, et al. Two methods for estimating limits to large-scale wind power generation. *Proc Natl Acad Sci USA* 2015;112(36):11169–74.
- [35] Marvel K, Kravitz B, Caldeira K. Geophysical limits to global wind power. *Nat Clim Change* 2013;3:118–21.
- [36] Jacobson MZ, Archer CL. Saturation wind power potential and its implications for wind energy. *Proc Natl Acad Sci USA* 2012;109(39):15679–84.
- [37] Adams AS, Keith D. Are global wind power resource estimates overstated? *Environ Res Lett* 2013;8:015021.
- [38] Pryor SC, Barthelmie RJ. Climate change impacts on wind energy: a review. *Renewable Sustainable Energy Rev* 2010;14(1):430–7.
- [39] Klink K. Trends in mean monthly maximum and minimum surface wind speeds in the coterminous United States, 1961 to 1990. *Clim Res* 1999;13(3):193–205.
- [40] Smits A, Tank A, Konnen GP. Trends in storminess over the Netherlands, 1962–2002. *Int J Climatol* 2005;25(10):1331–44.
- [41] Xu M, Chang C-P, Fu C, Qi Y, Robock A, Robinson D, et al. Steady decline of east Asian monsoon winds, 1969–2000: evidence from direct ground measurements of wind speed. *J Geophys Res Atmos* 2006;111(D24):8.
- [42] McVicar TR, Van Niel TG, Li LT, Roderick ML, Rayner DP, Ricciardulli L, et al. Wind speed climatology and trends for Australia, 1975–2006: capturing the stilling phenomenon and comparison with near-surface reanalysis output. *Geophys Res Lett* 2008;35(20):6.
- [43] Vautard R, Cattiaux J, Yiou P, Thepaut JN, Ciais P. Northern Hemisphere atmospheric stilling partly attributed to an increase in surface roughness. *Nat Geosci* 2010;3(11):756–61.

This page intentionally left blank

Chapter 5

The Future of Wind Energy Development in China

Pei-yang Guo¹, Dan-yang Zhu¹, Jacqueline Lam^{1,2},
and Victor O.K. Li^{1,2}

¹*The University of Hong Kong, Hong Kong, China*, ²*The University of Cambridge, Cambridge, United Kingdom*

Email: jcklam@eee.hku.hk

5.1 INTRODUCTION

Globally, energy is generated mainly from the nonrenewable sources. This has resulted in serious environmental pollution and health degradation. By contrast, renewable energies (RE) are clean, sustainable, and emit fewer pollutants and greenhouse gases (GHG) [1]. REs include wind, solar, biomass, geothermal and hydrothermal, all of which occur naturally on our planet. Like all renewable forms of energy, wind generates green electricity and provides a solution to reducing GHGs. It is expected that wind will provide more than 20% of global electricity demand by 2050 [2]. The growth of installed global wind capacity from 17.4 GW in 2000 to 432.4 GW in 2015 is a strong indication that this target will be met [3].

As the biggest GHG emitter in the world, China is facing increasing pressure to cut carbon emissions. The recent slowdown in economic development has prompted China to look for alternative economic solutions and develop new energy industries which include wind. In less than two decades of development, China's installed wind energy capacity has reached the stage of being greater than that of any other country in the world. In this chapter, we will first review the status of China's wind energy development, with a brief introduction of the electricity and wind energy market in China. Secondly, we identify the barriers and drivers to the country's wind energy development. Lastly, we outline the possible future pathways for achieving a sustainable wind energy industry in China.

5.2 WIND ENERGY DEVELOPMENT IN CHINA

5.2.1 Overview

Since 1979, the Chinese economy has increased at an average annual rate of 10%, doubling every 7 years. To maintain this high rate of economic growth, China needs to continue expanding its electricity supply. However, viable options of electricity generation are few. China is rich in coal reserves, but limited in gas and oil supply. Electricity generation based on coal is highly polluting and carbon-intensive, thus creating significant political and international pressure [4]. There is an urgent need for China to change from high-carbon to low-carbon electricity generation.

China has so far achieved remarkable progress in wind energy development. Wind power now represents 3.3% of the overall power generation [3]. This is largely due to the country's vast wind resources [5], relative technological maturity, and relatively low cost, compared to other renewable resources. From 2001 to 2015, China's accumulated wind power generation capacity increased from 404 MW to 148 GW (Fig. 5.1). The new installed wind energy capacity increased to 32 970 MW in 2015, thus securing China's global leading position in installed wind capacity [3]. Wind energy has constituted a key component of China's RE strategy and is expected to play an increasingly significant role in China's energy mix.

5.2.2 Electricity Market and Wind Energy Market in China

5.2.2.1 Electricity Market and Wind Energy Market

China's electricity market is heavily regulated. On the supply side, the government has established an on-grid tariff for each province. Each power plant must sell its outputs to the two national grid companies via the on-grid tariff. The grid companies then transmit and distribute the electricity to local utilities, which are subsidiaries of the two grid companies. On the demand side,

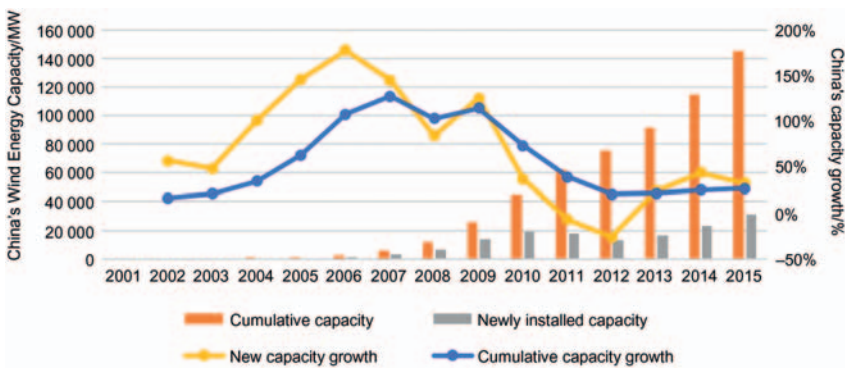


FIGURE 5.1 China's wind energy capacity development 2001–15 [3].

consumers purchase electricity from local utilities at fixed prices set by the local governments. Since 2015, China has started revamping the electricity market and has attempted to liberalize electricity supply [6]. However, such reforms have only just begun. The main electricity transactions conducted between power plants and two grid companies are still controlled by the central government.

According to the energy law in China, electricity produced by wind farms should all be taken up by the two national grid companies and purchased at a price stated by the feed-in-tariff (FIT). The FIT is set at a much higher price than the on-grid tariff applicable to thermal plants. All consumers must purchase electricity at a state-sanctioned fixed price, which includes surcharges for renewables, regardless of the proportion of renewables represented in the overall electricity package.

Two different pricing schemes have been introduced to the electricity market in China over the past decade to boost the integration of onshore wind to the grid: auctioning and FIT. The auctioning scheme was introduced in 2003, when the National Development and Reform Commission (NDRC) organized national concession tendering for selected projects and picked winners based on the lowest bidding price. However, it soon became evident that this process was dominated by the state-owned enterprises (SOEs), which submitted bids at very low prices to secure projects. SOEs were keen to win these projects because (1) they were required by the government to purchase wind capacity to meet their renewable installation target; (2) they were able to compensate for wind project loss with revenues from conventional generation; (3) some parties hoped to win the bid first and postponed the development until the cost of wind power technology becomes sufficiently low. Such practices conducted by SOEs carried unintended consequences: the tariffs were too low to cover the project cost; auction winners resorted to corner-cutting to reduce costs; and private investments were forced to exit the nascent wind power industry. After a few unsuccessful attempts to reform the auctioning process, the Chinese government eventually decided to abandon onshore wind auctioning.

Since 2009, FIT has been introduced to replace auctioning. China is divided into four regions based on wind resources and the existing grid infrastructure. Under each region, a benchmark price for wind power is issued by NDRC. Each tariff consists of two parts: a fixed on-grid tariff and a renewable subsidy. The fixed on-grid tariff is paid by the national grid companies. The renewable subsidy is covered by a national renewable fund, sustained by a surcharge levied on electricity consumers and fiscal transfer from the government. A high, fixed FIT has been considered by wind developers as one of the most important drivers of wind capacity installation [7].

Recently, a new renewable quota (the government has refrained from framing it as a “quota,” though it is a quota by nature) has been proposed, which will link closely with existing FIT [8]. The new regulation requires

nonhydro renewables to generate 9% of consumed electricity by 2020. To achieve the renewable target, NDRC has stipulated the amount of renewables that each province should share; this ranges from 5% to 13%. The regulation also requires that all power companies should share a minimum of 9% electricity output from the renewables by 2020, complemented by policy issues such as tradable green certificates issued by the local governments, whenever relevant, in order to meet the renewable quota. Before the new regulatory package has been successfully implemented at the local level, its effectiveness in stimulating the increasing penetration of wind and other renewables into the national grid and local utilities remains to be proven.

5.2.2.2 Key Players in the Wind Energy Market in China

China's wind industry is shaped by five key types of stakeholders, including the wind developers, the wind turbine manufacturers, the central government, the local governments, and the national and local grid companies. Because of the strong role the state plays in the electricity market in China, the central and the local governments are dominant players shaping the wind energy market. The national and local grid companies are under the direct control of the state and the local governments.

5.2.2.2.1 Wind Energy Developers

Wind energy developers in China consist primarily of the state-owned power generation companies. The unique feature of China's electricity system dates back to 2002, when its electricity market was restructured to allow competition in electricity supply. Five state-owned companies were spun off from the State Grid Corporation (SGC), then, the only vertically integrated utility. Since then, China's electricity generation has been dominated by five corporations plus a number of new entrants, most of which are SOEs such as Shenhua and CR power. After China increased the renewable penetration by taking up wind auctioning in 2003, these companies rapidly expanded their installed wind capacities via their deep pockets and their ability to subsidize the low strike price of wind renewables by the revenues obtained from non-renewables. Only one new entrant has been able to obtain significant market share from any state-owned companies. This being Tianrun, a private power company specialized in wind power development and a subsidiary of Goldwind, the leading wind turbine manufacturer in China.

5.2.2.2.2 Wind Turbine Manufacturers

Chinese wind turbine manufacturers top the world's wind energy market in terms of installed wind capacity. In 2015, among the top 10 companies achieving the highest installed wind capacity, five are Chinese [9]. Such outstanding performance can mostly be attributed to the rapid wind power

expansion in China, which relies predominantly on domestically produced wind turbines.

Chinese wind manufacturers started developing wind turbines at a much later stage than their European counterparts. Local wind turbine manufacturing began production in the mid-1990s. In 1996, the Chinese government unveiled a set of policy initiatives to speed up wind technology capacity. Chinese manufacturers gradually acquire advanced technologies via joint ventures or technology licensing and secure competitive positions in global turbine manufacturing [10,11]. A major policy reform was introduced in 2005, which required that 70% of wind turbine components be manufactured in China [12]. Though this policy was eventually abolished 5 years after the introduction due to international pressure, it significantly boosted the market share of domestic manufacturers and encouraged technology transfer from frontrunner companies in China. China has gradually reduced its reliance on imported turbine technologies and has accumulated its own innovative capacity [11]. Chinese manufacturers are capable of producing large turbines of comparable size to their European counterparts.

5.2.2.2.3 The Central Government

The central government, including NDRC and the National Energy Agency, are the primary national policy-making bodies taking charge of wind power development and planning in China. Before 2010 when auctioning was applied on wind power pricing, NDRC was responsible for planning concession bidding, for any wind projects that exceed 50 MW. After China has adopted FIT, NDRC retains the authority to approve any wind projects that exceeded this threshold, while delegating the local government the authority to approve any projects that falls below the threshold. However, the over-heated response of the local governments to approve wind projects that fall below the threshold, prompted NDRC, in 2011, to retake its authority to approve all types of wind projects. From 2013, NDRC decides to delegate the authority of wind projects approval back to the local governments, while retaining its overarching control over wind development planning. The central authority lays out plans for scheduled installation for individual provinces and coordinates transmission line construction [13].

5.2.2.2.4 The Local Governments

In parallel with the central government, the local governments have much control over local wind energy development. They are given the authority to propose annual plans for total local power generation, which will dictate the maximum wind capacity that each local province should take up. Before 2011, the local governments also gained considerable power on wind capacity installation as they enjoyed the authority to approve any wind projects falling

below 50 MW. For the local authorities, wind energy development is not taken as a zero-sum game; there are potentials to boost local employment and economic growth, and increase the local authority's tax revenue. However, some local governments also hold the belief that coal-fired electricity has a higher potential to boost local employment and economy [14]. Whenever there is an oversupply of electricity, local governments often attempt to save coal-fired power generation, at the expense of wind power development, via wind curtailment.

5.2.2.2.5 Grid Companies

Grid companies are tasked with ensuring grid access and priority dispatch of wind power. China's transmission and distribution are dominated by two national grid companies, namely, the National Grid and the Southern Power Grid. These two grid companies are not competitors as they are serving different regions. Local utility companies are subsidiaries of these two national companies, and follow closely the policies laid down by their parent companies. Grid companies make a profit from procuring and selling electricity at state-sanctioned prices. They pay the on-grid tariff for wind electricity at the same rate as their coal counterpart, whereas the difference between the FIT price and on-grid tariff is covered by the renewable fund. The renewable fund is supported by government subsidies and surcharge levied on the consumers.

5.3 WIND ENERGY DEVELOPMENT IN CHINA: BARRIERS AND DRIVERS

The wind energy output in China is less than satisfactory in view of the massive wind capacity installed. This can be witnessed by comparing wind development in China with that of the United States. In 2015, the installed wind energy capacity in China was double that of the United States [3]. However, the wind energy output generated in China was slightly lower than that of the United States, and only 186 TW h of wind energy output was generated in 2015, as compared to 190 TW h generated in the United States. The mismatch in wind energy capacity and output is due partly to the fact that wind resources are intrinsically less abundant in China [15,16]. Other factors beyond scarcity of wind resource have also contributed to the less well-performed wind energy output, including poor grid connectivity and wind curtailment [14,15,17]. In Sections 5.3.1 and 5.3.2, we will highlight the barriers to and drivers of wind energy development in China, and provide an account of the relatively less well-performed wind energy output in China.

5.3.1 Barriers to Wind Energy Development in China

5.3.1.1 Overcapacity in Nonrenewable Power Plants

Overcapacity in electricity generation from nonrenewables has become increasingly evident due to the slowdown in economy in China. The cooling effect on capacity investment is closely linked to its long history of capacity shortage. In the 1980s, after the introduction of the open door policy, electricity demand increased dramatically and most provinces began experiencing severe electricity shortage. Industrial users in China were only allowed to access electricity only on government-planned schedules, depending on how much capacity was generated in total. Such move went against the generally accepted international practice [18]. To spur capacity investment, the central government liberalized electricity supply, allowing provincial governments and private companies to build their own power plants. Preferential pricing was introduced to fix procurement price at a rate that guaranteed revenues. Such measures have produced huge financial incentives for grid companies to invest in generation capacity. Over the last few decades, the growth in electricity supply has gradually been catching up with the growth in electricity demand.

As a result of the recent economic slowdown in China, with growth rate dropping from double digits to single digits, ranging from 6% to 7% over the last few years, electricity demand followed the same pattern. However, capacity investment irrationally grew in spite of the economic trend. Growth in investment capacity outstripped electricity demand. In 2015, electricity demand increased marginally by 0.5% [19], while the total installed capacity increased by more than 10% [20].

Overcapacity implies that wind energy will play an increasingly weaker role in electricity generation. Gansu, a remote inland province in Northwest China, has an installed capacity of 27 GW of wind and solar energy, in addition to the 104 TW h thermal or hydro [21]. Given that its average annual electricity demand is 109 TW h, without cutting thermal power or hydro generation or transmitting the excessive capacity to other provinces, installed wind energy capacity could hardly be put into any meaningful use in Gansu. This is also true for other provinces that display similar electricity supply and demand characteristics.

5.3.1.2 Wind Curtailment

Wind curtailment is a particularly acute challenge to wind energy integration in China. Wind curtailment refers to the situation where the output of wind plants is reduced to a level below its maximum generation capacity. China has experienced curtailment since 2010 and curtailment reached its peak of 17% in 2012 (Fig. 5.2). After a brief remission in 2013 and 2014, the curtailment rate increased in 2015, and is expected to increase further in 2016.

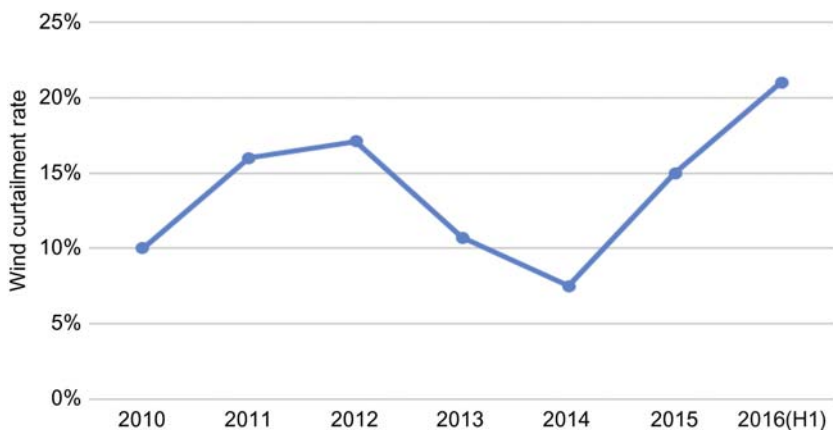


FIGURE 5.2 Wind curtailment rate in China: 2010–16 [15,23].

In some places, curtailment rate reached as much as 39% [3]. The severity of wind curtailment in China is staggering when compared to other RE development leaders such as Germany, which had a curtailment rate of below 1% in 2013 [22].

Wind curtailment should be considered within the context of China's priority dispatch policy. Internationally, procurement of output from generation sources other than wind is not guaranteed. The various generation sources are dispatched based on the structure of competitive wholesale market, such as the United States and Germany; or local policies or regulations, such as China. Under the priority dispatch policy, however, system operators are obliged to dispatch wind output first before they dispatch other sources. In China, the Renewable Energy Law provides that RE such as wind be awarded a dispatch priority, which means that grid companies must procure all power from wind developers at the FIT price.

However, in reality, priority dispatch has not been strictly implemented. Local governments sometimes misinterpret or distort the policy in favor of thermal power generation, which has been taken as a more important means for enhancing economic growth and employment [14]. Local policies that attempt to restrict wind power development include setting the total generation hours for wind power, ordering the wind developers to purchase generation rights from thermal power plants, thereby forcing wind power to compete with thermal power in the newly established electricity market. This situation would not occur in other countries as hefty compensation has to be paid to wind farm owners for every kilowatt hour the operator fails to procure. In China, because no penalty or compensation is required legally in case of any wind procurement failure, the local governments are free to interpret the priority dispatch provision, resulting in a violation of priority dispatch.

5.3.1.3 Poor Grid Connectivity

Poor grid connectivity arises from geographic distribution of wind farms and the centralized development of generation capacity. A key feature of China's wind power is centralized utility-scale generation. Large wind farms are mostly located in the vast inland regions, including North China, the Northeast, and the Northwest ("Three North" regions), where wind resources are abundant. Because of the sheer expansion and sparse distribution of population in these regions, wind energy needs to be transmitted across thousands of miles before consumption. Very often, wind generation within these inland provinces greatly outstrips demand, making it necessary to export excessive energy to coastal or southern provinces, and triggering the need for long-distance transmission.

Transmission planning often lags behind the speed of wind capacity installation. The time spent in obtaining official approval of new transmission lines greatly exceeds that of new wind power development. Construction of new transmission lines has to go through onerous planning, environmental impact, and feasibility assessments before it is assessed by various divisions of the central government [17]. Besides, huge delay may occur due to the lengthy process involved in land acquisition. Long-distance transmission also requires considerable coordination among the local governments, whenever transmission lines have to pass through their own jurisdictions [4]. In comparison, planning for wind projects is relatively easy. The local governments have much say on the installation of new wind capacity and the approval procedures are often simple and easy. The speed of installing wind turbines thus often outpaces that of constructing transmission lines.

5.3.1.4 Lack of a Well-Functioned Ancillary Service Market

Integrating renewables calls for flexible power sources to provide ancillary services. Wind energy outputs are inherently variable and uncertain. Therefore, the power system must be flexible enough to accommodate the rapid change. However, power supply flexibility is low in China. Coal-fired power plants dominate the power generation, accounting for 67% of total electricity supply [24]. Unlike gas power which could ramp up and down quickly, coal-fired power plants are usually designed to serve base load and run at a constant output. Large deviation from the designed output is often seen as ill-advised as it reduces efficiency, increases costs, and lowers equipment lifetime [25]. As such, no coal-fired power plants will be motivated to provide ancillary service for renewables without proper compensation.

China lacks a well-functioned ancillary service market to provide power plants with incentives to balance the grid. In other countries with a large share of coal power, such as Germany, any plant capable of providing ancillary service is eligible to enter the market. At a time when renewable output changes drastically, the price of ancillary service provision would surge to

an extremely high level to compensate for the sudden change. This price signal would encourage investment in flexible power source such as natural gas, and provide the necessary financial incentives for coal-fired power plants to retrofit and increase flexibility. However, in China, such market design is still largely elusive. Very often, coal-fired power plants are required by the government to provide ancillary service free of charge. In some regions where remuneration schemes do exist for ancillary service, the payment is often low and fixed by the government. The incentive for investment in flexibility remains weak.

5.3.1.5 *Lack of Demand Response and Energy Storage*

Demand response (DR) offers a promising solution to increase power system flexibility from the demand side. DR refers to all intentional modifications on consumers' electricity consumption patterns such as altering the duration of use, the level of instantaneous demand, and the total electricity consumption [26]. DR programs enable timely adjustment of consumer demand according to electricity supply conditions, which helps to accommodate intermittency of electricity output and levels out its variation. The DR programs that are most relevant to wind energy integration include direct load control (DLC), interruptible or curtailable load (IL), demand side bidding or buyback program, and emergency DR programs.

China's DR development is in its infancy. China has installed DLC and IL in some coastal provinces only. Because of the lack of electricity wholesale market, DR programs are rolled out under the strong supervision of the government, which would set the amount and price for curtailment. The state-owned grid companies are responsible for implementing the DR programs. However, because the grid companies earn profits from the fixed price difference of electricity procurement and sales, they are reluctant to promote DR as curtailment from DR would reduce their revenues. DR is therefore undervalued as a tool to integrate wind energy to the grid in China.

China also lacks energy storage technologies, particularly thermal storage, that can level wind output variation through absorbing and releasing wind energy from the grid. Such technologies are particularly important given the prevalence of combined heat-and-power (CHP). CHP has been promoted by the government for decades due to its high efficiency in heat and electricity generation. However, most CHP plants are not designed for flexibility; the proportion of electricity output to heat output is fixed. As a result, CHPs could not be ramped down during peak wind output seasons because residents are relying on them for heating. In principle, thermal energy storage could effectively decouple electricity generation from heat production, allowing CHP power plants to vary electricity output without affecting heat supply, thus enabling CHP plants to respond flexibly to variation in wind output. However, such thermal energy storage system is not yet available in China.

5.3.1.6 Differential Priorities Between the Central Government and the Local Governments

The policy objectives of promoting wind energy differ between the central and the local governments. The central government values increasing wind energy share to reduce emissions and enlarge economic benefits. The local governments, however, prioritize on large-scale investment of wind power and wind turbines, partly for local economic development and for extending their personal ambitions. Given that the performance of local officials is tied to local economic growth, large-scale wind energy projects that involve huge financial investment are preferred by the local governments. Wind power investment becomes a desirable option for local governments to strengthen their own political portfolio. Sometimes, the local governments would push for wind investment even when such development has proven to be redundant from environmental or economic perspectives.

The tussle between the central government (mainly NDRC) and the local governments is most evident in the transfer of authority for wind project approval. Before 2011, all wind projects above 50 MW had to obtain the approval from the NDRC. To circumvent the approval procedure, the local governments came up with a strategy of dividing a large wind project to smaller ones for wind projects below 50 MW. A rush to wind power installation by the local governments soon resulted in severe wind curtailment. To control the rush for wind investment, NDRC began asserting its authority over all wind projects from 2011. In 2013, however, under the banner of “streamlining administration and delegating power” proposed by the new administration, project approval authority was re-delegated to local governments. Nevertheless, the NDRC still tries to control wind development pace by issuing an annual wind development plan [13].

The relationship among the local governments is characterized by increasing protectionism. Provinces experiencing electricity overcapacity are not able to export the excessive power to other provinces experiencing power shortages. This is because local governments believe that importing electricity will reduce the local need for new capacity investment, thus hurting local employment and economy [14]. An example is the construction of a long-distance transmission line, which connects the wind power plants in Gansu province to the southern provinces of Hunan, Hubei, and Jiangxi. Government officials from the receiving provinces displayed their reluctance in purchasing wind energy from Gansu. Instead, they continued to approve new generation plants in order to reduce the import of electricity.

5.3.1.7 Vested Interests Between Coal Companies and the Government

Local governments are influenced by their vested interest in coal companies. Local governments have to balance the interests of coal-fired plants, which

dominate generation and contribute immensely to local economy and taxation. Wind energy will impact on coal-fired power plants and the local governments in the following ways:

1. An increase in wind dispatch would crowd out a share of output that would otherwise belong to coal. This is particularly evident in places where large centralized wind capacity is installed. For example, in Gansu province, if its total wind capacity of 12.5 GW operates at its legally guaranteed 1800 hours year⁻¹ [27], the average utilization hours of coal-fired power plants would be reduced by 1406 hours year⁻¹. This would slash the revenue of coal-fired plants by 30% and value-added tax by at least 30%. (The calculation is based on the assumption that the average utilization hour of coal-fired power plants is 5000 hours year⁻¹. The calculation for valued-added tax is based on the formula provided by Ref. [13].)
2. Accommodating wind intermittency increases ancillary service costs borne by coal-fired power plants. Integrating wind energy to the grid requires the provision of ancillary services by coal-fired power plants, such that the thermal power outputs can vary based on variation in wind outputs. In China, many provinces still demand compulsory ancillary service from coal-fired power plants. In the few provinces that do offer compensation for ancillary services, coal-fired generators are required to share the compensation [14]. An increase in wind integration would adversely impact the total revenue of coal-fired power plants.
3. From the perspective of local governments, coal-fired power plants contribute more in terms of employment and economic growth [14].

As a result, in face of an oversupply of electricity, the local governments are either inclined to compromise on the priority dispatch rule or invite the wind power generators to share profits with the coal-fired power plants. These measures have exacerbated the wind curtailment and thwarted the integration of wind energy to the grid. In [Section 5.3.2](#), we will outline the existing drivers of wind energy development in China.

5.3.2 Drivers of Wind Energy Development in China

5.3.2.1 Energy Coordination

Tackling wind curtailment requires coordination among capacity installation, transmission planning, and consumer demand. In particular, transmission must keep up with capacity installation. New wind energy projects should not be undertaken if the output could not be utilized or otherwise matched by demand.

Starting from 2015, China begins improving the coordination of energy sources. The central government tries to control the overheated capacity

installation with an annual development plan [13]. It provides a guideline that decides on the total planned capacity for each province according to wind resource endowment and severity of curtailment. Provincial governments are held responsible for approving individual projects and arranging grid connections and transmission within the province. The NDRC plans the large interregional transmission lines. Plans are under way to shift wind development from the remote regions, the “Three North,” to the south, where wind output could be transmitted and utilized by load within a short distance. Ultrahigh voltage (UHV) transmission lines are scheduled to deliver wind energy from inland regions to the south.

5.3.2.2 Coal-Fired Power Plants’ Retrofit and Energy Storage

China still has to rely on coal power to reduce wind output variation, as coal power still dominates electricity generation and China has very limited flexible energy sources other than natural gas. At present, coal power in China is highly inflexible. Most coal-fired power plants could only ramp down to a minimum level of 60%–70% rated output, while in western countries such as Denmark such level could reach as low as 20% [25]. For the CHP power plants that are dominant in the north, they are often not allowed to ramp down the output, as they are badly needed for heating. Wind energy is therefore frequently curtailed because few coal-fired power plants in China can provide high flexibility in energy output.

Recently, 15 pilot programs addressing coal-fired power plant generation flexibility enhancement were set up in regions with severe wind curtailment [28]. It is expected that through retrofits, the coal-fired power plants could further ramp down by an additional 20% of rated output. Recent regulations also seek to enhance the flexibility of CHP plants with thermal storage. Traditional CHP plants will be complemented with hot water tanks, which serve to decouple electricity output and heat output [29]. Pilot programs on electrical storage have also been launched in the “Three North” region. These pilots will allow electrical storage to be compensated for their ancillary service [30]. Though these programs are still in their infancy and are small scale, they can potentially increase generation flexibility when massively deployed.

5.3.2.3 Smart Demand Response

Smart DR utilizes smart infrastructure and management system to increase demand flexibility. Currently, the Chinese government is aggressively pursuing smart infrastructure deployment. China is committed to roll out new advanced meters with smart functionalities to 90% of all users by 2020 [31]. In 2015 alone, more than 90 million units were installed [32].

Equipped with smart infrastructure, the electricity system presents abundant opportunities for smart DR. Four pilot cities have been chosen for DR programs; these are Beijing, Suzhou, Tangshan, and Foshan [33]. Jiangsu has

already rolled out its first interruptible load program that could respond to contingency events within seconds [34]. China has established an annual demand side management target which requires utilities to achieve an annual saving of at least 0.3% in sales volume and 0.3% in demand [35]. Wind energy integration is set to benefit immensely from these measures.

5.3.2.4 Emerging Ancillary Service Market

China has made some progress in setting up ancillary service markets, though it is less than satisfactory. In 2006 a new regulation by NDRC was implemented to require generators to be compensated for the ancillary service they provide above the legally required level [36]. Before 2006, all ancillary services were provided free of charge. Up till now, nearly all regional grids have established rules on ancillary service compensation. Usually the rules will define an obligatory ancillary service level, above which payment would apply. Some provinces adopted a fixed formula. For example, the southern grid provides that thermal plants could receive RMB 3 (kW h)^{-1} for plants operating at 40%–50% of rated capacity, and RMB 6 (kW h)^{-1} for 30%–40% of rated capacity [37]. Some other provinces went further to allow market pricing. For example, the northeast grid has established that provincial and regional ancillary service markets should adopt the market pricing.

5.3.2.5 Carbon-Trading and Carbon Reduction Target

Carbon trading is an important instrument for internalizing the external costs of air pollution. Zero-emission wind power produces energy that contributes to the efforts to combat climate change. However, plants producing non-RE freely emit at zero cost as the cost associated with emissions is not reflected in its pricing. As a result, wind energy is at a price disadvantage. A fundamental approach to rectify such free-riding behavior is to let the thermal power plants pay for carbon emissions through carbon trading. By setting a legally binding carbon reduction target and assigning permits for each thermal power plant, plants with emissions exceeding their caps must purchase permits from others who meet or exceed the emission target. In this way, wind energy and thermal energy are put on a level playing field where they could compete fairly. Given that traditional regulatory, nonmarket-based command and control policies perform less well in reducing carbon, carbon trading has been increasingly hailed as a possible option on the national policy agenda [38]. Several pilot carbon-trading markets have been established at the subnational level, with different degrees of success. However, there is still no nationwide emission cap and furthermore, current programs merely serve to demonstrate the compatibility of carbon trading with China's carbon control regime [39]. Much commitment by the government is still needed to push the way forward for carbon trading.

5.4 THE FUTURE OF WIND ENERGY DEVELOPMENT IN CHINA

Despite efforts introduced by the government to overcome barriers, several challenges have yet to be fully addressed. Present implemented measures are insufficient in addressing the poor compliance with the priority dispatch measures. In terms of grid connectivity, although the annual development plan delineates the responsibilities of local governments to promote transmission line construction and introduce UHV transmission, transmission approval and construction procedures are still cumbersome. In addition, reform that could address the political tussle between the central and local governments is particularly difficult to carry out. We recognize that such barriers will not be overcome in the short term. Rather, it requires stakeholder engagement and reform over a long period of time. However, we believe that the following technologies and mechanisms reform, if followed through, would greatly improve the integration of renewable to the electricity supply system in the future.

5.4.1 Distributed Generation Deployment and Proactive Transmission Planning

Grid-connection delay and geographic mismatch between generators and loads could be alleviated by distributed generation deployment and proactive transmission planning [15]. Proactive transmission planning has been widely implemented in the United States, and the option of exporting excess output in China could be supported by the UHV lines. Some scholars have shown that proactive construction of large-scale transmission line is more cost efficient than smaller transmission investments on individual projects [40]. Distributed generation can be found in the eastern regions of China, where low-speed wind resources abound and electricity demand is substantial. With the distributed energy system installed near a load center, it could achieve greater energy conservation, lower investment cost, and a flexible operation pattern [41]. The savings in the transmission cost and curtailment loss outweigh the higher energy generation cost under relatively low wind speed [15]. In the future, distributed wind generation is more likely to be integrated with solar generation, establishing the “wind and solar” complementary power generation system [42].

5.4.2 Offshore Wind Power Planning

While the remarkable achievement of the Chinese wind power industry is attributed to onshore wind power, the geographic mismatch of generation and demand places heavy burden on transmission and grid planning. Since there are abundant offshore wind resources along the southeast coastline

where electricity demand is strong, the trend of promoting offshore wind power development is inevitable [43]. Scholars have suggested several approaches to offshore wind power development in China, including: (1) improving independent research and development in wind technologies (e.g., wind turbine manufacture, installation, and construction) through spiral interactive innovation; (2) modifying and upgrading the policy framework, especially the tariff policy and the financial subsidy policy; (3) encouraging the local governments to guide the development through a market-based mechanism; and (4) integrating wind energy to the grid [44]. While China is still at the infancy stage in offshore wind power development, it is predicted that offshore wind power will reach a mature stage before 2020 [45].

5.4.3 Smart Grid

Smart grid will contribute to advance the integration of the renewables through advanced information, communication, and management technologies [46,47]. A typical smart grid system consists of variable energy sources, energy storage, power electronic interface, power control, and power grid load [48]. Based on the metering records of consumers' energy consumption, the trend in wind power penetration in the local grid distribution system could be predicted [49]. On the other hand, electricity generation is presently monitored and controlled remotely via Advanced Metering Infrastructure and Supervisory Control and Data Acquisition. Smart homes, intelligent buildings, and electrical vehicles can also serve as smart grid components. For instance, electric vehicles can be considered as a distributed energy storage unit [48]. The European Union is moving into the field of smart grid proactively, and China is making similar moves. The SGC of China has committed to invest RMB 101 billion in developing smart grid technology during the period 2009–20 [50].

5.4.4 Merit-Order-Based Dispatch

The merit-order-based dispatch tends to give priority to power plants to deliver and dispatch according to marginal generation costs. Because of the close-to-zero marginal cost of wind, a merit-order-based dispatch would favor the purchase of power from wind farms. The conventional energy sources would then compete for the remaining demand not covered by the renewables (hard coal and fuel oil, etc.) In China, the dispatch order was characterized by inefficient dispatch, implying that the grid company would try to distribute equal shares of operating hours to all thermal power plants [51]. Since 2009, an energy-saving and environmentally friendly generation dispatching (ESGD) model, which preestablishes the dispatch order based on pollutant emission, has been carried out in five provinces [52]. However, as an administrative measure, ESGD provides relatively small improvement.

It does not change economic incentives and potentially exacerbates center-provincial tensions [51]. A full market-based ESGD model would require bidding for dispatch, based on the marginal cost which may only be realized in the long-term future.

5.4.5 Pricing Improvement

As the pricing method for onshore wind energy in China, fixed FIT has advantages and disadvantages. The primary benefit of a fixed FIT is that it ensures investment certainty for wind projects, which will yield a price attractive enough for wind energy investment. However, a fixed FIT suffers from several drawbacks: (1) the pricing for wind energy is set by the government, thus carrying the potential of deviation from the lowest cost; (2) improperly priced FIT, together with priority dispatch, would create overheated investment in wind energy, overload transmission capacity, and add enormous burden to consumers. Such issues have begun to emerge in China. Since the establishment of a fixed FIT, the renewable surcharge has been increased from RMB 0.001 (kW h^{-1}) to RMB 0.019 (kW h^{-1}) by 2016. Since surcharge alone would not cover all the costs of FIT subsidies, the central government has to contribute tens of billions of RMB to close the gap.

The current FIT pricing mechanisms should be adjusted according to the status of wind energy development. First, for countries with limited wind penetration, the priority is to attract sufficient level of investment. FIT pricing that ensures investment certainty is preferred. This is evident from the experience of the United Kingdom, which has moved from a quota to a de facto FIT system. Secondly, for countries that have large shares of renewables, cost reduction is a more important consideration than quick deployment. These countries should consider reducing the subsidy and improving wind energy competitiveness using other policy instruments. For example, Germany has taken up a market premium approach from 2012 and is moving toward auctioning to allow more market competition.

Taking into account overcapacity and overheated wind investment, China ought to reform the fixed FIT system. China has experimented with auctioning and abandoned it because the state-owned electricity companies rushed to underbid each other. However, China should at least consider adding a digression factor to the fixed FIT, which would gradually reduce the subsidy for FIT price according to a predetermined rate. This would encourage cost reduction for wind energy production without losing the benefits of investment certainty.

5.5 CONCLUSION

Over the last two decades, China has made remarkable progress in wind energy development. China leads the world in wind capacity installation and

wind turbine manufacturing output. However, such a leading position has not resulted in a correspondingly superior wind energy output. China still suffers from transmission and grid connectivity challenges, alongside curtailment problems. The electricity system is not flexible enough to accommodate wind intermittency. The local and the central governments have different wind development priorities, resulting in irrational investment decisions and ineffective management.

At the moment, integration of wind energy to the grid is a key priority. China has already started to reform its transmission planning, increase system flexibility through retrofitting coal-fired power plants, introduce DR programs, and improve energy storage. To ensure the level playing field for wind and thermal power plants, a legally binding carbon reduction target and carbon-trading initiatives have been established. However, such initiatives have just begun and the road to full implementation is long. In the future, market reform in the electricity market should be continued, alongside merit-order-based dispatch and the development of a well-functioned ancillary market. Fixed FIT pricing system requires further optimization to prevent overheated wind development and to ease the burden on consumers. By addressing these key challenges, a clean, smart, and sustainable electricity system is foreseeable for China.

ACKNOWLEDGMENT

We gratefully acknowledge the editorial assistance of Miss Melody Ma, and the funding support of the Research Grants Council of HKSAR, under Grant No. 17403614.

REFERENCES

- [1] Peidong Z, Yanli Y, Yonghong Z, Lisheng W, Xinrong L. Opportunities and challenges for renewable energy policy in China. *Renew Sust Energy Rev* 2009;13:439–49.
- [2] Ydersbond IM, Korsnes MS. What drives investment in wind energy? A comparative study of China and the European Union. *Energy Res Soc Sci* 2016;12:50–61.
- [3] GWEC. Global wind report: annual market update 2015. GWEC, Brussels; 2016.
- [4] Kahrl F, Williams J, Jianhua D, Junfeng H. Challenges to China's transition to a low carbon electricity system. *Energy Policy*. 2011;39:4032–41.
- [5] McElroy MB, Lu X, Nielsen CP, Wang Y. Potential for wind-generated electricity in China. *Science* 2009;325:1378–80.
- [6] C. C. o. t. C. P. o. China. Notice of CPC Central Committee and the State Council on further deepening reform on the electricity market structure; 2015.
- [7] Lam J, Woo CK, Kahrl F, Yu W. What moves wind energy development in China? Show me the money!. *Appl Energ* 2013;105:423–9.
- [8] NDRC. Guideline on establishing national goal on renewable energy, <http://zfxgk.nea.gov.cn/auto87/201603/20160303_2205.htm>; 2016.
- [9] Shankleman J. China's Goldwind knocks GE from top wind market spot, <<http://www.bloomberg.com/news/articles/2016-02-22/china-s-goldwind-knocks-ge-from-top-spot-in-global-wind-market>>; 2016.

- [10] Liao C, Jochem E, Zhang Y, Farid NR. Wind power development and policies in China. *Renew Energy*. 2010;35:1879–86.
- [11] Dai Y, Xue L. China's policy initiatives for the development of wind energy technology. *Climate Policy* 2015;15:30–57.
- [12] NDRC. Notice on wind power development and management, <http://www.nea.gov.cn/2005-08/10/c_131052907.htm>; 2005.
- [13] NEA. Notice on improving the management of annual wind development; 2015.
- [14] Zhao X, Zhang S, Zou Y, Yao J. To what extent does wind power deployment affect vested interests? A case study of the Northeast China grid. *Energy Policy*. 2013;63:814–22.
- [15] Lu X, McElroy MB, Peng W, Liu S, Nielsen CP, Wang H. Challenges faced by China compared with the US in developing wind power. *Nat Energy* 2016;1:16061.
- [16] Zhou Y, Luckow P, Smith SJ, Clarke L. Evaluation of global onshore wind energy potential and generation costs. *Environ Sci Technol* 2012;46:7857–64.
- [17] Yang M, Patiño-Echeverri D, Yang F. Wind power generation in China: understanding the mismatch between capacity and generation. *Renew Energy*. 2012;41:145–51.
- [18] Kahrl F, Wang X. Integrating renewable energy into power systems in China: a technical primer. Beijing: Regulatory Assistance Project; 2014.
- [19] NEA. NEA publishes total electricity demand in 2015, <http://www.nea.gov.cn/2016-01/15/c_135013789.htm>; 2016.
- [20] NBS. Communiqué on economy and social development in 2015. National Bureau of Statistics, <http://www.stats.gov.cn/tjsj/zxfb/201602/t20160229_1323991.html>; 2016.
- [21] NDRC. Plan on renewable consumption near production site, <<http://www.ndrc.gov.cn/zcfbz/zcfbtz/201604/W020160411375906058336.pdf>>; 2016.
- [22] FNA. Monitoringbericht 2014. Federal Network Agency, <http://www.bundesnetzagentur.de/SharedDocs/Downloads/DE/Allgemeines/Bundesnetzagentur/Publikationen/Berichte/2014/Monitoringbericht_2014_BF.pdf?__blob=publicationFile&v=4>; 2014.
- [23] NEA. Status of on-grid wind [Online], <http://www.nea.gov.cn/n_home/jjg/xnys/fd/index.htm>.
- [24] CEC. Briefing on power industry statistics. China Electricity Council, <<http://www.cec.org.cn/guihuayutongji/gongxufenxi/dianliyunxingjiankuang/>>; 2016.
- [25] Martinot E. Grid integration of renewables in China: learning from the cases of California, Germany, and Denmark, <http://www.martinot.info/Martinot_CVIG_2015_DE-DK-CA.pdf>; 2015.
- [26] Albadi MH, El-Saadany E. Demand response in electricity markets: an overview. In: 2007 IEEE power engineering society general meeting; 2007.
- [27] NDRC. Notice on guaranteed procurement of wind and solar energy, <http://www.sdpc.gov.cn/gzdt/201605/t20160531_806133.html>; 2016.
- [28] NEA. Notice on enhancing accommodation of renewable power in Three-North regions, <http://zfxgk.nea.gov.cn/auto92/201602/t20160216_2202.htm>; 2016.
- [29] NEA. Notice on initiating pilot programs on increasing thermal power flexibility, <http://zfxgk.nea.gov.cn/auto84/201607/t20160704_2272.htm>; 2016.
- [30] NEA. Notice on initiating pilot programs on admission of electrical storage for ancillary service in the “Three North” region, <http://www.gov.cn/xinwen/2016-06/18/content_5083393.htm>; 2016.
- [31] NEA. Action plan on power distribution network construction and transformation for 2015–2020, <http://zfxgk.nea.gov.cn/auto84/201508/t20150831_1958.htm>; 2015.
- [32] Reportlinker. China smart electric meter industry report, 2016–2020; 2016.

- [33] NDRC and MoF. Interim management methods for a new central incentive fund in support of comprehensive demand side management (DSM) pilot cities, N. d. a. r. commission and M. o. Finance; 2012.
- [34] Xinhua. China's first grid-load interaction system goes into operation, <http://news.xinhuanet.com/fortune/2016-06/15/c_1119049318.htm>; 2016.
- [35] NDRC. Interim measures for assessment of grid companies on meeting the demand side management target; 2011.
- [36] SERC. Interim measures for the management of ancillary service by grid-connected power plant; 2006.
- [37] NEA. Notice on management of ancillary service in southern grid; 2015.
- [38] Lo AY. Carbon trading in a socialist market economy: Can China make a difference? *Ecol Econ* 2013;87:72–4.
- [39] Lo AY. Carbon emissions trading in China. *Nat Climate Change* 2012;2:765–6.
- [40] Mills A, Wiser R, Porter K. The cost of transmission for wind energy in the United States: a review of transmission planning studies. *Renew Sust Energy Rev* 2012;16:1–19.
- [41] Dong L, Liang H, Gao Z, Luo X, Ren J. Spatial distribution of China's renewable energy industry: regional features and implications for a harmonious development future. *Renew Sust Energy Rev* 2016;58:1521–31.
- [42] Ming Z, Shaojie O, Hu S, Yujian G, Qiqi Q. Overall review of distributed energy development in China: status quo, barriers and solutions. *Renew Sust Energy Rev* 2015;50:1226–38.
- [43] Feng Y, Lin H, Ho S, Yan Y, Dong J, Fang S, et al. Overview of wind power generation in China: status and development. *Renew Sust Energy Rev* 2015;50:847–58.
- [44] He D-X. Coping with climate change and China's wind energy sustainable development. *Adv Climate Change Res* 2016;7:3–9.
- [45] Zhao X-g, Ren L-z. Focus on the development of offshore wind power in China: Has the golden period come? *Renew Energy* 2015;81:644–57.
- [46] Gao M, Jian L, Li W, Yao X. A stochastic programming based scheduling and dispatch for smart grid with intermittent wind power. *Global J Technol Optim* 2016;vol. 2016:1–8.
- [47] Hossain M, Madlool N, Rahim N, Selvaraj J, Pandey A, Khan AF. Role of smart grid in renewable energy: an overview. *Renew Sust Energy Rev* 2016;60:1168–84.
- [48] Colak I, Full G, Bayhan S, Chondrogiannis S, Demirbas S. Critical aspects of wind energy systems in smart grid applications. *Renew Sust Energy Rev* 2015;52:155–71.
- [49] Keyhani A. Design of smart power grid renewable energy systems. New York, NY: John Wiley & Sons; 2016.
- [50] Giordano V, Gangale F, Fulli G, Jiménez MS, Onyeji I, Colta A, et al. Smart grid projects in Europe: lessons learned and current developments. JRC Reference Reports, Publications Office of the European Union; 2011.
- [51] Kahrl F, Williams JH, Hu J. The political economy of electricity dispatch reform in China. *Energy Policy* 2013;53:361–9.
- [52] Zhong H, Xia Q, Chen Y, Kang C. Energy-saving generation dispatch toward a sustainable electric power industry in China. *Energy Policy* 2015;83:14–25.

Chapter 6

Wind Power in the German System—Research and Development for the Transition Toward a Sustainable Energy Future

Matthias Luther¹, Kurt Rohrig², and Wilhelm Winter³

¹*Friedrich-Alexander-University of Erlangen-Nuremberg, Erlangen, Germany,*

²*Fraunhofer-Institut für Windenergie und Energiesystemtechnik IWES, Kassel, Germany,*

³*Tennet TSO GmbH, Bayreuth, Germany*

Email: matthias.luther@fau.de, kurt.rohrig@iwes.fraunhofer.de, wilhelm.winter@tennet.eu

6.1 INTEGRATION OF RENEWABLES IN GERMANY AND EUROPE

The use of renewable energy sources (RESs) and especially wind energy in Germany is based on both the considerations to achieve long-term independence of primary energy imports and the absolute need to reduce CO₂ emissions to a minimum by 2050 at the latest. The political goals set by the German Federal Government in 2011 are given in Table 6.1. Beside an ambitious reduction of the CO₂ targets, 80% of the electrical consumption is expected to be covered by renewables by 2050. Another important boundary condition for the transition of the German electricity system is the ongoing nuclear power phaseout by 2022.

A possible long-term development of the installed wind and photovoltaic (PV) capacity in Germany by 2050 is described in Ref. [1] and shown in Fig. 6.1. The current installed capacity of renewables meanwhile exceeds the annual peak load of about 80 GW of the German electricity system. Furthermore and due to the regional domination of wind generation in Northern Germany during low load conditions—approximately 35 GW—the regional wind generation is temporarily three to five times higher than the regional load.

TABLE 6.1 Energy Policy Goals in Germany

	Nuclear Energy	CO ₂ Targets (Basis 1990)	Renewable Energy		Reduction of Consumption			
			Gross End Energy	Electricity Generation	Primary Energy	Building Heating	End Energy Traffic	Electricity Consumption
2015	-47%							
2017	-54%							
2019	-60%							
2020		-40%	18%	35%	-20%	-20%	-10%	-10%
2021	-80%							
2022	-100%							
2030		-55%, -40% ^a	30%, 27% ^a	50%	27% ^a			
2040		-70%	45%	65%				
2050		-80%/-95%	60%	80%	-50%	-80%	-40%	-25%

Treibhausgas-Emissionsprojektionen bis zum Jahr 2020 für das BMU und UBA (Öko-Institut, 2011).
^aClimate and energy framework until 2030 by the European Council as of 24 October 2014.

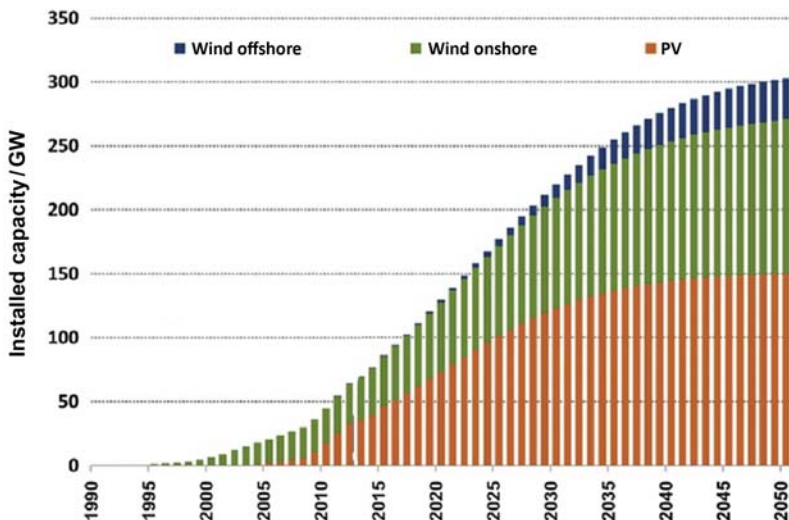


FIGURE 6.1 Prospective development of the wind and PV capacity in Germany until 2050. Trieb F. *Integration erneuerbarer Energiequellen bei hohen Anteilen an der Stromversorgung. Energiewirtschaftliche Tagesfragen*, 63. 2013;7:28–32.

Additionally, the total installed capacity of PVs with a significant higher in-feed in Southern Germany has meanwhile surpassed the installed amount of wind capacity.

During the past three decades, the technological achievements in research and development have made wind energy in Germany a powerful and sustainable building block of the energy industry. From both economic and environmental aspects, the transformation of the energy system to a renewable-based, decentralized energy supply, electricity will take over the central role and will also serve the heat and traffic sectors. From today's perspective, the three key phases of the transformation of the energy system are:

1. In the first completed phase, key technologies—in particular wind turbines (WTs) and PV and key techniques of biomass utilization—have been substantially developed, achieved significant cost reductions, and significantly promoted the launch to the energy markets. Today, over one-third of German electricity production is from renewable sources with 14% from wind energy.
2. The main task for the forthcoming next phase of energy transition is the complete integration of renewable energies. Volatile renewables require further development for their complete integration—both technical and economical—in an increasingly flexible overall system, covering all sectors of consumption: electricity, heat, and transport.
3. The third phase is characterized by a high degree of coverage of the country's total energy needs with renewable energy.

The technology involved in wind energy is the most developed among the renewable energies today. The resources are also seen worldwide more than adequate and they show the lowest electricity generation costs. The weakness of wind energy is the (regional) volatility, which is smoothed by wide-area use [2]. The reason for this is the strong spatial–temporal variability of the wind in Europe; local or regional occurring calms or high wind situations are never or very rarely recorded over long periods or for over large regions. Fig. 6.2 provides the study results for the regional in-feed of an individual wind cluster (“Pixel”) as well as for different geographical regions normalized on the total installed capacity for 2030 [3]. Therefore, energy deficits are often balanced at a certain time in one place by simultaneously occurring energy surpluses at a different location. This positive effect can be used only when the installed capacity covers more than the maximum power consumption in these regions and the energy surplus can be transported over long distances. This however requires the strengthening of existing and the construction of new electric transmission grids across Europe as well as regional grid reinforcements on the distribution level.

Offshore wind power generation provides huge advantages in terms of full-load hours and therefore can be considered as reliable power source. However, the deployed wind farms have to be widely spread over Europe seas and cost lines. Taking into account such a distributed offshore wind generation, wind fluctuations occurring over several timescales and locations can be reduced considering the power in-feed into the power system of Europe. Such a system would introduce reliable and sustainable energy to a highly integrated European energy system.

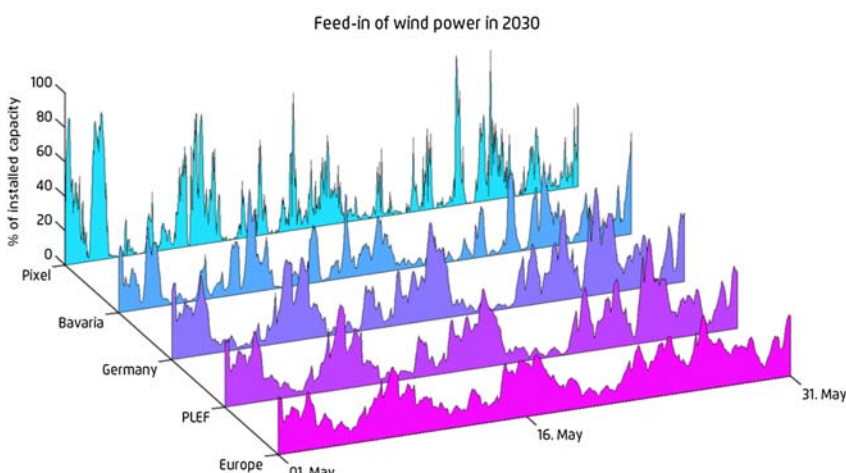


FIGURE 6.2 Fluctuation of wind power production for different spatial aggregation levels. AGORA Energiewende. *The European Power System in 2030: Flexibility Challenges and Integration Benefits*. 2015; 7.

6.2 ONSHORE AND OFFSHORE WIND DEVELOPMENT

Wind energy in Germany is making great strides. The year 2015 saw 63 GW of wind capacity newly installed across the globe—never before has the figure been so high. In 2014, 186.3 TW h, 3.3% of worldwide power consumption was covered by wind energy [3].

In 2015, German wind power plants produced 88 TW h, 53% more energy compared to 2014 (with 57.4 TW h). Wind energy thus represents a contribution of 14.5% of the total power consumption and 45% of the German renewable energy production [3].

In total, wind power plants with a capacity of about 6000 MW were installed in 2015 and put into operation. This leads to 45 000 MW capacity of wind power. The new installed onshore capacity in 2015 reached 3579 MW, so far the second highest figure after the record year of 2014 with 5188 MW. By 2015, offshore wind energy increased as well. At the end of the year 3283 MW (2280 MW installed in 2015) were already connected to the grid and contributed nearly 10% of the total wind power production.

For the first time in Germany, all renewable energies together provide the highest share of gross power consumption—32.6%. Renewables have now overtaken nuclear power plants (2012) and also the previously most important energy source, brown coal.

The development of the largest wind generators between 1985 and 2015 is shown in Fig. 6.3. Since the largest block sizes increased almost by a factor of 100, the corresponding annual energy production per generator was growing by a factor of 150 within the last 30 years.

For the analysis of turbines technology development, WT types are divided into category DD (direct drive), DD-PMSG (direct drive with permanent magnet generator), EESG (gear mechanism with external excitation synchronous generator), PMSG (gear mechanism with permanently excited generator), DFIG (gear mechanism with doubly fed asynchronous generator), IG (gear mechanism with asynchronous generator), CS (fixed speed WT), and others (turbine types with other concepts or inadequate level of detail). The name of a category is based upon the most concise feature of the concept. While previously the turbine market was characterized by fixed speed WTs, variable speed concepts are only being deployed nowadays. At 46%, direct-driven WTs (from the market leader Enercon) are the dominant type (Fig. 6.4). Also strongly represented are gear mechanisms with doubly fed induction generator (28%) and permanent magnet generator (18%).

The trend toward more powerful WTs is continuing—see Fig. 6.5. The 3–4 MW turbine class, with 48%, fell just short of the figure for the 2–3 MW turbine class which has been dominant for 10 years. This class reached a figure of 49% last year, presumably the last time it will experience the largest level of expansion. The 1–2 MW turbine class has for 5 years previously dominated the market. The WT capacity > 5 MW class continues to be limited to the E-126 model from the manufacturer Enercon—which is erected

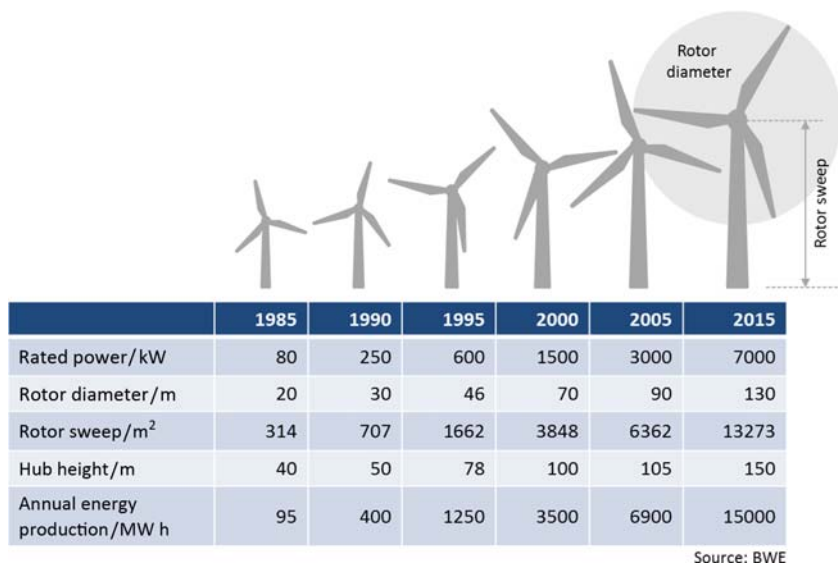


FIGURE 6.3 Development of the largest wind generators from 1985 till 2015.

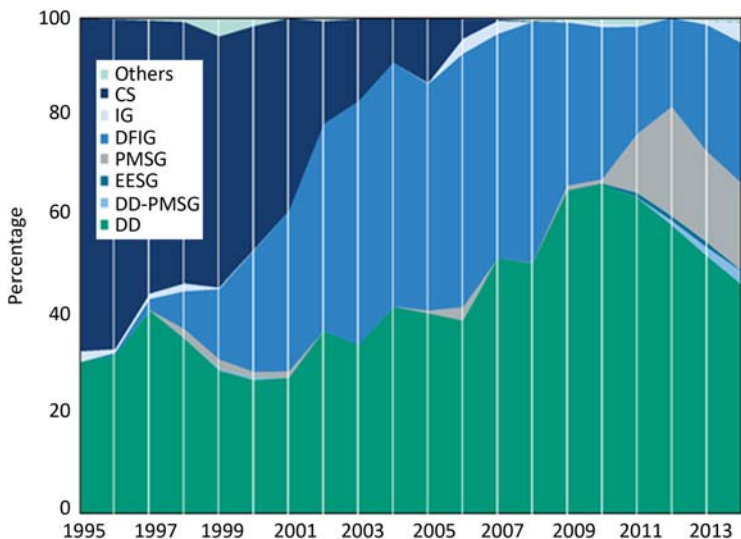


FIGURE 6.4 Development of WT technology. *Fraunhofer IWES. Wind energy report Germany, <www.windmonitor.de>; 2014.*

only occasionally. The average nominal capacity of WTs erected in 2014 was 2.68 MW, with 50% of WTs having a capacity of 2.3–3.1 MW. The total range of nominal capacity installed was between 0.5 and about 7.6 MW (Fig. 6.6).

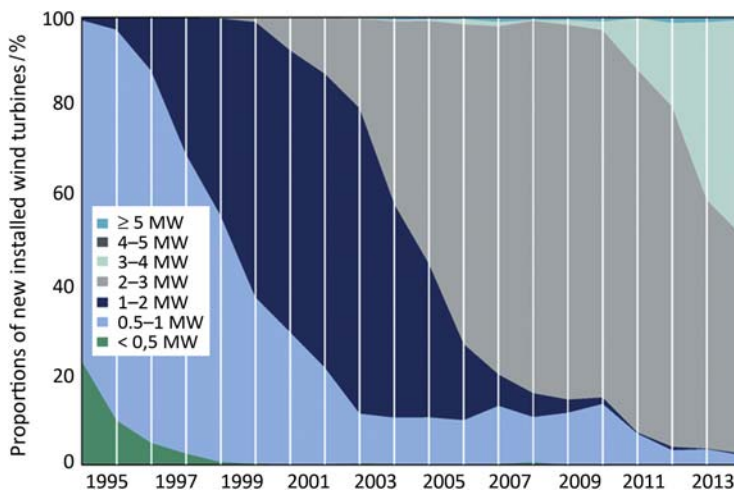


FIGURE 6.5 Development of WT classes. Fraunhofer IWES. Wind energy report Germany, <www.windmonitor.de>; 2014.

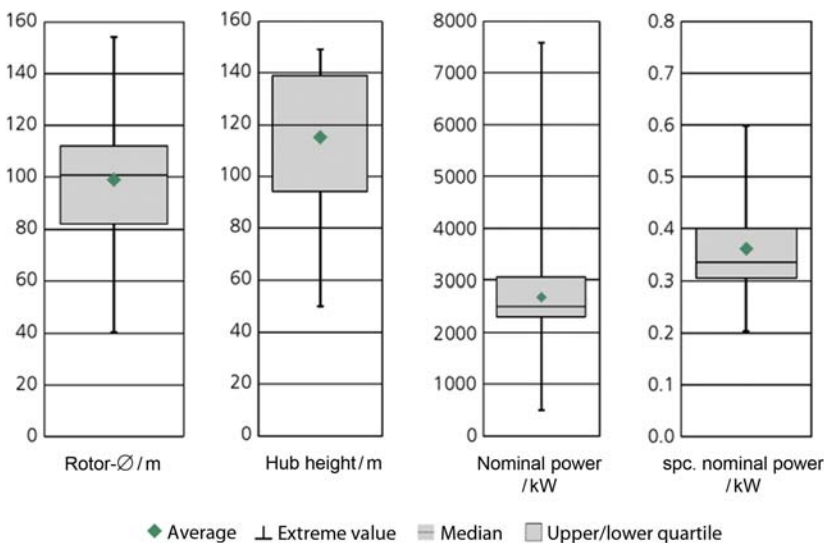


FIGURE 6.6 Turbine types and configurations. Fraunhofer IWES. Wind energy report Germany, <www.windmonitor.de>; 2014.

The last few years have seen a total of 44 different turbine types and configurations with different rotor diameters and hub heights erected in Germany. While the capacity level of turbines, barring a few exceptions, is restricted to an interval between 2.3 and 3.1 MW, adaptation to location-specific conditions takes place by varying rotor diameter and hub height.

Fig. 6.6 shows that the rotor diameters of turbines added in 2014 are in the 40–154 m range, with an average of 99 m. The largest rotor diameters on turbines designed for the onshore market are on the Enercon E-126 and Vestas V126 turbines, with rotor diameters of 127 and 126 m, respectively. Only the Siemens SWT6.0-154 and Senvion 6.2M152 are larger—but these are prototypes for the offshore market erected onshore.

The rotor diameter plays a key role in the capacity and the yield of a WT—this is because the rotor area determines the magnitude of available wind flow and amount of wind energy that can be converted into electrical energy. The variation options in turbine design can be seen very well by comparing the Enercon E-126 (7.6 MW) and Vestas V126 (3.3 MW). The nominal capacity differs by a factor of 2.3 for a virtually identical rotor diameter.

The most important interim goals for renewable energy have been met, but there are still a few challenges to be overcome. These include fluctuating feed-in levels, the concentration of wind energy in the north and PVs in the south, and the overall increasing share of renewable energies providing power require structural adaptation of the entire energy supply system. Furthermore, issues related to grid expansion, increase of storage capacities, flexibility of complementary power plants, the moving and capping of consumption and capacity peaks, and the continued expansion of renewables need to be addressed.

6.3 NETWORK OPERATION AND GRID DEVELOPMENT

The European Energy Supply for Electricity is undergoing fundamental changes. This includes strong moves away from a heavy reliance on fossil fuels as the primary energy source mainly provided by large synchronous generators connected to the transmission systems, toward a decarbonized future supply relying increasingly on variable RESs using nonsynchronous generation predominantly connected to the network via power electronics (PE) and extensively connected and deeply embedded in distribution networks. Some countries in Europe have already experienced times in which at some periods the national demand for electricity has been exceeded by the RES production alone. As this phenomenon continues to extend, the development of Europe-wide markets and system operation will facilitate greater sharing of resources. This new and varied generation mix changes power system characteristics leading to major system technical challenges in normal operation as well as during disturbed or even emergency operation.

Figs. 6.7 and 6.8 provide some operational snapshots for the German transmission system for January and May 2016 extracted from the database of the ENTSO-E Transparency Platform [4]. A comparison of both figures underlines the volatility of wind and PVs due to different weather conditions in different seasons.

Fig. 6.8 underlines the fact that during certain periods of the year the total in-feed of wind and PVs amounts to 85%–90% of the total load. Under

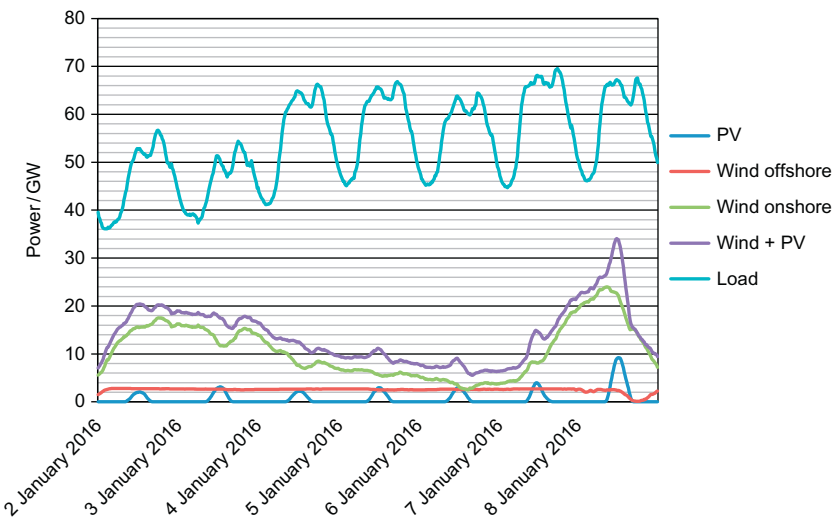


FIGURE 6.7 Wind and PVs in-feed vs network load for the German transmission system in January 2016.

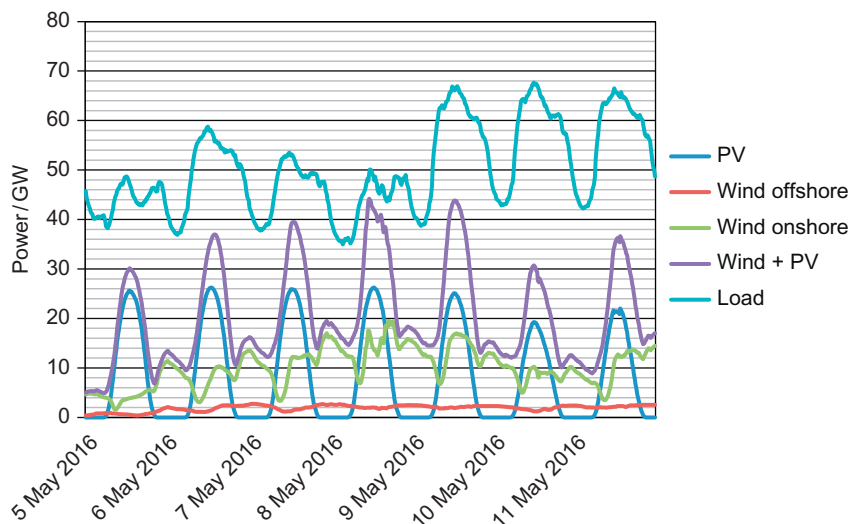


FIGURE 6.8 Wind and PVs in-feed vs network load for the German transmission system in May 2016.

consideration of the different regional distribution of the generation, the vertical network load becomes negative in specific network areas. Since the capacity of the German transmission system is limited in several areas, the daily operational practice by the German transmission system operators

(TSOs) is to perform congestion management mainly by re-dispatching measures for conventional and renewable generators. In 2015 the total cost for congestion management in the German transmission system amount to $\text{€}1.1 \times 10^9$ (1.1 billion Euros), which is nearly four times higher than in 2014 [5]. The dedicated energy volume for re-dispatching and countertrading increased from 5200 GW h in 2014 to 16 000 GW h in 2015.

Earlier investigations about wind integration from the system stability point of view have been analyzed and addressed [6–11]. From earlier experience and from today's system performance, maintaining a stable operation becomes a challenge in the face of an increasingly varied array of both conventional and emerging power systems. These future challenges already require a new framework and all participants of the energy market will have to face significant changes. This requires that traditional practices be reevaluated, new approaches be found, and that there must be much greater levels of cooperation and coordination.

The current network situation and the ongoing integration of renewables requires the development of an extended coordinated transmission system operation and network as well as the setting up of various network codes at European level.

The long-term planning of a transmission system in Germany is mainly based on three pillars:

1. The Grid Development Plan (GDP) 2025
2. The Offshore Grid Development Plan (O-GDP) 2025
3. The ENTSO-E Ten Year Network Development Plan (TYNDP).

The GDP 2025 deals with the expansion requirements of the German onshore transmission network. As stipulated by the German Energy Management Act, the four German TSOs are planning, developing, and building the grid of the future. The GDP is used to show how power generation in Germany can be successfully restructured and renewable energy can be integrated within 10 and 20 years. The corresponding O-GDP 2025 describes the expansion measures required to the offshore grid over the next 10 and 20 years. Both plans are analyzed, supervised, and finally approved of the German regulator (“Bundesnetzagentur”). Further information about the scenario framework, the methodology, and the detailed results from the analysis of the GDP can be taken from Ref. [12].

GDP and O-GDP have proposed several network reinforcements to be implemented by 2025. In addition to the strengthening of the 380 kV AC network, the GDP proposes high-voltage direct current (HVDC) connections in order to tackle the long-distance transmission requirements from north to south and to further strengthen the interconnectors with neighboring countries. Fig. 6.9 provides a scheme of the control areas of the German TSOs (Amprion, TenneT, 50Hertz and TransnetBW) including the interconnected



FIGURE 6.9 Scheme of the GDP and O-GDP approach including the controls areas of the German TSOs.

offshore areas in the North Sea and the Baltic Sea, and a scheme of the planned HVDC links with a capacity of 8–10 GW.

The GDP and O-GDP are an integrated part of the TYNDP prepared commonly by the European TSOs and endorsed by ENTSO-E every 2 years. The TYNDP 2014 describes how ENTSO-E proposes to integrate by 2030 up to 60% of renewable energy, respecting cost-efficiency and security through the planned strengthening of Europe's electricity power grid [13].

Another important cooperation at European level is the North Seas Countries Offshore Grid Initiative (NSCOGI) [14]. Established in 2010 by signing a Memorandum of Understanding between 10 Governments, the initiative has established three intergovernmental working groups on the design of a future grid, market mechanisms, and to support regional cooperation and ways to improve the planning process in the North Sea region.

6.3.1 Innovative Methods to Plan and Operate the Power System

In the future, a growing amount of PE will lead to a transition of the system to a structure with very low synchronous generation [15]. Due to large transit power flows and uncertainties, transmission systems are being operated under increasingly stressful conditions and are close to their stability limits. Together with the integration of large amounts of renewable generation with PE interfaces and addition of HVDC links into the power system, these challenges will necessitate a review of the operation and control of transmission networks.

6.3.1.1 *The Challenge for the Operation of the Transmission Grid in a New Power System Environment*

Tools, currently in use by TSOs for operational planning [16] and system operation, have to evolve in order to work in an environment that is characterized by large-scale integration of RESs with low predictability and limited controllability as well as a system operation close to its stability limits. The inclusion of new control equipment such as phase shifters and HVDC lines, and the development of a European Integrated Electricity Market with huge power flows over large distances, will bring further challenges [17].

6.3.1.2 *Dynamic Line Rating—The Way to Increase OHL Utilization*

The utilization of overhead lines (OHLs) has increased due to the increased transmission of electrical energy in Europe as well as a growing power production from regenerative energy producers [18]. The transmission capacities of OHLs are limited and in many cases there are already bottlenecks which restrict the flow of power.

A method to increase the OHL transmission capacity, depending on ambient weather conditions, will be described in the chapter. A dynamic rating system has been implemented into the operating process of a transmission system. The usability and the effect on the ampacity of OHLs have been verified for 380 kV lines.

Usually worst-case estimations for ambient weather conditions are used for OHL design. In many central European countries, a temperature of 35°C, a wind speed of 0.6 m s^{-1} and full sun radiation are assumed. At ambient conditions which are more favorable than the worst-case scenario, the conductors in a transmission line can carry more current without exceeding clearance limits.

For a flexible AC power system, dynamic line rating [19] is a useful approach in order to provide temporary additional transmission capacity while ensuring $(n - 1)$ security with higher loading of transmission lines. (The $(n - 1)$ criterion is a planning rule for transmission systems. For $(n - 1)$ security, the system must be able to sustain any single outage, including disconnection of any single generator, busbar or transmission element, and remains within performance limits as defined in the System Code concerned.) Good experience has already been gained by dissemination projects in Germany and Slovenia in order to improve reliability and safety of operating networks, especially in cases of increased power flows through existing transmission infrastructure.

6.3.1.3 *Impact of Reduced Inertia on Power System Frequency*

Frequency in a power system must lie within a predefined range, and not deviate too far from the frequency for which it was designed, so that

operational security is not compromised. If the frequency is not held near its nominal value, protection systems begin to active in order to protect machinery, and to keep the power system operational.

Large deviations in frequency are often caused by the tripping of large production units, which result in sudden imbalances in active power. Frequency can then drop by unacceptable amounts, resulting in the disconnection of production units and loads, producing a cascade effect which may lead to widespread power outages. As production units become large and larger, greater imbalances result, with larger possible frequency deviations.

Large synchronous generators help the power system to resist such system frequency deviations. All machines contribute to this resistance with their inertia. However, as renewable generation begins to replace conventional generation, the ability of the system to resist these deviations decreases.

In the near future it is expected that electricity will be produced more and more by wind and solar power plants. Additionally, aging thermal power plants will spend less time connected to the network. Therefore new control concepts such as direct voltage control of electronic power equipment will replace today's current source control mechanisms [20].

In order to control the power systems as efficiently as possible, more real-time information of inertia is needed. This real-time information needs to be sufficiently accurate. Possible countermeasures have been investigated in the Nordic countries such as real-time measurements of power plants by mitigating the impact of future production and consumption on inertia and frequency. However, further research and development work with a broader perspective will be necessary in the development of the project entitled “inertia, control, and protection of large power systems with a large amount of inverter-based components” within the framework of horizon 2020. This project is expected to cover all major issues related to the change in future power systems.

The suite of network codes which has been developed [21] will play a central role in creating the conditions which will allow a competitive, secure, and low carbon energy sector to develop and thrive.

Network codes are sets of rules which apply to one or more part of the electricity sector. The need for these codes was identified during the course of developing the third legislative package and Regulation 714/2009/EC and sets out the areas in which network codes are to be developed and the process for developing them. Based on Framework Guidelines written by the Agency for the Cooperation of Energy Regulators (ACER), ENTSO-E, in close cooperation with stakeholders, they have allocated 12 months in which to draft a network code on a particular subject. These network codes are assessed by ACER to ensure that they are in line with the Framework Guidelines and, once this is the case, they are submitted to the European Commission. Finally the network codes go through the comitology procedure

before becoming fixed in legislation. Network codes are intended to complement existing national rules by tackling cross-border issues in a systematic manner and, by creating a coherent and coordinated framework, represent a practical way of driving forward the adaptations in the energy system. Network codes are being developed in three areas.

6.3.2 The System Operation Network Codes

The purpose of the system operation network codes is to build on the close cooperation which exists today to provide a solid basis for coordinated and secure real-time system operation across Europe. Clearly system operation practices need to be developed in light of the connection requirements established in related network codes. The purpose of the system operation network codes is to define common pan-European operational standards for the existing and a future European electricity system, particularly as the penetration of renewable energy generation increases. The system operation network codes define the general operational criteria and procedures to be applied in and across all of Europe's synchronous areas. At the highest level, the system operation network codes aim to ensure security of supply and support for the efficient functioning of electricity markets.

FACTS (SVC, STATCOM, and TCSC among others) are PE-based technologies that are being installed on the power system for reactive power compensation and power flow control. It is worth noting that some of them (e.g., SVC and TCSC) have been installed with other objectives such as power oscillation damping. The reactive power regulation capability allows them to participate in ancillary services with the provision of being an active part of the system. In a system based on PE, it is important to determine their interaction with all the other devices and their impact on system stability.

Currently, energy storage is used for power balancing (mainly hydro) and in some cases for fast frequency response (as in the case of fly-wheel technologies). However, among those main time frames, there exists a gap that currently is filled by thermal or gas power plants. In a 100% RES-based power system, this gap must be provided by other generation (renewable) or by energy storage systems. Potential energy storage devices for providing ancillary services to the power system at different timescales must be researched and analyzed. Moreover, since energy storage systems tend to be integrated to the grid with a power converter, these systems may also provide reactive power regulation.

6.3.3 The Market-Related Network Codes

The market-related network codes, which cover the different time frames in which capacity is allocated and the balancing time frame (when the TSO is the only party active in the market), as well as rules for calculating cross-border

capacity in a coordinated manner and defining bidding zones, aim to introduce a standard set of market rules across Europe and promote the implementation of a competitive pan-European market (building on the very significant progress made by regional market integration projects). The aim is to create a relatively simple set of market rules which can promote effective competition, to minimize risks for all parties (particularly renewable generators who will benefit from markets close to real time) and to give incentives for market players to act in a way which is supportive to the efficient operation of the system and minimize costs.

6.3.4 The Connection-Related Network Codes

Investment decisions taken now will affect the power system for the next decades. The European energy system of 2020 is being built today and the foundations of the European energy system of 2050 are being conceived. As such, there is a need to make sure that all users are aware of the capabilities which their facilities will be required to provide—recognizing both the need for all parties to make a contribution to security of supply and the high cost of imposing requirements retrospectively. The grid connection codes therefore seek to set proportionate connection requirements for all parties connecting to transmission networks (including generators, demand customers, and HVDC connections). A stable set of connection rules also provides a framework within which operational and market rules can be developed.

One of main principles in the development of the Network Codes for Grid Connections (NCs RfG, DCC, and NC HVDC) is the goal of a consistent set of connection requirements for new generators, demand, and DC links, which take into account local system needs and inherent technical capabilities. Whereas this code details requirements for capabilities, it does not provide answers to operational or market-related issues. These rules can be found within the operational/market network codes, notably NCs Operational Security, Load Frequency Control and Reserves, Electricity Balancing and Emergency and Restoration, or appropriate national rules. It is also emphasized that whereas operational and market codes often reflect present needs, connection codes need to ensure future operational/market rules can be facilitated as well. The Network Code for “HVDC Connections and DC connected Power Park Modules” (NC HVDC) [22,23] contributes to a clear and nondiscriminatory way to connect large-scale RES, by means of HVDC links, to the European electricity grid, in order to sustain a reliable, efficient, sound, and secure transmission system that can make use of the technical opportunities of HVDC technology. The NC HVDC contains significant new requirements for some regions based on best practice in industry. Technical specifications are required to meet certain performance criteria necessary for this role in order to make the technologies capable of todays and future system needs.

HVDC is the preferred transmission technology for long distances and for connection of nonsynchronous systems. Several HVDC transmission systems have been developed worldwide mainly using line commutated converter technology (LCC-HVDC). Recent developments on voltage source converter technology (VSC-HVDC) may allow the power converters to provide additional services to the AC power systems where they are connected, including black-start capability (the process of restoring a power station to operation without relying on external electricity power), reactive power support, simple power reversal, and flexible operation. VSC-HVDC technology is the backbone technology for the development of a European Supergrid [24], to interconnect offshore power plants with different terrestrial systems. In addition, maintaining stable operation becomes a challenge in the face of an increasingly varied array of both conventional and emerging power system stability aspects. A major new challenge is coping with extremely weak power systems for some hours (during high RES production) followed a few hours later (during low RES production) with operation of a strong power system again supported by large centrally connected synchronous generators. Therefore, requirements for the new and varied generation mix are necessary to ensure that the power system characteristics can cope with the major system technical challenges in normal operation as well as during disturbed or even emergency operation. Demand connection code requires the capabilities for distribution systems and demand facilities in order to minimize deviations, for example, of frequency from its nominal value due to generation/load imbalances. In order to increase power system flexibility, demand side must be capable of providing flexibility. This flexibility may allow the system to maintain stability and operate in a more secure way. Demand flexibility may provide an additional way to ensure power balance by regulating the loads and consumptions as well as provide ancillary services (ASs). In order to provide these potential services, TSO–DSO interaction is needed. Demand-side response regardless of scale or connection voltage can contribute to correcting generation/load demand imbalance. Demand offered for demand-side management has already been selected by the demand facility owner and therefore is available for changes in demand. Adjustment of this demand in emergency situations for low-frequency demand disconnection (LFDD) and low-voltage demand disconnection (LVDD) purposes in advance of disconnection of other load demand is the most efficient, lowest consumer impact response in these circumstances.

6.4 FURTHER RESEARCH AND DEVELOPMENT FOR WIND POWER INTEGRATION

The necessary innovations concerning technology, infrastructure, and markets for the transformation of the power system can be reached only by

common and coordinated research and development [25]. The most important objectives for wind energy integration research are:

- Improve wind power forecasts by wide-area aggregation, probabilistic forecasts, and data assimilation with wind farm data.
- Enhance wind power plant capabilities to enable higher wind power penetration levels while maintaining adequate security of supply and power quality.
- Support grid planning and expansion by development of knowledge and tools suitable for high levels of wind power generation.
- Research tools, market rules, and power system regulations that promote cost-efficient operation and investments in power systems with major contributions from variable generation.
- Develop robust and stable control algorithms for PE devices in PE-dominated power systems.
- Analyze system needs for the integration of offshore grids for the onshore and offshore transmission system, respectively.
- Interoperability and analysis of interactions between HVDC systems and other connections.
- How to operate meshed offshore grids connected to all synchronous areas in Europe.
- Appropriate operational measures in order to cope with given uncertainties (market, renewables), optimization by using HVDC and FACTS, dynamic risk assessment.
- RES integration and coordinated approach in transmission and distributed systems.

6.4.1 New Control Concepts for PE-Dominated Power Systems

The rapid increase of renewable energy-based power generation and the ongoing implementation of smart grid concepts including the installation of new VSC-based HVDC systems is changing the dynamic characteristics of the entire power system in significant ways. For instance, when connecting offshore wind farms via HVDC links, new network constraints (e.g., the presence of harmonics under steady-state conditions) result in the adjustment of the protection schemes of cables. Moreover, with the increased penetration of renewables and HVDC links, one might rapidly reach, during some specific intraday periods, 100% penetration of PE, thus resulting in no mechanical inertia in the network (significant PE penetration already occasionally occurs in specific areas in continental Europe, e.g., Iberian Peninsula or Germany). Finally, following a major incident, the network (a control zone) could be partitioned into several areas, some of them with no synchronous machines. Such high penetration levels of PE result in four main categories of problems already encountered:

1. Modified dynamic behavior of the power system
2. Altered power quality

3. Interactions between the controllers of PE
4. Weaknesses of the existing protection schemes.

TSOs are faced with the task of finding appropriate solutions for the dynamic problems brought about by these changes. The European codes for grid connection define the necessary performance requirements with the cross-border implications of these changes in characteristics in mind. The HVDC connections, for example, should not lead to the degradation of existing levels of system reliability. For national level implementations, more detailed concepts have to be developed.

New hierarchical control concepts for integrating the advanced features of VSC-HVDC for voltage and reactive power control of the AC network must be developed and analyzed. This is based on the analysis of the fundamental control requirements in steady-state and under contingency situations. Fault ride-through capability and fast reactive power injection to support network voltage belong to the category of dynamic requirements, whereas steady-state operational requirements such as set point tracking involve slow changes. PE devices are usually operated as current source equivalent. The analysis of the today's voltage control approaches for PE devices shows that the current control concept in which the voltage control is performed via reactive current injection is not well suited for islanding operation or in case of PE-dominated power systems. However direct voltage control as already used for synchronous machines shift the characteristic of PE devices back to voltage source operation and is able to support in combination voltage and frequency stability issues.

6.4.2 Wind Power Forecasts

Wind power plants will be sited more and more across broader and new geographic areas, increasing the wind power forecasting challenge; new spatially joint models and forecast types are needed to accommodate the larger European level scale, including offshore and addressing least modeled effects such as sea-land breezes. Second, high penetration means that variable and uncertain wind power and other renewable sources will dominate markets and control rooms. Therefore, new probabilistic forecast types need to be designed for the necessary market and power system operator requirements. Real-life forecasting with these new algorithms will require more data than has been collected before, often at higher spatial and time resolution and lower latencies. Defining what data is needed for these algorithms is also needed.

The short- to medium-term wind power forecasting, using numerical weather forecasts combined with statistical (artificial intelligence) or physical methods, has experienced enormous progress in the last few years and are an integral part of today's energy supply [26].

The basis for a good wind power forecast is a reliable Numerical Weather Prediction (NWP) model. Unfortunately, the current NWP models do not satisfactorily fulfill the need in wind power forecast as wind speed prediction at WT hub height was not a primary aim of these models. Within the framework of the German project EWeLiNE [27–29], the aim of the NWP model of the German Weather Service COSMO-DE was to develop the needs of the renewable energy industry, namely wind power and PVs.

To improve a weather model, different strategies are possible: the parameterization of the model with respect to wind can be optimized by calibration of the model with wind measurements or the assimilation of measurements of wind speed and direction into the model.

All approaches have the same problem: wind speed measurements at hub height are required. In case of the assimilation, a new way is proposed in the project to directly include nacelle anemometer and wind power measurements from wind farms in the NWP-model assimilation procedure.

As wind power measurements are often more easily available as data from nacelle anemometers, the approach presented here includes in the first step, wind power measurements assimilated into the COSMO-DE model used by the German weather service.

The concept of integration of wind power forecasting into the NWP model, the construction of the forward operator with a new approach of fitting the power curve of a complete wind farm and the first results from the forecast of the NWP model are presented in Refs. [27–29].

Accurate forecasting of expected wind capacities is required in order to achieve improved integration of wind energy into transmission grids. Extreme values of wind power generation have strong impact on electricity prices (Fig. 6.10).

Precise wind power forecasts can reduce extreme price variations. Fig. 6.11 shows the graph of the error in the day-ahead forecast over recent years, based upon the disclosure obligations of TSOs for forecasted and projected current feed-in levels of wind energy (according to §17 Section 1 StromNZV (German Federal Ministry of Justice and Consumer Protection: Verordnung über den Zugang zu Elektrizitätsversorgungsnetzen (Stromnetzzugangsverordnung—StromNZV))). For Germany, the average root mean square error (RMSE) in relation to the average turbine capacity installed was 2.89% in 2014. The maximum positive discrepancy was 14.2%, and its negative equivalent –21.3%.

A decreasing tendency has been evident for the RMSE since 2010. The graph for the smallest German TSO, TransnetBW, represents an exception to this trend. The potential compensation effects mean the lower the forecast error is, the bigger the transmission grid is and the more WTs are installed in it (see Fig. 6.11). In addition to the higher forecast quality for TenneT and 50Hertz compared to Amprion and TransnetBW, it is reflected most of all in the comparison with the overall German error value. The small transmission grid and the low installed capacity consequently mean a far higher inherent susceptibility to errors at TransnetBW.

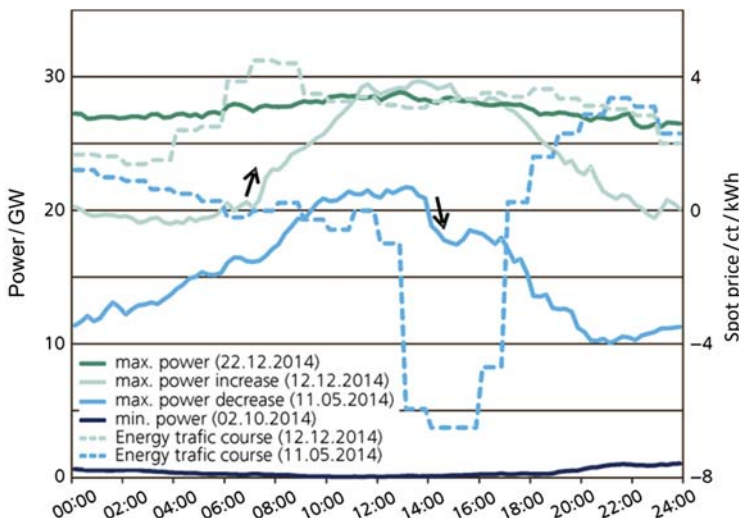


FIGURE 6.10 Extreme values of wind power and electricity prices. *Fraunhofer IWES. Wind energy report Germany, <www.windmonitor.de>; 2014.*

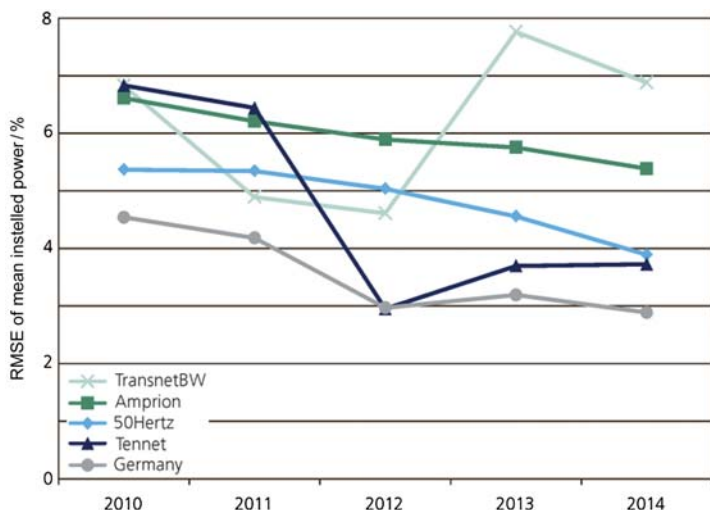


FIGURE 6.11 Development of wind forecast errors in Germany. *Fraunhofer IWES. Wind energy report Germany, <www.windmonitor.de>; 2014.*

6.4.3 Wind Farm Clusters

Wind power already has proven capabilities of providing ASs, as it complies with an increasingly demanding set of grid code requirements. However, most of the times, providing those services implies costs, related to the lost energy, since it is required to operate in a down-regulated mode. Future

research and development needs to demonstrate the participation of a wind power plant in a market for short-term reserves, and verify methods to understand how much the power from a wind power plant needs to be de-rated to guarantee a given firm reserve capacity for a given time horizon and with a given statistical significance.

For the provision of such services from wind power, a coordinated management of distributed wind farms aggregated to clusters will improve their capabilities in terms of system support. In such a system, controllability of nearly all components of the electrical equipment plays an important role in the operation of the power system. On one hand, this controllability gives the necessary flexibility to react on system responses over several timescales and events, but on the other hand, it introduces high complexity to the system and dedicated operation would be a hard task.

Aggregating distributed large wind farms to a cluster and controlling the cluster members is realized by the so-called wind cluster management system (WCMS). The system is able to allocate set points for distributed wind farms. While integrated in the control room of the system operator as well as in the energy management system (EMS), different control objectives can be achieved by means of the coordinated management of the cluster [30]. Possible beneficial operational aims are loss minimization, distinct reactive power exchange, reserve allocation, active power re-dispatch for higher voltage levels, fulfilling active power schedules, minimizing control actions of other devices like tap-changers, and the fulfillment of $(n - 1)$ security criterion. The structure of the system is shown in Fig. 6.12.

As shown in Fig. 6.12, the system contains forecast information of the wind farm clusters or neighboring clusters in the system as well, in order to achieve good coordination. The wind forecast itself requires the SCADA data of the wind farms. Also, in order to identify the condition of the power system, the WCMS has a connection to the state estimator of the control room and therefore is able to access measurement values that are received with the state estimators cycle time. The system borders to higher and lower voltage levels as well as neighboring systems areas can be sufficiently represented by electrical network equivalents.

The basic functions can be realized by adjusting the active power, or reactive power set points of the wind farm controllers within the cluster. Fig. 6.13 indicates the correction of an exemplary voltage violation during power system operation.

Based on the network equation as indicated in Fig. 6.13, a detected violation of the predefined voltage band is corrected by adjusting the reactive power set point of the cluster. The detection of violations takes place either within the limit check routine or the security assessment in the EMS of the control center, in which different outage scenarios are simulated and evaluated.

In a similar way, overloaded lines or other equipment-like transformers can be handled. In general, if the system operator can detect a congested line section

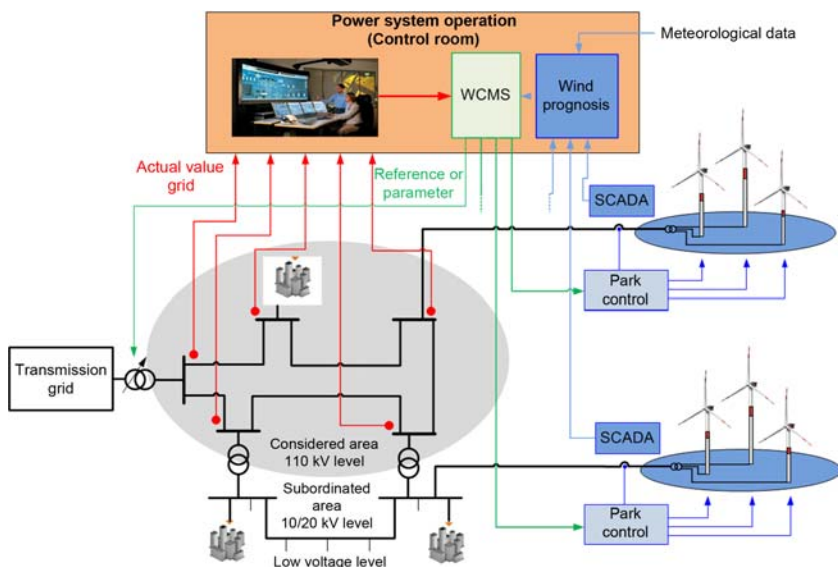


FIGURE 6.12 Wind cluster management system. Stock S, Faiella L, Rohrig K, Hofmann L, Knorr K. *Improving Grid Integration of Wind Energy Power Plants*. DEWEK, Bremen, 2012.

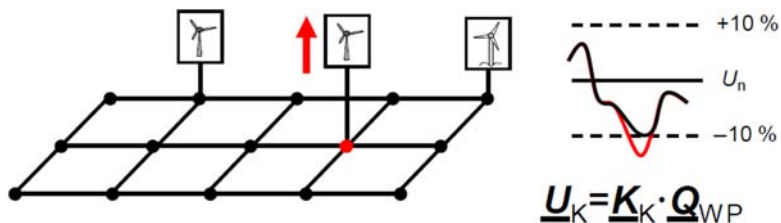


FIGURE 6.13 Correction of voltage violations. Hennig T, Loewer L, Faiella LM, Stock S, Jansen M, Hofmann L, Rohrig K. *Ancillary Services Analysis of an Offshore Wind Farm Cluster - Technical Integration Steps of a Simulation Tool*. EERA DeepWind' 2014, 11th Deep Sea Offshore Wind R&D Conference, Trondheim, 2014.

within the limit check or the security assessment of the EMS, the system operator can perform re-dispatches as corrective or preventive measures. The active power set points of already dispatched (according to the market condition) conventional power plants are adapted in such a way as to de-load the congested line. In principle, the set point of one plant in front of the congested line is lowered, while the active power mismatch of the system is tracked back by another power plant raising its active power production at the end of the line segment. If distributed wind farms are aggregated to clusters, sufficient amount of active power can be controlled. In such a way, the WCMS can also provide the re-dispatch functionality. Fig. 6.14 shows the re-dispatch principle.

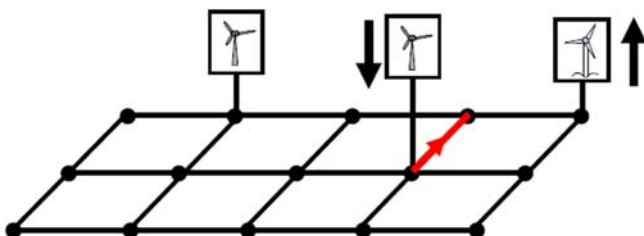


FIGURE 6.14 Correction of network congestions. Hennig T, Loewer L, Faiella LM, Stock S, Jansen M, Hofmann L, Rohrig K. Ancillary Services Analysis of an Offshore Wind Farm Cluster - Technical Integration Steps of a Simulation Tool. EERA DeepWind' 2014, 11th Deep Sea Offshore Wind R&D Conference, Trondheim, 2014.

Similar to the reactive power correction measures, the active power re-dispatch is performed using the network equations by transforming bus and branch variables during the sensitivity analysis. Both methods are based on the power flow formulation of the system.

6.4.4 Virtual Power Plants

For the further transformation of the electricity sector and for an adapted energy supply system, in addition to the network expansion and reinforcement, measures and solutions are needed to reduce the short-term, regional fluctuations of wind power feed-in. Here, storage technologies, the interaction of various RESs, and load management, even including the transport sector, are needed.

The coordination of different components of the electricity system is performed by the aggregation and processing of operational data from all units and their superior control by an EMS. These so-called virtual power plants (VPPs) offer new opportunities for demand-driven energy supply and to improve the flexibility of the consumer. But it is not only required to meet the energy needs at any time, but also to support the reliable operation of the energy system. The energy industry calls this capability of RES a power plant property.

The term power plant property for renewable energy systems indicates that the generation can be planned, controlled, and reliable, as required from the power system needs and that the renewable power plants must support the electric grid even when faults occur. These capabilities are based on the control of active and reactive power of the units [33] as well as the behavior during grid faults like the fault ride-through behavior. These measures to maintain grid stability are referred to as system services or ASs.

Since in the future, often situations will arise where at high wind or PV feed-in periods only a few or no conventional power plants in operation, it is imperative that RESs need to provide the ASs, to ensure security of supply.

It has been shown that modern plants for generating renewable electricity are able to provide ASs. The fact that these options do not or are rarely used is mainly due to three obstacles:

1. The fact that RES can provide AS is, even in the group of experts, not generally or only superficially known.
2. To allow the provision of AS by RES, partly extensive changes to the legal and economic conditions are necessary (e.g., prequalification rules, tendering periods, and technical requirements).
3. To make AS provision reliable, the various producers need to be linked and coordinated by appropriate control systems.

Research and development in the field of energy supply with high share of RES will have to deal with these topics. It is mandatory to develop concepts and mechanisms and create legal foundations which allow the necessary measures to maintain security of supply by ASs, secured by VPPs.

The main services, which may be provided by RES VPP, include in addition to the control power supply (frequency stability, secondary reserve power, and minute reserve) the reactive power (voltage support) and the network congestion management. Other services as the black-start capability are indeed important, but not the focus of current research and development challenges.

6.4.5 Sector Coupling Concepts

The coupling of the sectors electricity, heating, and transport is the key component in the successful transformation of the energy system. The sector coupling thereby effects two significant changes in the system:

1. The heat supply and the traffic can be powered by the electricity sector with renewable energy and so substitute the use of fossil fuels.
2. The coupling of the sectors leads to new, controllable loads in the electricity sector, and so causes an increased flexibility of the overall system.

The further development of renewable energy in the medium term leads to situations with serious surpluses and deficits in the power sector. In the electricity industry, the temporal course of the surpluses and deficits in the power sector is known as the residual load. The greater the fluctuations of the residual load in a region, the more electrical energy needs to be exchanged with the upper level (transmission system) or the neighboring region. Today, PV systems require derating at lunchtime and wind farms are curtailed in order to avoid network congestion. This wasted energy can be ideally used for the operation of heat pumps and the loading of e-cars. Prerequisite for a meaningful coupling is a predictive mode for heat pumps and an intelligent charging management with electric vehicles. Concerted, coordinated management of consumers in the sectors can largely be done with electricity price signals. For

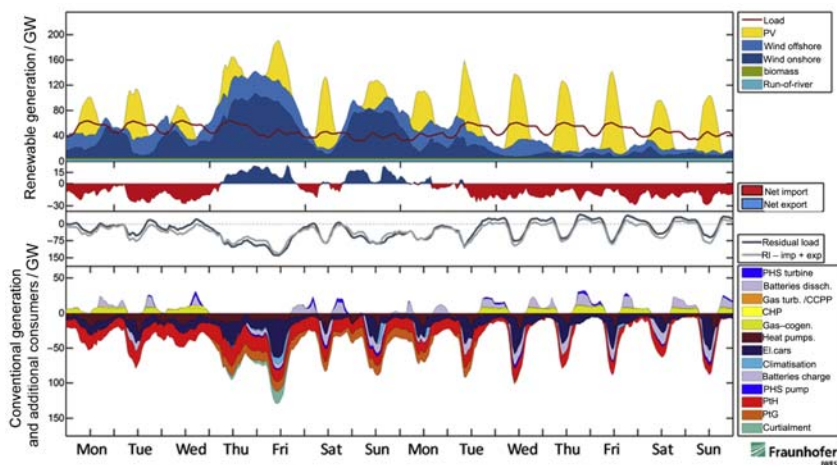


FIGURE 6.15 Energy production and demand in Germany 2050. http://www.energiesystemtechnik.iwes.fraunhofer.de/content/dam/iwes-neu/energiesystemtechnik/de/Dokumente/Veroeffentlichungen/2015/Interaktion_EEStrom_Waerme_Verkehr_Endbericht.pdf.

this purpose it is also necessary that the forecasts for wind and PV power are used in all sectors for energy management.

Fig. 6.15 shows the supply of RES in 2050 in Germany and the associated courses of traditional and new consumers. Behind this view is a scenario for Germany, that assumes an 83% reduction in greenhouse gases [34]. The electricity demand in this scenario is growing to 793 (TW h) a^{-1} , including heat pumps, e-cars, and OHL trucks. The consumption of e-cars is 110 TW h, including 45 TW h for OHL trucks. The maximum load is about 50 GW. The installed capacity for batteries is 15 and 12 GW for power-to-gas. The needed capacity for this scenario is 200 GW PV, 140 GW wind onshore, and 38 GW wind offshore.

In the load graph in the upper half of the picture, all producers and consumers are included that are not separately pictured in the lower half. The lower half shows mainly consumers, already existing today and expected to exist in future, taking some efficiency measures into account. The graphic represents the weeks 15 and 16 of the year.

6.4.6 European Wind Integration Projects and Studies

By 2020, the EU plans to produce 20% of its electricity from wind, with a much larger percentage beyond that. A few countries already have high wind penetration, but they have been able to do this largely by using conventional reserve power from neighbors with less ambitious renewable energy goals. However, in the future, it will no longer be possible to consider individual

wind power plants in isolation. In order to efficiently provide services delivered by conventional generators, it is necessary to consider large clusters of wind farms—both onshore and offshore as well as in different countries—as a single power plant. Conventional generation across Europe will be scarce or expensive, and the grid integration problem will become qualitatively different. The biggest challenge is that the controllability currently provided by conventional generation will come from large numbers of variable wind power plants, coordinated across great geographic, political, and electrical distances. Such coordination will require new tools, data, and procedures—the subject of several European studies and projects. There are already two major initiatives on the road toward the future pan-European power system:

1. The project *TWENTIES* demonstrates how new solutions can be used to support wind power integration. The project is dealing with pan-European impact and large-scale demonstrations (six demonstrated solutions with analyzed effects). One of three task focuses is on ASs with a total focus on grid impact of existing technology.
2. The *European Energy Program for Recovery* will support the offshore grid development subarea, i.e., projects in the “grid connection and power transmission.”

Furthermore, a couple of projects, studies, and other activities have worked out important solutions to foster wind energy integration in Europe:

- The main result of *IEA Task XXV* is a state-of-the-art report which is mainly a summary of national projects and experiences. The goal was to analyze and further develop the methodology to assess the impact of wind on power systems.
- The object of the *TRADEWIND* project was to assess the impacts of wind power in the European power systems. A new model was developed to analyze scenarios of up to 300 GW wind power in Europe. A trans-European power market and grid expansion will allow higher penetrations.
- The *EWIS* project emphasized that the integration of wind power is only realizable by joint activities and cooperation at European level. Therefore coordinated measures to reinforce the European grid as provided in EWIS are necessary. Apart from that, legal and market aspects have to be considered to maintain system security. Wind power control affords small wind integration costs compared to benefits.
- The *WindGrid* project attends to wind grid management, especially wind farm cluster systems and grid operation. The capabilities of wind farms were demonstrated by three zones with (1) high penetration, (2) low penetration, and (3) large power system with low wind energy penetration. The main goals are minimizing dispatching costs and modeling interconnected power systems to integrate large-scale wind farms into the network.

- The *PEGASE* project points out a pan-European network as a stochastic model operation including observation, planning, simulation, and improved security. It contains an interchange of information about large size networks. The study does not consider the capabilities of wind farms.
- The project *SAVEWIND* is a continuation of the ANEMOS and ANEMOS + projects. The aim of *SAFEWIND* is to substantially improve wind power predictability in challenging or extreme situations.
- The *EERA-DTOC* project combines expertise to develop a multidisciplinary integrated software tool for an optimized design of offshore wind farms and clusters of wind farms.
- The *e-highway 2050* project developed a top-down planning methodology to provide a first version of a modular and robust expansion of the Pan-European Electricity Network from 2020 to 2050, in line with the pillars of European energy policy.
- The *NSON* project will analyze and evaluate different market and network connection alternatives of Northern Seas regard to their impact on the German as well as the overarching European energy supply system. Use of energy-related simulations, novel mathematical optimization models, methods, and analysis of the European energy system are examined to demonstrate the feasibility and the energy-economic implications of different concepts.
- The *IRPWIND* project proposes a roadmap for coordinated steps to the transformation of the energy supply system. Besides the sustainable and well-coordinated grid extension and expansion on European level, the operation of the future supply system needs to be supported by precise and high-performance forecasts. This also requires a coordinated data and information exchange on European level, with high data security and reliability as well as fast accessibility. In the frame of *IRPWIND*, this proposal includes improving the prediction of wind power feed-in as the focus of activities for the integration of RES.
- In the framework of the Energy Concept 2050 by the German Government the large-scale federal research initiative, Kopernikus was launched in September 2016 by the Federal Ministry of Education and Research [35] with the aim to investigate and develop innovative technological and economical solutions for the transformation of the energy system. Within a period of 10 years, more than 230 partners from science, industry, and NGOs will work on the four research topics *new grid structure, storage of renewable energy, redesign of industrial processes, and system integration*. The results of the first phase are expected to be available by the end of 2019.

6.5 SUMMARY

Since the turn of the millennium, the energy supply in Germany is undergoing a challenging transformation. The shortages of conventional resources as well as the limitation of CO₂-emission account for new, sustainable, and affordable

energy concepts. Currently, the changes in electrical energy systems (power plant grid storage usage) are at the center of the transition process.

During the last three decades, wind energy has developed into one of the fundamental pillars of the electricity market. The current annual peak load and low load of the German electricity system amounts to 80 and 35 GW, respectively. At the end of 2015, the installed wind capacity in Germany amounts to 45 GW including 3500 GW of offshore installations. Additionally, the installed solar capacity from PVs is 45 GW. Long-term forecasts anticipate tremendous growing rates for both renewable resources up to 300 GW by 2050.

The transition of the electricity system from the integrated and thermal-based generation to volatile RESs requires new challenges for the entire system and in particular for the German and European TSOs. The ongoing wind power and PV integration alters the capacity limits of the German transmission and distribution grid resulting in day-by-day congestions. Short-term measures for more flexible operation, i.e., power flow control, generation management, demand-side management, or flexible line management, are used to provide a temporary relief. However, from a long-term perspective, network reinforcements, according to the German Network Development Plans and the TYNDP by ENTSO-E, are the only sustainable solutions to further integrate an increased capacity of generation from renewables. The long-term development plans reveal new hybrid system structures and therefore an indispensable analysis of new interactions and intersystem phenomena.

During the past 30 years, the wind energy in Germany has developed from small regional installations to a major cornerstone of the today's electricity generation. Earlier investigation concerning innovative generation concepts and system services of wind generators have paved the way for new technology concepts. Future research with respect to wind integration is dedicated to new tools and concepts of improved wind forecast systems, the integration of VPPs, as well as sector coupling concepts which will combine electricity, heat, and transport.

New grid concepts, the integration of further volatile RES and especially onshore and offshore wind power, require increasing reserve power as well as new economic energy conversion and storage concepts. Accordingly, current and future research activities need to be aligned to a global and interdisciplinary system planning and operation at the European level.

REFERENCES

- [1] Trieb F. Integration erneuerbarer Energiequellen bei hohen Anteilen an der Stromversorgung. *Energiewirtschaftliche Tagesfragen*, 63 2013;7:28–32.
- [2] Stappel M, Gerlach A-K, Scholz A, Pape C. The European power system in 2030: flexibility challenges and integration benefits. Berlin: AGORA Energiewende; 2015.
- [3] Fraunhofer IWES. Wind energy report Germany, <www.windmonitor.de>; 2014.
- [4] ENTSO-E Transparency Platform <<https://transparency.entsoe.eu>>.

- [5] Bundesverband der Energie- und Wasserwirtschaft (BDEW) e.V: *Redispatch in Deutschland*. Auswertung der Transparenzdaten April 2013 bis Juli 2016, Berlin, 9; August 2016.
- [6] Luther M, Radtke U. Operation and planning of grids with high levels of wind power. In: First world wind energy conference and exhibition. Berlin; July 4–8 2002.
- [7] König M, Luther M, Winter W. Offshore wind power in German transmission networks. In: Fourth international workshop on large-scale integration of wind power and transmission networks for offshore wind farms. Billund, Denmark; October 20–21 2003.
- [8] Luther M, Sassnick Y, Voelzke R. Influence of increased wind energy infeed on the transmission network. In: CIGRE conference. Paris, France; 2004.
- [9] Luther M, Radtke U, Winter W. Wind power in the German power system: current status and future challenges of maintaining quality of supply. In: Ackermann T, editor. Wind power in power systems. New York, NY: John Wiley & Sons; 2005. p. 233–55. ISBN:0-470-85508-8
- [10] Eriksen P, Ackermann T, Rodriguez J-M, Winter W. System operation with high wind penetration. IEEE Power Energ Mag 2005;11:65–74.
- [11] Luther M, Winter W. Wind power in the German power system: current status and future challenges of maintaining quality of supply. In: Ackermann T, editor. Wind power in power systems. 2nd ed. John Wiley & Sons; 2012. p. 549–67. ISBN:978-0-470-97416-2
- [12] Power grid development plan 2025 and offshore grid development plan 2025 Version 2015 <<http://www.netzentwicklungsplan.de/>>.
- [13] ENTSO-E Ten Year Network Development Plan <<http://tyndp.entsoe.eu/>>.
- [14] North Seas countries' offshore grid initiative—NSCOGI <<http://www.benelux.int/nl/ker-nthemas/energie/nscoxi-2012-report/>>.
- [15] Winter W, Elkington K, Bareux G, Kostevc J. A roadmap to 2020—pushing the limits. IEEE Power Energ 2015;13(1):60–74.
- [16] Grebe E, Kabouris J, Lopez S, Sattinger W, Winter W. Low frequency oscillations in the interconnected system of continental Europe. IEEE PES General Meeting; September 2010.
- [17] Winter W. Results of the EWIS study phase I. IEEE PES General Meeting, Pittsburgh, PA; 2007.
- [18] Van Hulle F, Smith JC, Winter W: Getting to higher levels of wind. IEEE PES Grid Integration and Transmission Magazine; June 2009.
- [19] Winter W. Integration of onshore and offshore wind power stations into the German extra high voltage grid. CIGRE Paris, France; 2006.
- [20] Erlich I, Winter W. Advanced grid requirements for the integration of wind turbines into the German transmission grid. IEEE Summer Meeting, Montreal, Panel Session, Invited Paper; 2006.
- [21] European Network Codes <www.entsoe.eu/major-projects/network-code-development/Pages/default.aspx>.
- [22] Winter W, Chan D, Norton M, Haesen E. Towards a European network code for HVDC connections and offshore wind integration. IEEE Xplore, No 15649937; September 2015.
- [23] Winter W, Bertolini P, Norton M, Urdal H. Requirements for HVDC connections and DC connected Power Park Modules in its role for a smarter and greener transmission system. Windintegration Workshop London; 2013.
- [24] Cornago A, editor. The European supergrid. Deventer, The Netherlands: Claeys and Casteels; 2015ISBN-13: 978-9077644263
- [25] ENTSO-E R&D Roadmap <www.entsoe.eu/publications/research-and-development-reports/rd-roadmap>.

- [26] Rohrig K, Lange B. Improvement of the power system reliability by prediction of wind power generation. IEEE Power Engineering Society General Meeting, Tampa; 2007.
- [27] Siefert M, Dobschinski J, Wessel A, Hagedorn R, Lundgren K, Majewski D. Development of innovative weather and power forecast models for the grid integration of weather dependent energy sources. In: Proceedings of the 12th international workshop on large-scale integration of wind power into power systems as well as on transmission networks for offshore wind power plants. London, UK; 2013.
- [28] Siefert M, Dobschinski J, Otterson S, Kanefendt T, Lundgren K, Ernst D, et al. Probabilistic wind power forecasts based on the COSMO-DE-EPS weather model. In: Proceedings of the 13th international workshop on large-scale integration of wind power into power systems as well as on transmission networks for offshore wind power plants. Berlin, Germany; 2014.
- [29] Vogt S, Dobschinsk J, Kanefendt T, Otterson S, Saint-Drenan Y-M. A hybrid physical and machine learning based forecast of regional wind power. In: Proceedings of the 14th international workshop on large-scale integration of wind power into power systems as well as on transmission networks for offshore wind power plants. Brussels, Belgium; 2014.
- [30] Rohrig K, Schlägl F, Jursa R, Wolff M, Fischer F, Hartge S, et al. Advanced control strategies to integration German offshore wind potential into electrical energy supply. In: Fifth international workshop on large-scale integration of wind power and transmission networks for offshore wind farms. Glasgow, Great Britain; 2005.
- [31] Stock S, Faiella L, Rohrig K, Hofmann L, Knorr K. Improving grid integration of wind energy power plants. Bremen: DEWEK; 2012.
- [32] Hennig T, Loewer L, Faiella LM, Stock S, Jansen M, Hofmann L, et al. Ancillary services analysis of an offshore wind farm cluster—technical integration steps of a simulation tool. EERA DeepWind' 2014, 11th deep sea offshore wind R&D conference. Trondheim; 2014.
- [33] Styczynski Z, Heyde C, Rohrig K, Rudion K. Renewable generation and reliability in the electric power network. Inform Technol 2010;52(2):90–9. Available from: <http://dx.doi.org/10.1524/itit.2010.0576>.
- [34] http://www.energysystemtechnik.iwes.fraunhofer.de/content/dam/iwes-neu/energysystemtechnik/de/Dokumente/Veroeffentlichungen/2015/Interaktion_EEStrom_Waerme_Verkehr_Endbericht.pdf.
- [35] Bundesministerium für Bildung und Forschung: *Kopernikus Projekte für die Energiewende* <<https://www.kopernikus-projekte.de/>>.

Part III

Wind Turbine Technology

This page intentionally left blank

Chapter 7

History of Harnessing Wind Power

Magdi Ragheb

University of Illinois at Urbana-Champaign, Urbana, IL, United States

Email: mragheb@illinois.edu

There is nothing new under the sun but there are lots of old things we do not know.

Ambrose Bierce, USA journalist, satirist

7.1 INTRODUCTION

President Abraham Lincoln, in the “Discoveries and Inventions” 1860 lecture, *New York Times*, November 22, 1936, is quoted as:

Of all the forces of nature, I should think the wind contains the largest amount of motive power ... Take any given space of the Earth's surface, for instance, Illinois, and all the power exerted by all the men, beasts, running water and steam over and upon it shall not equal the 100th part of what is exerted by the blowing of the wind over and upon the same place. And yet it has not, so far in the world's history, become properly valued as motive power. It is applied extensively and advantageously to sail vessels in navigation. Add to this a few windmills and pumps and you have about all. As yet the wind is an untamed, unharnessed force, and quite possibly one of the greatest discoveries hereafter to be made will be the taming and harnessing of it.

Wind power has been used since early history by mariners for sailing boats on rivers and lakes and then ships at sea. Since the early recorded history it has been used by successive cultures and civilizations. It is a fascinating field of study and captivates the interest of passionate creative and romantic people. Its future success depends on setting its footing on solid and realistic science, engineering and economics; and avoiding unrealistic dreams of perpetual motion machines and unrealistic romanticism.

Compared with modern machines powered by fossil fuels, wind machines depend on the wind as a fuel. Unfortunately, the wind is intermittent, unreliable, unsteady, and unpredictable and in some places on Earth it does not even blow at all. Yet, the advantage of the wind as a source of energy is that it is not just renewable, but infinite in magnitude originating in the Sun's fusion energy that is trapped in the Earth's atmosphere.

Windmills and water-driven mills were the only power generators for over 1200 years predating the 18th century's Industrial Revolution. They existed in antiquity in Egypt, Persia, Mesopotamia, and China. In the 7th century BC, king Hammurabi of Babylon implemented a plan to irrigate the fertile plains of the Euphrates and Tigris Rivers using vertical-axis wind machines [1].

Wind energy conversion has been reinvented many times in human history and is undergoing a new process of reengineering as the leading mechanically based renewable energy source. It is challenging the conventional energy sources into becoming a viable alternative to them. As fossil fuels are experiencing localized as well as global availability problems and peaking in their production and concerns about pollution and greenhouse-gas emissions, wind machines and generators are reclaiming with; new materials, electronic controls and advanced technology, an important share of the energy production field (Fig. 7.1).

The word "windmill" primarily refers to a wind-powered machine that grinds or mills grain such as wheat or corn and turns it into flour for bread making. This has been the most common function in addition to numerous other applications such as grinding of spices, lumber sawing, mines ventilation, iron and copper foundries power, gun-powder manufacturing, oil extraction from oil seeds, nuts and grains, converting old rags into paper, grinding



FIGURE 7.1 Modern wind turbines are replacing the iconic old American wind turbine technology on the American High Plains. *Photo: M. Ragheb.*

colored powders into dyes, manufacturing snuff tobacco and water pumping in Europe in the pre-Industrial Revolution era, and even lopping bee hives into towns under siege during warfare.

Holland has used windmills since AD 1350 to drain marshes and shallow lakes and turning them into productive agricultural land. They were coupled to an Archimedean screw, Egyptian noria, or Persian water wheel; all of them are early pump concepts which could elevate water to a height of 5 m. The noria's etymology comes from the Arabic: "Al Naoura" which literally means: "The wailing;" so-called because of the wailing sound it generates as it rotates. The "noria," is basically a water wheel that lifts water into an aqueduct carrying water to cities and fields using the flow energy of a water stream, similar to the modern hydraulic ram. It has a function similar to the chain pumps of which the "saqiya," literally "irrigator" in Arabic, which dates back to Babylonian (700 BC) and Pharaonic (4000 BC) times, is an example. Noria machines were in widespread use in the premedieval Islamic civilization before their evolution into the European windmills, and specimens are still in operation in some parts of the world today. Their introduction may have originated from Spain where Ibn Bassal (AD 1038–75) of Al Andalus (Andalusia) pioneered the use of a flywheel mechanism in the noria and saqiya to smooth out the delivery of power from the driving device to the driven machine [1].

Windmills were replaced by steam and internal combustion engines using fossil fuels ranging from coal to oil and natural gas as well as hydroelectric and nuclear energy. Nowadays wind turbines are primarily used in electrical power generation. The terminology "wind generators" becomes a more appropriate designation. Wind power has evolved from impulse or drag-driven heavy systems to light aerodynamic systems. The latter is not a modern concept, as it has been known to the ancient sailors and mariners and was applied to the development of sail windmills.

7.2 WIND MACHINES IN ANTIQUITY

Out of respect of the wind capability of destructiveness in tornadoes, hurricanes, typhoons, and storms, legends arose that the winds were imprisoned underground within the Earth and were released at the whim of a beneficent or malevolent deity. In ancient Greece, the god Aeolus was the ruler of the winds. Many primitive people thought that the wind could be controlled by magic. Control over the wind resources was reserved to the Royals in some societies, and later to the clergy [1].

In early Christianity, it was thought that the wind was God breathing to punish or reward the Earthly mortals. Mariners for centuries had legends dealing with their fears and superstitions about the wind. As early as 4000 BC, ancient Egyptian pottery depicts ships with square sails using the prevailing northerly wind to sail up the Nile River from north to south against its current.

During the ancient Egyptian Fifth Dynasty around 2500 BC, sailing ships advanced enough to go to sea and made trading trips along the East Coast of Africa to the land of Bunt. A relief on the walls of the Deir Al Bahari Queen Hatshepsut's temple in Luxor, Egypt, shows the sailboats sent on a trading and exploration expedition around the East coast of Africa. They sailed through an ancient canal dug to connect the Nile River to the Red Sea (Fig. 7.2). By 150 BC an account by Hero of Alexandria, Egypt in his *Spiritalia seu Pneumatica* describes a pneumatic application of a four-bladed wheel driven by the wind moving the piston of an air pump to blow the pipes of a musical organ with compressed air. A prayer wheel was used in Asia around AD 400 whose scoops caught the wind and rotated on a vertical shaft.

7.3 ISLAMIC CIVILIZATION WINDMILLS

Around 200–100 BC windmills with woven reed sails were used in the Middle Eastern region for grinding grain. The first documented invention of a real windmill occurred in the year AD 644 during the rule of the second Islamic Khaliph: Omar Ibn Al Khattab. A subject of Persian heritage, who proposed to him that he is able to build one, was commissioned by the Khaliph Omar Ibn Al Khattab to build a grain mill rotated by the wind.

The next written account comes from two Islamic geographers who tell of windmills built in the sandy and windy province of Seistan in present day Iran around AD 947. The first application had to do with drifting sand dunes which could bury whole villages and cities. To control the sand drifts, the people of Seistan ingeniously enclosed the sand drift or dune in a structure of timber

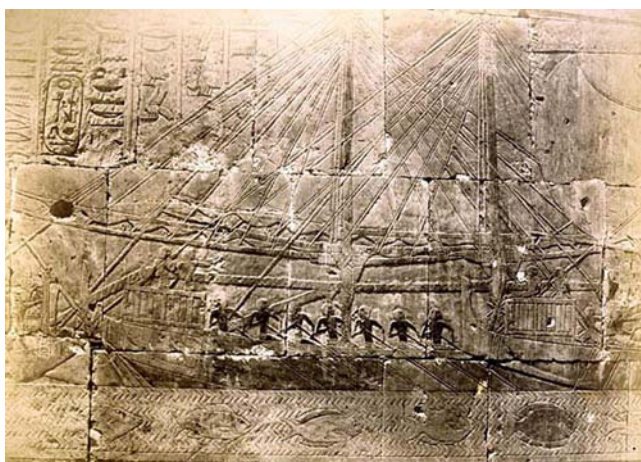


FIGURE 7.2 Relief of dual sail and rowing boats on the walls of the Deir Al Bahari's Queen Hatshepsut's temple in Luxor, Egypt, commemorating a trading expedition to the land of Bunt around the Eastern Coast of Africa.

and thorny bushes higher than the dune. In the lower part, they opened a door for the wind to enter and blow away the upper levels of sand in a vortex or tornado carrying the sand to be deposited evenly on the surrounding fields [1].

The Islamic geographer Ali Al Massoudi writes about Seistan in AD 947 that: “Wind turns mills which pump water from wells to irrigate the gardens. There is no place on Earth where people make more use of the wind.” Another Islamic scholar, Al Qazwini in AD 1283, describes how the people of Seistan used the wind to grind their wheat, as well as to control the drifting sand and to pump water. From that perspective, the region of Seistan can be considered as the birthplace of the eastern vertical-axis windmill in Islamic times ([Fig. 7.3](#)).

The Syrian cosmographer Al Damashqi (The Damascene) in AD 1300 describes in detail these vertical-axis windmills. They were erected in high places on top of hills, a mosque minaret or a tower in a castle. They were built as two-storied structures. The mill that turned and ground the grain into flour was at the upper story. The lower part contained the mill that was rotated by the blowing wind. The wheel turned one of two millstones in the upper section. Four slits existed in the walls of the first story with the outer part wider than the inner part. This formed ducts through which the wind blew from any direction. The ducted wind hit a reel with 6–12 cloth-covered arms rotating it. The reel moved the millstone that ground the grain. Other vertical windmills were used around the same time period in Afghanistan. They were driven by the prevalent north wind. A series of shutters and shields controlled the wind inlet [1].



FIGURE 7.3 Remaining vestiges of ancient vertical-axis windmills or “Panemones” at Seistan, near the border between Iran and Afghanistan. The rotors were made from cloth or bundles of reeds and wood.

Used originally in Persia and Afghanistan, windmills spread throughout the Islamic World and the Far East grinding grain and pumping water. They were adapted to crushing sugarcane for the manufacture of molasses and the extraction of sugar in Egypt. Centuries later, in the West Indies and the Caribbean Region, the West Indians hired Egyptian millwrights to establish the first sugar plantations. As Genghis Khan invaded Persia in the 12th century, the millwrights were induced to travel to China where bamboo horizontal mills with sails of matting adapted from Chinese sailing boats designs became common in the open fields. Superstition apparently suppresses their use today.

7.4 MEDIEVAL EUROPEAN WINDMILLS

The concept of the windmill first spread to Europe through the Islamic culture established in Morocco, at that time period referred to as Andalusia, to contemporary Portugal and Spain, by traders and merchants (Fig. 7.4). Another entry was through the trade routes through Russia and Scandinavia. A third route is attributed to the returning crusaders to Europe from the Middle East. A fourth way was through the Islamic Sicily into Italy.

The historian Mabillon in AD 1105 writes that a convent in France was allowed to construct watermills and windmills. Windmills according to him were becoming common in Italy in the 12th century. Questions aroused about whether the tithes for them belonged to the clergy. The controversy was decided in favor of the Church by Pope Celestine III. Mabillon recounts a story about an abbey in Northamptonshire, England in AD 1143 that was in a wooded area which was denuded over a period of 189 years: "That in the whole neighborhood there was no house, wind or water mill built for which timber was not taken from this wood." As wood was depleted for windmills construction, coal was used as a replacement energy source as a harbinger of the steam engine and the Industrial Revolution [1].

The first record of a windmill built in England was in Bury St. Edmunds in 1191. It was built in defiance of the then-vested authority and later destroyed by the Abbot. By the 14th century, the British monarchs watched the victories and defeats of their battling armies from the safety and high ground of the top of windmills scattered on the hills. A windmill was erected in Cologne, Germany in AD 1222. A windmill appeared in Siena Italy in AD 1237. Count Floris V in Holland granted the burghers of Haarlem the right to pay 6 shillings in tax for a windmill and 3 shillings for a horse mill in 1274.

In the 12–15th centuries the construction of windmills spread throughout central Europe all the way to Scandinavia reaching Finland in AD 1400. Windmills became the prime power movers all over Europe for grinding grain, pumping water, paper making, pressing oil from oil seeds, and sawing wood for ships and homes construction. The Dutch drainage mill was developed in Holland maintaining the land reclaimed from the sea, marshes, or shallow lakes. The Cistercian monks in France had introduced such a type of



FIGURE 7.4 Los Molinos at Consuegra, 77 km (48 miles) south of Madrid on the plains of Castilla-La Mancha, Spain. Windmills were so common by the end of the 16th century that the author Miguel de Cervantes recounts windmills and the encounter of his hero Don Quixote with them in La Mancha; which originally was an Arabic word meaning “dry, waterless land.” The wind flour mills were on the River Ebro and Don Quixote in his delusion mistook them as giants and charged them with his horse Rocinante and his squire Sancho Panza [1].

windmill to drain the lakes of their region. Peat was being mined for fuel needed by emerging cities, and this formed shallow lakes which grew in size over time and required systematic drainage by the 1300s. The first Dutch marsh mills were started by 1400. By 1600 there were 2000 of them operating to drain 0.8×10^6 ha (2 million acres) of land in Holland.

7.5 AEGEAN AND MEDITERRANEAN WINDMILLS

The windmills on the island of Crete, the Aegean Islands as well as Portugal and Spain were tower mills. The post mill which evolved into the tower mill was never observed in the Aegean area. Jib or triangular sails were typically used in the Iberian Peninsula and the Mediterranean. Their similarity to sailing ships is noticeable. They used 6–12 triangular cloth sails that were put up or down through roller reefing or by rolling them around the sail support. They were situated at the center of the mill or sheeted at mid-ship (Fig. 7.5).

The Aegean Islands windmills were small compared with the European windmills with a size of 4–12 m in diameter. The Dutch polder or scoop windmill measured about 29 m in diameter. They were placed four to twelve

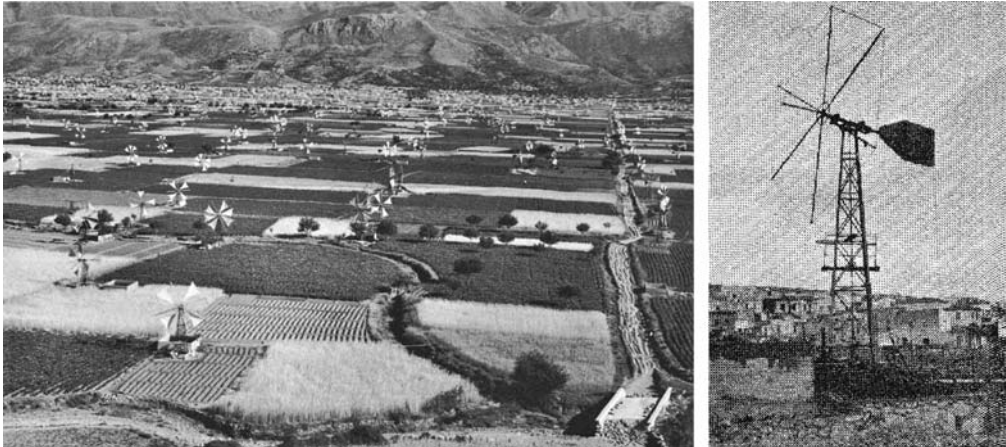


FIGURE 7.5 Sail water-pumping windmills harvesting the wind in large numbers on the island of Crete in the Mediterranean Sea.

in a row. Being efficient and well suited to the local conditions, they survived long after their use as wind power usage declined elsewhere.

Polders are low-lying tracts of land-forming hydrological entities that are surrounded by dikes or embankments. These are usually land reclaimed from a body of water such as an ocean shore or a shallow lake. They exist usually below sea level at river deltas, coastal areas, and fenlands and require constant drainage by opening sluices at low tide, by windmills in the past and pumps at present. The city of New Orleans in the United States is considered a polder area, seriously affected by flooding from hurricanes.

The earliest windmill structures were developed in the Middle East at the time of the Islamic Civilization and spread along the Mediterranean coast and in Persia around AD 500–900. Windmills technology was partly transferred to Medieval Europe by the returning crusaders in the 12th century. It developed there as the horizontal-axis design with tall structures on which the sails turned at a right angle to the ground.

Vertical-axis windmills are still being built in different parts of the world by enterprising farmers for irrigation and drainage purposes. A conventional aerodynamic sail and a Chinese impulse sail vertical-axis designs were built and used. An early description of a Chinese windmill was around AD 1219 by Yeh Lu Chu Tshai, a Chinese statesperson. Vertical-axis windmills using drag or impulse rather than cloth sails were built in Nebraska, United States around 1898 (Fig. 7.6).

Vertical-axis windmills have the advantage of a simple design consisting of six or more sails that are set upright upon horizontal arms resting on a tower or in the open, and which are attached to a vertical shaft positioned at the center. The sails are set in a fixed position that is oblique to the direction in which the wind will hit them. Their operation is independent of the direction from which the wind blows. Disadvantage of the vertical-axis design is that it may not be self-starting, and only one or two of the sails would catch the wind at any given time. The part of the sail catching the wind must then expend energy moving the dead weight of the part that is not catching it unless a shield configuration is adopted. Thus vertical-axis windmills are considered as less efficient than horizontal-axis windmills where the force of the blowing wind is evenly distributed on all sails [1].

7.6 DUTCH AND EUROPEAN WINDMILLS

European windmills were custom designed and built with the particular site and wind conditions taken into consideration. They were of primary importance in the life of rural Europe, grinding grain for flour and pumping water, so that they were installed before other structures were erected at European villages. Being erected on high ground to catch the wind from all directions, they were major landmarks seen from long distances by travelers.

The horizontal-axis machines were considered to possess a higher efficiency than the vertical-axis types; hence they were widely adopted in

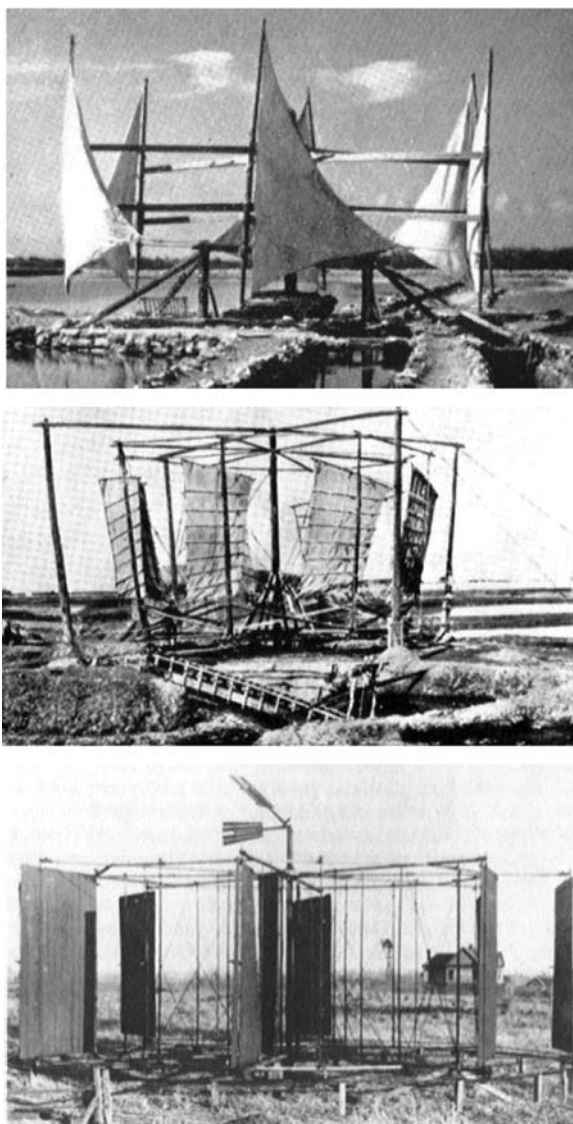


FIGURE 7.6 Conventional-sail vertical-axis wind irrigation turbine, using aerodynamic sails (top). Chinese-sail vertical-axis wind irrigation machine using impulse or drag sails (center). Merry-go-round drag-sails water-pumping mill at Lincoln, Nebraska, United States, 1898 (bottom).

Europe. The villagers personalized them and gave them individual names, much like boats today. The miller, doubling as a wind wright, commanded high authority, wealth, power, and respect in the village hierarchy. He usually charged the farmers a fraction of the grain being milled for his service.



FIGURE 7.7 Evolution of Dutch windmill designs: rotating cage post windmill with rotating lever wheel in the back and pegged wheel acted as a yaw mechanism to rotate the windmill to face the wind (left), tower design (Funenkade Olen windmill, Amsterdam, Holland) (center), and rotating-roof smock design for pumping drainage water (right).

This was supplemented by the flour dust accumulated on different parts of the windmill that he collected as a bonus. Being the richest man in town made him prominent politically. The miller's profession was a hazardous one particularly under stormy wind conditions. It required great skill and bodily strength climbing up the structure unfurling the sails for wind operation, or furling them to prevent the windmill arms from running away, damaging or destroying the windmill structure under wind gale conditions. With wooden windmills, the danger of fire was prominent through friction [1].

There evolved three types of European windmills ([Fig. 7.7](#)):

1. *Post design:* The post design refers to a massive upright post around which the entire body of the mill rotates in the direction of the blowing wind and was first described in AD 1270. The body of the mill supported the sails and the equipment. These designs were constructed out of wood. They used wood cog and ring gears to transmit the rotor blades rotation to a horizontal grindstone.
2. *Tower design:* This is also often referred to as the Dutch Mill. It was developed in the 14–15th centuries starting around 1390. The tower mill was installed on top of a tower of several stories. The construction material is brick with a wooden roof. It differs from the post mill in that instead of the whole windmill rotating around a central post, only its top or cap rotated to position or yawed the rotor blades to catch the wind. It formed an integral system for grain grinding and storage as well as the living quarters of the wind wright or wind smith and his family on the first story. The windmill needed continuous undivided attention while it was running, particularly under stormy conditions where the wind wright had to furl the sail on the blades and brake the mill to a stop. A runaway windmill is a

hazardous situation that if uncontrolled, would literally disintegrate the whole structure launching flying debris into neighboring structures; a hazard that exists in modern wind turbines. The post and the tower windmills had to be yawed manually to face the wind using a large wheeled lever at the back of the windmill. A lateral fan was added later to automate the yaw orientation of the mill into the prevailing wind direction.

3. *Smock design:* The smock design differs from the tower windmill in the construction materials used. The smock design has a stone base with a wooden upper section that is framed with weather boarding that is either tarred or painted. The name “smock” originates from the way these windmills’ appearance looks like the linen smocks worn at the time in Holland and Europe [1].

7.7 THE AMERICAN WINDMILL

This multiblade design appeared in Europe in the 17th century. Leupold Jacob from Leipzig in 1724 in a book: *Journal of Hydraulic Arts*, or in German: *Schauplatz der Wasser Künste*, introduced an eight-bladed self-regulating wind turbine that drove a single action piston water pump using a crankshaft and a tie rod. In an ingenious design, each blade was capable of pivoting around its own axis maintained by a spring system that is progressively extended in a high wind condition resulting in the rotor revolving in a gale no faster than in a moderate wind, avoiding the destructive situation of a runaway wind turbine (Fig. 7.8).

This design did not spread on the European continent, but rather on the American Great Plains. Starting in 1870, as a simple, economic, and a most successful design, it conquered the American continent and migrated back to

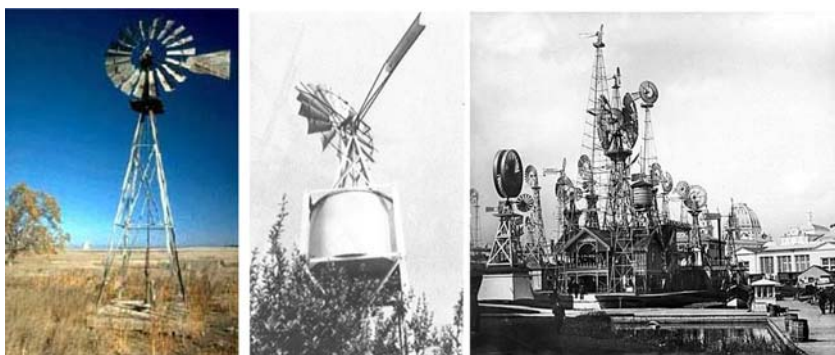


FIGURE 7.8 American water-pumping windmill used a ground water storage tank for cattle drinking (left). American water-pumping windmill with a tower water storage tank to feed gardens or steam locomotives. This is an example of a gravity pumped energy storage system (center). American Windmill versions competition at “The World Columbian Exposition,” Chicago, USA in 1893, as a commemoration of Christopher Columbus arrival to the New World 100 years earlier (right).

Europe and the rest of the world where it was named: “The American Windmill.” The most common windmill in America was built in the 19th century as a vertical steel structure topped with a rotating multibladed drag or impulse propeller that caught the wind. Its rotational motion is converted into linear motion that pumped water and stored it in a water tank for irrigation, cattle drinking, and water supply to steam locomotives.

The American Windmills were simple in construction and standardized in design. They could be easily dismantled, moved to other locations for reassembly. Their maintenance was simple amounting to addition of lubrication oil to the geared components, with parts that are interchangeable and could be cannibalized from one machine to another. The standardization led to the spread of the American Windmills in many altered versions in the American West as well as all over the world.

Early on, wooden slats were nailed to rims with tail rudders for orientation toward the wind or yawing. Instead of using a rudder, some designs used weather vanes operating downwind from the tower. Speed control was provided by spring and weight mechanisms and by feathering the blades to reduce the thrust in high winds. Around 1870, galvanized steel blades replaced the wooden slats allowing high speed operation that needed a reduction gear box to operate the reciprocal water pump at its required low speed [1].

The Halladay design introduced in 1854 evolved into the Aermotor and Dempster designs that became operational in different parts of the world. Starting 1850, about 6 million small turbines of 750 W (one Imperial horsepower) power or less were installed in the United States, primarily for water pumping for cattle and farm needs. Larger windmills with rotor diameters of up to 18 m diameter provided water for the steam boilers of the locomotives of the western railroads. This is really how the “American West was won”: through the windmill and the steam locomotive.

7.8 HISTORICAL DEVELOPMENTS

The earliest horizontal-axis windmills possessed short sails, which were made later longer and more efficient in catching the kinetic energy from the wind. As the sails were elongated, the axle or wind shaft on which they rotated had to be emplaced higher off the ground on the windmill structure or buck. Irrespective of their design, some common features exist in windmills. For horizontal-axis windmills:

1. A means of catching the wind through sails, arms, or rotor blades rotating around an axle.
2. A yaw mechanism to turn the sails, arms, or blades so that they face the wind. Otherwise, as the wind direction shifts, the windmill would stall.

3. A gear system and interlocking equipment transmitting the wind energy to the millstone, water pump, wood saw, or electrical generator that they are powering.

Vertical-axis windmills share the first and third features only since they catch the wind from all directions without the need to adjust them like in the case of the horizontal-axis windmills. The use of sails on the European windmills added an element of aerodynamic lift leading to higher rotor efficiency through its increased speed. The evolutionary perfection process took 500 years leading to windmills that have the components and features of the modern windmills.

Some windmills had aerodynamic brakes, spoilers, flaps, and leading edge airfoil sections that were precursors to the modern airplane wing. Features of modern airfoil rotor blades were incorporated through insight and trial and error: a nonlinear twist of the blades from their root to their tip, introducing a camber along the leading edge, emplacement of the blade spar at the quarter chord position at 25% of the way from the leading edge to the trailing edge, and designing the blade with its center of gravity at that same 1/4 chord position.

The simplest windmills sails are just cloth sails attached to the rotating arms or blades. Designs using multiple sails were used in the Mediterranean region such as at Alexandria, Egypt (Fig. 7.9). A design with small sails attached to multiple arms was used in Greece. With a small number of arms, large sails were used for a Portuguese, Spanish, and French windmills. Some were equipped with bells at the end of its rotating arms, generating an audible alarm for stray cattle or humans.

Better structural strength was achieved with wooden frames covered with cloth in what became known as common sails. Initially the cloth was only



FIGURE 7.9 Alexandria, Egypt's Moulins du Gabari (Al Qabbari), built on a hill overseeing the harbor of Alexandria, showing their furled sails.

placed over the frames or entirely removed. Later, a method for reefing or furling the cloth was developed to control the sail area depending on the wind speed. The common sails were light in weight and powerful but they had to be stopped by the mill wright furling the sail. Stopping the mill by an additional brake was needed. In many situations the wind became stronger than the brake could handle. The mill then could run out of grain and its millstones would now run dry, generating a spark shower igniting fires. Runaway wind turbines could also lead to vibration that would disintegrate the windmill wooden parts. In freezing weather, the cloth could become wet and frozen.

The wind wright had to skillfully ride out a storm much like a sailing ship's captain had to weather a storm at sea. One method to slow the sails in a high wind was to jam the grain into the millstones so that they act as a brake slowing down the sail rotation. A second method was to force the sails edge onto the wind. If the wind suddenly shifted, it could hit the windmill from behind with the sails and cause them to be blown off [1].

Combinations of wood and metal were used to prevent fires from friction of similar components. Many cloth sails lasted for as long as 40–50 years. Interestingly, the sails were built with a counterclockwise rotation, a tradition that endures today in most wind turbines, with rare exceptions.

Modern wind generators have evolved from a drag or impulse system into an airfoil system similar to airplane propellers and wings. Wood and glass epoxy, fiberglass, aluminum, and graphite composite materials are now used in their construction.

7.9 WINDMILLS APPLICATIONS

Barley- and rice-hulling windmills operated by hulling stones which were larger than the common millstones removing the thin outer cover of the grain kernel. They were grit stones with a few deep furrows with the grain flung out along them without being ground. Requiring heavier equipment and a stronger wind location than grinding mills, hulling mills were limited in number [1].

Different windmill applications required different specialized machinery. Oil mills pressed oil from oil seeds and nuts. Grinding mills ground spices. Saw mills sawed wood into planks for construction and ship building. Irrigation and drainage mills reclaimed the low lands of Holland or the Netherlands from the sea by drying out marches and shallow lakes. Polder drainage windmill designs used a scoop wheel or noria, and other designs used an Archimedean screw or “tambour.”

7.10 DISCUSSION

At the beginning of the 20th century, the first modern windmills driving electrical generators were introduced in France by Darrieus and then spread worldwide. The steam engine and then the internal combustion engine



FIGURE 7.10 Symbiotic coupling of nuclear and wind technologies views during winter and summer. The two units 2309 MWe Boiling Water Reactors LaSalle nuclear power plant near Marseilles, Illinois, United States operated by Exelon Nuclear corporation and the Grand Ridge Wind Farm operated by Invenergy LLC in the adjacent farmland near Ransom in Illinois, United States. The nuclear reactor and the wind turbines are both manufactured by the General Electric Company [7].

replaced sails on ships and mills. Both were more efficient than windmills using fossil fuels as a source of energy rather than the wind [1].

It is recognized that the renewable sources of energy are characterized by the use of a large labor supply providing job opportunities in high-population economies. Their implementation is rapid: it takes about 2 years in the United States for the implementation and production from wind parks projects since they only require local regulations, whereas other conventional energy sources such as coal and nuclear power stations require 10 years or more because they are bound by lengthy federal regulations [2–7].

A symbiotic coupling of wind technologies with other energy sources exists through sharing access to the electrical grid system. The two units 2309 MWe Boiling Water Reactors LaSalle nuclear power plant near Marseilles, Illinois, United States operated by Exelon Nuclear Corporation and the Grand Ridge Wind Farm operated by Invenergy LLC in the adjacent farmland near Ransom in Illinois, United States are jointly sited and connected to the same electrical grid system. The nuclear reactor and the wind turbines are both manufactured by the General Electric (GE) Company. The GE 1.5 MW SLE wind turbines have a hub height of 80 m and are net recipients of about 5 kW of electrical power from the grid on a standby basis, but then become net exporters of electricity into the electrical grid under favorable wind conditions (Fig. 7.10).

The world is embarking on a third industrial revolution: the Low Carbon Age; and wind power is being reinvented to help fill the need.

REFERENCES

- [1] Johnson GJ. *Wind energy systems*. Englewood Cliffs, NJ: Prentice Hall; 1985.
- [2] Ragheb M, Ragheb AM. Wind turbines theory-The Betz equation and optimal rotor tip speed ratio. In: Cariveau R, editor. *Fundamental and advanced topics in wind power*. InTech; 2011. <http://www.intechopen.com/articles/show/title/wind-turbines-theory-the-betz-equation-and-optimal-rotor-tip-speed-ratio>, ISBN: 978-953-307-508-2.

- [3] Ragheb AM, Ragheb M. Wind turbine gearbox technologies. In: Carriveau R, editor. Fundamental and advanced topics in wind power. InTech; 2011 <http://www.intechopen.com/articles/show/title/wind-turbine-gearbox-technologies>, ISBN: 978-953-307-508-2.
- [4] Ragheb M. Coupling wind power as a renewable source to nuclear energy as a conventional energy option. In: Invited paper submitted for presentation at the Academy of Sciences for the Developing World—Arab Regional Office, TWAS-ARO, 7th annual meeting seminar: “Water, nuclear and renewable energies: challenges versus opportunities” conference, Center for Special Studies and Programs, CSSP, Bibliotheca Alexandrina, Alexandria, Egypt, December 28–29, 2011, <<http://www.bibalex.org/CSSP/Presentations/Attachments/Coupling%20Wind%20Power%20as%20a%20Renewable%20Resource%20to%20Nuclear%20Energy%20as%20a%20Conventional%20Energy%20Option.pdf>>.
- [5] Kate Rogers K, Ragheb M. Symbiotic coupling of wind power and nuclear power generation. In: Proceedings of the 1st international nuclear and renewable energy conference (INREC10), Amman, Jordan, March 21–24, 2010.
- [6] Weisensee P, Ragheb M. Integrated wind and solar qattara depression project with pumped storage as part of desertec. In: The role of engineering towards a better environment, RETBE'12, 9th international conference, Alexandria University, Faculty of Engineering, December 22–24, 2012.
- [7] Ragheb M. Wind power systems: NPTE 475, Lecture Notes, <<http://www.mragheb.com/NPRE%20475%20Wind%20Power%20Systems/index.htm>>; 2016.

This page intentionally left blank

Chapter 8

Wind Turbine Technologies

Anca D. Hansen

Technical University of Denmark, Roskilde, Denmark

Email: anca@dtu.dk

8.1 INTRODUCTION

The wind turbine technology is a very complex technology involving multi-disciplinary and broad technical disciplines such as aerodynamics, mechanics, structure dynamics, meteorology as well as electrical engineering addressing the generation, transmission, and integration of wind turbines into the power system.

Wind turbine technology has matured over the years and become the most promising and reliable renewable energy technology today. It has moved very fast, since the early 1980s, from wind turbines of a few kilowatts to today's multimegawatt-sized wind turbines [1–3]. Besides their size, the design of wind turbines has changed from being convention driven to being optimized driven within the operating regime and market environment. Wind turbine designs have progressed from fixed speed, passive controlled and with drive trains with gearboxes, to become variable speed, active controlled, and with or without gearboxes, using the latest in power electronics, aerodynamics, and mechanical drive train designs [4]. The main differences between all wind turbine concepts developed over the years, concern their electrical design and control.

Today, the wind turbines on the market mix and match a variety of innovative concepts, with proven technology for both generators and power electronics [4]. The continuously increased and concentrated electrical penetration of large wind turbines into electrical power systems inspires the designers to develop both custom generators and power electronics [5,6] and to implement modern control system strategies.

8.2 OVERVIEW OF WIND TURBINE COMPONENTS

A wind turbine consists of a tower and a nacelle that is mounted on the top of a tower. The nacelle contains several components, which contribute with

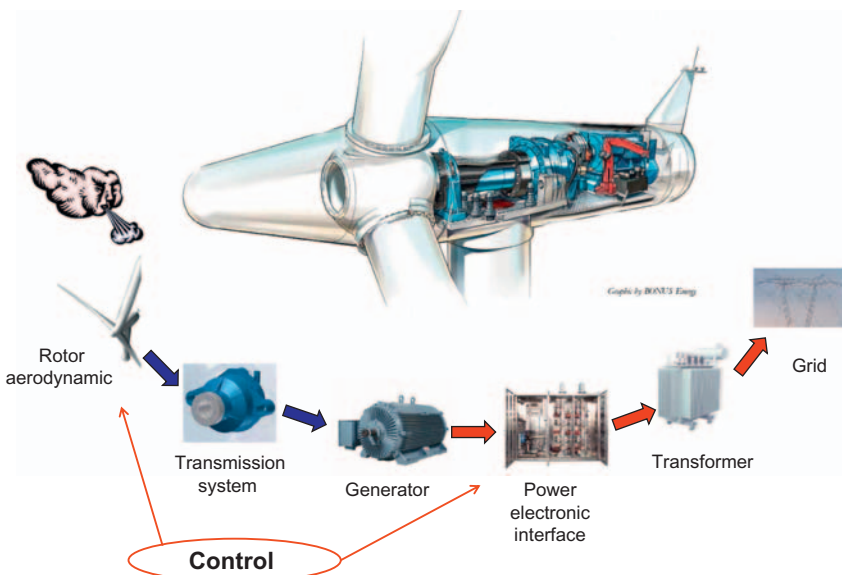


FIGURE 8.1 Wind turbine components—picture from Internet [7] adapted with additional illustrations.

their specific function in the energy conversion process from wind energy into electrical energy. Fig. 8.1 shows the main components of a wind turbine including the turbine rotor, transmission system (gearbox), generator, possible power electronics, control system, transformer, and finally its connection to the grid.

8.2.1 Aerodynamic Rotor

The aerodynamic rotor of a wind turbine captures the power from the wind and converts it to kinetic mechanical power. The aerodynamic rotor is mainly made up of a hub and blades, with the latter attached to the hub by mechanical joints. Modern wind turbines have typically two or three blades, made up by a matrix of fiber glass mats impregnated with polyester [8]. In the old wind turbines the blades can be firmly attached to the hub, while in the more modern ones the blades can be turned around their longitudinal axes.

8.2.2 Transmission System

As depicted in Fig. 8.1, the kinetic mechanical power from the aerodynamic rotor is transmitted to the generator through a transmission system, which typically consists of the rotor shaft, mechanical brake(s), and a gearbox.

The mechanical brakes are usually used as a backup system for the aerodynamic braking system of the wind turbine and/or as a parking brake once

the turbine is stopped. The aerodynamic brake system usually consists of turning the blade out of the wind, namely 90 degrees about the longitudinal axis of the blade.

The main purpose of the gearbox is to act as a rotational speed increaser; the gearbox of a wind turbine converts the slow high torque rotation of the aerodynamic rotor into the much faster rotation of the generator shaft. Depending on their geometrical designs, gearboxes are typically divided in two classes. The first one is the spur and helical gearboxes, which consists of a pair of gear wheels with parallel axes. The second one is the planetary gearbox which consists of epicyclic trains of gear wheels [9]. As the gearbox is continuously subjected to large and varying torques due to increased size of wind turbines and wind speed variability, the gearbox is the weakest link in the wind turbines, many of them failing in less than 2 years of operation [9]. As a result, in some of the newer wind turbines technologies, the gearbox has been removed, by designing generators, with a multipolar structure in order to adapt the rotor speed to the generator speed. The generator speed decreases by increasing number of pole pairs, and therefore the gearbox may not be necessary for multipole wind turbine generator systems, i.e., where number of pole pairs may be higher than 100.

8.2.3 Generator

The generator is an electromechanical component, which converts the mechanical power into electrical power. As indicated in Fig. 8.2, generators have typically a stator and a rotor. The stator is a stationary housing, which has coils of wire mounted in a certain pattern. The rotor is the rotating part of the generator and is responsible for the magnetic field of the generator.

A rotor can have a permanent magnet or an electromagnet, namely a magnetic field is generated on the rotor and rotates with the rotor. By its rotation, the rotor and thus its magnetic field pass the stator windings and

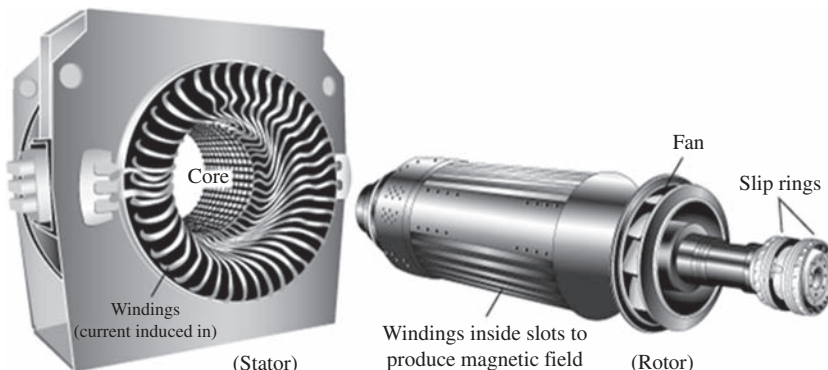


FIGURE 8.2 Generator's stator and torque. <<https://en.wikipedia.org/wiki/Stator>> [10].

induce a voltage in the terminals of the stator. When the magnetic field of the stator is following the magnetic field of the rotor, the generator is called synchronous, otherwise it is called asynchronous.

Two major types of generators used in the industry are: synchronous generator (SG) and asynchronous (induction) generator. Descriptions of synchronous and asynchronous generators can be found in many standard textbooks. For example, Refs. [4,13,14] provide a good overview regarding the different generator technologies currently used by the wind industry as well as future options for the design of wind turbine generators.

8.2.3.1 Synchronous Generator

The SG is a generator, which operates at the synchronous speed, dictated by the frequency of the connected grid, regardless of the magnitude of the applied torque. The magnetic field in the SG can be created by using permanent magnets or with a conventional field winding.

The speed of the SG is determined by the frequency of the rotating field and by the number of pole pairs of the rotor. If the SG has a suitable large number of poles (i.e., multipole structure) it can be used for direct-drive applications without the need of a gearbox.

The SG is more expensive and mechanically more complicated than an asynchronous generator of a similar size. However, it has one significant advantage compared with the asynchronous generator, namely, that it does not need reactive magnetizing current and thus no further power compensation equipment.

Two classical types of SGs are often used in the wind turbine industry:

- *Wound rotor synchronous generator (WRSG)* is the workhorse of the electrical power industry and therefore very well documented in the literature [13–15]. Its stator windings are connected directly to the grid and hence the rotational speed is strictly fixed by the frequency of the supply grid. The rotor winding, through which direct current (DC) flows, generates the exciter field, which rotates with synchronous speed.
- *Permanent magnet synchronous generator (PMSG)* has a wound stator, while its rotor is provided with a permanent magnet pole system. It has a high efficiency as its excitation is provided without any energy supply. However the materials used for producing permanent magnets are expensive and they are difficult to manufacture. Additionally, the use of permanent magnets excitation requires the use of a full-scale power converter in order to adjust the voltage and frequency of generation to the voltage and the frequency of transmission, respectively. Different topologies of PMSG are presented in the literature [16–18]. The most common types are the radial flux machine, the axial flux machine, and the transversal flux machine.

8.2.3.2 Asynchronous (Induction) Generator

The asynchronous generator has several advantages such as robustness, mechanical simplicity and as it is produced in large series, it also has a low price. The major disadvantage is that the stator needs a reactive magnetizing current. As the asynchronous generator does not contain permanent magnets and is not separately excited, it consumes reactive power in order to get its excitation. The reactive power may be supplied by the grid or by power electronics.

In the asynchronous generator, an electric field is induced between the rotor and the rotating stator field by a relative motion called slip, which causes a current in the rotor windings. The interaction of the associated magnetic field of the rotor with the stator field results in a torque acting on the rotor.

The rotor of an asynchronous generator can be designed as a short-circuit rotor (squirrel-cage rotor) or as a wound rotor [13]:

- *Squirrel-cage induction generator (SCIG)*—has been often used by the industry over the years, due its mechanical simplicity, high efficiency, and low maintenance requirements. As depicted in Fig. 8.3, the rotor of this generator has conducting bars embedded in slots and shorted in both ends by end rings. The electrical characteristics of the rotor can therefore not be controlled from the outside.

SCIG is very robust and stable generator, its speed changing by only a few percent as its slip varies with the changes in the wind speed. Wind turbines based on SCIG are typically equipped with a soft-starter mechanism and an installation for reactive power compensation, as SCIGs consume reactive power. SCIGs have a steep torque speed characteristic and therefore fluctuations in wind power are transmitted directly to the grid. These transients are especially critical during the grid connection of the wind turbine, where the inrush current can be up to seven to eight times the rated current.

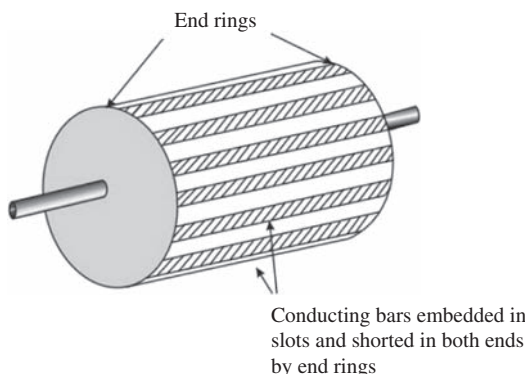


FIGURE 8.3 Squirrel-cage induction generator. <https://en.wikipedia.org/wiki/Squirrel-cage_rotor> [11].

In a weak grid, this high inrush current can cause severe voltage disturbances [25]. Through the soft starter, the generator is gradually connected to the grid in order to limit the inrush currents. The amount of reactive power for the generator varies depending on the wind conditions. This means that if the wind speed is high, the wind turbine can produce more active power, but only if the generator gets more reactive power. Without any electrical components to supply reactive power, the needed reactive power for the generator is taken directly from the grid and this might cause additional transmission losses and can, in some situations, make the grid unstable. To avoid this, capacitor banks or modern power electronic converters are typically used to provide the needed reactive power compensation.

- *Wound rotor induction generator (WRIG)*—the windings of the wound rotor can be externally connected through slip rings and brushes or by means of power electronic equipment (Fig. 8.4). This means that this generator has the advantage that its electrical characteristics can be controlled from the outside, and thereby a rotor voltage can be impressed.

By using power electronics, the power can be extracted or impressed to the rotor circuit and the generator can be thus magnetized from either the stator circuit or the rotor circuit. The disadvantage of WRIG is that it is more expensive than and not as simple and robust as the SCIG. Two WRIG configurations are mainly used in the wind industry:

- *OptiSlip or FlexiSlip induction generators* were often used in 1990s, as WRIGs with a variable external rotor resistance attached to the rotor windings, which can be changed by an optically controlled converter mounted on the rotor shaft, and hence the name. This optical coupling eliminates the need for costly slip rings that need brushes and maintenance. The range of the dynamic speed control depends on the size of the variable rotor resistance. Typically, the slip for OptiSlip is 10%, while for FlexiSlip it is about 16% [4].
- *Doubly fed induction generator (DFIG)*—has the stator windings directly connected to the constant frequency grid, while the rotor is connected to the grid through a back-to-back power converter.

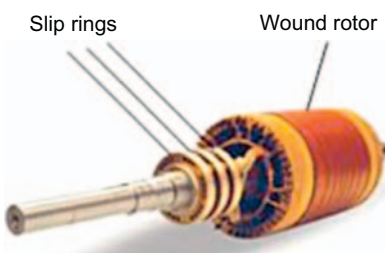


FIGURE 8.4 Wound rotor with slip rings. <[https://en.wikipedia.org/wiki/Rotor_\(electric\)](https://en.wikipedia.org/wiki/Rotor_(electric))> [12].

The size of this converter is related to the selected speed range, namely it is not a full-scale power converter, since typically only a fraction up to 70% of the speed range is utilized. The selection of the speed range is based on the economic optimization of investment costs and on increased efficiency. Thus the cost of the converter increases when the speed range around the synchronous speed becomes wider. DFIG has the ability to control independently its active and reactive power. A drawback of the DFIG is the inevitable need for slip rings [15,21].

8.2.4 Power Electronic Interface

The generator converts the mechanical power into electrical power, which is fed into the power grid through a power electronic interface [5,24]. As it is placed between the wind turbine generator and power grid, the power electronic interface should satisfy both generator and grid side requirements with a cost effective and easy maintenance solution. On the generator side, this interface ensures that the rotating speed of the turbine is continuously adjusted in order to extract maximum power out of the wind [17–19] following a maximum tracking point. On the grid side, the power electronic interface must comply with the grid codes [22] regardless of the wind speed, such as ability to control active and reactive power, frequency and voltage control.

The penetration of power electronics in wind turbine systems has been continuously growing since the 1980s, becoming gradually more and more advanced and bringing in significant performance improvements for the wind turbines—not only reducing the mechanical stress/loading and increasing the energy yield, but also enabling wind turbines to behave as active controllable components in the power system and support the grid similarly to the conventional power plants [21]. Nowadays, components can handle higher current and voltage ratings, the power losses decrease and the devices become more reliable.

The most commonly used power electronic interfaces in wind turbine applications over the years are:

- *Soft starter* is a simple and cheap power electrical component used in 1980s in wind turbines with SCIG to reduce the inrush current during wind turbines connections to the grid, thereby limiting the disturbances to the grid. Without a soft starter, the inrush current can be up to seven to eight times the rated current, which can cause severe voltage disturbances on the grid [24].
- *Capacitor bank* is an electrical component that supplies reactive power to the asynchronous generators of wind turbines [24]. Traditionally, mechanically switched capacitor banks are the easiest and most economical way to minimize the reactive power drawn by asynchronous generators from the grid. The generators of wind turbines can have a full load

dynamic compensation, where a certain number of capacitors are connected or disconnected continuously, depending on the average reactive power demand of the generator over a predefined period of time. As the reactive power demand of an asynchronous generator is strongly dependent on wind speed, the capacitor banks can often be triggered by an extreme number of switching events.

- *Frequency converter*, typically used in wind turbines since 2000, is a device which facilitates interconnection of two electrical systems with independent frequencies [24]. It makes it possible to adjust and control the generator frequency and voltage, and thus enhance wind turbines capability to behave and act as active components in the power system. A traditional frequency converter, also called an adjustable speed drive, consists of:
 - Alternating current (AC)/direct current (DC) conversion unit (rectifier) converts AC into DC, while the energy flows into the DC system;
 - Capacitors (energy storage);
 - DC/AC conversion unit (inverter) converts DC into AC, while the energy flows to the AC system.

During recent years different converter topologies (back-to-back/multilevel/tandem/matrix/resonant converters) have been investigated to test whether or not they can be used in wind turbines. The back-to-back converter is highly relevant to wind turbines today. It constitutes the state of the art and may therefore be used for benchmarking the other converter topologies. As discussed in Ref. [23], the matrix and multilevel converter are the most serious competitors to the back-to-back converter and thus are recommended for further studies.

8.2.5 Control System and Wind Turbine Control Capabilities

A wind turbine is typically equipped with a control system, necessary to assure a proper operation of the wind turbine under all operational conditions. The control system is meant to control and keep the wind turbine within its normal operating range by passive or active means. Passive controls use their own sensing and are exercised by use of natural forces, e.g., when the rotor “automatically” loses the aerodynamic efficiency (known as stall phenomena), when the wind speed exceeds a certain critical level. Active controls use electrical, mechanical, hydraulic, or pneumatic means and require transducers to sense the variables that will determine the control action needed. Typical variables which are monitored in a control system are wind speed, rotor speed, active and reactive power, voltage and frequency of the wind turbine’s point of connection. In addition, the control system must be able to stop the wind turbine, if necessary.

The overall goal of wind turbine active control is to maximize the power production and to reduce the structural loads on the mechanical components and thus their costs and life time consumption. At low wind speeds the control system has to ensure that the turbine produces optimal power, namely that the wind turbine is extracting power out of the wind with maximum efficiency. At high wind speeds, namely higher than the rated wind speed, the power production of the turbine should be limited to the rated power value and thereby reduce the driving forces on the blades as well as the load on the whole wind turbine structure.

All wind turbines are designed with some sort of power control [4]. Three options for the power output control are currently used: stall control, pitch control, and active stall control. The main differences between these options concern the way in which the aerodynamic efficiency of the rotor is limited during above the rated wind speed in order to prevent overloading.

- *Stall control (passive control)* is the simplest, most robust and cheapest power control method. Here the blades are firmly attached to the hub and the wind attack angle of the wings is fixed. The design of rotor aerodynamic causes the rotor to stall “automatically” (so losing efficiency) when the wind speed exceeds a certain level, i.e., rated value.
- *Pitch control (active control)* means that the blades can be quickly turned away from or into the wind as the power output becomes too high or too low, respectively. In contrast to stall control, pitch control requires that the rotor geometry changes and it is therefore more expensive due to its pitching mechanism and controller. The pitching system can be based on a hydraulic system, controlled by a computer system or an electronically controlled electric motor. The pitch control system must be able to adjust the pitch angle by a fraction of a degree at a time, corresponding to a change in the wind speed, in order to maintain a constant power output.
- *Active stall control*, as the name indicates, means that the stall of the blade is actively controlled by pitching the blades in the opposite direction than a pitch-controlled wind turbine does. This movement increases the angle of attack of the rotor blades in order to make the blades go into a deeper stall and into a larger angle of attack. In contrast to stall control, the active stall control has the advantage of being able to compensate for variations in the air density.

The wind turbines can also be classified according to their speed control ability into two significant classes such as fixed-speed wind turbines and variable-speed wind turbines.

- *Fixed-speed wind turbines* were the most common installed wind turbines in the early 1990s. Characteristic for these wind turbines is that they are equipped with a SCIG connected directly to the grid, a soft starter, and a capacitor bank for reduction of reactive power consumption. Regardless of the wind speed, the rotor speed of the wind turbine is almost fixed,

stuck to the grid frequency and cannot be changed. Fixed-speed wind turbines are designed to achieve maximum efficiency at one particular wind speed, namely at the most likely wind speed in the area where the wind turbine is placed. Fixed-speed wind turbines have the advantages of being simple, robust and reliable, well proven and with low cost of electrical parts. Its direct drawbacks are high mechanical stress, uncontrollable reactive power consumption, and limited power quality control [25].

- *Variable-speed wind turbines* have become the dominant type among the installed wind turbines during the past decade. Variable-speed operation can only be achieved by decoupling the electrical grid frequency and mechanical rotor frequency through a power electronic interface. Characteristic for these wind turbines is that they are designed to achieve maximum aerodynamic efficiency over a wide range of wind speeds. Within variable-speed operation, it is possible to continuously adapt (accelerate or decelerate) the rotational speed of the wind turbine to the wind speed, in such a way that the turbine operates continuously at its highest level of aerodynamic efficiency. The advantages of variable-speed wind turbines are an increased annual energy capture (this is about 5% more than the fixed-speed technology) and that the active and reactive power can be easily controlled [17–18]. They have also less mechanical stress, improved power quality and, not least, controllability and “grid friendliness,” which is a prime concern for the grid integration of large wind farms. The disadvantages are the additional losses due to power electronics that increase the component count and make the control system more complex. Beside these, they have also an increased cost due to the power electronics, which is about 7% of the whole wind turbine [17–19,26].

Fixed-speed wind turbines have been used with all three types of power control options by the industry. Until the mid-1990s, when the size of wind turbines reached the megawatt range, the stall control fixed-speed wind turbines, were the predominant type.

Pitch control applied to fixed-speed wind turbines has not been very attractive due to the large inherent power fluctuations at high wind speeds; the pitch mechanism is no fast enough to avoid power fluctuations in case of gusts at high wind speeds.

Active stall fixed-speed wind turbines have been popular in 1990s, due to their smooth limitation in power. However, as they have a very slow control, their success is strongly conditioned by their ability to comply with the stringent requirements impose these days by the utility companies.

The pitch control method has proved to be a very attractive option for variable-speed operation and for larger wind turbines than 1 MW. The variable-speed wind turbines are today only used in practice together with a fast pitch mechanism, due to power limitation considerations [4]. The reason why variable-speed stall or variable-speed active stall control wind turbines

are not considered is their lack of ability for rapid reduction of power. If such variable active stall controlled wind turbine is running at maximum speed and encounters a large wind gust, the aerodynamic torque can become critically large and may result in a run-away situation.

8.3 CONTEMPORARY WIND TURBINE TECHNOLOGIES

This section presents an overview of the contemporary wind turbine technologies with their configurations, characteristics, advantages, and drawbacks. Depending on the generator type, power electronics, power and speed controllability, the wind turbines can generally be categorized into four categories.

8.3.1 Fixed-Speed Wind Turbines (Type 1)

The fixed-speed wind turbine configuration uses a multiple-stage gearbox and a SCIG to convert the mechanical energy from the wind into electrical energy. This is the conventional concept applied by many Danish wind turbine manufacturers during the 1980s and 1990s, and therefore it is also referred as “Danish concept” [4].

As illustrated in Fig. 8.5, in this configuration the generator is directly connected to the grid via a transformer. Besides the generator, the electrical system of fixed-speed wind turbines also contains a soft starter for smoother grid connection and a capacitor bank for reactive power compensation.

Since SCIG operates in a narrow range around the synchronous speed, this turbine operates with almost constant speed, regardless of the wind speed. This concept has been very popular because of its relatively low price for mass production, its simplicity, and its robustness. However, as the fixed-speed wind turbine concept implies that the wind speed fluctuations are converted into mechanical fluctuations and consequently into electrical power fluctuations, this type of wind turbine experiences high mechanical and fatigue stress. Furthermore it has a limited power quality control, no control of its reactive power consumption, and no speed control to optimize its aerodynamic efficiency.

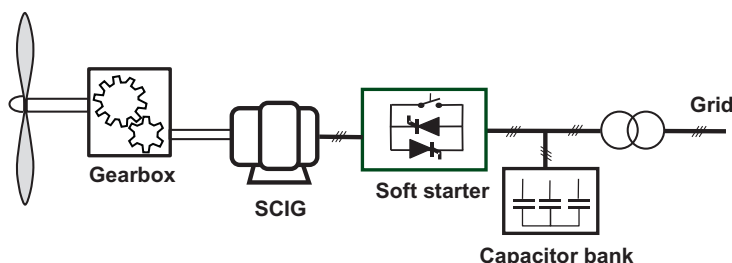


FIGURE 8.5 Fixed-speed wind turbine—Type 1.

A pole-changeable SCIG configuration corresponding to two rotation speeds has been used in some commercial wind turbines to increase the power production of these turbines, namely a generator winding set with typically 8 poles for low wind speeds and another one with 4–6 poles for medium and high wind speeds (typically 4–6 poles) [15,17].

8.3.2 Limited Variable-Speed Wind Turbines (Type 2)

This configuration corresponds to the limited variable-speed controlled wind turbine, known as OptiSlip or FlexiSlip. This type of wind turbine was promoted by the Danish manufacturer VESTAS since the mid-1990s up to 2006, and it has subsequently been used by the Indian manufacturer SUZLON [4].

As illustrated in Fig. 8.6, in this configuration the stator of a WRIG is directly connected to the grid, whereas the rotor winding is connected in series with a variable additional rotor resistance, which is controlled optically and is changed dynamically by power electronics. By changing the rotor resistance size, the speed of the turbine can be modified and thus a variable-speed operation can be achieved by controlling the energy extracted from the WRIG rotor. The size of this resistance defines thus the range of the variable speed (typically from 0% to 10%). However, some energy extracted from the controllable resistance is dumped as heat loss. This concept still needs a soft starter to reduce the inrush current and a reactive power compensator to provide the reactive power for the magnetization of the generator. The control system includes the control of the variable resistance and the pitch control of the blades.

The advantages are a simple circuit topology without slip rings and an improved operating speed range compared to that found in Type 1. To a certain extent, this concept can reduce the mechanical loads and power fluctuations caused by gusts. Some of the disadvantages are: limited speed range, as it is dependent on the size of the additional resistance; some power is

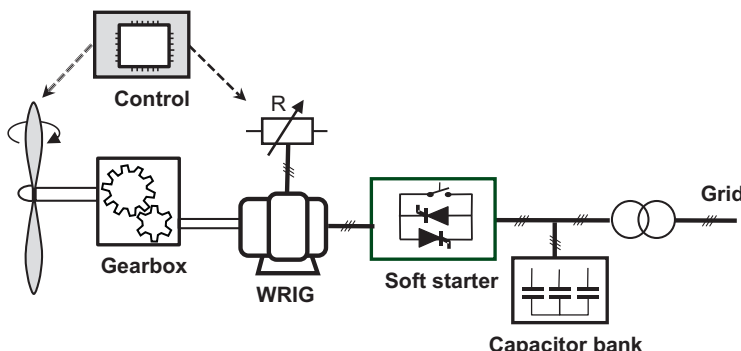


FIGURE 8.6 Limited variable-speed wind turbine—Type 2.

dissipated in the variable resistance as losses; and poor control of active and reactive power.

In summary, this concept partially solves the need for variable-speed operation to increase the aerodynamic efficiency. It is thus the first step toward the variable-speed wind turbine concept, which is the main dominating concept found in the market today.

8.3.3 Variable-Speed Wind Turbines With Partial-Scale Power Converter (Type 3)

Type 3 configuration denotes the variable-speed wind turbine concept with a DFID. It uses a partial-scale back-to-back power converter connected to the rotor of the generator, typically through slip rings. This concept supports a wide speed range operation, depending on the size of the power converter [19–20].

As illustrated in Fig. 8.7, the stator is directly connected to the grid, while the rotor is connected through a partial-scale power converter (rated at approximately 30% of nominal generator power). The power rating of this partial-scale converter defines the speed range (typically $\pm 30\%$ around synchronous speed). This converter decouples mechanical and electrical frequencies making variable-speed operation possible as it can vary the electrical rotor frequency. Moreover, this converter performs reactive power compensation and a smooth grid interconnection and therefore this configuration needs neither a soft starter nor a reactive power compensator. A slip ring is used to transfer the rotor power by means of a partial-scale converter. The power converter controls the rotor frequency, i.e., the rotor speed, enabling thus the variable-speed operation of the wind turbine [24,25]. Beside this, it also controls the active and reactive power of the generator. The control system includes the electrical control of the converter and the pitch controller of the blades to limit the power when the turbine is above the rated power.

This concept is naturally more expensive when compared with Type 1 and Type 2 solutions, however, it is still an attractive and popular option. The power converter enables the wind turbine to act as an actively

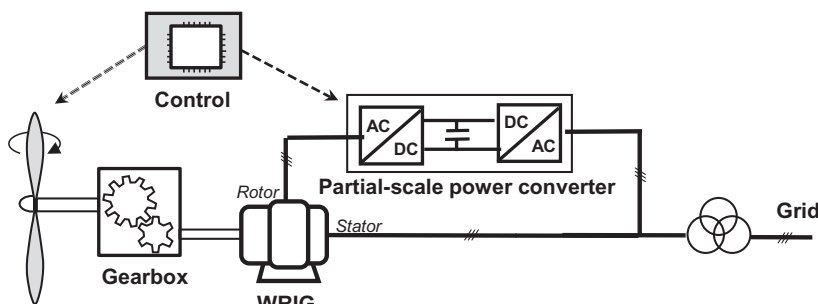


FIGURE 8.7 Variable-speed wind turbine with partial-scale power converter—Type 3.

controllable unit in the power system. Compared with Type 2, the rotor energy, instead of being dissipated, can be fed into the grid by the power electronic converter. It has a wider range of dynamic speed control compared to Type 2, depending on the size of the power converter. In addition to the fact that the converter is smaller, the losses are also lower. Its main drawbacks are the additional protection of the power converter in the case of grid faults and the use of slip rings, which requires a regular maintenance, and can result in machine failure and electrical loss [24,25].

8.3.4 Variable-Speed Wind Turbines With Full-Scale Power Converter (Type 4)

Type 4 corresponds to the variable-speed concept with full-scale power converter. The generator is connected to the grid through a full-scale power converter as illustrated in Fig. 8.8. The full-scale converter allows for the control of the generator in a speed range of up to 100%. Besides this it supports a smooth grid connection and reactive power compensation over the entire speed range. Similarly to Type 3, the control system of this concept includes the electrical control to control active and reactive power, as well as the pitch control to limit the rotor speed.

As depicted in Fig. 8.8, this concept can be implemented for different types of generator, namely the generator can be excited electrically (i.e., WRSG or WRIG) or by a permanent magnet (PMSG).

Some full variable-speed wind turbines systems have no gearbox—as depicted by the *dotted* gearbox in Fig. 8.8. In these cases, a direct-driven multipole generator is used [26]. The difference between wind turbines with and without gearbox is the generator rotor speed. The direct-driven multipole generator rotates at a low speed, because the generator rotor is directly connected to the hub of the aerodynamic rotor. The lower speed makes it necessary to produce a higher torque and therefore a large generator with large number of poles is needed. The wind turbine companies Enercon, Made, and Lagerwey supply this technology [27].

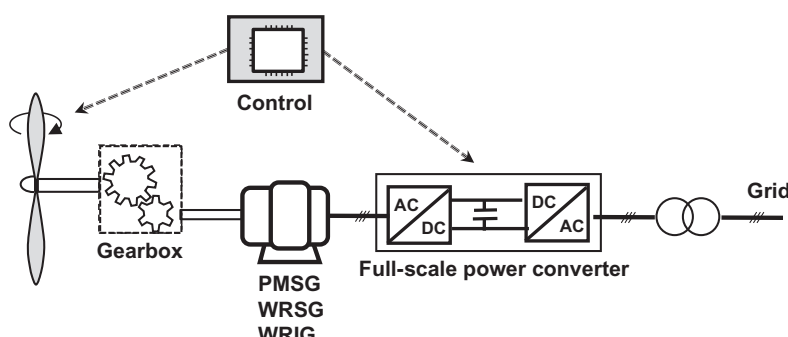


FIGURE 8.8 Variable-speed wind turbine with full-scale power converter—Type 4.

Compared with the Type 3 system, Type 4 has the advantages of a generator with: better efficiency; no slip rings; simpler or even removed gearbox; full power and speed controllability; as well as better grid support ability; and a less complex grid-fault ride-through capability. Some important benefits of removing the gearbox are reduced losses, lower costs, and increased reliability due to the elimination of rotating mechanical components.

Its main disadvantages are the more expensive converter (100% of rated power instead of 30%) and the losses in the converter, which are higher because all the power is processed by the power electronic converter. However the continuously decreasing cost of power electronics (roughly a factor of 10 over the past 10 years) and the absence of brushes might make this configuration the dominant one for development in the near future [28].

8.4 CONCLUSIONS

Over the years wind turbine technology has developed and reached a very reliable and advance level. The wind turbine technology have changed and progressed from fixed speed, stall controlled and with drive trains with gearboxes, to become variable speed, pitch-controlled and with or without gearboxes.

Today, the most dominating and promising wind turbine technologies are based on variable-speed operation concept. The increased interest in variable-speed wind turbines is due to the presence of the power electronics, which facilitate many attractive features, including reduced mechanical stress, increased power capture, as well as their ability to support the grid by complying with the increasingly onerous grid requirements. The presence of power electronics makes it thus possible for wind turbines to behave in a similar way to conventional power plants and hence actively support the grid.

As with all technologies, the future is difficult to predict. However, it is clear that future improvement of wind turbine technology will be strongly dependent on the further development of power electronics technology for wind power applications.

REFERENCES

- [1] Herbert GMJ, Iniyian S, Sreevalsan E, Rajapandian S. A review of wind energy technologies. *Renewable Sustainable Energy Rev* 2007;11:1117–45.
- [2] Chen Z, Blaabjerg F. Wind energy-the world's fastest growing energy source. *IEEE Power Electron. Soc. Newslett* 2006;18:15–19.
- [3] Li H, Chen Z. Overview of different wind generator systems and their comparisons. *Renewable Power Generation, IET* 2008;2:123–38.
- [4] Hansen AD. In: Ackermann T, editor. *Wind power in power systems*. 2nd ed. Chichester: John Wiley and Sons; 2010.
- [5] Chen Z, Guerrero JM, Blaabjerg F. A review of the state of the art of power electronics for wind turbines. *IEEE Trans Power Electron* 2009;24:1859–75.
- [6] Blaabjerg F, Liserre M, Ma K. Power electronics converters for wind turbine systems. *IEEE* 2011;48:708–19.

- [7] <https://www.google.dk/search?q=bonus+wind+turbine+picture&espv=2&biw=1280&bih=621&tbm=isch&tbo=u&source=univ&sa=X&ved=0ahUKEwis9Pj3iafNAhVGXCwKHZuSAqIQ7AkIOA#imgrc=kYwk2sNT_vaJ8M%3A>.
- [8] Mandell JF, Samborsky DD, Wang L, Wahl N. New fatigue data for wind turbine blade materials. In: ASME wind energy symposium, January 6–9 2003, Nevada USA.
- [9] Ragheb A, Ragheb M. Wind turbine gearbox technologies. In: Proceedings of the 1st international nuclear and renewable energy conference (INREC10), Amman, Jordan, March 21–24, 2010.
- [10] <<https://en.wikipedia.org/wiki/Stator>>.
- [11] <https://en.wikipedia.org/wiki/Squirrel-cage_rotor>.
- [12] <[https://en.wikipedia.org/wiki/Rotor_\(electric\)](https://en.wikipedia.org/wiki/Rotor_(electric))>.
- [13] Heier S. Grid integration of wind energy conversion systems. Chichester: Kassel University, John Wiley & Sons Ltd Germany; 1998.
- [14] Boldea I. The electric generators handbook—variable speed generators. Boca Raton, FL: Taylor & Francis; 2006.
- [15] Orabi M, El-Sousy F, Godah H, Youssef MZ. High-performance induction generator wind turbine connected to utility grid. In: Proc 26th Annu. INTELEC, Sep. 19–23, 2004. p. 697–704.
- [16] Alatalo M. Permanent magnet machines with air gap windings and integrated teeth windings, technical report 288. Sweden: Chalmers University of Technology; 1996.
- [17] Hansen LH, Helle L, Blaabjerg F, Ritchie A, Munk-Nielsen S, Bindner H, et al. Conceptual survey of generators and power electronics for wind turbines. Risø National Laboratory Technical Report Riso-R-1205(EN) Roskilde, Denmark; December 2001.
- [18] Parviainen A. Design of axial-flux permanent magnet low-speed machines and performance comparison between radial flux and axial flux machines [Ph.D. dissertation]. Acta universitatis Lappeenrantaensis; 2005.
- [19] Michalke G, Hansen AD, Hartkopf T. Modelling and control of variable speed wind turbines for power system studies. *Wind Energy* 2010;13:307–22.
- [20] Hansen AD, Sørensen P, Iov F, Blaabjerg F. Centralised power control of wind farm with doubly-fed induction generators. *Renewable Energy* 2006;31:935–51.
- [21] Muller S, Deicke M, De Doncker RW. Doubly fed induction generator systems for wind turbines. *IEEE Ind Appl Mag* 2002;8:26–33.
- [22] Altin M, Goksu O, Teodorescu R, Rodriguez P, Bak-Jensen B, Helle L. Overview of recent grid codes for wind power integration. In: Proc. of OPTIM'2010; 2010. p. 1152–1160.
- [23] Blaabjerg F, Teodorescu R, Chen Z, Liserre M. Power converters and control of renewable energy systems. In: Proc. 6th Int. conf. power electron, vol. 1; October 18–22, 2004. p. 1–20.
- [24] Erickson RW, Maksimovic D. Fundamentals of power electronics. Boulder, CO: Springer Science+Business Media; 2001.
- [25] Larsson A. The power quality of wind turbines [Ph.D. dissertation]. Goteborg: Chalmers University of Technology; 2000.
- [26] Dubois MR, Polinder H, Ferreira JA. Comparison of generator topologies for direct-drive wind turbines. *IEEE Nordic workshop on power and industrial electronics*. New York, NY: IEEE; 2000. p. 22–6.
- [27] Carlson O, Hylander J, Thorborg K. Survey of variable speed operation of wind turbines'. In: European union wind energy conference, Sweden; 1996. p. 406–409.
- [28] Kazmierkowski MP, Krishnan R, Blaabjerg F. Control in Power Electronics—Selected problems. London and New York, NY: Academic Press; 2002.

Chapter 9

Aerodynamics and Design of Horizontal-Axis Wind Turbines

Martin O.L. Hansen

Technical University of Denmark, Lyngby, Denmark

9.1 INTRODUCTION

A wind turbine is a device that transforms the kinetic energy in the wind into electricity, and the overall object is to make a machine that will survive all the expected loads in the design lifetime of typically 20 years and to produce electrical energy as cheap as possible, i.e., more formally to minimize the Levelized Cost of Energy (LCoE) and usually expressed in terms of dollars per kilowatt hour. To do this one must know something about the environmental input to the wind turbine as related to wind speed distribution, atmospheric turbulence and for an offshore wind turbine also a description of the sea state. Standards/norms, such as the International Electrotechnical Commission's document, IEC 61400-3, have been made that compiles all the load cases that must be considered in order to have a safe design.

The various environmental inputs and load cases must be transformed into forces including aerodynamic loads to verify the structural integrity of the wind turbine. Being able to calculate the aerodynamic loads is also needed to calculate the power production for a given wind speed and is thus an important element in the optimization process minimizing the LCoE. The objective of this chapter is to describe the aerodynamics of a wind turbine both qualitatively and quantitatively in order to have the tools for designing an aerodynamically efficient rotor. To fully follow all the derivations, requires a basic knowledge in fluid mechanics, but only at a fundamental level since exclusively the very basic conservation laws from classic physics are applied.

To understand the power contained in the wind one can consider an area normal to the wind velocity as shown in Fig. 9.1. After a time Δt the volume of air particles that has passed this area is $A \cdot V_o \cdot \Delta t$, (where A is the cross-

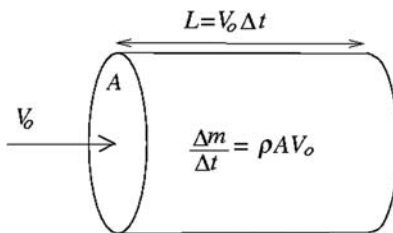


FIGURE 9.1 Air flow passing the area, A .

sectional area and V_o is the velocity) weighing $\Delta m = \rho \cdot A \cdot V_o \cdot \Delta t$ (where ρ is the density) and having a kinetic energy $E_{kin} = 1/2\Delta m V_o^2 = 1/2\rho V_o^3 A \Delta t$ and thus the available power (energy per time) in the wind is $P_{avail} = 1/2\rho V_o^3 A$. The available power is thus proportional to the density of the air, the rotor area, and very importantly the wind speed cubed, and it is the purpose of any wind turbine to transform as cheap as possible some of this into useful power.

9.2 A SHORT DESCRIPTION ON HOW A WIND TURBINE WORKS

To comprehend the equations used to compute the aerodynamic loads on a wind turbine rotor it is very useful first to learn how a wind turbine basically works. It is clear that a device is needed that will slow down the wind speed in order to extract kinetic energy from the air and at the same a torque must be created that eventually can drive an electrical generator. Both can be accomplished by a few spinning blades having cross sections shaped as conventional airfoils as shown in Fig. 9.2.

The upper part of Fig. 9.2 shows the rotor seen from the front and the lower part displays the unfolded cut in the rotor plane at the radial position, r , indicated by the dashed line and seen directly from above. The first thing to note in the lower part of Fig. 9.2 is that the wind speed approaching the rotor has been reduced by a factor $a \cdot V_o$, so that the apparent wind at the rotor plane is $(1 - a)V_o$. The in-plane velocity is mainly the rotational speed of the blade at the radial distance r from the rotor axis, ωr , (where ω is the angular velocity of the rotor) but also a small extra contribution, $a'\omega r$, is present, so that the effective tangential velocity experienced by the rotor is $(1+a')\omega r$. The two nondimensionalized velocities, a , and, a' , are called the axial- and the tangential induction factors, respectively, and if they were known, the relative wind, V_{rel} , approaching the rotor plane can be drawn in the so-called velocity triangle, see the lower left sketch in Fig. 9.2. By definition the lift is perpendicular and the drag parallel to the relative velocity as sketched in Fig. 9.2. The net aerodynamic loading is the vector sum of the lift and drag

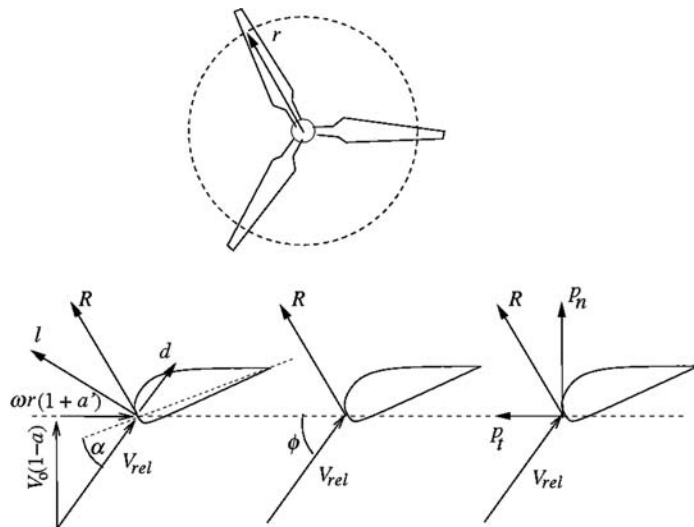


FIGURE 9.2 Local flow at the rotor blades at radial position r .

and denoted, R , in the figure and is the integral of the pressure and skin friction distribution on the airfoils at this radial position. It is seen that this resulting aerodynamic load vector has a component into the wind, p_n , and an in-plane component, p_t . The in-plane component, p_t , delivers the required torque to the shaft and the normal loading provides a contribution to the necessary thrust force that is reducing the wind speed in order to extract power from the wind. It is also, p_n , and, p_t , that are responsible for the induced wind speeds $a \cdot V_o$ and $a' \cdot \omega r$, since these are the reactions on the wind velocity from the blade loadings. This ends the qualitative description of how a wind turbine works and next will be shown how the aerodynamic loadings and induced velocities can be quantitatively determined and thus eventually be used as a design tool.

9.3 1D MOMENTUM EQUATIONS

The 1D momentum theory goes back more than 100 years and was developed by Froude and Rankine and is therefore often called the Rankine–Froude theory. The theory was originally developed for marine propulsion, but will be shown here for a wind turbine rotor. The rotor is modeled as a permeable disc with a normal load equally distributed over the rotor plane giving rise to a constant velocity profile in the wake. The integral of the normal loading can be integrated into one thrust force, T , as shown in Fig. 9.3. Only the flow confined by the streamlines touching the rotor tip is

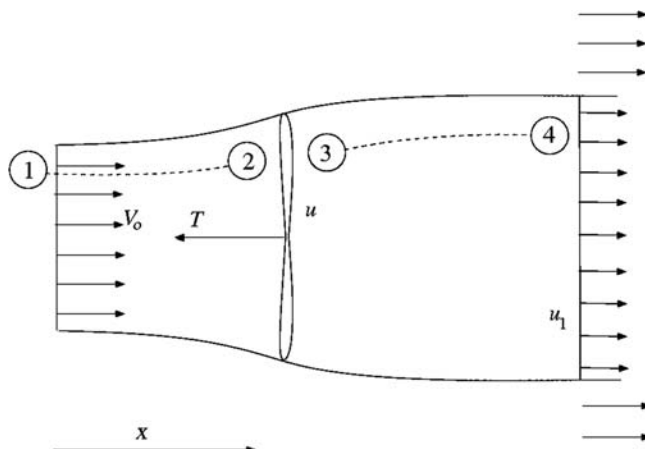


FIGURE 9.3 A simple wind turbine rotor model made as a permeable disc with constant loading giving basically a 1D flow.

affected by the thrust force and the free wind speed upstream is gradually being reduced to a lower value in the wake, as sketched in Fig. 9.3.

It is seen in Fig. 9.3 that the velocity due to the thrust force, T , is decreasing with the downstream distance and since the mass flow is the same at any downstream plane the streamlines have to expand. The undisturbed wind speed is denoted V_o , the reduced velocity in the rotor plane is u and the velocity in the wake is u_1 . According to Section 9.2 the velocity in the rotor plane u may also be written as $u = (1 - a)V_o$. Since there is no flow across the lateral streamlines touching the rotor tip the conservation of energy assuming no loss for the control volume confined by these are easily determined as

$$P = \frac{1}{2}\dot{m}(V_o^2 - u_1^2) = \frac{1}{2}\rho u A(V_o^2 - u_1^2) \quad (9.1)$$

where ρ is the density of the air, A the rotor area, and P the power extracted from the wind. In deriving Eq. (9.1) is assumed that the pressure at the outlet has recovered to the ambient pressure, since the streamlines are now parallel again and also that none of the mechanical energy is dissipated into heat. Furthermore, one may apply the Bernoulli equation along the streamline from 1 to 2 and again from 3 to 4 as indicated in Fig. 9.3.

$$\begin{aligned} p_o + \frac{1}{2}\rho V_o^2 &= p^+ + \frac{1}{2}\rho u^2 \\ p^- + \frac{1}{2}\rho u^2 &= p_o + \frac{1}{2}\rho u_1^2 \end{aligned} \quad (9.2)$$

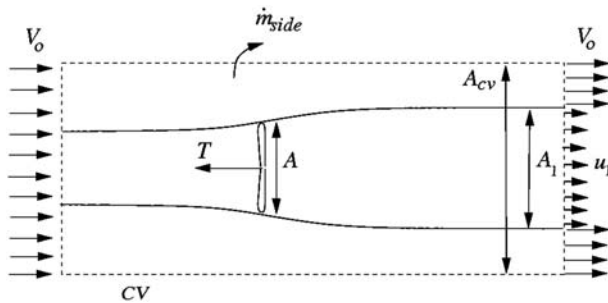


FIGURE 9.4 The *dashed line* indicates a cylindrical control volume enclosing the flow through the ideal wind turbine rotor and is used for evaluating relationship between the flow and thrust force.

where p_o denotes the ambient pressure, p^+ the pressure just upstream of the rotor, and p^- the pressure just behind the rotor. These equations may be combined to

$$\Delta p = p^+ - p^- = \frac{1}{2} \rho (V_o^2 - u_1^2) = \frac{1}{2} \rho (V_o + u_1)(V_o - u_1) \quad (9.3)$$

where Δp is the pressure drop over the rotor disc. Next a cylindrical control volume totally enclosing the flow through the rotor is considered as drawn by the *dashed line* in Fig. 9.4. Since the lateral boundary of this control volume is horizontal the pressure around the control volume can only contribute to an axial force at the in- and outlet planes, and here the pressure is assumed to be the ambient value. Therefore the net pressure force is zero and the only remaining force in the flow direction is the unknown thrust force, T . The lateral boundaries are no longer streamlines so there is a mass flow crossing the lateral boundaries of the control volume and that is carrying axial momentum. The conservation of axial momentum thus becomes

$$-T = \rho A_1 u_1^2 + \rho (A_{cv} - A_1) V_o^2 + \dot{m}_{side} V_o - \rho A_{cv} V_o^2 \quad (9.4)$$

And combining this with the conservation of mass

$$\dot{m}_{side} = \rho A_{cv} V_o - \rho A_1 u_1 - \rho (A_{cv} - A_1) V_o = \rho A_1 (V_o - u_1) \quad (9.5)$$

Yields

$$T = \rho A u (V_o - u_1) \quad (9.6)$$

Now since the thrust can also be expressed as the pressure drop over the rotor disc times the area the combination of Eqs. (9.3) and (9.6) gives:

$$u = \frac{1}{2} (V_o + u_1) \quad (9.7)$$

Since by definition $u = (1 - a)V_o$ Eq. (9.7) gives that the velocity in the wake becomes $u_1 = (1 - 2a)V_o$ and if this is introduced into Eq. (9.1) the power can written as:

$$P = 2\rho a(1-a)^2 V_o^3 A \quad (9.8)$$

The power is often nondimensionalized with the available power in the wind into the so-called power coefficient

$$C_p = \frac{P}{\frac{1}{2} \rho V_o^3 A} \quad (9.9)$$

And introducing Eq. (9.8) into (9.9) a simple expression is derived for an ideal power coefficient, C_p , assuming 1D flow and no losses

$$C_p = 4a(1-a)^2 \quad (9.10)$$

It is seen that the maximum value of Eq. (9.10) is $C_p = 16/27 \approx 60\%$ and occurs for $a = 1/3$. This is known as the Betz limit and is an upper theoretical value for the power coefficient of a wind turbine.

Also a thrust coefficient, C_T , is defined as:

$$C_T = \frac{T}{\frac{1}{2} \rho V_o^2 A} \quad (9.11)$$

And it can be shown that using the definition of the axial induction factor and Eqs. (9.6) and (9.7) that the thrust coefficient for an ideal rotor becomes

$$C_T = 4a(1 - a) \quad (9.12)$$

The value of the thrust coefficient giving the theoretical maximum power coefficient is thus $C_T = 8/9$.

Even though a real rotor is not ideal and cannot be modeled as simple as a permeable disc, the Eqs. (9.10) and (9.12) still tell us something about the maximum that can be achieved; this happens for a thrust force giving an axial induction factor of approximately $a = 1/3$. Measurements verify that Eq. (9.12) is valid up to approximately $a = 1/3$ and for higher values of the axial induction factor an empirical correlation called the Glauert correction is used, and one often used expression is:

$$C_T(a) = \begin{cases} 4a(1 - a) & \text{for } a < 0.3 \\ 4a \left(1 - \frac{1}{4}(5 - 3a)a \right) & \text{for } a \geq 0.3 \end{cases} \quad (9.13)$$

9.4 BLADE ELEMENT MOMENTUM METHOD

The blade element momentum (BEM) method as described by Glauert [1] is a generalization of the momentum theory coupled to the blade element theory often attributed to Drzewiecki. The blade element theory is that the flow past a given section is considered 2D and that the effective inflow velocity can be constructed as the vector sum of the incoming velocity and the rotational speed. However, when doing this one must also, as was shown by Glauert, include the induced velocities that are the reaction on the incoming flow from the aerodynamic blade loads. When doing this one can draw the so-called velocity triangle as shown in Fig. 9.5, where the induced velocity is included as \mathbf{W} , and where the axial component is given as aV_o (consistent with the 1D momentum theory) and the tangential component as $a'\omega r$. Provided that the induced velocity is known, one can calculate the size and direction of the relative velocity. Assuming locally a 2D flow past an airfoil and that the lift and drag coefficients are available as a function of angle of attack and the Reynolds number, the lift and drag can be calculated as will be shown later. The problem left is then to estimate the induced velocities that are in equilibrium with the aerodynamic loads, and this is exactly what the BEM theory does.

In BEM the loads and induced wind speeds are computed at a finite number of radial positions also denoted as elements. Furthermore, it is assumed that these elements are independent. A streamtube with thickness, dr , around each element is considered as shown in Fig. 9.6. The two lateral sides are assumed to be made up of streamlines and the partly empirical Eq. (9.13) is presumed also to be valid for the streamtube in Fig. 9.6. Furthermore, it is assumed that there are no azimuthal variations of the velocities at the outlet, u_1 , and in the rotor plane, u , which is only true if the thrust is also azimuthally constant corresponding to an infinite number of blades. A correction to this, denoted Prandtl's tip loss correction, is introduced later. But for the moment the equations are derived as if the aerodynamic loads are distributed evenly at the area of the strip cutting the rotor plane $dA = 2\pi r dr$. The thrust from one blade can be estimated from the blade element at the same radial position, r , from Fig. 9.7.

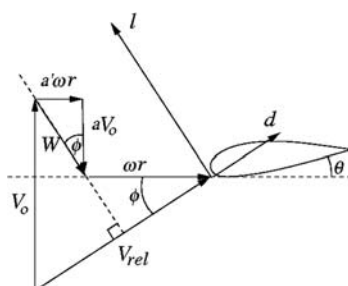


FIGURE 9.5 The velocity triangle used to compose the relative velocity approaching an element of the rotor at a radial distance, r , from the rotational axis.

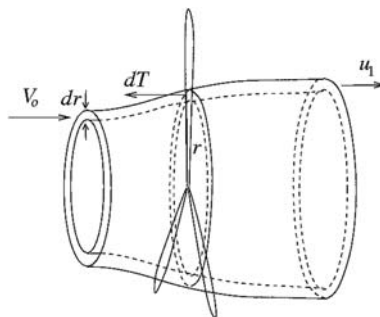


FIGURE 9.6 A streamtube of thickness, dr , intersecting the radial position, r , on the rotor plane.

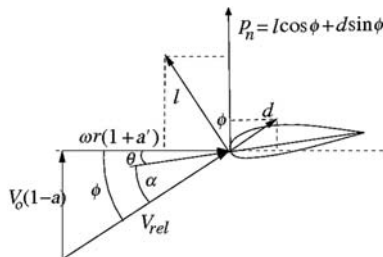


FIGURE 9.7 Velocities and aerodynamic loads at a blade element at a radial distance, r , from the rotational axis of rotation.

Provided that the axial and tangential induction factors, a and a' , are known the angle of the incoming relative wind with the rotor plane, ϕ , called the flow angle (Fig. 9.7) can be computed as:

$$\tan \phi = \frac{(1-a)V_o}{(1+a')\omega r} \quad (9.14)$$

And the size of the relative wind speed as

$$V_{rel}^2 = (1-a)^2 V_o^2 + (1+a')^2 (\omega r)^2 \quad (9.15)$$

Knowing the angle between the rotor plane and the airfoil chord, θ , the local angle of attack is

$$\alpha = \phi - \theta \quad (9.16)$$

The lift and drag coefficients are then found by a table look-up, $C_l(\alpha, Re)$ and $C_d(\alpha, Re)$, for the airfoil applied at this radial position, and from these the lift and drag (in units of $N m^{-1}$) can be computed as:

$$\begin{aligned} l &= \frac{1}{2} \rho V_{rel}^2 c C_l(\alpha, Re) \\ d &= \frac{1}{2} \rho V_{rel}^2 c C_d(\alpha, Re) \end{aligned} \quad (9.17)$$

Next, these aerodynamic loads are projected normal (see also Fig. 9.7) and tangential to the rotor plane as

$$\begin{aligned} p_n &= l \cos \phi + d \sin \phi \\ p_t &= l \sin \phi - d \cos \phi \end{aligned} \quad (9.18)$$

Finally, the thrust force at the streamtube in Fig. 9.6, can be calculated as

$$dT = B p_n dr \quad (9.19)$$

since p_n multiplied by dr is the force from one blade and B being the number of blades. Eq. (9.19) is nondimensionalized as in the definition for the thrust coefficient Eq. (9.11), but using the strip area of the streamtube intersecting the rotor plane and using Eqs. (9.18) and (9.17) to determine the normal load and introducing the solidity, $\sigma = Bc/2\pi r$

$$C_T = \frac{dT}{\frac{1}{2} \rho V_o^2 2\pi r dr} = \frac{\sigma(1-a)^2(C_l \cos \phi + C_d \sin \phi)}{\sin^2 \phi} \quad (9.20)$$

One can also apply the conservation of angular momentum for the control volume in Fig. 9.6 to find a relationship between a' and the torque from the aerodynamic loads noting that the angular velocity upstream of the rotor is 0 and $2a'\omega r$ in the wake

$$dM = mr2a'\omega r = 2\pi r dr \rho(1-a)V_o r 2a'\omega r = 4\pi r^3 \rho V_o \omega \cdot a'(1-a) dr \quad (9.21)$$

The torque can also be found directly from the tangential loads as:

$$dM = Br p_t dr = Br \frac{1}{2} \rho V_{rel}^2 c C_t dr = \frac{1}{2} \rho B \frac{V_o(1-a)\omega r(1+a')}{\sin \phi \cos \phi} r c C_t dr \quad (9.22)$$

Note that C_t in Eq. (9.22) is not the thrust coefficient but the tangential force coefficient given as:

$$C_t = C_l \sin \phi - C_d \cos \phi \quad (9.23)$$

From Eqs. (9.21) and (9.22) an expression for the tangential induction factor is derived

$$a' = \frac{\frac{1}{4 \sin \phi \cos \phi}}{\sigma C_t} - 1 \quad (9.24)$$

To describe the blade geometry one needs to have at some discrete radial positions (typically around 10–15 stations) the chord, $c(r)$, the twist, $\beta(r)$, and a table with the lift and drag coefficients as function of angle of attack. The chord, $c(r)$, is the local width of the blade, the pitch, θ_p , is the angle between the rotor plane and the tip airfoil and the twist the angle between a local airfoil along the blade and the tip airfoil as shown in Fig. 9.8.

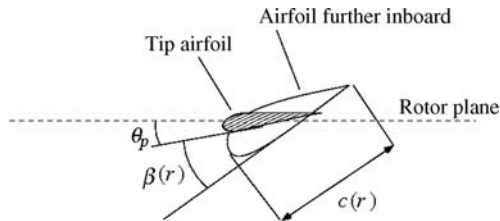


FIGURE 9.8 Sketch showing the chord, the twist and the pitch angle on a blade.

The angle between one blade element and the rotor plane θ in Eq. (9.16) is thus given as:

$$\theta(r) = \theta_p + \beta(r) \quad (9.25)$$

To evaluate the momentum equations from the control volume in Fig. 9.6, it has been assumed that there is no azimuthal variation of the induced velocities at the outlet, which would only be true for a rotor with infinite number of blades. Prandtl made a correction to the aerodynamic loads evaluated from the velocity triangle as in Fig. 9.7, so that when these are used for a rotor with infinite number of blades one gets approximately the same induction as for the real rotor with B blades. Prandtl evaluated the induced velocities from a lifting line model, where the blades are modeled as lines with a bound circulation distribution along the span. The local bound circulation can be estimated from Kutta–Joukowski theorem and the definition of the lift coefficient as:

$$\Gamma(r) = \frac{1}{2} V_{rel} c C_l \quad (9.26)$$

Next, there are vortices trailing from the blades and lying in a helical path as shown in Fig. 9.9 for a two-bladed rotor. The strength of the trailed vortices is given as the gradient of the bound circulation according to Helmholtz theorem. The only free parameter is then the helical pitch angle of the trailed vortex lines that must be specified, since the resulting induced velocities on the blades from this vortex system is a function of this pitch. But for a lightly loaded rotor the pitch can be approximated from the free wind speed and the angular velocity only. Knowing the geometry and the strength of the vortex lines the induced velocity, \mathbf{W} , can be computed on the blades using Biot–Savart law for every vortex line:

$$\mathbf{W} = \frac{\Gamma}{4\pi} \int \frac{d\mathbf{s} \times \mathbf{r}}{|\mathbf{r}|^3} \quad (9.27)$$

where Γ is the circulation of one vortex line, $d\mathbf{s}$, a small piece of the line with direction tangent to the line, and \mathbf{r} the radius vector from that small piece to the point where the induced velocity is evaluated.

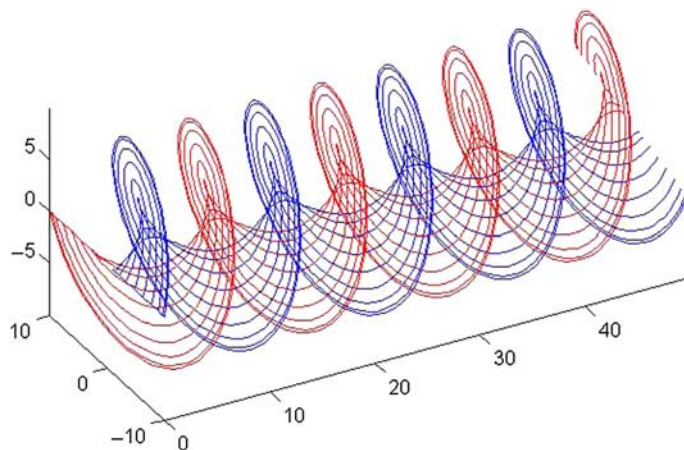


FIGURE 9.9 The vortex system behind a wind turbine rotor, $B = 2$.

Prandtl solved this system using potential flow and a simple assumption of the wake geometry and came up with a correction to the loads, so that the induction at the blades become the same as a rotor with an infinite number of blades. The loads from the velocity triangle shown in Fig. 9.7 is divided by a factor, F , denoted by Prandtl's tip loss correction, to model a system with an infinite number of blades that gives approximately the same solution as the vortex system shown in Fig. 9.9 for a finite number of blades. Then one can apply these loads to the momentum equations derived for an infinite number of blades:

$$F = \frac{2}{\pi} \arccos \left(\exp \left(-\frac{B R - r}{2 r \sin \phi} \right) \right) \quad (9.28)$$

where R is the rotor radius, r the local radius, and ϕ the local flow angle. When this correction is applied to the momentum equations (9.13) and (9.24) these become:

$$C_T(a) = \begin{cases} 4aF(1-a) & \text{for } a < 0.3 \\ 4aF \left(1 - \frac{1}{4}(5-3a)a \right) & \text{for } a \geq 0.3 \end{cases} \quad (9.29)$$

and

$$a' = \frac{1}{\frac{4F \sin \phi \cos \phi}{\sigma C_t} - 1} \quad (9.30)$$

Now one has finally, all the equations needed to calculate the aerodynamic loads on a wind turbine rotor for a given blade geometry.

9.4.1 The Blade Element Momentum Method

The necessary input for the BEM method is as follows. First one has to decide the number of elements, typically 10–15, and their radial positions. The airfoil data in the form of lift and drag coefficients at each station as function of angle of attack and possibly the Reynolds number, must be obtained. Furthermore, the chord and twist must be known at the elements. With the geometry given, one must also define the operational parameters in the form wind speed V_o , pitch angle θ_p , and rotational speed ω .

For each element:

1. Guess a value of the induction factors, a and a'
2. Calculate flow angle ϕ using Eq. (9.14)
3. Calculate angle of attack using Eqs. (9.16) and (9.25)
4. Determine lift and drag coefficients from tabulated airfoil data
5. Calculate Prandt's tip loss factor Eq. (9.28)
6. Calculate thrust coefficient using Eq. (9.20)
7. Calculate new value of axial induction factor a^{new} from Eq. (9.29)
8. Calculate tangential force coefficient using Eq. (9.23)
9. Solve Eq. (9.30) for a new value of the tangential induction factor a'^{new}
10. Compare the new values of a and a' with the values from previous iteration and if $|a^{\text{new}} - a^{\text{old}}| < \varepsilon$ stop else go back to Step (2) and calculate a new flow angle, etc.

The BEM method described above is the classical one derived by Glauert [1], and is sufficient for blade design. But for unsteady load estimation this must be complemented by more submodels to handle the dynamic response of the induced wind to time-varying loads from the angle of attack changing due to, e.g., atmospheric turbulence, tower passage, and wind shear. To read more about this is referred to textbooks such as Hansen [2], Manwell et al. [3], Burton et al. [4], and Schaffarczyk [5].

9.5 USE OF STEADY BLADE ELEMENT MOMENTUM METHOD

The BEM method can be used to analyze a given rotor design by computing the loads for varying operational parameters: angular velocity ω , pitch angle θ_p , and wind speed V_o . On a stall controlled wind turbine the blades are rigidly mounted to the hub and the pitch angle is thus constant. Further, an asynchronous generator is typically used where the rotational speed is almost constant, leaving only the wind speed as a free parameter. Fig. 9.10 shows the measured and computed power as function of wind speed for the Tellus 100 kW. The geometry for this rotor is reported in Schepers et al. [6]. It is seen that for low wind speeds where the angles of attack are also low and the local flow attached there is a very good agreement between the measured and computed power using 2D airfoil data. However, when using pure 2D

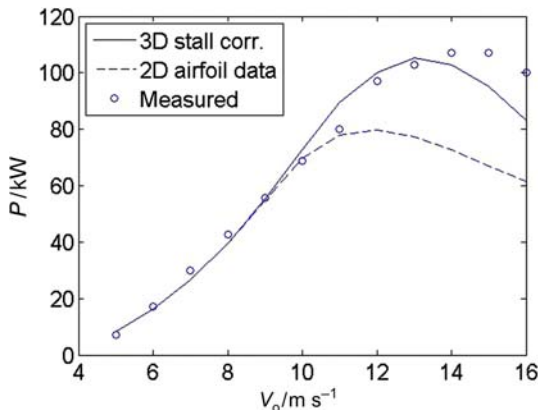


FIGURE 9.10 The measured and computed power curve for a 100 kW Tellus wind turbine as described in [6].

airfoil data the flow seems to stall too early with a resulting underestimation of the power at high wind speeds, and to improve the numerical results one must correct the 2D airfoil data in stall using a stall delay model that takes into account the effects of rotation on the stalled boundary layer. The model used here is found in Chaviaropoulos and Hansen [7] and alters the lift coefficient as:

$$C_{l,3D}(\alpha) = C_{l,2D}(\alpha) + 2.2 \cdot \left(\frac{c}{r} \right) \cdot \Delta C_l(\alpha) \quad (9.31)$$

$$\Delta C_l = C_{l,inv} - C_{l,2D}$$

where r is the radial distance to the rotational axis, c the chord, and $C_{l,inv}$ the inviscid lift coefficient. It should also be mentioned that the correction is only applied up to deep stall, where the 2D data are again applied. The Tellus turbine is a relatively small rotor with a radius of only 9.5 m and the rotational effects are thus stronger than on larger wind turbines, where the term (c/r) becomes small at the outer part of the blades. The overall blade data for the Tellus turbine is shown in Table 9.1 and the NACA 63 n-2nn airfoil is used, where the two last digits denote the thickness. 2D airfoil data can be found in airfoil catalogues, but are given in Ref. [6] for thicknesses 12, 15, 18, 21, and 25 and to find the actual airfoil data for a given thickness one has to interpolate between these 5 thicknesses. The rotational speed is 47.5 revolutions per minute (RPM) and the pitch angle is $\theta_p = -1.5$ degrees.

In Fig. 9.11 is shown the computed thrust force as function of wind speed for the stalled regulated Tellus wind turbine and it is seen that the thrust force increases with wind speed and stays high in high wind speeds, and in

TABLE 9.1 Global Blade Data for the 100 kW Tellus Wind Turbine as Described in Ref. [6]

Radial Position/m	Twist β /Degrees	Chord/m	Airfoil Thickness/%
2.70	15.0	1.090	24.6
3.55	9.5	1.005	20.7
4.40	6.1	0.925	18.1
5.25	3.9	0.845	17.6
6.10	2.4	0.765	16.6
6.95	1.5	0.685	15.6
7.80	0.9	0.605	14.6
8.65	0.4	0.525	13.6
9.50	0	0.445	12.6

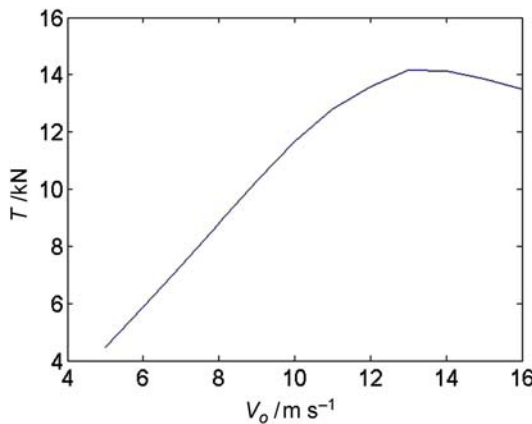


FIGURE 9.11 Computed thrust curve for the Tellus 100 kW wind turbine.

Fig. 9.12 is plotted the computed power and thrust coefficients. From Fig. 9.12 is seen that this wind turbine runs most efficiently between 6 and 9 m s^{-1} , where C_p is around 0.44.

Many large wind turbines are pitch regulated, where the entire blades can be pitched to alter the angles of attack along the blade and thus also the loads. An example of a pitch regulated wind turbine is the 2 MW Tjaereborg wind turbine as described in Hau et al. [8]. The blades are NACA44xx airfoils and the overall rotor geometry is summarized in Table 9.2. Again airfoil data are found in airfoil catalogues as, e.g., Abbott and Doenhoff [9] and

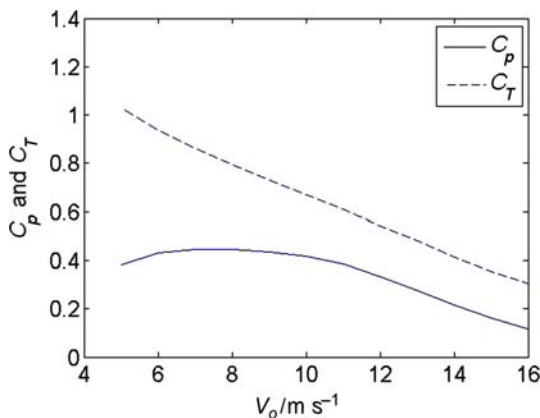


FIGURE 9.12 Computed thrust and power coefficients for the Tellus 100 kW wind turbine.

TABLE 9.2 Global Blade Data for the 2 MW Tjaereborg Wind Turbine as Described in Ref. [8]

Radial Position/m	Twist $\beta/\text{Degrees}$	Chord/m	Airfoil Thickness/%
6.46	8.0	3.3	30.58
9.46	7.0	3.0	24.10
12.46	6.0	2.7	21.13
15.46	5.0	2.4	18.70
18.46	4.0	2.1	16.81
21.46	3.0	1.8	15.46
24.46	2.0	1.5	14.38
27.46	1.0	1.2	13.30
28.96	0.5	1.05	12.76
30.46	0.0	0.90	12.22

then interpolated in thickness for a specific element. The nominal rotor speed at rated power is 22.36 RPM and the pitch can vary between -2 and 35 degrees. Since the blades are pitched when reaching rated power of 2 MW the amount of stall is small and there is no need to correct the airfoil data for 3D rotational effects. With the BEM code it is possible to compute the necessary pitch to exactly keep the rated power at high wind speeds by varying the pitch until it is reached (Fig. 9.13) and the corresponding power and thrust curves are shown in Figs. 9.14 and 9.15. Note that the thrust first

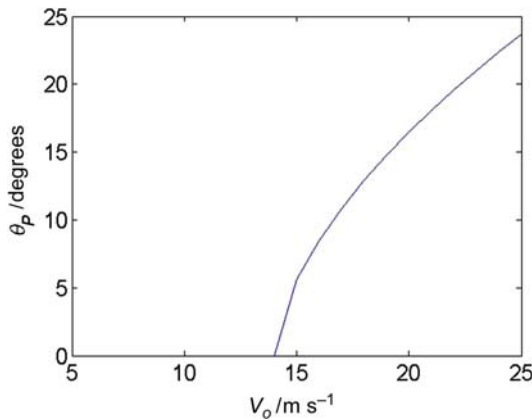


FIGURE 9.13 Computed pitch angle as function of wind speed for the 2 MW Tjaereborg wind turbine.

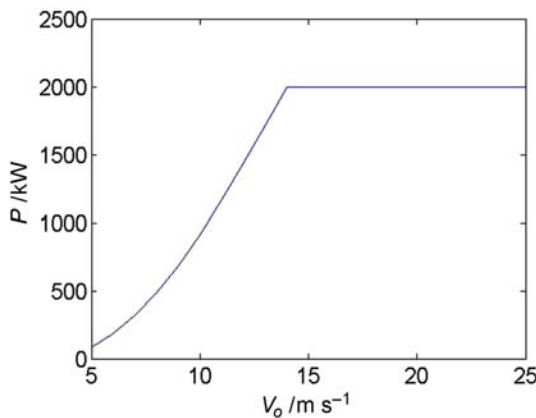


FIGURE 9.14 Computed power curve for the 2 MW Tjaereborg machine.

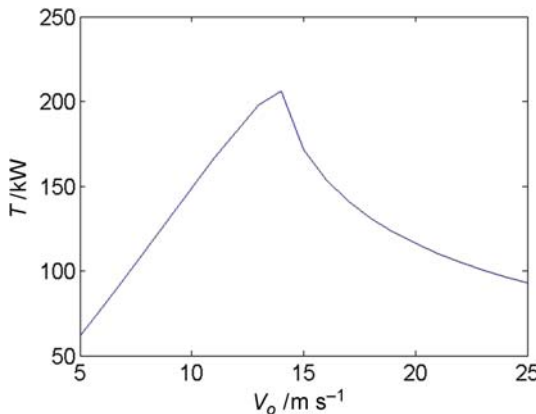


FIGURE 9.15 Computed thrust as function of wind speed for the Tjaereborg wind turbine.

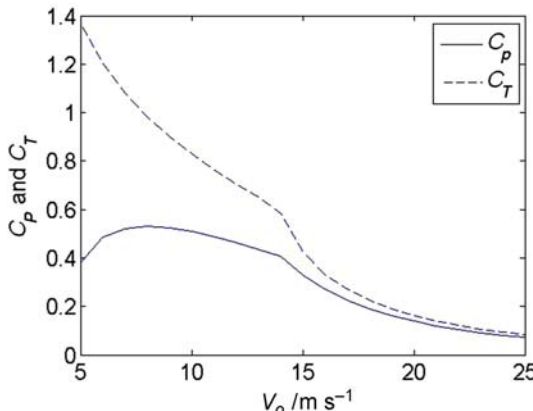


FIGURE 9.16 Power and thrust coefficients for the 2 MW Tjaereborg machine.

increases with wind speed but starts to decrease as soon as the blades are pitched toward lower angles of attack. Even though the Tjaereborg rotor is pitch regulated it is still only operating most efficiently at one wind speed ($C_{p,max} = 0.5$ at $V_o = 8 \text{ m s}^{-1}$) as shown in Fig. 9.16, where the power and thrust coefficients are plotted against wind speed.

Modern wind turbine can further vary the angular velocity within a certain range. And assuming that for a given wind turbine the power depends on the air density, the viscosity, the wind speed, the rotor radius, the angular velocity, and the pitch angle as

$$P = f(\rho, \mu, V_o, R, \omega, \theta_p) \quad (9.32)$$

one can derive that

$$C_p = f\left(\frac{\rho V_o R}{\mu}, \frac{\omega R}{V_o}, \theta_p\right) \quad (9.33)$$

The first parameter is the Reynolds number and this effect is small for large rotors and the second parameter is called the tip speed ratio λ . There is thus one combination of the tip speed ratio and pitch angle ($\lambda_{opt}, \theta_{p,opt}$) that for a given design gives the highest possible power coefficient, and requires that the rotational speed varies as

$$\omega(V_o) = \frac{\lambda_{opt}}{R} V_o \quad (9.34)$$

and that the pitch angle is kept at $\theta_{p,opt}$. Then the wind turbine will run at the highest possible efficiency for all wind speeds. However, this is in practice only possible up to a certain wind speed, since the rotational speed from Eq. (9.34) will become too large, so that the tip speed exceeds approximately $80-90 \text{ m s}^{-1}$ where the aerodynamic noise becomes unacceptable. For such

a turbine the power and thrust coefficients will be constant at their optimum value for the lower wind speeds and then start to decrease similar to Fig. 9.16, when the optimum tip speed ratio no longer can be kept as required by Eq. (9.34).

9.6 AERODYNAMIC BLADE DESIGN

Before describing a blade design process and how the BEM method can be used one needs first to define a good design. The object of any wind turbine related project is to reduce the price of producing 1 kW h considering the overall costs over the entire lifetime. To do this one must have a reliable cost model including, e.g., materials, manufacturing, and operation and maintenance cost, which is outside the scope of this chapter. Instead focus will be purely on obtaining an aerodynamically efficient rotor producing as many kWh m⁻² a⁻¹ (where a refers to annum) as possible, assuming this will also be the most economically profitable design. The actual design depends whether the turbine is stall regulated, pitch regulated, or variable speed pitch regulated. But in all cases one must combine the power curve $P(V_o)$, with a given site-specific wind distribution $h(V_o)$, where h is the actual annual number of hours in the wind speed interval $V_o \pm 0.5 \text{ m s}^{-1}$. The total annual energy production is the sum of $\sum h \cdot P$ (in units of kW h) for all wind speed intervals between start and stop. Especially for a stall-regulated wind turbine the actual design will depend strongly on the actual wind distribution at a given site. First one must decide on a rotor radius and the airfoils. Today there exist airfoils specifically designed for wind turbine blades as, e.g., the Risø-A1 (fixed rotor speed, stall, or pitch), Risø-B1 (variable speed and pitch control), and Risø-P (pitch regulated, variable, or constant rotor speed) families, see Ref. [10]. The shape of these airfoils were described by only a few degrees of freedom, DOFs, and a fifth order B-spline and the optimum values for the DOFs were found using a Simplex method optimizing various object functions, depending on whether the airfoil is to be used at the root, the mid, or tip of the blade. The aerodynamics for a given set of DOFs was determined using the XFOIL code [11]. The important properties for a wind turbine airfoil are summarized and prioritized in Table 9.3 (inspired by Fuglsang and Bak [10]) depending on its radial placement. It is clear that the main purpose of the root sections is to carry high bending moment and therefore the structural properties are most important, and hence the high thickness to chord ratio. However, also the geometrical compatibility is important, since these airfoils must morph smoothly with the geometries at the mid and tip part of the blade. At the outer part of the blade contributing mostly to the thrust and power production the aerodynamic properties such as high lift, high lift to drag ratio, benign poststall behavior, low roughness sensitivity and low noise are all very important. And the airfoils at the mid part of the blades should be able

TABLE 9.3 Relative Importance of Airfoil Properties

	Root	Mid Part	Tip
Thickness to chord ratio/%	>27	21–27	15–21
Structure	+++	++	+
Geometrical compatibility	++	++	++
Maximum roughness insensitivity		+	+++
High max lift coefficient		+	+++
Benign post stall behavior		+	+++
Low aerodynamic noise			+++

to both carry loads and produce power and be geometrically compatible with the root and tip airfoils. It is very important to verify the designs found using preferably both Computational Fluid Dynamics (CFD) and wind tunnel experiments, since XFOIL is based on the integral boundary layer equations not fully valid after stall, and therefore especially the real poststall behavior may be different. Further, it is possible to cure some of the bad aerodynamic properties of the thick root airfoils by applying vortex generators and Gourney flaps, see Ref. [12].

Now having decided on the airfoils one can start to think about how to design a good blade with respect to chord and twist distribution. The easiest and most straightforward design is a so-called one-point design, where the blade layout is calculated to obtain the highest possible power coefficient for one specific tip speed ratio and pitch angle. Since the BEM assumes that the different elements along the blade are independent they can be individually optimized to maximize the local power coefficient at each element, dC_p , defined as

$$dC_p = \frac{\omega dM}{\frac{1}{2} \rho V_o^3 2\pi r dr} \quad (9.35)$$

And can be combined with Eq. (9.22) to give

$$dC_p = \frac{B\lambda^2(1-a)(1+a')\frac{c}{R} \cdot \frac{r}{R} C_t}{2\pi \sin \phi \cos \phi} \quad (9.36)$$

The input to the design is a specified rotor radius, R , a given tip speed ratio, λ , and given airfoils along the blade. The design angle of attack, α_d , is for the radial element the one giving the highest lift to drag ratio and thus fixed. That means that also the lift and drag coefficients are fixed

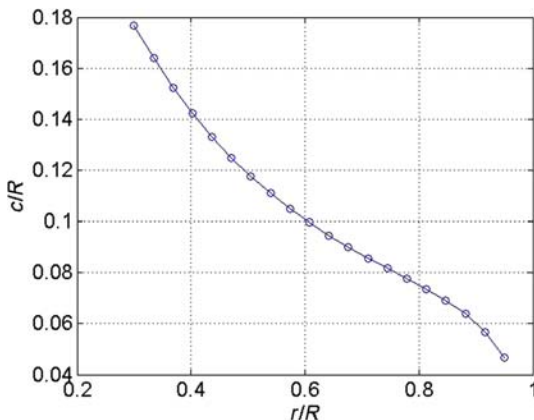


FIGURE 9.17 Dimensionless chord, c/R , for one-point design for parameters $\lambda = 6$, $B = 3$, $\alpha_d = 4$, $C_l = 0.8$, and $C_d = 0.012$.

corresponding their value at the design angle of attack. Now for every radial position following algorithm is made for various chord lengths.

1. Guess on a and a'
2. $\tan \phi = \frac{(1-a)R}{(1+a')\lambda r}$
3. $\theta = \phi - \alpha_d$
4. $C_n = C_l(\alpha_d)\cos \phi + C_d(\alpha_d)\sin \phi$ and $C_t = C_l(\alpha_d)\sin \phi - C_d(\alpha_d)\cos \phi$
5. $F = \frac{2}{\pi} \arccos \left(\exp \left(-\frac{B R - r}{2 r \sin \phi} \right) \right)$
6. Update a and a' using Eqs. (9.29) and (9.30)
7. Check convergence, if not go back to Step (2) with new values of a and a'
8. Calculate $dC_p(c/R)$ using Eq. (9.36)

Pick the value giving the highest local power coefficient and also note the local pitch, $\theta(r)$, and chord, $c(r)$ and continue with the next element. In Figs. 9.17 and 9.18 are shown the result using this one-point optimization for following parameters $\lambda = 6$, $B = 3$, $\alpha_d = 4$, $C_l = 0.8$, and $C_d = 0.012$. The overall power coefficient for this design is 0.44, which is not impressive and can be improved by choosing more efficient airfoils with less drag, especially for the outer part of the blade.

One could further improve the one-point design by slightly adjusting locally the twist angle at every element to maximize energy production in a wind speed interval, between 6 and 9 m s^{-1} where most energy is typically produced. To do so one can for each section calculate, using a BEM code, the local power production (kW m^{-1}) as function of twist angle and wind speed as

$$\frac{dP}{dr}(\theta, V_o) = B \omega r p_t \quad (9.37)$$

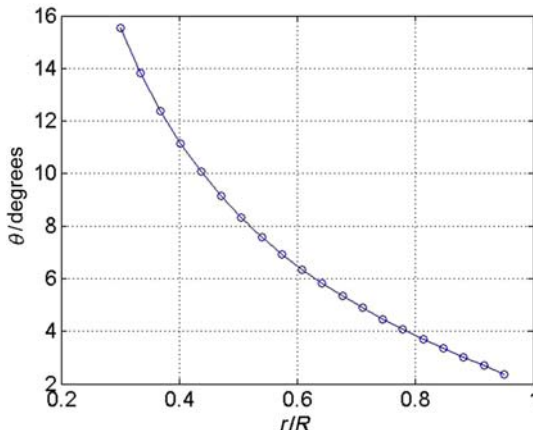


FIGURE 9.18 Twist distribution for one-point design for parameters $\lambda = 6$, $B = 3$, $\alpha_d = 4$, $C_l = 0.8$, and $C_d = 0.012$.

Next the produced energy in the chosen wind speed interval as function of twist angle is computed, $\frac{dE}{dr}(\theta)$ ($\text{kW h m}^{-1} \text{a}^{-1}$) (where a refers to annum) by combining the local power production with the annual number of hours in each wind speed interval as described earlier, and the twist angle producing most energy per meter blade is finally adopted.

An alternative one-point optimization would be to replace the BEM code with a lifting line using Eqs. (9.26) and (9.27) and letting the trailed vortex lines follow a helical pitch as shown in Fig. 9.9 and requiring that the axially induced velocity along the rotor blades should be constant. This would, however, give something very close the one-point optimized blade using the BEM equations, since these have been calibrated through Prandtl's tip loss correction to give approximately the same as this vortex model. Doing this, one should change the pitch of the helical wake iteratively as a function of the computed induction.

For a more complete optimization one could still use the BEM code to calculate the power and thrust as function of the rotational speed, the wind speed, the pitch angle, and the chord and twist distribution. The chord and twist distribution is then typically described by a limited number of DOFs, e.g., a spline and the BEM model is coupled to a formal optimization algorithm as, e.g., the Simplex method finding the geometry and operational parameters that maximizes the annual energy yield under certain constraints for a given wind distribution.

9.7 UNSTEADY LOADS AND FATIGUE

A big challenge for a wind turbine is that the loads are inherently unsteady, mainly due to atmospheric turbulence and gravity. The wind speed in one

fixed point in space is constantly due to atmospheric turbulence fluctuating around a mean value as, e.g., shown in Fig. 9.19 for a mean wind speed of $V_o = 18 \text{ m s}^{-1}$ and a turbulence intensity of $I = \sigma/V_o = 12\%$. When a wind turbine blade spins around in a turbulent wind field, both the size and direction of the wind velocity in the velocity triangle drawn in Fig. 9.7 is changing in time and thus also the aerodynamic loads. Furthermore, gravity gives a large one per revolution periodic load mainly in the edgewise direction of a blade, as indicated in Fig. 9.20. Other unsteady loads come from wind shear, tower passage and if the rotor in a wind farm is partly in the wake of an upstream turbine. Wind shear is when the wind speed increases with height so that the apparent wind speed is higher at the top position than when a blade half a revolution later is pointing down, and this gives a sinusoidal variation with the frequency of the rotation. The time it takes for a blade to pass the tower is small, but during this time the wind speed is reduced giving a sudden drop in the loads that acts as an impulsive loading.

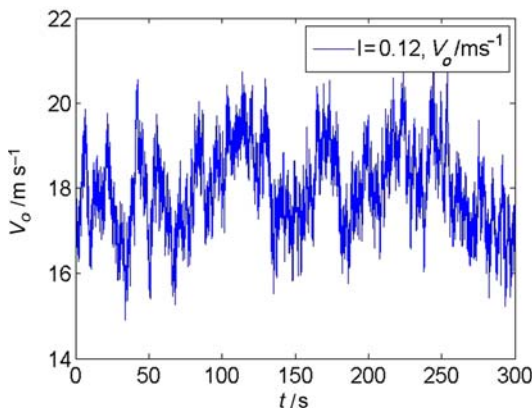


FIGURE 9.19 Example of a 5 minute time history of a turbulent wind speed measured in one fixed point in space, having a mean speed of $V_o = 18 \text{ m s}^{-1}$ and standard deviation $\sigma = 0.12 \cdot V_o = 2.2 \text{ m s}^{-1}$.

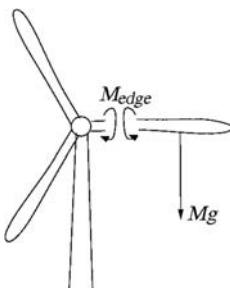


FIGURE 9.20 Simple drawing of edgewise bending moment due to gravity.

Further, the blades will respond elastically to the time-varying loads and the velocities from the vibrations also change the angles of attack and to solve for the time-dependent loads and deflections one needs to calculate in the time domain the coupled structural- and aerodynamic problem using a so-called aeroelastic code. To reduce the risk of a blade failure different norms exist, e.g., IEC 61400-3 that describe the load cases that a wind turbine is expected to experience during its design lifetime including: normal operation, extreme situations such as extreme wind and wave situations, fault conditions, starts and stops, etc. Each of these load cases must for a given design be simulated in time and the accumulated fatigue damage weighted with the expected occurrence of the various load cases must not lead to failure and also it must be checked that the ultimate loads do not cause any structural damage.

9.8 BRIEF DESCRIPTION OF DESIGN PROCESS

A typical design process will then be something like this. First, the wind turbine is designed combining a simple aerodynamic model as described in the previous sections with an optimization algorithm, where the object is to minimize the LCoE. Now for this design all the load cases described in the standards are then simulated aeroelastically in the time domain including the structural response to the time-varying loads and the extreme and fatigue loads are input to more advanced structural models, such as Finite Element Models (FEM), for the various components used in the turbine. If these FEM-based calculations reveal some structural problems one has to go back and change the design and redo all the cases to make new load input to the structural models, and so on until one believes to have an optimized design that with a very high probability will survive all the expected dynamic loads experienced during the entire design lifetime. Now, typically also the final blade design is checked using advanced flow solvers such as CFD codes to verify the aerodynamic loads found using the simpler models relying on tabulated airfoil data. And now the design has to physically be built and tested before it is allowed to be erected outside test stands and sold commercially.

REFERENCES

- [1] Glauert H. Airplane propellers. In: Durand WF, editor. Aerodynamic theory, vol. 4. Berlin: Springer; 1976. ISBN 0844606065.
- [2] Hansen MOL. Aerodynamics of wind turbines. 3rd ed. London and New York, NY: Routledge; 2015. ISBN 978-1-138-77507-7.
- [3] Manwell FM, McGowan JG, Rogers AL. Wind energy explained: theory, design and application. 2nd ed. New York, NY: Wiley; 2009. ISBN 978-0-470-01500-1.
- [4] Burton T, Jenkins N, Sharpe D, Bossanyi E. Wind energy handbook. 2nd ed. Wiley; 2011. ISBN 9781119993926.

- [5] Schaffarczyk AP. *Introduction to wind turbine aerodynamics*. Dordrecht: Springer; 2011. ISBN-13: 978-3642364082.
- [6] Schepers JG, Brand AJ, Bruining A, Graham JMR, Hand MM, Infield DG, et al. Rotor aerodynamics database, ECN-C--02-016 report; 2002.
- [7] Chaviaropoulos PK, Hansen MOL. Investigating three-dimensional and rotational effects on wind turbine blades by means of a quaso-3D Navier-Stokes solver. *J Fluids Eng* 2000;122:330–6.
- [8] Hau E, Langenbrinck J, Palz W. *WEGA large wind turbines*. Berlin: Springer; 1993. ISBN 978-3-642-52129-4.
- [9] Abbott IH, Doenhoff AE. *Theory of wing sections*. New York, NY: Dover; 1959. ISBN 9780486605869.
- [10] Fuglsang P, Bak C. Status of the Risø wind turbine airfoils. In: European wind energy conference, Madrid, 16–19 June, 2003.
- [11] Drela M. An analysis and design system for low Reynolds number airfoils, Low Reynolds number aerodynamics, vol. 54. Berlin: Springer; 1989. Notes in Eng.
- [12] Timmer WA, van Rooij RP. Summary of the Delft University wind turbine dedicated airfoils, AIAA-2003-0352. *J Sol Energy Eng* 2003;125(4):488–96.

Chapter 10

Vertical Axis Wind Turbines: Farm and Turbine Design

Robert Whittlesey

Exponent, Los Angeles, CA, United States

Email: rwhittlesey@exponent.com

10.1 VERTICAL AXIS WIND TURBINES HISTORY

Vertical Axis Wind Turbines (VAWTs) have traditionally been relegated to a niche category in the overall wind turbine market. Historically their advantage has been that they can generate power from wind that comes from any direction, in contrast to a Horizontal Axis Wind Turbine (HAWT), which must yaw to account for changes in wind direction. This advantage comes with an associated disadvantage compared to traditional HAWTs in terms of overall efficiency and power output. Many VAWT-focused start-up companies have been launched with great fanfare only to fail sometime later, as their designs are simply not efficient enough to compete with HAWTs—both on a power coefficient basis and on an economic basis (measured as dollars per kilowatt).

Despite their current place within the commercial market, VAWTs have a prominent place in wind turbine history. Indeed VAWTs were the very first type of wind turbines created, with examples of their construction appearing in ruins that date back to 200 BC in Persia [1]. These original turbines were generally directly linked to a millstone for grinding grain [2]. As a result of their orientation, this was accomplished without the use of gears. Furthermore it appears that the earliest designs relied on sail cloth for their blades rather than a rigid material. HAWTs did not appear until later in the 1300s [1]. Thus despite their current challenges, the persistence of the VAWT concept throughout history might give some hope to future VAWT designers regarding their potential.

The remainder of this chapter is divided into two primary sections: a discussion of VAWT wind farms and then a discussion of the relevant features that should be considered for optimal designs.

10.2 VERTICAL AXIS WIND FARMS

Historical understanding of the performance of wind turbines in a wind farm has been derived from extensive experience with HAWTs. It has been shown that as HAWTs are brought closer together in space, they will exhibit diminished performance—that is, for the same upstream wind conditions, they will produce less power [3]. This is primarily due to the wake of the upstream wind turbines adversely affecting lateral and downstream turbines.

With this understanding, wind farm developers are generally seeking ways of ensuring that HAWTs have maximum spacing to ensure optimal performance. Some general rules of thumb for HAWT wind farm design are to have at least 3 rotor diameters of separation between adjacent lateral wind turbines and at least 10 rotor diameters of downstream separation between adjacent wind turbines in the wind direction [3]. Even when these guidelines are followed, HAWTs will experience a deficit in performance when installed in a wind farm, relative to an isolated wind turbine installation.

With VAWTs it is unclear how performance would be affected when placed in a wind farm as the wake is fundamentally different than that of HAWTs. Experience, albeit based on HAWTs, would suggest that performance would decline. This question remained untested for many years, with good reason: if VAWTs are inferior to HAWTs in terms of efficiency, why would any wind farm developer want to fill their land with them? Thus it is not surprising that the current commercial market for VAWTs is several orders of magnitude smaller than HAWTs. However, recent research has shown that VAWTs in wind farms may actually be preferred to VAWTs operating in isolation [4]. Said differently, VAWTs in a wind farm could actually perform *better* than isolated VAWTs. This is markedly counter to historical experience with HAWT wind farms. This difference also means that the performance of a wind farm using HAWTs is not necessarily advantageous when compared to a farm using VAWTs.

10.2.1 Initial Research on VAWT Farms

The research paper that started this exploration into VAWT farms was published in 2010 [5]. In the paper, the goal was to examine whether bioinspiration could help improve the efficiencies of VAWT wind farms. The research revealed a unique configuration of counter-rotating pairs of VAWTs wherein the neighboring turbines were mutually beneficial. This configuration could generate more power from a given VAWT than the VAWT would in isolation. This is in stark contrast to the results obtained from HAWTs where interference from nearby turbines always results in a detriment to power production. The results, based on relatively simple simulations, were followed by field tests of full-scale VAWTs in the Antelope Valley of Los Angeles County, California, United States [4]. A schematic of the possible counter-rotating configurations are shown in Fig. 10.1.

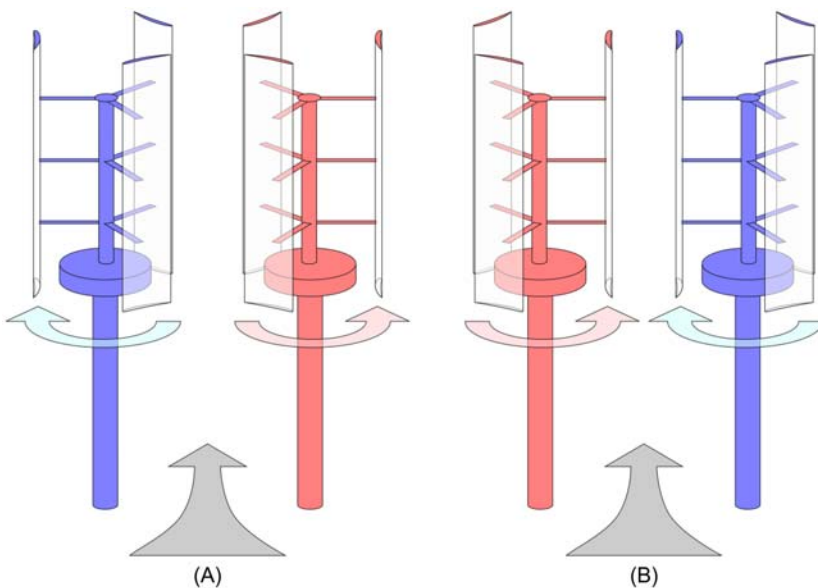


FIGURE 10.1 Schematic representation of two counter-rotating Vertical Axis Wind Turbines (VAWTs). In each figure, the blue turbine rotates clockwise (as viewed from above), whereas the red turbine rotates counter-clockwise. The turbines in figure (A) are depicted in the “doublet” configuration, whereas the turbines in figure (B) are in the “reverse-doublet” configuration.

Initial field results showed that, while VAWTs are much less efficient than HAWTs on an individual level, *“this deficiency is compensated (indeed, overcompensated) by the fact that VAWTs can be placed closer together”* [4]. Furthermore current research suggests that the reverse-doublet is preferred, as depicted in Fig. 10.1B, as turbines in this configuration appear to perform slightly better than turbines in a doublet configuration [6]. However, this result is tenuous, as the uncertainties in the calculations exceed the estimated difference in performance.

10.2.2 Power Density

One metric that was used to examine VAWT wind farms was the power density, which expresses the ratio of the power generated to the area of land used to generate it. The power density for a concentrated power generation facility, such as a coal or a nuclear power plant can be extremely high. However, for distributed generation systems like wind and solar, this metric is crucial to determining the efficiency of a system with respect to the ground it requires. The importance of the metric varies with the location of the generation system. In some areas, a large area of land is both available and has suitable wind for power generation, such as the state of Texas in the

United States. However, many island nations that use diesel fuel—a nonrenewable resource—for power generation do so because they have limited land available for power generation by renewables.

More specifically, the island of Grand Cayman has a land area of 200 km^2 (76 square miles) [7] and lists a power system that has a capacity of 145.75 MW [8]. This results in a power density of 0.74 W m^{-2} . Thus if one were to cover the entire island with some form of distributed energy production, the goal would be to ensure that the power density of the chosen technology exceeded 0.74 W m^{-2} . Of course, if only one-fourth of the island was available to contribute to power generation, then the power density requirement would increase to 3 W m^{-2} .

For reference, modern HAWT wind farms have a power density of $2\text{--}3 \text{ W m}^{-2}$ [4,9]. Thus for the island of Grand Cayman, one would have to cover one-fourth of the entire island with HAWTs (at the closest packing, approximately 3 rotor diameters laterally and 10 diameters downstream). However, Dabiri measured the power density of their VAWT wind farm to be an order of magnitude higher—up to 30 W m^{-2} [4]. If one chose a more conservative power density, say 10 W m^{-2} , for a VAWT wind farm on Grand Cayman, they would only need to cover 7.4% of the island. This is a substantial reduction in land area compared with the 25% required by a HAWT wind farm. This illustrates the potential value in using VAWTs in a wind farm, as the land area required is minimized.

It should be noted that these values are taken from the full-scale wind farm employed by Dabiri in his research. While the turbines were “full-scale,” they were only 1.2 kW turbines with a total height of 10 m. These are substantially smaller than the modern 1 MW turbines with a total height of 100–150 m.

The reason for the considerable increase in power density is still an area of research. However, the current hypothesis is that the wake downstream of the counter-rotating turbines recovers faster than one would expect [4]. This is based on previous studies of spinning cylinders, which found that vortex shedding and turbulence in the wake are suppressed, provided the rotation rate is high enough [10]. The counter-rotating VAWT is analogous to the spinning cylinders such that, when the tip-speed ratio is high enough, similar effects occur in the downstream wake and thus allow for tighter arrangements of VAWTs in a wind farm than is possible with HAWTs.

Substantial research is continuing to explore this aspect of VAWTs in particular. The reader is recommended to review the results for more details [11,12,13].

10.3 DESIGN GUIDELINES

In this section, general design guidelines will be explored to give the reader some useful information in designing their own turbine. In the field of

VAWTs there are a plethora of differing attitudes and approaches to designing the “ideal” wind turbine. In this section, the design choices will be oriented toward those that could be used most successfully in a counter-rotating wind farm arrangement, such as that discussed previously, as outside of a wind farm HAWTs have a marked advantage. These designs tend to be more “cylindrical” in shape. This is believed to be the most ideal for VAWT wind farms, due to the aforementioned analogy with rotating cylinders. Thus designs like the “Darrieus” wind turbine, which feature arc-shaped blades that connect directly to the rotor shaft, will not be discussed at length in this chapter. Those interested in reading more about the Darrieus-type wind turbine are suggested to consider alternative resources, especially Paraschivoiu’s book [14] and the work done by Sandia [15].

10.3.1 Power Coefficient

The design goal for VAWTs is no different than for HAWTs: to maximize power production. The most general way of expressing the efficiency of the system toward this goal is through the power coefficient, C_P , which is defined as:

$$C_P = \frac{P}{\frac{1}{2} \rho U^3 A}$$

where P is the power produced by the wind turbine, ρ is the density of the air, U is the freestream velocity, and A is the cross-sectional area of the wind turbine. This is the same equation used in calculating the efficiency of a HAWT, however the cross-sectional area is calculated slightly differently. Rather than using the area of the disk swept by the blades, one generally uses the diameter of the rotors multiplied by the length of the rotor blades, as shown in Fig. 10.2. As with HAWTs, many engineers strive to increase the power coefficient of any design, as this parameter represents the overall efficiency of a wind turbine.

10.3.2 Lift Versus Drag-Based VAWT

Unique to VAWTs there are two aerodynamic mechanisms used to turn the rotor. The “drag” mechanism is so-named as the torque developed by the rotor is principally due to unequal amounts of drag on the blades. One of the most popular drag-based VAWTs is known as the “Savonius” VAWT, in honor of the Finnish engineer Sigurd Johannes Savonius who first patented this style of turbine in 1925 [16]. Fig. 10.3 reproduces some of the figures from his patent. The Savonius VAWT is very robust in that it is simple to design and build; and can indeed produce power. However, it suffers from a substantial design flaw wherein a blade only produces positive torque (positive in the sense that the torque is suitable for producing power)

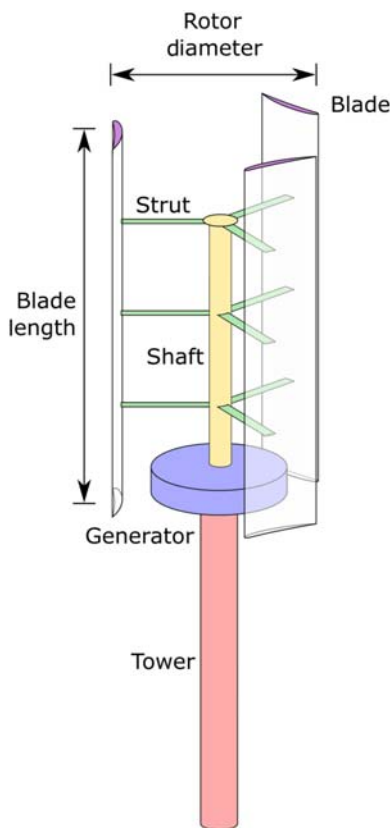


FIGURE 10.2 Schematic of a canonical, modern lift-based Vertical Axis Wind Turbine (VAWT). The blade is attached to the rotor shaft using the struts. The shaft is connected to the generator, where the mechanical energy is converted into electrical energy. This generator is installed on a tower, which elevates the structure in the air to ensure sufficient access to the wind resource. This drawing is not to scale.

during one half of the blade revolution—when the blade is moving in the same direction as the wind, i.e., “advancing.” When a blade is “retreating,” i.e., moving against the wind, it actually contributes negative torque and thus reduces the net torque applied to the generator. Thus a blade is only producing power during approximately half each revolution. It should be no surprise that this design, while robust and easy to make, is not a serious candidate for substantial power production.

An improvement in power production can be achieved through blades that produce positive torque during the entirety of the blade revolution. This design is known as a “lift” based VAWT. This type of VAWT has blades made of airfoils more-closely-resembling airplane wings. These are also sometimes referred to as “Darrieus-type” VAWTs, in honor of Georges Jean

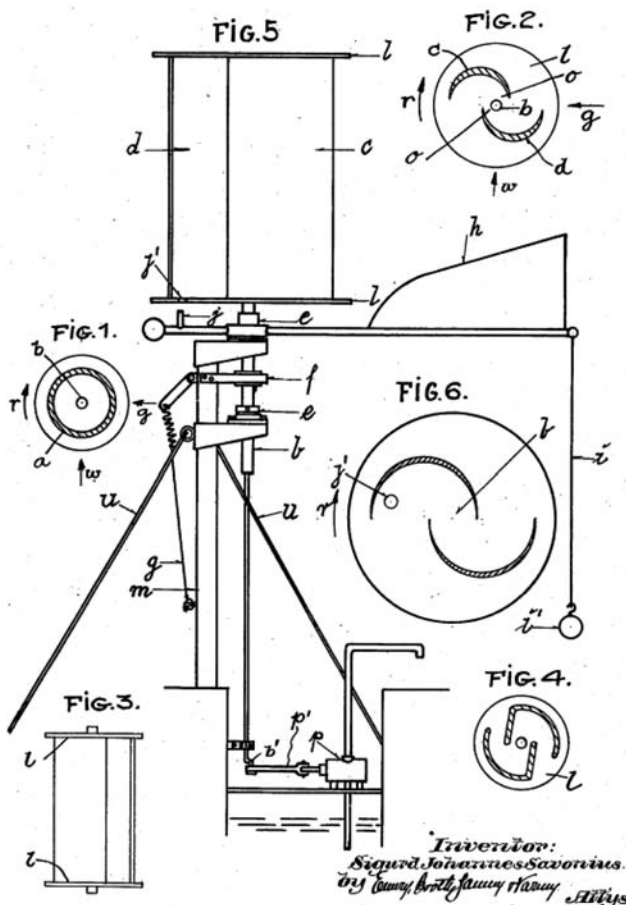


FIGURE 10.3 Figures from Savonius' patent illustrating his drag-based Vertical Axis Wind Turbine (VAWT) design [16].

Marie Darrieus, who patented this type of design in the United States in 1926 [17]. Fig. 10.4 shows the figures from Darrieus' patent filing. Based on the shape of these blades, they generally produce positive torque at every angle when they are operating in their optimal conditions. As a result lift-based VAWTs are generally more efficient than drag-based VAWTs. Most new commercially available VAWTs are based on the concept of aerodynamic lift in order to maximize the power production, but use different airfoil shapes than the “Darrieus” type. An example of a modern lift-based VAWT is shown schematically in Fig. 10.2. This type is also sometimes referred to as a “giromill” or “H-rotor” [18,19].

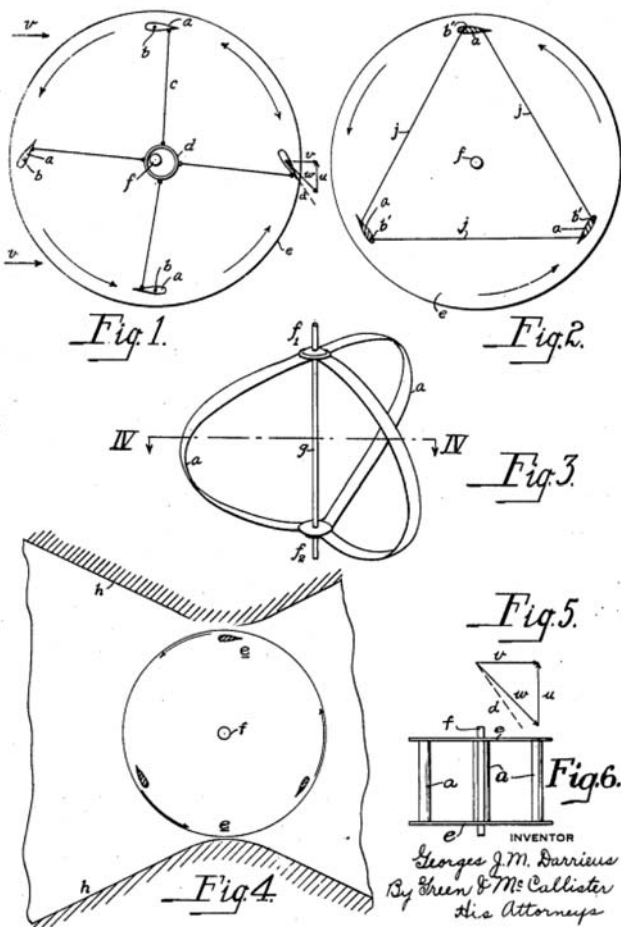


FIGURE 10.4 Figures from Darrieus' patent explaining the idea of a lift-based Vertical Axis Wind Turbine (VAWT) [17].

Despite the inherent power coefficient advantage of lift-based VAWTs, drag-based VAWTs are still being built, primarily by hobbyists who are more interested in learning about wind energy and building turbines themselves than in power production. Their interest is driven by the drag-based VAWT's simplicity and robustness to design imperfections. The power coefficient in lift-based VAWTs is so much higher than that of traditional drag-based VAWTs that a drag-based design is not normally relevant to any meaningful discussion with respect to wind farms. Thus the rest of this chapter will drop the prefix “lift-based” and simply refer to “VAWT” with the knowledge that we are referring to a lift-based VAWT, unless otherwise specified.

10.3.3 Starting

HAWTs and drag-based VAWTs are able to self-start. By contrast lift-based VAWTs have difficulty starting by themselves. The tip-speed ratio, λ , is defined as the ratio of the tangential velocity of the blade tip to the free-stream wind velocity. Fig. 10.5 plots the torque produced by the blades of a typical lift-based VAWT in one revolution, represented by the torque coefficient, C_Q , as a function of the tip-speed ratio. When the torque is positive the turbine continues to spin and power is produced. However, if the torque coefficient, C_Q , is negative, then the turbine eventually stops spinning on its own. The results show that there is a “dead-band” region through which the VAWT must be driven to get to the most efficient power production. Accelerating through this dead-band region requires power—the turbine must be driven by a motor at least to start.

The issue of the dead-band region has been addressed previously by electrically powering the turbine until the tip-speed ratio/wind speed was high enough for the turbine to self-spin [15, p. 15]. However, there are electrical and mechanical design challenges inherent in developing a system that turns the rotor in low wind. More recently, the industry has directed itself to developing self-starting designs. One such design involves the use of cambered airfoils (discussed later). However, even some designs with cambered airfoils still feature dead-band regions, which delay or impede self-starting [21].

Additionally, there are few start-up companies that have brought designs to market which attempt to address the self-starting issue through a hybrid turbine—by adding a smaller-radius drag-based VAWT to the shaft of a

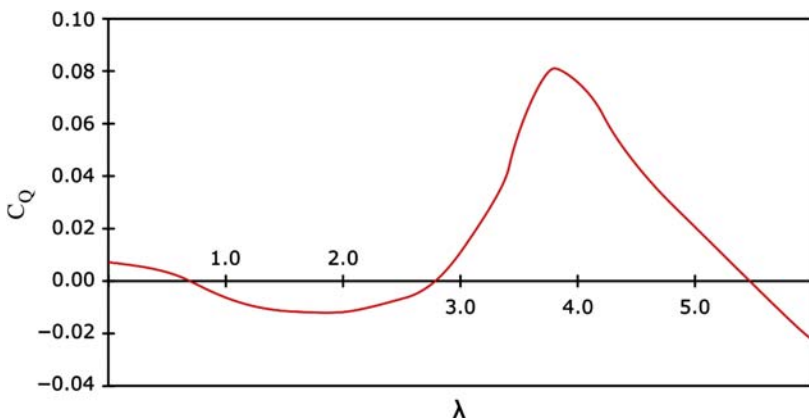


FIGURE 10.5 Nondimensional torque coefficient, C_Q , plotted against tip-speed ratio, λ . The dead-band region exists for tip-speed ratios between 0.6 and 2.8. *Figure adapted from Kirke B. Evaluation of self-starting vertical axis wind turbines for stand-alone applications, Ph.D. Thesis. Griffith University, Queensland, Australia; 1998 [20, p. 15].*

lift-based VAWT. While these designs have not been studied in depth, it is not expected that their power efficiency will be competitive.

10.3.4 Blade Airfoil Choice

By and large, the modern development of HAWT blades has been greatly aided by the many years of development of airplane airfoils for wings and propellers. More recently, the optimization of airfoils for HAWTs has become specific to the needs of wind turbines. VAWT blades have not been able to take advantage of the same research as the VAWT blades do not exist in the same environment as either wings or propellers. While there are many airfoils from which to choose as a basis for a VAWT blade, the aerodynamics of a VAWT are much more dynamic than a HAWT and require substantially more refinement to maximize performance. In particular, a VAWT experiences flow with a wide range of angle of attack during each rotation.

With this in mind, however, the choice of an airfoil is of paramount importance as “the power produced by a [VAWT] at different wind speeds [is] largely determined by its blade airfoil” (22, p. 494). One can use published literature as a starting point for airfoil design, but a final design would benefit greatly from additional research and development tailored to that specific design’s operating conditions. This will ensure the highest level of performance.

Based on the work done at Sandia National Laboratory [1, p. 17], most of the early studies of airfoils for VAWTs were using symmetric airfoils such as the NACA 00-series. Symmetric airfoils were used in the Sandia 34 m VAWTs that were used in the 1970s through 1990s. These airfoils can produce power; however, they suffer from the self-starting problem mentioned previously.

More recent research has considered cambered airfoils for VAWTs. A cambered airfoil, while increasing the drag a bit, has the potential to allow for self-starting of the VAWT in an entirely passive way [20, p. 319]. In the PhD thesis of Kirke, he writes: “*Cambered fixed pitch blades appear to offer the best combination of acceptable starting torque and peak performance with simplicity and low cost*” [20, p. 319].

For a given VAWT, the airfoil will have to be specifically tailored to ensure optimal performance. However, good starting points can be found in existing literature. Many have considered the Selig S1210 airfoil as a design basis. The Selig S1210 is intended to be a high-lift, low Reynolds number airfoil. In particular, Kirke studied the Selig S1210 but added “[it] is likely that a profile with even better characteristics [than the S1210] for VAWTs could be designed” [20, p. 320]. In other research, the Selig S1210 airfoil profile was studied and its ability to self-start was confirmed [23]. The blade profile of the Selig S1210 is shown in Fig. 10.6.

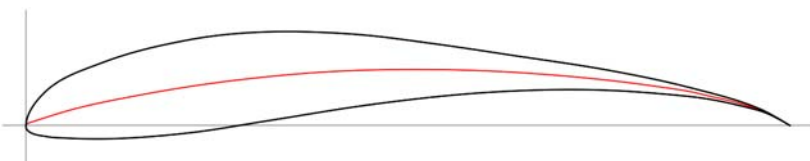


FIGURE 10.6 Selig S1210 airfoil profile. The mean camber line is in red.

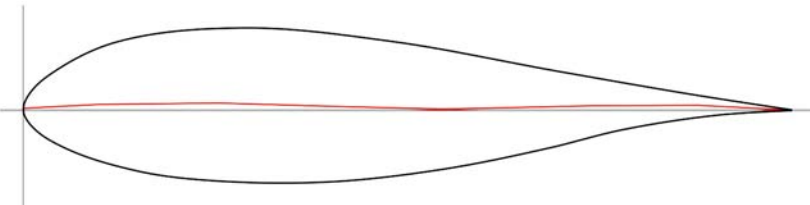


FIGURE 10.7 Delft University's DU 06-W-200 airfoil profile.

Thus the Selig S1210 may be an appropriate airfoil with which to start a new design since it is able to self-start, a rare feature among historical VAWTs.

Newer research thrusts in the realm of VAWT airfoils, however, have been focused on developing airfoils specifically for VAWTs. Claessens, for instance, has endeavored to improve the performance and self-starting characteristics as compared to the symmetric NACA airfoils and was able to find a number of improvements [24]. This work resulted in the “DU 06-W-200” airfoil, which is shown in Fig. 10.7. As an example of the success of this profile, it was reported to have been used in the commercially produced Windspire VAWT [21, p. 3], a turbine that self-starts. Interestingly, although the DU 06-W-200 airfoil is able to self-start, its degree of camber is far less than the heavily cambered S1210. We also do not yet have any direct comparisons of it to the Selig S1210 airfoil with respect to power production. The current state of research does not offer an explanation or verified model for prediction of power production or self-starting ability.

Thus it is hard to give accurate advice as to which blade profile (Selig S1210, Delft DU 06-W-200, or some other) is superior for wind farm use. Since both have been shown in the literature to offer good results, it seems reasonable to consider the merits intrinsic to each design. There may be compelling aspects of one’s design that suggest one blade design is a more appropriate starting point over the other. Some aspects to consider include the thickness of the blades with respect to structural stiffness (thicker blades being stiffer), ease of construction (e.g., the sharp trailing edge of the Selig S1210 may prove difficult to manufacture), weight (thinner blades being lighter), etc.

10.3.4.1 Blade Refinement

Having chosen a starting blade profile, one must further refine the airfoil design. Although the ultimate test is in the field with experiments, commercial development of a turbine will undoubtedly begin with simulations as the precursor to construction of prototypes and experiments, as minute changes to the airfoil geometry are far faster to execute with a computer than with a full-scale turbine.

In terms of simulations, VAWTs have extremely complex wake profiles that can easily make a simulation (such as one generated using a commercial software package such as FLUENT or Star-CCM) very time-consuming, computationally intensive to run, and subject to significant inaccuracies. As such, it may be beneficial to start with lower-fidelity simulations for exploration of overall concepts and to more quickly generate alterations to the airfoil design.

An appropriate means is to first develop and refine with the “cruder” tools and then move up. A likely testing progression would be to first select an airfoil profile with a simplified 2D analysis (e.g., RFOIL+VAWT performance simulation), refine it using a higher-fidelity Computational Fluid Dynamics (CFD) code (e.g., 3D simulations in Star-CCM, FLUENT, or OpenFOAM), and then lastly test the airfoil profile in a prototype turbine.

As an example, for the simplified 2D analysis, Claessons developed a unique method of simulating the airfoil performance by first running the airfoil profile through RFOIL and then using the results of the 2D airfoil profile to generate the VAWT performance using another software tool [25]. This method is undoubtedly faster than running a very high fidelity CFD simulation in 3D and would allow engineers to more quickly test a wide range of blade profiles and converge on a more optimal solution. For a more detailed discussion on the topic of VAWT modeling, see Paraschivoiu’s book [14].

10.3.4.2 Blade Orientation

For a symmetric blade, there is no issue of blade orientation. However, once a blade is cambered and becomes asymmetric the question arises: how does one install the blade? Is power production better with the camber toward or away from the axis of rotation? It is appropriate to note that the orientation of the blades *does* matter.

In his PhD thesis, Kirke suggests that the concave side of a cambered airfoil should face outward for optimal VAWT performance [20, p. 48 and p. 165]. This orientation is depicted in Fig. 10.2. This conclusion has been reached independently by others, including the author and some VAWT manufacturers, however, Kirke appears to be the first to have documented this observation.

The idea behind this is that, when installed in this configuration, the blade camber enables the airfoil to perform better during the upwind portion of the rotation cycle and worse during the downwind portion. The vast

majority of the power, 90%–95% according to Baker [26, p. 374], is generated during the upwind part of rotation. Thus in order to optimize power production, the camber orientation shown in Fig. 10.2 is best, where the concave side of the camber line faces outwardly. The increase in power production due to the camber on the upwind portion more than offsets the decrease during the downwind portion. If installed in the reverse, the blade, when oriented to produce the most energy, is actually in the downstream wake of other blades on the rotor. The increase in power production during the downwind portion is more than offset by the decrease in power production during the upwind portion.

10.3.5 Blade-Tip Vortices

Based on the canonical wind turbine shown in Fig. 10.2, a blade with straight ends at the top and bottom, as shown, will generate “blade-tip vortices” during each rotation of the rotor, much like an aircraft produces “wingtip vortices.” These vortices are known to be detrimental to performance by increasing the induced drag and, in a wind turbine, would decrease the power production.

One parameter that affects the strength of these vortices is the aspect ratio of the blades. The aspect ratio is defined as the length of the blade relative to its chord. In general it has been found that higher aspect ratio blades result in better performance, just as with aircraft wings, due to the reduction in reduced drag from tip vortices. As an example of this, Kirke’s prototype machine, with an aspect ratio of 7.5, performed much worse than his predictions, which were based on infinite-length blades. He concluded that the low aspect ratio of the blades was to blame. Subsequently he recommended blades with aspect ratios much higher than 7.5 [20, p. 320]. However, the likely reason for Kirke’s results was the production of blade-tip vortices, which were apparent in his aspect-ratio-of-7.5 design and are neglected in his infinite-length-blade-based predictions. VAWTs like that pictured in Fig. 10.2, in particular, have the effects of blade-tip vortices doubled compared to their HAWT brethren because the VAWT would generate blade-tip vortices from the tops and bottoms of the blades whereas a HAWT only has a single blade-tip vortex generated by each blade.

Thus increasing the aspect ratio of the blades by either elongating the blades or reducing the chord of the blades is one method of reducing the strength of the blade-tip vortices. Other means of reducing the blade-tip vortices can be found by the installation of winglets or an endplate/fence at the blade tip. Amato et al. conducted numerical simulations of various blade-tip devices to determine their effect on power coefficient [27]. Their study found that nearly all tip treatments resulted in power production improvements, however, a carefully designed winglet resulted in the highest power coefficient increase of approximately 7%. This is a marked improvement in power production for a passive device.

10.3.6 Blade Reynolds Number

The Reynolds number is a commonly used nondimensional parameter in fluid mechanics, which describes the ratio of inertial forces to viscous forces. In the context of VAWTs, the Reynolds number is defined using the kinematic viscosity of the air, the freestream velocity of the wind, and the chord length of the blade as follows:

$$Re = \frac{c \cdot U_\infty}{\nu}$$

where c is the chord length, U_∞ is the freestream velocity of the wind, and ν is the kinematic viscosity. Using this definition of the Reynolds number, Kirke suggests that low Reynolds numbers contribute to difficulty in the self-starting of a VAWT. Hence larger Reynolds numbers are desired. Additional research in this area by Brusca et al. found a similar result: increasing the Reynolds number increased the power coefficient of a given VAWT [18].

In practice, this advice is synonymous with ensuring that (1) the wind velocity magnitude is high and (2) the blade chord, which is proportional to the blade area, is large. However, it is not clear if the fault is in the wind velocity or if there is actually a Reynolds number dependence on performance (e.g., transition to turbulence or drag buckets). This should also be considered in more detail.

10.3.7 Turbine Mass

In general the turbine rotor mass is of particular concern as a design driver. The rotor mass is defined as all of the components which rotate: principally, the rotor shaft, the struts, and the blades. As the turbine rotor becomes more massive, all connecting systems must be upgraded, including the rotor shaft, the tower, and the foundation. Thus a lighter turbine mass is generally desired. Furthermore the lighter the blades and rotor are, the smaller the rotational moment of inertia of the VAWT rotor. This, in turn, allows the turbine to spin up and subsequently respond to wind gusts more quickly. Both of these features will then lead to greater power production and a higher capacity factor for the wind turbine.

The primary concern for a lighter turbine is one of structural or dynamic loads. Heavier, more massive blades are generally stronger and dampen vibrations better. Thus a trade-off must be made between a turbine that will ensure a safe, long operation, and one that is lighter and more responsive.

10.3.8 Turbine Diameter

For VAWTs, the turbine diameter as defined in Fig. 10.2, is a unique parameter that does not have a direct analog in the HAWT world. In the literature

there are currently no design guidelines to follow. However, the turbine diameter has an effect on aspects of the wind turbine performance. In particular, the larger the turbine diameter, the longer the blade struts must be to support the blades. Thus a larger diameter turbine is more massive and has a direct effect on the turbine inertia, as discussed earlier. Furthermore a larger turbine diameter results in a slower angular velocity, assuming the same tip-speed ratio. A slower angular velocity then may require that a gearbox be included in the design to ensure the angular velocity of the generator is sufficiently high for efficient power production.

Of course, the trade-off is that a smaller turbine diameter leads to higher centripetal forces on the rotor blades, at the same tip-speed ratio, as the centripetal force is proportional to $1/r$. Higher angular velocities also increase the propensity for fatigue failure of the blade struts due to more frequent cyclic loading. This is a special concern for VAWTs of this design, since the energy released in a blade liberation event is significant. An example of some VAWT failures due to blade liberation is available in Dabiri et al. [28].

10.3.9 Number of Blades

The concerns surrounding the number of blades in a VAWT are very similar to those surrounding the number of blades in a HAWT. Designs featuring fewer blades generate more “ripples” in the power output, whereas extremely high numbers of blades result in decreased power production due to drag. The lowest number of blades in a design has principally been 2 blades, as seen in the original Sandia turbines. However, many later embodiments have used 3 blades. There are commercial designs on the market featuring 4- and 5-bladed designs, such as those made by State of the Art Wind Technologies (SAWT).

The advantage of the increased blade numbers are increased rotor stability and a reduction in the “torque ripple” experienced by the 2-bladed design, particularly during low rotation rates [15, p. 38]. This results in a smoother power output. To expand upon this, Sutherland et al., while reflecting on the Sandia VAWT development, writes: “*...the use of 3 blades appears to be optimal ... adding more blades appears to add significant costs without reducing balance-of-system costs*” [15, p. 38]. Furthermore Kirke and Lazauskas suggest “*using at least 3 blades rather than 2*” with respect to vibration [29, p. 4]. Three blades have been featured in many other designs and studies [20,30]. A study comparing 3- and 6-bladed designs numerically, found that the power coefficient was higher for a 3-bladed design [31].

10.3.10 Struts

Struts are used to hold the blades to the main rotor shaft as shown in Fig. 10.2. They need to be strong in order to resist the aerodynamic, gravitational, and

centripetal forces exerted on the blades. However, they generally impede power production and decrease the power coefficient through their increased drag. Since drag scales with velocity to the second power and the linear velocity of a strut scales linearly with its radial position from the rotor shaft, most of the drag effect is concentrated at the connection to the blade. There are some advantages in choosing an aerodynamically “smooth” strut design or in covering the strut with a low-drag fairing, and the use of symmetric airfoil sections for fairing the struts is recommended [20, p. 212] [30]. In one demonstration turbine, the addition of aerodynamic fairings to round pipe struts resulted in a 15% increase in measured performance [15, p. 36].

The number and location of the struts is both a structural concern and an aerodynamic one. It is recommended to minimize the number of struts concomitantly with good structural design, as each strut removed eliminates some parasitic drag on the rotor and ultimately results in a higher power production.

10.4 SUMMARY

In conclusion the following points have been made regarding the design of VAWTs and how to aggregate VAWTs in wind farms:

- Counter-rotating VAWTs have been found to have substantially increased power density (W m^{-2}) over conventional HAWT wind farms
- VAWTs should be designed to use lift rather than drag as the basis of operation
- VAWTs can have difficulty self-starting, but careful airfoil selection and cambered airfoil profiles can alleviate these difficulties
- The Selig S1210 and DU 06-W-200 airfoil profiles have been shown to self-start and form a currently acceptable starting point for new blade airfoil designs
- Struts should be shaped to reduce aerodynamic drag
- Lower turbine rotor mass, larger aspect ratio blades (e.g., long “slender” blades), blade-tip devices (e.g., winglets), and 3-bladed rotor designs are preferred.

The VAWT field is relatively nascent compared to HAWTs. As more research is completed and published, some of the design guidance herein may be superseded as the technology improves. The reader is advised to always consider any new research that becomes available.

REFERENCES

- [1] Kaldellis JK, Zafirakis D. The wind energy (r)evolution: a short review of a long history. *Renewable Energy* 1887-1901;1011:36.
- [2] Shepherd D.G. Historical development of the windmill,” NASA Contractor Report 4337; 1990.

- [3] Hau E. *Wind turbines*. Berlin: Springer; 2013.
- [4] Dabiri JO. Potential order-of-magnitude enhancement of wind farm power density via counter-rotating vertical-axis wind turbine arrays. *J Renewable Sustainable Energy* 2011;3:1–12.
- [5] Whittlesey RW, Liska S, Dabiri JO. Fish schooling as a basis for vertical-axis wind turbine farm design. *Bioinspiration Biomimetics* 2010;5:1–6.
- [6] Kinzel M, Araya DB, Dabiri JO. Turbulence in vertical axis wind turbine canopies. *Phys Fluids* 2015;27(115102).
- [7] Cayman Islands Government. Location and geography, [Online]. Available: <<http://www.gov.ky/portal/page/portal/cighome/cayman/islands/locationgeography>>; 2016 [accessed 12.08.16].
- [8] Caribbean Utilities Corporation. Caribbean utilities corporation-operation & functional work, [Online]. Available: <<https://www.cuc-cayman.com/operation>>. [accessed 12.08.16].
- [9] MacKay DJ. *Sustainable energy—without the hot air*. England: UIT Cambridge; 2008.
- [10] Chan AS, Dewey PA, Jameson A, Liang C, Smits AJ. Vortex suppression and drag reduction in the wake of counter-rotating cylinders. *J Fluid Mech* 2011;679:343–82.
- [11] Araya DB. Aerodynamics of vertical-axis wind turbines in full-scale and laboratory-scale experiments. Pasadena, CA: California Institute of Technology; 2016.
- [12] Parneix N, Fuchs R, Immas A, Silvert F, Deglaire P. Efficiency improvement of vertical-axis wind turbines with counter-rotating layout. Hamburg: Wind Europe; 2016.
- [13] Ahmadi-Baloutaki M. Analysis and improvement of aerodynamic performance of straight bladed vertical axis wind turbines. Windsor, Ontario, Canada: University of Windsor Thesis; 2015.
- [14] Paraschivoiu I. Wind turbine design with emphasis on darrieus concept. Presses Internationales Polytechnique; 2009.
- [15] Sutherland HJ, Berg DE, and Ashwill TD. A retrospective of VAWT technology. Sandia Report SAND2012-0304, Sandia National Laboratories; 2012.
- [16] Savonius SJ. Rotor adapted to be driven by wind or flowing water. United States of America Patent US1697574A, August 13, 1925.
- [17] Darrieus GJM. Turbine having its rotating shaft transverse to the flow of the current. United States of America Patent US1835018A, October 01, 1926.
- [18] Brusca S, Lanzafame R, Messina M. Design of a vertical-axis wind turbine: how aspect ratios affects the turbine's performance. *Int J Energy Environ Eng* 2014;5:333–40.
- [19] Wahl M. Designing an H-rotor type wind turbine for operation on Amundsen-Scott South Pole station. Uppsala: Uppsala University Thesis; 2007.
- [20] Kirke B. Evaluation of self-starting vertical axis wind turbines for stand-alone applications, Ph.D. thesis. Queensland, Australia: Griffith University; 1998.
- [21] Basilevs Y, Korobenko A, Deng, Yan J, Kinzel M, Dabiri JO. Fluid-structure interaction modeling of vertical-axis wind turbines. *J Appl Mech* 2014;81 081006-1.
- [22] Islam M, Fartaj A, Carriveau R. Analysis of the design parameters related to a fixed-pitch straight-bladed vertical axis wind turbine. *Wind Eng* 2008;32(5):491–507.
- [23] Islam M, Ting DSK, Fartaj A. Desirable airfoil features for smaller-capacity straight-bladed VAWT. *Wind Eng* 2007;31(3):165–96.
- [24] Claessens MC. The design and testing of airfoils for application in small vertical axis wind turbines, M.S. Thesis. Delft University of Technology; 2006.
- [25] van Rooij R. Modification of the boundary layer calculation in RFOIL for improved airfoil stall prediction. Delft Report IW-96087R, Delft; 1996.
- [26] Baker J. Features to aid or enable self starting of fixed pitch low solidity vertical axis wind turbines. *J Wind Eng Ind Aerod* 1983;15:369–80.

- [27] Amato F, Bedon G, Raciti Castelli M, Benini E. Numerical analysis of the influence of tip devices on the power coefficient of a VAWT. *Int J Mech Aerosp Ind Mechatronic Manuf Eng* 2013;7(6):1053–60.
- [28] Dabiri JO, Greer JR, Koseff JR, Moin PM, Peng J. A new approach to wind energy: opportunities and challenges. *Phys Sust Energy* 2015;1652:51–7 2015.
- [29] Kirke BK, Lazauskas L. Limitations of fixed pitch Darrieus hydrokinetic turbines and the challenge of variable pitch. *Renew Enegy* 2011;36:893–7.
- [30] Kjellin J, Bulow F, Eriksson S, Deglaire P, Leijon M, Bernhoff H. Power coefficient measurement on a 12 kW straight bladed vertical axis wind turbine. *Renew Energy* 2011;36:3050–3.
- [31] Hassan S, Ali M, Islam M. The effect of solidity on the performance of H-rotor Darrieus turbine. International Conference on Mechanical Engineering; 2016.

Chapter 11

Multielement Airfoils for Wind Turbines

Adam M. Ragheb and Michael S. Selig

University of Illinois at Urbana-Champaign, Urbana, IL, United States

Email: adam.ragheb@gmail.com, aragheb@illinois.edu

11.1 INTRODUCTION

Multielement airfoil configurations hold the potential to increase the aerodynamic performance of the inboard section of a wind turbine blade [1]. In addition to improving the blade root aerodynamics, multielement airfoil arrangements also show promise to improving the transportability of large wind turbine blades and creating the ability to increase the spar cap separation to allow for an improved structural arrangement of the blades. Modern utility-scale wind turbines (1.5–10 MW rated power) have cut-in wind speeds between 3 and 5 m s⁻¹ and do not begin to operate at their rated power until wind speeds of between 10 and 15 m s⁻¹ are achieved. Increasing the lift coefficient of the inboard section of a wind turbine blade should aid in starting the wind turbine at lower speeds and will allow the turbine to produce its rated power at a lower wind speed. The turbine will be aided in starting at low speeds, also known as lowering the cut-in wind speed, through a larger tangential force coefficient C_t , which is a direct result of an increased lift coefficient C_l [2]. The tangential force coefficient, C_t , is the force coefficient that contributes to the torque of the wind turbine, and it is oriented normal to the rotor axis of rotation and is positive in the direction of the blade leading edge. The lift coefficient C_l is an aerodynamic quantity that is normal to the local flow. The resultant of the lift and drag coefficients may be decomposed into the aforementioned tangential force coefficient and the normal force coefficient C_n , which is parallel to the rotor axis of rotation. Additionally, the improvement of the blade root aerodynamics will allow for the axial induction factor to be increased to the Betz limit ideal operating condition of one-third [3] over a larger portion of the inboard section of the blade. These improvements would in turn increase the power output, increase the capacity factor, and open up new locations for wind turbines that would

otherwise be unsuitable for wind turbine placement. This chapter will discuss the benefits of multielement wind turbine blades as they relate to transportation and structural concerns, cover the results of multielement wind turbine blade studies conducted at the University of Illinois at Urbana-Champaign, and finally, will review multielement wind turbine blade work conducted by other research groups.

11.2 TRANSPORTATION BENEFITS

In regard to transportation, current wind turbine blades appear to have reached the maximum size that can be easily transported. Constructing a longer or thicker root section may render the blade incompatible with current transportation infrastructure. The most substantial limit in the design of utility-scale is the transportation cost, which grows rapidly for lengths of over 46 m and reaches prohibitive levels for blades over 61 m long [4,5]. Multielement configurations will allow for natural disconnect points on the blades, allowing the root section to be disassembled from the rest of the blade and the components to be transported to the wind farm site for assembly. These natural disconnect points will result in a simplification of the transportation process for a given blade radius and the ability to transport blades of larger radii as segmented blade sections. Fig. 11.1 presents a photograph of a wind turbine blade loaded onto an American Wind Transport Group, LLC truck for transport by road and depicts the difficulty of refueling a truck while transporting a wind turbine blade.



FIGURE 11.1 Photograph of wind turbine blade being transported by road (Top) and refueling of a blade-carrying truck (Bottom) in Walcott, Iowa.

The use of segmented blades for wind turbine applications has only recently begun, albeit for single-element airfoils. The first commercial wind turbine to use a segmented blade is the Gamesa G128, a wind turbine that is offered in 4.5 and 5.0 MW versions. The patented technology, termed “InnoBlade,” connects the two pieces of the 62.5 m blade with approximately 30 bolt channel fittings that are integrated into the blades [6]. By using a sectioned blade, Gamesa advertises that the tooling and equipment used to transport their 2–2.5 MW wind turbines can be used to transport the blades of the 5.0 MW wind turbine platform since no component is longer than 35 m [7].

Enercon also utilizes a segmented blade design on both their E115 and E126 wind turbines, pairing the technology with their innovative direct-drive annular generator [8]. The Enercon E115 blade comprises two glass fiber reinforced epoxy sections with an inner section of approximately 12 m in length and an outer section with a length of approximately 44 m. The 7.5 MW E126 wind turbine, on the other hand, has its inner blade section comprised of a primarily steel structure [9].

Multielement configurations will allow for natural disconnect points on the blades where the blade airfoils transition from a multielement arrangement to a single element, allowing the root section to be disassembled from the rest of the blade and the components to be transported to the wind farm site for assembly with little or no additional weight. These natural disconnect points will result in a simplification of the transportation process for a given blade radius or the ability to transport blades of larger radii. Additionally, if a blade were to be significantly damaged as a result of a hailstorm or leading edge erosion [10], components could more-easily be transported to the turbine location and if applicable, only the damaged section of the blade would need to be replaced.

11.3 STRUCTURAL BENEFITS

Current single-element wind turbine blades suffer from competing aerodynamic and structural requirements [11–13]. Aerodynamic requirements call for thinner airfoils while structural requirements call for thicker airfoils. These competing aerodynamic and structural requirements effectively cap the maximum size of wind turbine blades. The power rating of a wind turbine is proportional to the blade radius squared [3] while the weight and the required structural strength of a blade is proportional to the blade volume in accordance with the square-cube law; as a result, the blade weight grows faster than the power rating. The fact that the weight grows more rapidly than the power rating implies that a maximum economical size exists under the current structural configuration. In a multielement configuration with a strut (i.e., the well-separated cases of reference [1]), the strut and main element act in a biplane-like manner where an increased vertical separation between the two elements

will yield an aerodynamic benefit as well as an increase in the spar cap separation. An increase in spar cap separation is desirable because it offers increased structural benefits, including a stronger structure and decreased tip deflections [11–13]. By offering separate airfoil fairings for the upper and lower spar caps, well-separated multielement arrangements are able to solve the problem of competing aerodynamic and structural requirements. Multielement airfoil configurations may be tailored to facilitate even greater spar cap separations that could greatly improve the structural efficiency of the next generation of large multimegawatt wind turbines; this improved structural efficiency would effectively further raise the cap on the maximum achievable size of wind turbine blades. It should be noted that this style of multielement wind turbine blade would allow the design requirements for structural and aerodynamic considerations to be aligned whereas they currently compete with one another. This alignment of the design goals is due to the fact that in a biplane-like arrangement, the aerodynamic performance can be improved by increasing the vertical distance between the upper and lower blade sections; increasing the vertical distance is also desirable from a structural standpoint because the bending strength of an I-beam is proportional to the separation distance cubed. Limits, however, would eventually be reached on such blades in regard to torsional rigidity and tower clearance.

Structural investigations also attest to the benefits of multielement airfoil arrangements for the inboard sections of wind turbines. Studies conducted at the University of California, Los Angeles on a wind turbine blade with a biplane airfoil arrangement near the root show that such an arrangement is more structurally efficient than a single-element blade at loads from the incoming wind [13]. Compared to a conventional wind turbine blade, the use of a biplane arrangement makes it possible to construct a lighter blade that has an equal tip deflection [12]. While a biplane configuration of two NASA-designed 14%-thick supercritical SC(2)-0714 airfoils was found to have less total drag than the thick, single-element FFA-W3-301 wind turbine airfoil, a 30.1%-thick airfoil designed by The Aeronautical Research Institute of Sweden (FFA), one aspect of such a configuration that needs further study is the effect of the aerodynamic drag of the joint where the multielement arrangement would transition to a single-element arrangement [12]. It should be noted, however, that the SC(2)-0714 airfoil is designed to operate in the transonic regime; the airfoil was selected for study by Roth-Johnson and Wirz [12] because its box-like profile was expected to provide it with large principle area moments of inertia.

11.4 MULTIELEMENT WIND TURBINE BLADES

For the studies summarized in this chapter, the DU 00-W-401 airfoil geometry, a 40.1%-thick wind turbine airfoil designed by the Delft University Wind Research Institute in 2000, was used as a benchmark for gauging nominal spar

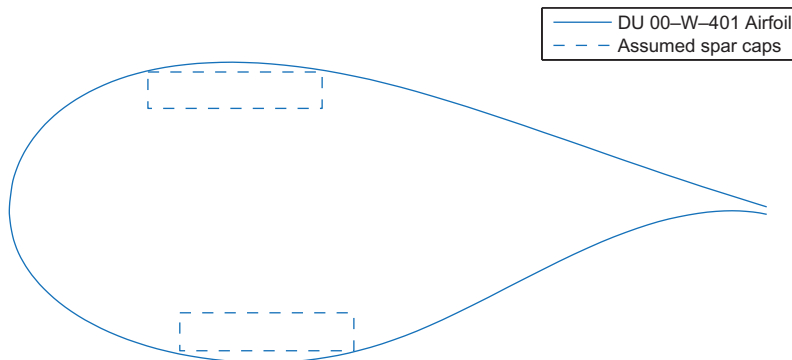


FIGURE 11.2 DU 00-W-401 airfoil and concept spar cap geometry. Taken from Ragheb AM, Selig MS. Multi-element airfoil configurations for wind turbines. In: Proceedings of the 29th AIAA applied aerodynamics conference, Honolulu, Hawaii, AIAA Paper 2011–3971; 2011.

cap spacing. Based on this geometry and examples in the literature [14] the location and dimensions of the top and bottom spar caps were approximated. The DU 00-W-401 airfoil section with the concept spar cap geometry is shown in Fig. 11.2. The 40.1% thick DU 00-W-401 wind turbine root airfoil was reported to have a maximum lift coefficient $C_{l,\max}$ value of around 1.04 at a Reynolds number $Re = 3.0 \times 10^6$ and $\alpha = 8.5$ degrees [15].

Normalized by the unit chord length of the airfoil, the nondimensional spar caps shown in Fig. 11.2, measure 0.23×0.048 with a separation of 0.27. The front of the top spar cap is located at $x/c = 0.183$ (18.3% of the distance from the airfoil leading edge to the trailing edge), and the front of the lower spar cap is located at $x/c = 0.225$. This concept spar cap geometry of these multielement configuration designs was greatly oversized to add ample flexibility and margin for the process of transformation of this concept from an academic study into a mass-producible commercial product. Two multielement airfoil configuration concepts are presented in this chapter. These configurations were designed with various combinations of slats, flaps, and struts arranged around a main airfoil element. In the second multielement geometry, the main airfoil element served as a fairing for the upper spar cap while the strut element faired the lower spar cap. Slats and flaps were located fore and aft of the main and/or strut elements, respectively. The entire arrangement was scaled to have a unit chord across all elements as shown in Fig. 11.3 and by the dotted chord line in Fig. 11.4. This scaling was done in order to allow for a direct comparison of the airfoil and multielement configuration lift coefficients.

The first multielement arrangement consists of a closely coupled multielement airfoil arrangement with a main element of similar thickness to existing wind turbine airfoils. The arrangement was denoted as the MFF arrangement; it contains a Main element and two Flap elements. This closely

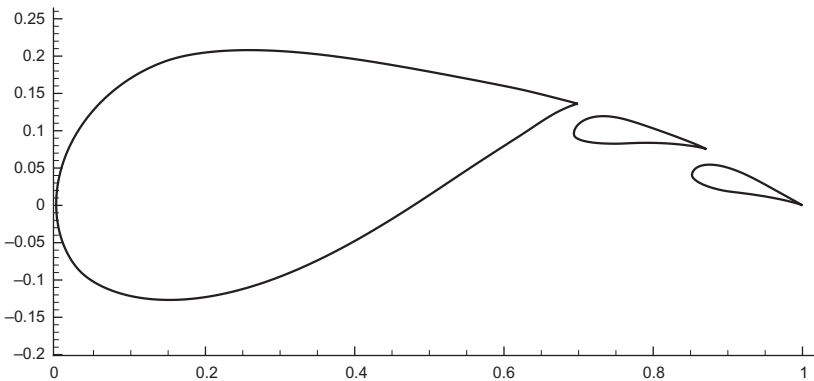


FIGURE 11.3 MFFS-018 multielement airfoil geometry as tested in references [16,17] with dimensions nondimensionalized by the unit chord length. Taken from Pomeroy BW, Williamson GA, Selig MS. Experimental study of a multielement airfoil for large wind turbines. In: Proceedings of the 30th applied aerodynamics conference, New Orleans, Louisiana; AIAA Paper, 2012–2892; 2012.

—	MFFS-018 Multielement airfoil
...	MFFS-018 Chord line
- - -	DU 00-W-401 and spar caps

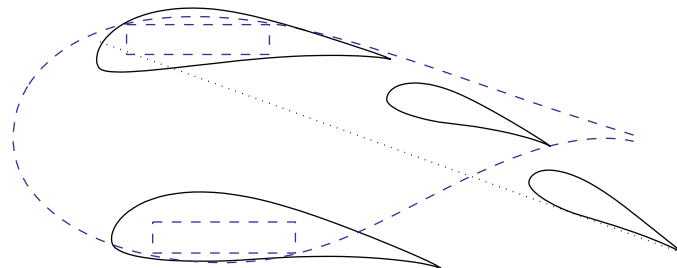


FIGURE 11.4 MFFS-018 multielement airfoil geometry. Taken from Ragheb AM, Selig MS. Multi-element airfoil configurations for wind turbines. In: Proceedings of the 29th AIAA applied aerodynamics conference, Honolulu, Hawaii, AIAA Paper, 2011–3971; 2011.

coupled arrangement was used in order to define an intermediate design concept between existing megawatt-scale wind turbine blade designs and a completely-redesigned well-separated multielement wind turbine blade as proposed by Ragheb and Selig [1]. Computational fluid dynamics (CFD) studies were conducted on this multielement airfoil by reference [16], and wind tunnel tests were tested on this geometry and derivatives of it in reference [17]; the airfoil geometry is presented in Fig. 11.3.

Narsipur et al. [16] conducted CFD analysis of the MFF-089 multielement geometry in ANSYS FLUENT at $Re = 1 \times 10^6$. While a number of different gap, overhang, and flap deflection angles were tested, all CFD

simulations of the configurations produced lift coefficient C_l values nearing 3.0 at an angle of attack of 18 degrees; values of the drag coefficient C_d at this angle of attack were around 0.035.

The second, more radical multielement arrangement presented herein consists of a double-slotted flap aft of a thin main element with a strut located beneath the main element. This configuration is presented in Fig. 11.4. The thin main element serves as an aerodynamic fairing for the upper spar cap and the strut element serves as a fairing for the lower spar cap. This well-separated multielement airfoil arrangement was named the MFFS and contains a Main element (M), two Flap elements (FF), and a Strut element (S). The MFFS family of designs evolved from the MFFS-018 arrangement, depicted in Fig. 11.4, of Ragheb and Selig [1] to offer an increased C_l/C_d when compared to the Delft University family of wind turbine airfoils [15,18] at C_l values up to 1.7. This configuration was developed with the goal of further increasing the lift over that of a single-flapped multielement arrangement. The second flap increased the camber relative to a single-slotted multielement airfoil configuration.

An inviscid multipoint inverse airfoil design method was used to develop and refine the multielement configurations. The PROFOIL [19–21] code and associated MFOIL graphical user interface was used to develop the configurations and to fine-tune the velocity profiles. The inviscid velocity profiles were adjusted in order to avoid the presence of strong adverse pressure gradients, which would be expected to lead to flow separation in an experimental or viscous computational investigation. The MFOIL user interface allows one to easily and rapidly account for changes to the structural constraints. The relocation of a spar cap or the addition of a rear spar would not preclude the user from getting significantly better aerodynamic results when compared to existing thick blade root airfoils, allowing a very great degree of freedom in the structural design of the blade. These multielement configurations were then analyzed using the viscous MSES [22–24] multielement computer program. The MSES code is an inviscid-viscous coupled solver. The performances, especially the C_l/C_d ratios and the stall characteristics, were compared with those of existing thick blade root airfoils at $Re = 3 \times 10^6$, which corresponds to the values encountered on utility-scale wind turbines.

Fig. 11.5 presents the flow properties across the multielement configuration. The left-hand figure of this pair of figures shows the pressure coefficient C_p distributions of the individual elements at $Re = 3.0 \times 10^6$ and angle of attack for the maximum lift-to-drag ratio, $\alpha_{C_l/C_d,\max}$, as determined by MSES [24]. The right-hand figure shows the nondimensional inviscid velocity distributions from MFOIL at the same α . These figures demonstrate that the adverse pressure gradients of the multielement arrangement were reasonable and no undesirable effects arose in the viscous case at the design point.

The aerodynamic performance of the MFFS-018 and DU 00-W-401 airfoils are compared in Fig. 11.6. These comparison data are from MSES

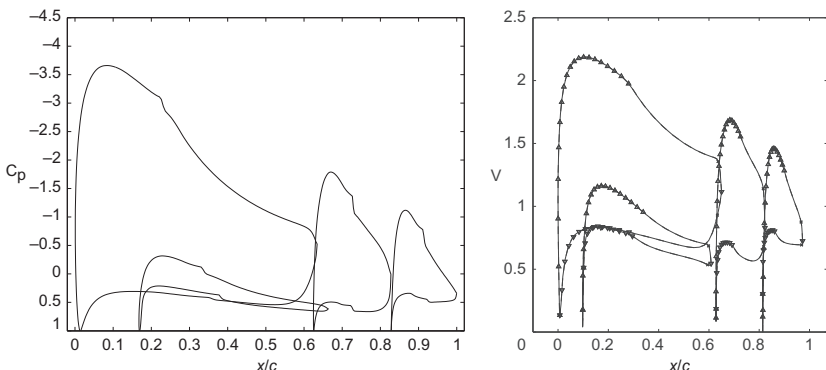


FIGURE 11.5 MFFS-018 viscous pressure coefficient (Left) and inviscid velocity normalized against the freestream velocity (Right) distributions at $C_l/C_{d,\max}$ ($\alpha = 12.9$ degrees, $C_l = 2.34$). Taken from Ragheb AM, Selig MS. Multi-element airfoil configurations for wind turbines. In: Proceedings of the 29th AIAA applied aerodynamics conference, Honolulu, Hawaii, AIAA Paper 2011–3971; 2011.

at $Re = 3.0 \times 10^6$. As determined by MSES, the DU 00-W-401 airfoil at $Re = 3.0 \times 10^6$ has a $C_l/C_{d,\max}$ of 82.9 at $C_l = 1.04$ and $\alpha = 6.5$ degrees. The MFFS-018 configuration shows a lift-to-drag ratio of $C_l/C_{d,\max} = 158.0$ at a lift coefficient of $C_l = 2.34$, which is a slightly greater lift-to-drag ratio than a single-flapped MFS configuration at a lower lift coefficient [1]. The MFFS-018 configuration appears to be well-suited for higher C_l values because it demonstrates the highest $C_l/C_{d,\max}$ of all the configurations analyzed in reference [1], but offers a C_l/C_d at $C_l = 1.7$ that is lower than single-flapped multielement arrangements. As shown in Fig. 11.6, the drop off of C_l/C_d beyond $C_l/C_{d,\max}$ was gentler than that of the DU 00-W-401 airfoil in the MSES simulations.

The MFFS airfoil arrangement was selected over a single-flapped configuration for a number of its benefits. The first benefit is that its double-slotted flap arrangement allows for a high degree of aerodynamic tunability to achieve high C_l/C_d ratios at specific C_l values. These specific C_l values would allow for operation at an optimal axial induction factor over a larger portion of the blade. Additionally, an increased separation between the two elements would yield an aerodynamic benefit because the strut and main element act in a biplane-like manner. An increase in spar cap separation is desirable because it offers increased structural benefits, including a stronger structure and decreased tip deflections [11–13]. By offering separate airfoil fairings for the upper and lower spar caps, this well-separated multielement arrangement is able to solve the problem of competing aerodynamic and structural requirements.

The design of the multielement airfoil families was an iterative process between airfoil and blade design. Using the MFF or MFFS, DU 91-W2-250,

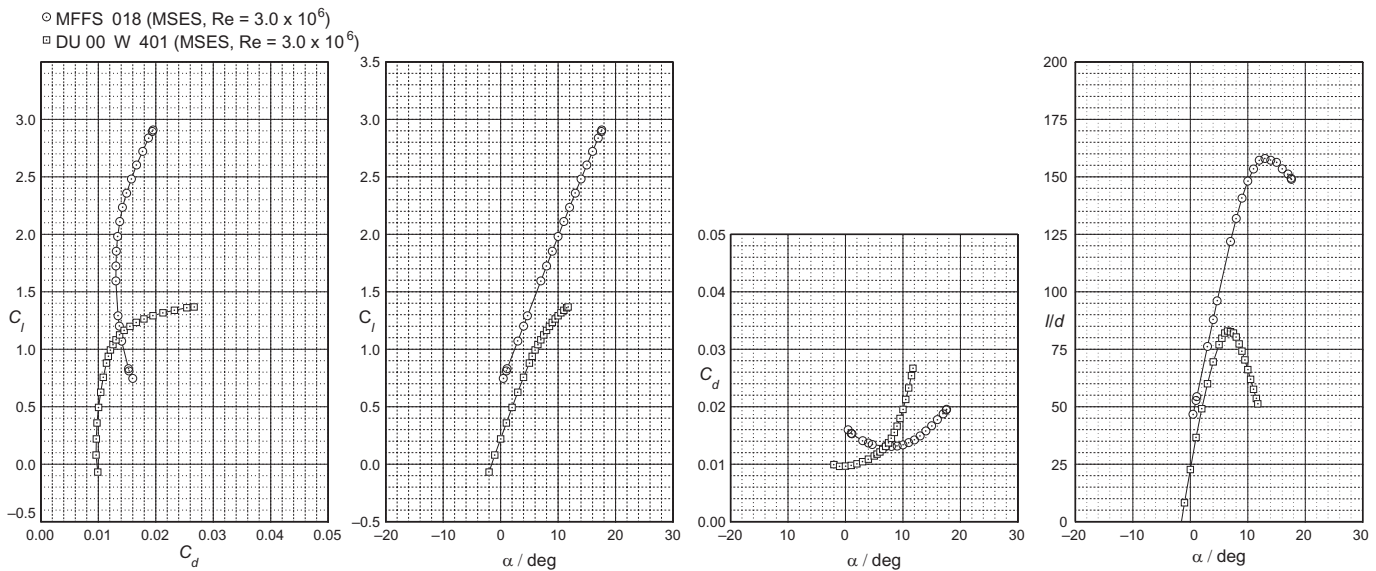


FIGURE 11.6 MFFS-018 lift and drag performance comparisons to the DU 00-W-401 at $Re = 3.0 \times 10^6$. Taken from Ragheb AM, Selig MS. Multi-element airfoil configurations for wind turbines. In: Proceedings of the 29th AIAA applied aerodynamics conference, Honolulu, Hawaii, AIAA Paper, 2011–3971; 2011.

DU 00-W-212, and DU 96-W-180 airfoils, an initial multielement blade was designed. The C_l distribution used to design the blade was chosen to produce a smooth chord distribution with no jagged edges or protrusions. This C_l distribution, along with the resulting chord, twist, and Reynolds number results from the PROPID [20] propeller analysis were used to determine the desired airfoil performance requirements for the multielement airfoils. The new airfoils would then be used in PROPID to modify the blade design. Results from PROPID were then used to define the new performance requirements for modifying the multielement airfoils. This process would be iterated upon until the airfoil and blade designs converged. Figs. 11.7 and 11.8 present the resulting MFS and MFFS multielement airfoil families, respectively, with correct twist and chord lengths normalized to the DU 91-W2-250.

While Figs. 11.7 and 11.8 present a cross-sectional view of the candidate wind turbine blades, a conceptual drawing of what a multielement wind turbine blade based on the MFFS family of airfoils would look like is presented in Fig. 11.9 for clarification. The MFF-089 and MFFS-026 multielement blade root airfoils were designed in MSES for wind tunnel testing [17] in the University of Illinois subsonic low-turbulence wind tunnel at Reynolds numbers between 0.75×10^6 and 1×10^6 . For ease of manufacturing, the two flap elements of the MFF-089 are identical to the two flap elements of the MFFS-026 [17]. The MFF-130 multielement airfoil was designed to produce a high C_l/C_d ratio at $C_l = 1.3$ and $Re = 10 \times 10^6$. The MFF-140 was designed

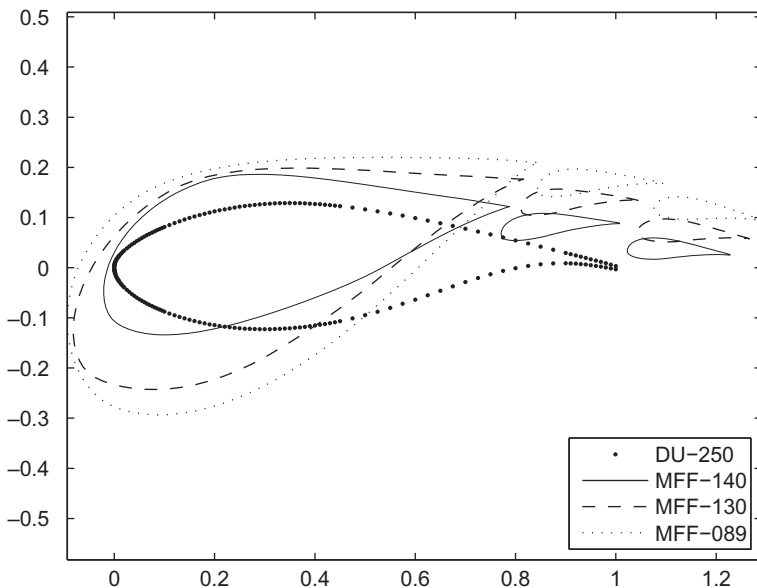


FIGURE 11.7 MFF family of airfoils coplotted with 25%-thick DU airfoil at shear and twist locations used for blade analysis (dimensions nondimensionalized by unit chord length).

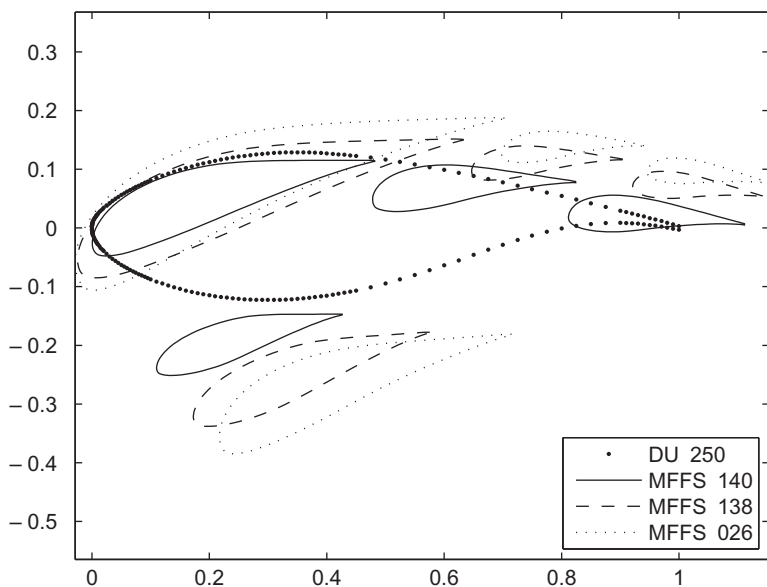


FIGURE 11.8 MFFS family of airfoils coplotted with 25%-thick DU airfoil at shear and twist locations used for blade analysis (dimensions nondimensionalized by unit chord length).

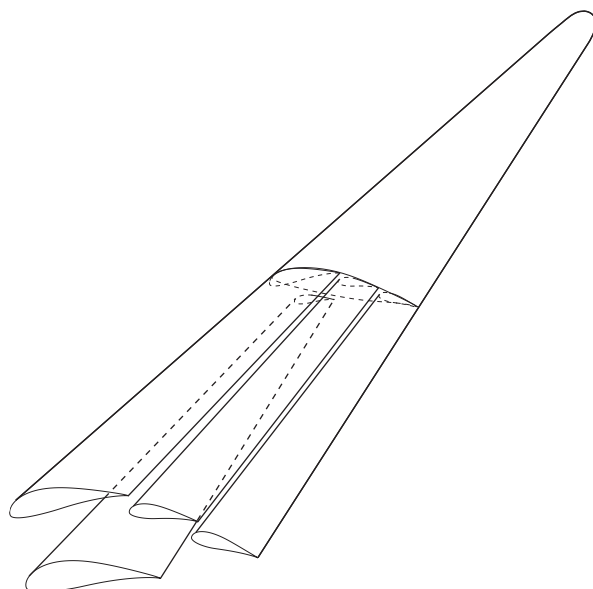


FIGURE 11.9 Conceptual drawing of a double-slotted (MFFS) multielement wind turbine blade.

for $C_l = 1.1$ at $Re = 11 \times 10^6$. The MFFS-138 was designed for a high C_l/C_d at $C_l = 1.5$ and $Re = 9.5 \times 10^6$ while the MFFS-140 was designed for $C_l = 1.25$ at $Re = 11 \times 10^6$.

All airfoil data presented herein were from the MSES flow solver. This program is known to especially overpredict the lift performance of thick airfoils such as the DU and MFF airfoils used for the inboard section of the baseline blade [25,26]. This characteristic was observed when the MSES predictions for the DU airfoils and the MFF-089 multielement airfoil arrangement were compared to unpublished wind tunnel results and published CFD results [16]. Because of the overpredicted lift performance of thick airfoils, the performance of a baseline conventional blade with thick airfoils would be overpredicted, and thus the gains achievable through the use of multielement airfoils on the inboard sections of a wind turbine blade would not be accurately modeled. Even with this overprediction of the baseline performance, PROPID simulations of a three-bladed 10 MW wind turbine with a diameter of 176 m (577 ft.) showed increases in GAEP of approximately 1%, with larger increases existing at lower wind speeds. This candidate wind turbine was designed to operate at a tip-speed ratio of 8.7 and at 9.8 revolutions per minute (RPM). The maximum blade chord of the baseline was capped at 4.9 m (16 ft). Based on the size of the concept wind turbine, it would likely be of the direct-drive variety [8] and would most probably be located offshore.

To conduct PROPID simulations, the desired C_l distribution for the blade design was chosen to create a blade with a typical chord distribution. The locations of the airfoils along the span of the blade were chosen to maximize the lift-to-drag ratio along the blade and to ensure a smooth twist and thickness distribution. To show the benefits of using the MFF family of airfoils, a blade was designed and analyzed using PROPID. The baseline 10 MW blade was used as a starting point, and the thick DU airfoils were replaced by the MFF airfoils. Only the inboard section of the blade was modified, so that from the DU 91-W2-250 airfoil (located at the 47% blade station) to the tip, the baseline and multielement blade designs are the same.

Aerodynamically the MFF and MFFS multielement airfoil configurations are superior to typical thick root airfoil sections of modern megawatt-scale wind turbines in many respects. When compared with a traditional section, these multielement configurations are capable of producing much higher maximum lift coefficients, with C_l values of up to 3.0 compared to the $C_{l,\max} = 1.04$ for the 40.1% thick DU 00-W-401 airfoil. Moreover, these multielement airfoil configurations produce much higher lift-to-drag ratios on account of both higher lift and much lower drag, with increases between 40% and 90% in $C_l/C_{d,\max}$ over the DU 00-W-401. At $C_l = 1.7$, the MFS-104 multielement configuration produced the greatest percent gain in C_l/C_d with a 60.7% increase over the DU 00-W-401 airfoil. The value of $C_l = 1.7$ was selected as a realistic value for the inboard section of a wind turbine blade; significantly larger C_l values would greatly exceed current blade structural limits. As demonstrated by the SMFS case of references [1,27–29],

the addition of a slat results in an increase in the $C_l/C_{d,\max}$ value of a multielement arrangement, but this comes at the cost of a sharper drop off in C_l/C_d above $C_l/C_{d,\max}$ when compared to a nonslatted multielement arrangement. By moving the strut element farther below the main and flap elements, the $C_l/C_{d,\max}$ value may be increased as a larger amount of lift is generated by the main element.

Based on the MSES results and preliminary PROPID results, the use of multielement airfoils is very promising. Multielement airfoils allow the lift coefficient and lift-to-drag ratios of the inboard section of a wind turbine blade to be increased. This results in a number of aerodynamic benefits. The axial induction factor can be increased to be closer to the ideal Betz value of one-third [3] near the inboard portion of a wind turbine blade. Additionally, the increased lift near the hub will allow for a larger tangential force coefficient C_t [2], which, in turn, will provide the turbine with increased torque from the root section and will create the potential for a lower cut-in wind speed and increased power output at low wind speeds. This reduction of the cut-in wind speed will help to increase the capacity factor, and may allow new locations to be opened up for wind turbines that may not be economically viable with conventional single-element wind turbine blades.

11.5 OTHER MULTIELEMENT WIND TURBINE RESEARCH

A number of studies have been performed into the potential benefits of adding slats to the inboard sections of wind turbine blades [27–31]. These studies were performed because due to the large thickness of the blade root as required by structural constraints, the aerodynamically suboptimal airfoils [1] produce loadings on the blade root section that are significantly lower than those corresponding to the maximum energy capture [28]. Gaunaa et al. [28] performed computational investigations on rotor slats for the regime defined by $0.1 > r/R > 0.3$ for the Light Rotor baseline 10 MW reference wind turbine rotor, where r/R is the radial location on the rotor (r) normalized by the rotor radius (R). Using 3D CFD, a significant modification of the flow field of the inner rotor region was observed. These changes caused by the addition of slats to the inboard region of the rotor were calculated to increase the C_p by 1% with a corresponding C_T increase of 2% [28].

In an earlier work, Gaunaa et al. [29] articulated that the material costs, stand still loads, and maximum chord length as determined by transportation requirements have caused the center part of utility-scale wind turbine blades to be loaded at significantly less than the optimal power production loading condition. Simply increasing the chord length near the hub would help resolve these issues, but issues of cost, transportation, and extreme structural loads limit this idea to academic studies. Thus the motivation for investigating the retrofit of slats to existing wind turbine blades was created. Using a Blade Element Momentum (BEM) based approach to evaluate the 2D CFD-optimized slat designs, it was estimated that the retrofit of slats to the root

section of a candidate 10 MW turbine would likely yield a greater than 1% increase in the annual energy production [29].

In general slats were investigated as additions to a previously designed rotor because the design problem is simplified due to the involvement of fewer degrees of freedom [29]. A later study by Jaume [30] investigated both a slat superimposed upon, and integrated into the geometry of, the DU 91-W2-250 airfoil developed by the Delft University of Technology [15]. It should be noted that this airfoil is located at $r/R = 43\%$ and is 25% thick. By adding a leading edge slat, the angle of attack range over which the airfoil performed efficiently was increased. Additionally, the maximum lift coefficient was increased by 64.8% and the critical angle of attack was increased by 9 degrees [15]. A downside to the addition of the slat is that the drag is greatly increased as low angles of attack. Jaume et al. [15] report that the optimization procedure used to design a slat for the DU 91-W2-250 will be applied to the five remaining airfoils of their reference blade in order to determine the preferred spanwise extent of retrofittable slats. In regard to thicker airfoils, the addition of a slat, based on the NACA 22 airfoil, to the 30% thick DU-97-W-300 airfoil was studied by Eisele and Pechlivanoglou [31]. Zahle et al. [27] used 2D CFD to optimize the shape of a slat for a 40% thick wind turbine airfoil [27].

While a large number of academic studies have been discussed, two current industry studies are of note. GE has researched placing a hemispherical dome over the inner parts of a wind turbine in its Energy Capture Optimization by Revolutionary Onboard Turbine Reshape (ECO ROTR) and has shown that this concept has improved the performance of the wind turbine. This dome concept was tested in 2012 in the Gust wind tunnel at the University of Stuttgart in Germany. The results were promising enough that starting in 2013, a full-scale test program was initiated. A geodesic dome 20 m in diameter weighing 20 tonnes was installed on a 1.7 MW 100 m diameter space frame tower (SFT) turbine in Tehachapi, California. On May 25, 2015, the dome was installed on the wind turbine, and it was reported that the turbine performance would be evaluated over a 4-month period.

The second industry study of note is the multirotor concept introduced by Vestas in April 2016. Vestas claims that by installing four smaller rotors on a main tower, the scaling rules of wind turbines can be challenged; they report that transport and installation challenges can be mitigated through this novel concept. Work on this project is being conducted in cooperation with the Technical University of Denmark as a research partner, and a concept demonstrator is being installed at the Risø site near Roskilde, Denmark.

11.6 DISCUSSION

Multielement airfoils for wind turbines hold great promise. In addition to increasing the aerodynamic efficiency of wind turbines, they also show strong promise for resolving transportation issues associated with large blades.

In regard to the structural considerations, the use of multielement airfoil configurations will allow for the currently competing aerodynamic and structural requirements to now be aligned. Whereas with current thick single-element airfoils, aerodynamic requirements push for a thinner airfoil and structural requirements push for a thicker airfoils, with the use of multielement airfoils with a main and strut element, both aerodynamic and structural requirements call for an increased vertical separation between the elements. While the join location where the wind turbine blade would transition from a multielement airfoil to a single element will add some weight, weight will be saved at the root section through the improved structural arrangement. Additionally, this heavy transition section will bring with it the ability to assemble the blades onsite in segments, which will ease transportation concerns.

Focusing on the aerodynamic aspects of the use of multielement airfoils on wind turbines, the potential for better start-up performance exists due to a higher C_t from higher lift airfoils as well as increased blade efficiency from more closely matched ideal operating conditions along the blade. Altogether these aerodynamic advantages are expected to increase the efficiency of the wind turbines through both increased energy production and reductions in blade material and mass, with an ultimate result of a lower cost of energy. Finally these multielement configurations demonstrated the desirable characteristic of a gentler drop off in C_l/C_d beyond $C_l/C_{d,max}$ when compared to the DU 00-W-401 airfoil.

By replacing the thick root airfoils with a multielement airfoil arrangement over the inboard 47% blade span on a wind turbine, the annual energy production of a 10 MW scale turbine can be increased by at least 1%. This increase is due to the larger C_l/C_d ratios attainable by the multielement arrangements and is only a minimum value due to the overprediction of the thick airfoil performance values. The blades with a multielement root also had larger C_l values inboard allowing for a more optimal axial induction factor closer to the hub. This increased inboard lift is expected to provide more torque at the root which in turn will result in a lower cut-in wind speed. Multielement wind turbine blades can be designed to have at least the same blade thickness near the hub as the conventional baseline design while maintaining improved performance. The use of a well-separated blade design for the root section introduced both the ability to increase the spar cap separation to create a stronger structure and the potential for natural disconnect points to allow for simplified transportation of large blades to the turbine sites. The MFFS design was successfully designed to be thicker than the baseline, both in terms of absolute thickness and t/c ratio, and a thicker blade allows for a stronger spar structure.

ACKNOWLEDGMENTS

Support for some of this research was provided by GE Energy and the UIUC Department of Aerospace Engineering. Dr. Robert Deters from the Department of Engineering

Sciences at Embry-Riddle Aeronautical University conducted the PROPID wind turbine simulations mentioned in this chapter.

REFERENCES

- [1] Ragheb AM, Selig MS. Multi-element airfoil configurations for wind turbines. Proceedings of the 29th AIAA applied aerodynamics conference, Honolulu, Hawaii, AIAA Paper 2011–3971; 2011.
- [2] Fuglsang P, Bak C, Gaunaa M, Antoniou I. Design and verification of the Riso-B1 airfoil family for wind turbines. *J Solar Energy Eng* 2004;126:1002–10.
- [3] Ragheb M, Ragheb AM. Fundamental and advanced topics in wind power. Wind turbines theory - the Betz equation and optimal rotor tip speed ratio. Rijeka, Croatia: INTECH; 2011. p. 19–38.
- [4] Griffin DA, Ashwill TD. Alternative composite materials for megawatt-scale wind turbine blades: design considerations and recommended testing. Proceedings of the 41st aerospace sciences meeting and exhibit, Reno, Nevada, AIAA Paper 2003–0696; 2003.
- [5] Cotrell J, Stehly T, Johnson J, Roberts JO, Parker Z, Scott G, et al. Analysis of transportation and logistics challenges affecting the deployment of larger wind turbines: summary of results. National Renewable Energy Laboratory, Technical Report NREL/TP-5000–61063, Golden, CO; 2014.
- [6] Sobie B. Wind energy innovation: segmented blades-navigant research, <<https://www.navigantresearch.com/blog/wind-energy-innovation-segmented-blades>>; 2014 [accessed June 2016].
- [7] Gamesa. Gamesa 5.0 MW Innovating for Reliability, <<http://www.gamesacorp.com/recursos/doc/productos-servicios/aerogeneradores/catalogo-g10x-45mw-eng.pdf>>; 2015 [accessed June 2016].
- [8] Ragheb AM, Ragheb M. Fundamental and advanced topics in wind power. Wind turbine gearbox technologies. Rijeka, Croatia: INTECH; 2011. p. 189–206.
- [9] De Vries E, Buist J. Turbines of the year-rotor blades-windpower monthly. <<http://www.windpowermonthly.com/article/1225377/turbines-year--rotor-blades>>, Published December 24, 2013, [accessed June 2016].
- [10] Fiore G, Selig MS. Simulation of damage for wind turbine blades due to airborne particles. *Wind engineering* 2015;39:399–418.
- [11] Wirz RE, Johnson PM. Aero-structural performance of multiplane wind turbine blades. Proceedings of the 29th AIAA applied aerodynamics conference, Honolulu, Hawaii, AIAA Paper 2011–3025; 2011.
- [12] Roth-Johnson P, Wirz RE. Aero-structural investigation of biplane wind turbine blades. *Wind energy* 2014;17:397–411.
- [13] Roth-Johnson P, Wirz RE, Lin E. Structural design of spars for 100-m biplane wind turbine blades. *Renewable energy* 2014;71:133–55.
- [14] Jackson KJ, Zuteck MD, van Dam CP, Standish KJ, Berry D. Innovative design approaches for large wind turbine blades. *Wind energy* 2005;8:141–71.
- [15] Timmer W, van Rooij R. Summary of the Delft University wind turbine dedicated airfoils. *J Solar Energy Eng* 2003;125:448–96.
- [16] Narsipur S, Pomeroy BW, Selig MS. CFD analysis of multielement airfoils for wind turbines. Proceedings of the 30th applied aerodynamics conference, New Orleans, Louisiana, AIAA Paper 2012–2781; 2012.

- [17] Pomeroy BW, Williamson GA, Selig MS. Experimental study of a multielement airfoil for large wind turbines. Proceedings of the 30th applied aerodynamics conference, New Orleans, Louisiana, AIAA Paper 2012–2892; 2012.
- [18] van Rooij R, Timmer W. Roughness sensitivity considerations for thick rotor blade airfoils. *J Solar Energy Eng* 2003;125:468–78.
- [19] Selig MS, Maughmer MD. Multipoint inverse airfoil design method based on conformal mapping. *AIAA J* 1992;30:1162–70.
- [20] Selig MS, Maughmer MD. Generalized multipoint inverse airfoil design. *AIAA J* 1992;30:2618–25.
- [21] Gopalaranthy A, Selig MS. Low-speed natural-laminar-flow airfoils: case study in inverse design, *AIAA. J Aircr* 2001;38:57–63.
- [22] Drela M, Giles MB. Viscous-Inviscid Analysis of Transonic and Low Reynolds Number Airfoils. *AIAA J* 1987;25:1347–55.
- [23] Drela M. Design and optimization method for multi-element airfoils. Proceedings of the AIAA/AHS/ASEE aerospace design conference, Irvine, California, AIAA Paper 93-0960; 1993.
- [24] Drela M. A User's Guide to MSES 3.05. MIT Department of Aeronautics and Astronautics, July, 2007.
- [25] Somers DM, Maughmer MD. Design and experimental results for the S414 airfoil. U.S. Army Aviation Research, Development and Engineering Command: Aviation Applied Technology Directorate, Fort Eustis, Virginia, RDECOM TR 10-D-112; 2010.
- [26] Duque EPN, Johnson W, vanDam CP, Cortes R, Yee K. Numerical predictions of wind turbine power and aerodynamic loads for the NREL Phase II combined experiment rotor, AIAA Paper 2000–0038; 2000.
- [27] Zahle F, Gaunaa M, Sorensen NN, Bak C. Design and wind tunnel testing of a thick, multi-element high-lift airfoil. Proceedings of EWEA 2012—European Wind Energy Conference & Exhibition, Copenhagen, Denmark, European Wind Energy Association (EWEA); 2012.
- [28] Gaunaa M, Zahle F, Sorensen NN, Bak C, Rethore PE. Rotor performance enhancement using slats on the inner part of a 10 MW rotor. Proceedings of EWEA 2013—European Wind Energy Conference & Exhibition, Vienna, Austria, European Wind Energy Association (EWEA); 2013.
- [29] Gaunaa M, Zahle F, Sorensen NN, Bak C. Quantification of the effects of using slats on the inner part of a 10 MW rotor. Proceedings of EWEA 2012—European wind energy conference & exhibition, Copenhagen, Denmark, European Wind Energy Association (EWEA); 2012.
- [30] Jaume AM, Wild J. Aerodynamic design and optimization of a high-lift device for a wind turbine airfoil. New results in numerical and experimental fluid mechanics X. Switzerland: Springer; 2016. p. 859–69.
- [31] Eisele O, Pechlivanoglou G. Single and multi-element airfoil performance simulation study and wind tunnel validation. Wind energy – impact of turbulence. Berlin, Germany: Springer; 2014. p. 17–22.

This page intentionally left blank

Chapter 12

Civil Engineering Aspects of a Wind Farm and Wind Turbine Structures

Subhamoy Bhattacharya

University of Surrey, Guildford, United Kingdom

Email: s.bhattacharya@surrey.ac.uk

12.1 ENERGY CHALLENGE

With the discovery of shale gas (fracking) and lowering of oil price, it is predicted that reliance of oil (often termed as oil age) may have gone. With the increasing use of electric cars and wind turbine, it may be argued that this change of moving toward low carbon energy (LCE) is irreversible and quite similar to the transition from *Stone Age* to *Bronze Age*. Offshore wind energy is considered promising technology to move toward LCE.

12.2 WIND FARM AND FUKUSHIMA NUCLEAR DISASTER

12.2.1 Case Study: Performance of Near Shore Wind Farm During 2012 Tohoku Earthquake

A devastating earthquake of moment magnitude $M_w 9.0$ struck the Tohoku and Kanto regions of Japan on March 12 at 2:46 p.m. which also triggered a tsunami, see Fig. 12.1 for the location of the earthquake and the operating wind farms. The earthquake and the associated effects such as liquefaction and tsunami caused great economic loss, loss of life, and tremendous damage to structures and national infrastructures but very little damage to the wind farms. Extensive damage was also caused by the massive tsunami in many cities and towns along the coast. Fig. 12.2A shows photographs of a wind farm at Kamisu (Hasaki) after the earthquake and Fig. 12.2B shows the collapse of pile-supported building at Onagawa. At many locations (e.g., Natori, Oofunato, and Onagawa), tsunami heights exceeded 10 m, and sea walls and other coastal defense systems failed to prevent the disaster.

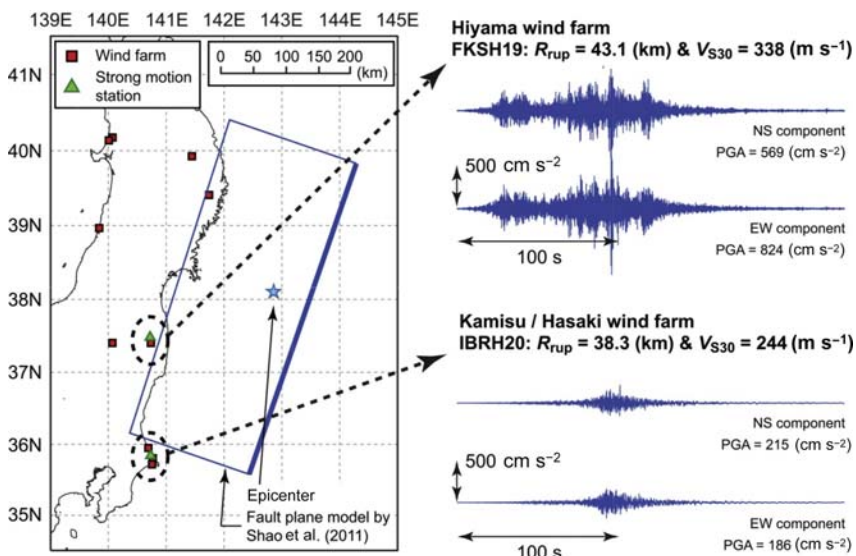


FIGURE 12.1 Details of the 2012 Tohoku earthquake and locations of the wind farms [10].

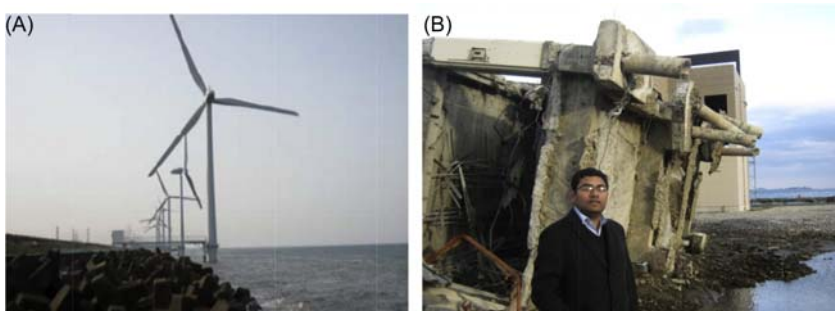


FIGURE 12.2 (A) Photograph of the Kamisu (Hasaki) wind farm following the 2012 Tohoku earthquake; and (B) collapse of the pile-supported building following the same earthquake.

The earthquake and its associated effects (i.e., tsunami) also initiated the crisis of the Fukushima Dai-ichi nuclear power plants (NPPs). The tsunami, which arrived around 50 minutes following the initial earthquake was 14 m high which overwhelmed the 10 m high plant sea walls flooding the emergency generator rooms causing the power failure of active cooling system. Limited emergency battery power ran out on March 12 and subsequently led to the reactor heating up and the subsequent meltdown leading to the release of harmful radioactive material to the atmosphere. Power failure also meant that many of the safety control systems were not operational. The release of radioactive materials caused a large scale evacuation of over 300 000 people and the cleanup costs is expected to be of the order of tens of billions of

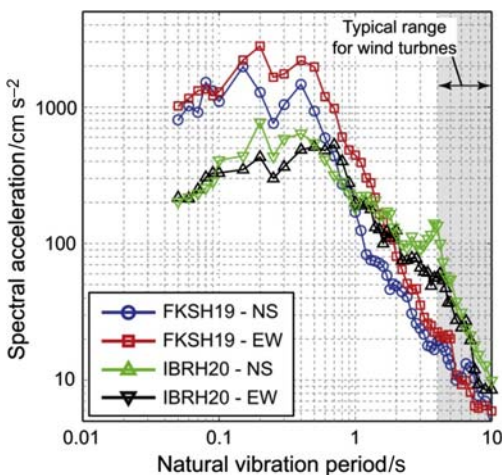


FIGURE 12.3 Power spectra of the earthquake and natural frequency of wind turbines.

dollars. On the other hand, following/during the earthquake the wind turbines were automatically shut down (like all escalators or lifts) and following an inspection—they were restarted.

12.2.1.1 Why Did the Wind Farm Stand Up?

Recorded ground acceleration time-series data in two directions (North–South (NS) and East–West (EW)) at Kamisu and Hiyama wind farms (FKSH 19 and IBRH20) are presented in Fig. 12.3 in frequency domain. The dominant period ranges, of the recorded ground motions at the wind farm sites, were around 0.07–1 seconds and on the other hand the periods of the offshore wind turbine systems are in the range of 3 seconds. Due to nonoverlapping of the vibration periods, these structures will not get tuned in and as a result they are relatively insensitive to earthquake shaking. However, earthquake-induced effects such as liquefaction may cause some damages. Further details can be found in Bhattacharya and Goda [1]. Further details of dynamics of wind turbine structures together with the effects of foundation flexibility can be found in Adhikari and Bhattacharya [2,3], Bhattacharya and Adhikari [4], Bhattacharya et al. [5,6,7], and Lombardi et al. [8].

ASIDE: One may argue, had there been few offshore wind turbines operating, the disaster may have been averted or the scale of damages could have certainly been reduced. The wind turbines could have run the emergency cooling system and prevented the reactor meltdown. In this context, it is interesting to note that there are plans to replace the Fukushima NPP by a floating wind farm. The project is in advanced stage whereby involving a 2 MW semi-sub floating turbine which has been operational for few years. An innovative 7 MW oil pressure drive type wind turbine on a three-column semi-sub floater has recently been tested.

12.3 WIND FARM SITE SELECTION

Fig. 12.4 shows the operating or planned wind farms along UK coast. Fig. 12.5 on the other hand shows wind farms along the coasts of United Kingdom and Europe together with the installed capacity. This section of the chapter will detail the considerations for choosing a particular site.

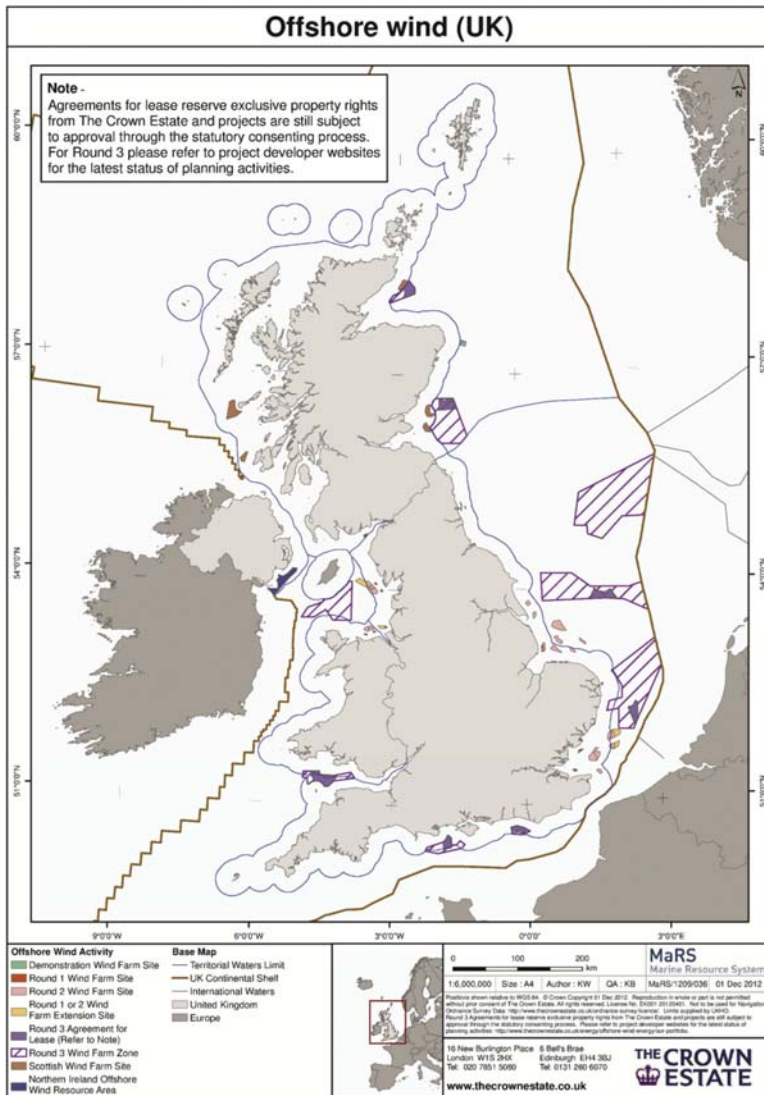


FIGURE 12.4 Offshore wind farms around United Kingdom.

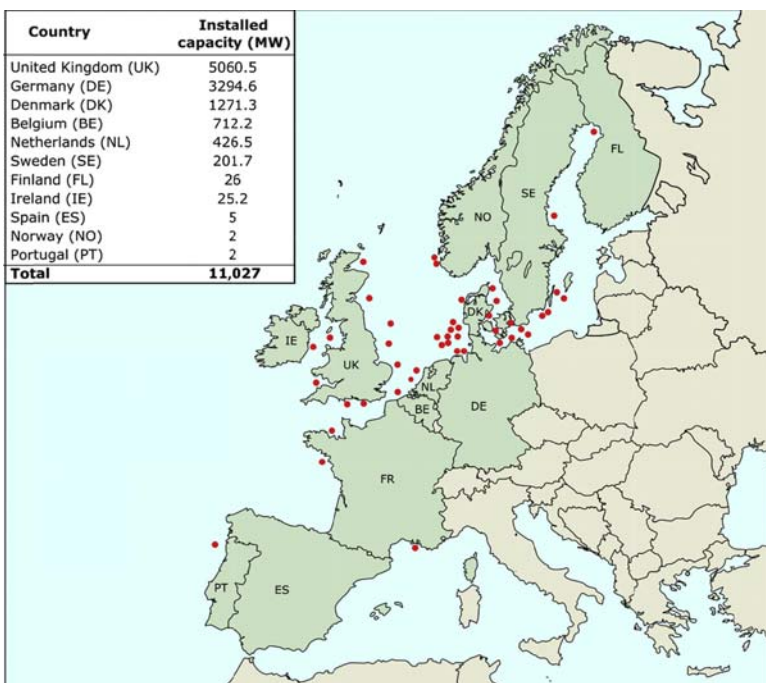


FIGURE 12.5 Wind farms in Europe.

The main considerations are:

1. *Wind resources:* A thorough knowledge of wind resources in an area is fundamental as it allows an estimation to be made on the wind farms productivity and therefore the financial viability of the project. As a thumb rule, a project is not financially viable if the average wind speed at the hub height is below 6 m s^{-1} and it is considered a safe investment if the average wind speed at the hub is more than 8.5 m s^{-1} .
2. *Marine aspects:* Marine aspects would include water depth, wave spectrum at the site (wave height, wave period), current and tide data, exposure to waves and sediment transport, identification of scour-related issues and if scour protection is needed. Often installation of foundations creates obstacles in the local flow pattern of water which may create turbulence leading to a scouring effect.
3. *Environmental impact:* For all wind farm, an EIA (Environmental Impact Assessment) must be completed as a part of the planning process and it covers the physical, biological, and human environment. This would involve collecting all types of existing environmental data and assessing for all the potential impacts that could arise due to the construction and operation of the wind farm. The impacts can range from favorable to less

favorable to detrimental. Potential aspects on the biological environment include marine mammals, sea birds that use the area on a regular basis, birds from nearby areas that pass through the area during flight, fish, etc. Other aspects include effect of flora and fauna during the construction (e.g., noise due to piling or operating noise), electromagnetic field generated by subsea cable. Human environment include a change of landscape. Marine archeology aspects such as ship wreck are also taken in consideration. To carry out the assessment, samples of seabed may be collected and analyzed for worms, barnacles, or other species.

4. *Power export/grid connection:* One of the important deciding factor is the location of onshore grid connections. The deciding factor includes the length of submarine cable required which is dependent on the turbine layout, substation location, identify export cable routing (landfall), risk assessment of buried cables, and the transformer options—alternating or direct current.
5. *Economics:* Modeling of capital costs and leveled cost of energy (LCOE) is a function involving many parameters: depth of water, distance from shore, wind speed at the site, port and harbor facilities near the site, socioeconomic condition and access to skilled labor, location of national grid, and hinterland for the proposed development.
6. *Navigation:* This navigation risk assessment survey investigates whether or not there is a need for exclusion zone due to fishing or navigation or military operations. Cables connecting the wind farms and the export cables are buried to depths of 2–3 m to avoid risk of entanglement with nets.
7. *Consents and legislations:* Depending on the country, the consent requirements may change. For example, in the United Kingdom, any development more than 100 MW is classified as significant infrastructure project and requires development consent order from IPC (Infrastructure Planning Commission). These rules are subject to amendment and currently the final decision rests with the Secretary of State for Energy and Climate Change.

12.3.1 Case Studies: Burbo Wind Farm (see Fig. 12.6 for location)

The Burbo wind farm was fitted with 3 MW wind turbines of Vestas V80 make.

The location of Burbo wind farm is influenced by the following:

1. Average wind speed more than 7 m s^{-1}
2. Shallow water depth 0.5–8 m at low tide
3. Good seabed condition for construction of foundation
4. Close to entrance of Mersey river
5. Proximity to Liverpool port
6. 6.4 km from Sefton coastline
7. Safe distance from navigation channel

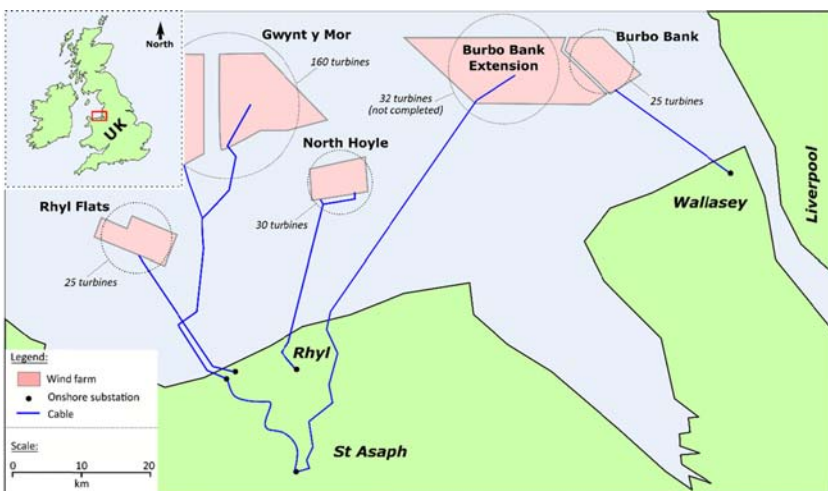


FIGURE 12.6 Location of the Burbo wind farm.

8. Onshore export cable traveled 3.5 km underground to a substation to be fed in the grid.

The following consents were taken for Burbo:

1. Consents are Section 36 of Electricity Act 1989 for wind turbine and cabling
2. Consent under Section 34 of Coastal Protection Act 1949 for Construction in navigable waters
3. Permission from Port Authority
4. Permission under Section 57 of the Town and Country Planning Act 1990 for onshore cabling, inter connection facilities, and substation
5. License under Section 5 of Food and Environment Protection Act 1985 for the siting of Wind Turbines and deposit of scour protection material

12.3.2 ASIDE on the Economics

Currently, many of the wind farms are operating from the subsidy provided by the government. For example, in the United Kingdom, there are schemes such as CfD (Contract for Difference) are in use. However, in order to be sustainable, large wind farms are to be constructed to achieve the economy of scales with the aim to produce electricity at the lowest possible cost. Therefore the cost of electricity from different sources are compared using LCOE or SCOE (Society's Cost of Energy). As many of the installation, operation and maintenance (O & M) will be carried out in rougher waters, time in construction is also a driving factor for site selection. Therefore every cost that increases part of the construction has to be lowered in such a

manner that an optimal method for the construction and installation will be established.

12.4 GENERAL ARRANGEMENT OF A WIND FARM

[Fig. 12.7](#) shows the components of a typical wind farm. The turbines in a wind farm are connected by interturbine cables (electrical collection system) and are connected to the offshore substation. There are export cables from offshore to the onshore. [Figs. 12.8 and 12.9](#) show photographs of some of the components. [Fig. 12.8A](#) shows the photograph of a wind farm with many wind turbines and a substation. [Fig. 12.8B](#) shows the details of the substructure of a monopile with J tubes for the electrical collection system. [Fig. 12.9](#) shows the photograph of a jacket supported substation.

12.5 CHOICE OF FOUNDATIONS FOR A SITE

The choice of foundation will depend on the following: site conditions (wind, wave, current, seabed condition, ground profile, water depth, etc.), available fabrication and installation expertise, operation and maintenance, decommissioning laws of the land, and finally economics. The definition of an ideal foundation is as follows:

1. A foundation which is capacity or “*rated power*” specific (i.e., 5 or 8 MW rated power) specific but not turbine manufacturer specific. In other words, a foundation designed to support 5 MW turbine but can support turbines of any make. There are other advantages in the sense that turbines can be easily replaced even if a particular manufacturer stops manufacturing them.
2. Installation of a foundation is not weather sensitive, i.e., not dependent of having a calm sea or a particular wind condition. The installation of the first offshore wind farm in the United States took more time due to the unavailability of a suitable weather window.
3. Low maintenance and operational costs, i.e., needs least amount of inspection. For example, a jacket type foundation needs inspection at the weld joints.

It is economical to have a large number of turbines in a wind farm to have the economy of scales and therefore it also requires a large area. If the continental shelf is very steep, grounded (fixed) turbines are not economically viable and a floating system is desirable.

12.6 FOUNDATION TYPES

Foundations constitute the most important design consideration and often determines the financial viability of a project. Typically foundations cost

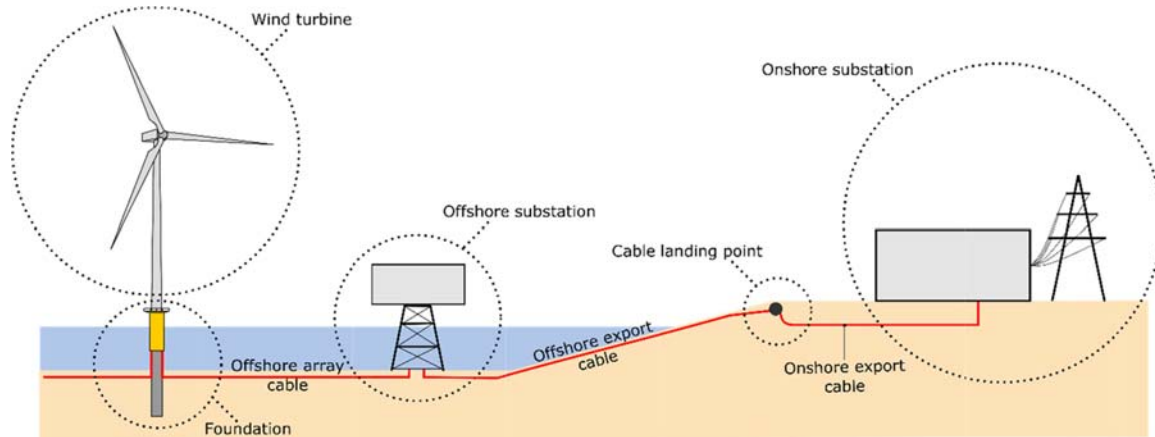


FIGURE 12.7 Overview of a wind farm.



FIGURE 12.8 (A) Wind farm with offshore substation; and (B) turbine J tubes for interturbine cables and electrical collection system.

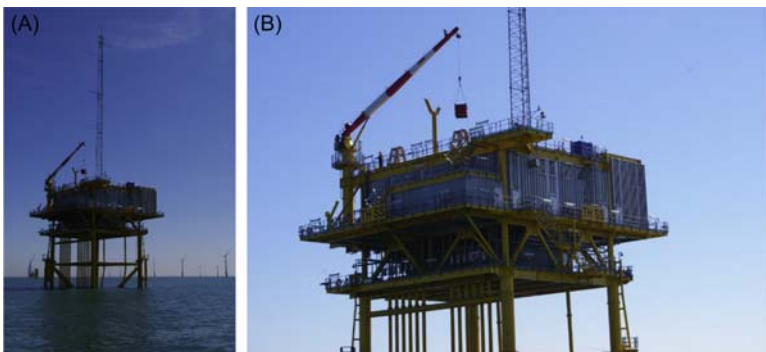


FIGURE 12.9 Offshore substation.

25%–34% of the whole project and there are attempts to get the costs down. Many aspects must be considered while choosing and designing the foundation for a particular site. They include: ease to install under most weather conditions, varying seabed conditions, aspects of installation including vessels and equipment required, and local regulations concerning the environment (noise). Fig. 12.10 shows a schematic diagram of a wind turbine supported on a large diameter column inserted deep into the ground (known as monopile). This is the most used foundation so far in the offshore wind industry due to its simplicity.

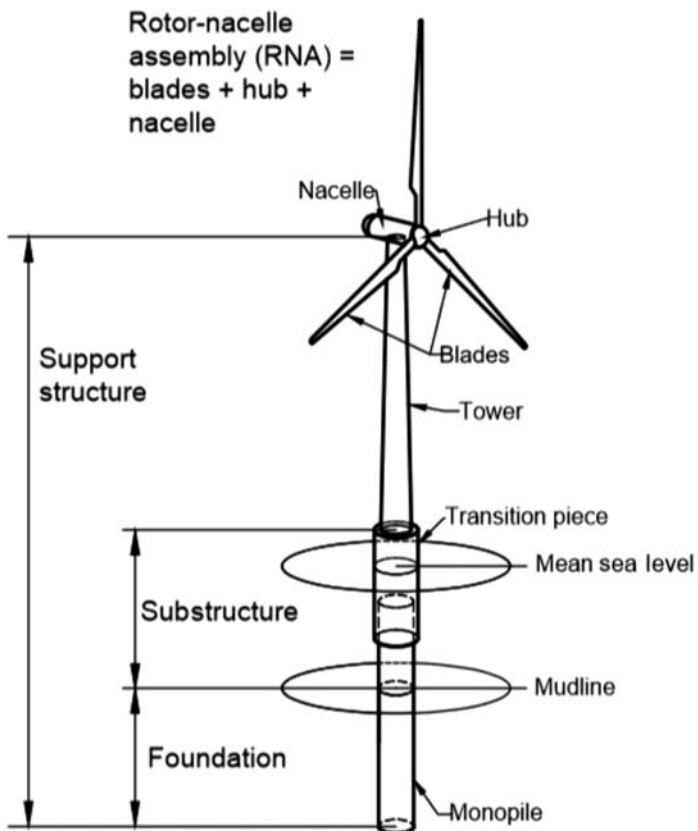


FIGURE 12.10 Monopile foundation.

Fig. 12.11 shows the various types of foundations commonly used today for different depths of water. Monopiles (Fig. 12.11C), gravity-based foundations (Fig. 12.11B), and suction caissons (Fig. 12.11A) are currently being used or considered for water depths of about 30 m. For water depth between 30 and 60 m, jackets or seabed frame structures supported on piles or caissons are either used or planned. Floating system is being considered for deeper waters, typically more than 60 m. However, selection of foundations depends on seabed, site conditions, turbine and loading characteristics, and the economics and not always on the water depth.

The substructure can be classified into two types:

1. Grounded system or fixed structure where the structure is anchored to the seabed. Grounded system can be further subdivided in two types in the terminology of conventional foundation/geotechnical engineering: shallow foundation (gravity base solution and suction caisson) and deep foundation.

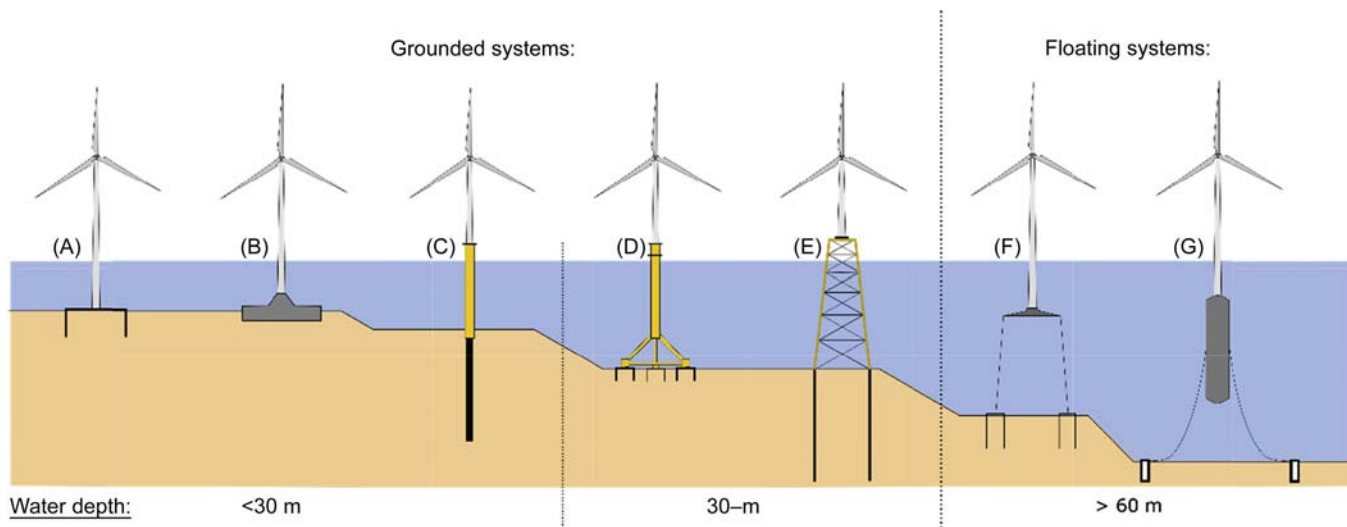


FIGURE 12.11 (A) Bucket/suction caisson; (B) gravity based; (C) monopile; (D) tripod on bucket/suction caisson; (E) jacket/lattice structure; (F) tension leg platform; and (G) spar buoy floating concept.

2. Floating system where the system is allowed to float is anchored to the seabed by a mooring system. Floating systems have certain ecological advantage in the sense that the foundations leave a very low seabed footprint, easy to decommission and maintain as the system can be deanchored and floated out to a harbor.

12.6.1 Gravity-Based Foundation System

The gravity foundation is designed to avoid uplift or overturning, i.e., no tensile load between the support structure and the seabed. This is achieved by providing adequate dead load to provide stability to the structure under the action of overturning moments. If the dead loads from the support structure and the superstructure (tower + RNA) are not sufficient, additional ballast will be necessary. The ballast consists of rock, iron ore, or concrete. Installation of these foundation often requires seabed preparation to avoid inclination. The gravity-based structure in most cases are constructed in situ concrete or with precast concrete units. The gravity-based concept can be classified into the two types depending on the method of transportation and installation:

1. Crane free solution also known as “float-out and sink” solution: These types of foundations will be floated (either self-buoyant or with some mechanism) and towed to the offshore site. At the site, the foundation will be filled with ballast causing it to sink to the seabed. This can be attractive solutions for sites having very hard or rocky soil condition. This operation does not require a crane and thus known as a “crane free” solution.
2. Crane-assisted solution: In this type, the foundation does have the capacity to float and is therefore towed to the site onboard a vessel. They are then lowered to the seabed using cranes. An example is the Thornton Bank, shown in [Fig. 12.12](#) where the shape of the gravity-based substructure is compared to a champagne bottle.

12.6.2 Suction Buckets or Caissons

Suction buckets (sometimes referred to as suction caissons) are similar in appearance to a gravity-based foundations but with long skirts around the perimeter. Essentially, they are a hybrid foundation taking design aspects from both shallow and pile foundation arrangements. A caisson consists of a ridged circular lid with a thin tubular skirt of finite length extending below, giving it the appearance of a bucket. Typically, such foundations will have a diameter to length ratio (D/Z) of around 1 making them significantly shorter than a pile but deeper than a shallow foundation. A sketch of a suction caisson with terminology can be seen in [Fig. 12.13](#). Suction caissons themselves



FIGURE 12.12 GBS from Thornton Bank Project.

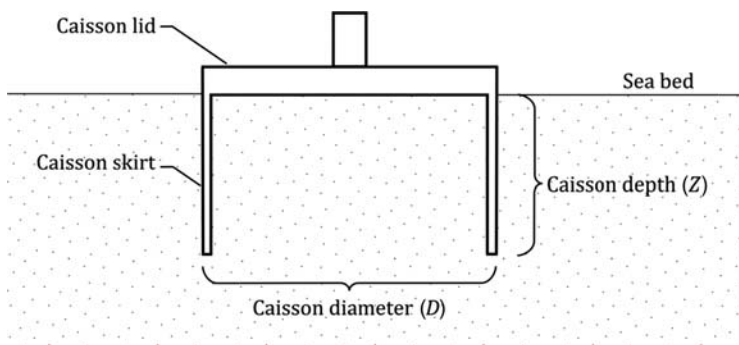


FIGURE 12.13 Typical layout of a suction caisson foundation.

are a fairly recent development in the offshore industry. Caissons first came into use around 30 years ago as foundation structure for offshore oil and gas production platforms.

12.6.3 Pile Foundations

Single large diameter steel tubular pile also known as monopile is the most common form of foundation for supporting offshore wind turbines. Fig. 12.14 shows the monopile type of foundation which is essentially a large steel pile (3–7 m in diameter) driven into the seabed with a typical penetration depth of 25–40 m. A steel tube, commonly called the transition piece (TP) is connected to the steel pile and the tower is attached to it. The TP supports the boat landings and ladders used for entering the turbine.



FIGURE 12.14 Large diameter monopile.

Currently, this type of foundation is extensively used for water depths up to 25–30 m.

These foundations can be reliability driven into the seabed using a steam or hydraulically driven hammer and the practice is very standardized due to the offshore oil and gas industry. The handling and driving of these foundations requires the use of either floating vessels or jack-up vessels which must be equipped with large cranes, a suite of hammers, and drilling equipment. If the ground profile at the site contains stiff clay or rock, drive–drill–drive procedure may need to be adopted. Pile driving results in noise and vibrations. Therefore the installation of the turbine (Nacelle and Rotor) is always carried out after the piling has been completed.

12.6.4 Seabed Frame or Jacket Supporting Supported on Pile or Caissons

Often a seabed frame or a jacket supported on piles or caissons can act as support structure and they can be classified as multipods ([Fig. 12.15](#)).



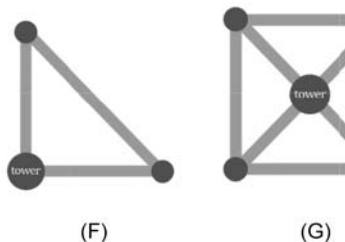
(A)

(B)

(C)

(D)

(E)



(F)

(G)

(H)

FIGURE 12.15 Multipod foundations. (A) Tetrapod caisson; (B) asymmetric tripod caisson; (C) jacketed caisson; (D) tripod caisson; (E) tripod pile; (F) asymmetric tripod plan; (G) jacket foundation plan; and (H) tripod foundation plan.



FIGURE 12.16 Different type of support structure for a wind farm in China.

Multipods have more than one point of contact between the foundation and the soil. Soil embedded elements may include flexible piles, gravity bases, and suction caissons can also be used. Fig. 12.16 shows an example from a wind farm in China. Further details on the foundations used in China can be found in [Chapter 13](#), Civil Engineering Challenges Associated With Design of Offshore Wind Turbines With Special Reference to China.

12.6.5 Floating Turbine System

The floating system can be classified into three main types ([Fig. 12.17A](#)):

1. Mooring stabilized TLP (tension leg platform) concept: This type of system is stabilized with tensioned mooring and is anchored to the seabed for buoyancy and stability.
2. Ballast stabilized *spar buoy* concept with or without motion control stabilizer: This type of system will have a relatively deep cylindrical base providing the ballast whereby the lower part of the structure is much heavier than the upper part. This would raise the center of buoyancy about the center of gravity of the system. While these are simple structures having a low capex cost, it needs a deeper draft, i.e., deeper water and is not feasible in shallow water. Motion stabilizer can be used to reduce the overall tilt of the system
3. Buoyancy stabilized semi-submersible: This concept is a combination of ballasting and tensioning principle and consumes a large amount of steel ([Fig. 12.17B](#)).

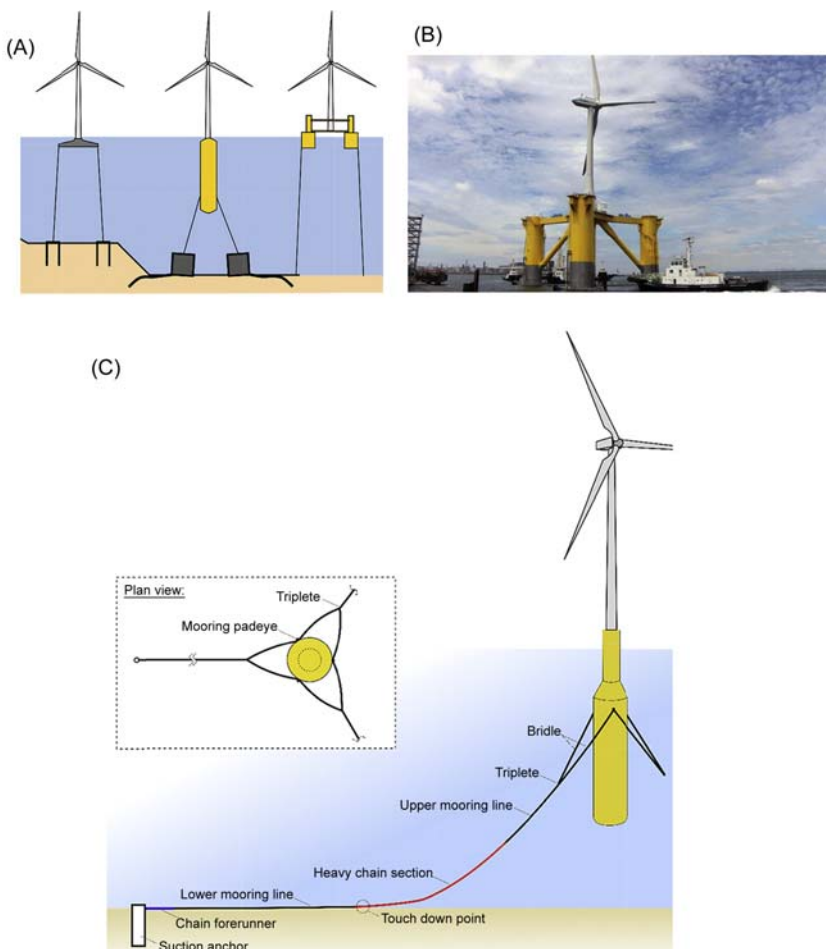


FIGURE 12.17 (A) Three main types of floating system to support wind turbine generator; (B) semi-submersible foundation for offshore Fukushima (Japan); and (C) details of Hywind Wind Turbine Installation which is Spar buoy—Floating system.

There are varieties of anchors that can be used to moor the floating system and they can be classified into surface anchors and embedded anchors. Example of surface anchors is a large heavy box containing rocks or iron ore and the holding capacity depends on the weight of the anchor itself and the friction between the base of the anchor and the seabed. On the other hand, examples of embedded anchors include anchor piles (Fig. 12.17A–C) which are floating wind turbine concepts suitable for deeper waters. Fig. 12.17B shows the floating concept (semi-sub) implemented in a wind farm in Japan (offshore Fukushima) and Fig. 12.17C shows the Hywind concept (spar).

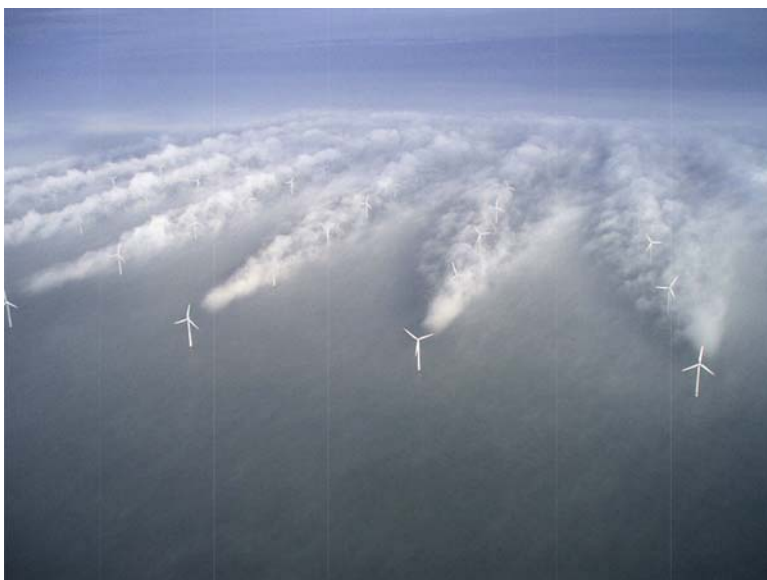


FIGURE 12.18 Wake turbulence. Photo credit: Vattenfall Wind Power, Denmark.

12.7 SITE LAYOUT, SPACING OF TURBINES, AND GEOLOGY OF THE SITE

Wind turbines in a wind farm are spaced to maximize the amount of energy that can be generated without substantially increasing the CAPEX (Capital expenditure, i.e., upfront cost). If the farm is significantly spread out, i.e., large spacing of the turbines, the interarray cable length will increase. The spacing is therefore an optimization problem between compactness of the wind farm (which minimizes the CAPEX cost due to subsea cables) and the adequate separations between turbines so as to minimize the energy loss due to wind shadowing from upstream turbines. Fig. 12.18 shows the aerial photo of wake turbulence behind individual wind turbines that can be seen in the fog of the Horns Rev wind farm off the Western coast of Denmark.

The geometric layout of a wind farm can be a single line of array, or a square or a rectangular configuration. Due to advanced methods for optimization having different constraints as well as site conditions, different layout pattern is increasingly being used. Typically, the spacing between turbines is equivalent to 3–10 times the rotor diameter and it depends on the prevailing wind direction. The spacing should be larger than 3–4 rotor diameter perpendicular to the prevailing wind direction and 8–10 diameters for direction parallel to the wind direction. For example, for a prevailing South Westerly wind direction (which is typical of Northern Ireland), a possible site layout for a wind farm located in the area is shown in Fig. 12.19. The spacing along

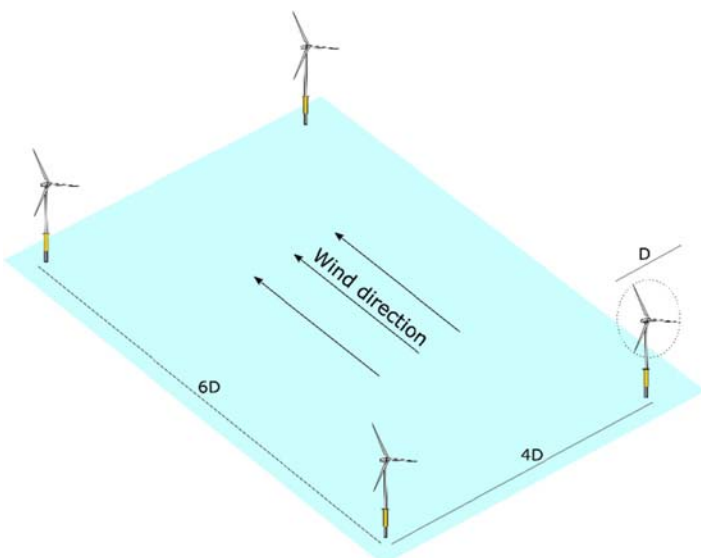


FIGURE 12.19 Spacing of turbines.

the wind direction is kept at 6 times the rotor diameter (6D) but for across the wind, the spacing can be kept bit lower (4D).

Due to the large spacing of the turbines (typically 800–1200 m apart), a small to medium size wind farm would extend over a substantial area. Typical size for a modern day wind farm is $20\text{ km} \times 6.5\text{ km}$ (e.g., Sandbank wind farm of German North Sea). Due to the large coverage of area for a wind farm, there may be significant variation in the geological and subsurface conditions as well as practical restraints. Examples include sudden drop in the sea floor causing change in water depth, paleochannels, change in ground stratification, submarine slopes, presence of foreign objects such as shipwrecks, location of important utility lines (gas pipeline, fiber optic cables), etc. A detail site investigation programme consisting of geotechnical and geophysical tests is carried out to establish a 3D geological model which often dictates the layout.

12.7.1 Case Study: Westermost Rough

Fig. 12.20 shows the ground profile from Westermost Rough Offshore Wind Farm (located in the United Kingdom) approximately 8 km off the Yorkshire coast, near the town of Withernsea following Kallehave et al. [9]. It may be observed that the monopile passes through different geology denoted in the figure. Therefore the foundation consists of monopiles of varying length, wall thickness and diameter. This also shows that not only geotechnical but also geological study needs to be carried out.

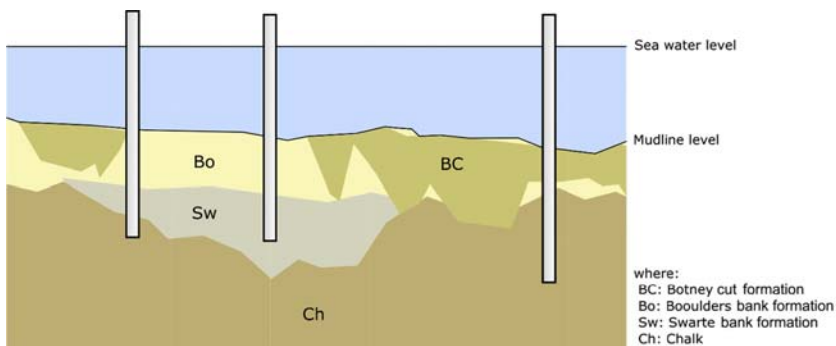


FIGURE 12.20 Monopile foundation in Westermost Rough. Adapted from Kallehave et al. [9].

12.7.2 Economy of Scales for Foundation

Monopiles are currently preferred for water depths up to 30 m. The simple geometry makes it possible to automate the manufacturing and fabrication process and the typical manufacturing cost related to monopile steel is 2 euros per kilogram. Welding can be carried out by robots and installation is relatively simple. However, if the diameter become large (knowns as XL or XXL piles which are over 8 m in diameter and weighs 1200 tonnes), the transportation and installation becomes challenging and limits the number of installation contractors that can carry out the work. Innovations are underway to install large diameter piles using a vibro method where a foundation is installed through the vibration of the soil and thus effectively liquefying the soil around it.

An alternative to large diameter monopiles is the 3 or 4 legged jacket on small diameter piles. Steel for jackets cost around 5 euros per kilogram to manufacture, which is more than double that of monopiles due to many tubular joints which are often welded manually.

Gravity-based foundations are cheaper to manufacture as compared to steel but requires a large fabrication yard and storing area. As concrete foundations will be much heavier than an equivalent steel foundation, large crane and vessels are required for installation. For an offshore site where the surface ground is rock, gravity-based structure will be a preferred choice; this is the situation in French waters.

Due to the vast size of a wind farm, there will be varying seabed condition including water depth and distance from the shore. As a result, the loads on the foundations will change and ideally the best design will be to design each foundation individually which will give rise to a customized foundation design for each turbine location. However, from economic point of view, it is desirable to have few foundation types so that the overall economy is

achieved and the process of fabrication and installation can be carried out efficiently using the same installation vessel. Most North European developers prefer one type of foundation (either monopiles or jackets) on a site. This consideration often dictates the layout of the farm to avoid deeper water or soft locally available mud.

REFERENCES

- [1] Bhattacharya S, Goda K. Use of offshore wind farms to increase seismic resilience of nuclear power plants. *Soil Dyn Earthquake Eng* 2016;80:65–8. Available from: <http://dx.doi.org/10.1016/j.soildyn.2015.10.001>.
- [2] Adhikari S, Bhattacharya S. Dynamic analysis of wind turbine towers on flexible foundations. *Shock Vib* 2012;19:37–56.
- [3] Adhikari S, Bhattacharya S. Vibrations of wind-turbines considering soil-structure interaction. *Wind Struct Int J* 2012;14:85–122.
- [4] Bhattacharya S, Adhikari S. Experimental validation of soil–structure interaction of offshore wind turbines. *Soil Dyn Earthquake Eng* 2012;31(5–6):805–16.
- [5] Bhattacharya S, Lombardi D, Muir Wood DM. Similitude relationships for physical modelling of monopile-supported offshore wind turbines. *Int J Phys Model Geotech* 2012;12(2):58–68.
- [6] Bhattacharya S, Cox J, Lombardi D, Muir Wood D. Dynamics of offshore wind turbines supported on two foundations. *Geotechnical Eng Proc ICE* 2013;166(2):159–69.
- [7] Bhattacharya S, Nikitas N, Garnsey J, Alexander NA, Cox J, Lombardi D, et al. Observed dynamic soil–structure interaction in scale testing of offshore wind turbine foundations. *Soil Dyn Earthquake Eng* 2013;54:47–60.
- [8] Lombardi D, Bhattacharya S, Muir Wood D. Dynamic soil-structure interaction of monopile supported wind turbines in cohesive soil. *Soil Dyn Earthquake Eng* 2013;49:165–80.
- [9] Kallehave D, Byrne BW, LeBlanc Thilsted C, Mikkelsen KK. Optimization of monopiles for offshore wind turbines. *Philos Trans R Soc* 2015;A 373:2035. <http://dx.doi.org/10.1098/rsta.2014.0100>.
- [10] Shao G, Li X, Ji C, Maeda T. Preliminary results of the March 11, 2011 Mw 9.1 Honshu Earthquake. Santa Barbara: University of California; 2011. Available at: http://www.geol.ucsb.edu/faculty/ji/big_earthquakes/2011/03/0311/Honshu_main.htmlS.

Chapter 13

Civil Engineering Challenges Associated With Design of Offshore Wind Turbines With Special Reference to China

Subhamoy Bhattacharya¹, Lizhong Wang², Junwei Liu³, and Yi Hong²

¹*University of Surrey, Guildford, United Kingdom*, ²*Zhejiang University, Zhejiang Sheng, China*,

³*Qingdao University of Technology, Qingdao Shi, China*

Email: s.bhattacharya@surrey.ac.uk

13.1 OFFSHORE WIND POTENTIAL IN CHINA

Due to the rapid and consistent economic growth and prosperity, the demand for energy in China has grown enormously. Due to the extensive coastline and to comply with the global climate agreements, offshore wind power sector has been expanding. The wind power industry has been growing steadily since 2006. Up to about 2010, the turbines were mostly built onshore in areas with high wind speed (e.g., Xinjiang Province) and offshore potentials were not investigated. However, the 12th Five Year Plan (2011–15) of the PRC (People Republic of China) Government gave a boost to expand the offshore capability and the target was to develop offshore wind turbine (OWT) farms of 5 GW capacity by 2015 and 30 GW capacity by 2020. Furthermore, there was an announcement of a “National Offshore Wind Power Development and Construction Plan (2014–16)” to develop offshore wind farms in Chinese waters/China Sea. Fig. 13.1 shows the location of the development of the wind farms in Chinese waters.

China completed the first OWT installation (Suizhong 35-1 Oil Field Turbine) in 2007. Subsequently, the first offshore wind farm in Asia was developed in 2010 through the Donghai Bridge 100 MW Offshore Wind Power Demonstration Project. In 2010, a wind farm was also constructed in the intertidal area of Longyuan Rudong. After successful construction and operation of the first three wind farms, a large number of wind farm projects

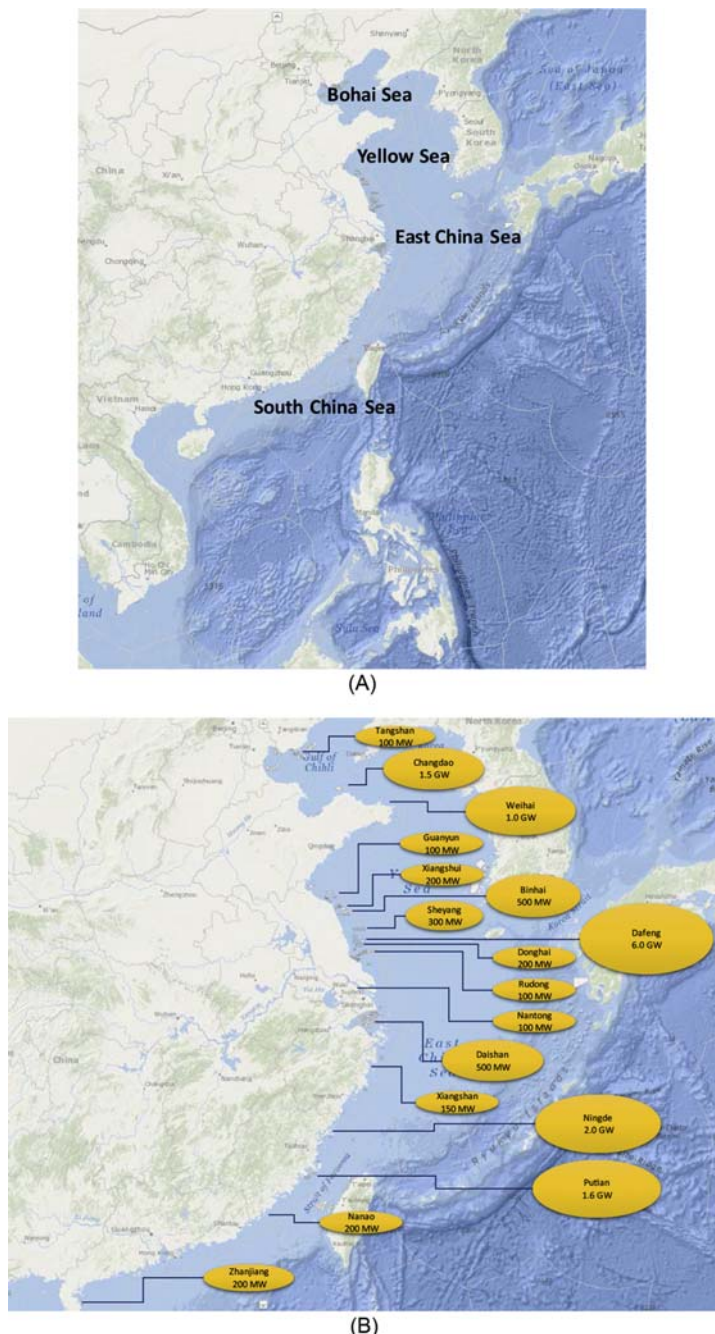


FIGURE 13.1 (A) A map showing the main developments of offshore wind projects in China. (B) Locations and capacities of offshore wind farms in China.

TABLE 13.1 Offshore Wind Farms in China

Development Status	No. of Farms
Fully commissioned	23
Partial generation	2
Under construction	11
Preconstruction	8
Consent authorized	>100

were consented/authorized and construction is under way. [Table 13.1](#) provides the statistics of the work in progress.

As shown in [Fig. 13.1A](#), there are five main sea areas in China: (1) Bohai Sea (enclosed sea); (2) Yellow Sea; (3) East China Sea; (4) South China Sea, and (5) Taiwan Strait. The locations and capacities of offshore wind farms (in operation or still under construction) in China are illustrated in [Fig. 13.1B](#).

The long stretch of China Sea is becoming attractive for many scientific surveys related to wind energy, as a result of the rapid development of economy in the adjoining areas, leading to energy demand. As the wind speed offshore is much larger and stable than that onshore counterpart, offshore wind power developments in these zones are attracting serious investors. The three main economic zones (Beijing Zone, Yangtze River Delta, and Pearl River Delta) are also very close to the long coastline of China, and is therefore convenient for electricity transport to the regional economic zones. Therefore, these sea regions are suitable for construction and application of offshore wind farms.

The distributions of offshore wind farms in those five sea regions are different on both number and density. It can be seen from [Fig. 13.1](#) that offshore wind farms are densely distributed along Yellow Sea coast and Hangzhou Bay. However, compared with Yangtze River Delta Economic Region (around Shanghai), there are few offshore wind farms in Pearl River Delta Economic Region (Guangzhou–Hong Kong). [Table 13.2](#) provides statistics of the distribution of the projects in China Sea.

13.2 DYNAMIC SENSITIVITY OF OWT STRUCTURES

OWTs, due to their shape and form (i.e., a long slender column with a heavy mass as well as a rotating mass at the top), are dynamically sensitive because the natural frequencies of these slender structures are very close to the excitation frequencies imposed by the environmental and mechanical loads [\[1\]](#).

TABLE 13.2 Offshore Wind Farms in China Sea

Offshore Wind Development	Fully Commissioned	Partial Generation	Under Construction	Preconstruction
Bohai Sea	4	0	2	1
Yellow Sea	14	0	0	1
East China Sea	3	2	6	3
Taiwan Strait	2	1	2	3
South China Sea	0	0	1	0

Fig. 13.2 shows a simple mechanical model of the whole system including the different components and the design variables. In the model, the foundation is replaced by four springs: K_L (lateral spring), K_R (rocking spring), K_V (vertical spring), and K_{LR} (cross-coupling spring). The stability and deformation of the system is very much dependent on these four springs; a few things may be noted regarding these springs:

1. The properties and shape of the springs (load–deformation characteristics) should be such that the whole structure should not collapse under the action of extreme loads and the deformation is acceptable under the working loads.
2. The values of the springs (stiffness of the foundation) are necessary to compute the natural period of the whole structure as this is a linear Eigen value analysis. Further details on the analysis required can be found by Adhikari and Bhattacharya [2] and Adhikari and Bhattacharya [3].
3. The values of the springs will also dictate the overall dynamic stability of the system due to its nonlinear nature. It must be mentioned that these springs are not only frequency dependent but also change with cycles of loading due to dynamic soil–structure interaction. Further details on the dynamic interaction can be found in the work of Bhattacharya et al. [4,5].

Fig. 13.3 shows typical wind and wave power spectral densities (PSDs) for offshore sites which essentially describe the frequency content of dynamic excitations from wind turbulence and waves. The graph also shows the turbine’s rotational frequency range (1P) and the turbine’s blade passing frequency range (3P) for a range of commercial wind turbines of different capacities (2–8 MW). A simplified way of translating the wind turbulence spectrum and the wave spectrum into mudline bending moment spectra through linear transfer functions has been presented by Arany et al. [6] The

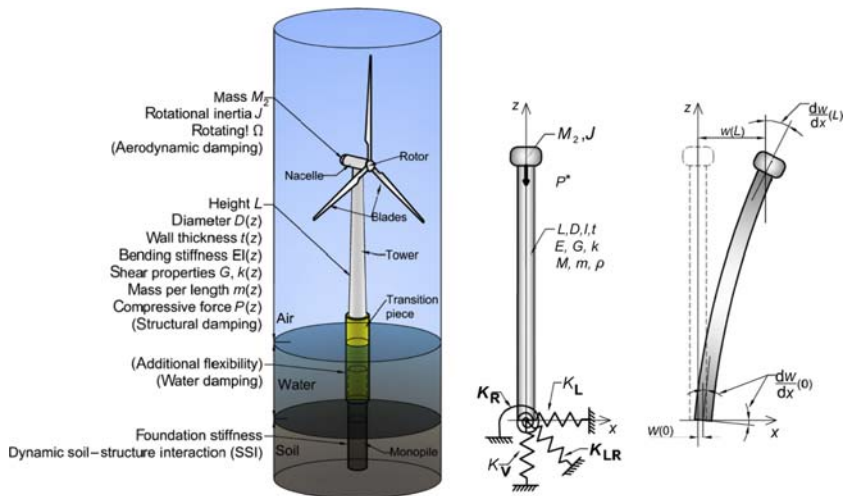


FIGURE 13.2 Simplified mechanical model of an OWT.

peak frequencies of loading have been shown to coincide with the peak frequencies of wind turbulence and waves. However, loads at the 1P and 3P frequencies can also be observed through effects such as aerodynamic and mass imbalance of the rotor and rotational sampling of turbulence by the blades, for 1P and 3P loads, respectively [6,7]. Further details on the estimations of the loads can be found in work by Bhattacharya [6,8]. For the widely used soft–stiff design, the target Eigen frequency (for practical purposes, the first natural frequency) is a frequency in the narrow gap between 1P and 3P. Fig. 13.3 also shows measured natural frequencies of a wide array of OWTs from several different wind farms across Europe (see Table 13.3 for the nomenclature on the wind turbine structure for which the measured natural frequencies are shown). The figure clearly shows the trend that the target natural frequencies of heavier turbines (8 MW) are indeed closer to the excitation frequencies of the wave and wind, making these structures even more sensitive to dynamics. It is of interest to review the codes of practice in this regard. DNV code [9] suggests that first natural frequency should not be within 10% of the 1P and 3P ranges. It is apparent from Fig. 13.4 that for soft–stiff design, the first natural frequency of the wind turbine needs to be fitted in a very narrow band (in some cases the 1P and 3P ranges may even coincide leaving no gap) which is a significant challenge.

13.3 DYNAMIC ISSUES IN SUPPORT STRUCTURE DESIGN

The schematic diagram of a wind turbine system model shown in Fig. 13.2 is relevant to the study of the overall system dynamics which is important for many design calculations such as Eigen frequencies and fatigue. In

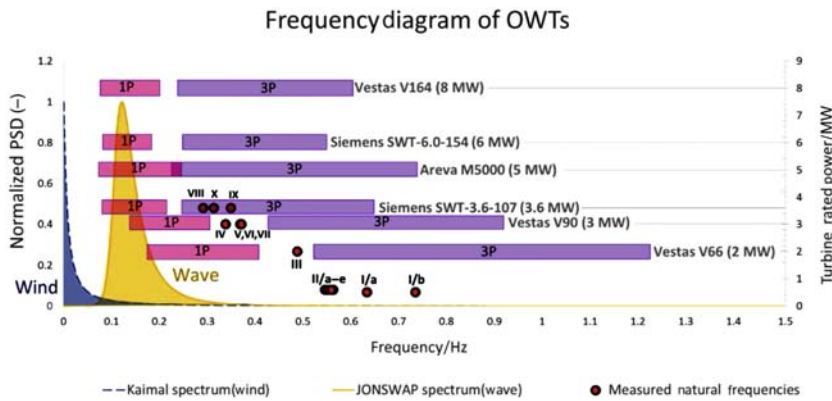


FIGURE 13.3 Typical wind and wave spectra, rotational speed (1P) and blade passing (3P) frequency bands for six commercial turbines and measured natural frequencies of the OWTs (given in Table 13.3).

In practice, the support structure is the whole structure that supports the heavy turbine, i.e., the components below the rotor nacelle assembly (RNA) which includes the tower, substructure, and foundation. The foundation is defined as the part of the support structure that is embedded in the ground below the mudline. The tower is typically a tubular tapered column. As the natural frequencies of these systems are very close to the forcing frequencies, the dynamics pose multiple design challenges and the scale of the challenges will vary depending on turbine types and site characteristics. These issues are briefly mentioned in the next section.

There are two main categories of modern wind turbines based on the operational range:

1. Variable rotational speed machines have an operational speed range (1P range).
2. Constant rotational speed wind turbines that operate at a single rotational speed (fixed 1P).

Variable speed machines have 1P and 2P/3P frequency bands which must be avoided, as opposed to a single frequency (applicable to constant rotational speed machines). They are more restrictive from the point of view of foundation design as the forcing frequency is a band rather than a unique value. The turbines currently used in practice (under operation) are variable speed machines. Fig. 13.3 shows the 1P and 3P bands for typical OWTs ranging from 2 MW (not in production anymore) turbines to commercially not yet available 8 MW turbines. It may be observed from Fig. 13.3 that for most wind turbines, 1P and 3P excitation cover wide frequency bands. To avoid these ranges, the designer of the support structure has three options from the point of view of the stiffness of the tower and the foundation:

TABLE 13.3 Analyzed Offshore Wind Farms With the Used Wind Turbines and Soil Conditions at the Sites

No.	Wind Farm Name and Location	Turbine Type and Rated Power	Soil Conditions at the Site
I	Lely offshore wind farm (The Netherlands)	NedWind 40/500 two-bladed 500 kW study purpose wind turbine	Soft clay in the uppermost layer to dense and very dense sand layers below
II	Irene vorrink offshore wind farm (The Netherlands)	NordtankNTK600/ 43 600 kW study purpose wind turbine	Soft layers of silt and clay in the upper seabed to dense and very dense sand below
III	Blyth offshore wind farm (United Kingdom)	Vestas V66 2 MW industrial OWT	Rocky seabed (weathered bedrock)
IV	Kentish flats offshore wind farm (United Kingdom)	Vestas V90 3 MW industrial OWT	Layers of dense sand and firm clay
V	Barrow offshore wind farm (United Kingdom)	Vestas V90 3 MW industrial OWT	Layers of dense sand and stiff clay
VI	Thanet offshore wind farm (United Kingdom)	Vestas V90 3 MW industrial OWT	Fine sand and stiff clay
VII	Belwind 1 offshore wind farm (Belgium)	Vestas V90 3 MW industrial OWT	Dense sand and stiff clay
VIII	Burbo bank offshore wind farm (United Kingdom)	Vestas V90 3 MW industrial OWT	Saturated dense sand
IX	Walney 1 offshore wind farm (United Kingdom)	Siemens SWT-3.6-107 3.6 MW industrial OWT	Medium and dense sand layers
X	Gunfleet sands offshore wind farm (United Kingdom)	Siemens SWT-3.6-107 3.6 MW industrial OWT	Sand and clay layers

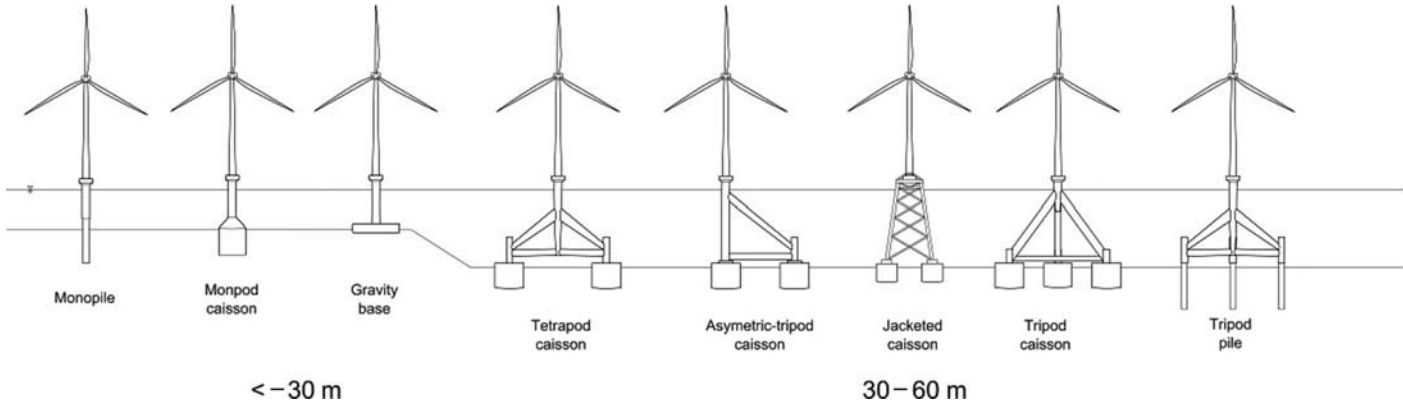


FIGURE 13.4 Figure showing different types of foundations for fixed (grounded) systems.

1. Soft–soft structures, whereby the natural frequency lies below the 1P frequency range. This design is typical for floating offshore platforms but are practically impossible to achieve for fixed (grounded) structures. Also, soft–soft fixed structures would likely be subject to high dynamic amplification of wave load response.
2. Soft–stiff structures, whereby the natural frequency lies above the 1P frequency and below 3P frequency range. This is the typical design choice for practical bottom fixed structures, such as monopile founded OWTs. All wind turbines in Fig. 13.3 are designed soft–stiff.
3. Stiff–stiff structures, whereby the natural frequency lies above the 3P range. Such designs are typically considered to have a massive support structure and therefore uneconomic.

It is quite clear from Fig. 13.3 that designing a soft–stiff system which avoids both the 1P and 3P frequency bands is challenging because of the tight tolerance of the target natural frequency. Indeed, some OWTs with a wide rotational speed range, such as the Areva M5000 5 MW in Fig. 13.3 with 0.075–0.25 Hz (4.5–14.8 rpm), do not even have a gap between 1P and 3P and they are overlapping. Modern wind turbines often feature a sophisticated pitch control system designed to leap frog the rotational frequency range that would cause resonance of the structure due to the corresponding 3P frequency. For example, if the rotational speed range is 5–13 rpm, equivalent to 0.083–0.216 Hz, then the 3P frequency band is 0.25–0.65 Hz. If the structural natural frequency is 0.35 Hz, then the pitch control may regulate the rotational speed such that the corresponding 3P frequency avoids $\pm 10\%$ of the structural natural frequency, i.e., the frequency band 0.315–0.385 Hz to comply with the DNV code [9]. This would result in a jump in the rotational speed from 6.3 to 7.7 rpm, avoiding operation between these values. Obviously, this is also not without cost, both in terms of initial cost, maintenance, and power production.

The second issue is the top head mass, i.e., the mass of the RNA (i.e., M_2 in Fig. 13.2). With increasing capacity of the turbine, the mass of the RNA increases and the natural frequency will also decrease keeping other factors constant. Furthermore, the hub height is also higher due to longer blades (associated with heavier turbines) which increase the flexibility of the taller towers causing further reduction in the natural frequency. This trend can also be seen in Fig. 13.3, the target natural frequency of wind turbines (in soft–stiff design) with higher power output is typically lower. Fortunately, the large rotor diameter wind turbines also tend to have lower rotational speeds. This is because of the fact that for optimum power production, the tip speed ratios (ratio of the speed of the tip of the blades and the incoming wind speed) are maintained at a favorable value, also to avoid blade damage. Furthermore, the top head mass is dependent on the choice of drive (with or without gearbox). Direct drive wind turbines do not need gearboxes, and thus significant weight

reduction can be achieved (theoretically). However, the weight reduction is not obvious because the power of an electric generator is proportional to its rotational speed.

13.3.1 Importance of Foundation Design

Designing foundations for OWTs are challenging as these are dynamically sensitive structures in the sense that natural frequencies of these structures are very close to the forcing frequencies of the wind, wave, and 1P (rotor frequency) and 2P/3P (blade shadowing frequency) loading. Typically, for the widely used soft–stiff design (target frequency of the overall wind turbine is between 1P and 2P/3P), the ratio of forcing frequency, f_f , to natural frequency, f_n , is very close to 1 and as a result is prone to dynamic amplification of responses such as deflection/rotation which may enhance the fatigue damage, thereby reducing the intended design life. Therefore, a designer apart from accurately predicting the natural frequency of the structure must also ensure that the overall natural frequency due to dynamic soil–structure interaction does not shift toward the forcing frequencies making the value of f_f/f_n even closer to 1. Therefore, foundations are one of critical components of OWTs not only because of the overall stability of the structure but also due to financial viability of the project. Foundation selection plays an important role in the overall concept design for offshore wind farms as there are large financial implications attached to the choices made. The selection of foundation type and the design is a complex task, which strongly depends not only on the site characteristics (wind, wave, ground type), turbine type, but also on the maturity and track record of the design concepts. Fig. 13.4 shows different types of foundations either in use or proposed to be used. One of the main aims of a foundation is to transfer all the loads from the wind turbine structure to the ground safely and within the allowable deformations. Guided by Limit State Design philosophy, the design considerations are to satisfy the following:

- 1. Ultimate limit state (ULS):** The first step in design is to estimate the maximum loads on the foundations (predominantly overturning moment, lateral load, and the vertical load) due to all possible design load cases and compare with the capacity of the chosen foundation. For monopile type of foundations, this would require computation of ultimate moment, lateral and axial load-carrying capacity. Therefore, inevitably, ULS design consideration will provide the minimum dimension (length and diameter) of the monopile and also the wall thickness required. The input required for such calculations are site characteristics (e.g., wind and wave data) and turbine data. At some sites, some other loads (e.g., ice load or earthquake loads) may need to be considered. Particularly, in Chinese waters, the loads from extreme events such as typhoon may govern.

- 2. Target natural frequency (Eigen frequency) and serviceability limit state (SLS):** This requires the prediction of the natural frequency of the whole system (Eigen frequency) and the deformation of the foundation at the mudline level (which can be further extrapolated to the hub level) over the lifetime of the wind turbine. As natural frequency is concerned with very small amplitude vibrations (linear Eigen value analysis will suffice), the deformation of the foundation will be small and prediction of initial foundation stiffness would suffice for this purpose. Therefore, the second major calculation is the determination of stiffness of the foundation. Closed form solution to obtain the foundation stiffness for rigid monopiles as well as flexible monopiles are developed by Shadlou and Bhattacharya [10] and used by Arany et al. [11] for simplified design of monopiles. These foundation stiffness values can be used to estimate the deformation (pile head rotation and displacement) in the linear range and natural frequency of the whole system.
- 3. Fatigue limit state (FLS) and long-term deformation:** This would require predicting the fatigue life of the monopile as well as the effects of long-term cyclic loading on the foundation.
- 4. Robustness and ease of installation:** This step will ascertain that the foundation can be installed and that there is adequate redundancy in the system [12].

Typically, foundations cost between 25% and 34% of the overall cost. For the North Hoyle project in the United Kingdom, the cost of foundation was 34% [13], and it has been reported that the development of Atlantic Array wind farm did not go ahead and one of the main reasons was the expense of the foundation. Foundations for wind turbines can be classified into two main types: fixed (or grounded to the seabed) and floating. While most of the currently installed or operating turbines are supported on fixed/grounded foundation system, research and development of floating foundations are under way. Fig. 13.4 shows the different types of grounded system (fixed to the seabed foundation system) either in use or proposed and will constitute the main part of this chapter.

Compared to the design of OWTs in North Sea, additional challenges are posed on wind turbine design in China, due to the presence of the unfavorable yet widely distributed soft clayey seabed in the Chinese waters. It is well recognized that soft clays (frequently encountered in Chinese waters) are much more susceptible to stiffness degradation [14], than stiff clay and dense sand (typically founded in North Sea, see Table 13.3), at a given undrained cyclic loading. In other words, natural frequencies of wind turbine structures in Chinese water is more likely to be altered by the environmental loadings than those of the turbines in North Sea, causing the former to be more sensitive to dynamics. Figs. 13.5–13.7 show fixed foundations used in Chinese waters and Fig. 13.8 shows the method of installation.

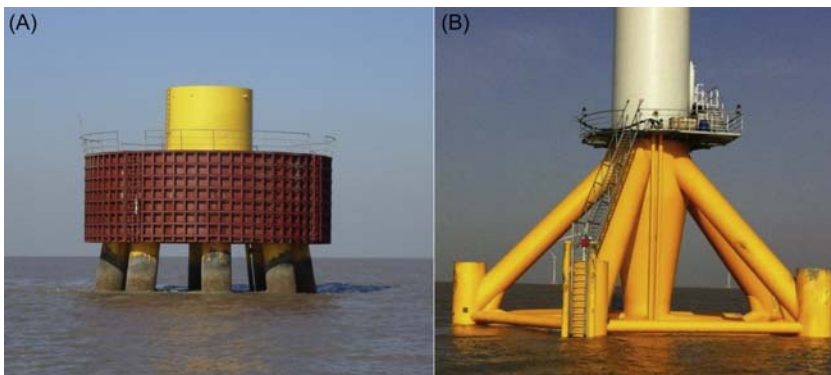


FIGURE 13.5 Foundations supporting wind turbines used in Chinese waters: (A) Group of eight piles supporting a high-rise pilecap used in soft soil sites. (B) Multipod foundation.



FIGURE 13.6 Large-scale prestressed concrete bucket foundation in water depth of 6 m (the caisson dimensions are 30 m in diameter and 7 m in depth).

13.4 TYPES AND NATURE OF THE LOADS ACTING ON THE FOUNDATIONS

13.4.1 Loads Acting on the Foundations

The loads acting on the wind turbine tower are ultimately transferred to the foundation and can be classified into two types: static or dead load due to the self-weight of the components and the dynamic loads (or in some instances this can be cyclic). However, the challenging part is the dynamic loads acting on the wind turbine and is discussed as follows:

1. The lateral load acting at the hub level (top of the tower) from the rotating blades produced by the turbulence in the wind. The magnitude of dynamic component depends on the turbulent wind speed.



FIGURE 13.7 Rudong intertidal wind farm.



FIGURE 13.8 Installation of wind turbine in China.

2. The load caused by waves crashing against the substructure very close to the foundation. The magnitude of this load depends on the wave height and wave period;
3. The load caused by the vibration at the hub level due to the mass and aerodynamic imbalances of the rotor. This load has a frequency equal to the rotational frequency of the rotor (referred to as 1P loading, as defined in [Section 13.2](#)). Since most of the industrial wind turbines are variable speed machines, 1P is not a single frequency but a frequency band

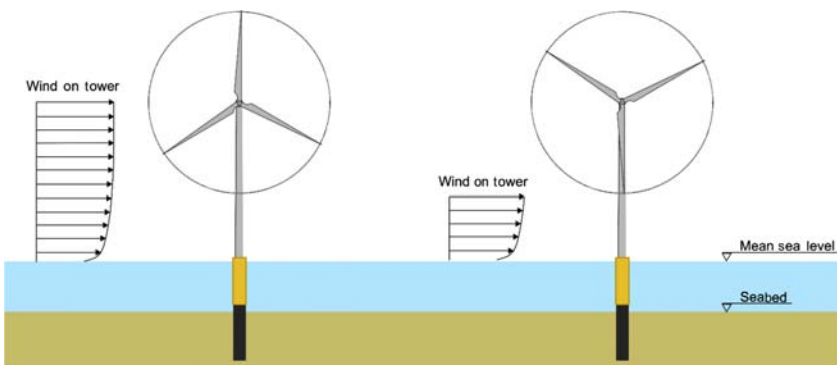


FIGURE 13.9 Blade shadowing load on the tower (3P load). The left-hand diagram shows the wind load on the tower when the blades does not shadow the tower.

between the frequencies associated with the lowest and the highest rpm (revolutions per minute).

4. Loads in the tower due to the vibrations caused by blade shadowing effects (referred to as 2P/3P, as defined in [Section 13.2](#)). The blades of the wind turbine passing in front of the tower cause a shadowing effect and produce a loss of wind load on the tower, as shown in [Fig. 13.9](#). This is a dynamic load having a frequency equal to three times (3P) the rotational frequency of the turbine for three-bladed wind turbines and two times (2P) the rotational frequency of the turbine for a two-bladed turbine. The 2P/3P loading is also a frequency band like 1P and is simply obtained by multiplying the limits of the 1P band by the number of the turbine blades.

The turbulent wind velocity and the wave height on sea are both variables and are best treated statistically using PSD functions. In other words, instead of time domain analysis, the produced loads are more effectively analyzed in the frequency domain whereby the contribution of each frequency to the total power in wind turbulence and in ocean waves is described. Representative wave and wind (turbulence) spectra can be constructed by a discrete Fourier transform from site-specific data. However, in absence of such data, theoretical spectra can be used. The DNV standard specifies the Kaimal spectrum for wind and the JONSWAP (Joint North Sea Wave Project) spectrum for waves in OWT applications.

It is clear from the above discussion that designing soft–stiff wind turbine systems demands the consideration of dynamic amplification and also any potential change in system frequency due to the effects of cyclic/dynamic loading on the system, i.e., dynamic–structure–foundation–soil interaction. Typically, the first modal frequency of the wind turbine system lies in the range of 75%–120% of the excitation frequencies (see [Fig. 13.3](#)) and as a result, dynamic amplifications of responses are expected.

Clearly, for soft–stiff design, any change in natural frequency over the design/operation period of the turbine will enhance the dynamic amplifications which will increase the vibration amplitudes and thus the stresses and fatigue damage on the structure. Therefore, fatigue is one of the main design drivers for these structures. Predicting fatigue damage is undoubtedly a formidable task due to complexity associated with the uncertainty in the dynamic amplification (owing to changes in system characteristics over time and number of cycles), randomness of the environmental loading and last but not the least, the impact of climate change.

13.4.2 Extreme Wind and Wave Loading Condition in Chinese Waters

Typhoons, which can lead to failure or even collapse of wind turbines, hit the region of East and South China Sea almost every year, but rarely occur in the North Sea. Typhoons can have a negative effect on wind turbine system ranging from fracture of blades, damage to braking system, and yielding of tower and even excessive rotation foundation. However, the direct effect of a typhoon is loss of power supply and emergently shut down which may damage the weakest part (e.g., blade and nacelle). It is therefore necessary to understand the wind condition in the Chinese waters and this section provides a brief summary.

Bohai Sea: The total area of Bohai Sea in China is approximately 77 284 km² and is classified into four parts: west, middle, Jinzhou, and Suizhong. Bohai Sea is the only inner sea region of China and is a shallow sea with average water depth of about 18 m. In winter, due to the flow of cold air from Siberia, the average wind speed is about 6–7 m s⁻¹. On the other hand, in summer, due to warm airflow from Western Pacific Ocean, the average wind speed is 4–5 m s⁻¹. In August, the wind speed is quite low. In this sea, wind farms are located in Jinzhou and the predominant wind directions for high wind speeds are southeast and southwest with mean annual wind speed of 7.21 m s⁻¹ (100 m height over sea level). Typhoons and cyclones are not normal in the Bohai Sea and the wind condition is stable throughout the year. The Bohai Sea has a cold climate and in the winter period, the onshore near coastline is almost frozen for 3–4 months.

Yellow sea: The total area of Yellow Sea is 380 000 km² and comprises Shandong, Jiangsu, and Korean Peninsula. There are many offshore wind farms built along the coastline in Yellow Sea from north to south. In winter, the wind is stable but in summer it varies in both magnitude and direction. Typhoons are very frequent in summer throughout the Shanghai area, which is located in the south of the Yellow Sea. The annual average wind speed in the north of the Yellow Sea is 6.80–6.88 m s⁻¹ but in the south, the value is larger and the average value is 7.45–7.55 m s⁻¹.

East China Sea: The total area of East China Sea is 770 000 km² and is comprised of the continent coastline of Japan and Taiwan. There are many

offshore wind farm projects located in Hangzhou Bay. The annual mean wind speed tested at 100 m in height over sea level is generally around $9.6\text{--}9.8 \text{ m s}^{-1}$ at the exit of Hangzhou Bay. However, in terms of frequent typhoon phenomena in summer from May to September each year, wind speed remains unstable and the amplitudes are quite large, even greater than 14 m s^{-1} . The cyclone effect is very important and governs the design of an OWT.

Taiwan Strait: Taiwan Strait is one part of East China Sea, connected with South China Sea in the south of China. In summer, it is common to see strong winds (e.g., typhoons) which damage the cities and structures along the coastline. Usually typhoons in summer time will come from southeast and the wind speed is quite high. The annual wind speed in Taiwan Strait is about $11.5\text{--}13 \text{ m s}^{-1}$ and is even higher when a typhoon appears (20 m s^{-1} or more). Each year, typhoons are responsible for serious damage to the economy and to structure in Taiwan and in particular to Fujian and Zhejiang, located on the two sides of Taiwan Strait.

South China Sea: The total area of South China Sea is about $3\ 500\ 000 \text{ km}^2$. It is surrounded by the continent of South China mostly, northeast to Taiwan Strait, southwest to Singapore Strait. Most of the wind projects are newly built or under construction. It is also common to see strong wind (e.g., typhoon) and high rainwater during each summer. The annual mean wind speed in South China Sea is $9\text{--}11 \text{ m s}^{-1}$. When typhoon comes, the wind speed is usually over 17 m s^{-1} (at 100 m in height). [Table 13.4](#) summarizes the wind condition in the Chinese waters.

13.4.2.1 Case Study: Typhoon Related Damage to Wind Turbines in China

Zhejiang Province, located on the west of East China Sea, experienced 23 typhoons since 1997 (the starting year of wind farming projects), causing hundreds of millions of dollars of economic loss. It is of interest to discuss the effects of August 10, 2006, Typhoon “*Saomai*” which had wind speeds

TABLE 13.4 Wind Condition Summary in China Seas

Sea Name	Wind Speed Range/ m s^{-1}	Mean Wind Speed/ m s^{-1}
Bohai Sea	6.4–8.2	7.45
Yellow Sea (north)	6.8–7.5	6.86
Yellow Sea (south)	7.0–8.2	7.48
East China Sea	7–11	9.68
Taiwan Strait	11.5–13	12.04
South China Sea	8.8–9.8	9.18

of 68 m s^{-1} that devastated many wind farms. This is the most powerful typhoon to hit China over the past 50 years; it killed 104 people and left at least 190 missing. Furthermore, it blacked out cities and destroyed over 50 000 houses in the southeast part of the country. Fig. 13.10 show the Hedingshan wind farm in Zhejiang province (before the cyclone) along with the aerial photograph of the typhoon. The typhoon destroyed 28 wind turbine structures and blades which included five collapsed towers (600 kW turbines) with a total loss of about 70 million RMB (Figs. 13.11–13.13).

13.4.2.1.1 Wave Condition

Bohai Sea, Yellow Sea, East and South China Sea are connected to each other, in a bow shape from north to south along the China coastline. Tropical and sub-tropical monsoon climate also influences the wave height in China Sea. Thus, in

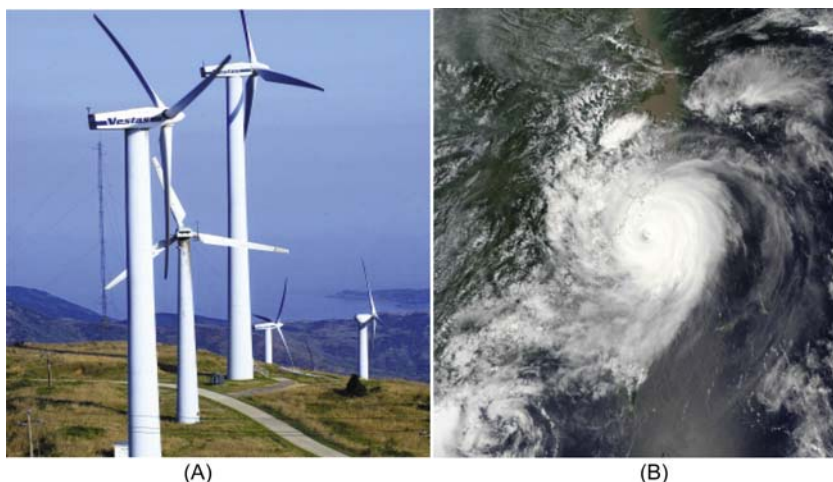


FIGURE 13.10 (A) Hedingshan wind farm (before typhoon Saomai). (B) Aerial view of the typhoon.



FIGURE 13.11 Damages to blades and tower due to hurricane Saomai.



FIGURE 13.12 Damages to the connections due to hurricane Saomai.



FIGURE 13.13 Damages to the foundations due to hurricane Saomai.

Chinese offshore wind farm projects, sea waves are a major influence in the design. The wave height distribution in South China Sea is variable owing to the large sea area. High wave height occur in the northeast of South China Sea and in the southeast of the Indo-China Peninsula, with wave heights of 2.4–2.6 m. The maximum significant wave height is however larger than 2.8 m in the west of the Luzon Strait. Comparatively, the significant wave height in the north is less than 2 m. Wave period ranges from 6 to 10 seconds. [Table 13.5](#) provides the distribution of wave height and period for the Chinese waters.

13.5 GROUND CONDITIONS IN CHINESE WATERS

Ground condition is fundamental in designing wind turbine foundations. There are many elements that should be considered: The depth of seawater, salinity

TABLE 13.5 Wave Height and Period in the Chinese Waters

China Sea	Region	Wave Height/m	Wave Period/s
Bohai Sea	Bohai Strait	1.2	4.8
	Others	<1	<4.5
Yellow Sea	North	1.2	5
	Center	1.4	5
	South	1.6	6
East China Sea	Shanghai coastline	1.6	6
	Zhejiang coastline	1.8	7
	Taiwan Strait	2.4	9
South China Sea	Luzon Strait	2.8	10
	Indo-China Peninsula	2.6	8
	Others	<2	6

content in ocean, and ground stiffness variation with depth. Generally, the ground condition in China Seas is not as stiff as that in North Europe. A summary of the ground conditions is given in the following sections.

13.5.1 Bohai Sea

Bohai Sea is a low-lying land settled by North China Plain, where the soil consists of sediments brought from mountains and Yellow River and is soft silty clay or clayey silt. The drilling of a borehole is the usual method used for underground geology surveys. There are many records of boreholes in Bohai Sea and a typical profile (from top to bottom) is as follows:

1. *Soft clay silt (Layer 1)*: The depth of this layer varies and typically 0–7.4 m in the Western Bohai.
2. *Mucky clay to silty clay (Layer 2)*: In this layer, the clay is changing from soft to stiff, with materials of mucky clay, silt, and loose sand. The depth of clay layer varies (thickness 2.5–9.0 m in Western Bohai), center Bohai (thickness 4.0–10.0 m), Jinzhou (thickness 2.7–14.8 m), and Suizhong (thickness 0.8–5.8 m).
3. *Combination of silty clay, clay, and loose sand (Layer 3)*: Again the thickness of this layer varies: 2.5–7.0 m in Western Bohai.
4. *Fine sand and silt*: In this layer, the main material is fine sand, combined with silty sand and clay. The stiffness is that of medium dense sand. The thickness in the western Bohai Sea is 4.0–15.0 m, in the center of Bohai it is 4.0–13.0 m, in Jinzhou it is 3.0–15.0 m and in Suizhong it is 0–14.2 m.

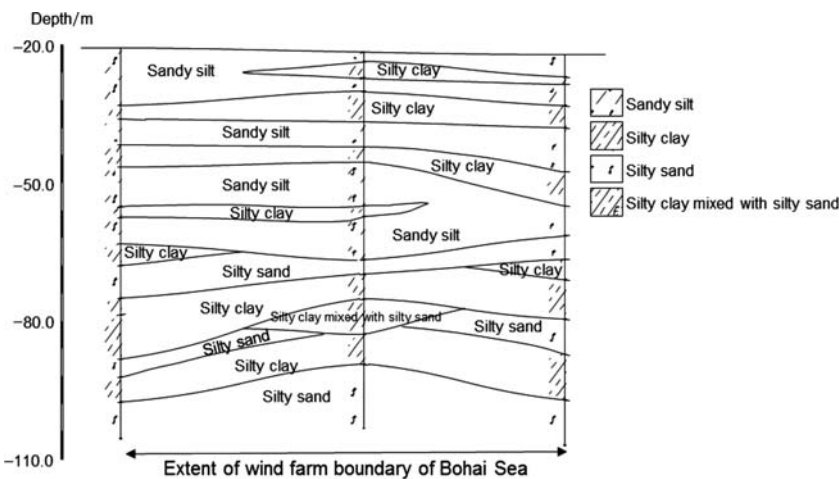


FIGURE 13.14 Ground profile in Bohai Sea wind farm.

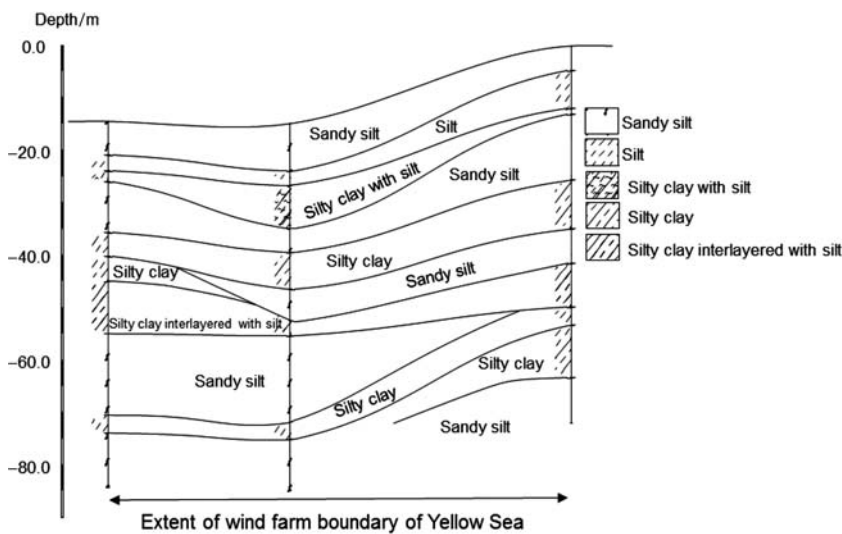


FIGURE 13.15 A section of a ground profile in Yellow Sea showing the extreme geology.

5. *Clay*: In this layer, the clay is quite stiff and hard, combined with some silty clay. The thickness in western Bohai is 2.0–18.0 m, in the center of Bohai it is 3.0–15.0 m, in Jinzhou it is 3.0–17.0 m, and in Suizhong it is 0–15.0 m.
6. *Fine sand and silt*: In this layer, the main material is fine sand, combined with silty clay where the layer is thin. The stiffness is quite dense. The thickness in western Bohai is 5.0–11.0 m, in the center of Bohai it is 6.0–15.0 m, in Jinzhou it is 7.0–15.0 m, and in Suizhong it is 12.0–18.0 m.

A typical ground profile for Bohai Sea is shown in Fig. 13.14 and it is clear that the ground is variable. On the other hand, Figs. 13.15 and 13.16

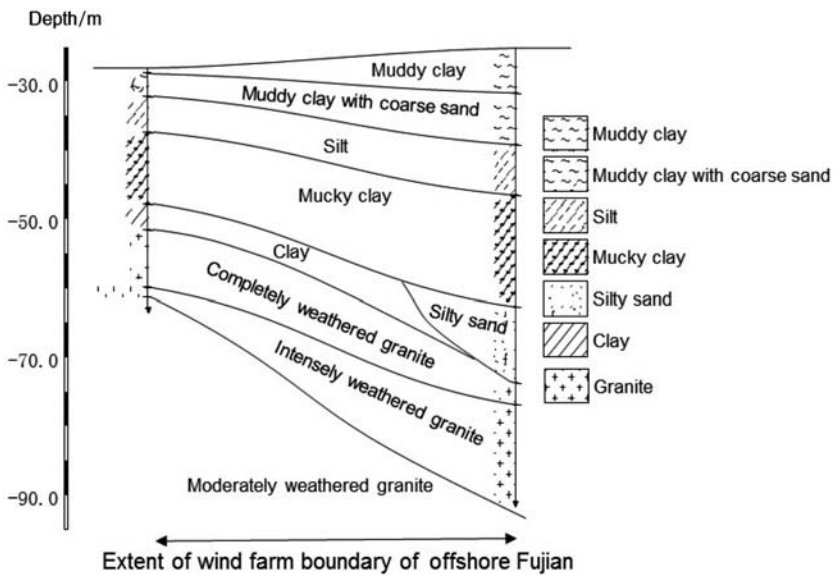


FIGURE 13.16 Ground profile in offshore Fujian Sea (Taiwan Strait).

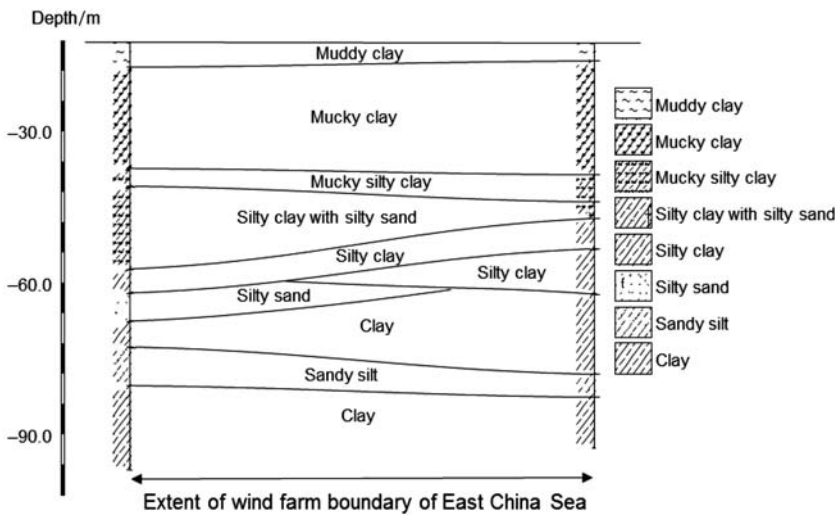


FIGURE 13.17 A section of the ground profile in East China Sea.

show ground profiles for Yellow Sea and Fujian Sea, respectively. It is evident that the ground profiles are variable which calls for detailed site investigation to minimize risks during construction. Multilayering soft marine sediments are also widely formed in the regions in and adjacent to East China Sea [15,16]. A typical ground profile in East China Sea is illustrated in Fig. 13.17.

TABLE 13.6 A Typical Ground Profile in South China Sea

Position No.	Depth/m	Soil
1	0–4.2	Silty clay
	4.2–19.4	Laminated soil
	19.4–40.0	Silty clay
2	0–3.0	Sandy soil
	3.0–7.4	Silty clay
	7.4–27.0	Laminated soil
	27.0–35.3	Silty clay
3	0–1.9	Silty clay
	1.9–2.6	Silty sand
	2.6–5.5	Silty clay
	5.5–9.0	Sandy soil
	9.0–15.0	Laminated soil
	15.0–39.8	Silty clay
4	0–1.5	Sandy soil
	1.5–4.9	Silty clay
	4.9–7.0	Silty sand
	7.0–13.7	Laminated soil
	13.7–25.4	Silty clay
	25.4–40.6	Sandy soil

Table 13.6 provides the multilayered ground profile in South China Sea. A general observation can be made that the ground profile in Chinese waters is variable and it shows the importance of a comprehensive site investigation.

13.5.2 Seismic Effects

Fig. 13.18 shows the map of China, which includes three major earthquake locations. It is of interest to note that the location of the earthquakes of February 4, 1965, Haicheng and July 28, 1976, Tangshan were close to the Bohai Sea. The effect of an earthquake on a wind turbine structure can be summarized as follows:

1. Loose to medium dense sandy soil around the foundation may liquefy which will affect the behavior of the foundation. In the case of monopile



FIGURE 13.18 Location of three major earthquakes in China.

foundation not having sufficient embedment in nonliquefiable soil beneath the liquefiable soil, there may be settlement which may cause tilting or in extreme situation a bearing failure. The time period of the wind turbine structure will increase owing to liquefaction and the structure will shift away from the predominant frequency of the earthquake causing higher displacement at the nacelle level.

2. Clay soils may soften depending on the layering/ground profile and the earthquake type. It may either attenuate or amplify the motion experienced by the structure.
3. Behavior of intermediate soils, i.e., sandy silt or silty sand, or silty clay under seismic loading is difficult to predict and advanced element tests and characterization are required. Cyclic triaxial tests can be carried out to assess the liquefaction potential of the soils.

13.6 A NOTE ON SLS DESIGN CRITERIA

Serviceability criteria will be defined based on the tolerance requirements for the operation of the wind turbine and is often described as “turbine manufacturer requirements.” Ideally, these should be turbine specific, i.e., size and the hub height, gear boxed, or direct drive. Typically, these tolerances are specified in some codes of practice (e.g., DNV) or a design specification

supplied by the client which may be dictated by the turbine manufacturer. Some of the specific requirements are:

1. Maximum allowable rotation at pile head after installation. DNV code specifies 0.25 degree limit on “tilt” at the nacelle level.
2. Maximum accumulated permanent rotation resulting from cyclic and dynamic loading over the design life.

An example of a method to predict the required foundation stiffness.

For a wind farm, it has been estimated that the maximum moment at the mudline level is 125 MN m and if the allowable tilt is 0.25 degree at the foundation level, one can therefore estimate the rotational foundation stiffness required as given in Eq. (13.1):

$$K_R = \frac{125 \text{ MN m}}{4.36 \times 10^{-3} \text{ rad}} = 28.6 \text{ GN m rad}^{-1} \quad (13.1)$$

This is a very large number and would require a large diameter monopile or equally alternative multiple pod foundations. In this context it may be mentioned that SLS criteria impact the foundation design and thereby costs. It has been reported that floating wind turbines are allowed to tilt by up to ± 5 degrees in the worst sea states. Therefore, it is necessary to understand the stringent criteria of 0.25 degrees for grounded wind turbine system. A value of 0.25 degree represents a horizontal deflection of 349 mm for a typical 80 m tower. Clearly, a less stringent tilt criterion will save on the foundation costs and installation time and make wind energy cheaper.

13.7 CHALLENGES IN ANALYSIS OF DYNAMIC SOIL–STRUCTURE INTERACTION

OWT are new types of offshore structures and are unique in their features. The most important difference with respect to oil and gas installation structures is that they are dynamically sensitive (as explained in Section 13.2) and moment resisting. Fig. 13.19 shows a typical monopile supported wind turbine and a pile supported fixed offshore jacket structure. There are, however, obvious differences between those two types of foundations. Piles for offshore structures (such as oil and gas platform) are typically 60–110 m long and 1.8–2.7 m in diameter and monopiles for OWTs are commonly 30–40 m long and 3.5–6 m in diameter. Degradation in the upper soil layers resulting from cyclic loading is less severe for offshore oil and gas platform piles which are significantly restrained from pile head rotation, whereas monopiles are free-headed. The commonly used design method using a beam on nonlinear Winkler springs (“ p – y ” method in API code or DNV code) may be used to obtain pile head deflection under cyclic loading, but its use is limited for wind turbines because of the following:

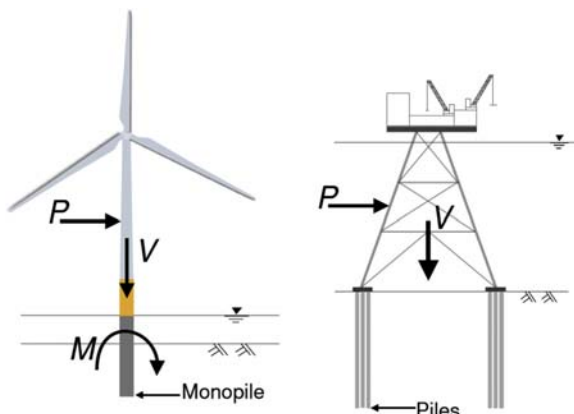


FIGURE 13.19 Monopile supported wind turbine and piles supported oil and gas platform.

1. The widely used API model is calibrated against response to a small number of cycles (maximum 200 cycles) of flexible piles for offshore fixed platform applications. In contrast, for a real OWT 10^7 – 10^8 cycles of loading are expected for the rigid piles over a lifetime of 20–25 years.
2. Under cyclic loading, the API or DNV model always predicts degradation of foundation stiffness in sandy soil. However, recent work by Bhattacharya and Adhikari [17], Cuéllar et al. [18], and Leblanc [19] suggested that the foundation stiffness for a monopile in sandy soil will actually increase as a result of densification of the soil next to the pile.
3. The ratio of horizontal load (P) to vertical load (V) is very high in OWTs when compared with fixed jacket structures.

While OWT structures are designed for an intended life of 25–30 years, little is known about their long-term dynamic behavior under millions of cycles of loading. While it is possible to monitor existing OWT installations at a reasonable cost, full-scale testing is very expensive. An alternative method is to carry out a carefully planned scaled dynamic testing to understand the scaling/similitude relationships which can be later used for interpretation of the experimental data and also for scaling up the results to real prototypes. There are mainly two approaches to scale up the model test results to prototype consequences: first is to use standard tables for scaling and multiply the model observations by the scale factor to predict the prototype response and the alternative is to study the underlying mechanics/physics of the problem based on the model tests recognizing that not all the interaction can be scaled accurately in a particular test. Once the mechanics/physics of the problem is understood, the prototype response can be predicted through analytical and/or numerical modeling in which the physics/mechanics discovered will be implemented in a suitable way. The second approach is particularly useful to study the dynamics of OWTs as it involves complex dynamic

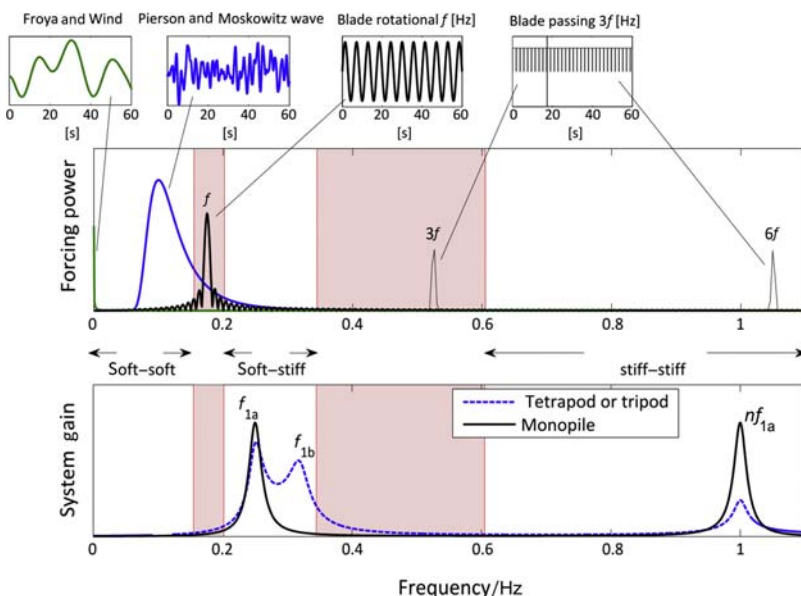


FIGURE 13.20 Relationship between effect of natural frequency of tripod and monopile on the forcing frequencies.

wind–wave–foundation–structure interaction and none of the physical modeling techniques can simultaneously satisfy all the interactions to the appropriate scale. Ideally, a wind tunnel combined with a wave tank on a geotechnical centrifuge would serve the purpose but this is unfortunately not feasible. It is recognized that not all physical mechanisms can be modeled adequately and therefore those need special consideration while interpreting the test results. As dynamic soil–structure interactions of wind turbines are being studied, stiffness of the system is a top priority. Bhattacharya et al. [4,5,20] carried out experimental testing of a 1:100 scaled wind turbine to characterize the free dynamics of the system and to study the long-term behavior under the action of the dynamic loading.

The following conclusions could be reached from the study:

1. The change in natural frequencies of the wind turbine system may be affected by the choice of foundation system, i.e., deep foundation or multiple pods (symmetric or asymmetric) on shallow foundations. Deep foundations such as monopiles will exhibit sway-bending mode, i.e., the first two vibration modes are widely spaced—typical ratio is 4.5. However, multiple pod foundations supported on shallow foundations (such as tetrapod or tripod on suction caisson) will exhibit rocking modes in two principle planes (which are of course orthogonal). Fig. 13.20 shows the dynamic response of monopile supported wind turbine and tetrapod foundation plotted in the loading spectrum diagram.

2. The natural frequencies of wind turbine systems change with repeated cyclic/dynamic loading. In the case of strain-hardening site (such as loose to medium dense sandy site), the natural frequency is expected to increase and for strain-softening site (such as normally consolidated clay [21–23]) the natural frequency will decrease.
3. The results showed that the multipod foundations (symmetric or asymmetric) exhibit two closely spaced natural frequencies corresponding to the rocking modes of vibration in two principle axes. Furthermore, the corresponding two spectral peaks change with repeated cycles of loading and they converge for symmetric tetrapods but not for asymmetric tripods. From the fatigue design point of view, the two spectral peaks for multipod foundations broaden the range of frequencies that can be excited by the broadband nature of the environmental loading (wind and wave) thereby impacting the extent of motions. Thus the system life span (number of cycles to failure) may effectively increase for symmetric foundations as the two peaks will tend to converge. However, for asymmetric foundations, the system life may continue to be affected adversely as the two peaks will not converge. In this sense, designers should prefer symmetric foundations to asymmetric foundations.

13.8 FOUNDATION DESIGN

While design guidelines are available for offshore oil and gas installation foundations, its direct extrapolation/interpolation to OWT foundation design is not always possible, the reasons of which is explored in the earlier section. There are two reasons: (1) The foundations of these structures are moment resisting, i.e., large overturning moments at the foundation which are disproportionately higher than the vertical load. (2) The structure is dynamically sensitive and therefore fatigue is a design driver. This section therefore explores a simplified foundation design methodology which may be used during option engineering or preliminary design for foundations supporting OWTs.

1. Compute the maximum mudline bending moment considering the different load combinations. The overturning moments due to 1P (misalignment) and 3P (blade shadowing) may be neglected in this step.
2. Based on the allowable tilt criteria for the particular project, determine the foundation stiffness required as discussed in [Section 13.6](#). This is the minimum stiffness that is required to satisfy the SLS.
3. It is then required to check the ULS criteria, i.e., the foundation capacity. If the foundation is not adequate, the size must be increased.
4. The soil surrounding the foundations will be subjected to tens of millions of cycles of cyclic and dynamic loading of varying strain as well as varying frequency. It must be ensured that the soil remains in the linear

elastic range so as not to alter the dynamic stiffness of the foundation. For detailed design, resonant column testing is recommended to find the threshold strains of the ground. Further details on the use of the threshold strain concept in monopile design can be found in the work by Lombardi et al. [24].

5. Beam on nonlinear Winkler model or finite element analysis can be carried out and it must be ensured that the $p-y$ curves in soil are within the linear elastic section at all depths. However, 3D finite element analyses are recommended to understand the strains around the foundation.
6. It is now required to obtain stiffness of the foundation to calculate natural frequency of the whole system to check where the overall system is placed: soft–soft, soft–stiff, or stiff–stiff (see Fig. 13.3). If the natural frequency is not acceptable, the design parameters such as foundation stiffness, tower stiffness, and mass may be altered so that the desired frequency is obtained. This is an iterative process.
7. The foundation stiffness may change over the lifetime of the wind turbine due to soil–structure interaction which will have an impact on the natural frequency of the system and tilt. If the ground is sandy site, the natural frequency to be expected to increase and if it is a clay site, the natural frequency may decrease. If the site is layered (as often encountered in Chinese waters, see Figs. 13.14–13.17), the change in natural frequency cannot be ascertained a priori and depends on various factors including the geometry of layering. Engineers need to carry out calculations to predict the change in frequency which is also necessary to compute the fatigue loading.

13.8.1 Challenges in Monopile Foundation Design and Installation

Monopiles have been predominantly used to support wind turbine generators (WTGs) in water depths up to 30 m. However, there are discussions with regard to the use of monopiles in deeper water depths termed as “XL” monopile. Preliminary calculations suggest that 10 m diameter monopiles weighing 1200 t (where t refers to metric tonnes) may be suitable for 45 m water depth and of course dependent on ground conditions. However, the use is uncertain due to the following: (1) no codified cyclic design to predict long-term tilt; (2) lack of redundancy in foundation system and therefore chance of single-point failure; (3) installation costs and lack of adequate specialized vessels; (4) connection between foundation, transition piece, and the tower. Some of these aspects are described in further detail as follows:

1. *Lack of redundancy*: Monopiles are “overturning moment” resisting structures and there are two main components: (1) overturning moment arising from the thrust acting at the hub level; (2) overturning moment due to the wave loading. Also these two moments can act in two different planes

and will vary constantly depending on the time of the day and time of the year. Monopiles are rigid piles and the foundation collapse can occur if the soil around the pile fails, i.e., there would be rigid body movement. If the foundation starts to tilt, it is very expensive to rectify.

2. *Cyclic (rather dynamic) design of monopile:* The response of monopile under cyclic/dynamic load is not well understood and there is lack of guidance in codes of practice. If cyclic design is incorrect, monopile can tilt in the long term. If the tilt is more than the allowable limit, the turbine may need a shutdown. Monopile design is usually (also wrongly) carried out using API design procedure calibrated for flexible pile design where the pile is expected to fail by plastic hinge [25].
3. *Issues related to installation of monopiles:* Large monopile installation requires suitable vessel availability as well as specialized heavy lifting equipment. Other issues are noise refusals, buckling of the pile tip, drilling out, grouted connections. If the site contains weak rock (siltstone/sandstone/mudstone) and where the local geology shows bedrock or hard glacial soils at shallow depths, drive–drill–drive techniques may be required, with subsequent increases in cost and schedule. It must be mentioned here that driving reduces the fatigue life.

13.8.2 Jacket on Flexible Piles

There has been a considerable interest in jacket-type structures for deeper water applications but is perceived to being expensive due to the amount of steel required. However, jackets supported on piles can be considered as a safe solution due to excellent track record of good performance in offshore oil and gas industry. Offshore oil and gas industries have been using long flexible piles (diameters up to 2.4 m) which are easy to drive and the necessary vessels are available (relatively as opposed to vessels to install monopiles). This aspect will drive down the TIC (time in construction) costs regarding piling and also large vessels are not required for pile installation. However, there are costs associated with jacket installation. One of the requirements is the optimization of the jacket so as to consume minimum steel. There are two types of jacket—normal jacket and twisted jacket. The advantage of twisted jacket over normal jacket is fewer numbers of joints and therefore less fatigue issues.

13.9 CONCLUDING REMARKS

OWTs are new types of offshore structure characterized by low stiffness (as a result flexible and having low natural frequency) and therefore sensitive to the dynamic loadings. Additional challenges are imposed on OWTs in China over and above those in North Sea, as the turbines in China are subjected to much harsher environmental loadings (particular typhoon and earthquake)

and are founded on softer and more complex multilayering seabed. This chapter discusses the complexity involved in designing the foundation of these structures. It has been shown that design guidelines available for offshore oil and gas installation foundations cannot be direct extrapolated/interpolated to OWT foundation design. It is also highlighted that any extrapolation from the design experiences for wind turbine foundations in North Sea to those in China should be treated with great caution.

REFERENCES

- [1] Guo Z, Yu LQ, Wang LZ, Bhattacharya S, Nikita G, Xing YL. Model tests on the long-term dynamic performance of offshore wind turbines founded on monopiles in sand. *J Offshore Mech Arct Eng* 2015;137(4) 041902-1-11.
- [2] Adhikari S, Bhattacharya S. Dynamic analysis of wind turbine towers on flexible foundations. *Shock Vib* 2012;19:37–56.
- [3] Adhikari S, Bhattacharya S. Vibrations of wind-turbines considering soil–structure interaction. *Wind Struct Int J* 2011;14:85–112.
- [4] Bhattacharya S, Cox J, Lombardi D, Muir Wood D. Dynamics of offshore wind turbines supported on two foundations. *Geotech Eng Proc ICE* 2013;166(2):159–69.
- [5] Bhattacharya S, Nikitas N, Garnsey J, Alexander NA, Cox J, Lombardi D, et al. Observed dynamic soil–structure interaction in scale testing of offshore wind turbine foundations. *Soil Dyn Earthquake Eng* 2013;54:47–60.
- [6] Arany L, Bhattacharya S, Macdonald J, Hogan SJ. Simplified critical mudline bending moment spectra of offshore wind turbine support structures. *Wind Energ* 2015;18:2171–97. Available from: <http://dx.doi.org/10.1002/we.1812>.
- [7] Burton T, Jenkins N, Sharpe D, Bossanyi E. *Wind energy handbook*. Chichester, West Sussex: John Wiley & Sons; 2001.
- [8] Bhattacharya. Challenges in the design of foundations for offshore wind turbines. IET reference; 2014.
- [9] DNV (Det Norske Veritas). *Guidelines for design of wind turbines*. 2nd ed. London: DNV; 2002.
- [10] Shadlou M, Bhattacharya S. Dynamic stiffness of monopiles supporting offshore wind turbine generators. *Soil Dyn Earthquake Eng* 2016;15–32. <<http://dx.doi.org/10.1016/j.soildyn.2016.04.002>>.
- [11] Arany L, Bhattacharya S, Macdonald J, Hogan SJ. Design of monopiles for offshore wind turbines in 10 steps. *Soil Dyn Earthquake Eng* 2017;92:126–52. ISSN 0267-7261, <<http://dx.doi.org/10.1016/j.soildyn.2016.09.024>>.
- [12] Wang LZ, Yu LQ, Guo Z, Wang ZY. Seepage induced soil failure and its mitigation during suction caisson installation in silt. *J Offshore Mech Arctic Eng* 2014;136. 011103-1-11.
- [13] Carter. North Hoyle offshore wind farm: design and build. *Energ Proc Inst Civil Eng EN1 2007* 2007;21–9.
- [14] Li LL, Dan HB, Wang LZ. Undrained behaviour of natural marine clay under cyclic loading. *Ocean Eng* 2011;38(16):1792–805.
- [15] Hong Y, Ng CWW, Chen YM, Wang LZ, Chan VSY. Field study of down drag and drag load of bored piles in consolidating ground. *J Perform Construct Facil, ASCE* 2015; <[http://dx.doi.org/10.1061/\(ASCE\)CF.1943-5509.0000790](http://dx.doi.org/10.1061/(ASCE)CF.1943-5509.0000790)>, 04015050.

- [16] Ng CWW, Hong Y, Liu GB, Liu T. Ground deformations and soil–structure interaction of a multi-propelled excavation in Shanghai soft clays. *Géotechnique* 2012;63(12):912–1007.
- [17] Bhattacharya S, Adhikari S. Experimental validation of soil–structure interaction of off-shore wind turbines. *Soil Dyn Earthquake Eng* 2011;31(5–6):805–16.
- [18] Cuéllar P, Georgi S, Baeßler M, Rücker W. On the quasi-static granular convective flow and sand densification around pile foundations under cyclic lateral loading. *Granular Matter* 2012;14(1):11–25.
- [19] Leblanc C. Design of offshore wind turbine support structures—selected topics in the field of geotechnical engineering. Denmark: Aalborg University; 2009.
- [20] Bhattacharya S, Lombardi D, Muir Wood DM. Similitude relationships for physical modelling of monopile-supported offshore wind turbines. *Int J Phys Model Geotech* 2011;11(2):58–68.
- [21] Wang LZ, He B, Hong Y, Guo Z, Li LL. Field tests of the lateral monotonic and cyclic performance of jet-grouting reinforced cast-in-place piles. *J Geotech Geoenvir En ASCE* 2015;141(5) 06015001.
- [22] He B, Wang LZ, Hong Y. Capacity and failure mechanism of laterally loaded jet-grouting reinforced pile: field and numerical investigation. *Sci China Technol Sci* 2015;59(5):763–76.
- [23] He B, Wang LZ, Hong Y. Field testing of one-way and two-way cyclic lateral responses of single and jet-grouting reinforced piles in soft clay. *Acta Geotech* 2017; Available from: <http://dx.doi.org/10.1007/s11440-016-0515-z>.
- [24] Lombardi D, Bhattacharya S, Muir Wood D. Dynamic soil–structure interaction of monopile supported wind turbines in cohesive soil. *Soil Dyn Earthquake Eng* 2013;49:165–80.
- [25] Hong Y, He B, Wang LZ, Wang Z, Ng CWW, Masin D. Cyclic lateral response and failure mechanisms of a semi-rigid pile in soft clay: centrifuge tests and numerical modelling. *Canadian Geotechnical Journal* 2017; Available from: <http://dx.doi.org/10.1139/cgj-2016-0356>.

This page intentionally left blank

Chapter 14

Numerical Methods for SSI Analysis of Offshore Wind Turbine Foundations

Susana Lopez-Querol¹, Liang Cui², and Subhamoy Bhattacharya²

¹*University College London, London, United Kingdom*, ²*University of Surrey, Guildford, United Kingdom*

Email: s.bhattacharya@surrey.ac.uk

14.1 INTRODUCTION

Offshore wind turbine installation is a unique type of structure due to its geometry (i.e., mass and stiffness distribution along the height) and the cyclic/dynamic loads acting on it. There are four main loadings on the offshore wind turbine: wind, wave, 1P, and 3P, see Fig. 14.1. Each of these loads has unique characteristics in terms of magnitude, frequency, and number of cycles applied to the foundation. The loads imposed by the wind and the wave are random in both space (spatial) and time (temporal) and therefore they are better described statistically. Apart from the random nature, these two loads may also act in two different directions. 1P loading is caused by mass and aerodynamic imbalances of the rotor and the forcing frequency equals the rotational frequency of the rotor. On the other hand 2P/3P loading is caused by the blade shadowing effect and is simply two or three times the 1P frequency. Fig. 14.1 shows the typical waveforms of the four types of loads. On the other hand, Fig. 14.2 presents a schematic diagram of the main frequencies of the loads together with the natural frequency of two Vestas V90 3 MW wind turbines from two wind farms: Kentish Flats and Thanet (UK).

Fig. 14.3 describes schematically the mechanism to be considered at the design stage guided by Limit State Design philosophy. A commentary on the diagram is given further.

1. Ultimate Limit State (ULS): The first step in the design is to estimate the maximum loads on the foundations (predominantly overturning moment,

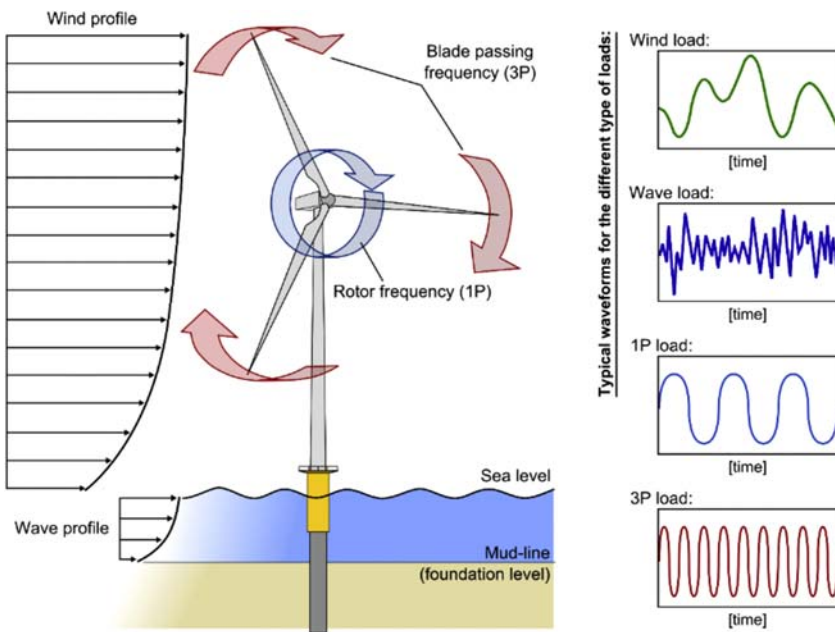


FIGURE 14.1 External loads acting on an offshore wind turbine, along with their typical waveforms.

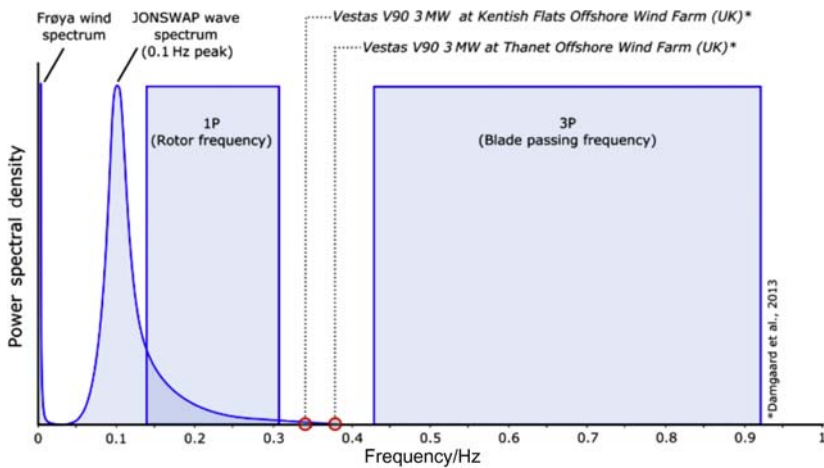


FIGURE 14.2 Forcing frequencies plotted against power spectra densities for Vestas V90 3 MW wind turbines.

lateral load and the vertical load) due to all possible design load cases and compare with the capacity of the chosen foundation. For monopile type of foundations, this would require computation of ultimate moment, lateral and axial load carrying capacity.

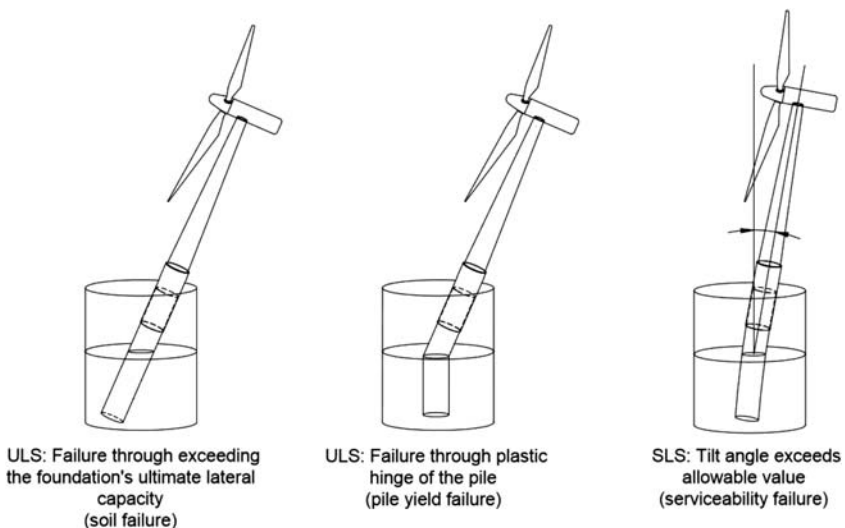


FIGURE 14.3 Examples of ULS and SLS failure (Arany et al. [1]).

2. Target Natural Frequency (Eigen Frequency) and Serviceability Limit State (SLS): This requires the prediction of the natural frequency of the whole system (Eigen Frequency) and the deformation of the foundation at the mudline level (which can be further extrapolated to the hub level) over the lifetime of the wind turbine.
3. Fatigue Limit State (FLS) and long-term deformation: This would require predicting the fatigue life of the monopile as well as the effects of long-term cyclic loading on the foundation.
4. Robustness and ease of installation: This step will ascertain that the foundation can be installed and that there is adequate redundancy in the system.

One of the major uncertainties in the design of offshore wind turbines is the prediction of long-term performance of the foundation, i.e., the effect of millions of cycles of cyclic and dynamic loads on the foundation. The three main long-term design issues are:

1. Whether or not the foundation will tilt progressively under the combined action of millions of cycles of loads arising from the wind, wave, and 1P (rotor frequency) and 2P/3P (blade passing frequency). It must be mentioned that if the foundation tilts more than the allowable, it may be considered failed, based on SLS criteria and may also lose the warranty from the turbine manufacturer. The loads acting on the foundation are typically one-way cyclic and many of the loads are also dynamic in nature. Further details of the loading can be found in Arany et al. [1].

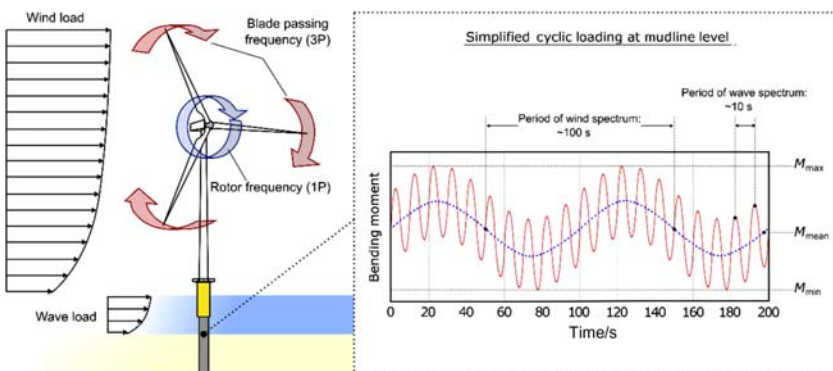


FIGURE 14.4 Loads acting on a typical offshore wind turbine foundation and typical mudline moment.

2. It is well known from literature that repeated cyclic or dynamic loads on a soil causes a change in the properties, which in turn can alter the stiffness of foundation, see Bhattacharya and Adhikari [2] and Bhattacharya [3]. A wind turbine structure derives its stiffness from the support stiffness (i.e., the foundation) and any change in natural frequency may lead to the shift from the design/target value and as a result the system may get closer to the forcing frequencies. This issue is particularly problematic for soft–stiff design (i.e., the natural or resonant frequency of the whole system is placed between upper bound of 1P and the lower bound of 3P) as any increase or decrease in natural frequency will impinge on the forcing frequencies and may lead to unplanned resonance. This may lead to loss of years of service, which is to be avoided.
3. Predicting the long-term behavior of the turbine taking into consideration wind and wave misalignment aspects [4,5].

The SLS and ULS modes of failure are schematically described in Fig. 14.3. ULS failure (which can also be described as collapse) can be of two types: (1) where the soil fails; (2) where the pile fails by forming a plastic hinge [6,7]. On the other hand, in SLS failure, the deformation will exceed the allowable limits. While the ULS calculations can be carried through standard methods, the SLS calculations and long-term issues requires detailed understanding of the Cyclic Soil–Structure Interaction as well as Dynamic Soil–Structure Interaction.

Fig. 14.4 shows a typical mudline bending moment acting on a wind turbine. Typically in shallow to medium deep waters, the wind thrust loading at the hub will produce the highest cyclic overturning moment at the mudline. However, the frequency of this loading is extremely low and is in the order of magnitude of 100 seconds (see Fig. 14.4). Typical period of wind turbine structures being in the range of about 3 seconds and therefore

no resonance of structure due to wind turbulence is expected resulting in *cyclic* soil–structure interaction (SSI) [8,9].

On the other hand, the wave loading will also apply overturning moment at the mudline and the magnitude depends on water depth, significant wave height and the peak wave period. Typical wave periods will be in the order of 10 s (for North Sea) and will therefore have *dynamic* SSI. A calculation procedure was developed by Arany et al. [1] and the output of such a calculation will be relative wind and the wave loads; an example is shown in Fig. 14.4. It is assumed in the analysis that the wind and the wave are perfectly aligned which is a fair assumption for deeper water further offshore projects (i.e., fetch distance is high). Analysis carried out by Arany et al. [1] showed that the loads from 1P and 3P are orders of magnitude lower than wind and wave but they will have highest dynamic amplifications. The effect of dynamic amplifications due to 1P and 3P will be small amplitude vibrations. Resonance has been reported in operational wind farms in German North Sea, see Hu et al. [10]. Furthermore there are added SSIs due to many cycles of loading and the wind–wave misalignments. Typical estimates will suggest that offshore wind turbine foundations are subjected to 10–100 million load cycles of varying amplitudes over their lifetime (25–30 years). The load cycle amplitudes will be random/irregular and have broadband frequencies ranging several orders of magnitudes from about 0.001–1 Hz.

Based on the previous discussion, the SSI can be simplified into two superimposed cases and is discussed as follows:

1. Cyclic overturning moments (typical frequency of 0.01 Hz) due to lateral loads of the wind acting at the hub. This will be similar to a “*fatigue type*” problem for the soil and may lead to strain accumulation in the soil giving rise to progressive tilting. Due to wind and wave load misalignment, the problem can be biaxial. For example, under operating condition, for deeper water and further offshore sites, wind–wave misalignment will be limited for most practical scenarios. Wave loading, on the other hand, will be moderately dynamic as the frequencies of these loads are close to the natural frequency of the whole wind turbine system (typical wind turbine frequency is about 0.3 Hz).
2. Due to the proximity of the frequencies of 1P, 3P, wind, and wave loading to the natural frequency of the structure, resonance in the wind turbine system is expected and has been reported in German Wind farm projects [10,11]. This resonant dynamic bending moment will cause strain in the pile wall in the fore-aft direction, which will be eventually transferred to the soil next to it. This resonant type mechanism may lead to compaction of the soil in front and behind the pile (in the fore-aft direction).

Deformation of the pile under the action of the loading described in Fig. 14.4 will lead to 3-dimensional soil–pile interaction as shown

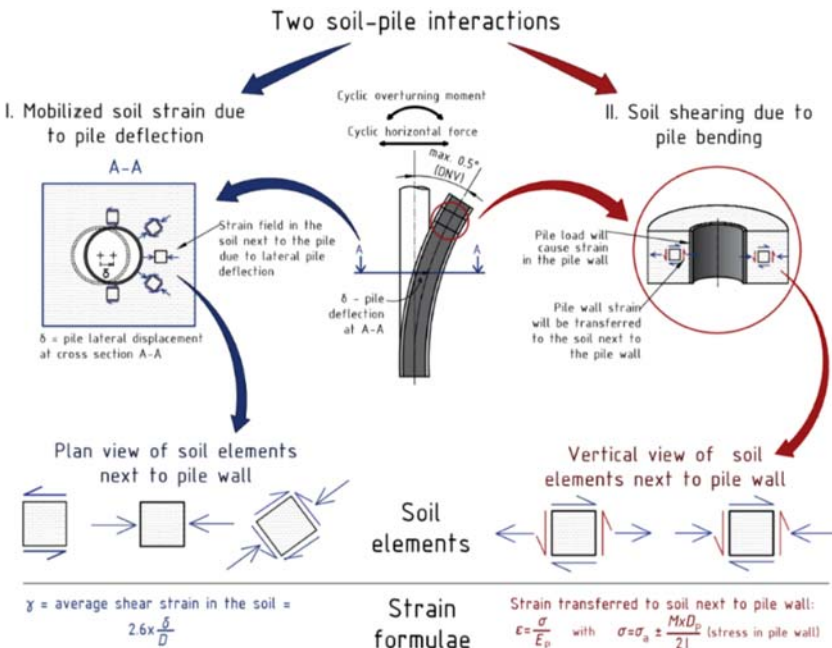


FIGURE 14.5 Two types of soil–pile interaction on a monopile supported wind turbine.

schematically in Fig. 14.5. Simplistically there would be two main interactions: (1) due to pile bending (which is cyclic in nature) and the bending strain in the pile will transfer (through contact friction) strain in the soil, which will be cyclic in nature; (2) due to lateral deflection of the pile there will be strain developed in the soil around the pile. Fig. 14.5 shows a simple methodology to estimate the levels of strains in a soil for the two types of interactions and is given by Eqs. (14.1 and 14.2). The average strain in the soil at any section in a pile due to deflection can be estimated using Bouzid et al. [12] as follows:

$$\gamma = 2.6 \frac{\delta}{D_p} \quad (14.1)$$

where δ is the pile deflection at that section (for example A-A in Fig. 14.5) and D_p is the pile diameter.

On the other hand, the shear strain in the soil next to the pile due to pile bending can be estimated using Eq. (14.2).

$$\gamma_1 = \frac{M \times D_p}{2 \times I \times E_p} \quad (14.2)$$

where M is the bending moment in the pile, I is the second moment of area of pile, and E_p is the Young's Modulus of the pile material. It must be mentioned that Eq. (14.2) assumes that 100% of the strain is transmitted to the

soil, which is a conservative assumption and calls for further study. In practice this will be limited to the friction between the pile and the soil.

14.1.1 Need for Numerical Analysis for Carrying out the Design

The previous section showed a simplified procedure to estimate SSI. However, this approach is grossly oversimplified and has limitations in the sense that the changes in soil properties due to cyclic loading cannot be considered. Also whether or not the foundation will progressive tilt cannot be studied. While the two simple interaction phenomena (i.e., due to pile bending and to lateral deflection of the pile) are taken into consideration, other aspects, such as interface opening (gap formation) or possible impacts between pile and soils during the dynamic loading cannot be accounted for. Moreover, the nature of dynamic loadings is complicated due to the wind–wave misalignment. These considerations make it necessary to use numerical simulations, which allow one to precisely define the geometry of the problem and can also encompass different types of soils. Furthermore changes in the behavior of the soils surrounding the pile is expected to occur as a consequence of the repetition of cycles. Advanced constitutive models, suitable to reproduce different aspects of cyclic/dynamic behavior, are therefore required for analysis. Classical elastoplastic models cannot estimate the accumulation of plastic volumetric strains due to the repetition of cycles (densification). Therefore advanced constitutive laws capable of simulating the plastic strains in soils not due to the magnitude of the loading, but due to the repetition of cycles are needed [13–15].

14.2 TYPES OF NUMERICAL ANALYSIS

Different types of numerical analysis ranging from very simple and practical to more theoretical and standardized can be carried out depending on the application. The methods can be classified into three groups: (1) Simplified where closed form solutions are used and useful during the conceptual and financial feasibility stage; (2) Standard method where code-based calculations are carried out. In the context of monopile, the standard analysis is the $p-y$ analysis (nonlinear Beam on Winkler Foundations), Winkler [16]; (3) Advanced analysis that requires specialist knowledge and expertise. In the detailed design stage, advanced analysis is necessary to predict the long-term prediction. The aim of this chapter is to present advanced numerical models that are suitable to model the SSI [17].

14.2.1 Standard Method Based on Beam on Nonlinear Winkler Spring

The American Petroleum Institute (API) code prescribes a methodology known as “ $p-y$ ” method, which is widely used for design of offshore piles.

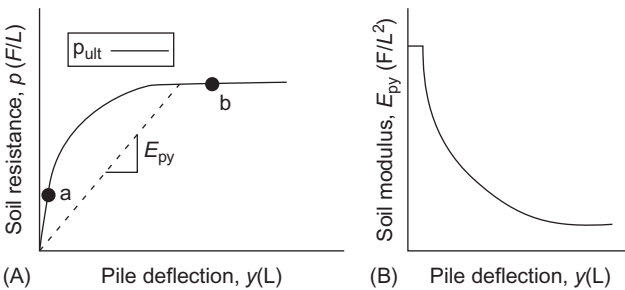


FIGURE 14.6 Examples of p - y curves [18].

This is a subgrade modulus method with nonlinear depth dependent load—deformation characteristics representing the pile—soil interaction. This procedure is calibrated to provide the worst case scenario for the foundation behavior under static and cyclic loading. The p - y curve has been adopted in most offshore standards (like API, 2007; GL, 2005; DNV, 2004 or ISO,) as it has been considered, for many years, as the best method available to determine the displacements of the head of the pile under various loading conditions. Fig. 14.6 represents a typical p - y curve and in the figure, from a to b, an increase in the loading carries an increasing rate of degradation. This nonlinear behavior can be determined empirically or using field tests, under either static or monotonic loading conditions. On the other hand, Fig. 14.6B shows the degradation suffered by the soil as the pile deflection increases [19,20,21].

Terzaghi [22] demonstrated that the linear relationship between p and y (from the origin to a in Fig. 14.6A) was only valid for values of p lower than a half of the ultimate bearing capacity of the soil [22]. This criteria is assumed in the construction of the p - y curves by many methodologies. API (2007) [23] takes into account a number of factors for the construction of the curves, which can be summarized as follows:

1. Type of soil: Basically either sandy or clayey material, considering their different properties.
2. Type of loading: Monotonic or cyclic loading.

Some other aspects, such as the effects of pile installations in the soils and the scour, are taken into account, although it is fully recognized that these factors require further analysis and research.

The main limitations of this API (2007) are:

1. The p - y curve is a procedure verified for piles up to 2 m diameter [19] and this is one of the main limitations of this methodology, as the monopiles in OWT currently have diameters of around 6 m. Extrapolation of a calibrated method is not advisable in geotechnical engineering. Achmus and Abdel-Rahman [19] demonstrated that p - y curve underestimates the

deflections of piles, compare to some numerical simulations. Other researches also demonstrate that $p-y$ curve overestimates the pile–soil stiffness for large diameter piles [24].

2. The nonlinear behavior expected for very high loads in large diameter piles are not covered by this methodology, because the calculated displacements are small if related to the pile diameter (although they can be very big in absolute terms) [19].
3. When the piles are installed in layered soil, the material is taken as continuous and the interaction between the different layers is neglected. This limitation does not occur when the curves are derived on the basis of full-scale tests [18].
4. The subgrade reaction coefficient, k , does not contain any effect related to the flexural stiffness of the pile or the type of loading.

Computational simulations are the alternative to overcome those limitations. Different trends in these methodologies and few worked out examples are presented next, in order to address their suitability and reliability.

14.2.2 Advanced Analysis (Finite Element Analysis and Discrete Element Modeling) to Study Foundation–Soil Interaction

14.2.2.1 Different Soil Models Used in Finite Element Analysis

To account for accumulated strains in the numerical simulations, it is necessary to employ a suitable constitutive model, capable of reproducing realistic soil behavior when subjected to cyclic/dynamic loading conditions. Simple elastoplastic models are usually based on one yield surface without hardening (e.g., the Mohr Coulomb model), with isotropic hardening (e.g., the Cam-Clay model), or on two yield surfaces (isotropic loading and deviatoric loading), e.g., Lade's. They are ideal and efficient on simulating the soil behavior under monotonic conditions, but not suitable to model cyclic loading. Essentially, in such models, plastic deformations start to appear for a certain magnitude of loading, usually higher than the amplitude of the cycles, and hence, the simulated soil behavior remains elastic under that limit, which is against experimental evidences particularly for granular soils [25]. Fig. 14.7 shows the different phenomenon, which can take place in soil during cyclic loading.

Plastic phenomenon for cyclic loading can either be based on “constant stress amplitude” (so called stress controlled) or “constant strain amplitude” (strain controlled). The phenomenon called “adaptation” refers to less dissipation of energy in each cycle of loading as the number of cycles increases, until convergence to nondissipative elastic cycles. On the other hand “accommodation” refers to change of the dissipation of energy from the beginning with an irreversible cumulative deformation and evolves toward a stabilized cycle. This is experienced in laboratory experiments for drained

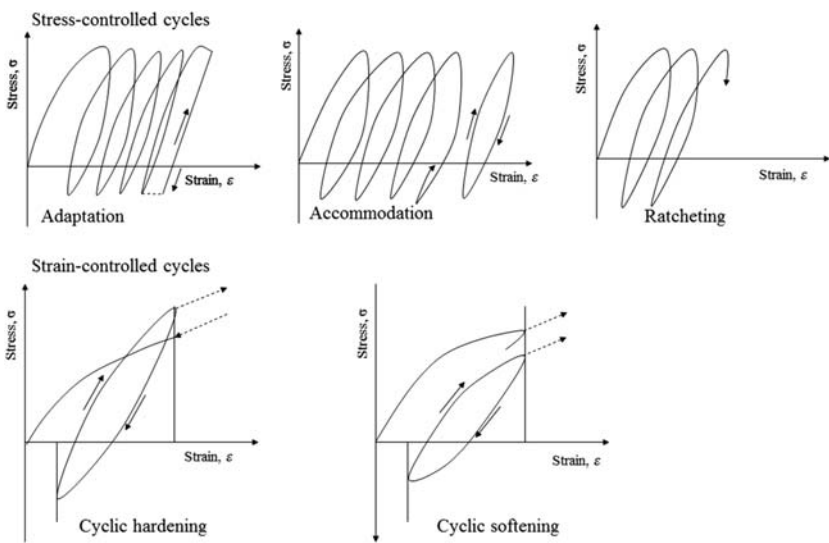


FIGURE 14.7 Different cyclic behaviors. After [25].

samples. “Ratcheting” is an irreversible strain accumulation, which keeps the same shape as that of the beginning [25].

Constant strain amplitude cyclic loading phenomenon results in the cyclic hardening or softening. Cyclic hardening occurs when there is an increase in the cyclic stress amplitude with an increase in the number of cycles, e.g., densification during testing of drained soil. On the contrary, cyclic softening occurs when there is a reduction in the cyclic stress amplitude as the number of cycles increases, e.g., an increase in pore pressure during the testing of undrained soil samples (decrease in the effective stress).

In one of the examples presented in this chapter, a kinematic hardening law has been employed by coupling the elastic moduli and a hardening parameter. Kinematic hardening is used to model plastic ratcheting, which is the build-up of plastic strain during cyclic loading, as previously explained. Other hardening behaviors include changes in the shape of the yield surface in which the hardening rule affects only a local region of the yield surface, and softening behavior in which the yield stress decreases with plastic loading. The kinematic hardening model only involves one plastic mechanism with a smooth yield surface. For nonlinear modeling, the material behavior is characterized by an initial elastic response, followed by plastic deformation and unloading from the plastic state. The plasticity is as a result of the microscopic nature of the material particles and includes shear loading that causes particles to move past one another, changes in void or fluid content that result in volumetric plasticity, and exceeding the cohesive forces

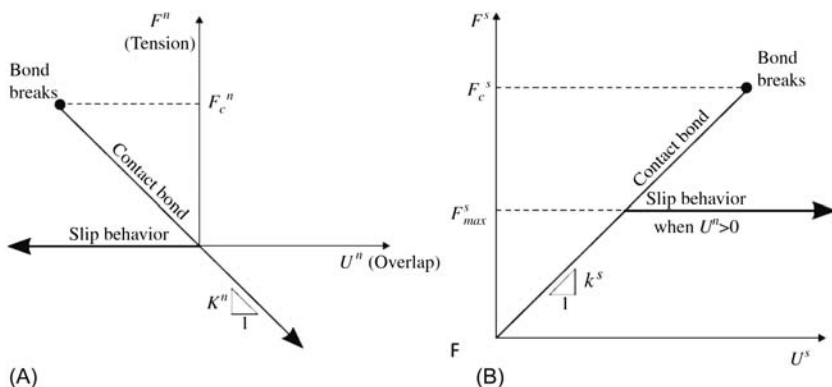


FIGURE 14.8 Force-displacement behavior for contact occurring at a point [28]. (A) Normal component of contact force, (B) Shear component of contact force.

between the particles or aggregates. The material is defined by model materials subject to loading beyond their elastic limit. See Refs. [25,26] for more details.

14.2.2.2 Discrete Element Model Analysis Basics

Originally proposed by Cundall and Strack [26], Discrete Element Method (DEM) simulates granular materials as assemblies of individual particles, which respond to given load conditions. The interactions between particles are simulated by contact laws, e.g., linear contact model, Hertz-Mindlin contact model [27], and parallel bond model, where the normal and tangential contact forces are dependent on the overlap and relative displacement between two contact particles (Fig. 14.8). The contact forces, accelerations, velocities, and displacements of all particles are updated in each small time step using the central difference time integration method. Stresses and strains are then calculated from the contact forces within a representative volume element (RVE) or along a boundary. The DEM is superior to other numerical methods (e.g., Finite Element Method (FEM)) as it allows the direct monitoring of change in soil stiffness, and more importantly it offers a method to analyze the micromechanics, which underlies the stiffness changes. Fig. 14.9 shows a flowchart of a typical DEM calculation.

14.3 EXAMPLE APPLICATION OF NUMERICAL ANALYSIS TO STUDY SSI OF MONOPILE

This section of the chapter shows different applications of numerical analysis to investigate phenomenon related to long-term performance as explained in Section 14.1.

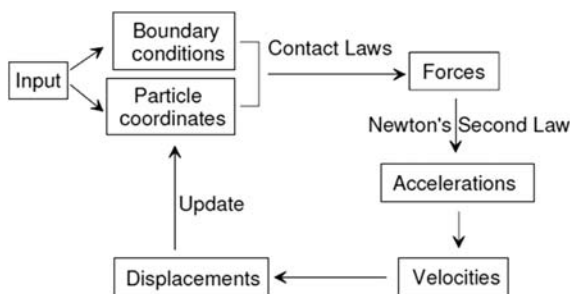


FIGURE 14.9 Flowchart to illustrate the calculation cycles performed in discrete element simulations.

14.3.1 Monopile Analysis Using DEM

An analysis of monopile–soil interactions and stiffness variations were carried out using an open-sourced DEM code modified and validated in previous studies (Cui [29], Cui et al. [30], O’Sullivan et al. [31]). More details can be found in Cui and Bhattacharya [32]. A DEM model of a soil tank ($100\text{ mm} \times 100\text{ mm} \times 50\text{ mm}$) was firstly created, which was filled with about 13 000 spherical particles of radii in the range of 1.1–2.2 mm. The particles were deposited under gravity. The pile was 20 mm in diameter and was embedded to a depth of 40 mm by removing particles located in the space, which was to be occupied by the pile. Particles were allowed to settle down again following the installation of the pile. Once the soil particles were settled down in the soil tank, cyclically horizontal movements were assigned to the pile to simulate the cyclic movements of OWT monopile due to the cyclic loadings. Translational movements rather than rotational movements were assigned to the pile at this stage. Three different strain amplitudes, 0.1%, 0.01%, and 0.001%, were chosen to examine the effects of strain levels. For each strain amplitude two types of cyclic loading were applied: symmetric cyclic loading with strains in the ranges of $(-0.1\%, 0.1\%)$, $(-0.01\%, 0.01\%)$, and $(-0.001\%, 0.001\%)$ and asymmetric cyclic loading with strains in the ranges of $(0, 0.2\%)$, $(0, 0.02\%)$, and $(0, 0.002\%)$. As constrained by the computational costs, 500 cycles were simulated for strain amplitude of 0.1% and 1000 cycles were simulated for other strain amplitudes. The simulation parameters are listed in Table 14.1.

The resultant horizontal stress applied on the pile versus the horizontal strain of soil is illustrated in Fig. 14.10. It can be observed that the stress–strain curves forms hysteresis loops, indicating the energy dissipations during the cyclic loading. It is also interesting to observe that, though the stresses in the first half cycle for the asymmetric cyclic loading is positive, it reduced to negative when the strain goes to zero. Following a few cycles, the minimum negative stress approaches the same magnitude as the maximum positive stress. Moreover the magnitude of stresses and the shape of the hysteresis loops for both symmetric cyclic loading and asymmetric

TABLE 14.1 Input Parameters for Discrete Element Method (DEM) Simulation

Parameters	Value
Soil particle density $\rho_s/\text{kg m}^{-3}$	2650
Particle sizes/mm	1.1, 1.376, 1.651, 1.926, 2.2
Interparticle frictional coefficient (μ)	0.3
Particle-boundary frictional coefficient (μ)	0.1
G_s (Hertz-Mindlin contact model) (Pa)	2.868×10^7
Poisson's ratio	0.22
Initial void ratio/e	0.539

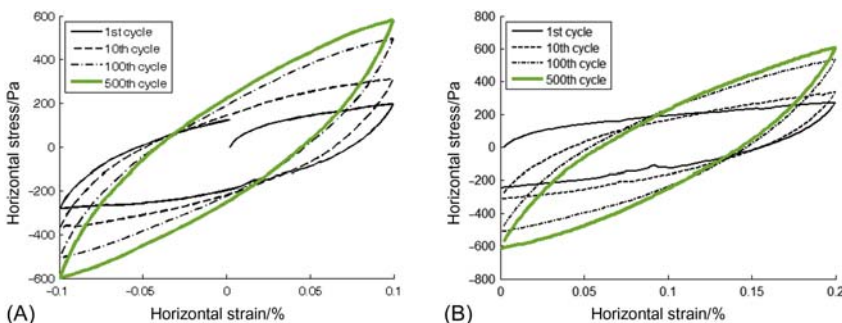


FIGURE 14.10 Hysteresis loops formed by stress–strain curves during cyclic loadings. (A) Strain (-0.1% , 0.1%), (B) Strain (0 , 0.2%) [32].

cyclic loading are almost identical after many cycles. The system under asymmetric cyclic loading behaves the same as symmetric cyclic loading with the same strain amplitude after many cycles, indicating that the strain amplitude, rather than the maximum strain, dominates the long-term cyclic behavior.

The secant Young's Modulus of soil in each cycle was calculated by determining the slope of a line connecting the maximum and minimum points of each full loop and is shown in Fig. 14.11. It is evident that the secant Young's Modulus of soil increased during the cyclic loading. The initial stiffness of asymmetric cyclic loading is lower than that of symmetric cyclic loading with the same strain amplitude due to higher maximum strain applied. However, following a few cycles, the stiffness for both types of cyclic loading approaches the same value. The Young's Modulus versus horizontal strain in the first half cycle and in the 500th cycle for strain amplitude of 0.1% is shown in

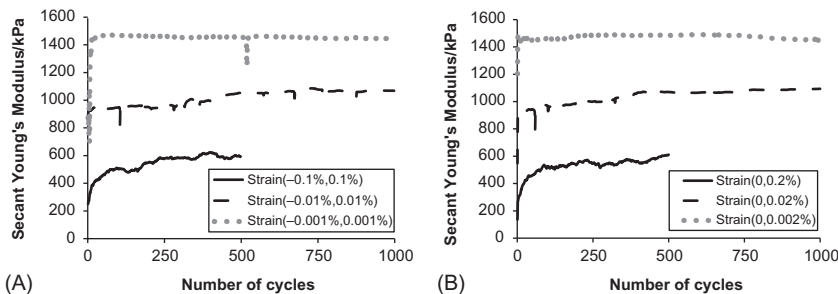


FIGURE 14.11 Secant Young's Modulus of soil at the end of each cycle. (A) Symmetric loading, (B) Asymmetric loading [32].

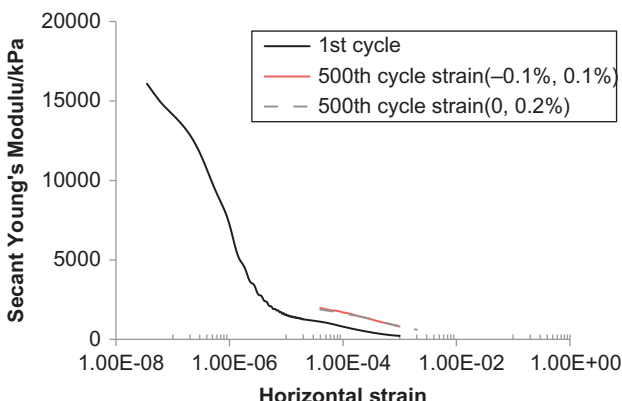


FIGURE 14.12 Secant Young's Modulus versus horizontal strain [32].

Fig. 14.12. The stiffness-strain curve in the first cycle displays the similar “S” shape as expected for the shear modulus-shear strain curve. Following cyclic loadings, all stiffness at different strain levels increases significantly.

To illustrate the ground settlement, plots of incremental soil particle displacements in the symmetric cyclic loading with strain amplitude of 0.1% in the first 50 cycles and in the next 50 cycles are given in Fig. 14.13. Each arrow in the plot starts from the original center of a particle and ends at the new center at the end of a given cycle. It is evident that soil particles surrounding the pile moved downwards, causing ground settlement. Soil densification around pile is the main reason causing the increase of soil stiffness. It also clear that the soil particle displacements are only significant in the first 50 cycles, underlying the significant increase in the soil stiffness in the first 50 cycles. In the current DEM simulations samples with same initial void ratio of 0.539 (medium dense sample) all showed densification behavior and stiffness increase under cyclic loading. It would be interesting to investigate soil behaviors and stiffness evolutions for a wide range of initial void ratios in the future study.

The evolutions of average radial stress in representative cycles are illustrated in Fig. 14.14. Due to the soil densification, the radial stress increased

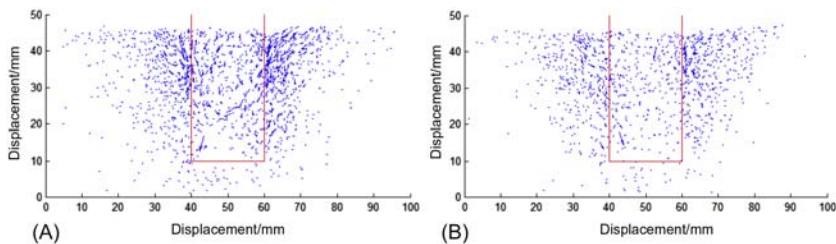


FIGURE 14.13 Incremental soil displacements at the end of the given cycle (Unit: mm) [32].
(A) 1st–50th cycles and (B) 51th–100th cycles.

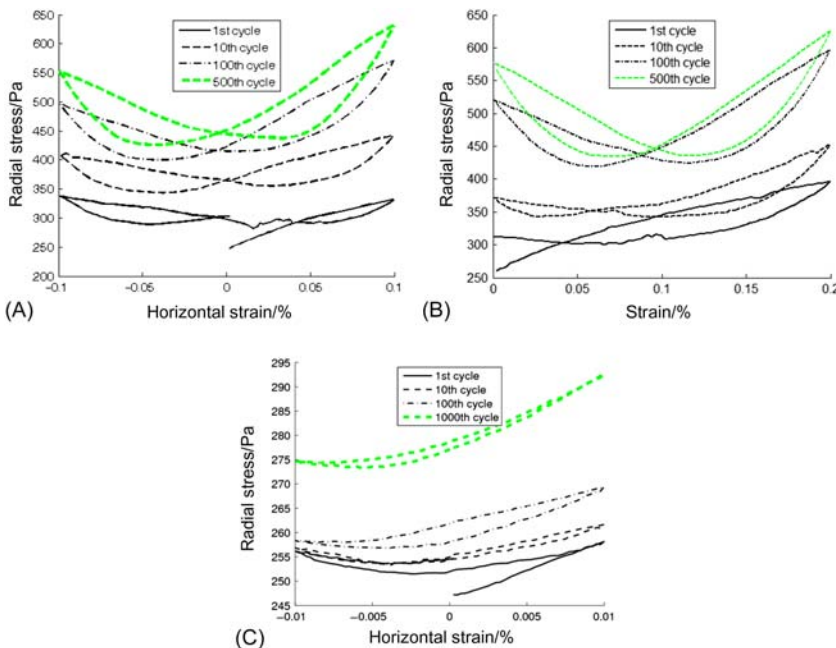


FIGURE 14.14 Evolution of average radial stresses in representative cycles [32]. (A) Strain $(-0.1\%, 0.1\%)$, (B) Strain $(0, 0.2\%)$, and (C) Strain $(-0.01\%, 0.01\%)$.

significantly for strain amplitude of 0.1% under cyclic loading. The shapes of the radial stress–strain curves are quite different for different strain amplitude. For symmetric cyclic loading with 0.01% strain amplitude (Fig. 14.14C), the radial stress increases at positive strain values, but decreases slightly at negative strain values. However, for 0.1% strain amplitude (Fig. 14.14A), the radial stress increases at both positive and negative strains, forming a “butterfly” shaped curve. It is also interesting to observe that, for the asymmetric cyclic loading (Fig. 14.14B), the stress–strain response in the first few cycles is different from that in the correlated

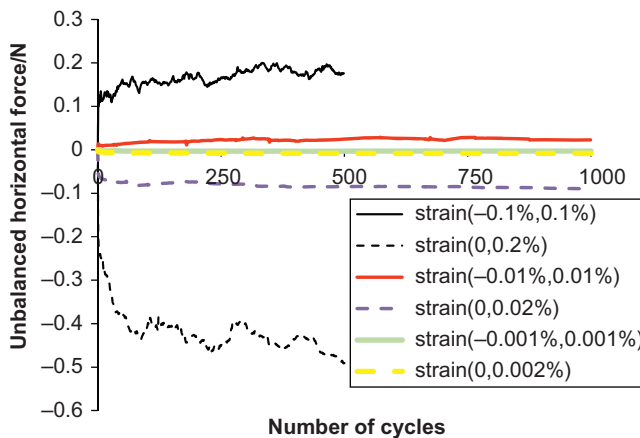


FIGURE 14.15 Evolution of unbalanced horizontal force on the pile at the end of each cycle [32].

symmetric cyclic loading. However, it eventually evolves to the same “butterfly” shape after many cycles. It confirms again that the influence of different maximum strain of a cyclic loading can be eliminated after many cycles and the dominant factor for cyclic soil response is strain amplitude.

The evolution of unbalanced horizontal force at the end of each cycle is illustrated in Fig. 14.15. It is evident that the unbalanced horizontal force is more significant with increasing strain amplitude. It can also be seen that the unbalanced force for asymmetric cyclic loading is much larger in magnitude and is oriented in the opposite direction compared with that for symmetric cyclic loading. It is because, for asymmetric cyclic loading pile only moves to the right side and compresses the soils on the right side significantly, therefore the horizontal force on the pile at the end of each cycle is oriented to the left. However, for the symmetric cyclic loading, the pile compressed the soils on both sides to the same strain level. At the end of a full cycle, the residual horizontal force is oriented to the right. In the presented study monopile was driven to move by a predefined constant velocity. It is more realistic to simulate the free motions of monopile under the action of resultant external force/moment, including the interaction force/pressure between the monopile and the soil.

14.3.2 Monopile Analysis Using FEM Using ANSYS Software

This section of the chapter presents the analysis of a monopile embedded 30 m in a cylindrical soil layer (90 m wide, 45 m deep), see Fig. 14.16. The steel pile is open ended with a wall thickness of 90 mm and a diameter of 7.5 m. It is worth noting that monopile diameters of up to 7 m are designed to maintain serviceability of the wind energy converters over several years as a result of harsh environmental conditions offshore. The monopile

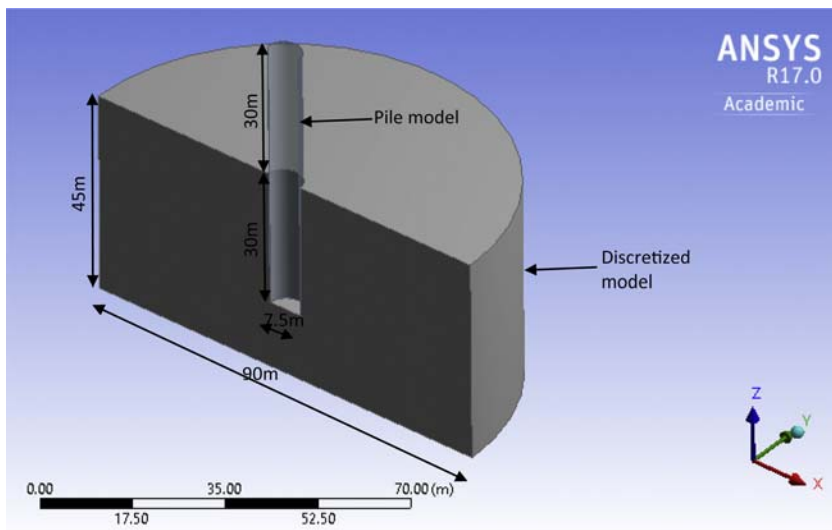


FIGURE 14.16 3D view of the monopile system.

extended 30 m above the sea bed to the point where it was loaded and driven 30 m into the sea bed where the water depth was 10 m. The software ANSYS 17.0 was used to create the 3D model of wind turbine foundation. Static Structural Analysis was used to analyze static conditions, while the Transient Structural was used for the cyclic load.

The soil–pile model took advantage of the symmetry in geometry and load, hence, only one half of the soil-pile model was modeled, as shown in Fig. 14.17 which means that the transversal displacements at the symmetry plane was set to zero. A fine mesh size was selected for the system as shown in Fig. 14.17 resulting in 50 622 nodes and 36 816 elements. Previous studies demonstrated that the minimum number of elements required for an accurate enough model of monopile wind turbine foundations may be in the range of 30 000–40 000. The interaction between pile and structure was modeled as a frictional interface with friction coefficient of 0.4.

The time step was taken as 0.5 second, which was derived by the integration time step (ITS) method [33]. The force was applied by an idealized system described by Bryne and Housby [34] with a generalized loading case for a 3.5 MW turbine in which a 4 MN horizontal load and a 6 MN vertical load applied 30 m above the soil surface was used. This can be represented as:

$$F(t) = F_{\max} \sin(2\pi ft) \quad (14.3)$$

The one-way lateral load was applied with a sinusoidal character of 0.1 Hz (typical frequency ranges in these infrastructures are 0–1 Hz for

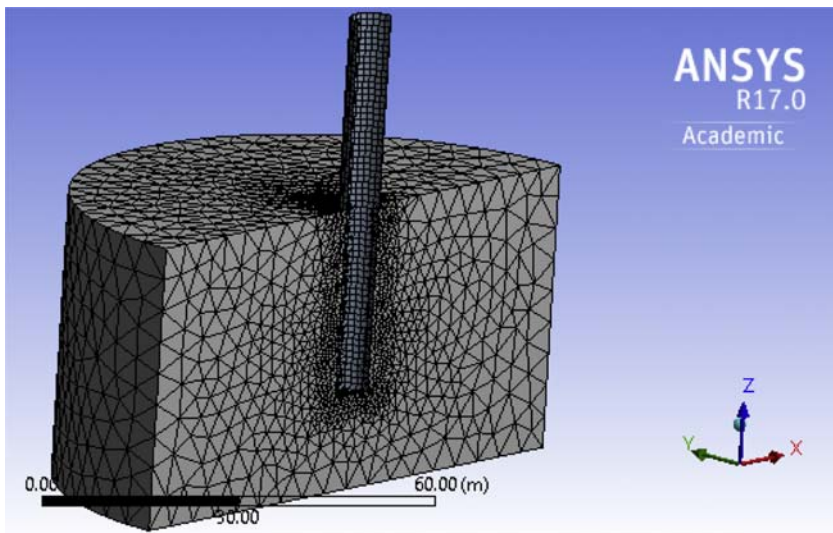


FIGURE 14.17 Mesh sizing of the system.

environmental loads and 5–200 Hz for machine loads [34]). At fixed end time, t of 1000 seconds was used, this gave 100 cycles (frequency = 0.1 Hz), which was used in analyzing the results. The input parameters for the pile were calibrated for offshore installation in United Kingdom using typical test results while those obtained after calibration for the soil are shown in Table 14.2. The steel monopile was represented as a linear-elastic, isotropic, homogeneous material. For the soil properties, the Kinematic Hardening law, have been employed.

The elastic modulus of the soil was derived from Janbu (1963) as presented in Eq. (14.2):

$$E = 60 \text{ MPa} \times \left(\frac{5}{6}\right) \times (\sqrt{2}) \times \left(\frac{\sigma_y}{\sigma_{at}}\right)^{\lambda} \quad (14.4)$$

where σ_y denotes the soil vertical effective stress, and σ_{at} is the atmospheric pressure.

The plot of the applied horizontal load versus the pile-head displacement for dynamic loading, $p-y$ (Fig. 14.18) shows a progressive inclination of the hysteretic loops, for every subsequent increase in the number of cycles, resulting in an increasing pile-head displacement. Similar trend can be observed in the result reported in Ref. [13], although that analysis was carried out for a clayey soil under the influence of a two-way lateral loading, which resulted in equal but opposite pile displacements in both directions. This result trend can be referred to as accommodation cyclic behavior (previously presented in this chapter) and is mostly found in laboratory experiments [25].

TABLE 14.2 Soil Model Material Parameters for Medium Dense Sand (after [19])

Parameter	Symbol	Value
Oedometric stiffness parameter	κ	600
Parameter for the elastic modulus (eq. 14.4)	λ	0.55
Poisson's ratio	ν	0.25
Unit buoyant weight/kN m ⁻³	γ'	15.5
Internal friction angle/deg	ϕ'	35
Dilation angle/deg	ψ	5
Cohesion/kN m ⁻²	c	0.1
Yield surface parameter	α	0.127
Yield surface parameter/kPa	k	1.8
Plastic potential	β	4.05×10^{-2}
Hardening law/MPa	C	22
	D	1200

A closer observation of pile-head displacement (Fig. 14.19) shows an increase in the displacement with time. This can be observed in drained cyclic tests with an increase in density (densification) [25]. However, instabilities caused by alternating degradation and compaction are observed at the earlier cycles, causing negative displacement accumulation at the initial stages of loading. The pile-head displacement at the end of the first cycle equals 1.36 cm and 2.06 cm at the end of 100 cycles, which is the maximum displacement of the sea bed in front of the pile. This gives a total increased displacement of 0.7 cm. The accumulation rate from the 1st to the 100th cycle equals 1.51 cm. The displacement accumulation per cycle reduces drastically for the first 10 cycles, and then tends toward zero as the number of cycles increase, because at deflections larger than that of static loading, the value of soil resistance, p , decreases sharply due to cyclic loading, while afterwards it remains pretty much constant [18]. This is as a result of the kinematic hardening parameter, as also reported in Ref. [25], which stated that the cycles become reversible until a complete stabilization is reached for very high numbers of cycles. Similar results are observed along radial stress paths [35,36].

A comparison of the load-displacement response at the pile head between results from finite element modeling (static and dynamic) and API $p-y$ curve method is provided in Fig. 14.20. The dynamic loading is represented by the curve for 1st, 50th, and 100th cycle. From Fig. 14.20, it is observed that at

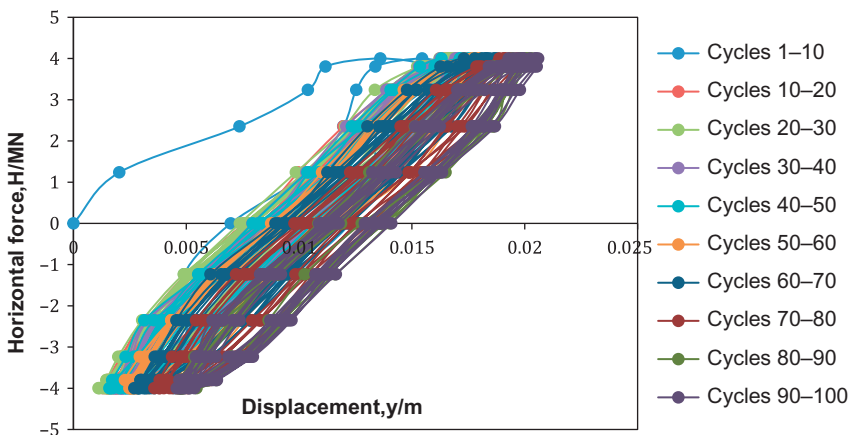


FIGURE 14.18 $p-y$ Curve obtained from harmonic loading.

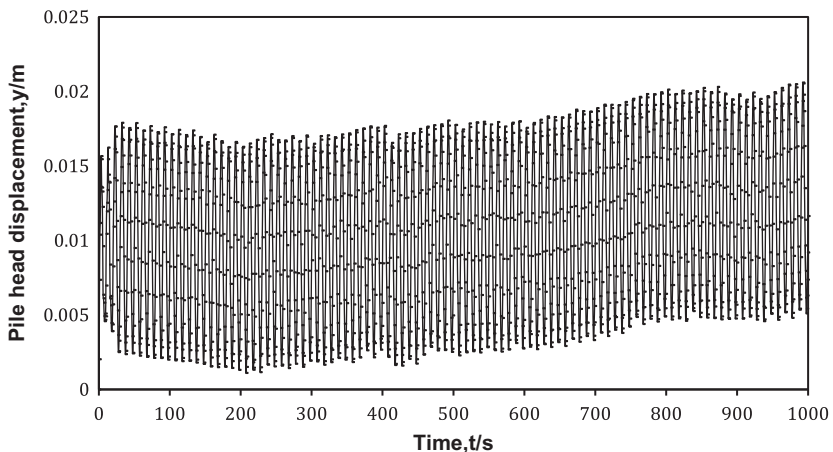


FIGURE 14.19 Plot of pile-head displacement with time.

very low lateral-horizontal forces, the API method is in agreement with numerical simulations for static loading and 1st cycle dynamic loading. This supports the statement that the API method is a pseudo static approach [18]. However, at low lateral-horizontal forces and high number of cycles, the API method underestimates the pile displacement. This can be observed by the difference in pile displacements between the API method and numerical simulations; calling Δ to the displacement obtained when the applied load is 4 MN, we can see that Δ equals 0.3 cm for the 1st cycle, 0.8 cm for the 50th cycle, and 1 cm for the 100th cycle. This underestimation of the pile displacement by the API method at low lateral displacement was also observed by Hearn [37]. This also

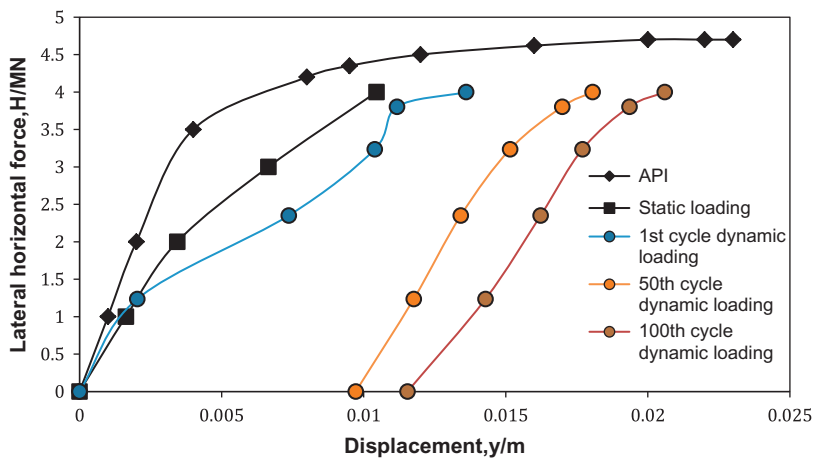


FIGURE 14.20 Comparison plot of the $p-y$ curve between the American Petroleum Institute (API) method and numerical simulations.

represents the conclusion presented by Yang et al. [38] who stated that “the cyclic bearing capacity may be significantly lower than the static bearing capacity.” This is true as the displacement increases with an increase in the number of cycles. Thus the displacement as a result of several cycles goes farther away from the displacement from static load/one cycle, since there is an accumulation of volumetric strains in the soil surrounding the pile. The plot also shows that the curve for the static loading and the 1st cycle dynamic loading are similar but the difference in pile displacement at the maximum applied lateral load of 4 MN is 0.3 cm. This gives a percentage difference of 30%. This may be because simulations for transient analysis are based on division of time or steps: therefore, there is a progressive accumulation of residual errors with an increase in the number of time steps [39].

REFERENCES

- [1] Arany L, Bhattacharya S, Macdonald J, Hogan SJ. Design of monopiles for offshore wind turbines in 10 steps. *Soil Dyn. Earthq. Eng.* 2017;92:126–52. <<http://dx.doi.org/10.1016/j.soildyn.2016.09.024>>.
- [2] Bhattacharya S, Adhikar S. Experimental validation of soil–structure interaction of offshore wind turbines. *Soil Dyn. Earthq. Eng.* 2011;31(5–6):805–16.
- [3] Bhattacharya S. Challenges in design of foundations for offshore wind turbines. *IET J. Eng. Technol Ref.* 2014;9. <<http://dx.doi.org/10.1049/etr.2014.0041>>, Online ISSN 2056-4007.
- [4] Bhattacharya S, Lombardi D, Muir Wood D. Similitude relationships for physical modelling of monopile-supported offshore wind turbines. *Int. J. Phys. Model. Geotech.* 2011;11(2):28–68.
- [5] Guo Z, Yu L, Wang L, Bhattacharya S, Nikitas G, Xing Y. Model tests on the long-term dynamic performance of offshore wind turbines founded on monopiles in sand. *J. Offshore Mech. Arctic Eng.* 2015; Paper No: OMAE-14-1142; <<http://dx.doi.org/10.1115/1.4030682>>.

- [6] Bhattacharya S, Cox JA, Lombardi D, Muir Wood D. Dynamics of offshore wind turbines on two types of foundations. *Proceedings of the Institution of Civil Engineers: Geotechnical Engineering* 2012;166:159–69. Available from: <http://dx.doi.org/10.1680/geng.11.00015>.
- [7] Bhattacharya S, Nikitas N, Garnsey J, Alexander NA, Cox J, Lombardi D, et al. Observed dynamic soil–structure interaction in scale testing of offshore wind turbine foundations. *Soil Dyn. Earthq. Eng.* 2013;54:47–60.
- [8] Arany L, Bhattacharya S, Macdonald J, Hogan SJ. Simplified critical bending moment spectra of offshore wind turbine support structures. *Wind Energy* 2014. Available from: <http://dx.doi.org/10.1002/we.1812>.
- [9] Arany L, Bhattacharya S, Macdonald JHG, Hogan SJ. Closed form solution of Eigen frequency of monopile supported offshore wind turbines in deeper waters incorporating stiffness of substructure and SSI. *Soil Dyn. Earthq. Eng.* 2016;83:18–32. ISSN 0267-7261, <<http://dx.doi.org/10.1016/j.soildyn.2015.12.011>>.
- [10] W.-H. Hu, S. Thöns, S. Said, W. Rücker Resonance phenomenon in a wind turbine system under operational conditions, in: A. Cunha, E. Caetano, P. Ribeiro, G. Müller (Eds.), *Proceedings of the 9th International Conference on Structural Dynamics, EURODYN 2014*, Porto, Portugal, June 30–July 2, 2014, ISSN: 2311–9020, ISBN: 978-972-752-165-4.
- [11] Nikitas G, Vimalan N, Bhattacharya S. An innovative cyclic loading device to study long term performance of offshore wind turbines. *Soil Dyn. Earthq. Eng.* 2016;82:154–60.
- [12] Bouzid D. p-y Curves from stress-strain of a soil: FE assessment. *Geomech. Eng.* 2013;5:379–99. Publisher: Techno-Press; <<http://dx.doi.org/10.12989/gae.2013.5.5.379>>.
- [13] P. Cuéllar, Pile foundations for offshore wind turbines: numerical and experimental investigations on the behaviour under short-term and long-term cyclic loading, PhD Thesis, Technical University of Berlin, (2011).
- [14] Wichtmann T, Niemunis A, Triantafyllidis Th. Strain accumulation in sand due to cyclic loading: drained triaxial tests. *Soil Dyn. Earthq. Eng.* 2005;25(12):967–79. Available from: <http://dx.doi.org/10.1016/j.soildyn.2005.02.022>.
- [15] Blazquez R, Lopez-Querol S. Generalized densification law for dry sand subjected to dynamic loading. *Soil Dyn. Earthq. Eng.* 2006;26(9):888–98. Available from: <http://dx.doi.org/10.1016/j.soildyn.2005.09.001>.
- [16] E. Winkler Die Lehre von der Elasticitaet und Festigkeit mit besonderer Rucksicht auf ihre Anwendung in der Technik fur polytechnische Shulen, Bauakademien, Ingenieure, Maschinenbauern, Architekten, etc. Verlag von H. Domenicus, Prag. (1867).
- [17] McClelland B, Focht JA. Soil modulus for laterally loaded piles. *Trans. Am. Soc. Civil Eng.* 1958;123(2954):1049–86.
- [18] Reese CL, Van Impe FW. *Single Piles and Pile Groups Under Lateral Loading*. Second ed. CRC Press/Balkema; 2001.
- [19] Achmus M, Abdel-Rahman K. Finite element modelling of horizontally loaded monopile foundations for offshore wind energy converters in Germany. *Proc Int Symp Front Offshore Geotech ISFOG 2005*;391–6. Available from: <http://dx.doi.org/10.1201/NOE0415390637.ch38>.
- [20] Ashour M, Norris G. Modeling lateral soil-pile response based on soil pile interaction. *J. Geotech. Geoenviron. Eng.* 2000;126(5):420–8.
- [21] H. Matlock, Correlations of design of laterally loaded piles in soft clay. in: *Proceedings of the II Annual Offshore Technology Conference*, Houston, Texas (OTC 1204) (1970) 577–594.

- [22] Terzaghi K. Evaluation of coefficients of subgrade modulus. *Geotechnique* 1955;297–326.
- [23] API (2007), Recommended practice for planning, designing and constructing fixed offshore platforms – working stress design, API Recommended Practice, 2A-WSD (RP 2A-WSD), (2007).
- [24] Wiemannand J, Lesny K. Design aspects of monopiles in German offshore wind farms. Chapter 37. Frontiers in offshore geotechnics proceedings of the international symposium on frontiers in offshore geotechnics (IS-FOG 2005), 19–21 Sept 2005, Perth, WA, Australia.
- [25] Cambou B, Hicher P-Y. Elastoplastic modeling of soils: cyclic loading. In: Hicher P-Y, Shao J-F, editors. Constitutive modeling of soils and rocks. London, UK: ISTE; 2008. Available from: <http://dx.doi.org/10.1002/9780470611081> ch4.
- [26] Cundall P, Strack O. A discrete numerical model for granular assemblies. *Geotechnique*. 1979;29(1):47–65.
- [27] Mindlin R, Deresiewicz H. Elastic spheres in contact under varying oblique forces. *ASME J. Appl. Mech.* 1953;20:327–44.
- [28] Itasca PFC2D manual 4.0, 2008.
- [29] L. Cui, Developing a virtual test environment for granular materials using discrete element modelling, PhD Thesis, University College Dublin, Ireland (2006).
- [30] Cui L, O'Sullivan C, O'Neill S. An analysis of the triaxial apparatus using a mixed boundary three-dimensional discrete element model. *Geotechnique* 2007;57(10):831–44.
- [31] O'Sullivan C, Cui L, O'Neil S. Discrete element analysis of the response of granular materials during cyclic loading. *Soils Found.* 2008;48(4):511–30.
- [32] Cui L, Bhattacharya S. Soil-monopile interactions for offshore wind turbine. *Eng. Comput. Mech.* 2016;169:171–82.
- [33] R.W. Hamming Digital filters (Prentice-Hall signal processing series), (1977).
- [34] Byrne BW, Housby GT. Foundations for offshore wind turbines. *Philos. Trans. A Math. Phys. Eng. Sci.* 2003;361:2909–30. Available from: <http://dx.doi.org/10.1098/rsta.2003.1286>.
- [35] Sa'don NM, Pender MJ, Abdul Karim AR, Oreense R. Pile head cyclic lateral loading of single pile. *Geotech. Geol. Eng.* 2014;32:1053–64. Available from: <http://dx.doi.org/10.1007/s10706-014-9780-5>.
- [36] Jardine RJ, Yang ZX, Foray P, Zhu B. Interpretation of stress measurements made around closed-ended displacement piles in sand. *Géotechnique* 2013;63:613–27. Available from: <http://dx.doi.org/10.1680/geot.9.P.138>.
- [37] E. Hearn, Finite element analysis of an offshore wind turbine monopile, Master's Thesis, Dept Civil Environ Eng Tufts Univ. Medford, MA, (2009). <[http://dx.doi.org/10.1061/41095\(365\)188](http://dx.doi.org/10.1061/41095(365)188)>.
- [38] Yang M, Ge B, Li W, Zhu B. Dimension effect on p-y model used for design of laterally loaded piles. *Procedia. Eng.* 2016;143:598–606. Available from: <http://dx.doi.org/10.1016/j.proeng.2016.06.079>.
- [39] T. Wichtmann, Explicit accumulation model fpr non-cohesive soils under cyclic loading, Inst Für Grundbau Und Bodenmechanik:274, PhD thesis, University of Karlsruhe, Germany, (2005).

This page intentionally left blank

Chapter 15

Reliability of Wind Turbines

Shuangwen Sheng¹ and Ryan O'Connor²

¹National Renewable Energy Laboratory, Golden, CO, United States, ²eDF Renewable Energy, Denver, CO, United States

Email: Shuangwen.sheng@nrel.gov

15.1 INTRODUCTION

Modern utility-scale wind turbines are complex systems that include both hardware components—structural, mechanical, electrical, thermal, and hydraulic—and software components. They are designed to convert kinetic energy from wind to electrical power for 20–25 years. The development of modern large wind turbines dates back to the 1970s and 1980s and has expanded dramatically during the past few decades with the global cumulative installed wind power generation capacity reaching 430 gigawatts (GW) by the end of 2015 [1,2]. The evolution, however, has been profoundly influenced by reliability and availability issues [2], ranging from structural collapses in the early prototypes to the recent premature component failures on commercial wind turbines. The encouraging fact is that nowadays most modern land-based wind turbines can achieve an availability of about 98% and mean time between failures (MTBFs) of more than 7000 hours, implying a failure rate of a little over 1 failure(s)/turbine per year [2]. The challenge is a few overhauls or replacements of major components are normally needed, throughout the design life of a modern wind turbine, despite the fact that structural components, such as the foundation and tower, can normally last longer. These overhauls or replacements of major components which are infrequent but typically associated with long downtime, compounded with frequent failures of other components that have short downtime, lead to increased operation and maintenance (O&M) costs of wind turbines and subsequently, the cost of energy (COE) for wind power. The cost can increase as wind turbines age and become much higher for offshore wind plants. Based on European experience, on average, the availability of offshore wind plants is about 7% lower than land-based plants [3], and the O&M costs for an offshore wind plant are twice the cost of a land-based plant [4]. As a

result, there is a clear need for the wind industry to improve reliability and reduce O&M costs, especially when turbines are installed offshore.

There are a few different factors to consider when improving turbine reliability and reducing O&M costs, such as design [5], testing [6], and O&M [7]. The wind turbine application is uniquely featured by a stochastic duty cycle, which is similar to automotive applications, and an expected long asset lifetime, which is more similar to aerospace applications. It is also characterized by difficult access, remote and regional resources, strained supply chains, and new functional requirements. The majority of wind turbine components are designed to be dependable and have no redundancy. For example, a typical wind turbine has about 5000 parts, which can lead to around half a million possible turbine failures at a wind plant with 100 turbines. Current turbine design standards focus on component survival against damage from hazards throughout a turbine design lifetime. This is compounded by the use of custom parts, and designer's behaviors are driven by certification, not regulation. Reliability demonstration is difficult as specific designs and parts become obsolete. Reputation of a turbine technology also has an influence, which is supported by anecdotes, analysis, witness to failures, and reporting. Oftentimes severe events are overstated. A lack of reliability increases capital expenditures through overdesign, excessive prototyping and testing, and warranty and insurance requirements; increases financing costs due to uncertainties, operational expenditures from both scheduled and unscheduled events; and reduces annual energy production.

Once turbines are installed in a wind plant, the main opportunity for COE reduction lies in improvement of O&M practices, which is the perspective taken in this chapter. The intention of this chapter is to highlight the current reliability statistics of wind turbines, and present the opportunities for the wind industry O&M to benefit from reliability engineering, such as warranty, maintenance, supply-chain, and risk management. The motivation is that reliability engineering is ready to be widely adopted and practiced by the wind industry and it can help reduce O&M costs without much delay. The authors hope that the materials presented in this chapter can help stimulate the integration of reliability engineering methods by the global wind industry and benefit O&M. This chapter is not intended to provide a comprehensive discussion on wind turbine reliability or O&M practice improvements through condition-based maintenance or prognostics and health management, for which the audience can refer to such books as Ref. [2].

Given that wind turbines have various types of components, a wind turbine reliability evaluation needs to consider them accordingly. However, this chapter focuses on mechanical components and uses them to demonstrate the potential benefits of reliability engineering to wind. In addition, different sectors of the wind industry may have different interests in terms of wind turbine reliability. For example, manufacturers may be more interested in

improving wind turbine reliability through design improvements; whereas owners and operators may be more interested in improving wind turbine reliability through O&M practice enhancements. This chapter takes the owners' and operators' perspective, focusing on reliability analyses to determine efficient maintenance practices [8]. Specifically, failure analysis identifies certain component failure rates and life characteristics over time or operating conditions to help determine maintenance or component replacement intervals. If root causes for certain failures were identified, these failure modes could be mitigated through either O&M practices or replacements with improved products. Another type of practice, such as failure-mode-effect-criticality analysis (FMECA), performed for product design or improvements, can also be conducted to benefit O&M [9].

In the next few sections, a brief discussion on terminology and reliability metrics is provided. Then, the current status of wind turbine reliability is presented. Next, the reliability life data analysis that can potentially benefit wind plant O&M, including data collection, model development, and forecasting, is discussed. Two case studies are then presented to illustrate how the life data analysis can be utilized to benefit wind plant O&M. The chapter concludes with some final remarks on potential opportunities to improve wind turbine reliability.

15.2 FUNDAMENTALS

15.2.1 Terminology

15.2.1.1 Reliability

Reliability is the *probability* that a product or a system will perform its *intended functions* satisfactorily (i.e., without failure and within specified performance limits) for a *specified length of time*, when operating under *specified environmental and usage conditions* [10]. Depending on the perspective, reliability can be inherent as designed and manufactured or operational as observed in the field [11]. To use wind turbines as the context, the product or system can be a wind turbine or a turbine component. The specified length of time is normally treated as the design life of 20–25 years for a wind turbine, which only specifies the duration and is not a complete reliability statement. Two other factors in the definition are to perform intended functions and under specified conditions. Reliability is a probability that changes if the application or design is changed. When wind turbine reliability is discussed, often it is based on anecdotes, not thorough and systematic life analyses using data collected from the field. A failure occurs when the intended functions of a wind turbine component cannot be performed satisfactorily.

For complex machines like a wind turbine, reliability of the entire turbine is affected by the reliabilities of its subsystems, including both hardware and

software, and how those components are connected. When analyzing the reliability of a wind turbine or a wind turbine subsystem like a gearbox, it is recommended to use a comprehensive and normalized grouping of components according to their functions and positions. One method is to use reliability block diagrams [12], which show the functional components and their relationships within a wind turbine. They consider the relationship of all competing and independent failure modes impacting the components on a wind turbine. The reliability of a wind turbine is also affected by environmental conditions, such as wind and wave conditions in offshore wind plants. It is worth noting that improvements in major turbine subsystem or component reliability alone are not sufficient and the impacts of connecting components on reliability also need to be considered. The economies of wind turbines and other independent power generation plants generally prohibit the use of redundant components (This does not include safety equipment.). In addition, low-level actionable components in wind turbines are generally nonrepairable, implying when failed, the components cannot be repaired without a maintenance intervention. All components must function for the wind turbine to generate electricity. This dependency on all turbine subsystems and components negatively impacts the reliability of a wind turbine as it leads to lower system reliability than individual component reliability. For more information on system and component reliability, please refer to [Chapter 6](#) in Ref. [13].

15.2.1.2 Metrics

To evaluate the reliability of a wind turbine, its major turbine components normally need to be grouped into three categories: structural, electrical, and mechanical. The reason for this grouping is because they typically need different reliability evaluation metrics and methods. For structural components, such as the blades, tower, and foundation, the probability of failure can be used as the metric and evaluated using structural reliability theory [14,15]. For electrical and mechanical components, their life is assumed to follow the classical bathtub curve. Its failure rate, λ , is a very popular measure, which is normally treated as the inverse of $MTBF$. These metrics can be calculated using classical reliability theory [13]. Some work on wind turbine reliability evaluation by integrating structural subsystems with electrical and mechanical components was reported in Ref. [16]. This chapter focuses on the mechanical components.

Below is a brief list of metrics and expressions that are useful for reliability evaluation, as stated in [Chapter 1](#) of Ref. [2].

- Mean time to failure: $MTTF$ (nonrepairable components)
- Mean time to repair or replacement: $MTTR$
- Logistic delay time: LDT
- Downtime: $MTTR + LDT$

- Mean time between failure: $MTBF = MTTF + MTTR + LDT$ (repairable systems, such as a wind turbine or a wind turbine gearbox)
- Failure rate:

$$\lambda = \frac{1}{MTBF} \quad (15.1)$$

- Repair rate:

$$\mu = \frac{1}{MTTR} \quad (15.2)$$

The $MTTF$ often is used on nonrepairable turbine components that need to be replaced after they fail. These are often the lowest level actionable components within a wind turbine. For a wind turbine gearbox or the entire turbine, which are both composed of many low-level actionable components, $MTBF$ is more appropriate. Among these metrics, $MTBF$, or failure rate, and downtime are often used in the wind industry to evaluate relative improvements of turbine reliability. No matter which metric is used, the key is to trend the chosen metric over time. On the other hand, using $MTTF$ or $MTBF$ alone is not sufficient [17] for reliability engineering analysis. When discussing wind turbine reliability within the community of peers, reliability engineers are better served by expressing the reliability in terms of life distributions and parameters, which will be discussed in [Section 15.4](#).

15.2.2 Taxonomy

Different parties may use various sets of taxonomies when talking about wind turbines. In terms of reliability, it is essential to know the taxonomy and chain of dependability in wind turbines. The set of taxonomy introduced by the ReliaWind consortium is adopted in this chapter. It uses a five-level system to describe a wind plant and the definitions include [2]:

- System, which could be the wind plant including wind turbines, substation, and cables
- Subsystem, which could be an individual wind turbine or a substation at the wind plant
- Assembly, which could be the gearbox in a wind turbine or the high-voltage system in the substation
- Subassembly, which could be the high-speed shaft in the gearbox
- Component, which could be the high-speed shaft bearing.

The set of taxonomy is also helpful when conducting reliability data collection. For more details on this set of taxonomy, please refer to Chapter 11 in Ref. [2]. If cost analysis is also of interest, refer to the land-based and offshore wind plant cost break down structures developed by the National Renewable Energy Laboratory (NREL) in Appendixes E and F of Ref. [18].

15.2.3 Failure Types

Wind turbine components are nonrepairable during operation and function similar to a chain under tension. All components must survive or the turbine fails. The length of the chain is not constant for all wind turbine designs [19]. The chain shown in Fig. 15.1 includes 14 major components common to many modern wind turbines: three blades, three pitch bearings, a hub, main bearing, main shaft, gearbox, generator, main frame, yaw bearing, and tower. Some turbine designs may include more or fewer major components [19].

Component life cycle reliability needs to consider all independent failure modes of the component. Wind turbine components commonly suffer from four types of failures: infant, premature, random, and wear out.

Infant failures are those events mostly due to wear-in problems or quality defects from the material manufacturing process. These types of failures are more likely to occur early in life and have a decreasing incidence rate with age. Preventing all infant failures is prohibitively expensive and every turbine manufacturer must allow some defect rate for each component. The allowable defect rate is a function of the manufacturer's quality management and risk assessment. For wind project owners, the majority of infant failures are mitigated by a supplier warranty. Performing life data analysis on infant failures provides the wind turbine owners with a way to measure the quality management of the supplier and to understand the value of a supplier warranty.

Premature failures include those events due to a latent defect in the design, manufacturing process, or application (including maintenance activities). Premature failures are often detected after some period of operation and may progress to show signs of degradation and wear before functional failures. Axial cracks are a common premature failure of wind turbine gearbox bearings. Corrosion is another premature failure seen on wind turbine components. Premature failures can impact a small or a large portion of an aging turbine population and these failures often disrupt operations like a “bump in the road,” or in extreme cases may be like a “fall from a small cliff.”

Random failures are expected to appear throughout the wind turbine life cycle. These failures are caused mostly by an unlikely string of preceding

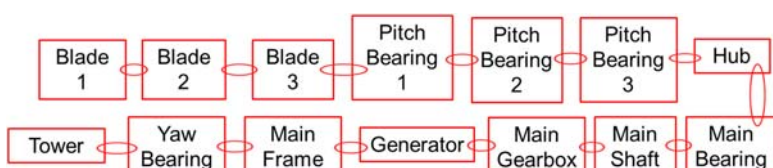


FIGURE 15.1 Figurative chain of dependability showing the relationship of major equipment in a wind turbine [19].

events, which can be an overload event like a 50 year extreme gust or a lightning strike. The rate of a random failure is constant regardless of the equipment age. As with infant failures, it is prohibitively expensive to over-design wind turbine components to survive all likely random, extreme failures. Experienced owners and original equipment manufacturers with a large fleet of wind turbines expect some failures due to random strength exceedances. The risk of these random failures is typically mitigated by insurance. Life data analysis of random failures provides wind turbine owners with a method to quantify their wind turbine insurance needs.

As strange as it may sound, wear-out failures are the way in which owners hope wind turbine components fail. If a majority of the failures are wear out, it is likely that the owner has selected a quality manufactured product, operated and maintained the asset effectively, avoided random failures from a host of causes, and finally failed the components by “old age.” This is the ideal way a component will break down at the end of its life and the failure for which the component lifetimes are often specified (e.g., a 20 year design life refers to the classic fatigue wear out of materials). These failures are more likely to happen later in the life cycle and life data analysis of this type of failures helps owners plan for maintenances and spare parts.

Table 15.1 provides a list of failure modes typically seen in major wind turbine assemblies, i.e., gearboxes, blades, pitch bearings (A wind turbine typically has three pitch bearings, which are treated together as an assembly.), and generators, by grouping according to the four failure types discussed earlier. For each failure mode, a failure mechanism is present and needs to be modeled and analyzed [16]. It is clear that reliability analysis of wind turbines can be conducted at different levels, for various components, and on certain failure modes. As a result, when analyzing or discussing wind turbine reliability, it is beneficial to specify as many of the details as possible.

The stacked bar plot in [Fig. 15.2](#) shows the relative behavior of these common failure types for a large population of wind turbine equipment, i.e. parts or components. Note that there is a possibility of experiencing any of these types of failures at any time in the life cycle of a large population of wind turbine equipment.

15.3 CURRENT STATUS

To accurately evaluate the current status of wind turbine reliability, it is necessary to calculate consistent metrics based on data collected through standardized practices, including analysis and reporting. However, these types of metrics, such as *MTBF*, are typically not easy, if not impossible, to get in the wind industry, especially for relatively older projects. Nevertheless, wind turbine reliability is so critical that there are various benchmarking efforts around the globe. This section gives a brief overview of these efforts, along

TABLE 15.1 Typical Failures Seen in Major Turbine Assemblies

Failure Types	Assemblies			
	Gearboxes	Blades	Pitch Bearings	Generators
Infant	<ul style="list-style-type: none">● Gear mesh● Timing errors● Macrogeometry● Skidding● Abrasion● Adhesion● Foreign object debris/damage● Bearings● Mounting failure● Macrogeometry● Skidding● Abrasion● Adhesion● Thermal runaway● Foreign object debris/damage	<ul style="list-style-type: none">● Composite delamination● Adhesive bond line failure● Mounting error● Transportation and handling● Lightning protection system● Laminate wrinkles	<ul style="list-style-type: none">● Mounting failure● Actuation system failure● Seal failure	<ul style="list-style-type: none">● Insulation failure● High-resistance connection
Premature	<ul style="list-style-type: none">● Gear mesh● Micropitting● Nonconforming inclusions● Grinding temper● Tooth interior fatigue failure● Corrosion● Lubricant degradation● Microgeometry errors	<ul style="list-style-type: none">● Bond line cracks● Leading-edge erosion (accelerated)● Composite delamination● Laminate wrinkles● Blade add-on failures e.g., spoilers, vortex generators● Moisture ingress and icing	<ul style="list-style-type: none">● Raceway fatigue cracks● Cage bunching● Raceway contact ellipse spill● Inadequate lubricant/maintenance● False brinelling● Actuation system failure	<ul style="list-style-type: none">● Wedge failure● Bearing failure● Insulation failure● Dust/debris buildup● Slip-ring failure

	<ul style="list-style-type: none"> ● Bearings <ul style="list-style-type: none"> ● Irregular white etching areas raceways ● Grinding temper raceways and rollers ● Nonconforming inclusions raceways and rollers ● Skidding ● Micropitting ● Cage failure ● Raceway creep ● Shoulder and lip fatigue ● Corrosion ● Lubricant degradation ● Preload errors ● Microgeometry errors 	<ul style="list-style-type: none"> ● Balancing mass rupture ● Lightning protection system 		
Random	<ul style="list-style-type: none"> ● Gear mesh <ul style="list-style-type: none"> ● Characteristic load exceedance ● Material strength exceedance ● Nonconformity from allowable defect rate ● Foreign object debris/damage following routine service ● Nacelle fire ● Bearings <ul style="list-style-type: none"> ● Characteristic load exceedance ● Material strength exceedance ● Foreign object debris/damage following routine service ● Nonconformity from allowable defect rate ● Nacelle fire 	<ul style="list-style-type: none"> ● Characteristic load exceedance ● Material strength exceedance ● Nonconformity from allowable defect rate ● Nacelle fire ● Lightning strike overload ● Pitch bearing failure ● Tower strike 	<ul style="list-style-type: none"> ● Characteristic load exceedance ● Material strength exceedance ● Nonconformity from allowable defect rate ● Nacelle fire ● Actuation system failure 	<ul style="list-style-type: none"> ● Low-voltage, high-current event ● Lightning surge; nacelle fire

(Continued)

TABLE 15.1 (Continued)

Failure Types	Assemblies			
	Gearboxes	Blades	Pitch Bearings	Generators
Wear	<ul style="list-style-type: none">● Gear mesh<ul style="list-style-type: none">● Bending fatigue● Surface fatigue● Bearings<ul style="list-style-type: none">● Subsurface rolling contact fatigue	<ul style="list-style-type: none">● Bond line fatigue failures: edge loading● Root fatigue cracks: flap and edge loading● Leading-edge erosion● Foreign object debris buildup● Composite fatigue failure● Hardware fatigue	<ul style="list-style-type: none">● Raceway rolling contact fatigue● Gear mesh bending fatigue● Gear mesh surface fatigue	<ul style="list-style-type: none">● Insulation fatigue● Bearing failure

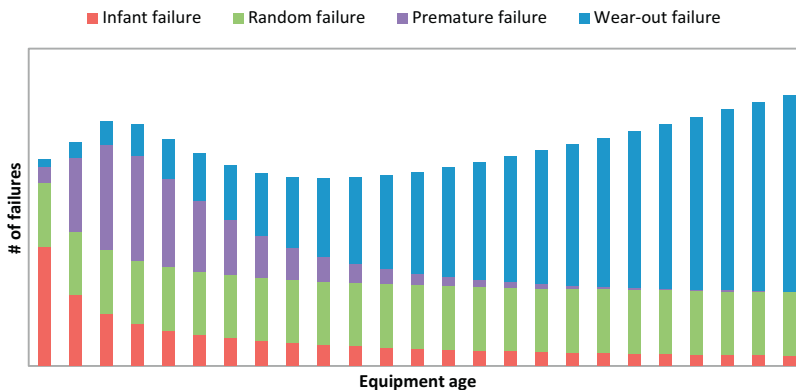


FIGURE 15.2 Common failure types for wind turbine equipment over the project life cycle [19].

with a survey of several recent publications, highlighting where the industry is in terms of turbine reliability.

A detailed survey of reliability data collection and analysis efforts was reported in Ref. [20]. It was observed that most efforts in this area were conducted in Europe, represented by Wissenschaftliches Mess- und Evaluierungsprogramm (WMEP) [21], Landwirtschaftskammer Schleswig-Holstein (LWK) [22], VTT [23], Vindstat [24], WindStats [25], and ReliaWind [26]. WMEP was the earliest among these efforts and started in 1989. Similar efforts in the United States were not started until about 2010, represented by Continuous Reliability Enhancement for Wind (CREW) [27], and a project conducted by Det Norske Veritas-Keuring van Elektrotechnische Materialen te Arnhem (DNV KEMA) and Germanischer Lloyd (GL) Garrard Hassan under the sponsorship of NREL [28]. Another effort from the United States is the gearbox failure database [29], which was started as part of the Gearbox Reliability Collaborative [30] project and focuses on gearbox failure modes and possible root causes. One recent data collection and analysis effort in Europe was formed in 2016 and called Wind energy-Information-Data-Pool (WInD-Pool) [31]. It is clear that there are variations among different reliability data collection and analysis efforts and there is a need for the wind industry to develop and adopt a standardized approach. To correctly understand results reported by different data collection efforts, it is necessary to consider the population of turbines each database recorded, including turbine age, technology, site location, etc.

Based on a majority of the European data collection and reporting efforts discussed earlier, Fig. 15.3 shows the compiled downtime contribution from different subsystems [32]. The top three contributors are the power module, drivetrain module, and rotor module, among which drivetrain and rotor modules are typically more expensive to repair due to the crane costs.

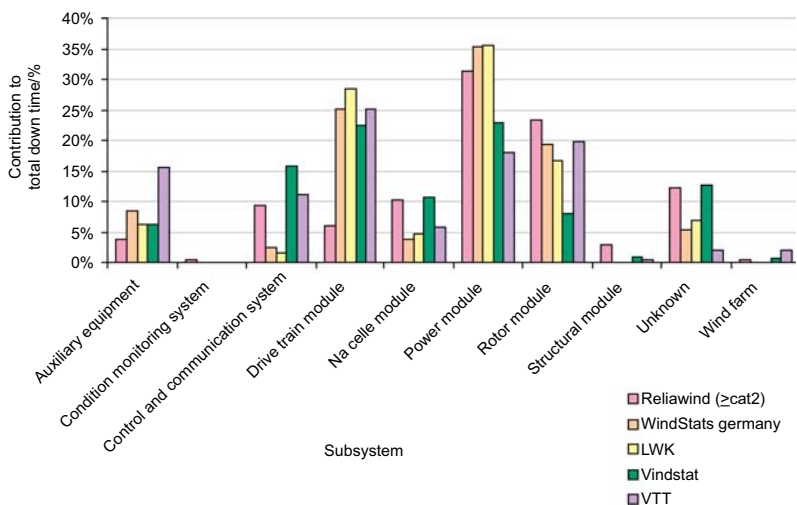


FIGURE 15.3 Downtime contribution from different subsystems based on a few European data collection efforts [32].

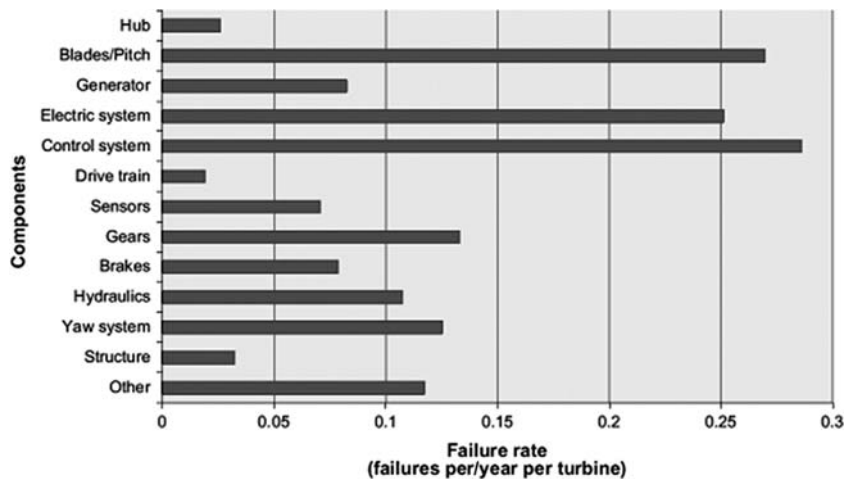


FIGURE 15.4 Average failure rate versus wind turbine components [33].

Fig. 15.4 shows the cumulative failure rate [33] and it can be observed that the control system has the highest failure rate, closely followed by the blades/pitch and electric system. A medium cumulative failure rate group is shown to include the gears, yaw system, hydraulics, brake, generator, sensor, and others. The hubs, drivetrains, and structures all have low failure rates. The study [33] also showed that medium size direct-drive wind turbines have

more frequent electrical and electronic failures but higher availability than geared turbines.

A few observations from the aforementioned efforts in the United States include [20]:

- The 2012 CREW data shows the top four identifiable drivers in terms of the average number of events per turbine were the rotor/blades, electric generator, balance of plant, and controls, and the top four identifiable drivers in terms of the mean downtime per event were the braking system, controls, yaw, and power distribution. The unidentified events caused the longest downtime per event, indicating the need to clarify what it specifically covers to better understand the downtime drivers.
- The data collected by DNV KEMA and GL Garrard Hassan (newly formed DNV GL) shows from 1999 to 2011 the average yearly replacement rates for gearboxes was about 5% and peaked in years 4, 5, and 8. Generators were about 3.5% and peaked in years 6 and 7, and blades were about 2% and peaked in years 1 and 5.
- The gearbox failure data collected in 2013 and 2014 shows that wind turbine gearboxes could fail in drastically different ways. Bearing and gear failures were concentrated in the parallel stages, and the top gearbox failure mode was high-speed or intermediate bearing axial cracks.

For offshore wind turbines, generators and converters were observed to have higher failure rates than land-based turbines [34]. Assuming that the definition of failures is similar in Refs. [33] and [34], the average failure rate for an offshore wind turbine is approximately 10 failures/turbine per year by a wind plant's third operational year, more than five times the land-based failure rate. For offshore wind turbines, the subassemblies/components that fail the most are the pitch/hydraulic system, the "other" component group (i.e., door/hatch, cover, bolts, lightning protection system, and lift), and the generator [34]. Offshore wind turbines show a stronger correlation between rising average failure rates and rising average wind speeds than land-based wind turbines [34].

There are a few conservative observations in terms of current wind turbine reliability status that can be made [2,20]:

- Mature technologies have lower failure rates and new technologies have higher failure rates
- Failure rates of 1–3 failure(s)/turbine per year are common for land-based wind plants
- Failure rates vary with turbine configurations and benefits from direct-drive wind turbines versus geared wind turbines are not yet conclusive
- The power module fails more frequently than other modules, but the drivetrain or rotor module failures typically have higher downtime and costs

- Offshore wind plants require improved reliability due to potential higher failure rates and longer downtime per failure event.

A typical wind plant has tens or hundreds of turbines, thereby generating a huge amount of data continuously. As a result, there are opportunities to make use of information technologies to standardize data collection practices and better harvest data, gaining knowledge so the reliability and availability of wind plants can be improved. One such opportunity is life data analysis based on reliability engineering, which can provide immediate benefits to wind plant O&M if appropriately adopted and practiced. It will be addressed in the next section.

15.4 RELIABILITY ENGINEERING

Reliability engineering is concerned with equipment life cycle management. Life data analysis is one of the most powerful tools in reliability engineering [13]. It provides a forward look based on past and present observations. There are several approaches available for performing life data analysis and this section presents one approach that is well-suited for wind turbine technology. Similar to other properties of the equipment, e.g., rating, ampacity, and height, if appropriate life data are not captured and analyzed, reliability cannot be evaluated, controlled, and improved. To benefit from reliability engineering through life data analysis, the practices typically include three steps: data collection, model development, and failure forecasting. For the analysis, it is helpful to clearly define the reliability relationships among turbine components. As shown in Fig. 15.1, the dependability between a series of major turbine components is illustrated through a system reliability block diagram. It features a representative wind turbine configuration including a gearbox, a generator, three blades, three pitch bearings, and assumes the failures that occurred to these components are independent [12].

15.4.1 Data Collection

Wind turbine equipment records and failure reports can be highly variable, from the level of detail and format to data integrity. Fortunately for wind turbine reliability engineers, there are often several data sources, such as supervisory control and data acquisition (SCADA), inspection reports, and maintenance work orders, that are available to investigate and characterize equipment records for life data analysis. One challenge with the life data analysis is that it may take more than 80% of the effort to collect and validate data. Another challenge is inconsistent definitions of failure events, as they may vary throughout the life cycle of a wind turbine or for different purposes, even within an organization. In addition, there are no mandatory

and standardized practices for reliability data collection to support systematic life analysis.

Analysts should plan to drill down the turbine equipment hierarchy to the lowest actionable element. Developers of wind projects consider the wind turbines and balance-of-plant equipment as the lowest actionable items. Long-term owners and operators of wind projects are interested in the major assemblies and subassemblies in the wind turbines and balance-of-plant subsystems. A manufacturer may consider the raw materials and surface finishes the lowest actionable level to track data.

The data collection begins by evaluating the major failures that are likely to happen during the life cycle of a wind turbine and the repairs that the wind turbine owner is likely to perform. Regardless of the equipment being analyzed, the data requirements for life data analysis can be satisfied with tracking just two fields: age and failure status. In practice, it is helpful to record a minimum of four fields for all equipment:

- Installation date
- Last known operating date
- Status
- Equipment key.

The *installation date* is the first day the equipment enters service. For original equipment, this is the first day generation is reported through the SCADA system or otherwise assumed as the commercial operating date (COD) of the turbine. For replacement equipment, this is the date when the turbine returns to service following a repair. The *last known operating date* is either: (1) the date the equipment was taken offline, or (2) the latest date turbine operation can be verified. For most modern wind turbines, the operating status can be verified in real time, and the *last known operating date* can therefore be updated constantly for equipment in service. Together, the *installation date* and *last known operating date* provide the bounds to measure the component's lifetime *usage*. For developing reliability models as functions of load cycles or other age measures, these two dates are useful to bound queries of a lifetime SCADA database. For convenience, equipment age is often measured with calendar time as it translates well with maintenance planning and risk analyses. The benefit of collecting the *installation date* and the *last known operating date* is the ability to measure lifetimes in several different ways.

The *status* identifies the state of the equipment on the *last known operating date*. Entries for the *status* field identify equipment as either a *failure* event, *F*, or a *suspended* event, *S*. Suspended events, or *suspensions*, are cases when the equipment has not failed by the specific failure mechanism being analyzed. *Suspensions* may be the default *status* when the equipment was commissioned as it is still in service, or may be equipment removed preventively, or otherwise failed by another failure mode than the one being

analyzed. Strict failure logic should be used to categorize the *status* for each equipment record. The *equipment* key links the equipment record with an instance on a wind turbine at a plant. All asset and plant records and properties are related to the equipment through this field.

Failure and repair events are unwelcome by wind plant owners and operators, but reliability engineers normally view them as opportunities to improve knowledge. The reliability engineers need to stay aware of all equipment status changes in the fleet and ensure that the necessary detail is recovered for all failure and repair events as accurately as possible. Some questions and details to consider when recording failure and repair events include:

- *When and how was the failure detected?* A failure is called an event, but it is often a process. Damage can be detected in several ways as it progresses to a failure. Catastrophic failures can be detected by turbine faults or local landowners reporting noticeable problems with surrounding turbines. Progressive failure events may be detected in the same ways earlier in the failure process, and also by routine maintenance, prognostics and health management systems, or during an offline inspection campaign. Recording the failure detection method lets owners evaluate the most popular methods for each failure mode and compare how alternative methods of detection correlate with subsequent repair event costs and production losses. Reliability engineers can analyze *when* and *how* the failure modes are detected to inform owners of the best methods to manage the failure mode risks and mitigate losses.
- *When was the turbine taken offline to replace the failed equipment?* This date is equivalent to the *last known operating date* for the failed equipment. This date can be on, after, or even before the failure detection date. If the offline date is the same as the failure detection date, the equipment was likely run to failure. If the offline date is after the failure detection date, the failing equipment may have been operated and monitored while the replacement was being planned. If the offline date is before the failure detection date, the turbine was most likely taken offline due to some other cause and the component was determined to require replacement.
- *When was the failed equipment replaced?* This is the date when the turbine returns to service following the replacement of the failed equipment. Together, the *offline date* and *replacement date* allow the reliability engineers to measure the total event downtime and production losses.
- *What is the failure mode of the failed equipment?* A failure mode describes how the equipment fails. Wind turbine equipment can fail by many independent and competing failure modes, as illustrated in [Table 15.1](#). Recovering the failure mode detail can require considerable time and resources, but categorizing and grouping events by failure modes allows the reliability engineers to develop the most informative

and specific reliability models. In a system reliability analysis, the reliability engineers develop a specific reliability model for each distinguishable failure mode of the equipment.

- *What type of maintenance was done?* The maintenance type can be either corrective, preventive, or planned preventive. Corrective maintenance is performed on equipment that has functionally failed or is unfit for service. Preventive maintenance is performed to replace equipment on the condition of some other event, with no indication of catastrophic failure on the equipment replaced. For example, when gearbox replacement is determined as necessary for a wind turbine, the main shaft bearing may be replaced at the same time as a preventive maintenance practice. Planned preventive maintenance is recorded when replacements are scheduled or planned based on early detection of the failure process. The maintenance type field helps owners to group and analyze total event downtimes and detection methods.

To facilitate the data collection and subsequent model development and life forecasting, an equipment and an event recording database typically needs to be developed. When developing such a database, it is necessary to consider how the data will be accessed and maintained. It is recommended to use a central repository if planning to perform routine analysis for a large fleet of equipment, as this helps to organize and manage the data entries.

15.4.2 Model Development

Good data collection facilitates efficient model development. But first, it is important to discuss what differentiates the models. Reliability models are functions of time that show the evolution of equipment risk of failures. The reliability models are lifetime distributions that can be expressed in several forms, all of which define the distribution of a continuous random variable lifetime t . These forms include but are not limited to:

- Reliability function $R(t)$
- Unreliability function $Q(t) = 1 - R(t)$
- Probability density function $f(t)$
- Hazard rate function $h(t) = f(t)/R(t)$.

Detailed expression of these forms for some common lifetime distributions are shown in [Table 15.2 \[35\]](#).

The hazard rate function, also known as failure rate in reliability, is perhaps the most popular expression of a lifetime distribution (The hazard function goes by several aliases: in reliability it is also known as the hazard rate or failure rate. In actuarial science, it is known as the force of mortality or force of decrement. In point process and extreme value theory it is known as the rate or intensity function. In vital statistics it is known as the age-specific

TABLE 15.2 Various Forms of Reliability Models for Different Lifetime Distributions

Lifetime Distribution	Parameters	$R(t)$	$f(t)$	$h(t)$	$Q(t)$
Exponential	$\lambda > 0$	$e^{-\lambda t}$	$\lambda e^{-\lambda t}$	λ	$1 - e^{-\lambda t}$
Weibull	$\eta > 0; \beta > 0$	$e^{-\left(\frac{t}{\eta}\right)^\beta}$	$\frac{\beta}{\eta} \left(\frac{t}{\eta}\right)^{\beta-1} e^{-\left(\frac{t}{\eta}\right)^\beta}$	$\frac{\beta}{\eta} \left(\frac{t}{\eta}\right)^{\beta-1}$	$1 - e^{-\left(\frac{t}{\eta}\right)^\beta}$
Gamma	$\lambda > 0; \kappa > 0$	$1 - I(\kappa, \lambda t)$	$\frac{\lambda(\lambda t)^{\kappa-1} e^{-\lambda t}}{\Gamma(\kappa)}$	$\frac{\lambda(\lambda t)^{\kappa-1} e^{-\lambda t}}{\Gamma(\kappa)[1 - I(\kappa, \lambda t)]}$	$I(\kappa, \lambda t)$
Lognormal	$-\infty < \mu' < \infty; \sigma' > 0$	$\int_{\ln(t)}^{\infty} \frac{1}{\sigma' \sqrt{2\pi}} e^{-\frac{1}{2} \left(\frac{x-\mu'}{\sigma'}\right)^2} dx$	$\frac{1}{\sigma' \sqrt{2\pi}} e^{-\frac{1}{2} \left(\frac{t-\mu'}{\sigma'}\right)^2}$	$\frac{f(t)}{R(t)}$	$1 - R(t)$
Log-logistic	$\lambda > 0; \kappa > 0$	$\frac{1}{1 + (\lambda t)^\kappa}$	$\frac{\lambda \kappa (\lambda t)^{\kappa-1}}{[1 + (\lambda t)^\kappa]^2}$	$\frac{\lambda \kappa (\lambda t)^{\kappa-1}}{1 + (\lambda t)^\kappa}$	$1 - \frac{1}{1 + (\lambda t)^\kappa}$

I is the gamma function; I is the incomplete gamma function.

death rate, and in economics its reciprocal is known as Mill's ratio.) due to its intuitive interpretation of the amount of reliability risk associated with a component at time t . The shape of the failure rate function indicates how the equipment ages. An increasing failure rate shows equipment is more likely to fail as time passes. This is common with mechanical items that undergo wear or fatigue. A decreasing failure rate means equipment is less likely to fail as time passes. This can occur with computer software or with some metals that work-harden through use and increase strength with time. Failure rates can follow a bathtub shape wherein equipment reliability improves initially then degrades as time passes. Failure rates can even follow an upside-down bathtub shape. The shape of the failure rate function is useful in determining the appropriate distribution to use when modeling equipment lifetimes. The lifetime distributions can be classified by their modeling capabilities for different behaviors of failure rate functions. Table 15.3 shows the classification of some common lifetime distributions for modeling strictly increasing failure rates, strictly decreasing failure rates, bathtub-shaped failure rates, and upside-down bathtub-shaped failure rates. The classification can be used as a guideline to choose the appropriate life distributions for different types of failure rates when starting the modeling efforts. However, the final distribution that can give the best possible modeling results may only be determined through a systematic evaluation based on the methods to be introduced next.

The reliability engineers rely on their experiences with failure mechanisms and lifetime data to determine the appropriate lifetime distribution(s) for the analysis. Two common methods used to analyze time-to-failure data sets and develop lifetime distributions are *Rank Regression* and *Maximum Likelihood Estimation (MLE)*. In short, rank regression solutions find the distribution that minimizes the error between observed values and expected values of unreliability, whereas MLE solutions find the distribution that is

TABLE 15.3 Classification of Lifetime Distributions

Lifetime Distribution	Increasing Failure Rate	Decreasing Failure Rate	Bathtub-Shaped Failure Rate	Upside-Down Bathtub-Shaped Failure Rate
Exponential	Yes	Yes	No	No
Weibull	Yes $\beta \geq 1$	Yes $\beta \leq 1$	No	No
Gamma	Yes $\kappa \geq 1$	Yes $\kappa \leq 1$	No	No
Lognormal	No	No	No	Yes
Log-logistic	No	Yes $\kappa \leq 1$	No	Yes

TABLE 15.4 Common Methods Used to Analyze Lifetime Data

Maximum Likelihood Estimation	Rank Regression
Find the distribution most likely to produce the historical data	Find the distribution resulting in the shortest distance between the expected values and the observed values
Estimate parameters independent of any ranking of failure time	Requires rank estimates of each failure time
Considers all equipment in the estimation of parameters; not just failures	Based on total sample size and failure order number
Best with censored data	Best with complete data

most likely to reproduce the historical data set. Both methods develop parametric lifetime distributions that handle a random continuous variable lifetime. These two methods are compared in [Table 15.4](#) and the selection of the method is based on the properties of the data set. MLE is the preferred method to develop lifetime distributions when analyzing the *censored* data (Wind turbine equipment lifetime data are often incomplete with *censored* observations. A *censored* observation occurs when only a bound is known on the time to failure. *Censoring* is seen frequently with lifetime data because it is impractical to observe all of the equipment failures.) for wind turbine equipment [\[35\]](#).

Development of the reliability model using the MLE method begins with an assumed distribution that could fit the data set representing reliability for one turbine subsystem or component at either a plant or a fleet level. This initial distribution may be determined based on prior knowledge of the failure mechanism and equipment lifetimes, e.g., by following recommendations given in [Table 15.3](#). Often prior knowledge is missing and this initial assumption is left up to the reliability engineers. Still, reliability software can make this initial guess programmatically without inputs from the analysts and this initial guess typically has little impact on the final results. The initial distribution is used to evaluate the likelihood that the historical events in the data set would occur if the distribution truly characterized the equipment lifetimes. The measure commonly used to characterize the distribution with the data set is called the *log-likelihood* value. A *log-likelihood* value is calculated based on the equipment record *status* and *age* and the assumed distribution. For *failure* records the log-likelihood value, L_F is calculated by:

$$L_F = \ln f(t) \quad (15.3)$$

and for *censored* data records (i.e., *suspensions*) the log-likelihood value, L_S is:

$$L_S = \ln R(t) \quad (15.4)$$

Log-likelihood values are calculated for all *failure* and *suspension* records in the data set and these values are summed to show the total log-likelihood value, L , as:

$$L = \sum L_F + \sum L_S \quad (15.5)$$

The reliability engineers then iterate on the distribution and calculate a new log-likelihood value for each record. The sum of the log-likelihood values for the new distribution is compared with the sum from the initial distribution. The distribution with the *maximum log-likelihood* value is ranked best for the data set. More and more iterations are made by the analysts with the goal to find the distribution that maximizes the log-likelihood value for the data set. Typically, this iterative process is aided with computer software evaluating thousands, or even millions, of potential distributions for the data set. The results from the MLE method are a lifetime distribution that can serve to estimate equipment lifetimes and fully describe the reliability of the equipment throughout its life cycle.

15.4.3 Forecasting

Data collection and equipment lifetime estimates alone can inform many decisions wind plant owners need to make. But, decision-makers rely on reliability engineers to understand how the equipment reliability impacts their assets. Forecasting is the primary reason to perform life data analysis and this section discusses an approach to apply the data collection and model development efforts for performing these failure forecasts.

Recall that the probability of failure for mechanical equipment is typically a continuous value starting from 0 and increasing monotonically to 1 over time. If we know that some equipment has operated for some period of time, t_0 , and has not failed [status = S], the *probability of failure* over some additional operating time, t , is still a continuous value starting from zero at age t_0 that increases to one as t approaches infinite. This value is known as the *conditional probability of failure* and is what wind turbine reliability engineers use to forecast failures. Often the *conditional probability of failure* is found easier by solving for the *conditional reliability* and then taking the mathematical (The term in brackets [] is known as the *conditional reliability*) complement:

$$Q(t_0 + t|t_0) = 1 - \left[\frac{R(t_0 + t)}{R(t_0)} \right] \quad (15.6)$$

where $Q(t_0 + t|t_0)$ is the *conditional probability of failure* for some additional service time, t , provided the equipment has operated without failure for time,

t_0 , and $R()$ is the *reliability function*. For a population of similar equipment at a wind project, the total number of equipment failures in a period of time is equal to the sum of the *conditional probabilities of failure* for all equipment during that time such that:

$$n(t) = \sum_{i=1}^U Q_i(t_0 + t|t_0) \quad (15.7)$$

where $n(t)$ is the *total number of failures* expected during some additional time, t , for a population of U total equipment and Q_i is the *conditional probability of failure* for each i th instance of equipment in the at-risk population. Equipment is *at risk* if it did not fail at t_0 and is expected to be operating during the time, t .

At a very high level, the top business decisions involve values of just two types: time and currency. Regardless of the units used in the failure forecast, all forecast results should be presented with respect to calendar time or the asset life cycle cost.

When a reliability engineer performs a failure forecast based on *causal measures* other than calendar time, such as total production or load cycles, the reliability engineer must forecast the duty cycle of the *causal metric* with respect to calendar time before presenting the failure forecast. This approach adds complexity and uncertainty to the failure forecast but it also offers higher fidelity and sensitivity for modeling application stress profiles, consistent with the diurnal and seasonal variability common to wind projects.

15.5 CASE STUDIES

To demonstrate the reliability engineering life data analysis method discussed in [Section 15.4](#), two case studies are presented in this section: one on gearbox spares planning and the other on pitch bearing maintenance scheduling.

15.5.1 Gearbox Spares Planning

An example wind project with 10 turbines has an inventory with one spare gearbox. Its asset manager wants to know if the project will likely need another spare gearbox in the next 2 years. She asks for a forecast showing the expected failures of the gearbox equipment at this project. The reliability engineer plans to provide the failure forecast by computing the *conditional probability of failure* for each gearbox at the project in the next 2 years. First, the data collection effort brings in gearbox equipment records with the *status*, the *age* in calendar days, and other classifying details about the design and application. Review of the data set shows this project has 10 gearboxes of varying ages at risk in the next 2 years. The reliability engineer happens to have access to a larger data set of assets under management and she finds 313 similar instances of gearbox equipment and lifetime records.

The reliability engineer reviews the censored lifetime data from the total 323 gearbox records and identifies a common gearbox failure mode in the records. For each record, she delineates the age and assigns a failure status: F for failure or S for suspension, based on her failure mode criteria. She selects three initial distributions to model the time-to-failure data and decides to use the MLE method to analyze the data. To execute the MLE method, she develops a logic that first evaluates the status of each record and then calculates the log-likelihood value for that record. If the record status is S for *suspension*, she calculates the natural log of the reliability function at the age of the record. Or if the record status is F for *failure*, she calculates the natural log of the probability density function at the age of the record. She then uses software to iterate the parameters for the distributions with a goal to maximize the log-likelihood values. An excerpt of the MLE solutions for the data set is shown in [Table 15.5](#) along with the log-likelihood values calculated for some of the equipment records. Evaluating the maximum log-likelihood values between the three distributions, the reliability engineer chooses the Weibull distribution with a slope of 1.402 and scale parameter of 13 088 days as the best reliability model for the gearbox lifetime data.

Now that the reliability engineer has collected the data and developed the reliability model, she is ready to run the failure forecast. She lists out the current age of the gearboxes at her project as t_0 along with the age of each gearbox in 2 years from now as $t_0 + t$. Note, because the equipment age and reliability model units are in calendar days, the expected future age in 2 years is deterministic, but this is not always the case for other aging metrics (e.g., production forecasts are probabilistic). The failure forecast results for the 10 gearboxes over the next 2 years are shown in [Table 15.6](#) along with informative measures of the current and future reliability for each gearbox.

Finally, the reliability engineer adds the number of failures expected for all gearboxes and compares this sum to the number of gearboxes available in inventory. In this case, the reliability engineer advises the asset manager that the project is expected to suffer less than one gearbox failure from the identified common failure mode in the next 2 years and a gearbox spare is likely not needed.

15.5.2 Pitch Bearing Maintenance Scheduling

At another project, the wind turbines are suffering a fatigue failure of pitch bearings that can result in catastrophic losses if undetected. This project cannot tolerate a catastrophic loss and the asset manager wants to know how often to inspect the pitch bearings to mitigate the risk. The nominal maintenance plan requires an offline inspection of each turbine every 6 months but the failure rate of the pitch bearings at this project suggests more frequent inspections are needed. The reliability engineer plans to use life data analysis and a risk-based inspection approach to find out an appropriate maintenance interval for this project.

TABLE 15.5 Example Spreadsheet Results of MLE Analysis With Three Lifetime Distributions

	Distribution	Weibull	Lognormal	Gamma
	Parameter 1	1.402	1.434	9320
	Parameter 2	13 088	9.583	1.459
Equipment age/days	Failure Status	Log-Likelihood	Log-Likelihood	Log-Likelihood
985	S	-0.027	-0.031	-0.02779
1492	S	-0.048	-0.058	-0.04987
1491	S	-0.048	-0.058	-0.04983
810	F	-10.280	-10.001	-10.2264
1812	S	-0.063	-0.076	-0.06541
1505	F	-10.059	-9.845	-10.0167
⋮	⋮	⋮	⋮	⋮
	Total Log LK	-530.5	-534.7	-531.0

The risk-based inspection approach requires a failure forecasting model and some additional data for calculation of risks. These data includes the cost of inspection, the failure mode detectability, and the planned replacement cost and catastrophic event cost, which the reliability engineer normally gathers or assumes. The “cost” terms here are inclusive of the material and labor costs plus the lost production revenue during the event downtime. The detectability shows the likelihood of detecting failures with the inspection.

The reliability engineer prepares outlooks of two maintenance strategies: the first showing the catastrophic risk of a “do-nothing” run-to-failure strategy and the other showing the risk of a preventive maintenance strategy through offline inspections. The catastrophic risk is the calculated product of the expected failures and the cost of a catastrophic event. The preventive maintenance costs include the sum of the total cost of the inspections, the expected replacement costs when failures are found during inspections, plus the risk of a catastrophic loss from misdetection during offline inspections. Because the project cannot tolerate catastrophic risk, the reliability engineer sets the preventive maintenance costs equal to the catastrophic risk to determine the most appropriate interval for the offline inspections.

The reliability model for the pitch bearing failure at this project is found, using the MLE method, to be a lognormal distribution with a log-mean of 8.12 log days and a log-standard deviation of 0.454 log days. The current age of the pitch bearings at the project is 560 days. The cost of an offline inspection is \$750 and the detectability of the failure with this inspection is 95%. The cost of a planned replacement of the pitch bearing failure is \$325 000 and the cost of a catastrophic event is \$650 000. The reliability engineer evaluates the risk outlooks for the two maintenance strategies as shown in Fig. 15.5 and advises the asset manager that a 36 day inspection interval is equivalent in cost to the run-to-failure strategy and has the highest likelihood for detecting a failure and avoiding a catastrophic loss.

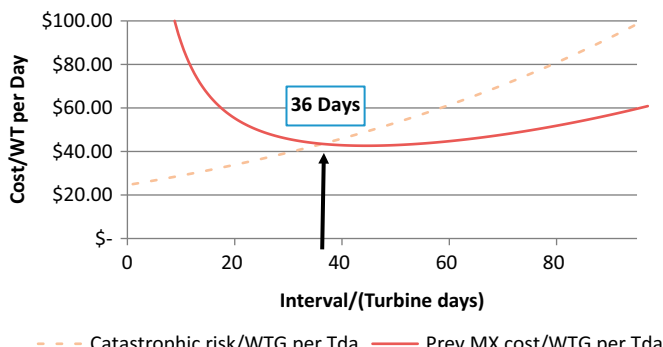


FIGURE 15.5 Pitch bearing maintenance strategies.

15.6 CONCLUSIONS

This chapter briefly discussed fundamentals for wind turbine reliability and the current industry status. Then, the reliability engineering method for life analysis was presented in detail and illustrated through two case studies. An owner and operator's perspective is taken and mechanical components are used to exemplify the potential benefits of reliability engineering analysis to wind plant O&M. It is worth noting that if there were appropriate resources, these analyses can be practiced by the wind industry now to gain tremendous benefits in terms of O&M risks and finance.

Wind turbine reliability is a complex issue. Many components are involved that can fail in vastly different ways, as well as unique operational conditions, long life expectations, and thin economic margins. However, in order to make wind power competitive and successful, the industry has to improve both turbine and plant reliability. This improvement is even more critical for the offshore wind industry. The areas of focus can start with mission-critical and costly assemblies. An immediate beneficial opportunity for the wind industry is through the adoption of reliability engineering life data analysis as discussed in this chapter. To truly address the wind turbine reliability challenge in a systematic and thorough manner as a global industry, all parties along the entire wind turbine supply chain have to come together and share data and knowledge in a fashion beneficial to both the partner and the entire industry. The task is challenging but rewarding.

ACKNOWLEDGMENTS

The contribution from the National Renewable Energy Laboratory to this work was supported by the U.S. Department of Energy under Contract No. DE-AC36-08GO28308. Funding for the work was provided by the DOE Office of Energy Efficiency and Renewable Energy, Wind Energy and Water Power Technologies Office. The support from eDF Renewable Energy is greatly appreciated.

The U.S. Government retains and the publisher, by accepting the article for publication, acknowledges that the U.S. Government retains a nonexclusive, paid-up, irrevocable, worldwide license to publish or reproduce the published form of this work, or to allow others to do so, for U.S. Government purposes.

REFERENCES

- [1] Global Energy Research Council. Global wind report 2015. [Online] <http://www.gwec.net/wp-content/uploads/vip/GWEC-Global-Wind-2015-Report_April_22_04.pdf>.
- [2] Tavner P. Offshore wind turbines reliability availability and maintenance. The Institution of Engineering and Technology, UK; 2012.
- [3] Tavner P. Offshore wind turbine reliability, supergen wind training, Manchester, UK; 2011.
- [4] International Renewable Energy Agency. Renewable energy technologies: cost analysis series, vol. 1, Power Sector, Wind Power, May; 2012.

- [5] Guo Y, Bergua R, van Dam J, Jove J, Campbell J. Improved wind turbine drivetrain designs to minimize the impacts of non-torque loads. *Wind Energy* 2015;18(12):2199–222.
- [6] Guo Y, Keller J, LaCava W. Planetary gear load sharing of wind turbine drivetrains subjected to non-torque loads. *Wind Energy* 2015;18(4):757–68.
- [7] Sheng S. Monitoring of wind turbine gearbox condition through oil and wear debris analysis: a full-scale testing perspective. *Tribol. Trans.* 2016;59(1):149–62.
- [8] Gonzalez D, Wagner PD, Wisniewski R, Lein PJ, MacDiarmid A, Rose D, et al. The impact of “Green” technology on system reliability. Utica, NY: Reliability Information Analysis Center; 2012.
- [9] Andrawus J, Watson J, Kishk M, Adam A. The selection of a suitable maintenance strategy for wind turbines. *Wind Eng.* 2006;30(6):471–86.
- [10] Rademakers et al. Reliability analysis methods for wind turbines, Task 1 of the project: probabilistic safety assessment for wind turbines. [Online] <<ftp://ftp.ecn.nl/pub/www/library/report/1992/c92018.pdf>>.
- [11] Safie F. Understanding the elements of operational reliability a key for achieving high reliability, presented at trilateral safety and mission assurance conference, Cleveland, OH, October 26–28; 2010.
- [12] IEC 61078. Analysis techniques for dependability—reliability block diagram and boolean methods; 2006.
- [13] O'Connor PDT, Kleyner A. Practical reliability engineering. 5th ed. John Wiley & Sons, Ltd; 2012.
- [14] Gintautas T, Sørensen, JD. Integrated system reliability analysis. [Online] <http://www.innwind.eu/-/media/Sites/innwind/Publications/Deliverables/D1_34_REPORT_revised_2015.ashx?la=da>.
- [15] Winterstein SR, Veers P. SAND94-2459. A numerical analysis of the fatigue and reliability of wind turbine components. Albuquerque, New Mexico: Sandia National Laboratories; 2000.
- [16] Kostandyan EE. Reliability modeling of wind turbines: exemplified by power converter systems as basis for O&M planning. Ph.D. Thesis. Alborg University; 2013.
- [17] Schenkelberg F. Replace after MTTF time to avoid failures—Right? [Online] <<http://nomtbf.com/2016/09/replace-mttf-time-avoid-failures-right>>.
- [18] Mone C, Smith A, Maples B, Hand M. Cost of wind energy review. Golden, NREL; 2015 [Online] <<http://www.nrel.gov/docs/fy15osti/63267.pdf>>.
- [19] O'Connor Ryan. Approach to quantify the inherent reliability of a wind turbine system. AWEA Windpower; 2014.
- [20] Sheng S. Report on wind turbine subsystem reliability—a survey of various databases. Golden, NREL; 2013 [Online] <<http://www.nrel.gov/docs/fy13osti/59111.pdf>>.
- [21] Tavner P, Spinato F, van Bussel GJW, Koutoulakos E. Reliability of different wind turbine concepts with relevance to offshore application, presented at the European wind energy conference, March 31–April 3, Brussels, Belgium; 2008.
- [22] Pettersson L, Andersson J-O, Orbert C, Skagerman S. RAMS-database for wind turbines—pre-study, Elforsk Report 10:67; 2010.
- [23] Wind energy statistics in Finland. [Online] <<http://www.vtt.fi/proj/windenergystatistics/?lang=en>>.
- [24] Carlsson F, Eriksson E, Dahlberg M. Damage preventing measures for wind turbines—phase 1 reliability data, Elforsk Report 10:68; 2010.
- [25] Windstats Newsletter, vols. 16–25, Q1; 2003–Q4; 2012.

- [26] Wilkinson M, Hendriks B. Report on wind turbine reliability profiles, ReliaWind deliverable D. 1. 3; 2011.
- [27] Peters V, Ogilvie A, Bond C. CREW database: wind plant reliability benchmark, SAND2012-7328; 2012.
- [28] Lantz E. Operations expenditures: historical trends and continuing challenges, presented at AWEA wind power conference, May 5–8, Chicago, IL, NREL/PR-6A20-58606; 2013.
- [29] Sheng S. Gearbox reliability database: yesterday, today and tomorrow. Wind turbine tribology seminar, Chicago, IL. [Online] <<http://www.nrel.gov/docs/fy15osti/63106.pdf>>; 2014.
- [30] Link H, LaCava W, van Dam J, McNiff B, Sheng S, Wallen R, et al. Gearbox reliability collaborative project report: findings from phase 1 and phase 2 testing. [Online] <<http://www.nrel.gov/docs/fy11osti/51885.pdf>>; 2011.
- [31] <http://windmonitor.iwes.fraunhofer.de/windmonitor_en/6_Projekte/7_wind-pool/>.
- [32] Lange M, Wilkinson M, van Delft T. Wind turbine reliability analysis. Presented at the 10th German wind energy conference, November 17–18, Bremen, Germany; 2010.
- [33] Pinar Pérez JM, García Márquez FP, Tobias A, Papaelias M. Wind turbine reliability analysis. Renew. Sustain. Energy Rev. 2013;23:463–72.
- [34] Carroll J, McDonald A, McMillan D. Failure rate, repair time and unscheduled O&M cost analysis of offshore wind turbines. Wind Energy 2016;19(6):1107–19.
- [35] Leenmis, Lawrence M. Reliability probabilistic models and statistical methods, 2nd ed.; 2009.

This page intentionally left blank

Chapter 16

Practical Method to Estimate Foundation Stiffness for Design of Offshore Wind Turbines

Saleh Jalbi, Masoud Shadlou, and Subhamoy Bhattacharya

University of Surrey, Guildford, United Kingdom

Email: S.Bhattacharya@surrey.ac.uk

16.1 INTRODUCTION

Fig. 16.1 shows a typical itemized cost of different components of an offshore wind farm and it is clear that the foundation is one of the most expensive item covering almost 34% of the overall cost. One of the main reasons of this high cost is the uncertainty associated with long-term loading conditions, ground profile, and lack of track record of performance on these structures. Research is currently under way to reduce the cost of foundations thereby reducing LCOE (levelized cost of energy). The principle aim of a foundation is to transfer all the loads from the wind turbine structure to the ground safely and within the allowable deformations. Guided by limit state design philosophy, the design considerations are to satisfy the following:

1. *Ultimate limit state (ULS)*: This is to ensure that the maximum loads on the foundations are much lower than the capacity of the chosen foundation. This calculation is dependent on the strength of the soil.
2. *Target natural frequency (Eigen frequency) and SLS*: This requires the prediction of the natural frequency of the whole system (Eigen frequency) and the deformation of the foundation at the mudline level. As natural frequency is concerned with very small amplitude vibrations, linear Eigen value analysis will suffice. The deformation of the foundation will be small and prediction of initial foundation stiffness would suffice for this purpose. This requires determination of stiffness of the foundation.
3. *Fatigue limit state (FLS) and long-term deformation*: This would require predicting the fatigue life of the monopile as well as the effects of long-term cyclic loading on the foundation. Again this step requires stiffness of the foundation.

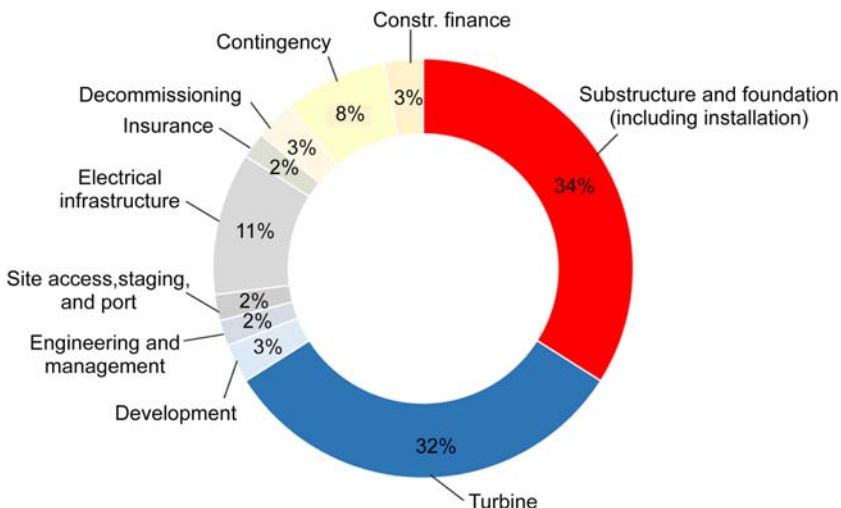


FIGURE 16.1 Cost of different components of a typical offshore wind farm.

4. *Robustness and ease of installation:* This step will ascertain that the foundation can be installed and that there is adequate redundancy in the system.

Design of foundation is an iterative process and Fig. 16.2 shows a flowchart for design of monopiles suggested by Arany et al. [1]. It is clear from the flowchart that foundation stiffness plays a key role in the design. This chapter therefore focuses on the different methods of estimating the foundation stiffness and this is one of the critical parameter for design.

Fig. 16.3 shows a mathematical model where the foundation is replaced by a set of springs: K_V (vertical stiffness), K_L (Lateral stiffness) K_R (Rocking stiffness), and K_{LR} (cross-coupling). The input required to obtain K_L , K_R , and K_{LR} are: (1) pile dimensions; (2) ground profile, i.e., soil stiffness along the length of the pile. In this context, it must be mentioned that the foundation stiffness is required for two calculations: Deformation (deflection ρ and rotation θ at mudline) and natural frequency estimation.

Few points may be noted regarding these springs:

1. The properties and shape of the springs (load–deformation characteristics, i.e., lateral load–deflection or moment–rotation) should be such that the deformation is acceptable under the working load scenarios expected in the lifetime of the turbine. Further details of shape of these springs associated with stress–strain of the supporting soil can be found in Bouzid et al. [2].
2. The values of the springs (stiffness of the foundation) are necessary to compute the natural period of the structure using linear Eigen value

Simplified design procedure of offshore wind turbine monopiles

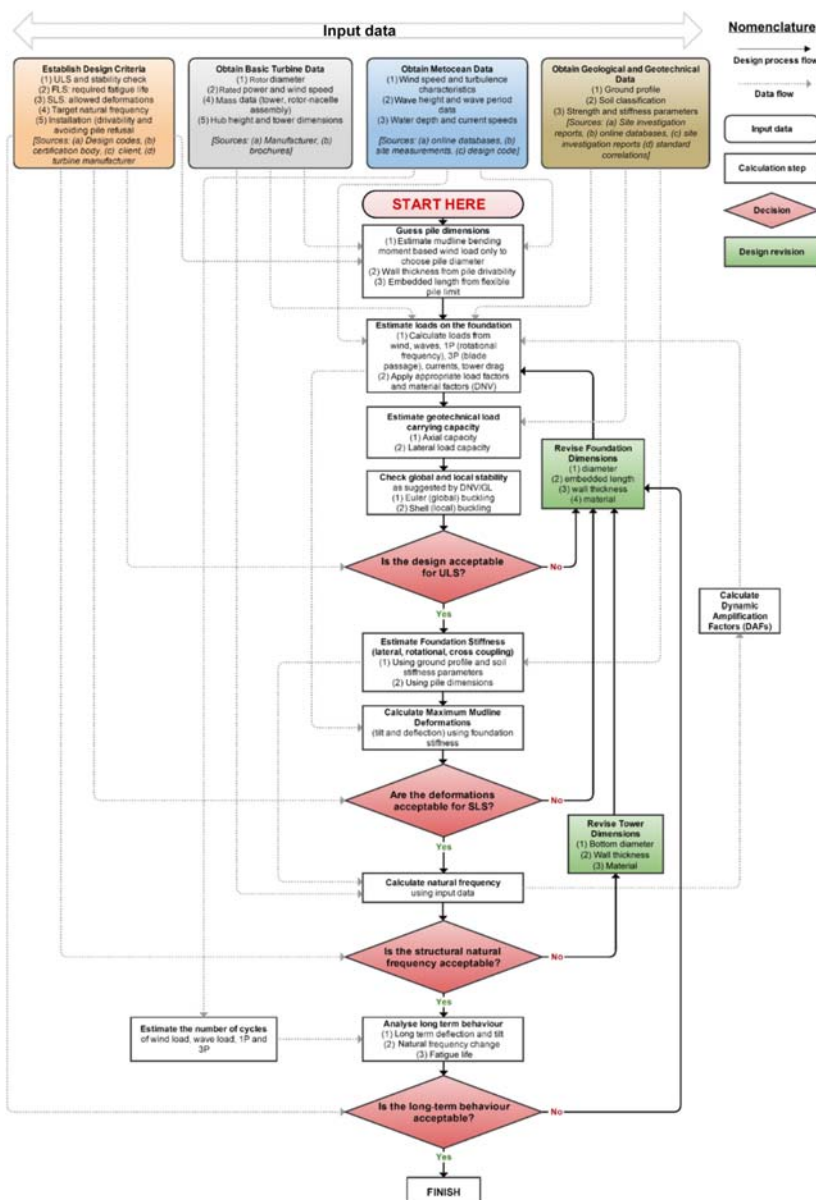


FIGURE 16.2 Flowchart of the design process for monopole.

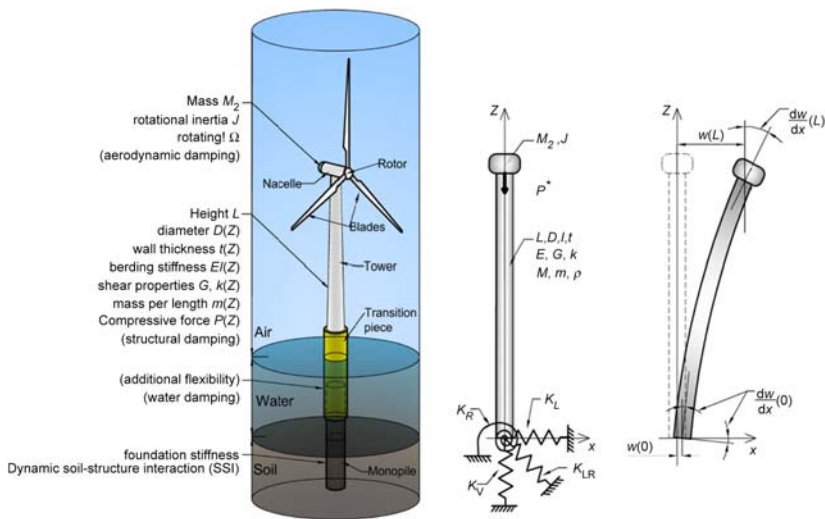


FIGURE 16.3 Mathematical model and importance of foundation stiffness.

analysis. Further details on the analysis required can be found by Adhikari and Bhattacharya [3]; Adhikari and Bhattacharya [4]; Arany et al. [5]; and Arany et al. [6].

The values of the springs will also dictate the overall dynamic stability of the system due to its nonlinear nature. It must be mentioned that these springs are not only frequency dependent but also change with cycles of loading due to dynamic soil–structure interaction. Further details on the dynamic interaction can be found by Bhattacharya et al. [7]; Bhattacharya et al. [8]; Bhattacharya [9]; Lombardi et al. [10]; Zania [11]; and Damgaard et al. [12].

16.2 METHODS TO ESTIMATE FOUNDATION STIFFNESS

In this section three methods are discussed:

1. *Simplified method:* Closed-form solutions for foundation stiffness can be obtained for simple ground profiles, see Fig. 16.4. Any spreadsheet programs or even a simple calculator can be used to compute them and typically time take is only few minutes. This method can be useful in the preliminary design and during the optimization stage or even financial feasibility study. In this context it must be remembered that foundation constitutes 34% of the overall cost.
2. *Standard method:* This is one of the most common methods used in industry, see Fig. 16.5. Foundation–soil interaction is represented by a set of discrete Winkler springs where the spring stiffness is obtained

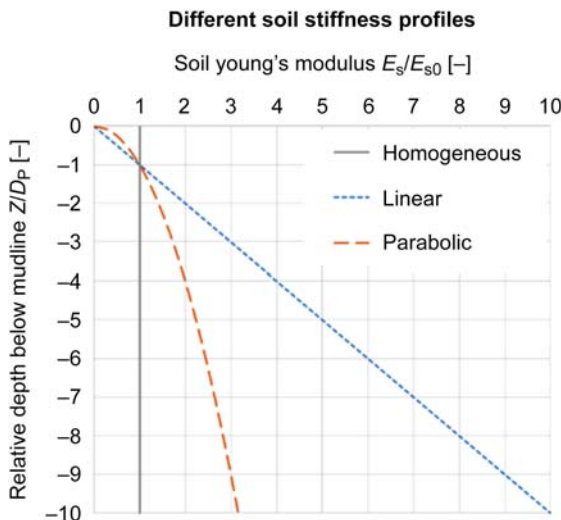


FIGURE 16.4 Homogeneous, linear, and parabolic soil stiffness profiles.

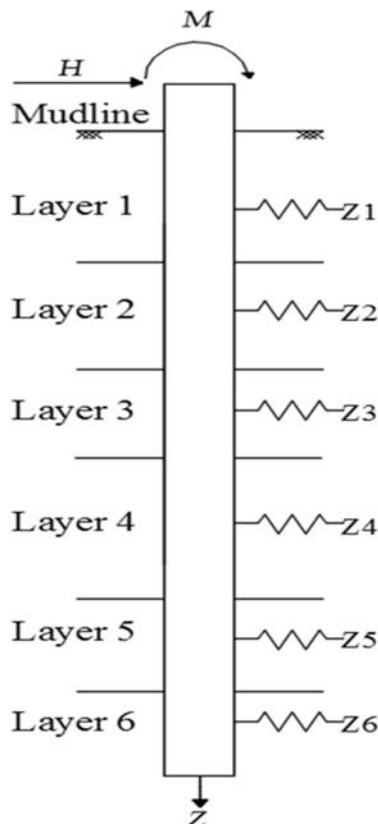


FIGURE 16.5 Monopile supported on discrete Winkler springs.

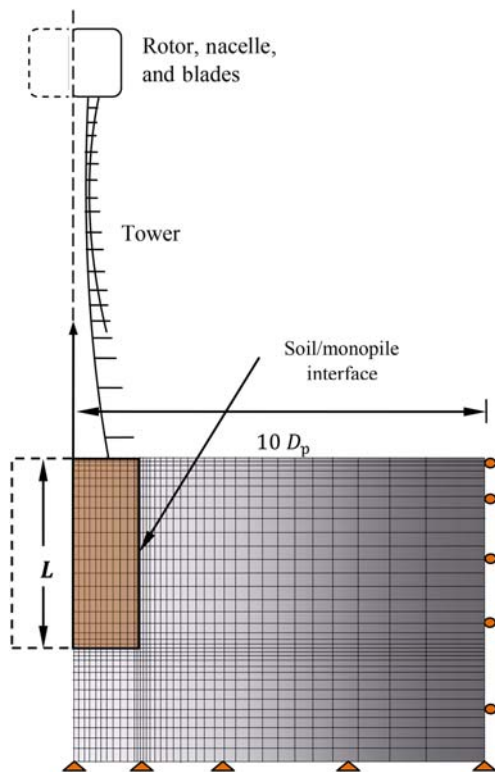


FIGURE 16.6 Finite element method.

through $p-y$ curves which are provided in different design standards. Standard software are available at reasonable costs to carry the analysis and will only take few hours to carry out an analysis. *Complex ground soil profiles can be analyzed for standard soils, i.e., sand and clay.* Few soil parameters are required and the effects of cyclic load are taken empirically.

3. *Advanced methods:* These are continuum models (Fig. 16.6) and advanced 3D finite element software packages or programs are necessary. Such packages are expensive, computationally demanding, and require experienced engineer to run the simulations. These models are *versatile and can model complex ground profile and any type of soils.* Cyclic loading can also be applied.

16.2.1 Simplified Method (Closed-Form Solutions)

Closed-form solutions have been proposed by Shadlou and Bhattacharya [13]. Values of K_L , K_R , and K_{LR} are summarized in Tables 16.1 and 16.2 for

TABLE 16.1 Formulas for Stiffness of Monopiles Exhibiting Rigid Behavior

Ground Profile (See Fig. 16.4)	K_L	K_{LR}	K_R
Homogeneous	$3.2 \left(\frac{L}{D_p} \right)^{0.62} f_{(vs)} E_{SO} D_p$	$-1.8 \left(\frac{L}{D_p} \right)^{1.56} f_{(vs)} E_{SO} D_p^2$	$1.65 \left(\frac{L}{D_p} \right)^{2.5} f_{(vs)} E_{SO} D_p^3$
Parabolic	$2.65 \left(\frac{L}{D_p} \right)^{1.07} f_{(vs)} E_{SO} D_p$	$-1.8 \left(\frac{L}{D_p} \right)^2 f_{(vs)} E_{SO} D_p^2$	$1.63 \left(\frac{L}{D_p} \right)^3 f_{(vs)} E_{SO} D_p^3$
Linear	$2.35 \left(\frac{L}{D_p} \right)^{1.53} f_{(vs)} E_{SO} D_p$	$-1.8 \left(\frac{L}{D_p} \right)^{2.5} f_{(vs)} E_{SO} D_p^2$	$1.59 \left(\frac{L}{D_p} \right)^{3.45} f_{(vs)} E_{SO} D_p^3$

* $f_{(vs)} = 1 + 0.6|v_s - 0.25|$

TABLE 16.2 Tables for Monopiles Exhibiting Flexible Behavior

Ground Profile (See Fig. 16.4)	K_L	K_{LR}	K_R
Homogeneous	$1.45 \left(\frac{E_p}{E_{SO}} \right)^{0.186} f_{(vs)} E_{SO} D_p$	$-0.3 \left(\frac{E_p}{E_{SO}} \right)^{0.5} f_{(vs)} E_{SO} D_p^2$	$0.19 \left(\frac{E_p}{E_{SO}} \right)^{0.73} f_{(vs)} E_{SO} D_p^3$
Parabolic	$1.015 \left(\frac{E_p}{E_{SO}} \right)^{0.27} f_{(vs)} E_{SO} D_p$	$-0.29 \left(\frac{E_p}{E_{SO}} \right)^{0.52} f_{(vs)} E_{SO} D_p^2$	$0.18 \left(\frac{E_p}{E_{SO}} \right)^{0.76} f_{(vs)} E_{SO} D_p^3$
Linear	$0.79 \left(\frac{E_p}{E_{SO}} \right)^{0.34} f_{(vs)} E_{SO} D_p$	$-0.27 \left(\frac{E_p}{E_{SO}} \right)^{0.567} f_{(vs)} E_{SO} D_p^2$	$0.17 \left(\frac{E_p}{E_{SO}} \right)^{0.78} f_{(vs)} E_{SO} D_p^3$

* $f_{(vs)} = 1 + 0.6|v_s - 0.25|$

rigid and flexible piles for three types of ground profile: homogenous, linear, and parabolic, see Fig. 16.4. Homogeneous soils are soils which have a constant stiffness with depth such as over-consolidated clays. On the other hand, a linear profile is typical for normally consolidated clays and parabolic behavior can be used for sandy soils. It may be observed from Table 16.1 that the stiffness term is a function of the aspect ratio (L/D_p) of the pile and soil stiffness (E_{S0}) and this is a characteristic of rigid behavior. Table 16.2 is a function of relative pile–soil stiffness (E_p/E_s). Further details of classification of rigid and flexible piles in relation to monopile application can be found by Shadlou and Bhattacharya [13].

16.2.2 Standard Method

Traditionally in the offshore industry, a nonlinear p – y method is employed to find out pile head deformations (deflection and rotation) and foundation stiffness. The approach can be found in API [14] and also suggested in DNV [15]. Originally it was developed by Matlock [16]; Reese et al. [17]; O’Neill and Murchinson [18], and the basis of this methodology is the Winkler approach [2] whereby the soil is modeled as independent springs along the length of the pile, see Fig. 16.5. The p – y approach uses nonlinear springs and produces reliable results for cases in which it was developed, i.e., small diameter piles and for few cycles of loading. The method is not validated for large diameter piles, in fact, using this method, underprediction of foundation stiffness has been reported by Kallehave and Thilsted [19], who also proposed an updated p – y formulation. Many researchers have recently worked on developing design methodologies for the large diameter more stocky monopiles with length to diameter ratios typically in the range between 4 and 10.

16.2.3 Advanced Method

In this method, soil–structure interaction is carried out using 2D and 3D FEA (finite element analysis) and different sophisticated soils models can be used. This requires advanced soil testing to feed the soil parameters. It is important to note that such models usually require not only knowledge but also expertise and experience. It is not advisable to use this method during the preliminary and optimization stages due to the high cost and the time required for calculation. This method best serves as a final check to a few optimized cases as results obtained are usually of high accuracy. Fig. 16.6 shows a typical section through a finite element model with various degrees of freedom showing the soil mass, the pile, the pile–soil interface, and the boundary conditions.

16.3 OBTAINING FOUNDATION STIFFNESS FROM STANDARD AND ADVANCED METHOD

The analysis method presented in Sections 16.2.2 and 16.2.3 are numerical methods and the output from such analysis will be pile head load–deflection and moment–rotation curves. However, following Fig. 16.3, three stiffness terms (K_L , K_R , and K_{LR}) are required to carry out dynamic and SLS calculations. This section of the chapter explains a simple methodology to extract the stiffness terms from the analysis results obtained in Sections 16.2.2 and 16.2.3.

While K_L (lateral stiffness, i.e., force required for unit lateral deflection and the unit is MN m^{-1}) and K_R (rocking stiffness is the moment required for unit rotation and the unit is MNm rad^{-1}) are easy to appreciate and visualize, the cross-coupling term (K_{LR}) is more involved and arises from matrix compliance. Arany et al. [5] showed cross-coupling stiffness (K_{LR}) of the foundation is an important parameter and must be considered for dynamic analysis of monopiles. Gazetas [20] explains the coupling effect in foundations as a consequence of the inertia of the structure and where the foundation center of gravity is above the center of soil reaction pressure. This means as the structure is being displaced laterally, an inertial force arises at the center of gravity and produces a net moment thereby rocking occurs. It is therefore necessary to explain the cross-coupling term (K_{LR}) through a simple cantilever beam example as shown in Fig. 16.7.

Fig. 16.7A shows a cantilever beam subjected to a moment at the free end (M) causing deflection (ρ_1) and rotation (θ_1). On the other hand, Fig. 16.7B shows another cantilever beam where the lateral load (P) at the tip causes deflection (ρ_2) and rotation (θ_2). The expressions for deflection and rotation are given by Eqs. (16.1) and (16.2).

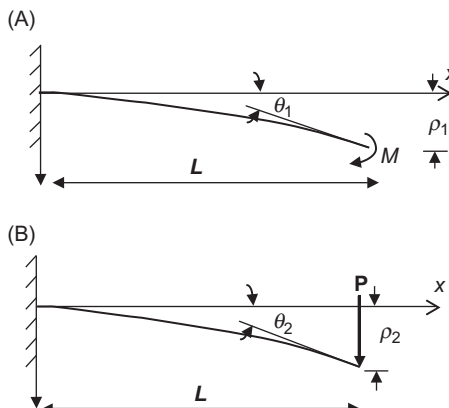


FIGURE 16.7 Explanation of cantilever cross-coupling term. (A) Cantilever beam subjected to a moment; (B) Cantilever beam subjected to a point load.

$$\rho_1 = \frac{ML^2}{3EI} \quad \theta_1 = \frac{ML}{EI} \quad (16.1)$$

For a point load

$$\rho_2 = \frac{PL^3}{3EI} \quad \theta_2 = \frac{PL^2}{2EI} \quad (16.2)$$

It is clear that both the moment and the point load produce a rotation as well as a deflection and in effect the rotation caused by the point load or the deflection caused by the moment is indicative of the cross-coupling stiffness term. By definition, the stiffness is the force/moment required to move the body by a unit displacement/rotation respectively, and thus for this example K_{11} is the stiffness resisting the point load, K_{12} and K_{21} are cross-coupling stiffness, and K_{22} is the stiffness resisting rotation. For “unit” values for P and M , the stiffness terms are given by Eqs. (16.3) and (16.4).

$$K_{11} = \frac{1}{\rho_2} = \frac{1}{\frac{1 \times L^3}{3EI}} = \frac{3EI}{L^3} \quad K_{12} = \frac{1}{\theta_2} = \frac{1}{\frac{1 \times L^2}{2EI}} = \frac{2EI}{L^2} \quad (16.3)$$

$$K_{21} = \frac{1}{\rho_1} = \frac{1}{\frac{1 \times L^2}{2EI}} = \frac{2EI}{L^2} \quad K_{22} = \frac{1}{\theta_1} = \frac{1}{\frac{1 \times L}{EI}} = \frac{EI}{L} \quad (16.4)$$

It may be noted that the cross-coupling stiffnesses K_{12} and K_{21} are equal for the same magnitude of loading. This method can be extended to the results obtained from standard and advanced methods to find the three stiffness terms (K_L , K_{LR} , and K_R). Typically (pile head load)—deflection and (pile head moment)—rotation curves are nonlinear depending on the soil type. However, the linear range of the curves can be used to estimate pile head rotation and deflection based on Eq. (16.5) and one can understand the importance of cross-coupling term.

$$\begin{bmatrix} H \\ M \end{bmatrix} = \begin{bmatrix} K_L & K_{LR} \\ K_{LR} & K_R \end{bmatrix} \begin{bmatrix} \rho \\ \theta \end{bmatrix} \quad (16.5)$$

Eq. (16.5) can be rewritten as Eq. (16.6) through matrix operation where I (impedance matrix) is a 2×2 matrix given by Eq. (16.7).

$$\begin{bmatrix} \rho \\ \theta \end{bmatrix} = [I] \times \begin{bmatrix} H \\ M \end{bmatrix} \quad (16.6)$$

$$I = \begin{bmatrix} I_L & I_{LR} \\ I_{RL} & I_R \end{bmatrix} \quad (16.7)$$

To obtain the stiffness terms, a numerical model (either standard or advanced) could be analyzed for a lateral load (say $H = H_1$) with zero moment ($M = 0$) and obtain values of deflection and rotation (ρ_1 and θ_1). The results can be expressed through Eqs. (16.8) and (16.9).

$$\begin{bmatrix} \rho_1 \\ \theta_1 \end{bmatrix} = \begin{bmatrix} I_L & I_{LR} \\ I_{RL} & I_R \end{bmatrix} \times \begin{bmatrix} H_1 \\ 0 \end{bmatrix} \quad (16.8)$$

$$\rho_1 = H_1 \times I_L \Rightarrow I_L = \frac{\rho_1}{H_1} \quad \theta_1 = H_1 \times I_{RL} \Rightarrow I_{RL} = \frac{\theta_1}{H_1} \quad (16.9)$$

Similarly another numerical analysis can be done for a defined moment ($M = M_1$) and zero lateral load ($H = 0$) results are shown in Eqs. (16.10) and (16.11).

$$\begin{bmatrix} \rho_2 \\ \theta_2 \end{bmatrix} = \begin{bmatrix} I_L & I_{LR} \\ I_{RL} & I_R \end{bmatrix} \times \begin{bmatrix} 0 \\ M_1 \end{bmatrix} \quad (16.10)$$

$$\rho_2 = M_1 \times I_{LR} \Rightarrow I_{LR} = \frac{\rho_2}{M_1} \quad \theta_2 = M_1 \times I_R \Rightarrow I_R = \frac{\theta_2}{M_1} \quad (16.11)$$

From the above analysis (Eqs. (16.8)–(16.11)), terms for the I matrix (Eq. (16.7)) can be obtained. Eq. (16.6) can be rewritten as Eq. (16.12) through matrix operation.

$$[I]^{-1} \times \begin{bmatrix} \rho \\ \theta \end{bmatrix} = \begin{bmatrix} H \\ M \end{bmatrix} \quad (16.12)$$

Comparing Eqs. (16.5) and (16.12), it can be observed that the relation between the stiffness matrix and the inverse of impedance matrix (I) given by Eq. (16.13). Eqs. (16.14) and (16.15) are matrix operations which can be carried out easily to obtain K_L , K_R , and K_{LR} .

$$K = \begin{bmatrix} K_L & K_{LR} \\ K_{RL} & K_R \end{bmatrix} = I^{-1} = \begin{bmatrix} I_L & I_{LR} \\ I_{RL} & I_R \end{bmatrix}^{-1} \quad (16.13)$$

$$K = I^{-1} = \begin{bmatrix} \frac{\rho_1}{H_1} & \frac{\rho_2}{M_2} \\ \frac{\theta_1}{H_1} & \frac{\theta_2}{M_2} \end{bmatrix}^{-1} \quad (16.14)$$

$$K = \frac{1}{\left(\frac{\rho_1}{H_1} \times \frac{\theta_2}{M_2}\right) - \left(\frac{\rho_2}{M_2} \times \frac{\theta_1}{H_1}\right)} \times \begin{bmatrix} \frac{\theta_2}{M_2} & -\frac{\rho_2}{M_2} \\ -\frac{\theta_1}{H_1} & \frac{\rho_1}{H_1} \end{bmatrix} = \begin{bmatrix} K_L & K_{LR} \\ K_{RL} & K_R \end{bmatrix} \quad (16.15)$$

Therefore, mathematically, it is required to run only two cases, i.e., $p-y$ analyses or FEA to obtain the three spring stiffness. It is important to note that the above methodology is only applicable in the linear range and therefore it is advisable to obtain a load-deflection and moment-rotation curve to check the range of linearity. If the analysis is used beyond the linear range, underestimations of deflections and rotations will occur. Also the natural frequency of the whole system will be underestimated.

16.3.1 Example Problem (Monopile for Horns Rev 1)

The case study of Horns Rev 1 is used to show the application of the methodology. Various data on the case study can be found by Augustesen et al. [20]. The monopile foundation supports a 60 m long tower carrying a Vestas V80 2 MW wind turbine. The pile has a diameter of 4.0 m and varying wall thickness (WT in Fig. 16.8). The reported ultimate loads on the pile head were $H = 4.6$ MN and $M = 95$ MN.m. Table 16.3 provides a detailed description of the soil layers which was obtained through an extensive test program including geotechnical borings, cone penetration tests (CPTs), and triaxial tests given by

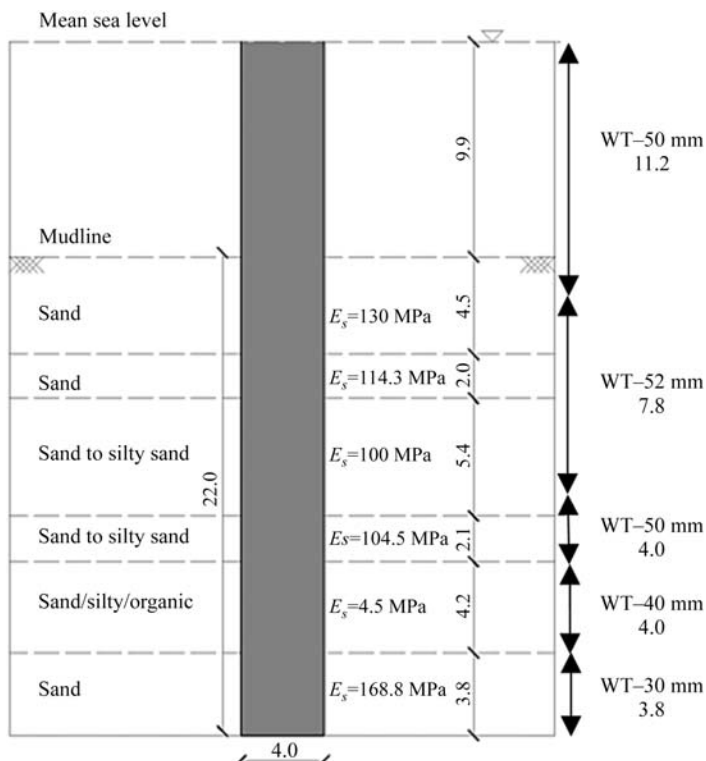


FIGURE 16.8 Pile details.

TABLE 16.3 Soil Properties

Soil Layer	Soil Type	Depth/m	E_s/MPa	$\phi/\text{degrees}$	$\gamma'/(kN \text{ m}^{-3})$
1	Sand	0–4.5	130	45.4	10
2	Sand	4.5–6.5	114.3	40.7	10
3	Sand to silty sand	6.5–11.9	100	38	10
4	Sand to silty sand	11.9–14.0	104.5	36.6	10
5	Sand/silt/organic	14.0–18.2	4.5	27	7
6	Sand	18.2→	168.8	38.7	10

Augustensen et al. [21]. ALP (Oasys) has been used for the $p-y$ analysis of the monopile which can compute deflections, rotations, and bending moments along the pile. Several other software packages such as PYGM and LPILE are available for this type of analysis, or can be solved numerically through a MATLAB program. In this study, $p-y$ curves along different depths are modeled in two ways: (1) elastic–plastic springs by taking the soil properties given in Table 16.3; (2) API recommended $p-y$ springs.

The API code provides the following formulations for sandy soils:

$$p = Ap_u \tanh\left(\frac{kz}{Ap_u}y\right) \quad (16.16)$$

where A is a factor that depends on the type of loading and p_u depends on the depth and angle of internal friction ϕ' .

However for the elastic–plastic model used in the study, the following equations were used to construct the $p-y$ curves.

$$p = ky \quad k = (E_s h) \quad (16.17)$$

where h is the midpoint of the elements immediately above and below the spring under consideration.

The plastic phase of the curve is given by:

$$F_p = (K_q \sigma'_v + c K_c) h D_p \quad (16.18)$$

where K_q and K_c are factors that depend on depth and ϕ' [22].

Fig. 16.9 shows the results obtained from the analysis.

It is evident from the Fig. 16.9 that the ULS loads lie within the linear range which means the deflections and rotations arising from such forces can be estimated using K_L , K_R , and K_{LR} . Table 16.4 summarizes the results for the analysis where two load cases have been applied ($H = 0.2 \text{ MN}$ and

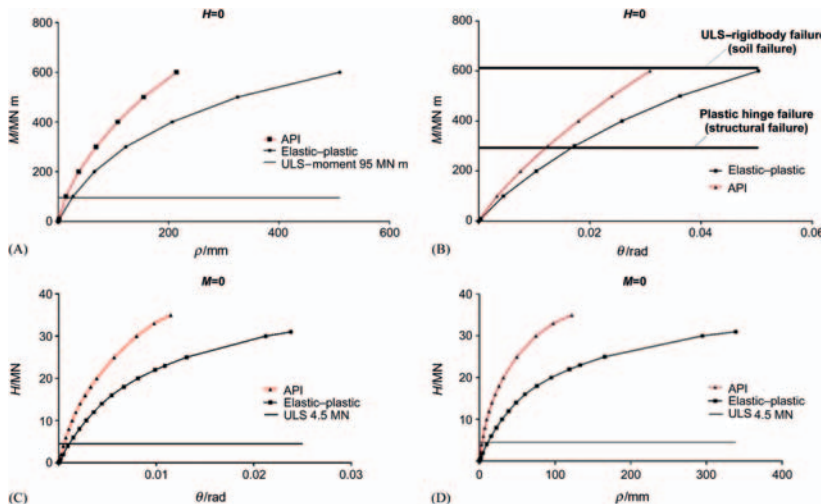


FIGURE 16.9 (A) Moment–deflection; (B) moment–rotation; (C) lateral load–rotation; and (D) lateral load–deflection curves.

$M = 0$), and ($H = 0$ and $M = 0.2 \text{ MN m}$) where the major steps are also shown. It may also be noted that Fig. 16.9B plots the ultimate capacity of the pile based on two considerations: (1) soil fails and the pile fails as rigid body failure and (2) pile fails by forming plastic hinge.

Using Eq. (16.13) and applying to the results obtained and shown in Table 16.4, stiffness terms as predicted by elastic–plastic model is given in Eq. (16.19).

Elastic–plastic formulation

$$I = \begin{bmatrix} 0.00215 & 0.00021 \\ 0.00021 & 0.000042 \end{bmatrix} \Rightarrow I^{-1} = K = \begin{bmatrix} K_L & K_{LR} \\ K_{RL} & K_R \end{bmatrix} = \begin{bmatrix} 894.1 & -4451.3 \\ -4451.3 & 46252.1 \end{bmatrix}$$

$$K_L = 894.1 \frac{\text{MN}}{\text{m}} \quad K_{LR} = -4451.3 \text{ MN} \quad K_R = 46252.1 \frac{\text{MN m}}{\text{rad}}$$

(16.19)

The same approach has been used for the API model and the results are shown in Eq. (16.20).

API formulation

$$I = \begin{bmatrix} 0.00075 & 0.00011 \\ 0.00011 & 0.00003 \end{bmatrix} \Rightarrow I^{-1} = K = \begin{bmatrix} K_L & K_{LR} \\ K_{RL} & K_R \end{bmatrix} = \begin{bmatrix} 3102 & -11823.7 \\ -11823.7 & 78275.5 \end{bmatrix}$$

$$K_L = 3102 \frac{\text{MN}}{\text{m}} \quad K_{LR} = -11823.7 \text{ MN} \quad K_R = 78275.5 \frac{\text{MN m}}{\text{rad}}$$

(16.20)

TABLE 16.4 Results from Analysis and Computation of I Matrix

It may be noted that the stiffness terms are quite different in the two formulations given in [Eqs. \(16.19\)](#) and [\(16.20\)](#). This is because the API formulation is empirical and is calibrated against small diameter piles and the extrapolation to large diameter piles is not validated or verified.

Finite element software package PLAXIS 3D was also used to evaluate the deflection and rotation due to the pile head loads. To save computational efforts space, half the pile was modeled ([Figs. 16.10](#) and [16.11](#)). A classical Mohr–Coulomb material model was set for the soil with the same stiffness and strength properties provided in [Table 16.3](#). For the pile material, elastic perfectly plastic model was used. Ten node tetrahedral elements were assigned to the soil volume and six node triangular plate elements were used for the pile. The interface between the soil and the pile was modeled with double noded elements. The soil extents were set as $20D_p$, and a medium fine mesh was used. The pile was extended by 21 m above the ground to simulate the effect of the applied moment. Similar plots such as that shown in [Fig. 16.9](#) were obtained. [Fig. 16.12](#) plots the deflection along the length of the pile obtained for $H = 4.6$ MN and $M = 95$ MN m.

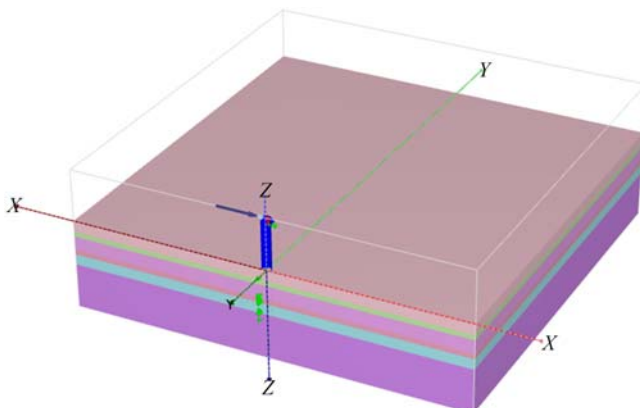


FIGURE 16.10 Geometry used in PLAXIS model.

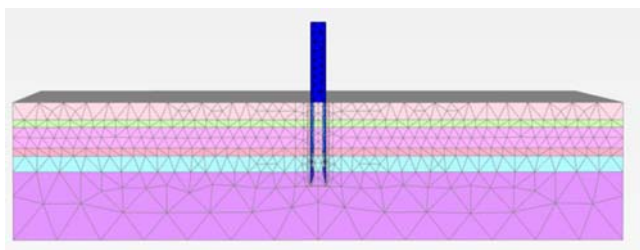


FIGURE 16.11 Mesh used in PLAXIS model.

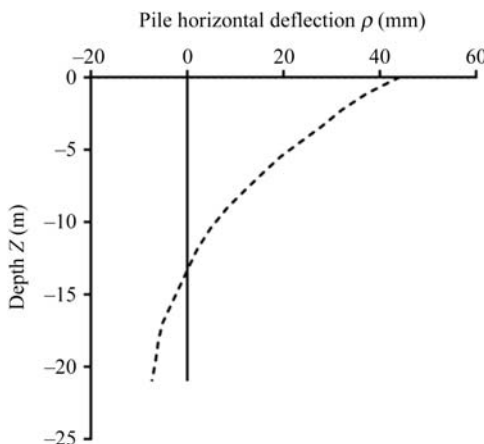


FIGURE 16.12 Plots the deflection of the pile obtained from the PLAXIS analysis for pile head loads of $H = 4.6 \text{ MN}$ and $M = 95 \text{ MN m}$.

16.4 DISCUSSION AND APPLICATION OF FOUNDATION STIFFNESS

Fig. 16.13 schematically shows the essence of the matrix operations presented in the earlier section. Essentially, the foundation is replaced by a set of springs which are obtained from lateral load/moment analysis of piles. This is quite similar to substructure method.

16.4.1 Pile Head Deflections and Rotations

Eq. (16.5) can be used to predict pile head deflections and rotations as shown in Eq. (16.21). It may be noted from Fig. 16.9 that the ultimate loads were within the linear range.

Elastic – plastic formulation

$$\begin{bmatrix} \rho \\ \theta \end{bmatrix} = \begin{bmatrix} 894.1 & -4451.3 \\ -4451.3 & 46252.1 \end{bmatrix}^{-1} \begin{bmatrix} 4.6 \\ 9.5 \end{bmatrix} = \begin{bmatrix} 0.03 \\ 4.8E-03 \end{bmatrix} \quad (16.21)$$

API formulation

$$\begin{bmatrix} \rho \\ \theta \end{bmatrix} = \begin{bmatrix} 3102 & -11823.7 \\ -11823.7 & 78275.5 \end{bmatrix}^{-1} \begin{bmatrix} 4.6 \\ 9.5 \end{bmatrix} = \begin{bmatrix} 0.014 \\ 3.5E-03 \end{bmatrix}$$

The results predict a deflection of 30 mm and a rotation of 0.280° (degree) using elastic–plastic model. On the other hand, the results predict 14 mm of deflection and 0.20° using API model. The advanced model based on PLAXIS 3D shown in Fig. 16.12 predicts a deflection of 42.5 mm and a rotation of 0.3° .

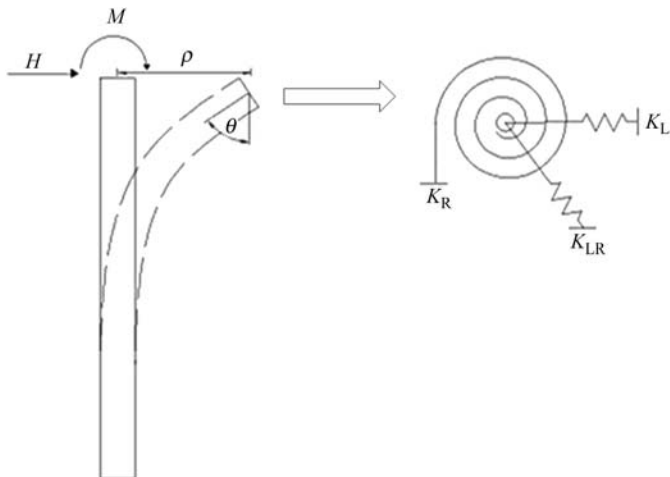


FIGURE 16.13 Simplified spring model.

16.4.2 Prediction of the Natural Frequency

These foundation stiffness values can be used to predict natural frequency following the method proposed by Arany et al. [1]. The steps are also shown as follows.

Step 1: Fixed based natural frequency of the tower

Calculate the bending stiffness ratio of tower to the pile:

$$\chi = \frac{E_T I_T}{E_P I_P} \quad (16.22)$$

Calculate the platform/tower length ratio:

$$\psi = \frac{L_s}{L_T} \quad (16.23)$$

Calculate the substructure flexibility coefficient to account for the enhanced stiffness of the transition piece:

$$C_{MP} = \sqrt{\frac{1}{1 + (1 + \psi^3)\chi - \chi}} \quad (16.24)$$

Obtain the fixed base natural frequency of the tower:

$$f_{FB} = \frac{1}{2\pi} C_{MP} \sqrt{\frac{3E_T I_T}{\left(m_{RNA} + \frac{33m_T}{140}\right)L_T^3}} \quad (16.25)$$

where the cross-sectional properties of the tower can be calculated as:

$$D_T = \frac{D_b + D_t}{2} \quad I_T = \frac{1}{8}(D_T - t_T)^3 t_T \pi \quad (16.26)$$

Step 2: Calculate the nondimensional foundation stiffness parameters

The equivalent bending stiffness of tower needed for this step:

$$q = \frac{D_b}{D_T} \quad f(q) = \frac{1}{3} \times \frac{2q^2(q-1)^3}{2q^2 \ln q - 3q^2 + 4q - 1} \quad EI_\eta = EI_{top} \times f(q) \quad (16.27)$$

where I_{top} is the second moment of area of the top section of the tower.

$$\eta_L = \frac{K_L L^3}{EI_\eta} \quad (16.28)$$

$$\eta_{LR} = \frac{K_{LR} L^2}{EI_\eta} \quad (16.29)$$

$$\eta_R = \frac{K_R L}{EI_\eta} \quad (16.30)$$

Step 3: Calculate the foundation flexibility factors

$$C_R(\eta_L, \eta_{LR}, \eta_R) = 1 - \frac{1}{1 + 0.6 \left(\eta_R - \frac{\eta_{LR}^2}{\eta_L} \right)} \quad (16.31)$$

$$C_L(\eta_L, \eta_{LR}, \eta_R) = 1 - \frac{1}{1 + 0.5 \left(\eta_L - \frac{\eta_{LR}^2}{\eta_R} \right)} \quad (16.32)$$

Step 4: Calculate the flexible natural frequency of the offshore wind turbine structure (OWT) system

$$f_0 = C_L C_R f_{FB} \quad (16.33)$$

Due to lack of the some aspects of tower data, a similar 2 MW wind turbine from North Hoyle has been used. [Table 16.5](#) summarizes the tower properties used for the calculations.

TABLE 16.5 Tower Properties

Top diameter/m	2.3
Bottom diameter/m	4.0
Wall thickness/mm	35
Tower height/m	70
Mass of RNA/t	100
Mass of tower/t	130

Note t refers to metric tonnes.

For simplicity the substructure flexibility coefficient (C_{MP}) is considered to be 1. Therefore, following Eqs. (16.22)–(16.33), we obtain:

$$D_T = \frac{D_b + D_t}{2} \Rightarrow \frac{4 + 2.3}{2} = 3.15 \quad I_T = \frac{1}{8} (3.15 - 0.035)^3 \times 0.035 \times \pi = 0.415 m^4$$

$$f_{FB} = \frac{1}{2\pi} \sqrt{\frac{3 \times 210E9 \times 0.415}{\left(100\ 000 + \frac{33 \times 130\ 000}{140}\right) 70^3}} = 0.385 \text{ Hz}$$

The fixed base frequency is therefore 0.385 Hz.

$$q = \frac{4}{2.3} = 1.74 \quad f(q) = \frac{1}{3} \times \frac{2 \times 1.74^2 (1.74 - 1)^3}{2 \times 1.74^2 \ln 1.74 - 3 \times 1.74^2 + 4 \times 1.74 - 1} = 3.56$$

$$EI_\eta = 210 \times \frac{1}{8} (2.3 - 0.035)^3 \times 0.035 \times \pi \times 3.56 = 119.4 \text{ GPa}$$

The nondimensional groups are:

$$\eta_L = \frac{0.8941 \times 70^3}{119.4} = 2568 \quad \eta_{LR} = \frac{-4.45 \times 70^2}{119.4} = -182.6$$

$$\eta_R = \frac{46.25 \times 70}{119.4} = 27.1$$



FIGURE 16.14 First mode of vibration.

The foundation flexibility coefficients are given as follows:

$$C_R(\eta_L, \eta_{LR}, \eta_R) = 1 - \frac{1}{1 + 0.6 \left(27.1 - \frac{-182.6^2}{2568} \right)} = 0.894$$

$$C_L(\eta_L, \eta_{LR}, \eta_R) = 1 - \frac{1}{1 + 0.5 \left(2568 - \frac{-182.6^2}{27.1} \right)} = 0.999$$

The natural frequency is therefore given by:

$$f_0 = 0.894 \times 0.999 \times 0.385 = 0.344 \text{ Hz}$$

16.4.3 Comparison With SAP 2000 Analysis

The system was modeled using SAP 2000 and a modal analysis is carried out to obtain the natural frequency. Nonprismatic beam elements of varying diameter were assigned to the tower while the soil–structure interaction was

represented by discrete linear Winkler springs. The spring stiffness values were taken from the soil properties (Table 16.3) and are a function of modulus of elasticity at the location of the spring and the spacing between two adjacent springs. A lumped mass was assigned at the tower head to model the dead mass of the RNA (rotor nacelle assembly). The first natural frequency recorded was 0.351 Hz and Fig. 16.14 shows the first mode of vibration.

NOMENCLATURE

- C_L, C_R Lateral and rotational flexibility coefficient
- C_{MP} Substructure flexibility coefficient
- D_b Tower bottom diameter
- D_p Pile diameter
- D_t Tower top diameter
- D_T Average tower diameter
- E_p Pile Young's modulus
- E_S Vertical distribution of soil's Young's modulus
- E_{SO} Initial soil Young's modulus at $1D_p$ depth
- $E_{I\eta}$ Equivalent bending stiffness for tower top loading
- f_0 First natural frequency (flexible)
- f_{FB} Fixed base (cantilever) natural frequency
- H Horizontal load at pile head
- I_p Pile second moment of area
- I_T Tower second moment of area
- K_L Lateral stiffness of the foundation
- K_{LR} Cross-coupling stiffness of the foundation
- K_R Rotational stiffness of the foundation
- L_p Pile embedded length
- L_S Platform height
- L_T Tower height
- M Applied moment at the pile head
- m_{RNA} Mass of rotor nacelle assembly
- m_T Mass of tower
- θ Pile head rotation
- t_T Tower wall thickness
- η_L Nondimensional lateral stiffness
- η_{LR} Nondimensional cross-coupling stiffness
- η_R Nondimensional rotational stiffness
- ρ Pile head deflection
- Ψ Length ratio
- χ Bending stiffness ratio
- v_s Soil Poisson's ratio
- ϕ' Soil angle of internal friction

REFERENCES

- [1] Arany L, Bhattacharya S, Macdonald J, Hogan SJ. Design of monopiles for offshore wind turbines in 10 steps. *Soil Dyn Earthq Eng* 2017;92:126–52 ISSN 0267-7261, <<http://dx.doi.org/10.1016/j.soildyn.2016.09.024>>.
- [2] Bouzid DA, Bhattacharya S, Dash SR. Winkler springs ($p-y$ curves) for pile design from stress-strain of soils: FE assessment of scaling coefficients using the mobilized strength design concept. *Geomech Eng* 2013;5:379–99. Available from: <http://dx.doi.org/10.12989/gae.2013.5.5.379>.
- [3] Adhikari S, Bhattacharya S. Vibrations of wind-turbines considering soil–structure interaction. *Wind Struct* 2011;14:85–112.
- [4] Adhikari S, Bhattacharya S. Dynamic analysis of wind turbine towers on flexible foundations. *Shock Vib* 2012;19:37–56.
- [5] Arany L, Bhattacharya S, Adhikari S, et al. An analytical model to predict the natural frequency of offshore wind turbines on three-spring flexible foundations using two different beam models. *Soil Dyn Earthq Eng* 2015;74:40–5. Available from: <http://dx.doi.org/10.1016/j.soildyn.2015.03.007>.
- [6] Arany L, Bhattacharya S, Macdonald JHG, Hogan SJ. Closed form solution of Eigen frequency of monopile supported offshore wind turbines in deeper waters incorporating stiffness of substructure and SSI. *Soil Dyn Earthq Eng* 2016;83:18–32 ISSN 0267-7261, <<http://dx.doi.org/10.1016/j.soildyn.2015.12.011>>. <<http://www.sciencedirect.com/science/article/pii/S0267726115003206>>.
- [7] Bhattacharya S, Cox JA, Lombardi D, Wood DM, Wood M. Dynamics of offshore wind turbines supported on two foundations. *Proc ICE-Geotech Eng* 2013;166:159–69. Available from: <http://dx.doi.org/10.1680/geng.11.00015>.
- [8] Bhattacharya S, Nikitas N, Garnsey J, et al. Observed dynamic soil–structure interaction in scale testing of offshore wind turbine foundations. *Soil Dyn Earthq Eng* 2013;54:47–60. Available from: <http://dx.doi.org/10.1016/j.soildyn.2013.07.012>.
- [9] Bhattacharya S. Challenges in the design of foundations for offshore wind turbines. Institute of Engineering and Technology, Engineering and Technology Reference; 2014. p. 9. Available from: <http://dx.doi.org/10.1049/etr.2014.0041> ISSN 2056-4007.
- [10] Lombardi D, Bhattacharya S, Muir-Wood D. Dynamic soil–structure interaction of monopile supported wind turbines in cohesive soil. *Soil Dyn Earthq Eng* 2013;49:165–80. Available from: <http://dx.doi.org/10.1016/j.soildyn.2013.01.015>.
- [11] Zania V. Natural vibration frequency and damping of slender structures found on monopiles. *Soil Dyn Earthq Eng* 2014;59:8–20. Available from: <http://dx.doi.org/10.1016/j.soildyn.2014.01.007>.
- [12] Damgaard M, Zania V, Andersen L, Ibsen LB. Effects of soil–structure interaction on real time dynamic response of offshore wind turbines on monopile. *Eng Struct* 2014;75:388–401. Available from: <http://dx.doi.org/10.1016/j.engstruct.2014.06.006>.
- [13] Shadlou M, Bhattacharya S. Dynamic stiffness of monopiles supporting offshore wind turbine generators. *Soil Dyn Earthq Eng* 2016;15–32. Available from: <http://dx.doi.org/10.1016/j.soildyn.2016.04.002>.
- [14] API, 2007. American Petroleum Institute API. Recommended practice for planning, designing and constructing fixed offshore platforms-working stress design, RP 2A-WSD, 2007.

- [15] DNV, 2014. Det Norske Veritas DNV. Offshore standard DNV-OS-J101: Design of offshore wind turbine structures. Technical report DNV-OS-J101, 2010.
- [16] Matlock H. Correlations for design of laterally loaded piles in soft clay. In: Proceedings of the second annual offshore technology conference; 1970.
- [17] Reese L.C., Cox W.R., Koop F.D. Analysis of laterally loaded piles in sand. Paper No. 2080. In: Proceedings of the sixth annual offshore technology conference; 1974.
- [18] O'Neill MW, Murchinson JM. An evaluation of $p-y$ relationships in sands. Houston, TX: University of Houston; 1983.
- [19] Kallehave D., Thilsted C.L. Modification of the API $p-y$ formulation of initial stiffness of sand. Offshore Site Investigation Geotechnique Integrated Geotechnologies—Present Future; 2012.
- [20] Gazetas G. Analysis of machine foundation vibrations: state of the art. Int J Soil Dyn Earthq Eng 1983;2:2–42 ISSN 0261-7277, <[http://dx.doi.org/10.1016/0261-7277\(83\)90025-6](http://dx.doi.org/10.1016/0261-7277(83)90025-6)>. <<http://www.sciencedirect.com/science/article/pii/0261727783900256>>.
- [21] Augustesen AH, Brødbæk KT, Møller M, Sørensen SPH, Ibsen LB, Pedersen TS, et al. Numerical modelling of large-diameter steel piles at Horns Rev. In: Topping BHV, Neves LFC, Barros RC, editors. Proceedings of the twelfth international conference on civil, structural and environmental engineering computing, No. 91. Civil-Comp Press Civil-Comp Proceedings; 2009.
- [22] Hansen J (1961). The ultimate resistance of rigid piles against transversal forces. Geoteknisk Institut, Bull, Copenhagen, Bull 12 < Tag as Book reference >.

Chapter 17

Physical Modeling of Offshore Wind Turbine Model for Prediction of Prototype Response

Domenico Lombardi¹, Subhamoy Bhattacharya², and George Nikitas²

¹*The University of Manchester, Manchester, United Kingdom, ²University of Surrey, Guildford, United Kingdom*

Email: domenico.lombardi@manchester.ac.uk

17.1 INTRODUCTION

OWTs are providing an increasing proportion of wind energy generation capacity because offshore sites are characterized by stronger and more stable wind conditions than comparable onshore sites. Owing to the higher capacity factor (i.e., ratio of the actual amount of power produced over a period of time to the rated turbine power) and decreasing levelized cost of energy (LCOE) (i.e., ratio of the total cost of an offshore wind farm to the total amount of electricity expected to be generated over the wind farm's lifetime), offshore wind turbines (OWTs) are currently installed in high numbers in Northern Europe. The industry is rapidly developing worldwide, particularly in countries such as China, South Korea, Taiwan, and Japan, whereas the United States has recently installed its first pilot offshore wind farm in Block Island. The design and construction of offshore turbines, however, are more challenging when compared with onshore counterparts, owing to the harsh environmental conditions existing at the offshore sites.

17.1.1 Complexity of External Loading Conditions

OWTs are characterized by a unique set of dynamic loading conditions that is schematically depicted in Fig. 17.1. These include: (1) load produced by the turbulence in the wind, whose amplitude is function of the wind speed; (2) load caused by waves crashing against the substructure, whose magnitude

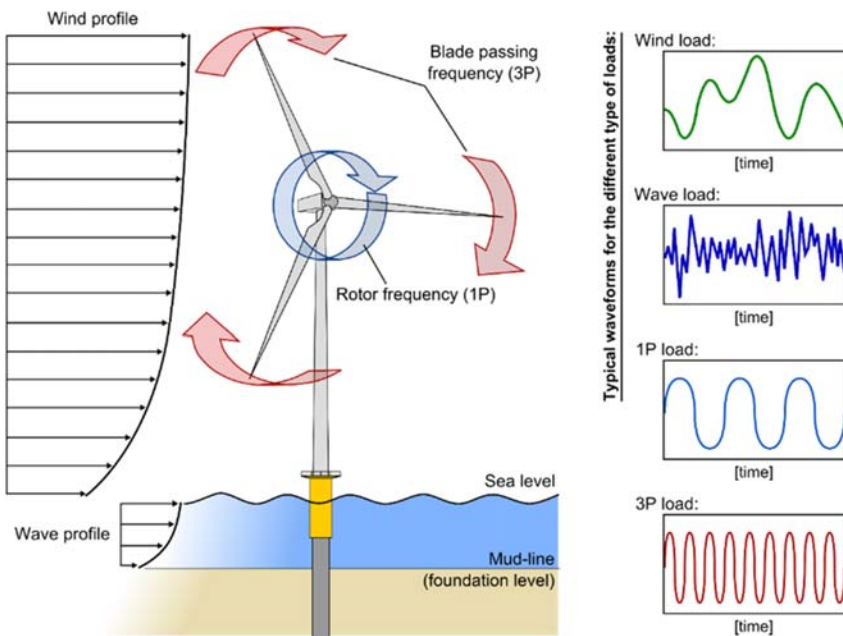


FIGURE 17.1 Typical loads acting on an OWT.

depends on the height and period of waves; (3) load caused by mass and aerodynamic imbalances of the rotor, whose forcing frequency equals the rotational frequency of the rotor (referred to as 1P loading in the literature); (4) loads in the tower due to the vibrations caused by blade shadowing effect (referred to as 3P loading in the literature), which occurs as each blade passes through the shadow of the tower.

The loads imposed by wind and wave are random in both space and time, as a result these are better described statistically by using the Pierson–Moskowitz wave spectrum and Kaimal wind spectrum, as shown in Fig. 17.2. It is clear from the frequency content of the applied loads that the designer in order to avoid the resonance of the OWT has to select a design frequency that lies outside the ranges of forcing frequencies. Specifically, the Det Norske Veritas (DNV) code [1] recommends that the natural frequency of the wind turbine should be at least $\pm 10\%$ away from the main forcing frequencies introduced earlier. Depending on the design value of natural frequency, three design approaches are possible, namely, soft–soft (natural frequency $< 1P$), soft–stiff (natural frequency between 1P and 3 P), and stiff–stiff (natural frequency $> 3P$).

It is worth noting that the design procedure requires an accurate evaluation of the natural frequency, which is dependent on the support condition (i.e., the stiffness of the foundation) that in turn relies on the strength and stiffness

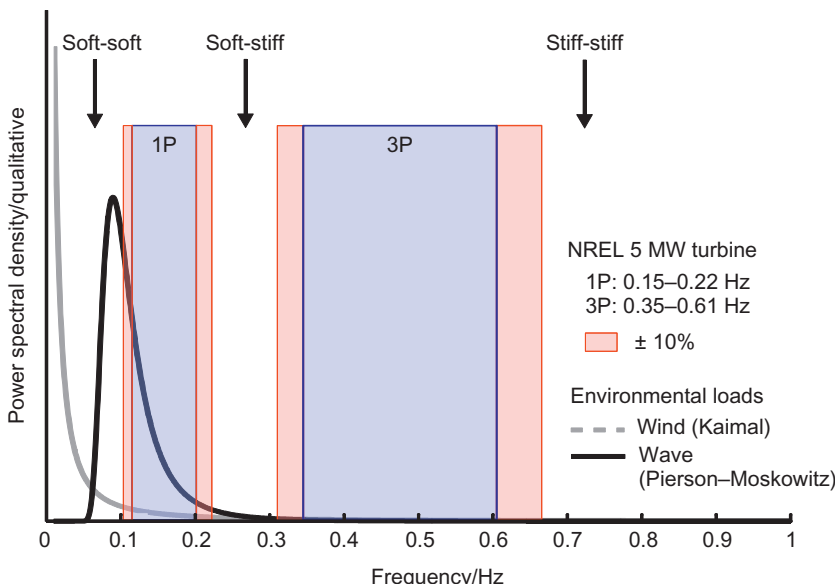


FIGURE 17.2 Qualitative power spectrum of main forcing frequencies and different design approaches considering an NREL (National Renewable Energy Laboratory) 5 MW wind turbine.

of the surrounding soil. Furthermore, as the natural frequencies of OWTs are very close to the forcing frequencies, the dynamics pose multiple design challenges because of the tight tolerance of the target natural frequency, whereby the scale of the challenges will vary depending on turbine types and site characteristics. Typical values of vibration characteristics and site characteristics of operating wind turbines are listed in [Table 17.1](#).

17.1.2 Design Challenges

There are two main aspects related to cyclic loading conditions, see Nikitas et al. [2], that have to be taken into account during design: (1) soil behavior due to nondynamic repeated loading, i.e., fatigue-type problem and this is mainly attributable to wind loading which has a very low frequency; (2) soil behavior due to dynamic loading which will cause dynamic amplification of the foundation response, i.e., the resonance-type problem. This is due mainly due to 1P and 3P loading but wave loading can also be dynamic for deeper waters and heavier turbines. A breakdown of the overall problem of soil–structure interaction into two types of soil shearing is schematically represented in [Fig. 17.3](#). The current codes of practice (e.g., DNV [1], American Petroleum Institute, API [2,3], Institute of Electrical Engineers, IEC [4]) for the design of monopile foundations of OWTs recommend the application of the p – y curves primarily for the evaluation of lateral pile

TABLE 17.1 Analyzed Offshore Wind Farms With the Used Wind Turbines and Soil Conditions at the Sites

No.	Wind Farm Name and Location	Turbine Type and Rated Power	Soil Conditions at the Site	Natural Frequencies ^a /Hz
I	Lely offshore wind farm (The Netherlands)	NedWind 40/500 two-bladed 500 kW study purpose wind turbine	Soft clay in the uppermost layer to dense and very dense sand layers below	0.63–0.74
II	Irene vorrlink offshore wind farm (The Netherlands)	Nordtank NTK600/43 600 kW study purpose wind turbine	Soft layers of silt and clay in the upper seabed to dense and very dense sand below.	0.55–0.56
III	Blyth offshore wind farm (United Kingdom)	Vestas V66 2 MW industrial OWT	Rocky seabed (weathered bedrock)	0.49
IV	Kentish flats offshore wind farm (United Kingdom)	Vestas V90 3 MW industrial OWT	Layers of dense sand and firm clay	0.34
V	Barrow offshore wind farm (United Kingdom)	Vestas V90 3 MW industrial OWT	Layers of dense sand and stiff clay	0.37
VI	Thanet offshore wind farm (United Kingdom)	Vestas V90 3 MW industrial OWT	Fine sand and stiff clay	0.37
VII	Belwind 1 offshore wind farm (Belgium)	Vestas V90 3 MW industrial OWT	Dense sand and stiff clay	0.37
VIII	Burbo bank offshore wind farm (United Kingdom)	Vestas V90 3 MW industrial OWT	Saturated dense sand (2090)	0.29
IX	Walney 1 offshore wind farm (United Kingdom)	Siemens SWT-3.6–107 3.6 MW industrial OWT	Medium and dense sand layers	0.35
X	Gunfleet sands offshore wind farm (United Kingdom)	Siemens SWT-3.6–107 3.6 MW industrial OWT	Sand and clay layers	0.31

^aEstimated based on Arany L, Bhattacharya S, Macdonald JH, Hogan SJ. Closed form solution of Eigen frequency of monopile supported offshore wind turbines in deeper waters incorporating stiffness of substructure and SSI. *Soil Dyn Earthq Eng* 2016;83:18–32 [16].

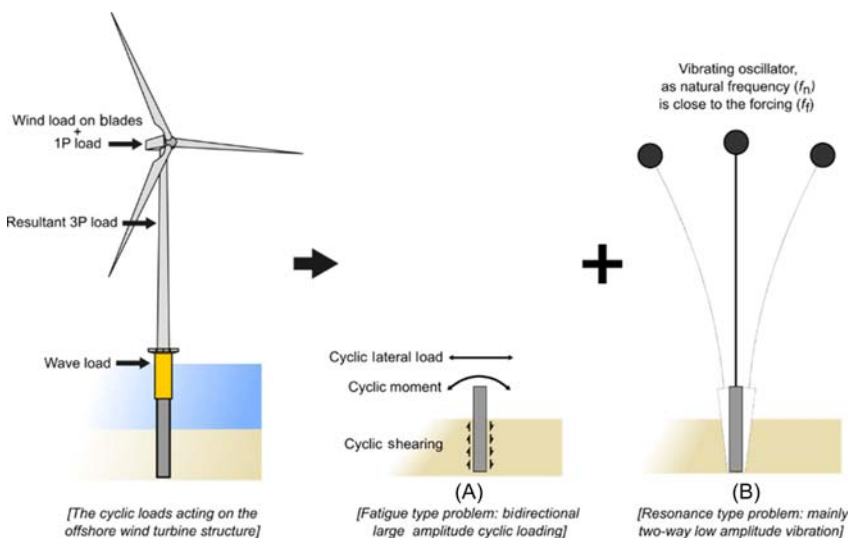


FIGURE 17.3 Breakdown of soil–structure interaction of OWTs into two types of problems.

capacity in the ultimate limit state. The codes provide limited guidance in predicting the change of the foundation stiffness and consequent change of natural frequency, which are both design drivers for serviceability limit state requirements.

Furthermore, it is important to note that the vibration of the foundation will induce cyclic strains in the soil in its vicinity. Under moderate-to-high amplitudes of cyclic loading, most soils change their stiffness and strength. In order to study the changes in soil stiffness due to these cyclic strains, the developing strain in the soil around the shear zone must be taken into consideration. Soils in offshore sites can be fully saturated and therefore pore pressures are likely to develop as a result of these cyclic strains. The pore pressure developed may dissipate to the surrounding soil depending on factors including frequency of loading, permeability of the soil, and diameter of the pile. Pore water pressure may also develop in unsaturated soils under cyclic shearing. It should be noted that due to the nature of the external excitation, wave and wind-induced loads may impose either one-way or two-way cyclic loading on the monopile, whereby one-way loading develops more soil deformation and consequently more change in foundation stiffness.

OWTs are relatively new structures without any track record of long-term performance. Therefore, the uncertainties of their long-term response pose additional challenges to developers and designers of offshore wind farms. In fact, monitoring of a limited number of installed wind turbines has indicated a gradual departure of the overall system dynamics from the design requirements (e.g., the data from Lely wind farm data [5]), which may lead to amplification of the dynamic response of the turbines, leading to larger tower

deflections and/or rotations beyond the allowable limits tolerated by manufacturer. The latter are often considered responsible for the damage observed in gearboxes and other electrical-rotating equipment.

17.1.3 Technical Review/Appraisal of New Types of Foundations

Foundations typically cost 25%–35% of an overall offshore wind farm project and in order to reduce the LCOE, new innovative foundations are being proposed. However, before any new type of foundation can actually be used in a project, a thorough technology review is often carried out to de-risk it. European Commission defines this through TRL (Technology Readiness Level) numbering starting from 1 to 9; see [Table 17.2](#) for different stages of the process. One of the early works that needs to be carried out is technology validation in the laboratory environment (TRL-4). In this context of foundations, it would mean carrying out tests to verify the long-term performance. It must be realized that it is very expensive and operationally challenging to validate in a relevant environment and therefore laboratory-based evaluation has to be robust so as to justify the next stages of investment. This is another motivation for scaled model testing.

17.1.4 Physical Modeling for Prediction of Prototype Response

Experimental investigations on physical wind turbine models can provide valuable information for understanding the dynamic behavior and long-term performance of OWTs. While physical modeling at normal gravity (often

TABLE 17.2 Definition of TRL

TRL Level as European Commission

TRL-1: Basic principles verified

TRL-2: Technology concept formulated

TRL-3: Experimental proof of concept

TRL-4: Technology validated in laboratory

TRL-5 Technology validated in relevant environment

TRL-6: Technology demonstrated in relevant environment

TRL-7: System prototype demonstration in operational environment

TRL-8: System complete and qualified

TRL-9: Actual system proven in operational environment

known as 1 g testing) can be used for modeling different loading conditions experienced by structures, its application in tackling soil–structure interaction needs additional consideration. In such cases, geotechnical centrifuge facilities are often used where 1: N scale model can be subjected to N g (N times earth gravity) to replicate the prototype stresses. However, OWTs are very complex structure involving aerodynamics (wind turbulence at the blades), hydrodynamics (wave slamming the tower and the part of the tower under water), cyclic, and dynamic soil–structure interaction. Ideally, a wind tunnel and a wave tank onboard a geotechnical centrifuge is suitable which seems to be unlikely with the current technology development. For such problems involving many interactions, where overall system dynamics and long-term performance needs to be studied, centrifuge is not well suited due to the unwanted parasitic vibration of geotechnical centrifuge and the lack of stable platform. Another important limitation of centrifuge facilities is the limited number of cycles that can reasonably be applied when compared with the expected number of cycles that a typical OWT experiences over its life span of 25 years, which is in the range 10^7 – 10^8 . This calls for alternative modeling techniques where a problem will be studied through a set of nondimensional groups and is explained in the next section.

17.2 PHYSICAL MODELING OF OWTs

Derivation of correct scaling laws constitutes the first step in an experimental study. The similitude relationships are essential for interpretation of the experimental data and for scaling up the results for the prediction of the prototypes' responses. As shown in Fig. 17.4, there are two approaches for deriving the scaling law relationships. The first is to use standard tables for scaling and multiply the model observations by the scale factor to predict the prototype response, see for example Wood [6]. The alternative is to study the underlying mechanics/physics of the problem based on the model tests, recognizing that not all the interactions can be scaled accurately in a particular test. Once the mechanics/physics of the problem are understood, the prototype response can be predicted through analytical and/or numerical modeling in which the physics/mechanics discovered will be implemented in

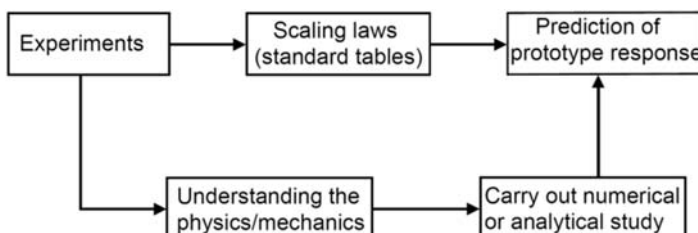


FIGURE 17.4 Reflective loop for physical modeling.

a suitable way. As shown by Bhattacharya et al. [7] and Lombardi et al. [8], the second method is well suited for investigating the dynamics of OWTs, which involves complex dynamic wind–wave–foundation–structure interaction and no physical modeling technique can simultaneously satisfy all the interactions at a single scale. Ideally, a wind tunnel combined with a wave tank on a geotechnical centrifuge would serve the purpose but this is unfortunately not feasible. Special consideration is required when interpreting the test results.

The design and interpretation of test carried out on a small-scale model require the assessment of a set of laws of similitude that relate the model to the prototype structure. These can be derived from dimensional analysis from the assumptions that every physical process can be expressed in terms of non-dimensional groups and the fundamental aspects of physics must be preserved in the design of model tests. The necessary steps associated with designing such a model can be stated as follows:

- To deduce the relevant nondimensional groups by thinking of the mechanisms that govern the particular behavior of interest at both model and prototype scale.
- To ensure that a set of crucial scaling laws are simultaneously conserved between model and prototype through pertinent similitude relationships.
- To identify scaling laws which are approximately satisfied, and those which are violated and which therefore require special consideration.

17.2.1 Dimensional Analysis

Dimensional analysis refers to a method of great generality and mathematical simplicity that can be conveniently used for studying phenomena that at first appear to be very complex but which can be qualitatively analyzed and described in more simplified terms [9]. Although the basis of dimensional analysis was set in the 19th century by Fourier in his work on the theory of the heat flow, only in the 20th century the method has been extensively used in different fields of physics and engineering. The approach is based on the concept of similarity, which in physical terms implies that that any phenomenon can be studied through a finite number of independent quantities expressed in a nondimensional form, i.e., unit-free. In this context, the aim of dimensional analysis is to determine these nondimensional quantities, which constitutes the first step in an experimental study.

17.2.2 Definition of Scaling Laws for Investigating OWTs

As discussed earlier, OWTs are dynamically sensitive structures because of the multiple frequencies that contribute to the complexity of the interaction of the foundation with the supporting soil. To study the dynamics and predict

the long-term performance of OWTs, the following phenomena have to be considered and correctly replicated in the model tests, namely:

- Vibration of the pile owing to the environmental loads will induce cyclic strains in the soil in the vicinity of the pile. In order to study the changes in soil stiffness owing to these cyclic strains, the developing soil strain around the field must be monitored. These soils are saturated and therefore pore pressures are likely to develop as a result of these cyclic strains. The pore pressure developed may dissipate to the surrounding soil, depending on the frequency of the loading.
- Changes in the soil stiffness owing to the cyclic loading may lead to changes in foundation stiffness, which in turn will alter the natural frequency of the system. Therefore the relationship between the foundation characteristics and the overall system dynamics, in other words, the soil–structure interaction, is important for overall system performance.
- Repeated cyclic stresses will be generated in the pile owing to cyclic loading. Therefore foundation fatigue is also a design issue.

Based on the above discussion, the following physical mechanisms are considered for the derivation of the nondimensional groups:

1. Strain field in the soil around a laterally loaded pile which will control the degradation of soil stiffness
2. Cyclic stress ratio (CSR) in the soil in the shear zone
3. Rate of soil loading which will influence the dissipation of pore water pressure
4. System dynamics, the relative spacing of the system frequency, and the loading frequency
5. Bending strain in the monopile foundation for considering the nonlinearity in the material of the pile
6. Fatigue in the monopile foundation.

17.3 SCALING LAWS FOR OWTs SUPPORTED ON MONOPILES

17.3.1 Monopile Foundation

Most of the OWTs currently in operation are supported on monopiles. Monopiles consist of tubular steel tubes having diameter in the range 3.5–10 m. The choice of monopiles results from their simplicity of installation and the proven success of conventional piles—characterized by smaller diameters, i.e., 1.5–3.0 m, in supporting offshore oil and gas infrastructures.

17.3.2 Strain Field in the Soil Around the Laterally Loaded Pile

Repeated shear strain may reduce the stiffness of saturated soils. Assuming that the changes in soil stiffness drive the long-term performance, the average

strain next to a pile is a governing criterion and must be preserved in order to ensure similar stiffness degradation in both model and prototype. The relevant nondimensional group can be derived by considering that the average shear strain field around a laterally moving pile is a function of pile head deflection (δ) and pile outer diameter (D), mathematically expressed by:

$$\varepsilon_s \propto \frac{\delta}{D} \quad (17.1)$$

Klar [10] suggested a value of 2.6 for the coefficient of proportionality between the average strain in the soil and the ratio of head deflection and pile diameter. However, there is a lack of consensus in the literature on this proportionality coefficient. The pile head deflection is a function of the external load (P), the shear modulus of the soil (G), and the pile diameter. Therefore, the average strain field in the soil around a pile can be expressed as a function of only three parameters (Fig. 17.5A):

$$\varepsilon_s = f(P, D, G) \quad (17.2)$$

The parameters in Eq. (17.2) can be used to obtain a dimensionless group as follows:

$$\varepsilon_s = f\left(\frac{P}{GD^2}\right) \quad \frac{[F]}{[FL^{-2}][L]^2} \quad (17.3)$$

Eq. (17.3) describes the nondimensional group that takes into account the strain field in the soil generated by a lateral loaded pile. Eq. (17.3) shows

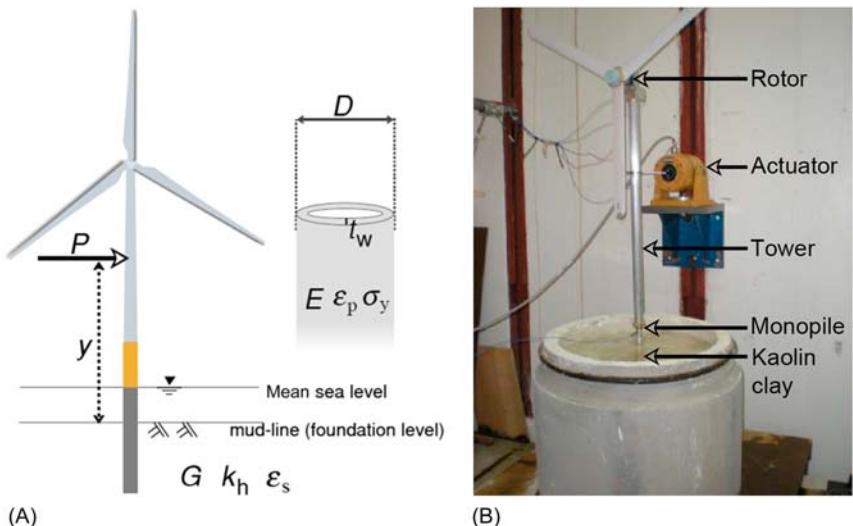


FIGURE 17.5 (A) Definition of the main parameters used in the nondimensional analysis. (B) Small-scale physical model of OWT used in the pilot studies.

that the strain in the soil is directly proportional to the horizontal load applied at the pile head, inversely proportional to the soil stiffness and inversely proportional to the square of the pile diameter.

17.3.3 CSR in the Soil in the Shear Zone

In geotechnical earthquake engineering, it is well established that degradation of a soil due to liquefaction-type failure is a function of CSR which is defined as the ratio of the shear stress to the effective vertical stress at a particular depth, defined in Eq. (17.4) [11]. The CSR can be expressed in Eq. (17.4):

$$\text{CSR} = \frac{\tau_{\text{cyc}}}{\sigma'_v} \quad (17.4)$$

$$\tau_{\text{cyc}} \propto \frac{P}{D^2} \frac{[F]}{[L]^2} \quad (17.5)$$

where τ_{cyc} is the cyclic shear stress imposed by the pile on the soil at a particular depth and σ'_v is the effective vertical stress on the soil at the same depth.

The vertical effective stress can be related to the shear modulus of the soil:

$$\sigma'_v \propto G \frac{[F]}{[L]^2} \quad (17.6)$$

It is usually found that G is proportional to σ'_v^n , where the exponent n is a function of the type of soil, varying from 0.435 to 0.765 for sandy soil, although a value of 0.5 is commonly used in practice. For clayey soil, the value of n is generally larger and usually taken as 1 [12].

Combining Eqs. (17.4)–(17.6), one can see that the nondimensional group expressed in Eq. (17.3) can also guarantee similarity of CSR. This leads us to a nondimensional group, expressed in Eq. (17.7a,b), that must be satisfied.

$$\left(\frac{P}{GD^2} \right)_{\text{model}} = \left(\frac{P}{GD^2} \right)_{\text{prototype}} \quad (17.7a)$$

It is interesting to note that using two different approaches based on average strain in the soil, and on the CSR, dimensional analysis leads to a unique nondimensional group given in Eq. (17.7a). It can be easily shown that considering the overturning moment (M) at the head of the foundation, i.e., pile head for example, the group in Eq. (17.7b) can equally be used.

$$\left(\frac{M}{GD^3} \right)_{\text{model}} = \left(\frac{M}{GD^3} \right)_{\text{prototype}} \quad (17.7b)$$

17.3.4 Rate of Soil Loading

Pore pressure generation and subsequent dissipation is a function of the frequency of loading exerted on the soil. The time (t) in which the pore pressure dissipates will be directly proportional to the soil permeability (k_h) and inversely proportional to characteristic length, e.g., monopile diameter:

$$t \propto \frac{k_h}{D} \quad (17.8)$$

Considering the variables in Eq. (17.8), one can obtain the only possible dimensionless group:

$$\left(\frac{k_h t}{D}\right) \frac{[LT^{-1}][T]}{[L]} \quad (17.9)$$

Replacing time by forcing frequency (f_f), the pore pressure dissipation is therefore correctly modeled when:

$$\left(\frac{k_h}{f_f D}\right)_{\text{model}} = \left(\frac{k_h}{f_f D}\right)_{\text{prototype}} \quad (17.10)$$

17.3.5 System Dynamics

In order to correctly simulate the system dynamics resulting from the interaction between the external loads (i.e., forcing frequency) and the wind turbine (i.e., natural frequency), the ratio between the forcing frequency and the natural frequency of the turbine should be of the same order in the physical model and prototype. The main forcing frequencies are (see also Fig. 17.2):

- Environmental loading: the predominant wave and wind forcing frequency is typically around 0.1 Hz.
- Rotor frequency: it represents the frequency of the blade rotation, and is generally indicated by 1P. As shown in Fig. 17.2, typical values are in the range of 0.15–0.22 Hz.
- Wind shielding effects of the blade on the tower: when the blade passes the tower, the shadowing effect of the wind load causes a cyclic load on the tower. This frequency is indicated by 3P (or 2P for a two-bladed rotor). Evidently the blade passing frequency is the product of the rotor frequency and the number of blades.

From Fig. 17.2 it may be noted that for any of the three design approaches possible (i.e., soft–soft, soft–stiff, and stiff–stiff), the ratio between the forcing and the natural frequency is close to 1. This aspect must be preserved also in the physical model. Therefore the nondimensional groups for the correct

modeling of the dynamics of the system can be expressed as a ratio between the forcing and natural frequency:

$$\left(\frac{f_f}{f_n}\right)_{\text{model}} = \left(\frac{f_f}{f_n}\right)_{\text{prototype}} \quad (17.11)$$

Lombardi et al. [8] pointed out that the two groups for “rate of soil loading,” given in Eq. (17.10), and “system dynamics,” given in Eq. (17.11), cannot be simultaneously satisfied with same pore fluid in model and prototype. It is obvious that both coefficient of permeability and diameter of the monopile affect the drainage condition. Modeling both the nondimensional groups together can be conveniently accommodated through the use of a different pore fluid such as silicone oil or methyl cellulose solution for the model tests.

17.3.6 Bending Strain in the Monopile

The strain in the monopile is a function of its mechanical properties and the characteristics of the external loads. As shown in Fig. 17.1, the external loads due to the wind and the waves can be conveniently modeled as a horizontal force acting at the distance y above the foundation level—see Figs. 17.3 and 17.5A. Making the assumption that the monopiles remains elastic, the strain in the pile wall will be a function given in Eq. (17.12).

$$\varepsilon_p = f(P, y, D, E, t_w) \quad (17.12)$$

where t_w is the pile wall thickness and E is the Young’s modulus of the pile.

The parameters in Eq. (17.12) can be combined to obtain a dimensionless group:

$$\varepsilon_p = f\left(\frac{Py}{ED^2 t_w}\right) \frac{[F][L]}{[FL^{-2}][L]^2[L]} \quad (17.13)$$

In order to correctly model the material nonlinearity of the pile, the non-dimensional group expressed in Eq. (17.14) must be preserved in the model and the prototype:

$$\left(\frac{Py}{ED^2 t_w}\right)_{\text{model}} = \left(\frac{Py}{ED^2 t_w}\right)_{\text{prototype}} \quad (17.14)$$

17.3.7 Fatigue in the Monopile

The stress in the monopile can be an important parameter influencing the fatigue phenomena. Fatigue relates to the degradation of the material after a large number of load cycles ($>10^7$ cycles). The design of an OWT must ensure that the fatigue limit state is satisfied. The fatigue in the monopile can be expressed as a function of the external load, pile diameter, pile wall

thickness, vertical distance between the application point of the load P and the pile head, and the yield stress of the material (σ_y):

$$f(P, D, t_w, y, \sigma_y) \quad (17.15)$$

The parameters in Eq. (17.15) can be combined to obtain a dimensionless group:

$$f\left(\frac{Py}{\sigma_y D^2 t_w}\right) \frac{[F][L]}{[FL^{-2}][L]^2[L]} \quad (17.16)$$

Eq. (17.16) represents the nondimensional group required to take account of the fatigue phenomenon. This can be correctly modeled when Eq. (17.17) is satisfied:

$$\left(\frac{Py}{\sigma_y D^2 t_w}\right)_{\text{model}} = \left(\frac{Py}{\sigma_y D^2 t_w}\right)_{\text{prototype}} \quad (17.17)$$

To explore the usefulness of these dimensionless groups derived so far, the next section of the paper describes typical results obtained from high-quality small-scale experiments.

17.3.8 Example of Experimental Investigation for Studying Long-Term Response of 1–100 Scale OWT

This section describes an example of experimental investigation carried out on a small-scale OWT. The experimental apparatus is shown in Fig. 17.5B, however, more details regarding the experimental arrangement can be found in Lombardi et al. [8]. As it can be seen from the figure, modeling of the environmental dynamic loads can be achieved by using an electrodynamic actuator fixed to the laboratory strong wall and connected to the tower. The blades are rotated by a DC electric motor to model the 1P loading, which also give some aerodynamic damping to the system. An alternative cyclic loading system is proposed by Nikitas et al. [2]. This consists of two identical interlocking gears where masses can be attached (see Fig. 17.4). The working principle of this cyclic loading device is based on the unbalanced rotation of eccentric masses and is presented schematically in Fig. 17.6. This counter-rotating eccentric mass of equal magnitude is able to produce a unidirectional cyclic load in Y axis only as the net force in X axis is zero due to cancelation of the equal and opposite forces. In the case when the two masses mounted on the interlocking gears are not equal, there will be a sinusoidal loading along two perpendicular directions (X and Y axes). The force resultants in X and Y axes for two cases when the masses are equal and unequal are presented in Fig. 17.7.

It may be noted that the excitation force produced by this device is dependent on three variables: mass of the weights attached to the gears (m), the radius of the gears (r), and the angular velocity of the gears (ω). The frequency (Hz) of the cyclic loading depends mainly on the angular velocity

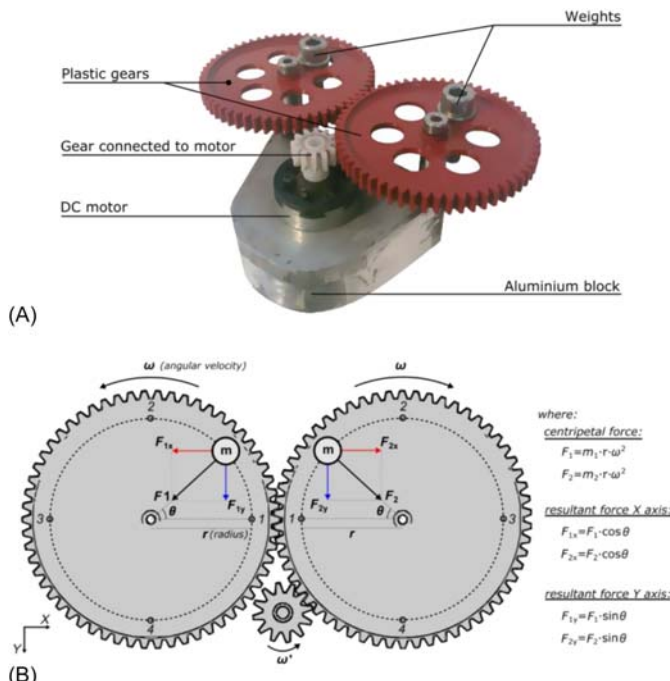


FIGURE 17.6 Cyclic loading system developed by Nikitas et al. [2]: (A) photograph depicting different components and (B) working principle.

which can be easily controlled by the voltage (V) of the power supply. In order to control the force in Y axis, the appropriate masses should be attached to the rotating gears, considering the fact that the radius remains the same. Also it is possible to change the frequency and the amplitude by just replacing the type and the diameter of the gears. Once the amplitude and the frequency of the cyclic loads are defined, the device is mounted on the tower to simulate the desired overturning moment at the level of the foundation.

In a typical offshore project, the largest contribution toward the overturning moment is due to the wind and the wave loads having different magnitude of overturning moment, frequency, and also the number of cycles. A way to address this loading complexity in a scaled model tests is by attaching two of these eccentric mass actuators, one to represent each load (frequency and amplitude) and placing them at the correct height in order to produce the desired scaled bending moment at the base of the model. The result of such an arrangement would provide realistic results of the foundation's long-term performance. Such a configuration is presented schematically in Fig. 17.8, where the wind and the wave are both acting along the same direction, i.e., collinear. There can be loading scenarios, when the wind and the wave may not be aligned and Fig. 17.9 shows a possible configuration that can be used for simulation.

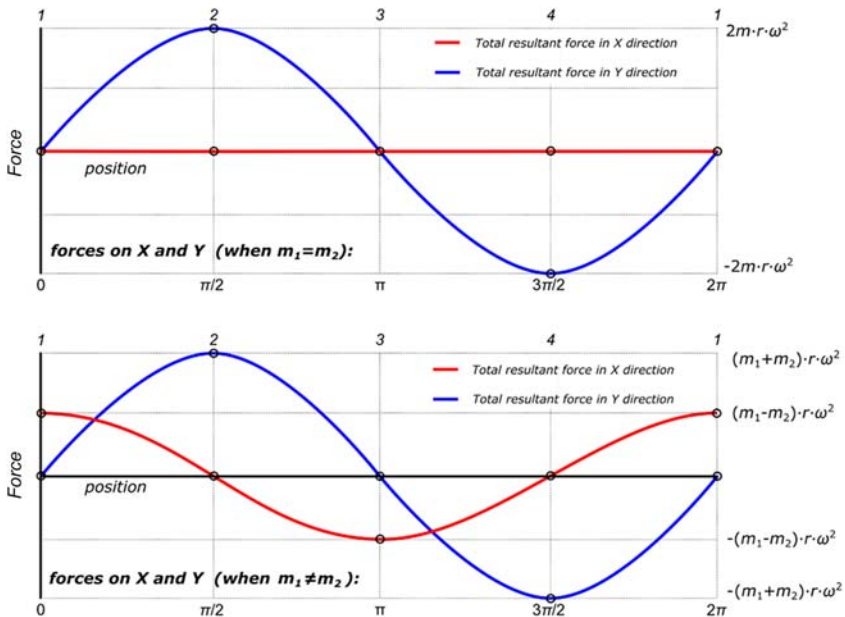


FIGURE 17.7 Force resultants in X and Y axes when the masses are equal (top) and not (bottom).

Typical results presented by Lombardi et al. [8] highlighted that the long-term behavior of OWTs supported on monopiles is strongly affected by the level of strain generated in the soil adjacent the foundation (given in Eq. 17.3), whereby larger strains result in higher variation in foundation stiffness and natural frequency of the system. Evidently, the potential change in vibration characteristics has to be appropriately taken into account in design and prediction of the long-term performance of OWTs.

17.4 SCALING LAWS FOR OWTs SUPPORTED ON MULTIPOD FOUNDATIONS

Offshore wind farm projects are increasingly turning to alternative foundations [13], which include jacket and multipod foundations. The scaling relations required to investigate such foundations need to take into account the geometric arrangement (i.e., characterizing the asymmetry). Thus, this section of the chapter incorporates the additional scaling laws required to study generic multipod foundations, such as the one depicted in Fig. 17.10.

The rules of similarity between the model and prototype that need to be maintained are as follows.

The dimensions of the small-scale model need to be chosen in such a way that similar modes of vibration will be excited in model and prototype.

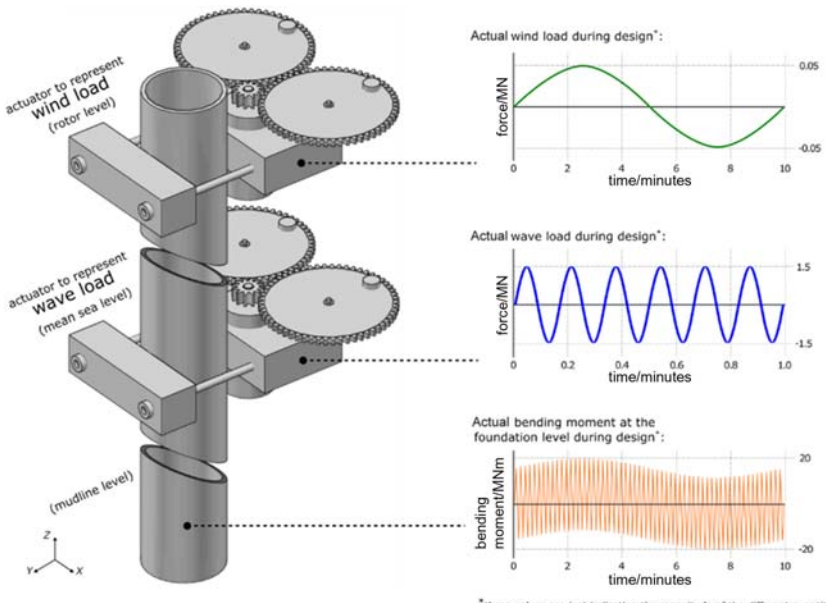


FIGURE 17.8 Configuration of two actuators to represent separately wind and wave loads, when these are acting along the same direction.

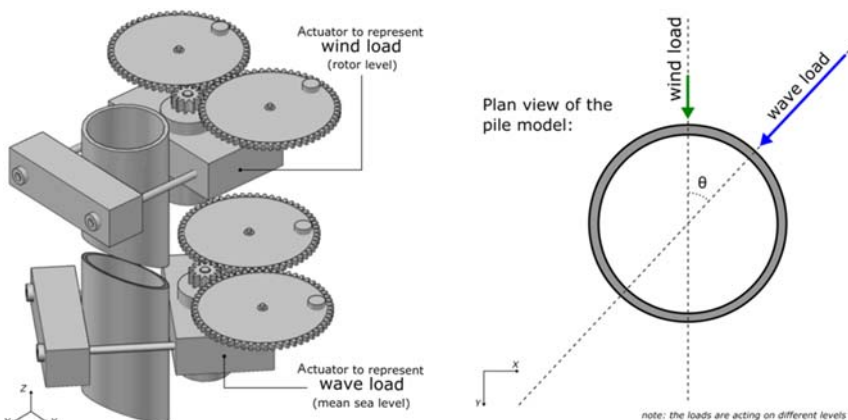


FIGURE 17.9 Configuration to study the wind–wave misalignment.

It is expected that rocking modes will govern the multipod (tripod or tetrapod suction piles or caissons) foundation and as a result relative spacing of individual pod foundations (b in Fig. 17.10) with respect to the tower height (L in Fig. 17.10) needs to be maintained (see Eq. (17.18)). This geometrical scaling is also necessary to determine the point of application of the resultant

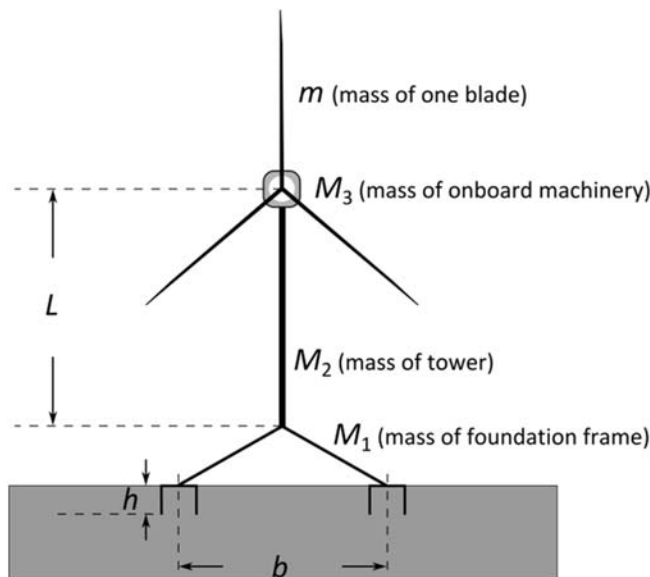


FIGURE 17.10 Schematic diagram for multipod foundation wind turbines.

force on the model. The aspect ratio of the caisson (diameter-to-depth ratio) should also be maintained to ensure the pore water flow is reproduced. This leads to the similitude relationship given in Eq. (17.19).

$$\left(\frac{L}{b}\right)_{\text{model}} = \left(\frac{L}{b}\right)_{\text{prototype}} \quad (17.18)$$

where L is the length of the tower and b is the spacing of the caissons.

$$\left(\frac{D}{h}\right)_{\text{model}} = \left(\frac{D}{h}\right)_{\text{prototype}} \quad (17.19)$$

where D is the diameter of the caisson and h is the depth of the caisson.

To model the vibration of the tower, the mass distribution between the different components needs to be preserved. In other words, the ratios $M_1:M_2:M_3:m$ in Fig. 17.10 need to be maintained in model and prototype.

$$(M_1:M_2:M_3:m)_{\text{model}} = (M_1:M_2:M_3:m)_{\text{prototype}} \quad (17.20)$$

The relative stiffness between suction caisson and the surrounding soil: The stiffness of the caissons relative to the soil needs to be preserved in the model so that the caisson interacts similarly with the soil as in the prototype. Caisson flexibility affects both the dynamics and the soil–structure interaction and as a result this mechanism is of particular interest. Based on the

work of Doherty et al. [14], the nondimensional flexibility of a suction caisson is given by:

$$\frac{Et}{GD} \quad (17.21)$$

where E is the elastic modulus of caisson skirt (GPa); t is the thickness of caisson skirt (mm); G is the shear modulus of surrounding soil (GPa); and D is the diameter of the caisson (m).

The above group can be derived from the expression of hoop stress (σ_θ) developed in a thin walled cylindrical pressure vessel given in Eq. (16.5).

$$\sigma_\theta \propto \frac{pD}{t} \quad (17.22)$$

noting that σ_θ is the stress in the caisson which is proportional to the elastic modulus of caisson skirt (E) and p is the pressure applied by the soil, dependent on the shear modulus. Therefore the following relationship should be maintained:

$$\left(\frac{Et}{GD}\right)_{\text{model}} = \left(\frac{Et}{GD}\right)_{\text{prototype}} \quad (17.23)$$

The loading encountered in a single caisson in a multipod foundation is a combination of vertical and horizontal load. For a combination of lateral and vertical load, a failure envelope given in Eq. (17.24) is often used in practice.

$$\left(\frac{V}{V_{\max}}\right)^i + \left(\frac{H}{H_{\max}}\right)^j = 1 \quad (17.24)$$

where H_{\max} is the bearing capacity in horizontal direction; V_{\max} is the bearing capacity in vertical direction; V is the vertical load on the individual caisson; and H is the horizontal load on the caisson with $i = j = 3$ (see Ref. [7]).

The nondimensional group to preserve is $\frac{V}{V_{\max}}$ which is proportional to $\frac{V}{\gamma'D^3}$ for sandy soil where γ' is the buoyant soil unit weight (kN m^{-3}) and D is the caisson diameter. The relationship for clay soil is given in Eq. (17.25c). Therefore the following relationship should hold:

$$\left(\frac{V}{V_{\max}}\right)_{\text{model}} = \left(\frac{V}{V_{\max}}\right)_{\text{prototype}} \quad (17.25a)$$

$$\left(\frac{V}{\gamma'D^3}\right)_{\text{model}} = \left(\frac{V}{\gamma'D^3}\right)_{\text{prototype}} \quad \text{for sandy soil} \quad (17.25b)$$

$$\left(\frac{V}{s_u D^2}\right)_{\text{model}} = \left(\frac{V}{s_u D^2}\right)_{\text{prototype}} \quad \text{for clay soil} \quad (17.25c)$$

Details of the derivation are provided in Ref. [7]. The lateral load acting on the caisson can be derived from the CSR in the shear zone next to the footing which is quite similar to the case for pile as derived in earlier for the monopile due to the fact that caissons and monopiles will act as a rigid body. This leads us to a nondimensional group (Eq. (17.26)) that must be satisfied.

$$\left(\frac{H}{GD^2}\right)_{\text{model}} = \left(\frac{H}{GD^2}\right)_{\text{prototype}} \quad (17.26)$$

17.4.1 Typical Experimental Setups and Results

A series of tests were carried by Bhattacharya et al. [13] to investigate the dynamics and long-term performance of small-scale OWTs models supported on multipod foundations (Fig. 17.11). Fig. 17.12 shows the asymmetric model arrangement in a typical setup. The results showed that the multipod foundations (symmetric or asymmetric) exhibit two closely spaced natural frequencies corresponding to the rocking modes of vibration in two principle axes. Furthermore, the corresponding two spectral peaks change with repeated cycles of loading and they converge for symmetric tetrapods but not for asymmetric tripods. From the fatigue design point of view, the two spectral peaks for multipod foundations broaden the range of frequencies that can be excited by the broadband nature of the environmental loading (wind and wave) thereby impacting the extent of motions. Thus the system life span (number of cycles to failure) may effectively increase for symmetric foundations as the two peaks will tend to converge. However, for asymmetric foundations, the system life may continue to be affected adversely as the two peaks will not converge.

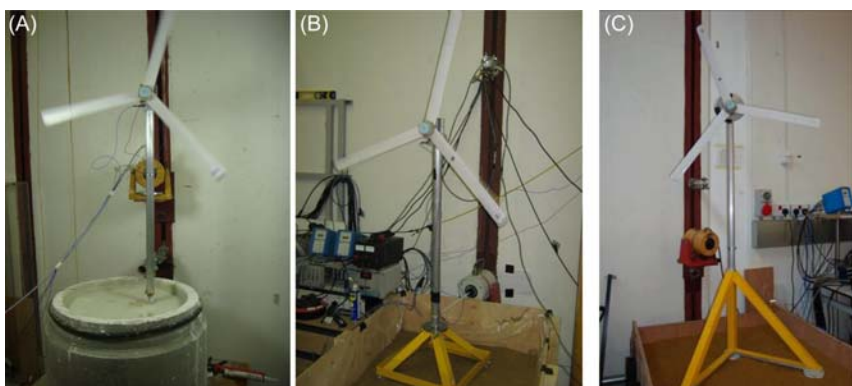


FIGURE 17.11 Small-scale wind turbine model supported on different types of foundation: (A) monopile; (B) symmetric tetrapod foundation; and (C) asymmetric tripod.

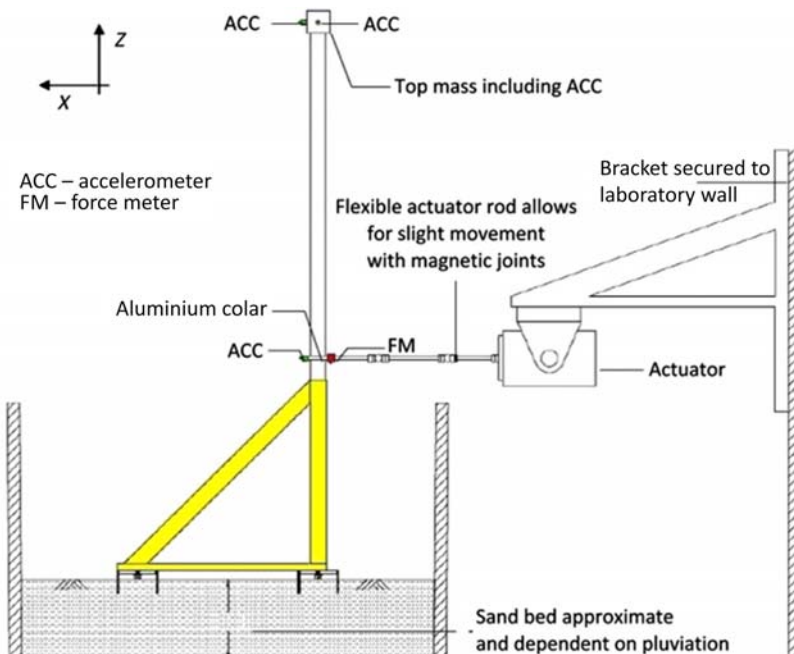


FIGURE 17.12 Schematic diagram of the test setup for asymmetric tripod [15].

In this sense, designers should prefer symmetric foundations to asymmetric foundations.

17.5 CONCLUSIONS

This chapter shows that small-scale experimental studies can be carried out to study complex dynamic soil–structure interaction problems where there is no prior information. The long-term performance of OWTs has been studied because there is a real concern regarding the effect on performance of changes in the foundation stiffness.

Mechanics-based nondimensional groups have been derived in order to study the various aspects of this problem and their validity has been verified using physical modeling.

REFERENCES

- [1] DNV GL AS. Design of offshore wind turbine structures. DNV-OS-J101, Det Norske Veritas; 2014.
- [2] Nikitas G, Vimalan NJ, Bhattacharya S. An innovative cyclic loading device to study long term performance of offshore wind turbines. *Soil Dyn Earthq Eng* 2016;82:154–60.

- [3] API. Recommended practice for planning, designing, and constructing fixed offshore platforms: working stress design. 20th ed. Washington, DC: American Petroleum Institute RP2A-WSD; 20072007
- [4] IEC 61400-1. Wind turbine generator systems—Part 1: Design requirements, 3rd ed; 2005.
- [5] Kuhn M. (2000). Dynamics of offshore wind energy converters on mono-pile foundation experience from the Lely offshore wind turbine. In: OWEN Workshop.
- [6] Wood DM. Geotechnical modelling. CRC Press; 2003. ISBN: 9780415343046.
- [7] Bhattacharya S, Lombardi D, Wood DM. Similitude relationships for physical modelling of monopile-supported offshore wind turbines. Int J Phys Model Geotech 2011;11(2):58–68.
- [8] Lombardi D, Bhattacharya S, Wood DM. Dynamic soil–structure interaction of monopile supported wind turbines in cohesive soil. Soil Dyn Earthq Eng 2013;49:165–80.
- [9] Lombardi D, Bhattacharya S, Ghosh S, Alexander NA. Fundam Eng Math. London: ICE Publishing; 2015.
- [10] Klar A. Upper bound for cylinder movement using “elastic” fields and its possible application to pile deformation analysis. Int J Geomech 2008;8(2):162–7.
- [11] Seed HB, Idriss IM. Simplified procedure for evaluating soil liquefaction potential. J Soil Mech Found Div 1971;97(SM9):1249–73.
- [12] Wroth CP, Randolph MF, Houslsby GT, Fahey M. A review of the engineering properties of soils with particular reference to the shear modulus, Report CUED/D-SOILS TR75. University of Cambridge; 1979.
- [13] Bhattacharya S, Cox JA, Lombardi D. Dynamics of offshore wind turbines supported on two foundations. Proc Inst Civil Eng Geotech Eng 2013;166(2):159–69.
- [14] Doherty JP, Houslsby GT, Deeks AJ. Stiffness of flexible caisson foundations embedded in non-homogeneous elastic soil. J Geotech Geoenvir Eng 2005;131(12):1498–508.
- [15] Bhattacharya S, Nikitas N, Garnsey J, Alexander NA, Cox J, Lombardi D, et al. Observed dynamic soil–structure interaction in scale testing of offshore wind turbine foundations. Soil Dyn Earthq Eng 2013;54:47–60.
- [16] Arany L, Bhattacharya S, Macdonald JH, Hogan SJ. Closed form solution of Eigen frequency of monopile supported offshore wind turbines in deeper waters incorporating stiffness of substructure and SSI. Soil Dyn Earthq Eng 2016;83:18–32.

Part IV

Generation of Electricity

This page intentionally left blank

Chapter 18

Energy and Carbon Intensities of Stored Wind Energy

Charles J. Barnhart

Western Washington University, Bellingham, WA, United States

Email: charles.barnhart@wwu.edu

18.1 THE NEED FOR STORAGE

The world needs affordable, accessible, sustainable, and low-carbon energy resources [1–3]. Of the renewable resources, solar PV and wind turbines have the highest technical potential to satisfy this need, but these technologies generate electricity from variable, weather-dependent resources [3–7]. Fig. 18.1 provides a compelling visualization of 30 days of superimposed power demand time series data (red) wind energy generation data (blue) and solar insolation data (yellow). Supply correlates poorly with demand. The amount of storage needed for operation of electrical grids incorporating increasing amounts of variable wind resources is a critical yet complicated question. It is complicated for two reasons: (1) the electrical grid, composed of myriad power sources and sinks is conducted as a whole in real-time, and (2) the number of technologies and practices, their varied and evolving characteristics, and their possible implementations under differing and shifting policy landscapes presents a grossly under-determined problem with several solutions.

Technologies and practices positioned to ensure grid-reliability include flexible conventional generation (natural gas combustion turbines and diesel generation sets), flexible renewable generation (curtailment, hydropower, concentrated solar power (CSP) with thermal storage), flexible load (demand-side management), energy storage, and resource sharing (diversity and trans-mission). In the future, when greenhouse gas emissions are constrained, flexible generation will need to be achieved using low-carbon energy supplies.

Studies have made efforts to determine the amount of renewable generation an electrical grid can support by bundling these technologies and practices into an abstract resource: grid flexibility, defined as the percentage of

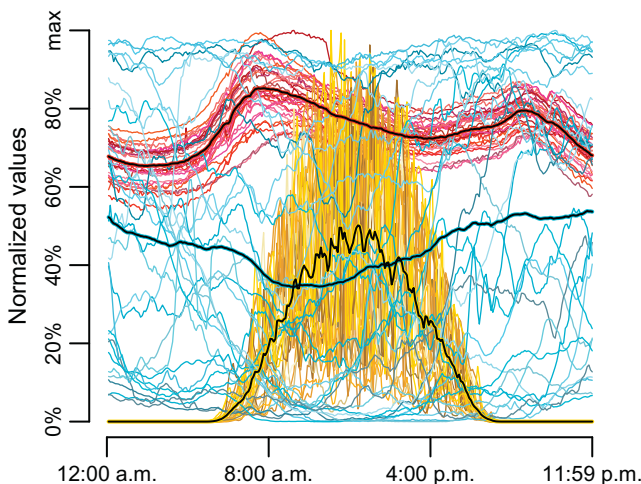


FIGURE 18.1 Wind power generation (blue), insolation (gold), and power demand (red) time series data provide a compelling visualization of renewable energy's intermittent correlation with demand. Thirty days of data collected in April 2010 are superimposed and normalized to their maximum values. Average values are in color highlighted black lines. *Data obtained from Bonneville Power Administration, Bonneville Power Administration, P.O. Box 3621, Portland, OR 97208–3621, <http://www.bpa.gov> and <https://transmission.bpa.gov/business/operations/Wind/baltwg.aspx>* (2011). Plot first published in Barnhart CJ, Dale M, Brandt A.R, Benson SM. *Energy & environmental science* 2013; 6: 2804–10.

generation and load capable of being readily dispatched or halted [5]. Less flexible grids harbor high percentages of so-called baseload generating plants such as nuclear, coal, and natural gas combined cycle plants. The amount of energy storage capacity required will depend firstly on grid flexibility. It will depend secondly on attributes of the renewable generation. The amount, type, mix, and degree of supply correlation affects how well supply satisfies demand. Today storage on power grids is dominated by pumped hydroelectric storage (PHS). **Table 18.1** lists worldwide storage capacity by power and energy. This chapter describes the effect storage has on the energy and carbon intensity of wind generated electricity. First, key storage characteristics are listed. Second, energy return ratio results are presented, and third, carbon intensity calculations and results are presented.

18.2 KEY CHARACTERISTICS FOR STORAGE

Energy storage incurs energetic costs and emits carbon to the atmosphere. Direct emissions of carbon are those associated with the round-trip efficiency and operation of the storage device. Indirect emissions are those resulting from the process of mining the materials and manufacturing the storage and flexible generation technologies. The energetic and carbon intensity values

TABLE 18.1 Global Storage Capacity

Technology	Power/MW	Energy/GW h
Li-ion	~ 20 [8]	0.06 ^a
NaS	365.3 [9]	2.191 ^{b,c}
PbA	~ 1 800 000 ^d	400 ^d
Flow (VRB, ZnBr)	3 [8]	0.024 ^c
Compressed air energy storage (CAES)	400 [10] (650 [10,11])	3.73 [12]
Pumped hydroelectric storage (PHS)	129 000 [8]	102 ^e

^aAssuming 3 hour storage.

^bAssuming NGK modulesRastler (2010) with 6 hour discharge.

^cAssuming PacifiCorp moduleRastler (2010) with 8 hour discharge.

^dAssuming total car batteries worldwide (1 billion) each 10 kg with practical power and energy densities of 180 W kg⁻¹ and 40 W kg⁻¹ yields 1.8 TW and 0.4 TW h of capacity.

^eIn 2008 United States had 21.5 GW PHS capacity that delivered 6288 GW h of energy, [13].

Source: Rastler D. Electricity energy storage technology options: a white paper primer on applications, costs, and benefits. Technical report, Electric Power Research Institute, Palo Alto; 2010; Reddy T, Linden D. Linden's handbook of batteries, McGraw Hill, New York; 2010; Succar S. Compressed air energy storage. In: Barnes FS, Levine JG editors. Large energy storage systems handbook. Boca Raton, FL: CRC Press; 2011; pp. 111–153 [Chapter 5]; Sandia National Laboratory. American recovery and reinvestment act: energy storage demonstrations. Technical report, Sandia National Laboratory Energy Storage Systems; 2011; RWE. Adele—adiabatic compressed air energy storage for electricity supply. Technical report, RWE Power AG, Essen/Köln; 2010.

for energy storage technologies were obtained from LCA and NEA studies [14–17]. Key characteristics for grid-scale storage are safety, affordability, reliability, longevity, and efficiency. Technologies that satisfy these criteria, in this analysis, include four electrochemical storage technologies: lithium-ion (LiB), sodium sulfur (NaS), traditional lead acid (PbA), vanadium redox flow batteries (VRB); two geological storage technologies; pumped hydroelectric storage (PHS); and compressed air energy storage (CAES).

Key net energy and carbon data are listed in Table 18.2. The energy intensity per unit energy storage capacity, ε_s (kWh_e/kWh_s), depends on the technology's depth of discharge (D), its total number of charge–discharge cycles (λ), and its cradle-to-gate embodied electrical energy requirement per unit capacity of energy delivered to storage (CTG_e).

Embodied energy accounts for energy expended in mining raw resources, manufacturing the device and delivering the device to point of use. The per cycle carbon intensity (g CO₂eq kW h⁻¹) for storage technologies were calculated by adding capital (GHG_{s,cap}) and operational greenhouse gas (GHG_{s,op}) emissions per unit of electrical energy delivered per cycle.

A critical attribute of an energy storage technology is its round-trip efficiency, η . The carbon intensity of the discharged electricity is $\geq 1/\eta$ times the carbon intensity of the input electricity. Using storage increases the

TABLE 18.2 Data Used in Net Energy Analysis of Storage Technologies

Technology	CAES	LiB	NaS	PbA	PHS	VRB
$\text{GHG}_{s,\text{cap}}/\text{kg} (\text{MW h})^{-1}$	19 400	600 960	687 500	153 850	35 700	161 400
$\text{GHG}_{s,\text{op}}/(\text{kg/MW h})^{-1}$	288	0	0	0	1.8	3.3
D , discharge depth	1	0.8	0.8	0.8	1	1
λ , cycles	25 000	6000	4700	700	25 000	10 000
η , efficiency	0.7 (1.36)	0.9	0.75	0.9	0.85	0.75
CTG_e	22	136	145	96	30	208
χ , Carbon multiplier	0.735 ^a	1.111	1.333	1.111	1.764	1.333
ε_s , Energy intensity	0.00088	0.028	0.039	0.17	0.0012	0.072

Definitions are in the text. Detailed analysis and references in Supplementary Materials.

^aCAES operation delivers more electricity that enters storage by combusting natural gas.

Sources: Denholm P, Kulcinski P. Life cycle energy requirements and greenhouse gas emissions from large scale energy storage systems. *Energy Convers Manage* 2004; 45:2153–72; Rydh C, Sandén B. Energy analysis of batteries in photovoltaic systems. Part I: Performance and energy requirements. *Energy Convers Manage* 2005; 46:1957–79; Sullivan JL, Gaines L. A review of battery life-cycle analysis: state of knowledge and critical needs ANL/ESD/10-7. Technical report, Argonne National Laboratory, Oak Ridge, TN; 2010.

carbon intensity of delivered electricity by a factor, χ , as listed in Table 18.2. χ is a carbon intensity multiplier. If storage is 90% efficient, the carbon intensity of the delivered electricity increases by 11%, $\chi = 1.11$. Manufacturing storage also incurs its own energetic and carbon costs.

Despite higher energy and carbon intensities when compared to PHS, electrochemical storage technologies present one clear advantage: energy density. Batteries are able to store several hundred times the amount of energy per unit mass and volume than PHS (Fig. 18.2). Additionally, batteries do not require geological features, i.e., steep topography, that PHS requires and therefore can be deployed anywhere including city centers, residences, and commercial buildings (Fig. 18.3).

18.3 NET ENERGY ANALYSIS OF STORING AND CURTAILING WIND RESOURCES

Curtailing renewable resources results in an immediate and obvious forfeiture of energy. However, flexible grid technologies can also consume significant amounts of energy in their manufacture and operation. These embodied energy costs are not as immediately apparent, but they are an energy sink from a societal perspective.

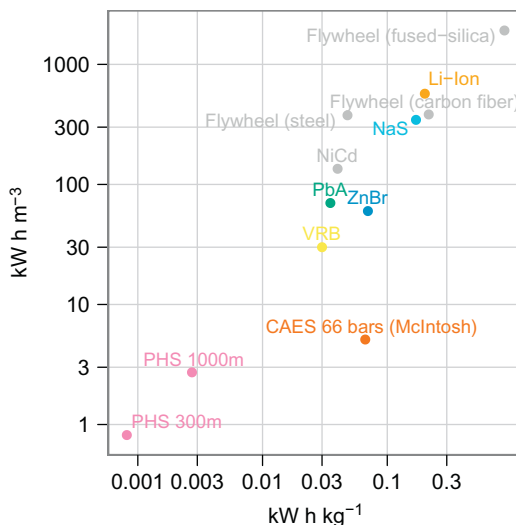


FIGURE 18.2 A plot comparing volumetric and specific energy densities for energy storage technologies. Data obtained for PHS and CAES are calculated, battery data from Ref. Reddy T, Linden D. Linden's handbook of batteries. McGraw Hill, New York; 2010 [9], flywheel data from Ref. Semadeni M. Storage of energy, overview. Encycl Energy 2004; 5:719–38 [18].

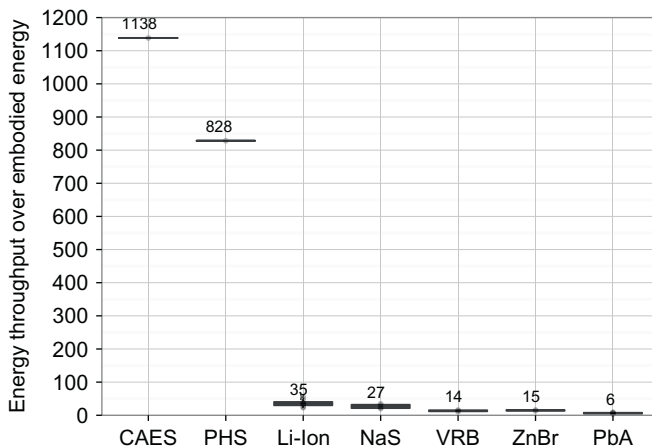


FIGURE 18.3 The total energy stored over the life of a storage device divided by the embodied energy required to manufacture the device provides a comparative metric for comparing societal energy costs. Higher values are better.

In this section, I compare the energetic costs of electrical energy storage (EES) to the energetic costs of curtailment. In lieu of storage or other means of grid flexibility, variable resources are curtailed during periods of oversupply or of strong market disincentives [19,20]. Consequently electricity is

squandered, capacity factors are reduced, and revenue for turbine owners in certain markets is lost. In Texas, e.g., 1.2%–17.1% of potential wind generation was curtailed on an annual basis between 2007 and 2012, equaling a total of 13 TW h of electrical energy [21]. Worldwide, curtailment rates are projected to increase as wind and solar comprise a larger fraction of the generation mix [5,21]. We ask whether or not storage provides societal net energy gains over curtailment. EES has significant value not quantified or analyzed in this study, including electricity market economics [22], insuring reliable power supplies to critical infrastructure [23], ancillary benefits to power grid operation [8], and application in disaster relief and war zone scenarios.

The results shown here were originally presented in Ref. [24], which presents a theoretical framework for quantifying how storage affects net energy ratios. This framework accommodates any type of generation or storage technology. Using Life Cycle Assessment (LCA) data for generation and storage technologies, we calculate which storage and generation technologies result in a net energy gain over curtailment. We present our data and results in terms of EROI: the amount of electrical energy returned per unit of electrical energy invested. A complete derivation of the methods and detailed results can be found in Ref. [24]. Fig. 18.4 shows calculated grid EROI values,

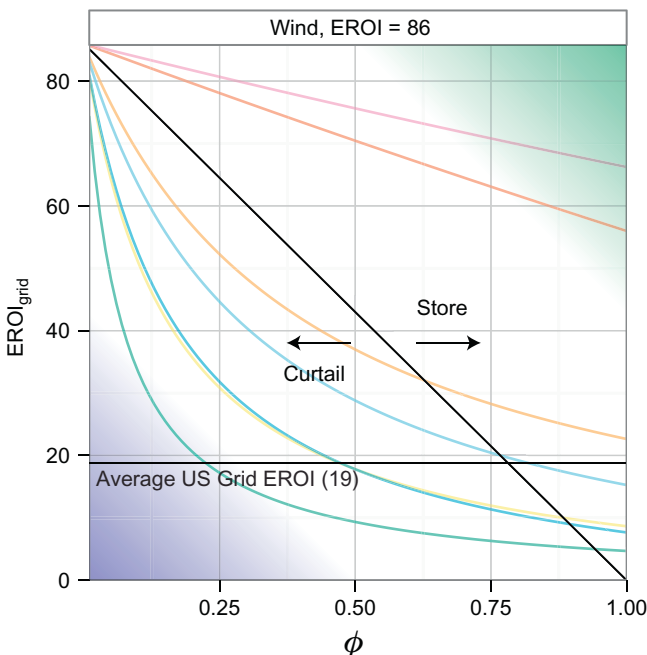


FIGURE 18.4 Grid $EROI_{\text{grid}}$ values as a function of storage or curtailment fraction, ϕ , and electrical energy storage (EES) technology paired with wind. Storage technologies in order of decreasing EROI values on right side of plot are as follows: PHS, CAES, Li-Ion, NaS, VRB, ZnBr, and PbA.

$\text{EROI}_{\text{grid}}$, for PV (top) and wind resources (bottom) used with storage technologies (colored lines) as a function of φ . The solid black line bisecting the plots indicates the EROI value due to curtailment, spanning a range from original resource EROI to zero. The green region to the right of this line indicates combinations of EROI , ESOIE , and φ in which storage yields better energy returns than curtailment, $\text{EROI}_{\text{grid}} > \text{EROI}_{\text{curt}}$. To the left, in blue, $\text{EROI}_{\text{grid}} < \text{EROI}_{\text{curt}}$, storage implementation is more energetically costly than simply curtailing the resource. Several interesting results emerge from Fig. 18.4. First, storage technologies with low ESOIE values, like PbA and ZnBr, reduce the grid EROI down much more severely than technologies with high ESOIE values, like PHS, CAES, and Li-Ion. Second, battery technologies paired with wind yield grid EROI values far below EROI values from curtailment alone for reasonable values of φ . However, these grid EROI values are greater than the average US power grid values ~ 20 . Ideally storage technologies that support generation resources should not diminish energy return ratios below curtailment energy return ratios for reasonable values of φ . This means that geologic storage technologies, not contemporary battery technologies, are much more favorable for storing electricity generated from wind power.

Curtailment of wind resources during times of excess generation is a viable form of grid flexibility. Curtailment rates of up to 30% yield carbon and energy intensities that are lower than respective pairings with electrochemical storage technologies. While curtailment appears to be an immediate waste of a resource, the life-cycle energy costs of storage are greater than curtailment at reasonable rates below about 30%. Avoiding curtailment may not lead to the most environmentally sound decisions. Curtailment is not the only option, nor is it ideal. Useful applications for excess electricity occur beyond the power grid. Excess electricity could be used for thermal storage, producing heat or ice for later use. Additionally, electricity could be used to pump or desalinate water, smelt metal ores, or manufacture goods. The energy is “stored,” i.e., embodied elsewhere in the economy.

18.4 THE CARBON FOOTPRINT OF STORING WIND ENERGY

Energy storage emits carbon to the atmosphere. Direct emissions of carbon are those associated with the round-trip efficiency and operation of the storage device. Indirect emissions are those resulting from the process of mining the materials and manufacturing the storage and flexible generation technologies. The carbon intensity values for energy storage technologies were obtained from LCA and NEA studies [14–17]. Carbon intensity values for the average US power grid emissions and subgrid emissions were obtained from Ref. [25] (Table 18.3).

The per cycle carbon intensity ($\text{g CO}_2\text{eq kW h}^{-1}$) for storage technologies were calculated by adding capital and operational greenhouse gas (GHG) emissions.

TABLE 18.3 Generation Technology Lifecycle

Emissions Resource	Reference and Notes kW h kgCO _{2eq} -1	Min	25th%	Median	75th%	Max
Wind	[26] On Shore (Harmonized) 107 Estimates from 44 studies	22	50	91	119	333
PV	[27] Crystalline Silicon PV Irradiation of 1700 kW h m ⁻² year ⁻¹ 41 Estimates from 13 studies	5	20	22	25	38
NGCC	[28] 51 Estimates from 42 studies Capital emissions: 1 g kW h ⁻¹	1.4	2	2.2	2.4	3
NGCT		1.2	1.3	1.5	1.8	1.9
NGCC	[28]	—	15	21	36	—

The life carbon intensity values for wind, PV, and gas. Here NGCC refers to natural gas combined cycle and NGCT refers to natural gas combustion turbine (sometimes called a peaker plant).

$$\text{GHG}_s = \text{GHG}_{s,cap}/(\lambda D) + \text{GHG}_{(1s,op)} \quad (18.1)$$

The storage technology's depth of discharge, D , modulates per cycle capital ($\text{GHG}_{s,cap}$) emissions from storage meaning that a shallow depth of discharge requires larger batteries (with associated manufacturing costs) to provide equivalent storage capacities. Values used in these calculations can be found in [Table 18.2](#).

The life-cycle carbon intensity of electricity delivered to the power grid from generation resources via energy storage technologies was calculated by summing per cycle storage carbon intensities with lifecycle generation carbon intensities.

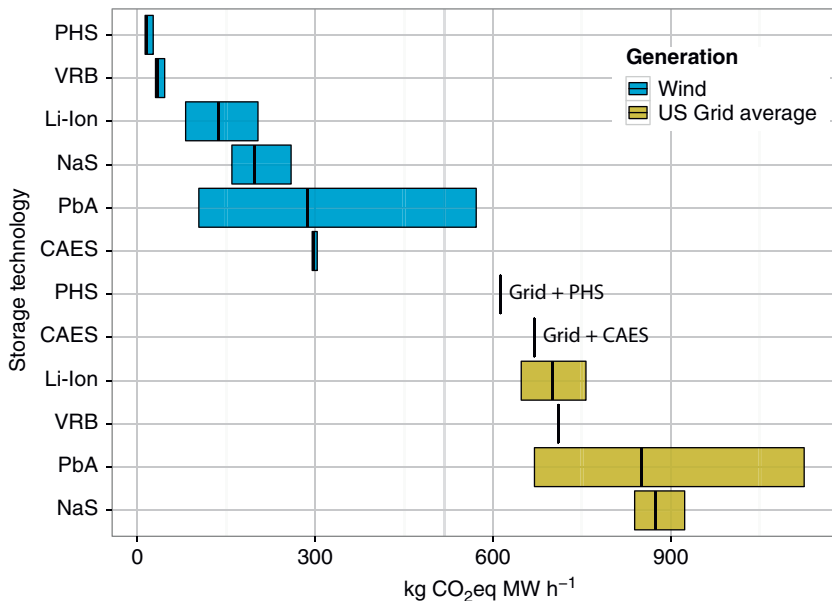


FIGURE 18.5 The carbon intensity of electricity provided from wind-charged storage technologies. For comparison, the carbon intensity of electricity provided from storage technologies charged by a hypothetical US average power grid (vertical line) is displayed on the right half of the bar chart.

$$\text{GHG}_g = \text{GHG}_s + \text{GHG}_r/\eta \quad (18.2)$$

Fig. 18.5 shows carbon intensity values in terms of $\text{kg CO}_{2\text{eq}}$ per electrical energy delivered to the power grid from various wind storage technology pathways. For reference, the average carbon intensity values for the US power grid (518 kg MW^{-1}) is shown. Additionally, carbon intensity values direct wind and grid-storage pairings are shown. All wind storage pairings emit less carbon than the US power grid average. The best performing storage technologies are PHS, VRB, and Li-Ion. The worst performing technologies are PbA and CAES, which emits carbon via natural gas combustion upon discharge.

18.5 CONCLUSIONS

Energy storage promises many benefits for electrical power grids and societal energy use in general. Our analysis shows how to calculate and compare their energy and carbon footprints. In conclusion the analyses presented in this chapter reveal the following insights:

1. Flexible power generation and energy storage come with a cost. Energy delivered from storage has greater carbon and energetic intensities than

energy delivered directly from power generation technologies, and depending on the technology, the energy and carbon penalties for storage can be large.

2. The energy and carbon intensities wind plus storage are far lower than for the US grid.
3. Not all storage technologies are created equal. PHS performs best and traditional lead acid batteries perform worst. CAES trades low energy intensity for high-carbon emissions associated with combustion of natural gas. LiB and VRB perform best among electrochemical storage solutions with LiB providing the lowest energy intensity and VRB the lowest carbon intensity. Traditional lead acid batteries perform poorly by these metrics. Although they have low energy requirements for manufacture, their low number of charge–discharge cycles leads to frequent replacement and a high-energy intensity of 0.17.
4. The curtailment of wind resources provides flexibility with lower carbon and energy costs in comparison to the implementation of energy storage technologies until curtailment rates exceed about 30%.

Energy storage and curtailment can provide the flexibility the power grid will require as the fraction of intermittent wind resource supply increases. This chapter shows the benefits of using systems-level energy intensity and carbon intensity analysis to compare performance of flexible options for wind [29]. Policy makers and consumers that consider the effects of deploying storage with wind can better identify environmentally sound solutions.

REFERENCES

- [1] Chu S, Majumdar A. Opportunities and challenges for a sustainable energy future. *Nature* 2012;488:294–303.
- [2] Cont J, Holtberg P, Doman LE, Smith KA, Sullivan JO, Vincent KR, et al. International energy outlook 2011, DOE/EIA-0484(2011). Technical report, U.S. Energy Information Administration, Washington, DC; 2011.
- [3] Kojm C. Global trends 2030: alternative worlds. National Intelligence Council; 2012. p. 160.
- [4] Lew D, Piwko D, Miller N, Jordan G, Clark K, Freeman L. How do high levels of wind and solar impact the grid? The western wind and solar integration study. Technical report December, National Renewable Energy Laboratory; 2010.
- [5] Denholm P, Margolis RM. Evaluating the limits of solar photovoltaics (PV) in traditional electric power systems. *Energy Policy* 2007;35:2852–61.
- [6] Marvel K, Kravitz B, Caldeira K. Geophysical limits to global wind power. *Nat. Climate Change* 2012;3:118–21.
- [7] Hand M, Baldwin S, DeMeo E, Reilly J, Mai T, Arent D, et al. Renewable electricity futures study. NREL TP-6A20-52409; 2012.
- [8] Rastler D. Electricity energy storage technology options: a white paper primer on applications, costs, and benefits. Technical report. Palo Alto: Electric Power Research Institute; 2010.

- [9] Reddy T, Linden D. *Linden's handbook of batteries*. New York: McGraw Hill; 2010.
- [10] Sandia National Laboratory. American recovery and reinvestment act: energy storage demonstrations. Technical report. Sandia National Laboratory Energy Storage Systems; 2011.
- [11] RWE. Adele—adiabatic compressed air energy storage for electricity supply. Technical report, RWE Power AG, Essen/Köln; 2010.
- [12] Succar S. Compressed air energy storage. In: Barnes FS, Levine JG, editors. *Large energy storage systems handbook*. Boca Raton, FL: CRC Press; 2011. p. 111–53. chapter 5
- [13] EIA. Electric power monthly April 2012. Technical report April, U.S. Energy Information Adminsitration; 2012.
- [14] Denholm P, Kulcinski P. Life cycle energy requirements and greenhouse gas emissions from large scale energy storage systems. *Energy Convers Manage* 2004;45:2153–72.
- [15] Rydh C, Sandén B. Energy analysis of batteries in photovoltaic systems. Part I: Performance and energy requirements. *Energy Convers Manage* 2005;46:1957–79.
- [16] Sullivan JL, Gaines L. A review of battery life-cycle analysis: state of knowledge and critical needs ANL/ESD/10-7. Technical report. Oak Ridge, TN: Argonne National Laboratory; 2010.
- [17] Barnhart CJ, Benson S. On the importance of reducing the energetic and material demands of electrical energy storage. *Energy Environ. Sci.* 2013;6:1083–92.
- [18] Semadeni M. Storage of energy, overview. *Encycl Energy* 2004;5:719–38.
- [19] Wiser R, Bolinger M. 2011 Wind technologies market report. Technical report August, U. S. Department of Energy; 2012.
- [20] Lannoye E, Flynn D, O'Malley M. Evaluation of power system flexibility. *IEEE Trans Power Syst* 2012;27:922–31.
- [21] Wiser R, Bolinger M. 2012 Wind technologies market report-DOE/GO-102013-3948. Technical report August, LBNL; 2013.
- [22] Budischak C, Sewell D, Thomson H, Mach L, Veron DE, Kempton W. Cost-minimized combinations of wind power, solar power and electrochemical storage, powering the grid up to 99.9% of the time. *J Power Sources* 2013;225:60–74.
- [23] Armand M, Tarascon JM. Building better batteries. *Nature* 2008;451:652–7.
- [24] Barnhart CJ, Dale M, Brandt AR, Benson SM. The energetic implications of curtailing versus storing solar-and wind-generated electricity. *Energy Environ Sci* 2013;6:2804–10.
- [25] EGRID. EGRID 2009 data; 2013.
- [26] Dolan SL, Heath GA. Life cycle greenhouse gas emissions of utility-scale wind power systematic review and harmonization. *J Indus Ecol* 2012;16:S136–54.
- [27] Hsu DD, Donoghue PO, Fthenakis V, Heath GA, Kim HC, Sawyer P, et al. Life cycle greenhouse gas emissions of crystalline silicon photovoltaic systematic review and harmonization. *J Ind Ecol* 2012;16:S122–35.
- [28] O'Donoghue PRO, Heath GA, Dolan SL, Vorum M. Life cycle greenhouse gas emissions of electricity generated from conventionally systematic review and harmonization. *J Ind Ecol* 2014;18:125–44.
- [29] Carabajales-Dale M, Barnhart CJ, Brandt AR, Benson SM. A better currency for investing in a sustainable future. *Nat Clim Change* 2014;4:524–7.

This page intentionally left blank

Chapter 19

Small-Scale Wind Turbines

Patrick A.B. James and AbuBakr S. Bahaj

University of Southampton, Southampton, United Kingdom

Email: a.s.bahaj@soton.ac.uk

19.1 INTRODUCTION

This chapter deals with micro and small wind turbines. Micro-wind turbines are typically defined as having a rated power up to 1.5 kW_p (where p refers to peak power) and their most widely used application is in yachts for battery charging. Small wind turbines are rated between 1.5 and 100 kW_p and are generally free standing, pole or tower mounted turbines. Small wind turbines at the lower end of this range are sometimes used in off-grid systems, but turbines above 20 kW_p are almost always grid connected (Fig. 19.1). The majority of micro and small wind turbines are horizontal axis three blade designs. Vertical axis small wind turbines (VAWT) represent a small fraction of the market despite their claimed performance benefits over horizontal axis turbines particularly in relation to turbulent wind response.

This chapter focuses on small wind turbines in the United Kingdom over the past decade (2005–15), which represents a period of “boom and bust” for building mounted micro-wind turbines in particular. The sector was trying to break out from yacht battery charging to the emerging grid connected micro-generation sector during this period (Figs. 19.2–19.5).

Grid connected micro-generation carries high-upfront capital costs, which is often the key barrier to commercial uptake. To encourage “early adopter” take up of a new technology, grants are often initially used to cover a fraction of the capital cost. Later as the market penetration of a technology grows, more radical policy approaches such as enabling businesses to apply enhanced capital allowances to micro-generation investment or feed in tariffs may emerge [2,3].

Grant subsidies are, however, not without their problems. Whilst they enable micro-generation technologies to become visible to the public and so encourage wider take-up, as a subsidy they financially reward installation of a system and not generation. This is a fundamental weakness of grant subsidies; it risks rapid deployment of a technology with potentially limited regard to the

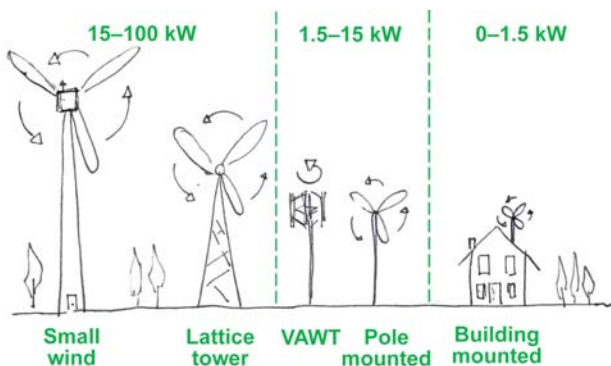


FIGURE 19.1 Small and micro-wind turbine scales, 1–100 kWp.

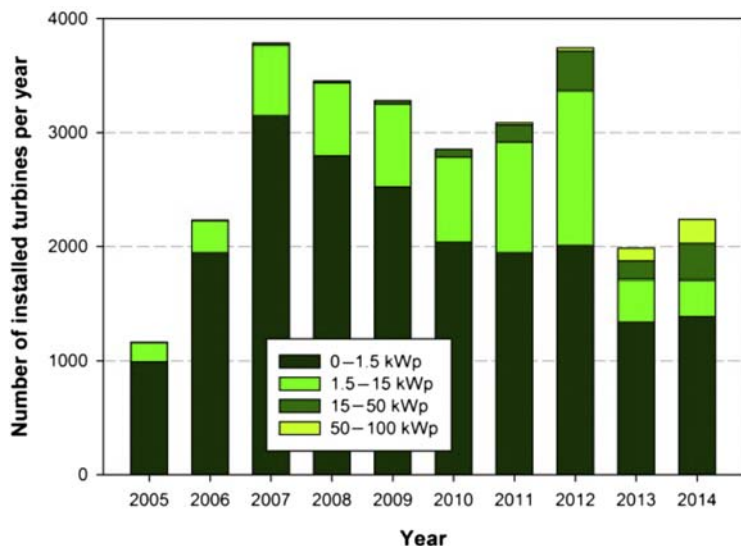


FIGURE 19.2 Number of installed small and micro-wind turbines per year by size category. 2005–14 in the United Kingdom. Data source RenewableUK (2015). Small and medium wind uk market report, RUK-003-5, March 2015 [1].

long-term performance. Poor energy yield performance is to the detriment of primarily the turbine owner but also to the grant funder in the longer term. The installer, however, has already been paid and whilst reputational damage may occur, this may take several years to emerge and will affect the wider industry.

In the case of micro-wind turbines, the predictive performance problem is exacerbated by the fact that the wind resource at a site is very difficult to quantify with any level of confidence without undertaking prior

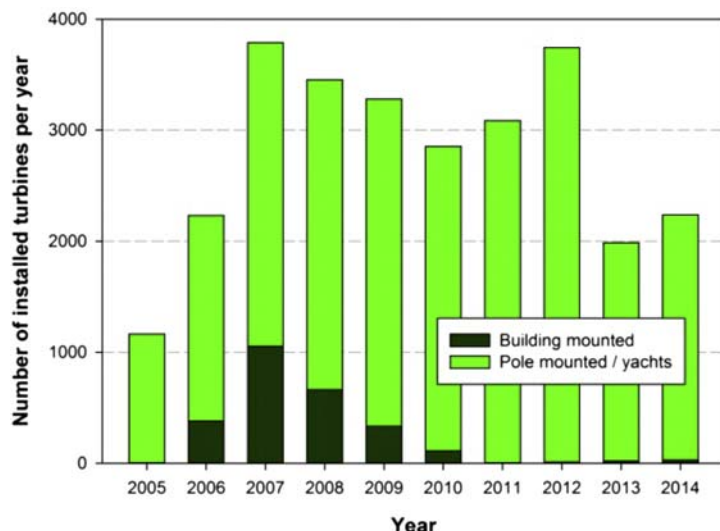


FIGURE 19.3 Number of installed small and micro-wind turbines per year by application sector, building mounted compared to pole mounted and marine. 2005–14 in the United Kingdom. Data source RenewableUK (2015). Small and medium wind uk market report, RUK-003-5, March 2015.

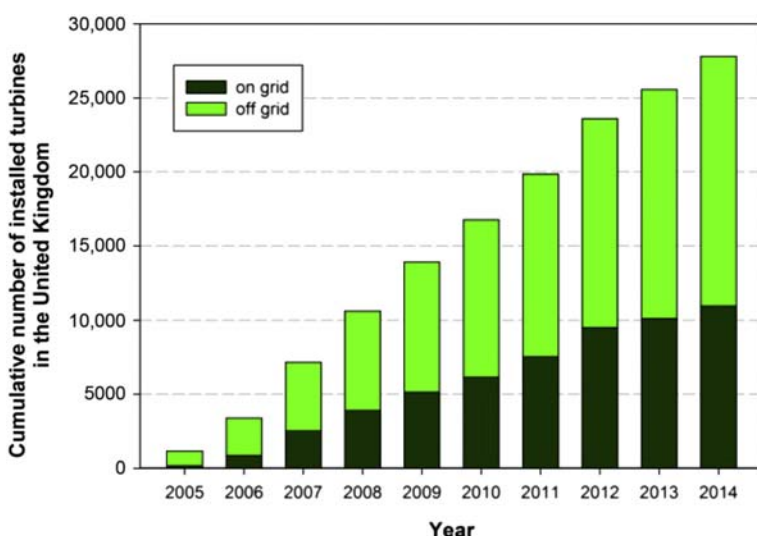


FIGURE 19.4 Cumulative number of installed small and micro-wind turbines both “on” and “off” grid. 2005–14 in the United Kingdom. Data source RenewableUK (2015). Small and medium wind uk market report, RUK-003-5, March 2015.

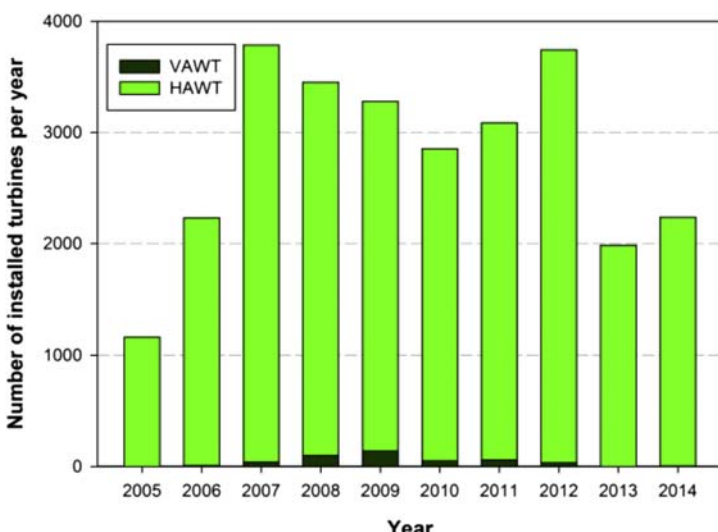


FIGURE 19.5 Number of installed horizontal axis (HAWT) and vertical axis (VAWT) small and micro-wind turbines ($<100\text{ kWp}$) per year. 2005–14 in the United Kingdom. *Data source RenewableUK (2015). Small and medium wind uk market report, RUK-003-5, March 2015.*

measurements. Field measurements are expensive to undertake, even placing an anemometer in an appropriate location for 6–12 months would cost at least £1000. This cost alone would make most micro-wind turbines financially unattractive. For installers undertaking site wind measurements also delays the actual deployment of the turbine and the installer payment.

Guidance documents in the United Kingdom at this time [4,5] stated that the threshold wind speeds should be 5 m s^{-1} for installation. The primary data source for this information was the Numerical Objective Analysis Boundary Layer (NOABL) wind speed modeling tool [6] and underlying UK weather station dataset. The NOABL tool was developed as a wind resource assessment for large-scale onshore wind turbines located in clean air, rural locations. The modeling interpolates wind speeds from meteorological weather stations across the entire UK assuming rural land form with no obstructions throughout. If NOABL is used to assess wind speeds without the use of correction factors to account for built form density, it will significantly overestimate the wind speed resource. The tool was never developed with micro-wind turbines as the application but it has become the starting point for site resource assessment and this was part of the problem in the United Kingdom.

In 2008 the British Wind Energy Association (BWEA), now RenewablesUK, published its annual report of the state of the micro-wind industry [7]. It is instructive to look at some of the data published for this year in terms of the claimed typical load factors for small wind turbines and market projections. In the United Kingdom, large onshore wind farms have an average

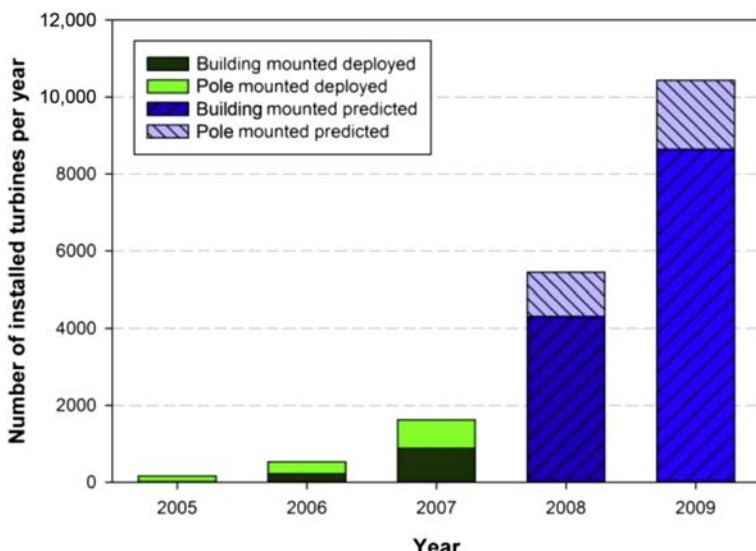


FIGURE 19.6 British Wind Energy Association (BWEA) Small wind report 2008. Annual building and pole mounted turbine installations (2005–07) and year 2007 projections for 2008 and 2009 (all sizes below 15 kWp). Data source British Wind Energy Association. BWEA small wind systems. UK Market Report 2008, (now renewableUK); 2008.

load factor of around 28% with offshore wind farms around 38% [8]. The 2008 BWEA report provides average Annual Energy Production (AEP) data, which corresponds to load factors of 10% and 17% for building mounted and small pole mounted wind turbines, respectively. The building mounted turbine market was predicted to grow by over 400% to about 11,700 turbines annum⁻¹ in the United Kingdom from 2007 to 2009 as highlighted in Fig. 19.6.

B&Q, a major DIY (Do-It-Yourself) retailer started to sell a 1.0 kWp wind turbine, the WS1000, produced by Windsave Ltd. in 2006. The micro-wind turbine was sold as a complete, fully installed system (turnkey solution of turbine, grid connected inverter and wiring). The total cost of the B&Q Windsave system was £1498 fully installed.

To stimulate the micro-generation sector, United Kingdom launched the Low Carbon Buildings Programme [9] in April 2006, funding projects across four streams: households, communities, medium scale, and large scale. In total the government funded $\text{£}91 \times 10^6$ (£91 million) of micro-generation demonstration projects. In relation to small wind, 940 wind turbines (0.5–50 kWp) were installed through LCBP (total wind turbine grant value $\text{£}4.7 \times 10^6$ (£4.7 million)), representing 4.9% of all micro-generation installations and 5.1% of the total budget.

1. *Households:* 762 wind turbine grants awarded at an average value of £2304, total LCBP cost of $\text{£}1.8 \times 10^6$ (£1.8 million). Maximum grant

subsidies were £1000 kW⁻¹ installed, up to a maximum of £5000 per installation subject to an overall 30% limit of the installed cost (exclusive of VAT). Forty-four grants with a value of £24 510 were returned (39 of which were building mounted turbines) due to de-installation of systems owing to issues of poor performance

2. *Communities*: 18 wind turbines, average grant £15 726
3. *Medium scale*: 27 wind turbines, average grant £17 809 and
4. *Large scale*: 1 wind turbine, average grant £32 924.

It is instructive to consider what the 2008 report BWEA claimed typical load factors [7] would mean for the economics of such a Windsave turbine.

$$\begin{aligned}\text{Annual generation (kWh)} &= \text{Load factor (\% / 100)} \times \text{rated power (kW)} \\ &\quad \times \text{hours in the year} \\ &= 0.10 \times 1.0 \times 8760 = 876 \text{ kWh a}^{-1}\end{aligned}$$

Considering the standard electricity tariff of 12p/kWh this generates an avoided import value of £105/annum.

With an LCBP grant of £500 on proof of installation, this would give a simple payback time of less than 10 years at a discount rate of 0%. At the time, residential solar photovoltaic (PV) systems were in comparison far more expensive at around £8000 for a 3 kWp system. There was also no feed in tariff in place at this point in the United Kingdom. In addition, an outlay of £1500 was seen by the micro-generation industry as a more affordable “discretionary” purchase for early adopters, compared with the far higher cost in 2006 of a home PV system.

By 2006, the micro-wind turbine market was growing rapidly in the United Kingdom, primarily driven by companies such as B&Q’s selling of the Windsave WS1000 turbine. However, concerns began to emerge about the claimed energy performance figures of turbines, especially in the built environment. The *WarwickWindTrial* study of 26 turbines in locations ranging from “theoretically poor” to “theoretically excellent” produced an average load factor of 4.1% in [10] 2009. The BWEA’s 2008 published average load factor figures of 10% (building mounted) and 17% (pole mounted) started to look very optimistic. B&Q suspended the selling of micro-wind turbines in February 2009 following the WarwickWindTrial report, pending the findings of the larger national micro-wind trial undertaken by the Energy Saving Trust [11].

In July 2009 the National Micro-wind Trial report, “*Location, Location, Location: Domestic small-scale wind field trial report*” was released [11]. B&Q offered all micro-wind turbine customers a full refund and free decommissioning of their system. Windsave, the supplier to B&Q filed for bankruptcy in September 2009 when B&Q effectively ended their relationship with them.

The 2008 BWEA Small wind systems report uses the assumption that building mounted or off-grid (on a boat) turbines (up to 1.5 kW) have an average load factor of 10% [7]. There is no differentiation in load factor regardless of the application. The assumed load factor increases to 17% for free standing, pole mounted turbines, but again is regardless of the application (1.5–10 kW).

This EST micro-wind field trial was established to address a number of key questions:

1. Are UK manufacturers' performance claims in terms of predicted annual electricity generation realistic?
2. What is the relationship between NOABL wind speed data for a location and measured turbine hub-height wind speeds? Are the proposed correction factors for NOABL wind speeds to real sites realistic?
3. How sensitive are micro-wind turbines to turbulence and to what extent does this compromise theoretical performance?
4. What is the future potential market for building mounted and pole mounted micro-wind turbines in the United Kingdom?

19.2 THE FUNDAMENTAL CONCERN FOR MICRO-WIND: THE WIND RESOURCE

The fundamental issue for micro-wind is the wind resource. It does not matter if a micro-wind turbine is able to rapidly respond to changing wind speeds or work well in turbulent wind if the overall wind resource is poor. To illustrate this issue, the example of the wind resource on the roof of a University of Southampton (UoS) building is considered (Fig. 19.7, weather station highlighted as yellow square). Southampton is located on the South Coast of the United Kingdom, it is a port city of around 250 000 people. The University is located to the north of the city in an urban area (orange square in Fig. 19.7). The weather station is on the top of a three storey building on the main campus. The prevailing wind is from the South West in the United Kingdom and in this direction the land falls away at the site as the campus is on a slope. The roof of the building would be considered to be fairly unobstructed in the prevailing wind direction for an urban environment (yellow arc in Fig. 19.7).

NOABL provides the predicted wind speed for any 1 km grid square in the United Kingdom at 45 m, 25 m, and 10 m above ground level (AGL). These wind speeds are for clean air, unobstructed terrain. The University of Southampton NOABL 1 km grid square reference 445,111 (SU4511), NOABL output: 45 m AGL = 6.5 m s^{-1} 25 m AGL = 6.0 m s^{-1} , 10 m AGL = 5.2 m s^{-1}

The NOABL-MCS correction factor [4] for the University of Southampton weather station anemometer would be $0.35 \times \text{NOABL} = 1.8 \text{ m s}^{-1}$, to account for built up location and an anemometer height of 2 m above the roof. This would correspond to a building mounted turbine where the turbine blade tip



FIGURE 19.7 A Location of University of Southampton weather station (top yellow) in the northern part of the port city of Southampton. The prevailing wind is from the South West (yellow arc) where the topography slopes away from the building. *Aerial images adapted from Google Earth.*

comes within 2 m of the roof during a rotation (dense urban 35% correction factor, see [Table 19.1](#)).

The Microgeneration Installation Standard MIS3003 issue 2.0 [4] has three wind speed categories as shown in [Table 19.1](#). The 2015 revision [12] increased this to five essentially splitting the rural category into three, to provide better prediction in the key rural sector and providing better hub-height correction. The underlying scaling factor analysis remains unchanged and relates to the work of Harris and Deaves in 1980 [13]. The stated threshold wind speed for installing a micro-wind turbine is 5.0 m s^{-1} , which this site achieves as a NOABL estimate, although with urbanization correction applied this estimate is reduced to 1.8 m s^{-1} . [Fig. 19.8](#) compares a NOABL wind speed average as a Weibull distribution with a shape factor of two with the observed wind speed data over a 12 month period. The observed wind speed has an average of 2.35 m s^{-1} and fits well to a Weibull distribution with a shape factor of two.

TABLE 19.1 NOABL MCS3003, Issue 2.0 (2010) Wind Speed Correction Factors for Level of Urbanization of a Site and Proximity of a Turbine to Roof and Nearest Obstructions

NOABL correction classification	Proximity of turbine to roof or nearest obstruction	Lowest point of turbine above roof (m)	NOABL wind speed scaling factor
Rural <i>Open country with occasional houses and trees</i>		12	100%
		7	94%
		2	86%
		0	82%
Low-rise urban/suburban <i>Typically town/village situations with other buildings well-spaced</i>		6	67%
		4	61%
		2	53%
		0	39%
Dense Urban <i>City centers of most closely spaced four-storey buildings or higher</i>		10	56%
		5	51%
		3	44%
		1	35%

Source: Scaling factors derived from data given in Harris RI, Deaves DM. The structure of strong winds. Wind engineering in the eighties, Proc. CIRIA Conference, London, November 12–13; 1980.

This one graph serves to highlight the issue for micro-wind, uncorrected clean air wind speeds are not appropriate and should not be used.

Fig. 19.9 compares the predicted yield of a Windsave WS1000 turbine if mounted at the position of the University of Southampton anemometer in terms of the NOABL wind speed and the measured anemometer. The power curve for the WS1000 turbine has been applied to the wind speed cubed but

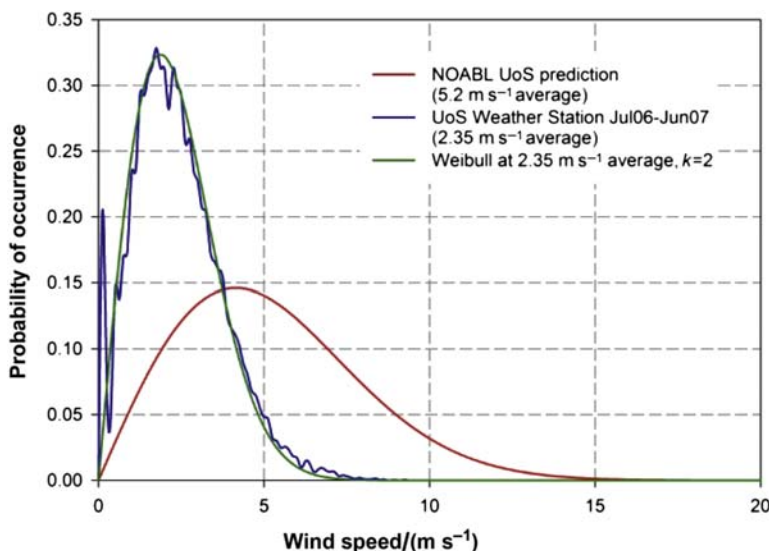


FIGURE 19.8 Comparison of NOABL wind speed estimate and measured data for the roof of B37, University of Southampton (UoS) (July 2006–June 2007).

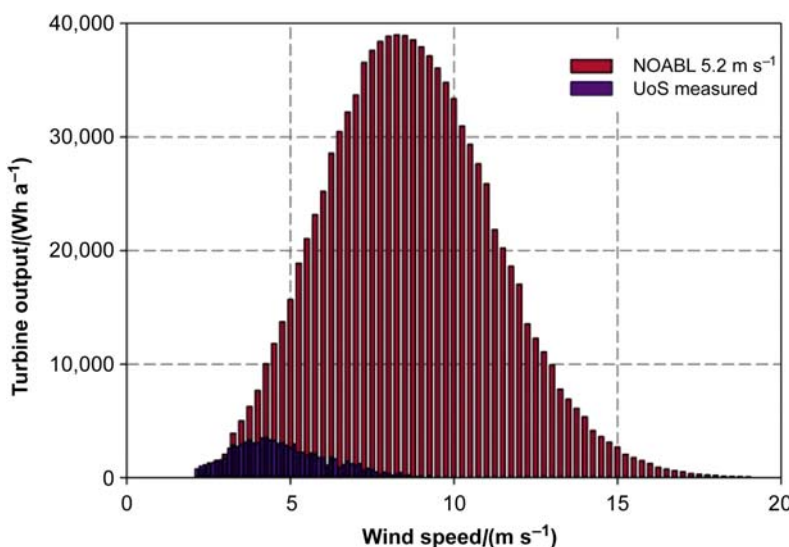


FIGURE 19.9 Comparison of predicted output (0.5 m s⁻¹ width wind speed binned distribution) from a WS1000 building mounted micro-wind turbine at the University of Southampton, comparing uncorrected NOABL prediction (836 kWh a⁻¹ and actual wind speed measurements (94 kWh a⁻¹, where “a” refers to annum).

with no cut-in or cut-out speed has been applied. The predicted energy output is shown as a binned distribution of the wind speed cubed (0.5 m s^{-1} bin width). The NOABL wind speed gives an estimated annual yield of 836 kWh a^{-1} , compared to 94 kWh that can be achieved for the actual wind resource. In reality the WS1000 turbine has a cut-in speed of 4.5 m s^{-1} so the potential generation is around a half of the estimated 836 kWh .

This analysis does not consider the power requirements of the inverter, which is a further complication for grid connected systems in particular. In the United Kingdom there are specific performance characteristics that inverters must comply with, for grid connection. Systems less than 16 A phase^{-1} (3.68 kWp single phase) follow guidance under Engineering Recommendation G83/2 (2012), (*Recommendations for the Connection of Type Tested Small-scale Embedded Generators (Up to 16 A per Phase) in Parallel with Low-Voltage Distribution Systems* [14]). Systems above 16 A need to be compliant to G59 [15]. In the case of G83/2 there is a requirement that a minimum reconnection period of 20 seconds occurs when an inverter senses the grid voltage and frequency within accepted limits. Therefore an inverter must always be synchronized with the utility grid to be able to immediately export generated power. In the case of PV, there is always enough DC power on even the dullest of days from a PV array to power the inverter and keep it synchronized. Micro-wind is more problematic; if the wind is infrequent and gusty, the inverter may be off and may not complete its synchronization cycle in time to export the potential generation from a gust. For this reason, a micro-wind inverter may take its synchronization power from the utility grid rather than the DC side as is the case with PV. In some of the field trial examples shown in this chapter, this can actually lead to a “negative load factor” where, in extreme cases, the parasitic load of the turbine is actually greater than the annual generation (see case study example of an *Urban Building Mounted Turbine*, Fig. 19.22). If we consider that an inverter might have a parasitic AC load of up to 10 W , this would correspond to approximately 88 kWh a^{-1} , which in the case of the University of Southampton’s example given earlier and Fig. 19.9, would cancel out all theoretical generation.

It is with these performance concerns in mind that the UK’s National Micro-wind Field Trial became established building on the work of the WarwickWindTrials [10]. Under the UK’s National Micro-Wind Trial nine different types of turbines were assessed; five building mounted and four pole mounted (Table 19.1). These turbines had predominantly either been installed through the Low Carbon Buildings Programme [9] or were Windsave turbines purchased through B&Q. Table 19.1 shows the specifications of the turbines and it is interesting to note that there is no specific wind speed at which manufacturers choose to rate their turbine. A total of 64 building mounted and 22 pole mounted turbines were monitored for a period of 12 months across urban, suburban, and rural locations (Table 19.2).

TABLE 19.2 Specifications of Micro-Wind Turbines That Participated in the UK's National Micro-Wind Field Trial

Turbine	Number in Trial	Diameter/ (m)	Rated Power/ (kW)	Rated wind speed/ (m s^{-1})	Cut-in wind speed/ (m s^{-1})	Cut-out wind speed/ (m s^{-1})
Building Mounted Turbines						
Air dolphin	5	1.8	1.0	12.0	2.5	50
Ampair 600	14	1.7	0.6	12.5	3.5	None
Eclectic D400	4	1.1	0.4	15.5	2.5	None
Swift	5	2.1	1.5	12.5	2.3	None
Windsave, WS1000	36	1.75	1.0	12.5	4.5	15
Free Standing, Pole Mounted Turbines						
Eoltec	5	5.6	6.0	11.5	2.7	None
Iskra AT5-1	6	5.4	5.0	11.0	3.0	None
Proven 2.5	4	3.5	2.5	12.0	2.5	None
Proven 6	7	5.5	6.0	12.0	2.5	None

NOTE: Specifications relate to micro-wind turbines installed at the time of the UK's National Micro-wind Field Trial (2008).

In addition to the fully monitored sites of UK's *National Micro-wind Field Trial*, monthly generation readings from an additional 68 micro-wind turbines were provided to the trial. Building mounted and pole mounted turbines are considered separately in the next two sections. The *UK's National Micro-wind Field Trial* study forms the basis of the data presented here and further information can be found in two *Energy Policy* publications by the authors [16,17].

19.3 BUILDING MOUNTED TURBINES

Fig. 19.10 shows the distribution of building mounted wind turbines in the United Kingdom for the national micro-wind field trial. Five case study sites are

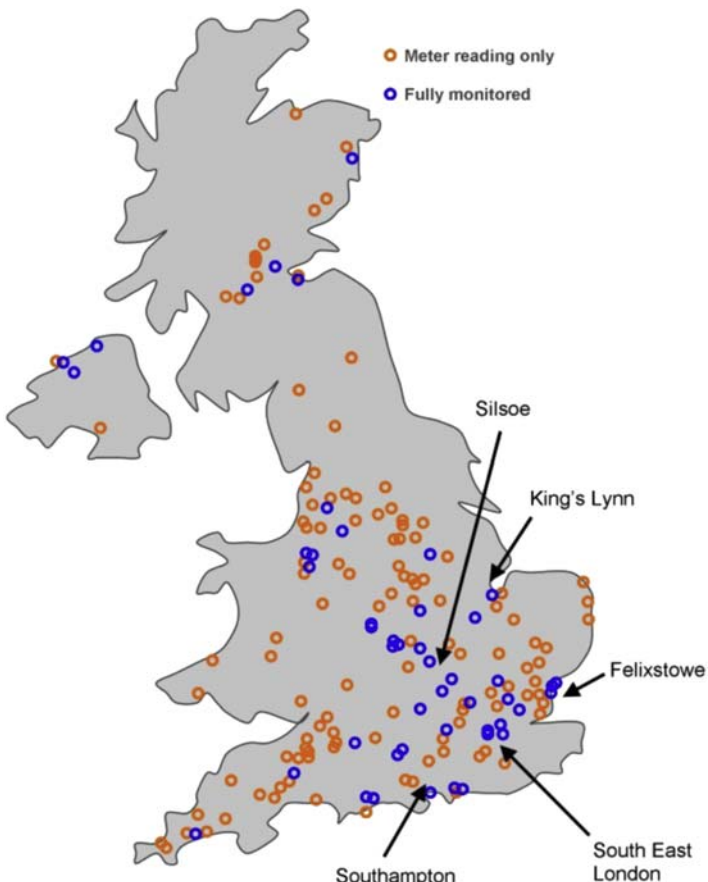


FIGURE 19.10 Location of building mounted turbines of the national micro-wind trial. Blue circles, Fully monitored sites; Orange circles, meter readings only. Five case study sites are highlighted: Southampton (Dense Urban), South East London (Dense Urban), Felixstowe (Low-rise urban/suburban), King's Lynn (Rural), and Silsoe (Rural).

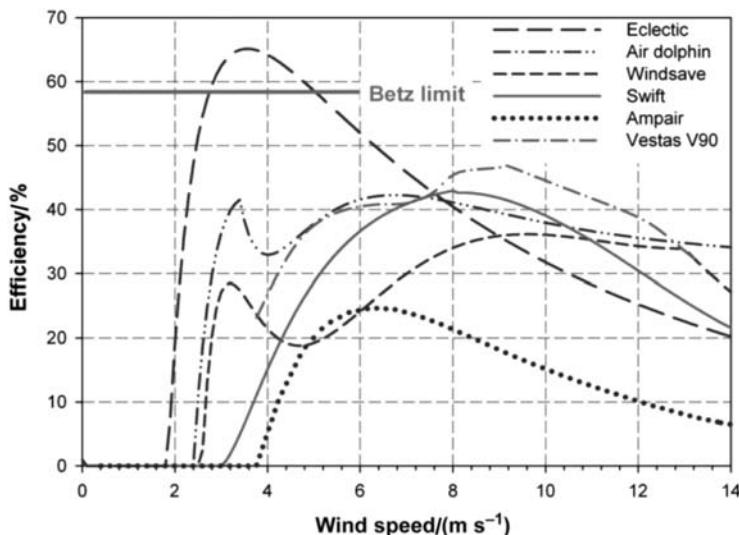


FIGURE 19.11 Calculated manufacturers' turbine efficiency as a function of wind speed from manufacturers' stated power curve (at time of field trial).

highlighted: Southampton (Dense Urban), South East London (Dense Urban), Felixstowe (Low-rise urban/suburban), King's Lynn (Rural), and Silsoe (Rural).

It is instructive to compare the manufacturer's published power curves of the various building mounted turbines with a commonly used large-scale turbine of the period, a 1.8 MW Vestas V90. Peak efficiencies at realistic wind speeds for operation (above 4 m s^{-1}) are around 40% and as you would expect are lower than that of the large V90 turbine (45%) and occur at a lower wind speed (Fig. 19.11). The corresponding AEP is shown in Fig. 19.12. The Windsave WS1000 is predicted to generate about 900 kWh a^{-1} for an average annual wind speed of 5 m s^{-1} . It is interesting to note that this AEP is similar to that of 1 kWp of roof mounted PV in the South of the United Kingdom [18], but obviously at higher capital cost that the micro-wind turbine.

The initial data monitoring testing for the field trial was undertaken at Silsoe in Bedfordshire. An industrial shed surrounded by low lying fields was used to assess the performance of a WS1000 turbine (Fig. 19.13).

Silsoe is not in a particularly windy location in the United Kingdom, with a stated NOABL wind speed of 4.6 m s^{-1} . The site is classified as rural and has a 2010 MIS3003 MCS 0.82 correction factor (3.8 m s^{-1}). Fig. 19.14 compares the 5 minute average anemometer measurements with turbine power over a period of four winter months (periods of highest wind speeds). The power curve shown is interpolated from the measured dataset and shows close agreement with the manufacturer's published data. It is interesting to

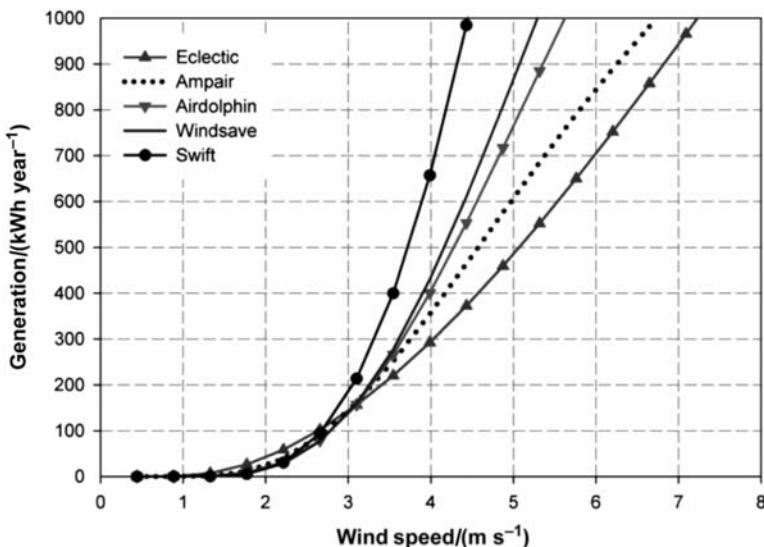


FIGURE 19.12 Annual Energy Production (AEP) estimates for building mounted wind turbines as a function of annual average wind speed, assumed Weibull distribution with a shape factor of 2.0.

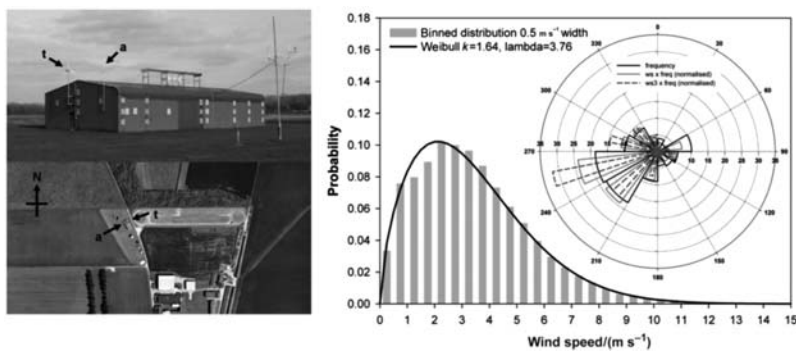


FIGURE 19.13 Windsave WS1000 turbine (*t*) and ultrasonic anemometer (Vaisala WMT50, *a*) on South West side of industrial shed surrounded by low lying fields. Silsoe site measured wind speed data, March 2008–February 2009. NOABL wind speed 4.6 m s^{-1} , NOABL-MCS (2010) 3.8 m s^{-1} [4.6].

note the scatter in power points above 5 minute average wind speeds of 11 m s^{-1} . This is where, over a 5 minute period the peak wind speed may exceed the cut-out speed of 15 m s^{-1} leading to a loss of output.

The measured wind speed distribution and turbine performance over a 12 month period (March 2008–February 2009) is shown in Figs. 19.13 and 19.15, respectively. The overall generation was 244 kWh (103 kWh m^{-2}

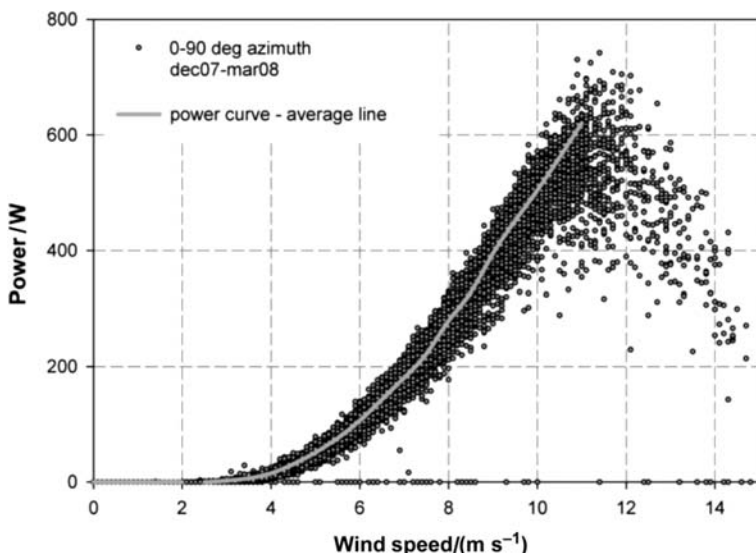


FIGURE 19.14 Comparison of WS1000 published power curve and Silsoe site measurements, 5 minute averages.

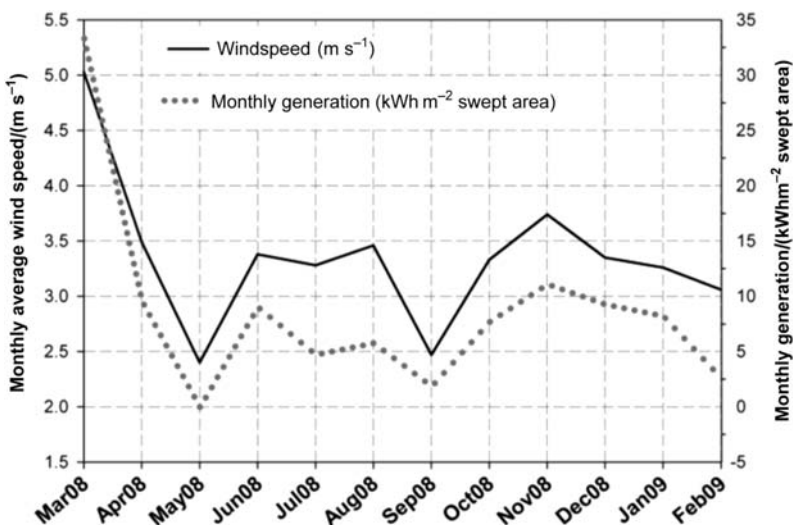


FIGURE 19.15 Twelve months of Silsoe site WS1000 micro-wind turbine performance data. March 2008–February 2009. Average wind speed 3.4 m s^{-1} , annual load factor 2.8%.

swept area), with an average wind speed of 3.4 m s^{-1} . This corresponds to a load factor of 2.8 %.

The data monitoring at the Silsoe site was reconfigured to record 1 second interval data of wind speed and power to assess the speed of response

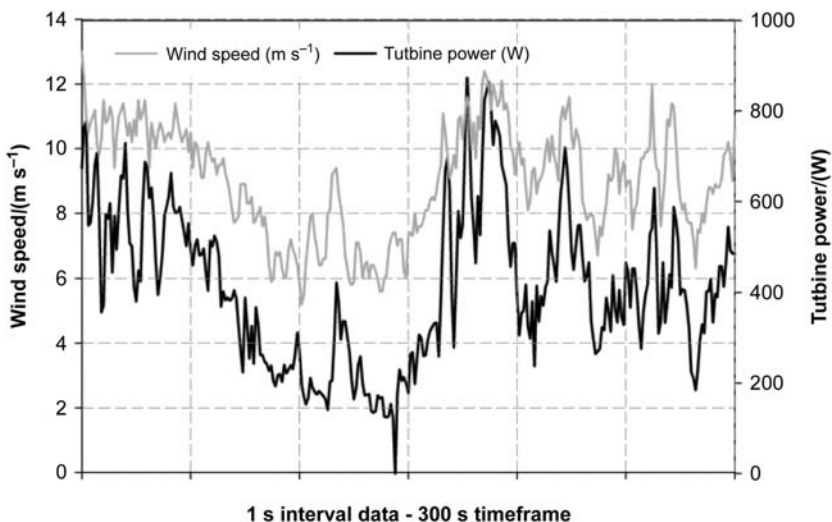


FIGURE 19.16 One-second interval wind speed and turbine power response, Windsave WS1000 turbine at Silsoe.

of the WS1000 turbine. Fig. 19.16 shows the wind speed and turbine power output over an example 300 s period. There is a clear correlation between wind speed and power output suggesting the response of the turbine is indeed fast of the order of seconds. If one compares the Turbulent Intensity, TI, defined as the (*standard deviation of wind speed over a 10 minute period*)/(*average wind speed over a 10 minute period*), over a 10 minute period with the output of the turbine, this rapid response is evident (Fig. 19.16).

Periods of high turbulent intensity corresponds to rapid changes in wind speed. The energy (proportional to wind speed cubed) in 10 minutes of high TI will be larger than for a low TI period. This is illustrated in Fig. 19.17, where the power output of the turbine as a function of TI (low and high) is shown. High TI periods produce greater power output from the turbine than periods of lower TI with the same average wind speed. The performance benefit of high TI reduces at higher wind speeds as it increases the probability of the cut-out wind speed (15 m s^{-1}) being reached in that 10 minute period.

19.3.1 Rural Building Mounted Turbine

- Fig. 19.18 shows a rural class site [4] building mounted turbine near King's Lynn. The prevailing wind is from the South West with an average wind speed of 3.65 m s^{-1} . The NOABL [6] and

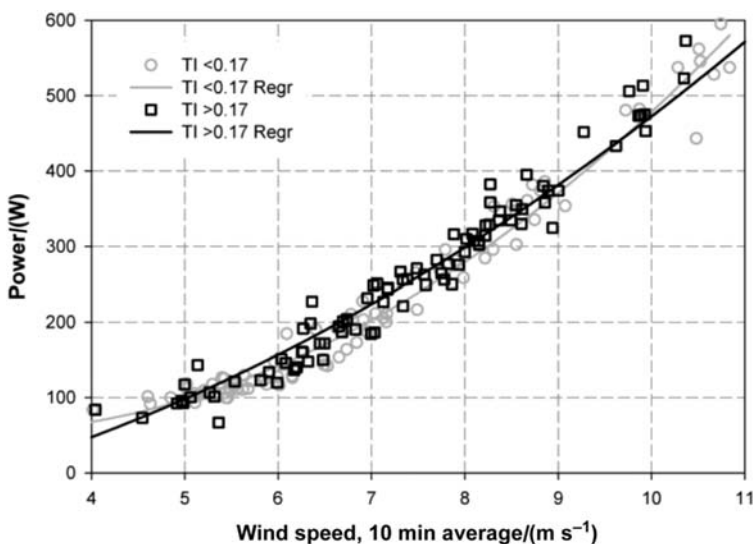


FIGURE 19.17 Power output as a function of wind speed turbulent intensity, TI, for a WS1000 turbine, averaged over a 10 minute period. Higher turbulent intensity results in higher power output from the turbine, demonstrating the rapid response of the turbine.

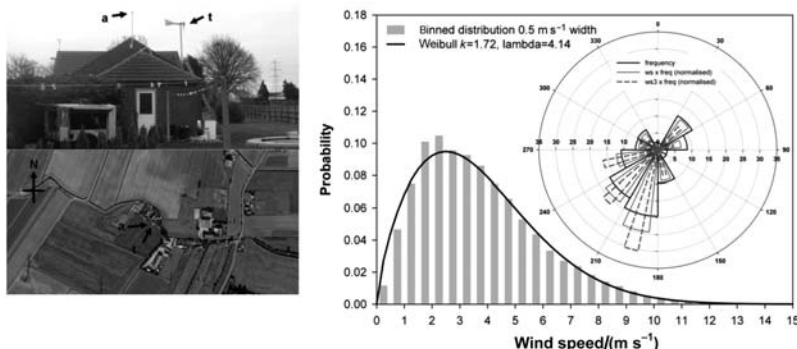


FIGURE 19.18 Windsave WS1000 turbine (*t*) and ultrasonic anemometer (Vaisala WMT50, *a*) on rural house near King's Lynn. Site measured wind speed data, March 2008–February 2009. Average wind speed 3.65 m s^{-1} . NOABL wind speed 5.0 m s^{-1} [6]. NOABL-MCS (2010) 4.3 m s^{-1} [4].

NOABL-MCS (2010) [4] wind speed estimates for the site are 5.0 and 4.3 m s^{-1} , respectively. The measured load factor, including inverter power draw was 3.1% over a 12 month monitoring period (Fig. 19.19).

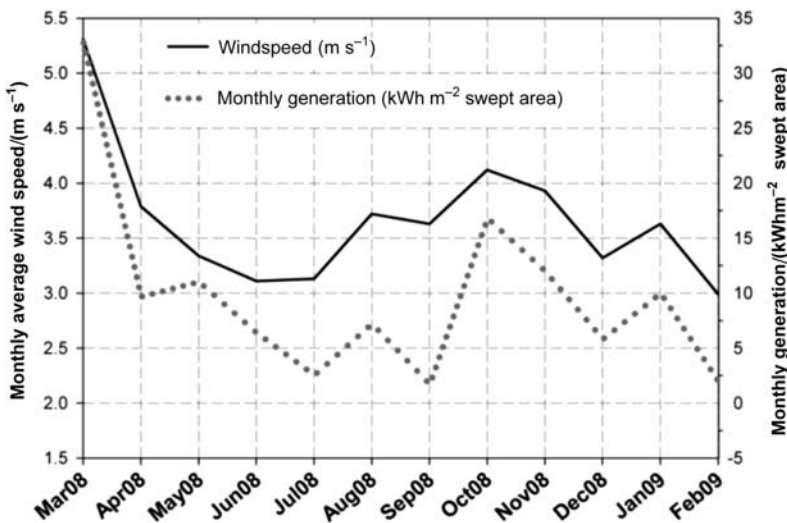


FIGURE 19.19 Measured wind speed at King's Lynn site and WS1000 wind turbine monthly output. March 2008–February 2009. Average wind speed 3.65 m s^{-1} , load factor 3.1%.

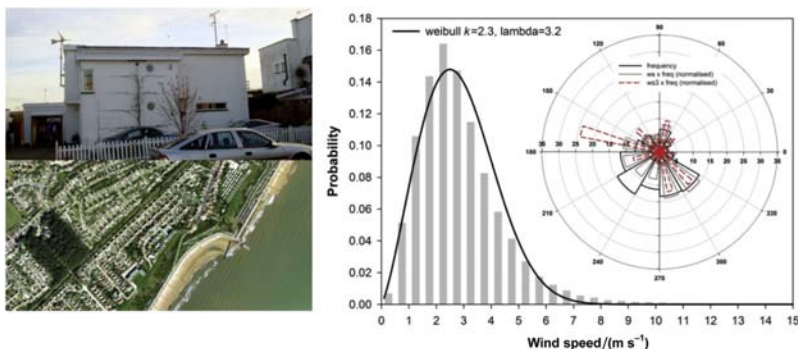


FIGURE 19.20 Windsave WS1000 turbine (*t*) and ultrasonic anemometer (Vaisala WMT50, *a*) on house in coastal town of Felixstowe. Measured wind speed data, March 2008–February 2009. Average wind speed 2.83 m s^{-1} . NOABL wind speed 5.7 m s^{-1} . NOABL-MCS (2010) 2.2 m s^{-1} [4.6].

19.3.2 Suburban Building Mounted Turbine

Fig. 19.20 shows a coastal, suburban turbine in Felixstowe on the East coast of the United Kingdom. The NOABL [6] and NOABL-MCS (2010) [4] wind speed estimates for the site are 5.7 and 2.2 m s^{-1} , respectively. The measured wind speed was 2.83 m s^{-1} which resulted in an annual load factor of 0.6% (Fig. 19.21).

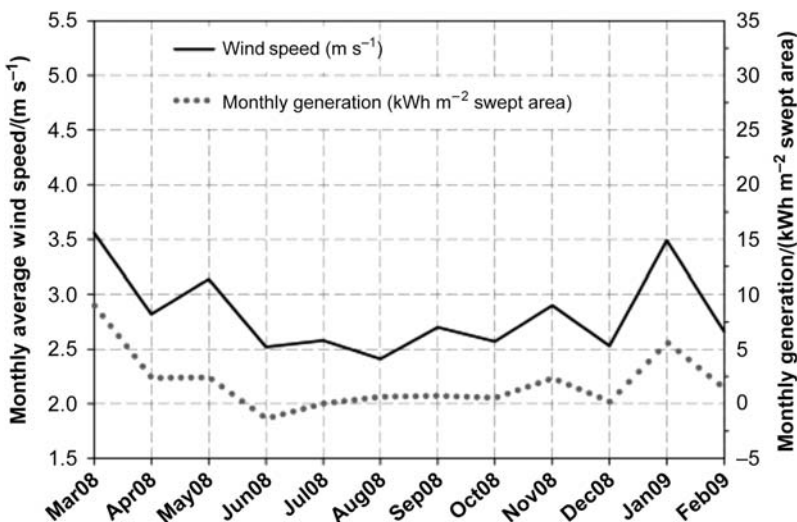


FIGURE 19.21 Measured wind speed at Felixstowe site and WS1000 wind turbine monthly output. March 2008–February 2009. Average wind speed 2.83 m s^{-1} , load factor 0.6%.

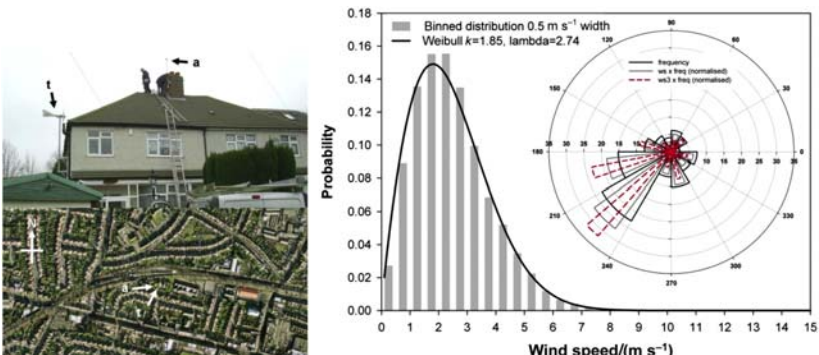


FIGURE 19.22 Windsave WS1000 turbine (*t*) and ultrasonic anemometer (Vaisala WMT50, *a*) on house in South London. Average wind speed 2.4 m s^{-1} . NOABL wind speed 5.0 m s^{-1} [6] and NOABL-MCS (2010) [4], 1.8 m s^{-1} .

19.3.3 Urban Building Mounted Turbine

Fig. 19.22 shows a highly urbanized site in South London. The turbine has been installed at the eaves height of the roof, whereas the wind speed anemometer is above the roof height. The NOABL and NOABL-MCS (2010) [4] wind speeds for the anemometer location are 5.0 and 1.8 m s^{-1} . The site is clearly not appropriate for micro-wind and this is reflected in the measured wind speeds and turbine output (Fig. 19.23). In this case, the parasitic AC demand of the inverter is actually greater than the generation of the turbine

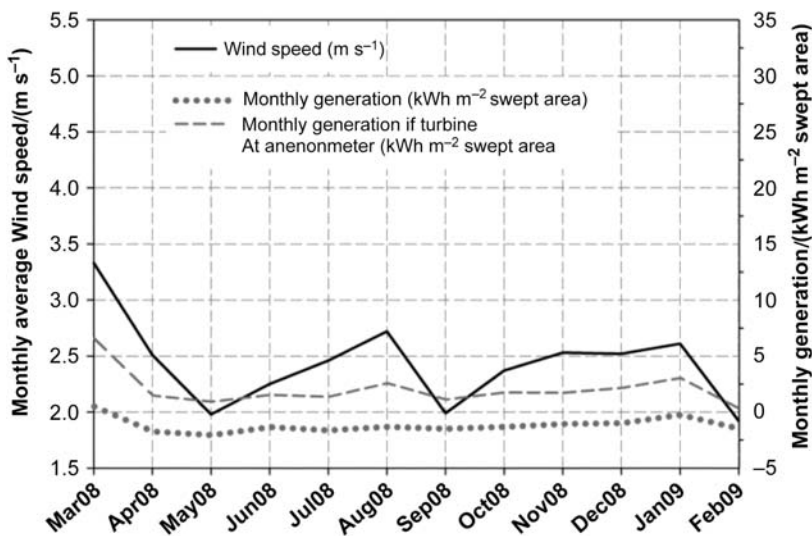


FIGURE 19.23 Measured wind speed at South London site and WS1000 wind turbine monthly output. March 2008–February 2009. Average wind speed 2.4 m s^{-1} , load factor -0.42% . Potential turbine generation if located at anemometer height is shown (dashed gray line).

resulting in an overall negative load factor. If the turbine has been located at the anemometer position, the higher generation would have just exceeded the inverter power requirements over the year.

19.3.4 Summary Findings: Building Mounted Turbines

Fig. 19.24 shows the performance analysis of the building mounted turbines. It is important to note that half of the urban turbines have a negative load factor (they consume more power than they generate over the year). The best performing rural wind turbines generated around $300 \text{ kWh m}^{-2} \text{ a}^{-1}$, which corresponds to a load factor of $\sim 8\%$. The field trial data has shown this very poor performance compared to the claimed typical load factor of 10%. Fig. 19.25 compares the measured wind speeds at the building mounted turbine sites with that predicted by NOABL-MCS [4]. The solid gray line shows a 1:1 (perfect) relationship between prediction and observation. For urban and rural sites there is a fairly even scatter on either side of the perfect fit line. The NOABL-MCS 2010 correction therefore appears appropriate for both Urban and Suburban sites. However, this correction merely serves to confirm that there is no wind resource in such locations. The threshold wind speed for installation of micro-wind turbine is 5.0 m s^{-1} . Only two sites in the trial achieved this design threshold, although no sites had a measured wind speed above 4.0 m s^{-1} . It appears that the NOABL-MCS 2010 [4] correction still represents an overestimate of wind resource for rural locations.

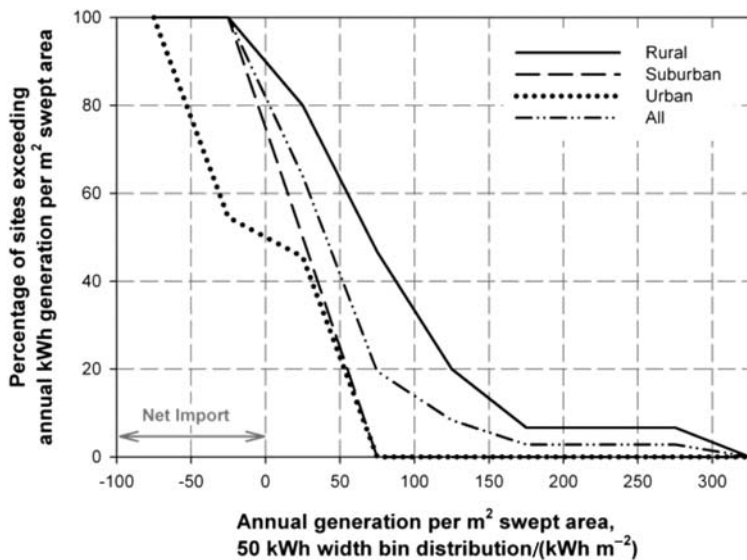


FIGURE 19.24 Binned distribution (50 kWh width) of building mounted micro-wind turbine sites, annual generation per square meter swept area, as a function of site type: Rural, Suburban, Urban.

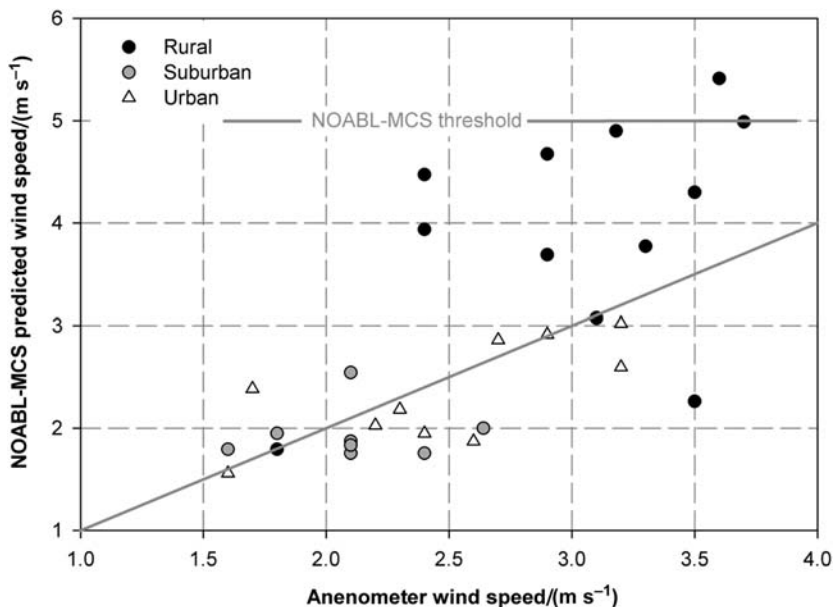


FIGURE 19.25 EST micro-wind trial building mounted turbine summary. Comparison between measured annual wind speeds at sites with NOABL-MCS 2010 estimates [4]. Rural NOABL-MCS 2010 correction [4] is seen to overestimate the wind resource.

19.3.5 Field Trial Observations: Pole Mounted Turbines

Fig. 19.26 shows the location of pole mounted turbines in the UK's National Micro-wind Trial. These are generally located on farmland in what would be considered as good wind resource locations.

The calculated manufacturer's efficiency curves and AEP as a function of wind speed are shown in Figs. 19.27 and 19.28. All the pole mounted turbines show very similar AEP predictions for the expected wind speed ranges (4.8 m s^{-1} annual average).

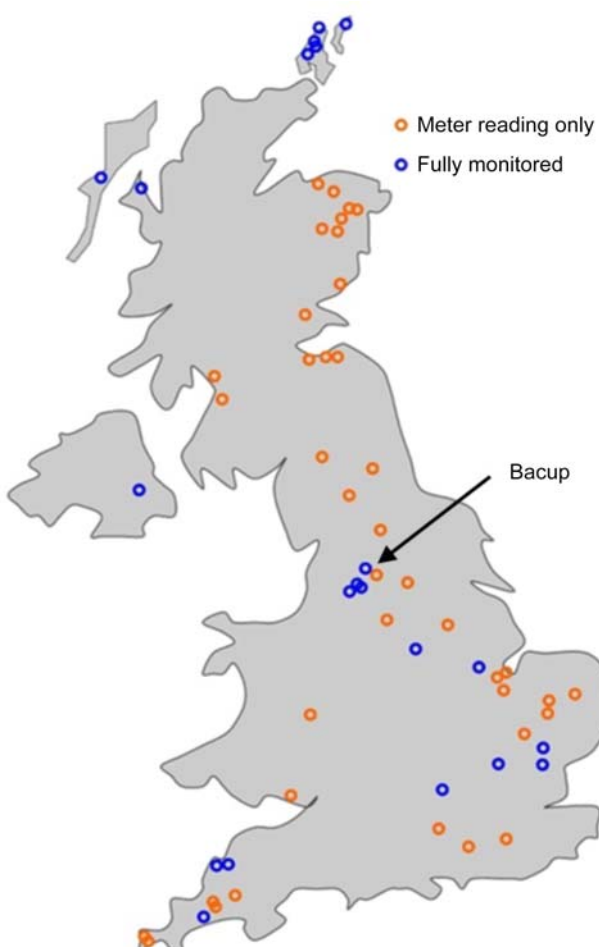


FIGURE 19.26 Location of Pole mounted turbines for UK's National Micro-Wind Trial. Case study site Bacup (Rural) is highlighted.

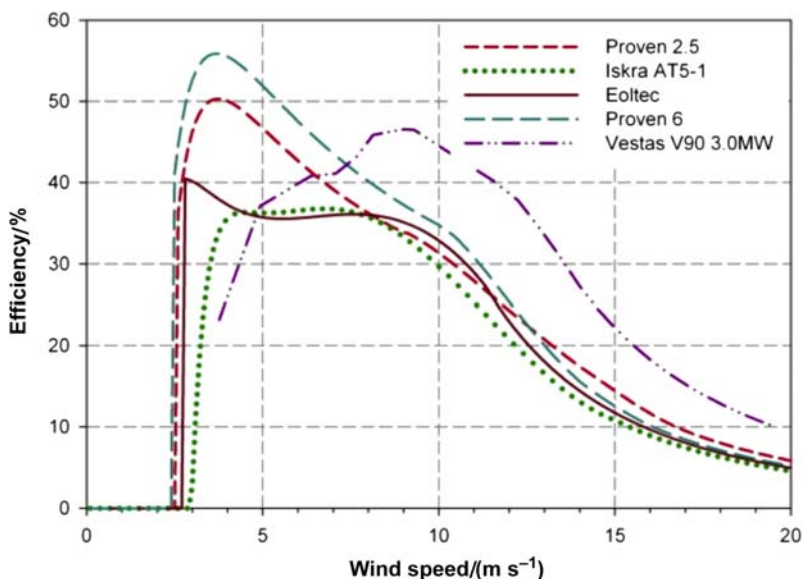


FIGURE 19.27 Calculated manufacturers' pole mounted turbine efficiency as a function of wind speed from manufacturers' stated power curve (at time of field trial).

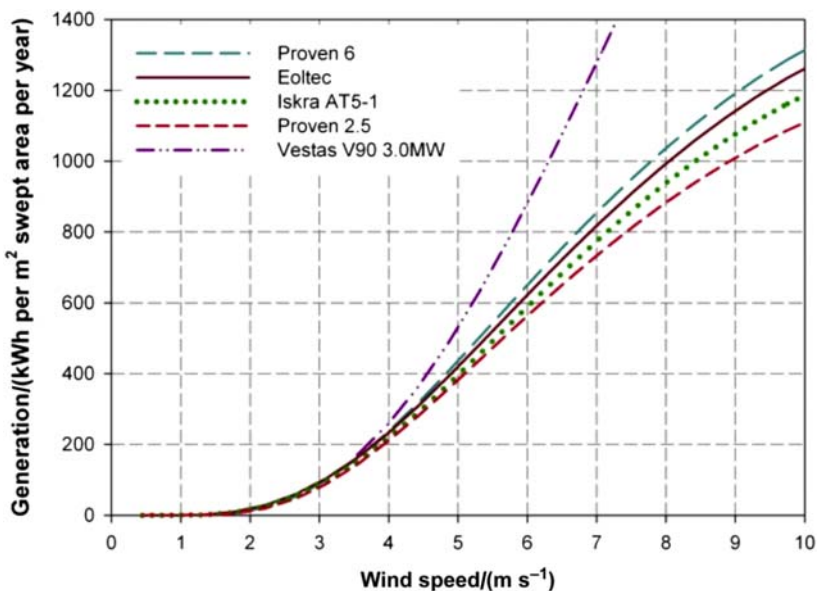


FIGURE 19.28 Annual Energy Production (AEP) estimates for pole mounted wind turbines as a function of annual average wind speed, assumed Weibull distribution with a shape factor of 2.0.

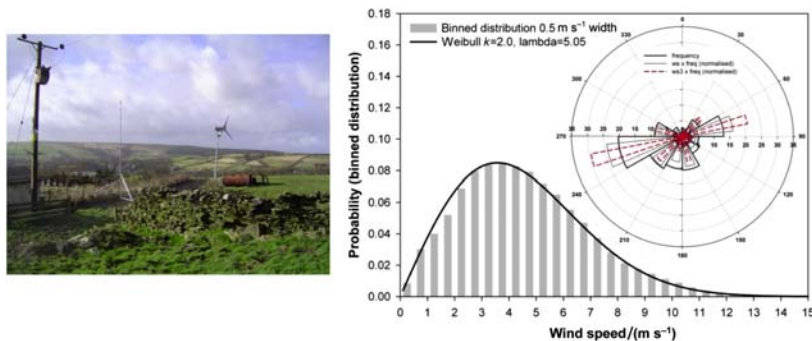


FIGURE 19.29 Proven 6 kW turbine and ultrasonic anemometer (Vaisala WMT50) on a farm near Bacup, South Pennines, Lancashire. Average wind speed 4.62 m s^{-1} . NOABL wind speed 7.7 m s^{-1} . NOABL-MCS 2010 wind speed 6.8 m s^{-1} .

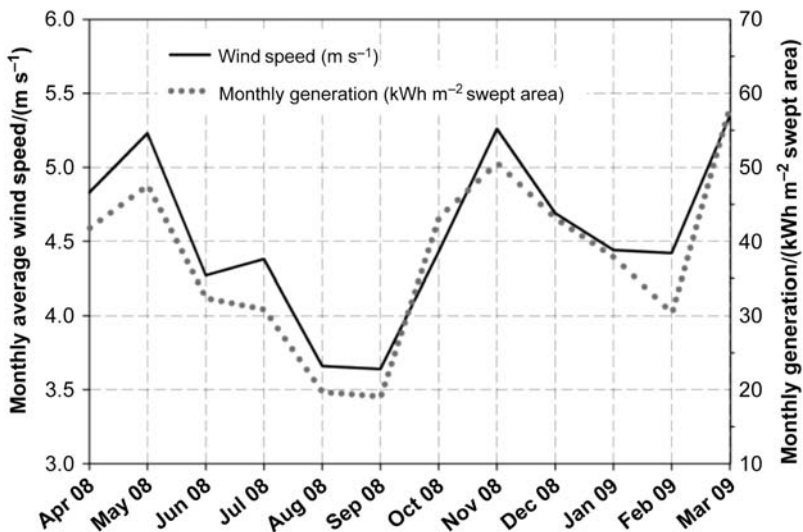


FIGURE 19.30 Measured wind speed at Bacup, South Pennines site and Proven 6 kWp wind turbine monthly output. March 2008–February 2009. Average wind speed 4.62 m s^{-1} , load factor 20.6%.

Fig. 19.29 shows a typical farm-based pole mounted turbine wind trial site. A Proven 6 kW turbine is located in a field near to the main farm buildings. Scaffold poles have been used to mount an anemometer at the same height as the turbine hub (12 m). The predominant wind speed direction is from the South West. The average wind speed of the site was 4.62 m s^{-1} compared to NOABL [6] and NOABL-MCS 2010 [4] estimates of 7.7 and 6.8 m s^{-1} . The load factor of the site was 20.6% (Fig. 19.30).

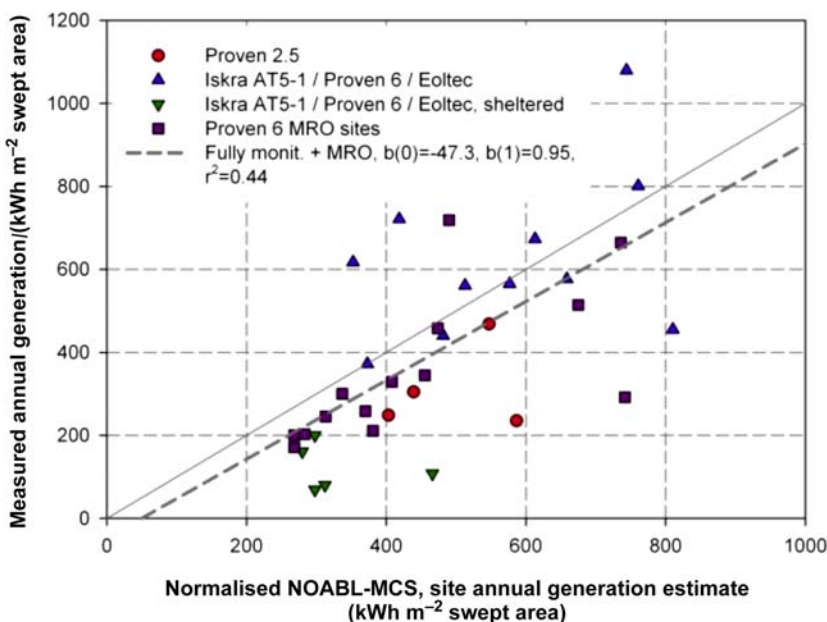


FIGURE 19.31 Comparison of NOABL-MCS [4] AEP estimate and measured annual generation across pole mounted turbines of the national micro-wind trial.

Fig. 19.31 compares the NOABL-MCS estimate of annual generation [4] with the measured performance of pole mounted turbines in the trial. Whilst there is still a high level of variability in site-specific prediction, the overall relationship is consistent.

19.4 THE FUTURE FOR MICRO-WIND

Pole mounted turbines were shown to perform well in the UK's National Micro-wind Trial. An average load factor of 19% was measured with the best turbine sites having load factors in excess of 30% (Orkney Islands). Rural landowners, especially farmers are a clear market for pole mounted turbines. The groundwork installation costs such as foundations and underground cable laying can in some cases be undertaken by the farmer at marginal cost. An assessment in 2009 by the authors of the potential pole mount turbine market in the United Kingdom was based around the premise of 50 kW_p being installed in each farm in the United Kingdom, which achieved a threshold wind speed [17]. For a threshold NOABL-MCS [4] wind speed of 5.0 m s^{-1} this suggested a resource-based potential UK market of around 87,000 farm sites (achieving a load factor threshold of 17%), predominantly in Scotland.

Feed in tariffs have transformed the micro-generation sector in the United Kingdom. Over the past 5 years, PV has become almost ubiquitous either on household roofs or ground mounted in fields. As of May 2016, there was 10,265 MW of PV capacity in the United Kingdom across 882,440 installations. Around 40% of this capacity is in the 5–25 MWp capacity range [19]. By comparison the cumulative number of small wind turbines (<50 kW) is very small. There are 4226 turbines in the range 1.5–15 kW and 749 in the 15–50 kW range, respectively, with an overall capacity of 52 MW. For all but the windiest of sites in the United Kingdom, PV will offer a better financial return and is a lower risk investment with an established supply chain and easy resource assessment. PV has a typical load factor of ~11% in the South of the United Kingdom, whereas an excellent pole mounted small wind site might achieve ~30%, but more typically 19%. The current grid connected PV cost is around £1265 kWp⁻¹ installed (10–50 kW range 2016), [20], whereas a high quality pole mounted turbine may be £5000–7000 kWp⁻¹ fully installed.

To qualify for feed in tariffs a system must be installed by an MCS certified contractor (Micro-generation Certification Scheme, [12]). As of June 2016, the most generous Feed in Tariff in the United Kingdom was 4.32 p kWh⁻¹ for generation from PV and 8.46 p kWh⁻¹ for generation from wind [21]. The overall economics are sensitive to the level of export to the grid, and therefore “avoided import,” which has a value of ~12 p kWh⁻¹. If we were to assume a 50% level of export for the case of PV and wind [22,23], a £5000 (kWp)⁻¹ turbine would need to have a load factor of ~28% to achieve the same financial payback time (14 years in each case at 0% discount rate). The twin issues of an unstable feed in tariff policy in the United Kingdom and the rapidly falling price of PV make the market challenging for small wind. This is outlined clearly in RenewableUK’s 2014 report “Small and Medium Wind Strategy: The current and future potential of the sub-500 kW wind industry in the UK,” which states that “*experience shows mounting challenges, and our industry is at a crossroads that will determine its future*” [24].

19.5 CONCLUSIONS

The main lesson from the UK’s National Micro-wind Trial study is born out in its formal report title “Location, Location, Location: Domestic small-scale wind field trial report.” It is that there is simply insufficient wind resource in urban and suburban locations [11]. Deploying micro-wind turbines in these locations will lead to very poor load factors (typically 2%) and in some cases they may even be negative due to the parasitic AC power draw of the inverter.

The study suggests that horizontal axis micro-wind turbines are able to respond quickly to changes in wind speed, in essence that turbulence is not

the key issue in relation to poor performance. The best performing rural building mounted turbines had load factors up to 8%, which is still less than PV in the United Kingdom. The building mounted turbine MCS correction factors for NOABL wind speeds [4] show good agreement for urban and suburban sites, but the NOABL-MCS rural value appeared high in this study.

Pole mounted turbines performed well in this study achieving the expected load factors (average 19%). The NOABL-MCS correction to wind speed for rural pole mounted turbines is far better, but still, on an individual site basis, can lead to a large over or under estimate of the resource.

For off-grid systems, wind and PV are complementary technologies having higher generation in different seasons of the year. In relation to grid connected systems, the dramatic reduction in the cost of PV, driven by generous feed in tariffs has transformed the micro-generation sector in the United Kingdom. This has made the economics of small grid connected wind much more difficult in a highly competitive market. The deployment of medium wind (100–500 kW) on rural farms is a sector, which has significant potential but is still in the very early phases of scale up in the United Kingdom. In 2014 211 turbines were deployed in the United Kingdom compared to just 18 in 2011 [1]. The long-term success of this market will depend on the feed in tariff policies in the United Kingdom and the relative cost of generation compared to PV.

ACKNOWLEDGMENTS

This work is part of the activities of the Energy and Climate Change Division and the Sustainable Energy Research Group (www.energy.soton.ac.uk). The work presented here was undertaken as part of the United Kingdom's National Micro-wind Trial. The field trial was developed and delivered with funding and support from a wide variety of stakeholders including the Energy Saving Trust (EST); The Scottish Government; DEFRA; B&Q; and the UK's main energy suppliers including EDF Energy, RWE Npower, NIE Energy, Centrica plc, ScottishPower Ltd., Scottish & Southern Energy, and E.on UK. These funders were represented on the project's advisory group and were influential in the trial's site selection and communications.

Aspects of this work formed the basis of the 2011 PhD study of Dr. Matthew Sissons entitled "Micro-wind power in the United Kingdom: Experimental datasets and theoretical models for site-specific yield analysis" [25].

REFERENCES

- [1] RenewableUK. Small and medium wind UK market report. RUK-003-5, March 2015; 2015.
- [2] Watson J, Sauter R, Bahaj AS, James PAB, Myers LE, Wing R. Unlocking the power house: policy and system change for domestic micro-generation in the UK. ISBN 1-903721-02-04; 2006. p. 1–32.

- [3] Watson J, Sauter R, Bahaj AS, James PAB, Myers LE, Wing R. Domestic micro-generation: economic, regulatory and policy issues for the UK. *Energy Policy* 2008;36(8):3095–106.
- [4] MIS3003. Requirements for contractors undertaking the supply, design, installation, set to work commissioning and handover of micro and small wind turbine systems issue 2.0; 26/08/2010.
- [5] Energy Saving Trust (EST). CE72: Installing small wind-powered electricity generating systems-Guidance for installers and specifiers; 2004.
- [6] NOABL. Numerical objective analysis boundary layer tool database, <<http://tools.decc.gov.uk/en/windspeed/default.aspx>>; 2016.
- [7] British Wind Energy Association. BWEA small wind systems. UK Market Report 2008, (now renewableUK); 2008.
- [8] DUKES Digest UK Energy Statistics. Chapter 6 Renewable sources of energy, <https://www.gov.uk/government/uploads/system/uploads/attachment_data/file/450298/DUKES_2015_Chapter_6.pdf>; 2015.
- [9] LCBP. Low carbon building programme, final report, DECC, <https://www.gov.uk/government/uploads/system/uploads/attachment_data/file/48160/2578-lcb-programme-2006-11-final-report.pdf>; 2011.
- [10] WarwickWindTrials. WarwickWindTrials final report, <<http://www.warwickwindtrials.org.uk/resources/Warwick+Wind+Trials+Final+Report+.pdf>>; 2009.
- [11] Energy Saving Trust (EST). Location, location, location: Domestic small scale wind field trial report; July 2009.
- [12] MIS3003. Requirements for contractors undertaking the supply, design, installation, set to Work Commissioning and Handover of Micro and Small Wind Turbine Systems Issue 3.4; 01/05/2015.
- [13] Harris RI, Deaves DM. The structure of strong winds, wind engineering in the eighties. Proceedings CIRIA conference, November 12–13th, 1980, London, UK.
- [14] G83/2,2012. G83: Recommendations for the connection of small scale embedded generators (up to 16 A per phase) in parallel with public low voltage distribution networks. Available from The Energy Networks Association: <www.energynetworks.org>; 2012.
- [15] G59/3, 2014. G59: Recommendations for the connection of embedded generating plant to the public electricity suppliers' distribution systems. Available from The Energy Networks Association: <www.energynetworks.org>; 2014.
- [16] James PAB, Sissons MF, Bradford J, Myers LE, Bahaj AS, Anwar A. Implications of the UK field trial of building mounted horizontal axis micro-wind turbines. *Energy Policy* 2010;38(10):6130–44.
- [17] Sissons MF, James PAB, Bradford J, Myers LE, Bahaj AS, Anwar A, et al. Pole-mounted horizontal axis micro-wind turbines: UK field trial findings and market size assessment. *Energy Policy* 2011;39(6):3822–31.
- [18] James PAB, Jentsch MF, Bahaj AS. Quantifying the added value of BiPV as a shading solution in atria. *Solar Energy* 2009;83(2):220–31.
- [19] DECC. Department of energy and climate change. Solar photovoltaics deployment, 30/06/2016, <<https://www.gov.uk/government/statistics/solar-photovoltaics-deployment>>; 2016.
- [20] DECC. Department of energy and climate change. Solar PV cost data, 23/07/2016, <<https://www.gov.uk/government/statistics/solar-pv-cost-data>>; 2016.
- [21] Ofgem. Feed in Tariff tables 01 July–30 September 2016, <<https://www.ofgem.gov.uk/environmental-programmes/feed-tariff-fit-scheme/tariff-tables>>; 2016.

418 PART | IV Generation of Electricity

- [22] Bahaj AS, Myers LE, James PAB. Urban energy generation: influence of micro-wind turbine output on electricity consumption in buildings. *Energy Buildings* 2007;39 (2):154–65.
- [23] Bahaj AS, James PAB. Urban energy generation: the added value of photovoltaics in social housing. *Renew Sust Energy Rev* 2007;11(9):2121–36.
- [24] RenewableUK. Small and medium wind strategy: the current and future potential of the sub-500kW wind industry in the UK; November 2014.
- [25] Sissons MF. Micro-wind power in the UK: experimental datasets and theoretical models for site-specific yield analysis. May 2011, PhD Thesis. University of Southampton; 2011.

Chapter 20

Integration Into National Grids

Jurgen Weiss and T. Bruce Tsuchida

The Brattle Group, Cambridge, MA, United States

Email: Jurgen.Weiss@Brattle.com, Bruce.Tsuchida@Brattle.com

20.1 WIND INTEGRATION: WHAT IT MEANS AND WHY WE NEED IT

Wind turbines dedicated to producing electric power have been in service since the late 19th century. By the 1930s, wind turbines were providing local electric power needs to various rural communities and farms in the United States. However, it was only in the 1970s that electric utilities recognized wind as a potential resource for producing bulk power, at least in part driven by the oil embargo and resulting high price of oil, which at the time was still a significant fuel used for power generation. In the United States, the Public Utility Regulatory Policies Act (PURPA) enacted in November 1978 promoted energy conservation and renewable energy, and provided incentives to explore the potential of wind. Still, the overall capacity of wind resources in the power generation industry remained low. The worldwide capacity of wind generation installed by electric utilities in 1990 was less than 2 GW. Only in the late 1990s did wind generation start to grow more rapidly and the technology was soon recognized as the “alternative” energy source. By 2015 the global installed capacity of this alternative resource exceeded 432 GW and is growing faster than ever, as shown in Fig. 20.1 [1]. The worldwide wind energy investment in 2015 has surged to approximately \$110 billion (USD), leading to nearly 64 GW of new wind capacity being installed in that year [2]. The United States was no exception to this trend, and today (as the end of 2015) it has nearly 74 GW (approximately 48 500 wind turbines) of installed onshore wind capacity. More than 66 GW of this cumulative wind capacity was installed between 2000 and 2015. Wind represents approximately 7% of total bulk power capacity of 1064 GW installed in the United States as of 2015 [3]. (In 2015, the 74 GW of wind installed in the United States produced approximately 191 GW h of power, or roughly 4.8% of the total power produced (3975 GW h) by utility-scale generation

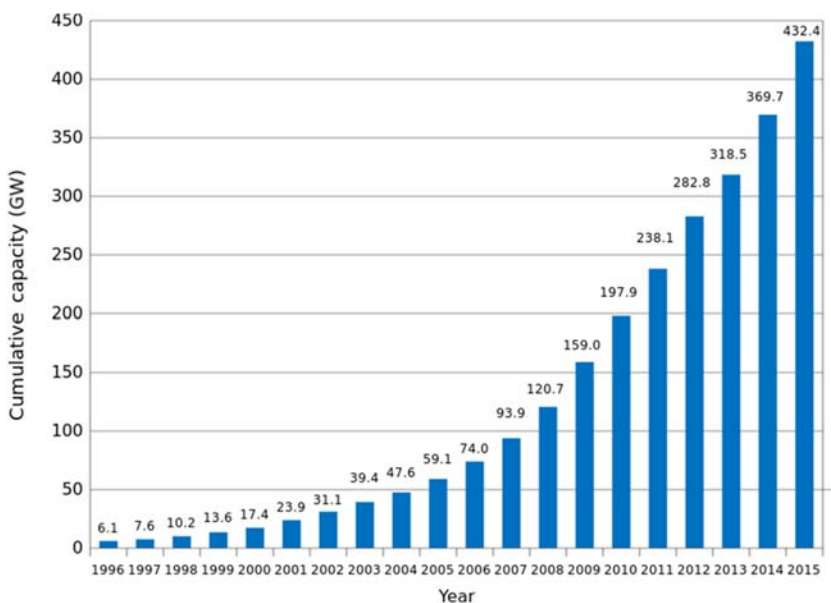


FIGURE 20.1 Cumulative global wind capacity installed by year.

resources [3]. Globally, wind production accounted for approximately 3.7% of total electricity production [4]).

The investments in wind were driven by a number of factors, including policy incentives aimed at reducing pollution from fossil fuel-based power generation—with many focused on reducing greenhouse gas (GHG) emissions. Some countries also view reducing reliance on imported fossil fuel as part of achieving energy independence, which in turn is often part of a larger national security strategy, as a reason for promoting wind. The rapidly declining cost of wind generation has also contributed to this growth. Today, onshore wind in locations with good wind resources is often one of the resources with the lowest levelized cost of energy among all commonly operated generation technologies [5]. Where costs are competitive, some view wind resources as a way to save money or at least provide some low-cost diversification away from volatile fossil fuel-driven electricity prices.

As a result of all of these forces, many countries, spanning the range from small islands to large interconnected systems, have been integrating these indigenous and variable resources into their generation portfolio. There are over 170 countries with future targets for renewable energy resources, with wind typically representing a significant portion. For example, in Europe, Germany has a renewable penetration target of 80% by 2050, Denmark has a target of achieving 100% by 2035, and Scotland is aiming for 100% renewable energy by 2020 [6]. In the United States, California and

New York both have mandates to generate 50% of electricity with renewable energy by 2030, and Hawaii 100% by 2045. Elsewhere, Alberta announced a clean energy target of 30% by 2030 and plans to install 5 GW of renewable resources [7]. Mexico, with its Energy Reform legislation enacted in December 2013, has set an ambitious annual target of 2 GW of wind capacity per year until 2023, Uruguay has a goal to generate as much as 38% of its power from wind by the end of 2017, the Indian government has committed to a target of 175 GW of renewables by 2022, including 100 GW of solar capacity and 60 GW of cumulative wind power capacity [8], and South Australia recently committed to a new target of zero net emissions by 2050 [9]. Discussions and negotiations at the United Nations Framework Convention on Climate Change have led over 190 countries to sign (and over 110 countries to ratify) the Paris Agreement that calls for reducing GHG emission globally. The agreement aiming at zero net emissions by 2050 indicates that the future generation portfolio is viewed globally to be largely comprised of non-GHG-emitting renewable resources, with wind and solar being the leading technologies (absent breakthroughs of other technologies) [10].

20.2 CURRENT/STANDARD MEASURES FOR WIND INTEGRATION

Wind generation technology captures the freely available but varying amount of wind that cannot be controlled (though the electricity serving the system can be managed, largely through curtailment). The exponential growth of wind capacity in the late 1990s to the 2000s has made it necessary for many system operators to recognize the operational and planning challenges brought on by the intermittent nature of wind.

At a fundamental level, the electric power system requires that production (generation) and consumption (demand) to be in balance at all times, even over extremely short time intervals (fractions of seconds, in practice). This creates two kinds of fundamental challenges. The first challenge is that production and consumption must be balanced under “normal” conditions, given the natural (and price-driven) fluctuations in consumption and to a lesser degree variation in production from conventional generation resources, such as seasonally fluctuating hydro generation. This challenge is potentially made harder by the variability of power production from wind resources due to fluctuations in weather conditions, and the limited ability to control the output from the wind resources, short of curtailment.

The second challenge is to maintain system security following a disturbance, such as the loss of a traditional generation resource or transmission element (such as a line or a transformer). Typically, wind resources do not directly increase this challenge—since most wind farms are smaller than the cause of such disturbances (typically a larger generation resources or

transmission element), and the system is designed and operated to be able to cope with such disturbances. However, wind resources may replace other traditional generation resources that are capable of responding to a disturbance through their ability to provide synchronized inertia, various frequency response, and replacement reserves. (In many US systems, frequency response is provided by governor response (primary frequency response) and automatic generation control (secondary frequency response). Replacement reserves that relieve these fast responses so the system can prepare for the next disturbance are often considered as tertiary.) Technological advances have enabled wind to provide some frequency response, but generally in a limited manner when compared to dispatchable (i.e., resources where the output can be increased or decreased by the plant or system operators) generation resources. As a consequence, the increase of wind resources replacing dispatchable resources can lead to frequency response challenges, especially for small systems at high levels of wind penetration.

Balancing the system under normal conditions remains operationally challenging on several time frames, from days (how much wind should the system operator count on and how much additional resources should be prepared if wind is not strong enough?) to hours (greater ramping needs in the 1- to 3-hour time frame), to seconds (frequency control), and becomes increasingly so as wind displaces more dispatchable generation resources. More generally, imbalances of any kind lead to frequency deviations, which if significant could lead to service interruptions (blackouts and damage to electrical equipment in the most severe case, if adequate protections are not in place). Even relatively small frequency deviations can harm the sophisticated manufacturing processes of today. Historically, this balance was met by controlling the production (generation) from mostly dispatchable resources via Automatic Generation Control (AGC) or similar control mechanisms that adjust power plant outputs based on the size of measured changes in frequency or area-wide supply–demand balance (after accounting for intertie flows with neighboring systems). Learning through experience, system operators could predict the change in consumption with a high level of accuracy and commit and dispatch these controllable generation resources, which were mostly thermal and hydro generation, to match predicted and actual consumption in real time.

However, as more wind resources were added to power systems, the cumulative variability of wind power production in some systems began to exceed the variability and uncertainty caused by short-term fluctuations of consumption. With production—previously controllable for nearly all system resources—now varying due to external factors (weather), the balancing of production and consumption became more difficult under both normal operating conditions and following system disturbances. The rapid expansion of wind in the early 2000s therefore explains why integration studies of wind

resources assessing the technical feasibility and the economic viability started to permeate the industry during this time period [11].

In the early days and at lower wind penetration levels, many integration studies were often technical feasibility studies focusing on maintaining the operational security, or the reliability, of the bulk power system. Reliability concerns include services that are critical to maintaining the operational security of the bulk power system during and after major disturbances (i.e., the second challenge discussed above). Primary issues include frequency response, system inertia, and frequency and voltage ride-through capabilities, all designed to ensure that following a disturbance, such as the sudden loss of a large generating unit, loss of a transmission line, rapid loss or restoration of renewable power due to sudden weather shifts, or a sudden and unexpected change in demand, power can be provided while maintaining frequency deviation within a narrow band [12]. (In the Eastern Interconnect (a 60 Hz system that approximately covers the eastern half of the United States and Canada), the system starts to respond when the frequency deviation exceeds ± 36 milli-Hertz (59.964–60.036 Hz), excluding time error corrections.) Because all resources (for both production and consumption) on the electric system are synchronized at the same frequency, frequency deviations can lead to cascading failures. For example, the tripping (failure) of a generator resource due to a decline in frequency can lead to a further reduction in frequency, causing more generator trips, and so on. Today, many systems have built in various protection schemes, such as load shedding via under-frequency relays and generation tripping via over-frequency relays, to avoid such situations.

Early wind machines used simple induction generators and were designed with the primary focus of capturing the free-flowing wind energy. These turbines provided no dynamic grid support in the event of a power system disturbance. This design led to wind generators having different response characteristics compared to conventional synchronous generators, and these alternative technologies were required to disconnect if frequency or voltage deviated from their nominal levels. Disconnecting a large quantity of wind resources could lead to the aforementioned cascading effects. In the United States, the Federal Energy Regulatory Commission (FERC), with considerable input from both the wind and the power systems industry, addressed this concern of cascading failure during certain system conditions by requiring all new wind turbines to ride through low-voltage events rather than disconnecting (Order 661A, 2005). (California and Hawaii are requiring ride-through capabilities from new distributed PV installations.) Today, disturbances, such as short-term small frequency or voltage deviations, rarely affect the operations of newer wind turbines, easing integration efforts. (A resource that lacks dynamic response capability does not help stabilize the power system when a disturbance occurs, and further displaces generation resources that could. This puts more stress on the remaining generator

resources that do provide the grid support services. Therefore equipping wind turbines with such capability remedies are twofold.) At the same time, technology has improved such that newer wind turbines can provide some of the frequency, inertia, and voltage control that have traditionally been provided by other dispatchable generators. (While most dispatchable generator resources provided inertia, only generators with AGC capability (or its equivalent) provided voltage support and frequency control.) With many of these technological capabilities now in place, the main focus of wind integration has begun to shift from worrying about the technical feasibility of accommodating wind under normal operating conditions and following system disturbances toward understanding the economics of wind integration, i.e., how increasing amounts of wind (and other non-GHG-emitting resources with variable output) can be integrated at least cost. (Dynamic response capabilities of wind turbines have evolved significantly over the past decade. Typical modern wind turbines are coupled to the power system with advanced electronics that allow operators to control wind turbine output at a faster rate (milliseconds rather than seconds) and more accurately compared to conventional synchronous generator resources. Furthermore, wind turbines provide some inertia, which is also controllable through the advanced electronics (inertia response from conventional synchronous generator resources are typically uncontrolled).) (Since improving technical capabilities do not change either the underlying variability of wind production or the continued possibility that short-term deviations from expected wind output need to be managed.)

At very low penetration levels of wind, the cost of integrating wind, i.e., the cost for the system to react to expected and unexpected wind output changes in ways that maintain system balance within acceptable bounds to provide reliable electricity supply, tends to be very low because the fluctuation of wind is dwarfed by fluctuation of demand. That is, while the variability of wind imposes a real cost, in the sense of using up some of the ability of the system to absorb (unexpected) fluctuations, it is easily absorbed, at least on large systems or systems with significant flexible resources such as hydro, without material adjustments from standard procedures. Considerations of the attractiveness of wind as a generation resource in this easy-integration context therefore tend to ignore any potential additional costs to manage the variability of power production from wind resources.

However, with penetration increasing, it eventually becomes necessary to make costly operational and potentially investment changes to accommodate the larger aggregate fluctuations from wind resources to keep production and consumption in balance. Potential operational changes include re-dispatching the power system by using more expensive generators capable of quickly changing output in response to changes to power production from wind or deviations of wind output relative to forecast. Potential investment changes include adding more flexible generation resources (generally more

expensive), and accounting for the wind capacity for generation capacity reserves. (Wind capacity is often discounted because wind resources are not always available. This requires the system to secure other resources for maintaining required/desired capacity reserve margins. Securing such resources under higher wind penetration levels could become costly because the net revenue from selling energy, which can offset the annual carrying charge, can be lower (because wind resources with lower marginal costs are dispatched before these resources).) Wind resource expansion decision now needs to include these adjustment costs.

While the specific methods and assumptions may vary, most wind integration studies estimate the cost of integrating wind by calculating the combined (net) variability of wind and demand (net-load variability) using time-synchronized data and evaluating how dispatchable resources will be used to match such variability to maintain system balance. Many studies point to improving ancillary service products (including reassessing their quantity) as one of the solutions to provide adequate response to the increasing magnitude and faster rate of output fluctuation from wind resources but also to fill in the gap that occurs when actual wind production deviates from forecast production. Some studies identify ways to increase the flexibility of existing resources through retrofitting these resources, or by adding new flexible resources of various types including storage. Studies for larger interconnected systems often highlight the benefit of better regional coordination for addressing net-load variability. Coordination within a region reduces net-load variability because it diversifies both load and wind profiles while allowing the system operator to seek the needed flexibility from a larger pool of resources. (Wind production profiles across different geographic locations are not perfectly correlated and the correlation declines with geographic distance. Hence, the combined variability of wind resources decreases by pooling wind generation in different locations, with benefits generally increasing the further apart wind resources are located, or the more diverse the geography around them. For instance, mountain ranges in Wyoming create significant lags and different directional patterns across wind farms located on different sides of those ranges. However, there are limits to the benefits of geographic diversification. For instance, while the overall wind production across ERCOT is somewhat smoother and more predictable than from any particular subregion, it is still a very volatile pattern and there are times (hours or longer) when essentially all of the wind production in the state goes off-line, or returns to high power, over short time frames. [13]. Sometimes the loss of power is not because the wind is not blowing, but because a widespread storm is making it blow too hard, above the operating limits of the plants. These can affect large areas, such as all of England [14].) A robust transmission system is often seen as key to such coordination. Some studies highlight the benefits of expanding the region itself, aiming for further increased diversification of wind and load

profiles and access to a larger pool of resources with flexibility. Regional coordination backed by a robust transmission system may also have additional benefits, such as increasing energy market competition and improving network resiliency, so such decisions are typically made in conjunction with other objectives.

The least-cost wind integration solution varies by system. In smaller and more isolated systems, procuring additional flexibility, mostly through ancillary services in the form of operating reserves, tends to be a key solution. As a consequence, some jurisdictions have been trying to put the economic burden of providing this flexibility on wind developers—by requiring renewable resources to provide some “firming” of its power or to manage their ramp rates. In response, alternative resource developers team up with flexible resources including natural gas or hydro generation resources or bundle their assets with storage technologies. In larger and more interconnected systems, flexibility is less critical due to the diversification benefits brought by transmission and regional coordination. Growing penetration of wind resources has thus led a number of power systems operators to rethink their process for adding transmission as a cost-effective tool for wind integration. (Transmission often has significant other benefits beyond wind integration.)

In recent years, the additional need for flexibility to integrate wind has led to significant increases in the flexibility of various dispatchable generators. In Ontario, for example, nuclear units, previously deemed inflexible in the United States and Canada, are now cycled to accommodate these alternative resources. At the same time, wind technologies have improved and many newer wind turbines can themselves provide the various grid support services, and some systems allow renewable generators to directly contribute to maintaining reliability, for example by providing certain ancillary services. (There are other reliability contributions, such as counting (even if partially) the capacity of wind resources toward meeting resource adequacy goals.) Overall, options for securing the needed flexibility have increased, and consequently the cost of securing the needed flexibility needs has declined.

In addition, the design of electricity markets has evolved in ways that help integrate wind and other variable resources. In the United States and Europe, liberalized wholesale markets have generally moved toward shorter dispatch cycles, mostly dispatching resources on 5-minute intervals. Shorter dispatch cycles reduce the uncertainty and duration of the period (and therefore the overall quantity) for which ancillary services must be provided. For example, the Electric Reliability Council of Texas (ERCOT), with nearly 16 GW of wind installed (as of March 2016) [15], identified moving the dispatch resolution from 15 to 5 minutes in late 2010 as “one of the main reasons why ERCOT has been successful in integrating renewables with minimal increase in Ancillary Services capacity” [16]. While this was likely a good idea regardless of wind integration, it complemented the introduction of many renewables onto the ERCOT system.

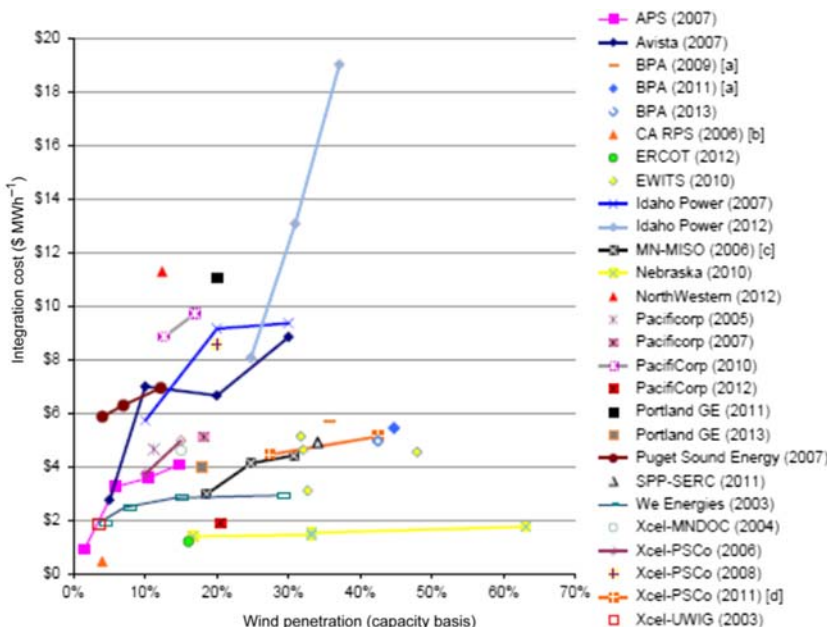
In addition to shorter dispatch cycles, several regional US markets including the Mid-Continent Independent System Operator (MISO) and Southwest Power Pool require variable resources to directly participate in the wholesale energy market as dispatchable resources. That is, a wind unit can bid into the energy market up to the cap based on its forecasted output and will be penalized (like any other dispatchable resource) if it cannot follow its dispatch signal. (Power systems operations differ significantly region by region. Most US markets centrally dispatch at least larger generating units by sending commands to individual generating units to increase, hold, or decrease output levels. In European markets, generators tend to self-dispatch, i.e., they react to market prices rather than direct dispatch signals. However, penalties can still arise through short-term imbalances caused by deviations of output from wind generation relative to anticipated and contracted electricity amounts.) MISO assumes that approximately 95% of wind energy's potential can be captured through economic dispatch. The traditional unit commitment cycle, typically performed day-ahead, has also been evolving. Many US markets, including PJM, have introduced intraday commitment to reduce the uncertainty associated with deviations of net load from forecast. Others, including the New York Independent System Operator, include wind resources in its commitment logic.

Some systems have tried to expand their regional footprint to maximize the geographical diversity benefits of renewable resources. Denmark, known as one of the world's leading wind countries, interconnects both with Germany and the Scandinavian countries. The larger footprint has helped integrate wind resources developed in and around Denmark. Other systems, such as the Germany market and Xcel Energy Colorado, have reduced the total variability of wind resources by aggregating all wind and/or solar output into one portfolio for output forecasting purposes, effectively reducing the real-time net-load variability and forecast deviations. For the same reason Spain also forecasts total wind output at the market level, rather than at the individual plant level.

Improvements in wind forecasting techniques have further reduced the forecast uncertainty. Technological advances in weather forecasting, together with better data on historical performance of renewable resources, allow significantly improved forecasting accuracy of wind generation. Forecasts today are much more accurate than they were 10 years ago and often include ramping forecasts to allow system operators to prepare for extreme events. In many cases the improvements in forecasting technique lead to operational changes. (There are other ways to take advantage of the improved forecasts. For example, better wind forecasts can be applied to improve load forecasts, especially in today's world where smarter infrastructure are being deployed at the customer site.) For example, Xcel Energy Colorado improved the wind forecast accuracy by 35% relative to previous forecast methods, informing both day-ahead and real-time operations. Since the introduction of

the improved methodology, Mean Absolute Error (MAE) in wind forecasting has decreased from 18.01% in 2009 to 11.04% by 2013 (a 38.7% reduction) [17]. Xcel Energy now coordinates the unit commitment, dispatch, and fuel purchase schedules for its traditional generation resources with wind forecasts and estimates that its $\text{US\$}6 \times 10^6$ ($\$6$ million (USD)) investment in improving wind forecast over 6 years has saved over $\text{US\$}60 \times 10^6$ ($\$60$ million (USD)) over the same period [18]. The California Independent System Operator and MISO have enhanced their ancillary service products and now include flexible ramping products designed for dealing with net-load ramping needs that are much steeper than historical load variation.

Overall, the worldwide experience with wind generation over the past two decades has led to a greater understanding of the characteristics of this renewable resource and the remedies needed for integrating it reliably and economically through the use of existing, and sometimes new, resources. Fig. 20.2 shows the estimated integration cost from a number of studies performed for US systems. Two observations can be made based on these studies. First, the estimated cost of integrating wind varies significantly across studies, ranging from less than $\$2$ (MW h) $^{-1}$ to more than $\$10$ (MW h) $^{-1}$.



[a] Costs in $\$/\text{MWh}$ assume 31% capacity factor.

[b] Costs represent 3-year average.

[c] Highest over 3-year evaluation period.

[d] Cost includes the coal cycling costs found in Xcel Energy (2011).

FIGURE 20.2 Estimates of wind integration costs from multiple US wind integration studies [20].

While many factors including changes in fuel and capital costs likely contribute to the wide range, the range of estimated integration costs is generally wider at higher penetration levels. The second observation is that, on average, estimates of integration costs are not increasing over time even though penetration levels have been increasing. For example, PacifiCorp has conducted four studies, in 2005, 2007, 2010, and 2012. The integration cost estimate of $\$4.5 \text{ (MW h)}^{-1}$ at a penetration level of about 10% in 2005 increased to $\$5 \text{ (MW h)}^{-1}$ at an 18% penetration level in 2007 and to nearly $\$10 \text{ (MW h)}^{-1}$ at a 15%–18% penetration level in 2010, but then decreased to only approximately $\$2.5 \text{ (MW h)}^{-1}$ at a penetration level slightly above 20% in 2012 [19]. While the integration costs will vary over time due to changing underlying assumptions for natural gas prices (and therefore shows a higher cost in 2010), it is also likely that progress is being made in understanding the characteristics of this alternative resource. Operators are improving the methodologies for estimating integration costs and are being helped by an expanded set of operational (and technology) options available for renewables integration.

Nonetheless, the mainstream integration approach has generally stayed inside the traditional framework of adjusting the production (generation) from dispatchable resources to meet the net load (i.e., demand net of wind and other noncontrollable generation resources).

20.3 THE FUTURE OF WIND INTEGRATION

The currently prevailing framework for wind integration is centered on the notion that increasing levels of wind generation and the associated output fluctuations are largely counterbalanced with the flexibility from traditional dispatchable resources. There are, however, at least three distinct developments that will likely limit the effectiveness for this framework at some point in the future.

First, wind is no longer the dominant alternative resource technology in many regions. Rather, the cost of other renewable technologies, particularly solar photovoltaic (PV) generation, has become much more competitive and has been entering the market at a rapid pace. PV technology has several advantages over wind. First, its generation profile tends to better match the general load profile—it generates more power during the daytime when it is needed, compared to wind resources in many parts of the world typically producing more in the early mornings when power is not needed as much. This profile difference now leads many to view solar PV as a complementary technology to wind. Also, the scalability and modularity of the technology enables fast and widespread deployment. Wind and solar currently dominate the global growth of renewable electricity production. In 2015, the combined share of investments between these two technologies comprised 90% of global renewable energy (excluding large hydro resources) investment of

nearly $\text{US\$}286 \times 10^9$ (\$286 billion (USD))—with solar at $\text{US\$}160 \times 10^9$ (\$160 billion (USD)) and wind at nearly $\text{US\$}110 \times 10^9$ (\$110 billion (USD)) [21]. Given its longer investment history and higher average capacity factor, wind still represents a larger portion of total installed capacity and production. (In 2015, annual energy production from wind exceeded 840 TWh, about 3% of global electricity production. By comparison, solar PV generated about 250 TWh, or about 1% of the global electricity production [21].)

Second, a combination of the improving economics of wind and solar and climate change related policy will likely require most existing fossil-fuel-based resources to be replaced with nonemitting resources over the next few decades. Therefore, most of the current fossil-fuel-based resources will likely eventually no longer be as available to help “integrate” renewable resources with variable output. At that point, various types of renewable resources, eventually storage, and almost certainly enhanced real-time demand management will likely become increasingly important for integrating each other. (It is also possible that gas turbine or steam turbine technology-based resources currently fueled by fossil fuel to continue providing the integration services (balancing the system dominated by variable resources such as wind and solar), by replacing the fossil fuel with renewable fuels such as biomass, biogas, and biofuels.) This will create both new challenges and opportunities. The loss of inertia, which is currently largely provided by fossil-fuel-based resources, likely represents a new challenge not addressed in many past integration studies. (As Fig. 20.2 shows, many of the earlier integration studies focused on renewable penetration levels that were typically lower than 40%–50%. With the awareness of global warming, several systems are exploring options to achieve significantly higher penetration levels to reduce GHG emissions. Such future systems are often expected to be primarily characterized by variable generation resources, such as wind and solar PV, which provide limited if any inertia. Therefore inertia has begun to be a focus of interest, especially on smaller systems.) Given the low tolerance for frequency fluctuations of the system, maintaining inertia, which acts to stabilize the system, can become critical, especially for smaller systems. Should the total quantity of inertia become lower than the system needs, it has to be made up either with new inertia provided from remaining non-fossil-fuel resources and possibly from demand resources. (These options include increasing loads with rotating mass (such as motor loads) and converting existing generators (with rotating mass) into synchronous condensers. Studies have identified other means to reduce the needs of inertia, including providing synthetic inertia from inverter-based generation or adjusting primary frequency response quantities from resources that respond faster than traditional resources (e.g., governors).)

The loss of traditional fossil-fuel-based resources providing flexibility and inertia may be accelerated due to the impact of higher penetration levels of renewable resources with near-zero marginal costs have on market prices.

In systems with wholesale energy markets and significant shares of renewable generation, market clearing prices have, on average, declined, and in some cases quite substantially. At the same time, the occurrence of negative market clearing prices has increased. Negative prices can occur when larger, less flexible units want to stay online in order to avoid high start-up and shut-down costs or when resources are willing to bid into the market at negative prices to assure being dispatched and thus receive output-based incentives, such as the US production tax credit for renewable resources, renewable energy credits (RECs), feed-in tariffs (FITs), or fixed price power purchase agreements. These price patterns impact the long-term economic viability of fossil-fuel-based resources that system operators currently rely on to provide the operational flexibility for integrating alternative resources such as wind. In systems dominated by fossil-fuel-based resources, planners and policy makers will therefore need to understand the conflicting pressures of the current framework—increasing renewable resources to replace fossil fuel requires securing the economic viability of fossil-fuel-based resources for providing ancillary services, at least until alternative technology options emerge at sufficient scale to be able to provide non-fossil-fuel-based alternatives.

Finally, led by the progress of solar PV, there is a significant trend toward locating generation sources much closer to the customer than has been observed traditionally. In many cases, resources are moving “behind the meter” and thus become less visible and less controllable for system operators, creating additional challenges with respect to balancing supply fluctuations. Solar PV is the most obvious generation technology to be located behind the meter because it is scalable: a small solar PV panel can generate just as much electricity per unit of surface area than a larger one. (This does not mean that solar PV does not benefit from economies of scale in construction, or that there are not other sources of efficiency gains. In fact, utility-scale solar PV projects can and tend to be substantially cheaper per unit of power output and per unit of avoided emissions than small residential systems. They tend to produce more output per panel since larger systems can be oriented more optimally toward the sun—they do not have to follow the slope of the roof and can also be tracking the sun. They also involve lower installation costs with lower inversion and control costs since they can be sized for a larger group of PV assets, rather than for individual roofs.) By contrast, small and medium-sized wind turbines are not as advanced as the more developed large-scale wind turbines and lack the high capacity factors enjoyed by their utility-scale siblings. Nonetheless, distributed wind has recently been gaining momentum as well. (Distributed wind operates at capacity factors that are generally higher than PV systems and also have the benefits of producing some power around the clock. Furthermore, daily wind production profiles tend to fit the residential demand profile better than solar PV because the peak residential demand in

many parts of the world often occurs after sunset. And distributed wind projects can be put in service much faster, typically within 2–9 months, compared to 2–4 years for land-based utility-scale wind farms and 8–12 years for offshore wind farms. Finally, wind does provide system generation inertia (needed for stability), and although limited, this could become critical for protecting some small-scale systems from disturbances. Therefore, while not as prominent as solar PV systems, distributed wind has started to gain momentum.)

Most distributed solar PV and wind systems serve the host load directly (behind the meter) and are not visible to the system operator. Yet the operational and planning issues caused by their variable output are the same as for the larger utility-scale resources. Today, many system operators are becoming aware of the growth in distributed resources and are trying to incorporate the associated uncertainty in their operations. One of the challenges is that imbalances on the distribution network cannot be remedied in the traditional way of controlling the output of dispatchable generators as done on the bulk transmission system—since most distribution systems do not have resources that are controlled by a system operator. Distribution level integration of wind and solar resources therefore likely represents new and important challenges that require further coordination of the operations of all resources, regardless of their interconnection point and controllability by the system operator (i.e., whether they are interconnected to the bulk transmission system and controlled by the system operator or interconnected to the distribution system, oftentimes behind-the-meter, and not controlled by the system operator).

In addition to these three developments related to wind and solar PV, the emergence of new storage technologies represents a significant change in the industry. (Many of these new storage technologies are portable and scalable, so that they do not require much space and can be installed quickly (within months, compared to years for new generation resources), even at remote locations, and they be designed to provide various services, including ancillary services and dynamic grid support.) Variable renewable resources are recognized as a force that creates opportunities for storage in many systems. The marginal cost difference between renewable and traditional fossil-fuel-based resources, the need for flexibility in operation, and in the early days the lack of voltage regulation capability or protection against low-voltage events by wind resources, has created such opportunities. These new storage technologies can respond to emerging opportunities in existing energy and ancillary service markets but are also a potential component of a changing framework of integrating the renewable resources.

The combined effect of these developments around wind and solar PV and storage is change to the current practice of system planning, particularly in smaller systems including island grids. For example, many of the smaller and isolated markets that have traditionally relied on fuel oil-based

generation resources have experienced very high and volatile power prices over the past decade. These systems have been seeing renewable resources as their remedy for a lower, more stable power price (and to some extent energy security). However, the limited demand, the lack of geographical diversity, and limited flexibility from existing resources have made it technically challenging for these systems to integrate higher amounts of renewable resources.

Several systems, including in particular island systems, have tried to increase load flexibility as renewable penetration levels increase. This can be done in the first instance by creating more centrally coordinated load management and associated opportunities for customers to be compensated for providing various system services. A more dramatic potential change pushing further along those lines would involve the electrification of other industries in a way that provides flexibility. Electrifying the transportation section and using electrical vehicles as a source of flexibility (such as by timing charging) is one example. Electrification of heating (and/or cooling, although most cooling today is already electrified) likely provides opportunities for using thermal storage (of water) to provide additional flexibility to integrate renewables while at the same time displacing fossil fuel consumption for heating. Allowing demand response to play a bigger role in managing system variability (and emergency situations) has been a theme in larger interconnected systems as well. (Other approaches under development in larger interconnected systems include dynamically managing the transfer capacity of transmission lines.) The proliferation of smarter infrastructure, much of it deployed at the customer site (smart meters, smart thermostats, smart appliances, all enabled by smarter software), enables participation of increasing amounts of demand in activities that help mitigate the variability of renewable generation. The incentives to provide demand response likely also rely significantly on improved price signals to end users, e.g., in the form of time-varying retail tariff structures and means to compensate end users for providing ancillary services.

Also, in a system primarily characterized by variable generation resources, such as wind and solar, transmission planning will likely need to take into account not only short-term reliability concerns, but increasingly how to allow access to promising areas for renewable energy development, i.e., areas where the wind blows and/or the sun shines a lot, and how to transport energy from renewable rich areas to load centers. The development of new transmission lines in Texas, the so-called Competitive Renewable Energy Zone (CREZ) lines and the current construction of high-voltage transmission lines in Germany to connect on- and offshore wind resources in the North to demand centers in the South are two examples of a trend that will likely need to accelerate.

All of these approaches represent a framework that differs significantly from the traditional framework for renewable integration. Rather than

addressing the challenges associated with incrementally growing wind (and other variable generation) capacity, it takes into account the broader ultimate objectives of renewable integration, such as to ultimately enable deep economy-wide GHG reductions. This more holistic approach therefore likely needs to involve other sectors, such as buildings (space and water heating) and transportation, which traditionally were not part of planning and operating the electric system. For instance, New York City's 80×50 initiative is one such integrated effort across sectors—buildings, energy, and transportation—to understand potential strategies for New York City to achieve an 80% reduction in GHG emissions by 2050 (thus 80×50). A number of other cities around the world, including Berlin, Copenhagen, and Vancouver, have committed to essentially 100% renewable energy use and at least 80% GHG reductions by mid-century [22]. In these examples, the phrase “alternative” energy source no longer applies because the entire system is designed around renewable resources, with wind often being the largest component.

20.4 CONCLUSIONS

Overall, the increasing shares of wind, solar PV, and other renewable resources, more and more of which are connected to the electricity grid by advanced power electronics, are part and parcel of the (r)evolution of power systems across the world. This evolution also includes increased levels of flexibility embedded elsewhere in the system, including controllable loads, electricity, and thermal storage technologies (with a growing share behind the meter) and transmission system interconnections and control procedures. The more distributed nature of wind, solar PV, and other forms of generation along with more active consumer participation are all contributing to a dramatic shift in the nature and characteristics of the electricity grid.

To plan a system that can accommodate large amounts of renewables at least cost, it will be important to consider a more holistic approach than traditional incremental approaches. Since many of the complementary approaches, including demand-side responses, storage, and various means of using renewable energy generators themselves to balance the system, are nascent and rapidly evolving, it is impossible to plan the “optimal” system today. It is therefore important to enable the development of complementary technologies, and to incorporate them into plans and markets as they mature. Also, given that in many parts of the world traditional fossil generation still represents the largest share of total production, a transition is needed that minimizes disruption along the way, both physically and financially. In many countries there are material institutional hurdles to implementing this holistic approach, which would consider (wholesale) renewables, retail technologies, and revised transmission planning as a complementary bundle of choices to be made jointly. In particular, responsibility for these choices tends to be dispersed across entities with different information sets and

different interests. Nonetheless, as the system continues to evolve toward higher levels of variable renewable resources, the accompanying industry framework must provide the appropriate signals to incentivize sufficient flexibility in both the operational and investment time horizons. Not only is a sufficient level of capacity required to meet future demand, but the nature of this capacity is fundamentally different from what was needed in the past, due to the emphasis on and the need for flexibility.

REFERENCES

- [1] Global Wind Energy Council <<http://www.gwec.net/wp-content/uploads/2012/06/Global-Installed-Wind-Power-Capacity-MW-%E2%80%93-Regional-Distribution.jpg>> [accessed November 2016].
- [2] United Nations Environment Programme, Bloomberg New Energy Finance <http://fs-unep-centre.org/sites/default/files/publications/globaltrendsinrenewableenergyinvestment2016lowres_0.pdf> [accessed November 2016].
- [3] US Energy Information Administration, Total electric power industry summary statistics, released November 2016 <https://www.eia.gov/electricity/annual/html/epa_01_02.html> [accessed November 2016].
- [4] REN21, Renewables 2016, Global Status Report.
- [5] Lazard Levelized Cost of Energy Analysis 9.0 <<https://www.lazard.com/media/2390/lazards-levelized-cost-of-energy-analysis-90.pdf>> [accessed November 2016].
- [6] The Scottish Government, 2020 Routemap for Renewable Energy in Scotland—Update, dated September 17, 2015 <<http://www.gov.scot/Resource/0048/00485407.pdf>> [accessed November 2016].
- [7] <<http://business.financialpost.com/news/energy/alberta-eyes-renewable-energy-boom-with-5000-megawatt-target-by-2030>> [accessed November 2016].
- [8] Global Wind Energy Council, Global Wind Report, Annual Market Update 2015 <http://www.gwec.net/wp-content/uploads/vip/GWEC-Global-Wind-2015-Report_April-2016_19_04.pdf> [accessed November 2016].
- [9] <<http://www.renewablessa.sa.gov.au/>> [accessed November 2016].
- [10] UNFCCC, The Paris Agreement <http://unfccc.int/paris_agreement/items/9485.php> [accessed November 2016].
- [11] For a summary of US integration studies, see the archive at <http://uvig.org/resources/#!/3700/u-s-regional-and-state-studies> (accessed November 13, 2016). See also European Wind Integration Study (EWIS), March 2010. For an overall summary of wind integration studies and their conclusions, see IEA, Expert Group Report on Recommended Practices: 16. Wind Integration Studies, 1. Edition 2013.
- [12] Reliability Guideline, North American Electric Reliability Corporation <www.nerc.com> [accessed November 2016].
- [13] Tom Konrad, Why Geographic Diversification Smooths Wind Power, April 2011 <<http://www.renewableenergyworld.com/articles/2011/04/why-geographic-diversification-smoothes-wind-power.html>> [accessed November 2016].
- [14] Jonathan Dennis, The University of Queensland Australia, Large Centralised Renewable Generation. Final Report, pp. 32–34 <<http://escornwall.com.au/reports/final-report-jonathan-dennis.pdf>> [accessed November 2016].
- [15] <http://www.ercot.com/content/wcm/lists/89475/ERCOT_Quick_Facts_33016.pdf>.

436 PART | IV Generation of Electricity

- [16] ERCOT, ERCOT Concept Paper: Future Ancillary Services in ERCOT, Draft Version 1. 1; 2013. p. 8.
- [17] Drake Bartlett, Xcel Energy, What is the value of a variable generation forecast? Xcel Energy, February 25, 2014.
- [18] Drake Bartlett, Xcel Energy, Utility Variable-Generation Integration Group Fall 2016 Forecasting Workshop presentation <www.UVIG.org>.
- [19] PacifiCorp, 2012 Wind Integration Resource Study, April 2013 <http://www.pacificorp.com/content/dam/pacificorp/doc/Energy_Sources/Integrated_Resource_Plan/Wind_Integration/2012WIS/2013IRP-AppendixH-2012WindIntegrationStudy_4-30-13.pdf> [accessed November 2016].
- [20] NREL. Wind Technologies Market Report (reproduced from Figure 52); 2013.
- [21] BP Global, Statistical Review of World Energy 2016—data workbook <www.bp.com/content/dam/bp/excel/energy-economics/statistical-review-2016/bp-statistical-review-of-world-energy-2016-workbook.xlsx> [accessed November 2016].
- [22] For an overview of 100% renewable energy cities and efforts, see <<http://www.go100percent.org/cms/>>.

Part V

Environmental Impacts of Wind Energy

This page intentionally left blank

Chapter 21

Life Cycle Assessment: Meta-analysis of Cumulative Energy Demand for Wind Energy Technologies

Michael Carbajales-Dale

Clemson University, Anderson, SC, United States

Email: madale@clemson.edu

21.1 INTRODUCTION

Technology assessment of energy production technologies is often computed in terms of financial cost. The US Department of Energy (DOE) and the National Renewable Energy Laboratory have been aggregating data on cost estimates for electricity generation in an online application: the Transparent Cost Database [1]. Two main metrics exist to assess the cost of, especially electricity generating, infrastructure investment: (1) *Overnight capital cost*—Combines all the capital cost data per unit of (peak) nameplate capacity without interest, as if built *overnight* [2], computed in \$ $(W_p)^{-1}$ (Units of nameplate capacity are presented with a subscript p to denote *peak* power.); (2) *Levelized cost of electricity* (LCOE)—Total costs (including annualized capital and yearly operating) divided by total energy service production [1], computed as \$ $(\text{kW h}_e)^{-1}$ (Electrical energy is denoted with subscript e , primary energy is denoted with a subscript p .).

This chapter will advance the benefits of computation of analogous metrics for energetic “costs” associated with electricity production by renewable energy technologies, such as cumulative energy demand (CED). The chapter then presents the results of a meta-analysis of CED during the various life-cycle stages of wind electricity production, in terms of capital energy cost (CEC)—equivalent to overnight capital cost (in Section 21.5.1), life-cycle energy cost (LCEC)—equivalent to LCOE (in Section 21.5.2). The

CED is also assessed by major component of the wind energy system (in [Section 21.5.4](#)) and trends in the parameters are assessed (in [Section 21.5.5](#)) to determine if there are systematic reductions (e.g., due to learning) occurring within the wind industry. This information is then brought together in [Section 21.5.6](#) where the net energy trajectory of the global wind industry is presented.

21.2 WIND ENERGY TECHNOLOGIES

Growth in installed capacity of wind has been rapid in the last decade with sustained growth rates of 20% during the period 2000–10. Global installed capacity of wind turbines, as depicted in [Fig. 21.1](#), increased over 25-fold from 16 GW in 2000 to over 400 GW in 2015. Around 97% of wind deployment is currently on land, though deployment is increasingly occurring offshore, in increasingly deeper waters, to make use of stronger and more steady winds.

The ratio of average power output to nameplate capacity $\left[\frac{W_{\text{avg}}}{W_p} \right]$ is termed the *capacity factor*. [Fig. 21.2](#) uses data from [\[5,6\]](#) to display the distribution in capacity factor for global installed capacity of wind. The peak in capacity factor occurs around 25%, meaning that a 1 MW_p wind turbine will have an annual electricity production of 2.2 GW h_e (year)⁻¹ (Generally speaking, offshore installations will have a higher capacity factor often greater than 35%).

The main technology for generating electricity from wind is the horizontal axis wind turbine, wherein airfoil-shaped blades spin around a central hub, which sits at the top of a central tower (Vertical axis wind turbines (VAWT) also exist, though generally not for the large, utility-scale turbines, ones as large as 6 MW have been built. Small-scale VAWTs (100–10 000 W) are favored in locations where wind direction changes rapidly and often, e.g., urban settings.). The size of wind turbines have increased from a hub height of less than 30 m in the early 1990s to a hub height of over 100 m today [\[7,8\]](#). Blade length has similarly increased. Power capacity is proportional to the area swept by the blades. The power that can be extracted from the wind is also proportional to the cube of the wind speed. As such there is benefit to increasing the size of wind turbines, both to increase the capture area, but also to take advantage of the more frequent, higher wind speed at greater height. Power capacity of wind turbines has increased by two orders of magnitude from around 100 kW during the 1990s to 10 MW today. The main components of the wind system are rotor, nacelle housing the gearing and generator, tower, foundation, and the balance of system. These are described briefly further.

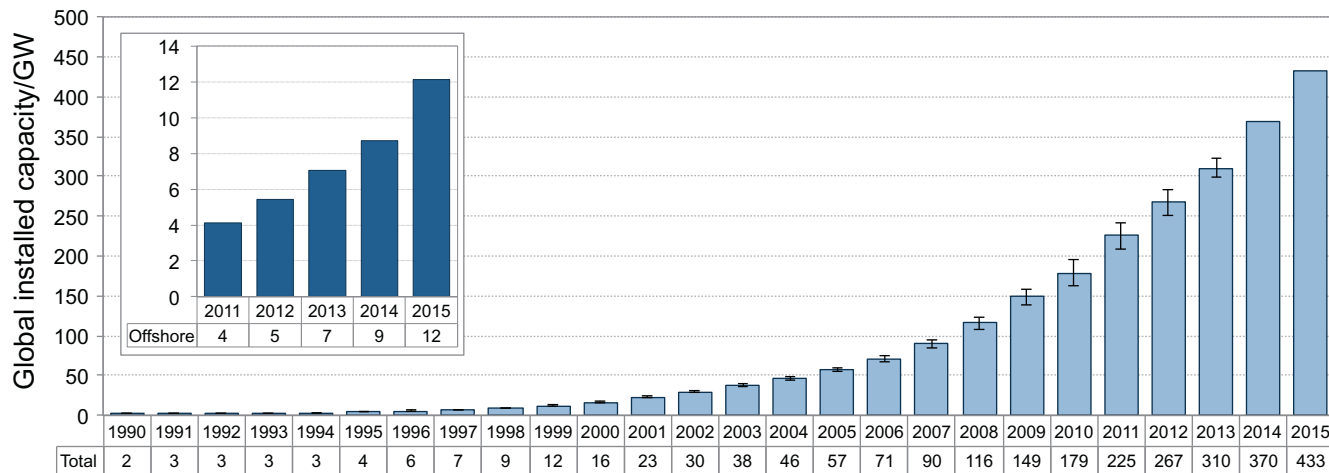


FIGURE 21.1 Global cumulative installed capacity (GW) of wind disaggregated by onshore and offshore. Compiled using data from GWEC. *Global Wind Statistics 2016, Technical Report, Global Wind Energy Council, Brussels, Belgium, <<http://www.gwec.net/global-figures/graphs/>>*; 2016 [Accessed 20.07.16]; EWEA. *Wind in our Sails—The coming of Europe's off-shore wind energy industry; 2011*; UN. *UN Energy Statistics Database, URL: <<http://data.un.org/Explorer.aspx?d=EDATA>>*; 2016 [accessed 25.07.16]; 2016; EIA. *International Energy Statistics, URL: <<http://www.eia.gov/countries/data.cfm>>*; 2016 [accessed 25.07.16]; [3–6].

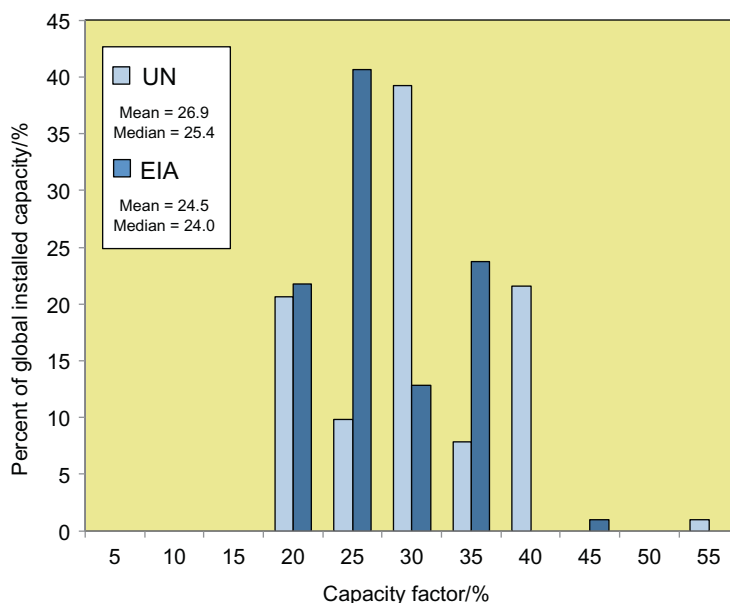


FIGURE 21.2 Distribution in global wind capacity factors using data from [5,6].

21.2.1 Rotor

The rotor is made up of the hub and blades.

21.2.1.1 Hub

The hub connects to the generator shaft by a bearing and also connects to the blades by bearing to allow control of the pitch of the blades. The hub is typically made primarily out of cast iron with a glass fiber reinforced polyester (or similar material) casing called the spinner [9].

21.2.1.2 Blades

The blades of modern turbines are aerofoils, which can reach over 50 m in length, comprising a main spar glued between two shell sections. Primary materials used in blades are carbon fibers and woven glass fibers infused with epoxy resins and polyurethane glue used to assemble the blade shell.

21.2.2 Nacelle

The nacelle houses the electricity generating equipment including gearbox (if geared), generator, foundation, cover, yaw system (a bearing system that allows the wind turbine to change direction to face the wind), and controls.

21.2.2.1 Gearing and Generator

The gearbox converts the low-speed rotation delivered by the blades to a high-speed (1500 rpm) rotation for electricity generation. Typical materials for the gearbox are iron and steel. The generator also consists mainly of iron and steel. Some manufacturers use lighter permanent magnets made from rare earth metals (e.g., neodymium or dysprosium) while others use heavier induction generators [9]. Although most wind turbines have gears, nongeared turbines are being built but must rely on heavier, low-speed generators.

21.2.2.2 Foundation and Cover

The nacelle foundation provides the floor of the nacelle and is often made from cast iron. The cover to the nacelle is typically made from a fiberglass, consisting of woven glass fibers, polyethylene, and styrene.

21.2.3 Tower

The hub height of turbines has increased significantly in recent decades with the tallest turbines reaching over 150 m. As such the turbine tower makes up a large proportion of the mass of the turbine. Typical materials are structural steel, which is rolled and welded into tower sections, or concrete.

21.2.4 Foundation

The foundation of wind turbines can change significantly, depending on the installation location. Onshore foundation designs include: tensionless pier, a cast-in-place concrete ring around 3–5 m in diameter and up to 10 m deep; anchor deep, a 2 m thick concrete ring supported by up to 20 steel anchors up to 15 m deep; and gravity spread, a broad steel-reinforced concrete disk up to 20 m in diameter [10]. Offshore designs include: gravity-based, using mass to prevent the turbine from tipping over; monopile, consisting of a single, hollow steel pile driven into the sea bed; tripod, consisting of a braced Y-frame and three, smaller piles into the sea bed; and floating, consisting of a floating ballast submerged and moored to the sea bed [11].

21.2.5 Balance of Systems

The balance of system comprises all of the other components and installations to allow the wind system to operate. This includes inverters (if the turbine puts out DC electricity), electrical control systems, operational buildings and roads, spare equipment (e.g., replacement blades) grid interconnection, and energy storage (if required).

21.3 LIFE-CYCLE ASSESSMENT

Life-cycle assessment (LCA) is a system of methodologies and tools to evaluate the physical flows and environmental impacts associated with the production of goods and provision of services over the full life cycle from extraction and processing of raw materials through manufacture, operation, and finally to disposal [12]. The LCA is divided into four main phases (1) *goal and scope*—Including the definition of the *functional unit*, which quantifies the service delivered by the product system, definition of system boundaries, clarification of assumptions and limitations, allocation methods (e.g., between coproducts), and impact categories; (2) *Life-cycle inventory* (LCI)—Tracking material and energy flows from and to the environment, often involving either the creation of a “bottom-up” model of the production process, the use of input–output tables, or some hybrid of the two; (3) *Life-cycle impact assessment* (LCIA)—Evaluating the environmental impacts of flows associated with the LCI including selecting appropriate impact categories, indicators and environmental impact models, classification, and measurement of impacts using a common metric to place different categories on an equivalent basis and; (4) *Interpretation*—Including identification of significant issues arising from the LCI and LCIA stages, evaluation of completeness, sensitivity and consistency, and conclusions, limitations and recommendations.

21.3.1 Cumulative Energy Demand

CED is an impact metric that “represents the direct and indirect energy use, including the energy consumed during the extraction, manufacturing and disposal of the raw and auxiliary materials.” [13, p. 2189] Certain environmental energy flows are not accounted, as such the wind flowing through the turbine is not included in the CED for wind-generated electricity.

We may define CED on the basis of either nameplate capacity (to give CEC) or lifetime electricity generation (to give LCEC). Mathematically, we may say

$$\text{CEC} \left[\frac{\text{MJ}_p}{W_p} \right] = \frac{\text{CED}}{K} \quad (21.1)$$

where K is the nameplate capacity of the device and

$$\text{LCEC} \left[\frac{kW h_p}{kW h_e} \right] = \frac{\text{CED}}{E} \quad (21.2)$$

where E is the energy delivered by the device over its lifetime.

21.3.2 Energy Payback Time

Energy payback time (EPBT) is the amount of time that an energy technology takes to deliver the amount of energy required over its life cycle [14]. Mathematically, we may define this as

$$\text{EPBT [years]} = \frac{\text{CED}}{\dot{E}} \quad (21.3)$$

where \dot{E} is the energy delivered by the device annually.

21.3.3 Fractional Reinvestment

The fractional reinvestment, f , defines the amount of electricity that an industry composed of devices with a certain EPBT must invest in deploying new devices to maintain a certain growth rate [15,16] (It should be noted that here EPBT is defined using a quality correction factor to directly compare electricity production with the energy investments, which we denote with a subscript e , where $\text{EPBT}_e = \text{CED}_e/E_e$). Mathematically we can define this as

$$f[\%] = r\text{EPBT}_e \quad (21.4)$$

where r is the industry growth rate in percent per year.

If $f > 100\%$, the industry is running in deficit, if $f < 100\%$, the industry can provide surplus electricity to society. Currently the global photovoltaic industry has a fractional reinvestment, $f_{PV} = 90\%$ meaning that only 10% of electricity production by the PV industry is available for other uses within society.

21.4 META-ANALYSIS

The areas of interest for this analysis are: energy requirements for production of capital infrastructure, *capital energy cost* (CEC), an analog to overnight capital cost, measured on a per unit of nameplate capacity bases; and total life-cycle energy requirements for the system, *life-cycle energy cost* (LCEC), an analog to LCOE, measure on a per unit of electricity production basis.

A recent meta-analysis and harmonization project was carried out by researchers at the National Renewable Energy Laboratory (NREL) and a number of other institutions to determine the distribution in greenhouse gas (GHG) emissions from a variety of electricity production technologies over their entire life cycle. Methodological details are provided in Heath and Mann [17]. The results have been published in a special issue of the *Journal of Industrial Ecology*. This analysis uses the NREL methodology to build upon previous meta-analyses, which have been done for the energy inputs to wind electricity production [7,8,15].

21.4.1 Literature Search

Searches were made of a number of publication types including peer-reviewed journals, industry reports, reports by national agencies, e.g., the US Department of Energy (DOE) and other work, e.g., conference papers and doctoral theses. The search terms included the “wind,” with the following phrases: “embodied

energy”; “cumulative energy demand”; “life cycle inventory”; “life cycle assessment”; “energy payback time”; “net energy ratio” (NER); “energy yield ratio” (EYR); “energy return on investment”; and “EROI.”

The initial search produced 120 items published since 2012. These were then passed to the screening process.

21.4.2 Literature Screening

A number of criteria were used to screen the initial results (1) the study should be in English; (2) the study should be original research or should reference data used; (3) the study should give data on wind turbine technologies; (4) the study should give numeric data on net energy metrics, e.g., CED, or net energy ratio (NER); and (5) the study should give sufficient information on assumptions and system boundaries to allow for harmonization. Cross-referenced estimates were also eliminated. The studies remaining after screening are presented in [Table 21.1](#) along with data from previous meta-analyses [\[7,8,15\]](#).

21.4.3 Harmonization of Study Boundaries and Data

A number of methods were used to allow comparison of results: Data given in terms of primary energy was changed to electricity equivalents using conversion factors given in the study. If no conversion factor was given, a standard conversion factor of 30% was used. If data was given in terms of an energy intensity, i.e., energy inputs per unit of electricity produced, e.g. $[MJ (kW h_e)^{-1}]$, this was converted to per unit capacity inputs by either: using the capacity factor, i.e., the ratio of the average power output to nameplate capacity of the system; or using the total lifetime electricity production of the system; or using the annual electricity production of the system and the lifetime of the system, if no lifetime was given, the system was assumed to have a nominal lifetime of 25 years.

21.5 RESULTS AND DISCUSSION

The raw data from the studies was used to calculate three metrics: CEC; LCEC; and EPBT, presented in [Table 21.1](#). Further data was collected from the studies to determine the proportion of CED that each of the major components comprised.

21.5.1 Capital Energetic Costs (CEC)

Capital costs include the energy requirements to extract and process all raw materials, manufacture, and install the capital equipment including any site preparation and grid interconnection. Units of measurement for CEC are primary energy inputs per unit of nameplate capacity $[MJ_p (W_p)^{-1}]$.

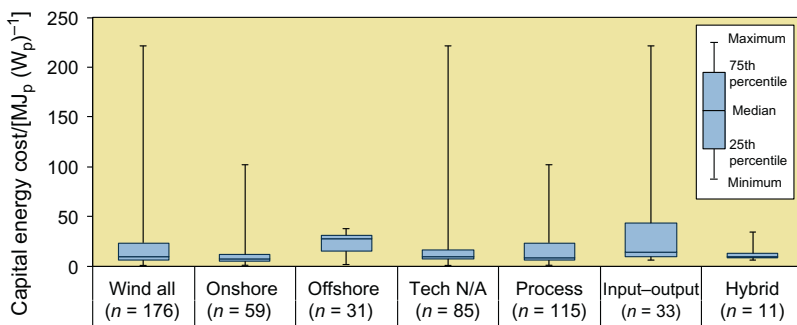


FIGURE 21.3 Capital energy cost (CEC) [$\text{MJ}_p (\text{W}_p)^{-1}$] different wind technologies (onshore, offshore, and unspecified) and when using different analysis methodologies (process-based, input–output, hybrid).

Fig. 21.3 shows the distribution in estimates of CEC for the various wind technologies and analysis methods. This presentation does not account for changes in these values over time but instead shows the distribution across all studies over the more than 40 year period. The boxes represent 25–50–75 percentiles and whiskers plot minimum and maximum values. Generally there is a large min–max range in the data, with much smaller interquartile range. Onshore wind tends to have a lower CEC than offshore wind (due to the added costs of offshore deployment). Input–output analysis tends to produce higher estimates with a larger range, whereas hybrid analyses produced the lowest range and median value.

21.5.2 Life-Cycle Energy Costs (LCEC)

LCEC includes all of the energy inputs over the full life cycle of the system, including end-of-life, normalized by the total lifetime electricity output from the system. The unit of measurement is primary energy per unit of electricity production [$\text{kW h}_p (\text{kW h}_e)^{-1}$]. Unlike the financial metric LCOE, no discounting of inputs and outputs has been made.

Fig. 21.4 shows the life-cycle energy requirements for onshore and offshore technologies and all of the different analysis methods. Similarly to CEC we find a wide range in the data. Again onshore has a lower median value than offshore and process analysis methods produce a lower variation in value.

21.5.3 Harmonization

During the harmonization procedure, parameter inputs that impact the calculation of performance metrics are substituted for standard values. We will harmonize the capacity factor and turbine lifetime to analyze the effect on LCEC. In Fig. 21.5A we see the unharmonized values of

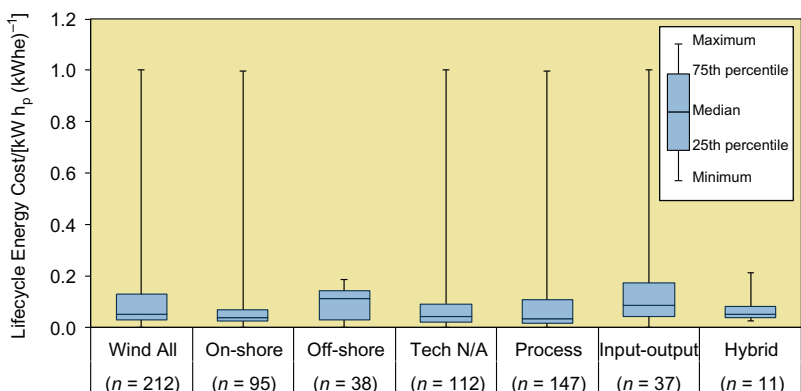


FIGURE 21.4 Life-cycle energy cost (LCEC) [$\text{kW h}_p (\text{kW h}_e)^{-1}$] of different wind technologies (onshore, offshore, unspecified) and when using different analysis methodologies (process-based, input—output, hybrid).

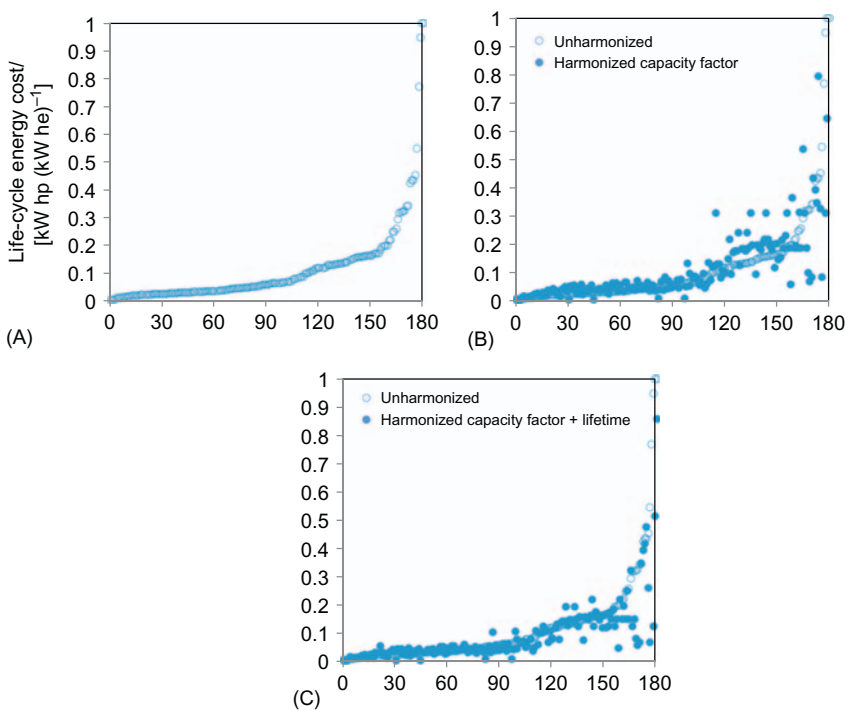


FIGURE 21.5 Harmonization of capacity factor and lifetime. (A) Unharmonized, (B) Harmonized capacity factor (25%), (C) Harmonized capacity factor and lifetime (25 years).

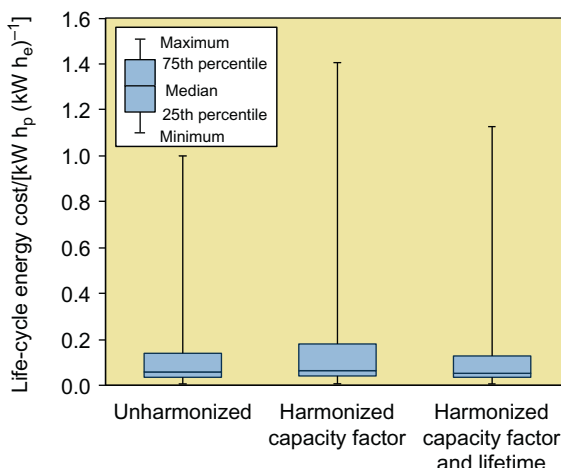


FIGURE 21.6 Life-cycle energy cost (LCEC) [$\text{kW h}_p (\text{kW h}_e)^{-1}$] of unharmonized data and after harmonization of capacity factor and lifetime.

LCEC computed using the data in the studies and ranked from smallest to largest. The corresponding distribution is shown in Fig. 21.6. We first replace the value for capacity factor used in the study, with a standard value of 25% (representing the global median value, as shown in Fig. 21.2) and recalculate LCEC, as shown ranked in Fig. 21.5B. As can be seen in the new distribution in Fig. 21.6 this step actually increased the min–max and interquartile range, and slightly increased the median value. We then replaced the turbine lifetime used in the study, with a nominal value of 25 years. The recalculated values for LCEC can be seen in Fig. 21.5C with the corresponding distribution again shown in Fig. 21.6. The min–max range has now decreased (though still not below the unharmonized range), however, the interquartile range has decreased below unharmonized.

21.5.4 Components

Many of the studies provide a breakdown of CED by different components. This data is presented in Table 21.2 with distributions presented in Fig. 21.7. Again there is a large distribution to the values. The tower contributes the highest median value to the overall CED (23%). Transport has the highest range in values, which is greatly influenced by both distance and the size of the system. Disposal presents an interesting case. Many studies give energy credits for recycling of turbine materials (primarily steel), leading to a negative value, as much as 50% of the overall value.

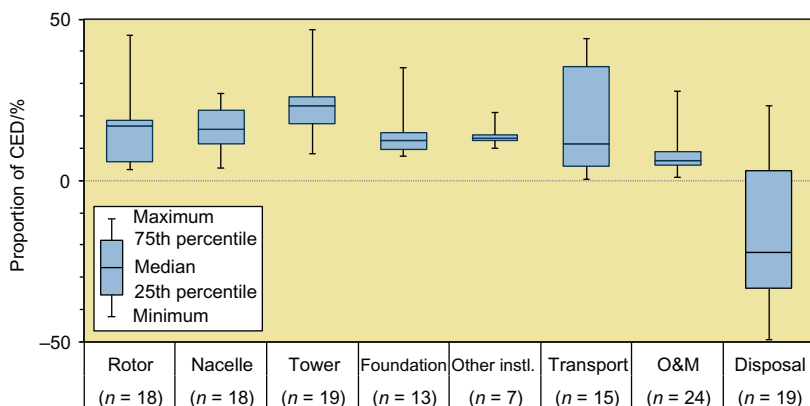


FIGURE 21.7 Proportion of cumulative energy demand (CED) made up by different components, based on data presented in Table 21.2. Disposal is often calculated to have negative embodied energy due to recycling credits.

21.5.5 Trends in Parameters

The distributions presented in Figs. 21.3–21.7, did not account for all physical attributes of the turbines or studies. For instance we might expect that larger turbines might have a lower CEC or that a turbine built today would have a lower CED than the equivalent turbine built 10 years ago.

To assess the relationship between CEC and turbine power rating, we present Fig. 21.8. CEC decreases as turbine rating increases.

We also expect that as installed capacity increases the industry decreases the cost of producing wind power systems. The energy learning curve for wind is depicted in Fig. 21.9 with a power curve fitted to the data. The learning rate is defined as the percent reduction in cost per doubling of installed capacity. The learning rate for the wind industry is approximately 5%.

21.5.6 Net Energy Trajectory of the Global Wind Industry

Combining data on CED and EPBT (including learning effects, see Section 21.5.5), as well as global wind industry capacity factors 21.2 and growth rate of installed capacity (see Fig. 21.1), we can determine the fractional reinvestment in each year. Combining these annual values we can develop the net energy trajectory for the global wind industry, as shown in

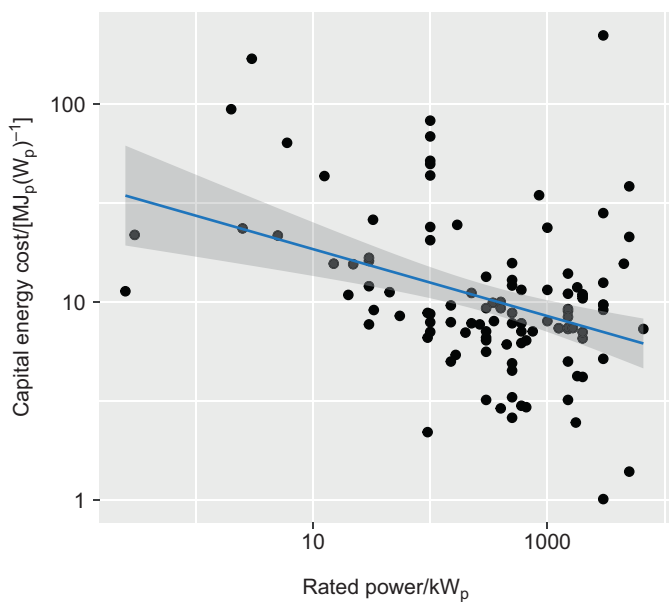


FIGURE 21.8 Estimates of capital energy cost (CEC) [$\text{MJ}_p (\text{W}_p)^{-1}$] as a function of the turbine rated power [kW_p] on a log–log scale with a power curve fitted to the data. CEC decreases as the power rating increases.

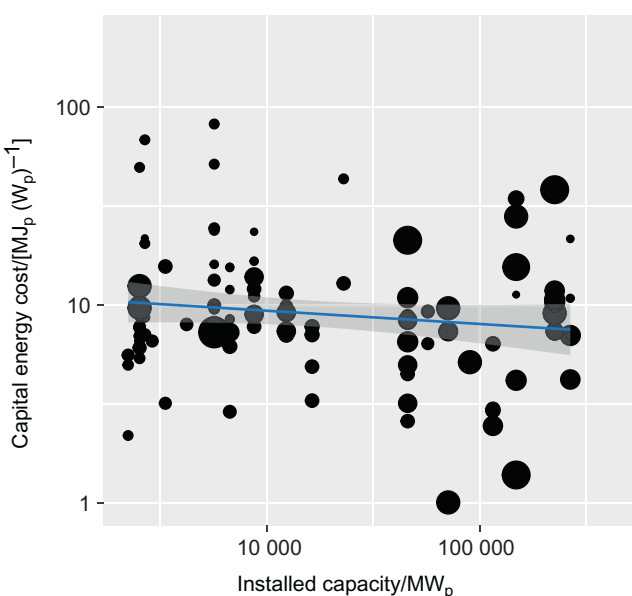


FIGURE 21.9 Estimates of capital energy cost (CEC) [$\text{MJ}_p (\text{W}_p)^{-1}$] as a function of the global installed capacity of wind [MW_p] on a log–log scale with a power curve fitted to the data. CEC decreases as the installed capacity increases.

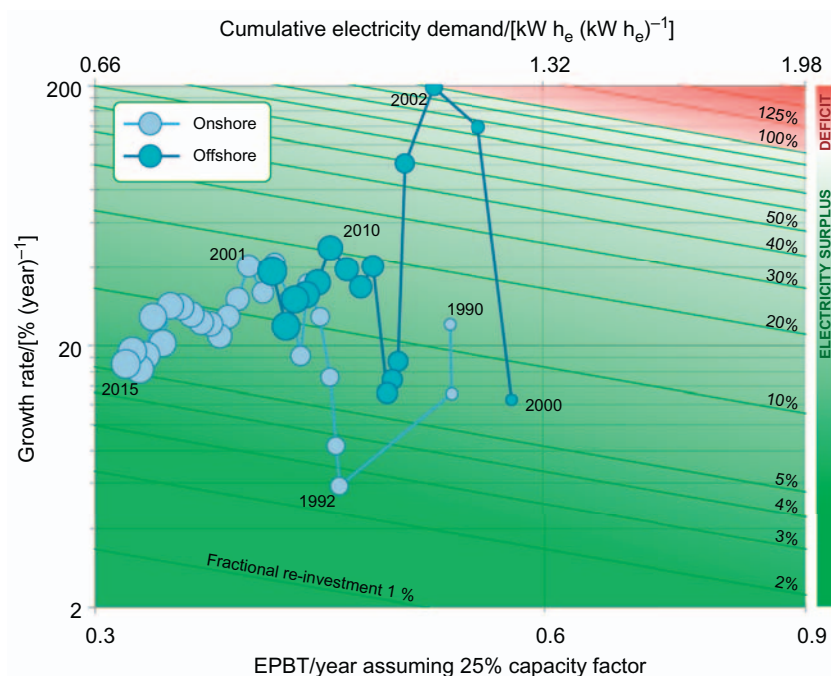


FIGURE 21.10 Net energy trajectories for the onshore and offshore wind industries.

Fig. 21.10 (It is worth noting that these values are based on a capacity factor of 25%. In reality offshore wind farms tend to have higher capacity factors (more like 35%–40%), so are likely to have shorter EPBT and correspondingly lower fractional reinvestment.).

As can be seen both the onshore and offshore wind industries are operating with low fractional reinvestment. The onshore industry currently has a growth rate of around 16 year^{-1} and wind turbines have an EPBT_e of just over 0.3 years, giving $f_{ON} = 5\%$. The offshore wind industry is currently growing more rapidly at a rate of around 40 year^{-1} and has a higher EPBT (since less offshore capacity has been installed) giving a higher fractional reinvestment, $f_{OFF} = 15\%$.

21.6 CONCLUSIONS

The results of meta-analysis of energy requirements (CED) for wind electricity production technologies has been presented. To facilitate the utility of this information, the metrics presented, CEC and LCEC, are direct analogies of financial metrics commonly used to characterize electricity production technologies, overnight capital cost and LCOE, respectively. The

meta-analysis also determined another commonly used metric for assessing wind turbines, EPBT.

The results showed a large variation in both CEC and LCEC. The results were then harmonized for both capacity factor (to the global median value of 25%) and lifetime (to a value of 25 years). Results showed an increase in the interquartile range after harmonization for capacity factor, which was decreased after subsequent harmonization of lifetime. We also presented a breakdown of CED by major component/life-cycle phase, which also showed a large range between studies. Disposal had the highest variation comprising between 22% and negative 50% if recycling credits were included.

Analyzing trends in the data showed that CEC decreases as a function of turbine power rating [W_p] and also as a function of global installed capacity with a learning rate of around 5%. This compares with a learning rate in the PV industry of over 20% [18,16].

All of this information was combined to calculate the net energy trajectory of the global wind industry. The industry is clearly a net electricity provider, both in terms of onshore as well as offshore installations, with both having fractional reinvestment rates of below 20%. In fact the industry could be growing at over 10 times its current rate and still be providing net electricity to society, over and above providing sufficient energy to meet its own needs.

ACKNOWLEDGMENTS

The author would like to acknowledge financial support from the Environmental Engineering & Earth Sciences department at Clemson University.

REFERENCES

- [1] DOE. Transparent cost database, 2012, URL: <<http://en.openei.org/apps/TCDB/>>; 2012 [accessed 16.12.12].
- [2] Koomey J, Hultman N. A reactor-level analysis of busbar costs for us nuclear plants, 1970–2005. *Energy Policy* 2007;35:5630–42.
- [3] GWEC, Global Wind Statistics. Technical report, Global Wind Energy Council, Brussels, Belgium, <<http://www.gwec.net/global-figures/graphs/>>; 2016 [accessed 20.07.16].
- [4] EWEA. Wind in our sails—The coming of Europe's off-shore wind energy industry; 2011.
- [5] UN. UN Energy Statistics Database, 2016. URL: <<http://data.un.org/Explorer.aspx?d=EDATA>>; 2016 [accessed 25.07.16].
- [6] EIA. International Energy Statistics, 2016. URL: <<http://www.eia.gov/countries/data.cfm>>; 2016 [accessed 25.07.16].
- [7] Lenzen M, Munksgaard J. Energy and CO₂ life-cycle analyses of wind turbines—review and applications. *Renewable Energy* 2002;26:339–62.
- [8] Kubiszewski I, Cleveland C, Endres P. Meta-analysis of net energy return for wind power systems. *Renewable energy* 2010;35:218–25.

- [9] Vestas. Life cycle assessment of electricity production from an onshore V90–3.0 MW wind plant; 2013.
- [10] Tong W. *Wind power generation and wind turbine design*. Wit Press; 2010.
- [11] Tsai L. An integrated assessment of offshore wind farm siting: a case 335 study in the Great Lakes of Michigan, Ph.D. thesis. The University of Michigan; 2013.
- [12] ISO. ISO 14040—environmental management - life cycle assessment - principles and framework; 1998.
- [13] Huijbregts MA, Hellweg S, Frischknecht R, Hendriks HW, Hungerbühler K, Hendriks AJ. Cumulative energy demand as predictor for the environmental burden of commodity production. *Environ Sci Technol* 2010;44:2189–96.
- [14] J.M. Teem. Erda, the option generator, In: Electron Devices Meeting, 1975 International, IEEE, 1975. pp. 275–278.
- [15] Dale M. A comparative analysis of energy costs of photovoltaic, solar thermal, and wind electricity generation technologies. *Appl Sci* 2013;3:325–37.
- [16] Carbajales-Dale M, Barnhart CJ, Benson SM. Can we afford storage? A dynamic net energy analysis of renewable electricity generation supported by energy storage. *Energy Environ Sci* 2014;7:1538–44.
- [17] Heath G, Mann M. Background and reflections on the life cycle assessment harmonization project. *J Ind Ecol* 2012;16:S8–11.
- [18] Dale M, Benson SM. Energy balance of the global photovoltaic (pv) industry—is the pv industry a net electricity producer?. *Environ Sci Technol* 2013;47:3482–9.
- [19] White S, Kulcinski G. Net energy payback and co₂ emissions from wind-generated electricity in the midwest. Madison, WI: Fusion Technology Institute; 1998.
- [20] Brown M, Ulgiati S. Energy evaluations and environmental loading of 360 electricity production systems. *J Cleaner Prod* 2002;10:321–34.
- [21] Gagnon L, Belanger C, Uchiyama Y. Life-cycle assessment of electricity generation options: the status of research in year 2001. *Energy Policy* 2002;30:1267–78.
- [22] Khan FI, Hawboldt K, Iqbal MT. Life cycle analysis of wind-fuel cell integrated system. *Renewable Energy* 2005;30:157–77.
- [23] Wagner HJ, Pick E. Energy yield ratio and cumulative energy demand for wind energy converters. *Energy* 2004;29:2289–95.
- [24] Tryfonidou R, Wagner H-J. Multi-megawatt wind turbines for offshore use: aspects of life cycle assessment. *Int J Global Energy Issues* 2004;21:255–62.
- [25] Lenzen M, Wachsmann U. Wind turbines in Brazil and Germany: an example of geographical variability in life-cycle assessment. *Appl Energy* 2004;77:119–30.
- [26] Elsam. Life cycle assessment of offshore and onshore sited wind farms; 2004.
- [27] Hondo H. Life cycle GHG emission analysis of power generation systems: Japanese case. *Energy* 2005;30:2042–56.
- [28] Ardente F, Beccali M, Cellura M, Brano VL. Energy performances and life cycle assessment of an Italian wind farm. *Renewable Sustainable Energy Rev* 2008;12:200–17.
- [29] Pehnt M. Dynamic life cycle assessment (LCA) of renewable energy technologies. *Renewable Energy* 2006;31:55–71.
- [30] Nalukowe BB, Liu J, Damien W, Lukawski T. Life cycle assessment of a wind turbine, report IN1800; 2006.
- [31] Vestas. Life cycle assessment of electricity produced from onshore sited wind power plants based on Vestas V82-1.65MW turbines; 2006.
- [32] Lee Y, Tzeng Y. Development and life-cycle inventory analysis of wind energy in Taiwan. *J Energy Eng* 2008;134:53–7.

- [33] Martinez E, Sanz F, Pellegrini S, Jimenez E, Blanco J. Life-cycle assessment of a 2-MW rated power wind turbine: CML method. *Int J Life Cycle Assess* 2009;14:52–63.
- [34] Weinzettel J, Reenaas M, Solli C, Hertwich EG. Life cycle assessment of a floating offshore wind turbine. *Renewable Energy* 2009;34:742–7.
- [35] Tremeac B, Meunier F. Life cycle analysis of 4.5 MW and 250 W wind 395 turbines. *Renewable Sustainable Energy Rev* 2009;13:2104–10.
- [36] Crawford RH. Life cycle energy and greenhouse emissions analysis of wind turbines and the effect of size on energy yield. *Renewable Sustainable Energy Rev* 2009;13:2653–60.
- [37] Fleck B, Huot M. Comparative life-cycle assessment of a small wind turbine for residential off-grid use. *Renewable Energy* 2009;34:2688–96.
- [38] Mithraratne N. Roof-top wind turbines for microgeneration in urban houses in New Zealand. *Energy Buildings* 2009;41:1013–18.
- [39] Chen G, Yang Q, Zhao Y. Renewability of wind power in China: a case study of nonrenewable energy cost and greenhouse gas emission by a plant in Guangxi. *Renewable Sustainable Energy Rev* 2011;15:2322–9.
- [40] Yang Q, Chen G, Zhao Y, Chen B, Li Z, Zhang B, et al. Energy cost and greenhouse gas emissions of a Chinese wind farm. *Procedia Environ Sci* 2011;5:25–8.
- [41] Vestas. Life cycle assessment of electricity production from a V80-2.0 MW Grid streamer wind plant; 2011.
- [42] Wagner H, Baack C, Eickelkamp T, Epe A, Lohmann J, Troy S. Life cycle assessment of the offshore wind farm *alpha ventus*. *Energy* 2011;36:2459–64.
- [43] Zimmermann T. Parameterized tool for site specific LCAs of wind energy converters. *Int J Life Cycle Assess* 2013;18:49–60.
- [44] Guezuraga B, Zauner R, Pölz W. Life cycle assessment of two different 2 mw class wind turbines. *Renewable Energy* 2012;37:37–44.
- [45] Kabir M, Rooke B, Dassanayake G, Fleck B. Comparative life cycle energy, emission, and economic analysis of 100 kw nameplate wind power generation. *Renewable Energy* 2012;37:133–41.
- [46] Raadal HL, Vold BI. GHG emissions and energy performance of wind power, LCA of two existing onshore wind farms and six offshore wind concepts. Report Ostfold Research, OR 24; 2012.
- [47] Demir N, Taşkin A. Life cycle assessment of wind turbines in pınarbaşı-kayseri. *J Cleaner Prod* 2013;54:253–63.
- [48] Greening B, Azapagic A. Environmental impacts of micro-wind turbines and their potential to contribute to UK climate change targets. *Energy* 2013;59:454–66.
- [49] Marimuthu C, Kirubakaran V. Carbon payback period for solar and wind energy project installed in India: a critical review. *Renewable Sustainable Energy Rev* 2013;23:80–90.
- [50] Rajaei M, Tinjum JM. Life cycle assessment of energy balance and emissions of a wind energy plant. *Geotech Geol Eng* 2013;31:1663–70.
- [51] Vestas. Life cycle assessment of electricity production from an onshore V100-2.6 MW wind plant; 2013.
- [52] Wagner H, Mathur J. *Introduction to wind energy systems—basics, technology and operation*. Springer; 2013.
- [53] Yang J, Chen B. Integrated evaluation of embodied energy, greenhouse gas emission and economic performance of a typical wind farm in China. *Renewable Sustainable Energy Rev* 2013;27:559–68.
- [54] Uddin MS, Kumar S. Energy, emissions and environmental impact analysis of wind turbine using life cycle assessment technique. *J Cleaner Prod* 2014;69:153–64.

- [55] Vestas. Life cycle assessment of electricity production from an onshore V105-3.3 MW wind plant; 2014.
- [56] Vestas. Life cycle assessment of electricity production from an onshore V117-3.3 MW wind plant; 2014.
- [57] Vestas. Life cycle assessment of electricity production from an onshore V126-3.3 MW wind plant; 2014.
- [58] Al-Behadili S, El-Osta W. Life cycle assessment of Dernah (Libya) wind farm. *Renewable Energy* 2015;83:1227–33.
- [59] Aso R, Cheung WM. Towards greener horizontal-axis wind turbines: analysis of carbon emissions, energy and costs at the early design stage. *J Cleaner Prod* 2015;87:263–74.
- [60] Martínez E, Blanco J, Jiménez E, Saenz-Díez J, Sanz F. Comparative evaluation of life cycle impact assessment software tools through a wind turbine case study. *Renewable Energy* 2015;74:237–46.
- [61] Matveev A, Shcheklein S. Life cycle analysis of low-speed multiblade wind turbine. *Int J Renew Energy Res (IJRER)* 2015;5:991–7.
- [62] Nagashima S, Uchiyama Y, Okajima K. Environment, energy and economic analysis of wind power generation system installation with input-output table. *Energy Procedia* 2015;75:683–90.
- [63] Noori M, Kucukvar M, Tatari O. A macro-level decision analysis of wind power as a solution for sustainable energy in the USA. *Int J Sustainable Energy* 2015;34:629–44.
- [64] Vargas A, Zenón E, Oswald U, Islas J, Güereca L, Manzini F. Life cycle assessment: a case study of two wind turbines used in Mexico. *Appl Therm Eng* 2015;75:1210–16.
- [65] Vestas. Life cycle assessment of electricity production from an onshore V100-2.0 MW wind plant; 2015.
- [66] Vestas. Life cycle assessment of electricity production from an onshore V112-3.3 MW wind plant; 2015.
- [67] Cheng VK, Hammond GP. Life-cycle energy densities and land-take requirements of various power generators: a UK perspective. *J Energy Inst* 2016;90(2):201–13.

APPENDIX A

TABLE 21.1 Results From Meta-analysis With Capital Energy Cost (CEC) [$\text{MJ}_p (\text{W}_p)^{-1}$], Life-Cycle Energy Cost (LCEC) ($\text{kW h}_p (\text{kW h}_e)^{-1}$) and Energy Payback Time (EPBT) (years)

Reference	Year	Location	Power rating/kW	Life/years	Turbine	Tech. ^a	Hub height/m	Rotor Diameter/m	Wind Speed/m/s	Operating	Capacity Factor/%	Analysis Type ^b	Scope ^c	CEC/ $[\frac{\text{MJ}_p}{\text{W}_p}]$	LCEC/ $\frac{\text{kW h}_p}{\text{kW h}_e}$	EPBT ^d /years
[7]	1977	USA	1500	30	2 blades	N/A	50	60	10.5	No	50.4	I/O	BCEMT	10.96	0.02	0.7
[7]	1980	UK	1000	25		ON		46	18.4	No	18.3	I/O	CM	11.54	0.08	2.0
[7]	1980	UK	1000	25		N/A		46	18.4	No	18.3	I/O	CM	23.65	0.16	4.1
[7]	1981	USA	3	20		N/A	20	4.3	10.1	Yes	26.8	I/O	CMO	169.03	1.00	20.0
[7]	1983	Germany	2	15		N/A				Yes	45.7	I/O	CM	93.99	0.43	6.5
[7]	1983	Germany	6	15		N/A				Yes	45.7	I/O	CM	63.58	0.29	4.4
[7]	1983	Germany	12.5	15		N/A				Yes	45.7	I/O	CM	43.24	0.20	3.0
[7]	1983	Germany	32.5	15		N/A				Yes	45.7	I/O	CM	26.05	0.12	1.8
[7]	1983	Germany	3000	20	2 blades	N/A	100	100		Yes	45.7	I/O	CM	221.72	0.77	15.4
[7]	1990	Denmark	95	20	3 blades	ON	22.6	19		Yes	25.2	PA	M	2.23	0.01	0.3
[7]	1990	Denmark	150	25		N/A				Yes	30.1	PA	M	4.99	0.02	0.5

(Continued)

TABLE 21.1 (Continued)

Reference	Year	Location	Power rating/kW	Life/years	Turbine	Tech. ^a	Hub height/m	Rotor Diameter/m	Wind Speed/ $\frac{m}{s}$	Operating	Capacity Factor/%	Analysis Type ^b	Scope ^c	$CEC/\left[\frac{Mj_p}{W_p}\right]$	$LCFC/\frac{kW\cdot h_p}{kW\cdot h_e}$	EPBT ^d /years
[7]	1990	Germany	300	20	3 blades	N/A	34	32	11.5	Yes	28.9	PA	CMT	5.64	0.03	0.6
[7]	1991	Japan	100	20		N/A				Yes	31.5	I/O	CMT	49.67	0.25	5.0
[7]	1991	Germany	30	20	2 blades	N/A	14.8	12.5	13	Yes	14.4	PA	CGMOT	7.70	0.08	1.7
[7]	1991	Germany	33	20	2 blades	N/A	22	14.8	11	Yes	29.4	PA	M	9.09	0.05	1.0
[7]	1991	Germany	45	20		N/A		12.5		Yes	33.5	PA	M	11.18	0.05	1.1
[7]	1991	Germany	95	20	3 blades	ON	22.6	19		Yes	20.5	PA	CGMT	8.80	0.07	1.4
[7]	1991	Germany	95	20	3 blades	N/A	22.6	19		Yes	20.5	PA	M	6.60	0.05	1.0
[7]	1991	Germany	100	20	2 blades	N/A	24.2	34	8	Yes	20.9	PA	M	7.89	0.06	1.2
[7]	1991	Germany	150	20	3 blades	N/A	30	23	13	Yes	25.6	PA	M	7.91	0.05	1.0
[7]	1991	Germany	165	20	3 blades	N/A	32	25	13.5	Yes	23.2	PA	M	5.42	0.04	0.7
[7]	1991	Germany	200	20	3 blades	N/A	30	26	13	Yes	21	PA	M	7.01	0.05	1.1
[7]	1991	Germany	225	20		N/A		27		Yes	39.9	PA	M	7.79	0.03	0.6
[7]	1991	Germany	265	20	2 blades	N/A	30.5	52	8.5	Yes	19	PA	M	7.68	0.06	1.3
[7]	1991	Germany	300	20		N/A		32		No	39.9	PA	M	9.32	0.04	0.7
[7]	1991	Germany	450	20	3 blades	N/A	36	35	18	Yes	20	PA	GM	6.06	0.05	1.0
[7]	1991	Germany	3000	20		N/A		80		No	34.2	PA	M	9.72	0.05	0.9

[7]	1991	Germany	3000	20	2 blades	N/A	100	100	12	Yes	30.4	PA	GM	12.45	0.06	1.3
[7]	1992	Japan	100	20		N/A				Yes	31.5	I/O	CMOT	68.51	0.34	6.9
[7]	1992	Japan	100	30		N/A		30	13	Yes	28	I/O	CMOT	8.74	0.03	1.0
[7]	1992	Japan	100	30		N/A		30	10	Yes	40	I/O	CMOT	20.46	0.05	1.6
[7]	1992	Germany	0.3	20	3 blades	N/A	11.6	1.5	9	Yes	38.8	PA	CDMOT	21.85	0.09	1.8
[7]	1992	Germany	300	20	3 blades	N/A	34	32		No	41.9	PA	CDGMOT	7.14	0.03	0.5
[7]	1993	Germany	300	20		N/A				Yes	22.8	PA	CDMOT	6.63	0.05	0.9
[7]	1994	Germany	500	20		N/A				Yes	27.4	I/O	CM		0.00	
[7]	1994	Germany	300	20		N/A				Yes	22.8	PA	MO(D)	3.16	0.02	0.4
[7]	1994	Germany	500	20	2/3 blades	N/A	41	39		Yes	36.5	PA	M	15.66	0.07	1.4
[7]	1995	UK	350	20	3 blades	N/A	30	30	15	Yes	30	PA	M	7.95	0.04	0.8
[7]	1996	Japan	100	30		N/A				Yes	20	I/O	CMO	82.27	0.43	13.0
[7]	1996	Japan	100	20	1984	N/A		30		Yes	18	I/O	CMO	51.60	0.45	9.1
[7]	1996	Japan	170	20		N/A		27		Yes	22.5	I/O	CMO	24.47	0.17	3.4
[7]	1996	Japan	300	20		N/A		28		Yes	18	I/O	CMO	13.36	0.12	2.4
[7]	1996	Japan	400	20		N/A		31		Yes	18	I/O	CMO	9.96	0.09	1.8
[7]	1996	Germany	1000	20	3 blades	N/A	55	54		Yes	18.5	I/O	CMO		0.00	
[7]	1996	UK	6600	20		N/A				Yes	29	I/O	CDMO	7.32	0.04	0.8
[7]	1996	Switzerland	30	20	2 blades	N/A	22	12.5	11.4	Yes	7.9	PA	CDGMOT	16.07	0.32	6.5
[7]	1996	Germany	100	20	3 blades	N/A	30	20		Yes	31.4	PA	CMO	23.86	0.12	2.4
[7]	1996	Switzerland	150	20	3 blades	N/A	30	23.8		Yes	7.6	PA	CDGMOT	9.59	0.20	4.0
[7]	1996	Germany	1000	20	3 blades	N/A	55	54		Yes	18.5	PA	CMO		0.00	

(Continued)

TABLE 21.1 (Continued)

Reference	Year	Location	Power rating/kW	Life/years	Turbine	Tech. ^a	Hub height/m	Rotor Diameter/m	Wind Speed/ $\frac{m}{s}$	Operating	Capacity Factor/%	Analysis Type ^b	Scope ^c	$CEC/\left[\frac{M_p}{W_p}\right]$	$LCFC/\frac{kW\cdot h_p}{kW\cdot h_e}$	EPBT ^d /years
[7]	1996	Germany	1000	20	3 blades	N/A	50	60		No	36.2	PA	CMO	7.98	0.03	0.7
[7]	1997	Denmark	15	20	1980	N/A	18	10		Yes	20.5	I/O	CMO	15.58	0.12	2.4
[7]	1997	Denmark	22	20	1980	N/A	18	10.5		Yes	19.9	I/O	CMO	15.50	0.12	2.5
[7]	1997	Denmark	30	20	1980	N/A	19	11		Yes	19	I/O	CMO	11.98	0.10	2.0
[7]	1997	Denmark	55	20	1980	N/A	20	16		Yes	20.6	I/O	CMO	8.55	0.07	1.3
[7]	1997	Denmark	600	20	3 blades	N/A	50	47	15	Yes	26.5	I/O	BCDEGMOT	6.19	0.04	0.7
[7]	1997	Denmark	1500	20	3 blades	OFF	55	64	17	No	38.4	I/O	CMO	7.27	0.03	0.6
[7]	1997	Denmark	400	20		N/A				Yes	22.8	PA	M(O)	2.88	0.02	0.4
[7]	1998	Germany	500	20	3 blades	N/A	44	40.3		Yes	29.6	I/O	CGMOT	12.12	0.06	1.3
[7]	1998	Germany	1500	20	3 blades	N/A	67	66		Yes	31	I/O	CGMOT	13.87	0.07	1.4
[7]	1998	Argentina	2.5	20		N/A				No	22	PA	CMT(O)	23.52	0.17	3.4
[7]	1998	Argentina	30	20		N/A				No	22	PA	CMT(O)	16.72	0.12	2.4
[7]	1998	Argentina	225	20		N/A				No	22	PA	CMT(O)	11.10	0.08	1.6
[7]	1998	Germany	500	20	3 blades	N/A	44	40.3		Yes	29.6	PA	CGMOT	7.84	0.04	0.8
[7]	1998	Germany	1500	20	3 blades	N/A	67	66		Yes	31	PA	CGMOT	9.01	0.05	0.9

[19]	1999	USA	342.5	30	Kenetech KVS-33	ON	36.6	32.9		Yes	24	I/O	(B)CDMOT	9.87	0.04	1.3
[19]	1999	USA	600	20	Tacke 600e	ON	60	46	6.1	Yes	31	I/O	(B)CDMOT	11.50	0.06	1.2
[19]	1999	USA	750	25	Zond Z-46	ON	48.5	46		Yes	35	I/O	(B)CDMOT	7.08	0.03	0.6
[7]	1999	Germany	1500	20		N/A	67	66		No	31	PA	CDGMOT	7.43	0.04	0.8
[7]	1999	India	1500	20	E-66	N/A	67	66		No	45.9	PA	CDGMOT	9.25	0.03	0.6
[7]	2000	Belgium	600	20		N/A				Yes	34.2	I/O	DM(O)	7.76	0.04	0.7
[20]	2000	Italy	2500	0		N/A				Yes		I/O	MCO		0.13	
[7]	2000	Belgium	600	20		N/A				Yes	34.2	PA	DM(O)	7.12	0.03	0.7
[7]	2000	Denmark	500	20	3 bladeS	OFF	40.5	39	16	Yes	40	N/A	MTCGOD	4.92	0.02	0.4
[7]	2000	Denmark	500	20		ON	41.5			Yes	40	N/A	MTCGOD	3.28	0.01	0.3
[7]	2001	Japan	100	25		N/A	30	30		Yes	34.8	I/O	CMT	43.55	0.16	4.0
[7]	2001	Brazil	500	20	3 blades; E40	N/A	44	40.3		Yes	29.6	I/O	CGMOT	12.88	0.07	1.4
[21]	2002	USA				N/A				No		N/A	TCO		0.01	
[22]	2003	Canada	500	20		N/A				No		PA	MCTOD		0.01	0.2
[22]	2003	Canada	500	20		N/A				No		PA	MCTOD		0.01	0.2
[22]	2003	Canada	500	20		N/A				No		PA	MCTOD		0.01	0.2
[23]	2004	Germany	500	20	Enercon E-40	ON	44	40.3		No	29	PA	MCTO	2.61	0.01	0.3
[23]	2004	Germany	500	20	Enercon E-40	ON	55	40.3		No	38	PA	MCTO	4.52	0.02	0.4
[23]	2004	Germany	500	20	Enercon E-40	ON	65	40.3		No	53	PA	MCTO	8.80	0.03	0.5
[23]	2004	Germany	1500	20	Enercon E-40	ON	67	66		No	32	PA	MCTO	3.15	0.02	0.3
[23]	2004	Germany	1500	20	Enercon E-40	ON	67	66		No	40	PA	MCTO	5.05	0.02	0.4
[23]	2004	Germany	1500	20	Enercon E-66	ON	67	66		No	52	PA	MCTO	8.41	0.03	0.5

(Continued)

TABLE 21.1 (Continued)

Reference	Year	Location	Power rating/kW	Life/years	Turbine	Tech. ^a	Hub height/m	Rotor Diameter/m	Wind Speed/m/s	Operating	Capacity Factor/%	Analysis Type ^b	Scope ^c	$\text{CEC}/\left[\frac{\text{Mj}_p}{\text{W}_p}\right]$	$\text{LCFC}/\frac{\text{kW h}_p}{\text{kW h}_e}$	EPBT ^d /years
[24]	2004	Germany	5000	20	Repower Systems AG	OFF	95	126.5	9.2	No	50	PA	MTCOD	21.31	0.7	0.3
[25]	2004	Germany	500		Enercon E40	ON	44	40.3	7.5	No		PA-I/O	MTCOD		0.12	
[25]	2004	Germany	500		Enercon E40	ON	55	40.3	7.5	No		PA-I/O	MTCOD		0.13	
[25]	2004	Germany	500		Enercon E40	ON	55	40.3	7.5	No		PA-I/O	MTCOD		0.16	
[25]	2004	Germany	500		Enercon E40	ON	55	40.3	7.5	No		PA-I/O	MTCOD		0.21	
[25]	2004	Germany	500		Enercon E40	ON	65	40.3	7.5	No		PA-I/O	MTCOD		0.20	
[25]	2004	Germany and Brazil	500		Enercon E40	ON	44	40.3	7.5	No		PA-I/O	MTCOD		0.04	
[25]	2004	Germany and Brazil	500		Enercon E40	ON	55	40.3	7.5	No		PA-I/O	MTCOD		0.05	
[25]	2004	Germany and Brazil	500		Enercon E40	ON	55	40.3	7.5	No		PA-I/O	MTCOD		0.06	
[25]	2004	Germany and Brazil	500		Enercon E40	ON	55	40.3	7.5	No		PA-I/O	MTCOD		0.08	
[25]	2004	Germany and Brazil	500		Enercon E40	ON	65	40.3	7.5	No		PA-I/O	MTCOD		0.08	
[25]	2004	Germany and Brazil	500		Enercon E40	ON	44	40.3	7.5	No		PA-I/O	MTCOD		0.04	

[25]	2004	Germany and Brazil	500		Enercon E40	ON	55	40.3	7.5	No		PA-I/O	MTCOD		0.04		
[25]	2004	Germany and Brazil	500		Enercon E40	ON	55	40.3	7.5	No		PA-I/O	MTCOD		0.05		
[25]	2004	Germany and Brazil	500		Enercon E40	ON	55	40.	7.5	No		PA-I/O	MTCOD		0.06		
[25]	2004	Germany and Brazil	500		Enercon E40	ON	65	40.	7.5	No		PA-I/O	MTCOD		0.06		
[25]	2004	Brazil	500		Enercon E40	ON	44	40.3	7.5	No		PA-I/O	MTCOD		0.03		
[25]	2004	Brazil	500		Enercon E40	ON	55	40.3	7.5	No		PA-I/O	MTCOD		0.03		
[25]	2004	Brazil	500		Enercon E40	ON	55	40.3	7.5	No		PA-I/O	MTCOD		0.04		
[25]	2004	Brazil	500		Enercon E40	ON	55	40.3	7.5	No		PA-I/O	MTCOD		0.05		
[25]	2004	Brazil	500		Enercon E40	ON	65	40.3	7.5	No		PA-I/O	MTCOD		0.05		
[25]	2004	Brazil	500		Enercon E40	ON	44	40.3	7.5	No		PA-I/O	MTCOD		0.03		
[25]	2004	Brazil	500		Enercon E40	ON	55	40.3	7.5	No		PA-I/O	MTCOD		0.03		
[25]	2004	Brazil	500		Enercon E40	ON	55	40.3	7.5	No		PA-I/O	MTCOD		0.03		
[25]	2004	Brazil	500		Enercon E-40	ON	55	40.3	7.5	No		PA-I/O	MTCOD		0.04		
[25]	2004	Brazil	500		Enercon E-40	ON	65	40.3	7.5	No		PA-I/O	MTCOD		0.04		
[26]	2004	Denmark	2000	20		ON	78			Yes	32.2	PA			6.54	0.03	0.6
[26]	2004	Denmark	2000	20		OFF	60			Yes	46.2	PA			10.93	0.04	0.8
[27]	2005	Japan	300	30		N/A				No	20	PA-I/O	CMO		6.41	0.03	1.0
[27]	2005	Japan	400	30		N/A				No	20	PA-I/O	CMO		9.32	0.05	1.5
[22]	2005	Canada		20		N/A				No		N/A			0.03	0.2	

(Continued)

TABLE 21.1 (Continued)

Reference	Year	Location	Power rating/kW	Life/years	Turbine	Tech. ^a	Hub height/m	Rotor Diameter/m	Wind Speed/ $\frac{m}{s}$	Operating	Capacity Factor/%	Analysis Type ^b	Scope ^c	$CEC/\frac{[M]_p}{W_p}$	$LCFC/\frac{kW\cdot h_p}{kW\cdot h_e}$	EPBT ^d /years	
[22]	2005	Canada		20		N/A				No		N/A			0.03	0.2	
[22]	2005	Canada		20		N/A				No		N/A			0.03	0.2	
[28]	2006	Italy	7260	20		ON	55	50		Yes		I/O	MTCOD		0.05	1.0	
[29]	2006	Germany	1500			N/A				No		N/A	MTCOD		0.03		
[29]	2006	Germany	1500			ON				No		N/A	MCOTD		0.03		
[29]	2006	Germany	2500			N/A				No		N/A	MTCOD		0.03		
[29]	2006	Germany	2500			OFF				No		N/A	MCOTD		0.03		
[30]	2006		3000	20		N/A				No	30.0	N/A			1.01	0.01	0.1
[31]	2006	Denmark	1650	20		ON				No	39.0	PA			7.38	0.03	0.6
[31]	2006	Denmark	3000	20		OFF	80			Yes	54.2	PA			9.66	0.03	0.6
[32]	2008	Taiwan	1750	20		N/A	60	60		Yes	42.6	N/A			2.46	0.01	0.2
[32]	2008	Taiwan	660	20		N/A	45	47		Yes	18.9	N/A			2.94	0.02	0.5
[32]	2008	Taiwan	600	20		N/A	46	43.7		Yes	30.9	N/A			2.99	0.02	0.3
[28]	2008	Italy	660	20		ON	55	50		Yes	19.0	N/A			6.39	0.06	1.1
[33]	2009	Spain	2000	20		N/A				No	22.8	N/A			4.18	0.03	0.6
[34]	2009		5000	20		OFF	100	116		No	53.0	PA			1.39	0.05	1.1

[35]	2009	France	0.25	20		N/A			No	5.5	N/A			11.32	0.33	6.6
[35]	2009	France	4500	20		N/A	124	113	No	30.0	N/A			15.59	0.08	1.6
[36]	2009		3000	20		N/A	80	90	No	33.0	PA-I/O			28.08	0.13	2.7
[36]	2009		850	20		N/A	60	52	No	34.0	PA-I/O			34.57	0.16	3.2
[37]	2009	Canada	0.4	20	Air-X micro turbine	ON	30	1.17	No	16.1	PA	MTCBaO	101.64	1.00	20.0	
[38]	2009	New Zealand	1.5	20	1.5 kW Swift turbine	ON		2	5.5–6.3	No	4.0	PA	MTCOD	13.81	0.55	10.9
[38]	2009	New Zealand	1.5	20	1.5 kW Swift turbine	ON		2	5.5–6.3	No	6.4	PA	MTCOD	13.81	0.34	6.8
[39]	2011	China	1250	20		ON	68	64	6.3	Yes	25.0	N/A		7.37	0.05	0.9
[40]	2011	China	1250	20		ON	68	64		Yes	24.9	PA-I/O		7.37	0.05	0.9
[41]	2011	Denmark	3000	20	VII12	ON	84		No	43.4	PA			9.12	0.03	0.7
[41]	2011	Denmark	2000	20	V-80	ON	80		No	47.2	PA			10.42	0.04	0.7
[41]	2011	Denmark	2000	20	V-90	ON	80		No	35.7	PA			10.70	0.05	1.0
[41]	2011	Denmark	1800	20	V100	N/A			No	42.5	PA			11.85	0.04	0.9
[42]	2011	Germany	5000	20	6 RePower 5M and 6	OFF			Yes	44.5	N/A			38.33	0.14	2.7
[43]	2011	Europe	2300	20	Multibrid M5000 Enercon E-82 E2	ON	97		No	25.3	PA	MCTGOD	4.51	0.03	0.6	
[43]	2011	Europe	2300	20	Enercon E-82 E2	ON			No	29.2	PA	MCTGOD	4.51	0.02	0.5	
[43]	2011	Europe	2300	20	Enercon E-82 E2	ON			No	36.5	PA	MCTGOD	4.51	0.02	0.4	

(Continued)

TABLE 21.1 (Continued)

Reference	Year	Location	Power rating/kW	Life/years	Turbine	Tech. ^a	Hub height/m	Rotor Diameter/m	Wind Speed/ $\frac{m}{s}$	Operating	Capacity Factor/%	Analysis Type ^b	Scope ^c	$CEC/\left[\frac{M_p}{W_p}\right]$	$LCF/\frac{kW\ h_p}{kW\ h_e}$	EPBT ^d /years
[44]	2012		1800	20		N/A				Yes	28.0	N/A		4.22	0.02	0.4
[44]	2012		2000	20		N/A				No	34.0	N/A		7.04	0.03	0.7
[45]	2012	Canada	100	25		N/A	37	21		Yes	24.0	N/A		7.06	0.04	0.9
[45]	2012	Canada	20	25		N/A	36.7	9.45		Yes	22.0	N/A		10.85	0.06	1.5
[45]	2012	Canada	5	25		N/A	36.6	5.5		Yes	23.0	N/A		21.64	0.12	2.9
[44]	2012		1800	20	1.8 MW gearless	ON	105	90	7.4	Yes	20.7	PA	MTCGOD	7.82	0.06	1.2
[44]	2012		2000	20	2.0 MW geared	ON	65	70	6	No	34.1	PA	MTCGOD	3.80	0.02	0.4
[45]	2012	Canada	5	25	Endurance (EN) 5 kW	ON	36.6	5.5		No	23.3	PA	MTCGOD	77.90	0.42	10.6
[45]	2012	Canada	100	25	Northern Power (NP) 100 kW	ON	37	21		No	22.4	PA	MTCGOD	39.07	0.22	5.5
[46]	2012	UK	5000	20	NREL 5 MW	OFF	90	126		No	46.0	PA	MTCGOD		0.00	1.6
[46]	2012	UK	5000	20	NREL 5 MW	OFF	90	126		No	46.0	PA	MTCGOD		0.00	1.8
[46]	2012	UK	5000	20	NREL 5 MW	OFF	90	126		No	46.0	PA	MTCGOD		0.00	2.7
[46]	2012	UK	5000	20	NREL 5 MW	OFF	90	126		No	46.0	PA	MTCGOD		0.00	2.2
[46]	2012	UK	5000	20	NREL 5 MW	OFF	90	126		No	46.0	PA	MTCGOD		0.00	1.7

[46]	2012	UK	5000	20	NREL 5 MW	OFF	90	126		No	46.0	PA	MTCGOD		0.00	1.5
[46]	2012	Norway	2300	20		ON				Yes	33.9	PA	MTCGOD		0.00	1.0
[46]	2012	Norway	2300	20		ON				Yes	33.9	PA	MTCGOD		0.00	1.0
[46]	2012	Norway	2300	20		ON				Yes	33.9	PA	MTCGOD		0.00	1.0
[46]	2012	Norway	2300	20		ON				Yes	33.9	PA	MTCGOD		0.00	0.8
[46]	2012	Norway	750	20		ON				Yes	24.4	PA	MTCGOD		0.00	1.4
[46]	2012	Norway	750	20		ON				Yes	24.4	PA	MTCGOD		0.00	1.4
[46]	2012	Norway	750	20		ON				Yes	24.4	PA	MTCGOD		0.00	1.3
[47]	2013	Turkey	330	20		N/A	50	33	13	N/A	16.3	PA	MCT	15.24	0.15	3.0
[47]	2013	Turkey	330	20		N/A	80	33	13	N/A	21.0	PA	0		0.00	2.8
[47]	2013	Turkey	330	20		N/A	100	33	13	N/A	25.8	PA	0		0.00	2.5
[47]	2013	Turkey	500	20		N/A	50	48	12	N/A	15.8	PA	0		0.00	2.9
[47]	2013	Turkey	500	20		N/A	80	48	12	N/A	20.6	PA	0		0.00	2.4
[47]	2013	Turkey	500	20		N/A	100	48	12	N/A	23.1	PA	0		0.00	2.3
[47]	2013	Turkey	810	20	N/A	50	53	13	N/A	16.6	PA	0		0.00	2.0	
[47]	2013	Turkey	810	20	N/A	80	53	13	N/A	21.3	PA	0		0.00	1.6	
[47]	2013	Turkey	810	20	N/A	100	53	13	N/A	23.5	PA	0		0.00	1.5	
[47]	2013	Turkey	2050	20	N/A	50	82	13	N/A	15.3	PA	0		0.00	1.5	
[47]	2013	Turkey	2050	20	N/A	80	82	13	N/A	19.8	PA	0		0.00	1.3	
[47]	2013	Turkey	2050	20	N/A	100	82	13	N/A	22.1	PA	0	8.46	0.06	1.2	
[47]	2013	Turkey	3020	20	N/A	50	82	17	N/A	10.3	PA	0		0.00	2.3	
[47]	2013	Turkey	3020	20	N/A	80	82	17	N/A	13.5	PA	0		0.00	1.8	

(Continued)

TABLE 21.1 (Continued)

Reference	Year	Location	Power rating/kW	Life/years	Turbine	Tech. ^a	Hub height/m	Rotor Diameter/m	Wind Speed/ $\frac{m}{s}$	Operating	Capacity Factor/%	Analysis Type ^b	Scope ^c	$CEC/\left[\frac{Mj_p}{W_p}\right]$	$LCFC/\frac{kWh_p}{kW h_e}$	EPBT ^d /years
[47]	2013	Turkey	3020	20	N/A	100	82	17	N/A	15.1	PA	0		0.00	1.8	
[48]	2013	UK	6	20	ON	9	5.5	5	no	14.8	PA	MTCGOD	29.90	0.32	6.4	
[48]	2013	UK	6	20	ON	9	5.5	5	no	18.3	PA	MTCGOD	29.90	0.26	5.2	
[48]	2013	UK	6	20	ON	9	5.5	5	no	19.0	PA	MTCGOD	29.90	0.25	5.0	
[48]	2013	UK	6	20	ON	9	5.5	5	no	21.7	PA	MTCGOD	29.90	0.22	4.4	
[48]	2013	UK	6	20	ON	9	5.5	5	no	24.0	PA	MTCGOD	29.90	0.20	4.0	
[48]	2013	UK	6	20	ON	9	5.5	5	no	27.4	PA	MTCGOD	29.90	0.17	3.5	
[48]	2013	UK	6	20	ON	9	5.5	5	no	30.8	PA	MTCGOD	29.90	0.15	3.1	
[48]	2013	UK	6	20	ON	9	5.5	5	no	34.2	PA	MTCGOD	29.90	0.14	2.8	
[11]	2013	Michigan	3000	20	Vestas VI12-3.0 MW	OFF	100		No	28.2	PA	MTCGOD	29.00	0.16	3.3	
[11]	2013	Michigan	3000	20	Vestas VI12-3.0 MW	OFF	100		No	30.1	PA	MTCGOD	20.97	0.11	2.2	
[11]	2013	Michigan	3000	20	Vestas VI12-3.0 MW	OFF	100		No	30.8	PA	MTCGOD	31.80	0.16	3.3	
[11]	2013	Michigan	3000	20	Vestas VI12-3.0 MW	OFF	100		No	31.6	PA	MTCGOD	34.47	0.17	3.5	

[11]	2013	Michigan	3000	20	Vestas VI12-3.0 MW	OFF	100			No	32.7	PA	MTCGOD	31.33	0.15	3.0
[11]	2013	Michigan	3000	20	Vestas VI12-3.0 MW	OFF	100			No	31.0	PA	MTCGOD	19.93	0.10	2.0
[11]	2013	Michigan	3000	20	Vestas VI12-3.0 MW	OFF	100			No	33.3	PA	MTCGOD	27.30	0.13	2.6
[11]	2013	Michigan	3000	20	Vestas VI12-3.0 MW	OFF	100			No	34.4	PA	MTCGOD	28.33	0.13	2.6
[11]	2013	Michigan	3000	20	Vestas VI12-3.0 MW	OFF	100			No	34.8	PA	MTCGOD	29.37	0.13	2.7
[11]	2013	Michigan	3000	20	Vestas VI12-3.0 MW	OFF	100			No	35.2	PA	MTCGOD	31.37	0.14	2.8
[11]	2013	Michigan	3000	20	Vestas VI12-3.0 MW	OFF	100			No	31.2	PA	MTCGOD	19.90	0.10	2.0
[11]	2013	Michigan	3000	20	Vestas VI12-3.0 MW	OFF	100			No	32.5	PA	MTCGOD	32.50	0.16	3.2
[11]	2013	Michigan	3000	20	Vestas VI12-3.0 MW	OFF	100			No	34.2	PA	MTCGOD	28.30	0.13	2.6
[11]	2013	Michigan	3000	20	Vestas VI12-3.0 MW	OFF	100			No	34.6	PA	MTCGOD	29.33	0.13	2.7
[11]	2013	Michigan	3000	20	Vestas VI12-3.0 MW	OFF	100			No	35.2	PA	MTCGOD	31.37	0.14	2.8
[11]	2013	Michigan	3000	20	Vestas VI12-3.0 MW	OFF	100			No	29.3	PA	MTCGOD	29.07	0.16	3.1
[11]	2013	Michigan	3000	20	Vestas VI12-3.0 MW	OFF	100			No	30.3	PA	MTCGOD	20.93	0.11	2.2
[11]	2013	Michigan	3000	20	Vestas VI12-3.0 MW	OFF	100			No	30.4	PA	MTCGOD	31.10	0.16	3.2
[11]	2013	Michigan	3000	20	Vestas VI12-3.0 MW	OFF	100			No	30.8	PA	MTCGOD	32.10	0.17	3.3
[11]	2013	Michigan	3000	20	Vestas VI12-3.0 MW	OFF	100			No	31.2	PA	MTCGOD	36.57	0.19	3.7
[49]	2013	India	1650	20		ON	75			Yes	21.0	PA-I/O	MTCGOD	7.40	0.06	1.1
[50]	2013	USA	1800	26	Vestas V90 turbine	ON		6.5–7		Yes	24.5	PA	MCTGO		0.00	1.0
[9]	2013	Europe	3000	20	Vestas V90-3.0 MW	ON	80	100	9.25	No	41.3	PA	MCTGOD	5.79	0.02	0.4

(Continued)

TABLE 21.1 (Continued)

Reference	Year	Location	Power rating/kW	Life/years	Turbine	Tech. ^a	Hub height/m	Rotor Diameter/m	Wind Speed/ $\frac{\text{m}}{\text{s}}$	Operating	Capacity Factor/%	Analysis Type ^b	Scope ^c	$\text{CEC}/\left[\frac{\text{M}_\text{hp}}{\text{W}_\text{p}}\right]$	$\text{LCOE}/\frac{\text{kWh}_\text{p}}{\text{kWh}_\text{e}}$	EPBT ^d /years
[51]	2013	Europe	2600	20	Vestas V100-2.6 MW	ON	80	90	8	No	38.4	PA	MCTGOD	6.73	0.03	0.6
[52]	2013	Germany	5000	20	Repower 5M and Multibrid M5000	OFF				Yes	46.2	PA	MCOD	38.33	0.13	2.2
[53]	2013	China	1500	20		N/A				No	25.8	PA	MCTGOD	5.49	0.03	0.7
[54]	2014	Thailand	0.3	20	300 W vertical axis	ON	36	0.25	12	No	4.3	PA	MTCOD	1.77	0.07	1.3
[54]	2014	Thailand	0.3	20	300 W vertical axis	ON	30	0.25		No	5.3	PA	MTCOD	1.77	0.05	1.1
[54]	2014	Thailand	0.3	20	300 W vertical axis	ON	30	0.25		No	20.5	PA	MTCOD	1.77	0.01	0.3
[54]	2014	Thailand	0.5	20	500 W horizontal axis	ON	36	1.7	12	No	5.8	PA	MTCOD	1.18	0.03	0.6
[54]	2014	Thailand	0.5	20	500 W horizontal axis	ON	30	1.7		No	7.2	PA	MTCOD	1.18	0.03	0.5
[54]	2014	Thailand	0.5	20	500 W horizontal axis	ON	30	1.7		No	40.7	PA	MTCOD	1.18	0.00	0.1
[55]	2014	Europe	3300	20	Vestas V2105-3.3 MW	ON	72.5	105	9.25	No	47.0	PA	MCTGOD	6.58	0.02	0.4

[56]	2014	Europe	3300	20	Vesta s V117-3.3 MW	ON	91.5	117	8	No	42.4	PA	MCTGOD	6.69	0.03	0.5
[57]	2014	Europe	3300	20	Vestas V126-3.3 MW	ON	117	126	7	No	37.2	PA	MCTGOD	7.81	0.03	0.7
[58]	2015	Libya	1650	20	M. TORESS (TWT 1.65/82), 3-bl	ON	71	82		Yes	42.4	PA	MTCGOD	6.36	0.02	0.5
[59]	2015		2100	0		N/A	70	80	12	No		PA	M	1.56	0.00	0.0
[59]	2015		1600	0		N/A	65	70	12	No		PA	M	1.77	0.00	0.0
[59]	2015		2700	0		N/A	80	90	12	No		PA	M	1.57	0.00	0.0
[60]	2015		2000	20	G8X Gamesa onshore wind	ON	70	80		No	22.8	PA	MCGOD		0.00	0.0
[61]	2015	Russia	4	10	WPI-5-4 24 blade turbine	ON	8.22	5	2	No	8.3	PA	MTCOD	24.66	0.95	9.5
[61]	2015	Russia	4	10	WPI-5-4 24 blade turbine	ON	8.22	5	3.6	No	24.5	PA	MTCOD	24.66	0.32	3.2
[61]	2015	Russia	4	10	WPI-5-4 24 blade turbine	ON	8.22	5	5.2	No	40.3	PA	MTCOD	24.66	0.19	1.9
[61]	2015	Russia	4	10	WPI-5-4 24 blade turbine	ON	8.22	5	6.5	No	49.3	PA	MTCOD	24.66	0.16	1.6
[61]	2015	Russia	4	10	WPI-5-4 24 blade turbine -	ON	8.22	5	7.8	No	56.0	PA	MTCOD	24.66	0.14	1.4
[61]	2015	Russia	4	10	WPI-5-4 24 blade turbine	ON	8.22	5	10.3	No	73.8	PA	MTCOD	24.66	0.11	1.1

(Continued)

TABLE 21.1 (Continued)

Reference	Year	Location	Power rating/kW	Life/years	Turbine	Tech. ^a	Hub height/m	Rotor Diameter/m	Wind Speed/ $\frac{m}{s}$	Operating	Capacity Factor/%	Analysis Type ^b	Scope ^c	$CEC/\left[\frac{M_p}{W_p}\right]$	$LCF/\frac{kW\ h_p}{kW\ h_e}$	EPBT ^d /years
[62]	2015	Japan	1650	20	Vesta V82-1.65 MW	ON				No	20.0	PA-I/O	MCGO	9.98	0.08	1.6
[63]	2015	US	2000	20	Vesta V80-2.0 MW	ON	78			No	32.2	PA-I/O	MTCO	14.13	0.07	1.4
[63]	2015	US	2000	20	Vesta V80-2.0 MW	OFF	60			No	46.2	PA-I/O	MTCO	10.53	0.04	0.7
[63]	2015	US	3000	20	Vesta V90-3.0 MW	ON	105			No	30.1	PA-I/O	MTCO	12.11	0.06	1.3
[63]	2015	US	3000	20	Vesta V90-30 MW	OFF	80			No	53.3	PA-I/O	MTCO	9.15	0.03	0.5
[64]	2015	Mexico	2000	20		ON		80		No		PA	MCD	0.67	0.00	0.0
[64]	2015	Mexico	2000	20		ON		80		No		PA	MCD	0.93	0.00	0.0
[65]	2015	Europe	2000	20	Vestas V100-2.0 MW	ON	80	100	8	No	47.9	PA	MCTGOD	7.56	0.03	0.5
[66]	2015	Europe	3300	20	Vestas V112-3.3 MW	ON	84	112	8	No	40.9	PA	MCTGOD	5.74	0.02	0.4
[67]	2016	Denmark	2000	20		ON				Yes	32.2	PA	MTCGOD	6.55	0.03	0.6
[67]	2016	Denmark	2000	20		OFF				Yes	46.2	PA	MCTGOD	10.94	0.04	0.8

^aTechnology: ON, onshore; OFF, offshore.^bProcess-based analysis (PA), input—output (I/O), or hybrid (PA-I/O).^cAs stated in study: business management (B), manufacture (M), transport (T), construction (C), grid connection (G), operation & maintenance (O), and decommissioning (D).^dNo quality correction between primary and electrical energy.

APPENDIX B

TABLE 21.2 Proportion of Cumulative Energy Demand (CED) Made Up by Different Components/percentage

Component	Unit	[33]	[37]	[39]	[43]	[44]	[44]	[45]	[45]	[45]	[47]	[11]	[11]	[11]	[9]	[51]	[53]	[55]	[56]	[57]	[63]	[63]	[63]	[65]	[66]		
Rotor	[%]	44.9		18.2	18.5	7.2	5.1				15.0	3.6	5.2	3.3	3.3	16.0	18.0	7.8	22.0	21.0	18.5				18.0	23.0	
Nacelle	[%]	12.8		15.9	24.6	11.0	23.6	53.7	60.4	45.0	27.0	4.3	6.2	4.0	3.9	16.0	15.0	23.5	20.0	19.0	16.5				16.0	22.5	
Tower	[%]	23.2	10.4	22.7	22.3	46.8	46.0				25.0	9.0	13.1	10.7	8.3	25.0	24.0	31.2	23.0	27.0	33.5				24.0	22.0	
Foundation	[%]	12.3		34.9	13.0	19.8	9.7				29.0					15.0	15.0		10.0	9.0	10.5				9.0	7.5	
Substation	[%]			0.4							1.0								0.2								
Energy storage	[%]			74.3				42.7	13.6	39.9						14.0	13.0		13.0	12.0	10.0				21.0	14.0	
Other buildings	[%]			1.2																							
Transport	[%]			13.4	0.7	2.0	7.0	7.0			1.0	38.2	11.5	11.3	13.7			0.4				32.5	38.0	39.0	44.0		
O&M	[%]	6.9		6.0	7.0	5.5	5.5	3.7	26.0	15.1	1.0	15.1	26.2	19.6	27.5	7.0	7.0		5.0	4.0	4.0	6.5	5.5	3.0	3.0	6.0	5.0
Disposal	[%]			28.7	1.0	3.1	3.1	49.4	44.5	35.8		23.1	8.7	8.7	10.3	20.0	20.0	46.7	22.2	33.3	33.3				33.3	25.0	

This page intentionally left blank

Chapter 22

Environmental and Structural Safety Issues Related to Wind Energy

Kaoshan Dai¹, Kewei Gao¹, and Zhenhua Huang²

¹Tongji University, Shanghai, China, ²University of North Texas, Denton, TX, United States

Email: kdai@tongji.edu.cn

22.1 INTRODUCTION

Wind power is one of the most mature renewable energy technologies, and industry has been experiencing accelerated growth during recent decades. However, wind energy developments are not free of environmental impacts. A poor understanding of these environmental impacts is a serious concern for the current wind energy industry, especially in developing countries and ecologically vulnerable regions. In addition, structural safety issues have gradually appeared, such as the structural reliability issues of wind turbine towers. In this chapter, the authors review the potential environmental impacts and structural safety issues associated with wind farm developments and identify potential methodologies to mitigate these adverse effects.

22.2 WIND-ENERGY-INDUCED ENVIRONMENTAL ISSUES AND COUNTERMEASURES

Wind power plants use wind turbines to convert wind energy into electrical or mechanical energies. The output power of a wind turbine is a function of air density, area swept by turbine blades, and wind speed [1]. The primary environmental issues related to wind turbines include avian safety, biosystem disturbance, noise, visual pollution, electromagnetic interference, and local climate changes [2,3]. These issues could be grouped into ecological effects, impacts on humans, and climate-related issues [4].

22.2.1 Effects on Animals and Mitigation Strategies

22.2.1.1 Birds and Bats

Birds can be killed by colliding with the rotating propellers of a wind turbine or they can suffer lethal injuries because of the collision with wind turbine towers, nacelles, or other structures in a wind farm such as guy cables, power lines, and meteorological masts [5].

Various factors influence wind-turbine-induced bird mortality, such as the wind turbine design and layout, bird species, and climatic variables. Examining the wind turbine design and layout, Orloff and Flannery [6] reported that the bird mortality rate was higher for three blade lattice turbines than for other turbine types. Smallwood and Thelander [7] indicated that the end of turbine strings (rows or columns of turbines on a wind turbine farm), the edge of the gap in turbine strings, and the edge of turbine clusters were the most dangerous sections of wind farms for flying birds. Sovacool [8] demonstrated that the bird mortality rate increased in regions where turbines were located on ridges or upwind slopes, or close to the bird migration routes. Holmstrom et al. [9] showed a significant correlation between the collision probability and the approaching angle between the bird flight path and the turbine orientation surface. Bird mortality is also associated with bird species [10]. Orloff and Flannery [6] observed that golden eagles, red-tailed hawks, and American kestrels were killed by wind turbines more often than turkey vultures and ravens. Langston and Pullan [11] suggested that one should consider diurnal and nocturnal species (different behaviors of birds during days and nights) when characterizing the sensitivity of the bird–wind turbine collisions. For the climate variables, Smallwood and Thelander [7] found that wind turbines killed more birds during winter and summer.

In addition to the mortality rates, another negative impact of wind turbines on birds is disturbance, including habitat destructions, barrier effects, and impacts on the bird breeding and feeding behaviors. For example, the construction of wind turbines and associated infrastructures may cause the destruction of local birds' habitat [11]. Some wind turbines can create physical barriers that deny birds' access to their natural feeding grounds and roosting locations. Noises and turbulent air currents produced by operations of wind turbines may scare birds away and narrow their territories, which can affect birds' foraging behaviors. Christensen et al. [12] studied the behavior of birds using radar tracks and concluded that 14%–22% of the observed birds increased their flying altitude to pass through the studied wind farm. Another research [13] found, through 10 years of collecting data on 47 eagle territories at western Norway, that coastal wind farms affected the breeding success rate of white-tail eagles.

A high mortality rate close to wind farms has been observed for bats as well. Wind turbines are associated with the mortalities of nearly a quarter of all bat species in the United States and Canada [14]. There are different

opinions among researchers on the reasons for these bat mortalities [15,16]. Early studies observed barotrauma-related internal hemorrhaging in over 50% of the dead bats near wind turbines, therefore, some researchers believed that the barotrauma and internal hemorrhaging caused by the sudden pressure drop near turbine edges were the main reason for the wind-turbine-induced bat mortalities [17]. More recent studies found that the impact trauma was actually responsible for the majority of the turbine-associated bat deaths [18]. Concerning the reasons why bats are attracted by wind turbines, Arnett et al. [19] explained that bats were attracted by ultrasound emissions and lights of wind turbines. Other researchers [20,21] believed that bats treated wind turbines as trees and tried to access them as potential roosting sites or the large amount of insects attracted by the high heat radiation of wind turbine nacelles caused hunting bats to aggregate around wind turbines. Regarding the factors related to wind-turbine-induced bat mortalities, Kunz et al. [22] found that there were almost twice as many dead bats in grassland areas than in agricultural landscapes or forested ridge tops. Marsh [23] indicated that wind farms on forested ridges were more dangerous for bats and many bats were killed during the 2-hour period after sunset during their autumn migration. A study by Barclay et al. [24] showed that the height of wind turbine towers was associated with the death toll of bats. A comprehensive bibliography associated with the wind-farm-induced bat mortalities up to 2008 could be found in Arnett et al. [25].

To reduce these bird and bat fatalities and disturbances, several mitigation strategies have been suggested, including restricting construction activities, improving structural designs, and optimizing site selections. Restricting construction activities to nonbreeding periods could be effective in helping to reduce the negative effects of bird disturbances [26]. Structural design improvements were effective in reducing bird mortalities as well [27]. For example, McIsaac [28] found that the pattern-painted wind turbine blades could increase the visual acuity of raptors. Marsh [23] proposed that wind turbine blades with night illuminations could be more visible to birds. However, Langston and Pullan [11] believed that the night illumination on wind turbines may attract birds, especially in bad weather conditions, and increase the chance of collision. Arnett et al. [19,29] found that there was no difference in bird or bat fatality rates for wind turbines with or without lighting. In addition to construction activity restrictions and structural designs improvements, the site selection of a wind farm is also important [8]. For example, Foote [30] proposed that bird flight activities in a zone of 200–500 m surrounding the planned wind farm location should be recorded and analyzed systematically, including flight heights, directions, species, and behaviors of birds. Carrete et al. [31] recommended assessments of the spatial distribution and aggregation activities of vulnerable bird species before starting wind farm constructions in order to minimize bird disturbances. Busch et al. [32] pointed out that, in addition to the technical improvements,

an international cooperative effort is also important to reduce the environmental impacts of global wind farm projects. A detailed discussion on mitigation methodologies for the environmental impacts of wind turbines can be found by Northrup and Wittemeyer [33].

22.2.1.2 *Marine Species*

Offshore wind turbines may impact marine species. Wind turbines and their scour protection may change the nearby fish distributions and wind farm constructions may create an artificial reef, which impacts the biodiversity of marine species. The construction of wind turbine foundations and the on-site erection of wind turbine towers may make seawater turbid and introduce additional objects on the seabed (blocking effect), which can cause damages to the benthic fauna and flora and block sunshine into the water. Berkenhagen et al. [34] indicated that the offshore wind farm constructions would induce a substantial effect on fisheries. In particular, the opportunities to catch valuable species would be considerably reduced. In addition to the blocking effect, the noise and the electromagnetic fields around operating wind turbines may lead to negative effects on fishes as well [35]. Marine mammals such as porpoises and seals may also react to wind farm noise and electromagnetic fields, especially during the construction phase [36,37]. The maintenance activities of wind turbines, such as part replacements or lubrications, may also impact on marine species by leaking oils or wastes into the surrounding seawater and polluting marine species living environments. With the increasing height of wind turbine towers and the increasing size of offshore wind farms, the environmental impacts of wind farms on fishes and marine mammals are becoming more evident.

22.2.2 Noise Problems and Possible Solutions

Noise is one of the major environmental hindrances for the development of the wind power industry and can induce sleep disturbances and hearing losses in humans. Exposure to high-frequency noises can trigger headaches, irritability, and fatigue, as well as constrict arteries and weaken immune systems. The public also can become annoyed or dissatisfied by the disturbing noises [38]. According to Van den Berg [39], during quiet nights, people reacted strongly to wind turbine noises in the range of 500 m surrounding a wind farm and experienced annoyance in the range of 1900 m surrounding a wind farm. The wind-turbine-induced visual and aesthetic impacts on the landscape could increase the public's annoyance [40]. However, due to the paucity of literature and the fact that annoyance can be caused by many other factors, the clear association between annoyance and wind turbine noises still needs more rigorous studies. Wind turbine noises could be categorized into tonal and broadband noises based on the noise frequencies and

aerodynamic and mechanical noises based on the noise sources. The total noise, measured by the sound pressure level, is a combination of mechanical and aerodynamic noises. The low-frequency noises (10–200 Hz) are considered as the substantial part of the noises with the larger modern turbines [41]. Many factors affect the wind-turbine-induced noise propagation and attenuation, such as air temperature, humidity, barriers, reflections, and ground surface materials. Background noise is another important factor. For example, noises can be perceived differently at night. The whooshing (amplitude-modulated noise from wind turbines) can be perceived as being more intense than during the daytime and even be heard as thumping because of the low human-made background noises and the stable atmosphere [1].

To control the noise level, governments and medical institutions have recommended minimum separation distances between wind farms and habitations or upper limit noise levels of dBA values that can be heard at the closest inhabited dwellings. Different criteria on these separation distances and noise dBA values have been provided by different countries and regions. Suitable criteria should be followed with a comprehensive consideration of specific local conditions for wind farm developments. To reduce the noise from wind turbines, improved blade design is a key issue. The application of upwind turbines is useful to reduce low-frequency noises [42]. The insulations inside the turbine towers can effectively mitigate the mechanical noise during the course of operation [43]. In addition to these technical measures, building wind farms close to noisy areas is another way to reduce the noise-induced problems [34].

22.2.3 Visual Impacts and Mitigation

A wind turbine blade may cast a shadow in the sunshine on its neighbor area. This shadow may induce an undesirable visual impact or even a disturbing flicker when a rotating blade casts a moving shadow on landscapes and houses [44]. In addition to the shadow and flicker issues, the negative visual impact of wind farms on landscapes is another factor that creates a negative opinion of the wind energy industry, in people's minds [45]. However, this problem is subjective. People's positive or negative attitude may depend on their perception of the unity of the environment, their personal feeling toward the effects of wind turbines on landscape, and their general attitude about the wind energy industry [46]. Evaluation of the visual impact of a wind farm is a difficult task. A survey study by Krohn and Damborg [47] showed that the public usually supports wind power and the renewable energy industry. However, the local residents may oppose building a new wind farm close to them, even though they know it will benefit the society. This is so called Not-In-My-Backyard syndrome (NIMBY).

Factors influencing the visual impact intensity of wind turbines include background nature, local landscapes, and landscapes between viewers and

turbines. For example, a wind turbine located on a hill may induce direct visual impact, but the intensity of the impact can be weakened when viewing from a higher position [48]. Therefore, when selecting wind farm sites, areas that are considered visually pleasing, especially on the coast, should be avoided. A simulation study conducted by Bishop and Miller [49] showed that in all weather and light conditions, the visual impact intensity of wind turbines decreases with increasing distances. The number of blades and the blade rotating directions of a wind turbine can influence its visual impact intensity as well. According to Sun et al. [50], a wind turbine with three blades is more acceptable than the one with two blades for people who are sensitive to visual impacts. Wind turbines with anticlockwise rotating blades generated stronger negative reactions from viewers [50]. The layouts of wind turbines in a farm, which can be categorized into regular and irregular layouts, can also affect their visual impact intensity. Generally, the regular layout created a better sense of visual regularity and consistency than the irregular layout, which may lead to a sense of chaos.

Four considerations were suggested to limit the wind farm visual impacts on landscapes during the design phase: (1) whether it is acceptable to change the landscape; (2) how visually dominant are the wind turbines on the landscape; (3) what is the relationship between aesthetics and the wind energy development; and (4) how important is the impact. To promote positive attitudes of local communities toward wind farms, public participations in the early stages of the planning and implementation of wind power projects are recommended, such as working together to seek solutions to the visual impact issues [46]. Design improvements can be used to mitigate the visual impact intensity of wind turbines. For example, the shadow flicker issue of wind turbines can also be predicted and avoided with an appropriate siting design of a wind farm. Layout design of wind frames and aesthetic design of wind turbines can also be helpful. The fewer the number of wind turbines and the simpler the layout, the easier it is to create a visually balanced, simple, and consistent image. Selecting an appropriate color for a turbine is important to mitigate its visual impact. Rather than painting turbines a color to camouflage them against their background, it is more suitable to choose a color to engage the turbines to suite the background at different views and in different weather conditions.

22.2.4 Climate Change and Considerations

Different studies have shown that wind turbines can impact local weather and regional climate such as the temperature and wind speed. Zhou et al. [51] studied 8-year satellite data in a region of west-central Texas equipped with 2358 wind turbines and reported a temperature increase of 0.724°C in the area. Barthelmie et al. [52] studied the recovery rate of the wind speed after it passed through a wind farm and reported a decreasing curve. Roy

and Traitor [53] believed that large wind farms induced cooling effects during daytime and warming effects at night as a result of the vertical air mixture near the ground surface. These cooling and warming effects altered the regional climate, and the change can induce a long-term impact on wildlife and regional weather patterns. In contrast, some other studies reported that wind farms were able to alleviate adverse climates such as sand storms, even though the effect was very limited [54].

Different analytical methods and models, such as the blade element momentum model, the vortex wake method, the computational fluid dynamics method, have been suggested for the wind farm climate studies to mitigate the meteorological impacts of wind farms [55]. For example, Keith et al. [54] proposed that, through improved rotor and blade designs and a proper design of turbine spacing and pattern, the rotor-generated turbulence of wind turbines can be mitigated and the hydro-meteorological impact of wind farms can be reduced.

22.3 STRUCTURAL SAFETY STUDIES FOR WIND TURBINE TOWERS

Along with the fast development of wind energy industry, today's wind turbines are much taller than their predecessors. Additionally more and more wind farms are located in strong earthquake zones and/or strong wind-prone regions. In recent years, many structural failures of wind turbines caused by extreme winds or strong earthquakes have been reported based on qualitative observations and phenomenological assessments. This section summarizes studies related to wind turbine tower structural safety problems.

22.3.1 Wind Turbine Tower Structural Performances Under Wind and Seismic Loads

Many structural failures of wind turbines caused by extreme environmental loadings have been reported and studied in recent years. For example, Ishihara et al. [56] studied the collapse of two wind turbine towers in Japan caused by the 2003 typhoon Maemi. Chou and Tu [57] analyzed the tower collapse and the rotor blade damage of a wind turbine in Taiwan caused by the 2008 typhoon Jangmi. Chen et al. [58] conducted a forensic engineering study on failures of several wind turbine towers in a coastal wind farm after a typhoon event.

The tower structures for modern megawatt wind turbines are generally over 60 m high. Therefore, wind turbine towers belong to tall structures, which are typically flexible and vulnerable to vibration fatigue damages caused by wind loads. Therefore, the structural design of a wind turbine tower is generally controlled by wind loads [59–61]. Design specifications such as Risø, GL, IEC [59–61] provide guidance for the design of wind

turbine towers. For example, IEC provides 22 design loading cases, including eight turbine operation conditions. During the design procedure, time history analysis can be adopted to accurately consider tower–blade coupling [62]. Design parameters for wind turbine towers are typically provided by manufacturers who designed the blades and turbines [63,64]. Blade rotation should be considered as an important parameter. Murtagh et al. [62] found that the vibration amplitude at the top of wind turbine towers under wind loads were underestimated if blade rotation was not considered. The reasons may be because the blade rotation can induce the centrifuging stiffening effect [62] and the aeroelastic damping effect [65] to the wind turbine structure and influence its vibration performances.

In addition to the extreme wind loads, the seismic performance of wind turbine towers is getting more attention of structural engineers and researchers because more wind farms are located in earthquake-prone areas. Previously, researchers [64,66] believed that the earthquake loads would not control the design of small wind turbine towers. However, recent studies [67] pointed out that the bending moment at the bottom of a wind turbine tower sometimes is controlled by earthquake loads. Therefore earthquake design should be conducted for wind turbine towers. For the earthquake design procedure, the response spectrum analysis and the time history analysis are the two main analysis methods. The response spectrum analysis method has been widely used to design all different types of structures due to its simplicity. However, when applying this method on the design of wind turbine towers, Nuta et al. [68] indicated some uncertainties and suggested that various factors need to be considered due to the low-damped feature of the wind turbine towers. The time history analysis method is more suitable for flexible (slender/tall) wind turbine tower structures. When selecting earthquake time history records for this analysis method, the effects of ground motion durations and soil characteristics should be considered [69]. The effects of the near-fault earthquakes (which have obvious pulse and directionality effects) [70] and the vertical earthquake motions [66,71] should also be included in the analysis if necessary. The advantage of the time history analysis method for wind turbine towers is that it can properly consider the structural nonlinearities and damping characteristics. For example, IEC [61] specified a 1% structural damping ratio for a parked wind turbine tower structure. The aerodynamic damping characteristics could also be involved in the analysis if necessary [71]. The aerodynamic damping is an extra damping induced by aerodynamic behaviors of blades at the operational conditions of wind turbines [72]. Some detailed earthquake design requirements could be found in different wind turbine design guidelines. For example, Risø [59] provided a single-degree-of-freedom model with a lumped mass for the earthquake analysis of wind turbine towers. The lumped mass is a concentrated mass point at the top of a turbine tower, which includes the masses of the blades, the turbine engine, and the top one-fourth

of the tower. GL [60] specified a return period of 475 years for earthquake analysis and required that at least the first three modes and six ground motions should be studied. IEC [61] explicitly stipulated that the participating mass in the seismic design should be more than 85% of the total mass of a wind turbine tower. Shaking table tests can help designers understand the seismic performances of a wind turbine tower structure. A typical shaking table test study of a wind turbine tower can be found by Prowell et al. [73], which verified the low-damped feature of the wind turbine tower structures.

22.3.2 Health Monitoring and Vibration Control of Wind Turbine Towers

In addition to the wind and earthquake studies, health monitoring and vibration control are also important for the structural safety of wind turbine towers. To monitor the health and control the vibration of a wind turbine tower structure, the modal parameters of the tower structure are needed. Modal testing is a commonly used procedure to identify the vibration modal parameters of a wind turbine tower. There are two excitation methods for the modal testing procedure: active excitation method and ambient excitation method. There are limited examples of using the active excitation method on wind turbine tower structures [74]. On the other hand, the ambient excitation method is feasible to identify the dynamic parameters of a wind turbine tower due to its large-scale feature. Velazquez et al. [75] estimated the dysfunction probability of a wind turbine tower based on ambient vibration measurements. Kusiak et al. [76] analyzed the collected ambient vibration data of a wind turbine tower and obtained a parametric model of the structure by using a genetic evolution algorithm. There are two hypotheses for using the ambient vibration testing: (1) the measured structure must be a linear time-invariant system [77,78] and (2) the input excitation must be white noise [77]. It seems that these two assumptions were not perfectly satisfied for wind turbine tower structures, especially when the turbine is operating. To solve this problem, Allen et al. [79] and Malcolm [80] proposed a method to simplify the wind turbine towers into a linear cycle time-variant structure and investigated the feasibility of applying the Coleman conversion method for this analysis.

Structural health monitoring of wind turbine towers can be applied to help assess their current structural performances, identify their structural damages, estimate their lifetime, and improve their structural reliabilities [81,82]. Structural health monitoring has been successfully utilized for wind turbine towers to identify structural damages, such as loose of high-tension bolts, resonance problems [81], and cracking [83,84]. Several structural health monitoring equipment has been developed to collect operational, environmental, and structural parameters of wind turbine towers [78,84–86]. Example case studies on structural health monitoring of wind turbine towers

can be found in Pavlov [87], Simarsly et al. [86], Rohrmann et al. [65], and Benedetti et al. [84]. For the analysis procedure of structural health monitoring, the change of vibration frequency method was popularly used to identify structural damages. However, for a large-scale wind turbine tower structure, the sensitivity of this change of vibration frequency method may not be good enough to effectively identify its structural damages due to modeling uncertainties, data noises, data processing errors, environment-induced changes, and blade rotation effects [82]. Kim et al. [88] reported that the sensitivity of vibration mode shapes typically is better than that of vibration frequencies. Therefore, the change of vibration mode shape method could be considered to identify structural damages of wind turbine towers. However, whether this method works or not is still unknown because noises and measurement errors always exist in actual data. In addition to the change of vibration frequency method, several advanced analysis methods have also been proposed, such as the wavelet method [89], the HHT [90], the genetic algorithm based on time domain measurements, the neural network method [91], and the statistical method [92].

The aforementioned structural health monitoring can provide information for timely maintenances of wind turbine tower structures. Structural vibration control technologies, on the other hand, can effectively depress structural vibrations of wind turbine towers, therefore reducing fatigue damages and preventing structural failures under extreme loadings. The selection of vibration control devices for wind turbine towers, unlike that of conventional dampers, should consider the effects of limited installation spaces inside the tubular tower, multidirection vibrations, and broadband vibration frequencies. Passive energy dissipation devices are the most popular used vibration control devices for wind turbine towers, which include tuning mass dampers (TMD), tuning liquid dampers (TLD), tuning liquid column dampers (TLCD), and circular tuning liquid column dampers (CTLCD). Many applications of these passive energy dissipation devices for structural vibration control of wind turbine towers have been reported along with the increasing height of modern wind turbine towers. For example, Murtagh et al. [93] designed a TLD based on the blade–tower coupling theory and installed it at the top of a wind turbine tower to reduce the abnormal vibration displacements of the tower; Karimi et al. [94] reported positive conclusions of a TLCD application on vibration controls of wind turbine towers. In addition to the passive energy dissipation devices, some conventional dampers specifically designed for tall and slender structures [95,96] and oil dampers [97] may also be applied for wind turbine tower structures. However, most of the aforementioned dampers and devices were only effective under a tuned condition, namely a certain frequency, usually the natural frequency of the first vibration mode. It is desirable that multiple frequencies of wind turbines, e.g., the fundamental frequency of the tower and the frequencies of the blade rotation, can be controlled. Therefore, some researchers proposed to use

particle dampers with broadband working frequencies and high durability features to control the wind turbine tower vibrations [98]. The particle dampers are based on the mechanism of friction and impact effects between particles, which is insensitive to temperature changes and flexible for deployment locations. Some other researchers are working on developing structural vibration control devices and technologies suitable for wind turbine towers under harsh operating environments.

22.4 SUMMARY

Renewable energy, a solution for global energy problems, can also impact the socioeconomic positively, such as diversifying energy supplies, increasing regional and rural development opportunities, and creating additional domestic industries and employment opportunities. However, renewable energy also induces some environmental and structural safety issues. These environmental and structural safety issues of wind turbines are controversial topics and should not be ignored. Minor issues today may cause disastrous effects in the future when wind energy becomes a major energy source.

This chapter summarized the environmental impacts of wind power industry and potential mitigation methods. As shown in this review study, it is recommended that the wind energy exploitation including related infrastructure constructions and facility operations should be evaluated for the economic, social, environmental, biological, and ecological influences. Suitable measures should be implemented to mitigate those negative impacts. Developers, planners, and government officials need to gather and communicate full information with the public to ensure that the projects are developed in a way that avoids or minimizes those negative impacts.

As the supporting structures of wind turbines, the safety of wind turbine towers is an important topic for researchers and engineers, which includes structure stabilities and fatigue resistances of wind turbine towers under operational vibrations, extreme wind loads, and earthquake effects. Tests and numerical simulations are the two basic research and design/analysis methods for wind turbine towers. For the numerical simulation, response spectrum and time history analysis are the two main procedures for calculating the resistances of wind turbine towers. The response spectrum procedure is more suitable for design/analysis because it is easy to apply and the time history analysis procedure is more suitable for research because it could get more data. For current research of wind turbine towers, the pulsating wind action for wind resistance studies and the tower coupling action for earthquake studies are the two popular topics. Health monitoring and vibration control of wind turbine towers is another significant research topic. Health monitoring identifies structural damages and vibration control mitigates structural vibrations. Effective health monitoring and vibration control technologies can help construct taller wind turbine towers under lower budgets.

ACKNOWLEDGMENTS

The authors would like to acknowledge supports from State Key Laboratory of Disaster Reduction in Civil Engineering (SLDRCE14-B-02), State Key Laboratory for Geomechanics and Deep Underground Engineering (SKLGDUEK1514), State Key Laboratory of Geohazard Prevention and Geoenvironment Protection (SKLGP2016K006), and Key Laboratory of Low-Carbon Conversion Science and Engineering, Shanghai Advanced Research Institute, Chinese Academy of Sciences, Key Laboratory of Energy Engineering Safety and Disaster Mechanics (Sichuan University) (EES201603), Ministry of Education, and International Collaboration Program of Science and Technology Commission of Shanghai Municipality (16510711300).

REFERENCES

- [1] Ellenbogen JM, Grace S, Heiger-Bernays WJ, Manwell JF, Mills DA, Sullivan KA, et al. Wind Turbine Health Impact Study: Report of Independent Expert Panel. MA: Massachusetts Department of Environmental Protection and Massachusetts Department of Public Health; 2012.
- [2] Lima F, Ferreira P, Vieira F. Strategic impact management of wind power projects. *Renew Sustain Energ Rev* 2013;25:277–90.
- [3] Tabassum-Abbas, Premalatha M, Abbasi T, Abbasi SA. Wind energy: increasing deployment, rising environmental concerns. *Renew Sustain Energ Rev* 2014;3:270–88.
- [4] Mann J, Teilmann J. Environmental impact of wind energy. *Environ Res Lett* 2013;8:1–3.
- [5] Drewitt AL, Langston RH. Assessing the impact of wind farms on birds. *Ibis* 2006;148:29–42.
- [6] Orloff SG, Flannery AMS. Available from: http://www.energy.ca.gov/windguidelines/documents/2006-12-06_1992_FINAL_REPORT_1989-1991.PDF Wind turbine effects on avian activity, habitat use, and mortality in Altamont pass and Solano County, wind resource areas. Tiburon, CA: BolSystems Analysis, Inc; 1992 [accessed August 2013].
- [7] Smallwood KS, Thelander CG. Development methods to reduce bird mortality in the Altamont pass wind resource area. Ojai, CA: Bioresource Consultants; 2004.
- [8] Sovacool BK. Contextualizing avian mortality: a preliminary appraisal of bird and bat fatalities from wind, fossil-fuel, and nuclear electricity. *Energ Pol* 2009;37:2241–8.
- [9] Holmstrom LA, Hamer TE, Colelazier EM, Denis N, Verschuy JP, Ruché D. Assessing avian-wind turbine collision risk: an approach angle dependent model. *Wind Eng* 2011;35:289–312.
- [10] Barrios L, Rodriguez A. Behavioural and environmental correlates of soaring-bird mortality at on-shore wind turbines. *J Appl Ecol* 2004;41:72–81.
- [11] Langston R.H.W., Pullan J.D. Windfarms and birds: an analysis of the effects of wind-farms on birds and guidance on environmental assessment criteria and site selection issues. Report T-PVS/Inf (2003) 12, by Bird Life International to the Council of Europe, Bern Convention on the Conservation of European Wildlife and Natural Habitats. RSPB/BirdLife in the UK. Available from: http://www.birdlife.org/eu/pdfs/BirdLife_Bern_wind-farms.pdf; 2003 [accessed June 2016].
- [12] Christensen TK, Hounisen JP, Clausager I, Petersen IK. Visual and radar observations of birds in relation to collision risk at the Horns Rev offshore wind farm. Denmark: National Environmental Research Institute, Ministry of the Environment; 2003.
- [13] Dahl EL, Bevanger K, Nygård T, Røkkaft E, Stokke BG. Reduced breeding success in white-tailed eagles at Smøa windfarm western Norway, is caused by mortality and displacement. *Biol Conser* 2012;145:79–85.

- [14] Ellison LE. 57 pp Bats and wind energy—a literature synthesis and annotated bibliography. U.S. Geological Survey Open-File Report 2012–1110. Reston, VA: US Geological Survey; 2012.
- [15] Maina JN, King AS. Correlations between structure and function in the design of the bat lung: a morphometric study. *J Exp Biol* 1984;111:43–61.
- [16] Grodsky SM, Behr MJ, Gandler A, Drake D, Dieterle BD, Rudd RJ, et al. Investigating the causes of death for wind turbine-associated bat fatalities. *J Mammal* 2011;92:917–25.
- [17] Baerwald EF, D'Amours GH, Klug BJ, Barclay RMR. Barotrauma is a significant cause of bat fatalities at wind turbines. Calgary, Alberta: Department of Biological Sciences, University of Calgary; 2008.
- [18] Rollins KE, Meyerholz DK, Johnson GD, Capparella AP, Loew SS. A forensic investigation into the etiology of bat mortality at a wind farm: barotrauma or traumatic injury? *Vet Pathol Online* 2012;49(2):362–71.
- [19] Arnett E.B., Erickson W.P., Kerns J., Horn J. Relationships between bats and wind turbines in Pennsylvania and West Virginia: an assessment of fatality search protocols, patterns of fatality, and behavioral interactions with wind turbines. A Final Report Prepared for the Bats and Wind Energy Cooperative. Bat Conservation International. Austin, TX; 2005.
- [20] Ahlén I. Available from: <http://docs.wind-watch.org/Ahlen-windturbines-bats-2003.pdf> Wind turbines and bats—a pilot study. Eskilstuna, Sweden: Swedish National Energy Administration; 2003 [accessed July 2014].
- [21] Long CV, Flint JA, Lepper PA. Insect attraction to wind turbines: Does colour play a role? *Eur J Wildlife Res* 2011;57:323–31.
- [22] Kunz TH, Arnett EB, Erickson WP, Hoar AR, Johnson GD, Larkin RP, et al. Ecological impacts of wind energy development on bats: questions, research needs, and hypotheses. *Front Ecol Environ* 2007;5:315–24.
- [23] Marsh G. WTS: the avian dilemma. *Renew Energ Focus* 2007;8(4):42–5.
- [24] Barclay RMR, Baerwald EF, Gruver JC. Variation in bat and bird fatalities at wind energy facilities: assessing the effects of rotor size and tower height. *Can J Zool* 2007;85:381–7.
- [25] Arnett EB, Brown K, Erickson WP, Friedler J, Hamilton BL, Henry TH, et al. Patterns of fatality of bats at wind energy facilities in North America. *J Wildlife Manage* 2008;72:61–78.
- [26] Pearce-Higgins JW, Stephen L, Douse A, Langston RHW. Greater impacts of wind farms on bird populations during construction than subsequent operation: results of a multi-site and multi-species analysis. *J Appl Ecol* 2012;49:386–94.
- [27] Smallwood KS, Karas B. Avian and bat fatality rates at old-generation and repowered wind turbines in California. *J Wildlife Manage* 2009;73:1062–71.
- [28] McIsaac H.P. Raptor acuity and wind turbine blade conspicuity. Available from: http://altamontsrc.org/alt_doc/raptor_acuity_and_wind_turbine_blade_conspicuity_mcissac.pdf; 2012 [accessed July 2013].
- [29] Arnett EB, Huso MMP, Schirmacher MR, Hayes JP. Altering wind turbine speed reduces bat mortality at wind-energy facilities. *Front Ecol Environ* 2011;9:209–14.
- [30] Foote R. The wind is blowing the right way for birds. *Renew Energ Focus* 2010;11(2):40–2.
- [31] Carrete M, Sanchez-Zapata JA, Benitez JR, Lobon M, Montoya F, Donazar JA. Mortality at wind farms is positively related to large scale distribution and aggregation in griffon vultures. *Biol Conser* 2012;145:102–8.
- [32] Busch M, Kannen A, Garthe S, Jessopp M. Consequences of a cumulative perspective on marine environmental impacts: offshore wind farming and seabirds at North Sea scale in

- context of the EU Marine Strategy Framework Directive. *Ocean Coastal Manage* 2013;71:213–24.
- [33] Northrup JM, Wittemyer G. Characterising the impacts of emerging energy development on wildlife, with an eye towards mitigation. *Ecol Lett* 2013;16:112–25.
 - [34] Berkenhagen J, Döring R, Fock HO, Kloppmann MHF, Pedersen SA, Schulze T. Decision bias in marine spatial planning of offshore wind farms: problems of singular versus cumulative assessments of economic impacts on fisheries. *Marine Policy* 2010;34:733–6.
 - [35] Kikuchi R. Risk formulation for the sonic effects of offshore wind farms on fish in the EU region. *Marine Pollut Bull* 2010;60:172–7.
 - [36] Thompson PM, Lusseau D, Barton T, Simmons D, Rusin J, Bailey H. Assessing the responses of coastal cetaceans to the construction of offshore wind turbines. *Marine Pollut Bull* 2010;60:1200–8.
 - [37] Dong Energy, Vattenfall, Danish Offshore Wind—Key Environmental Issues. The Danish Energy Authority and The Danish Forest and Nature Agency. Available from: http://mhk.pnln.gov/wiki/images/0/09/Danish_Offshore_Wind_Key_Environmental_Issues.pdf; 2006 [accessed October 2014].
 - [38] Rogers AL, Manwell JF. Available from: <http://www.minutemanwind.com/pdf/Understanding%20Wind%20Turbine%20Acoustic%20Noise.pdf> Wind turbine acoustic noise, wind turbines noise issues. Renewable Energy Research Laboratory; 2006 [accessed August 2013].
 - [39] Van den Berg GP. Effects of the wind profile at night on wind turbine sound. *J Sound Vib* 2004;277:955–70.
 - [40] Pedersen E, Persson WK. Perception and annoyance due to wind turbine noise—a dose-response relationship. *Acoust Soc Am* 2004;116(6):3460–70.
 - [41] Møller H, Pedersen CS. Low-frequency noise from large wind turbines. *J Acoust Soc Am* 2011;129(6):3727–44.
 - [42] Frey RC, Kollman JR. Literature search on the potential health impacts associated with wind-to-energy turbine operations. Fremont, OH: Ohio Department of Health; 2008.
 - [43] Binopoulos E, Haviaropoulos P. Available from: <http://www.cres.gr/kafe/publications/papers/dimoseyseis/CRESTRANSWINDENVIRONMENT.doc> Environmental impacts of wind farms: myth and reality. Centre for Renewable Energy Sources; 2012 [accessed July 2013].
 - [44] Harding G, Harding P, Wilkins A. Wind turbines, flicker, and photosensitive epilepsy: characterizing the flashing that may precipitate seizures and optimizing guidelines to prevent them. *Epilepsia* 2008;49:1095–8.
 - [45] Wolsink M. Wind power implementation: the nature of public attitudes: equity and fairness instead of “backyard motives”. *Renew Sustain Energ Rev* 2005;11:1188–207.
 - [46] Johansson M, Laike T. Intentions to respond to local wind turbines: the role of attitudes and visual perception. *Wind Energ* 2007;10:435–51.
 - [47] Krohn S, Damborg S. On public attitudes towards wind power. *Renew Energ* 1999;16:954–60.
 - [48] Paul Magoha K. Footprint in the wind? Environmental impacts of wind power development. *Refocus* 2002;3(5):30–3.
 - [49] Bishop ID, Miller DR. Visual assessment of off-shore wind turbines: the influence of distance, contrast, movement and social variables. *Renew Energ* 2006;32:814–31.
 - [50] Sun C, Wang Y, Li X, Ma S. Environmental impacts of wind power generation projects. *J Electr Power Sci Technol* 2008;23(2):19–23.

- [51] Zhou L, Tian Y, Roy SB, Thorncroft C, Bosart LF, Hu Y. Impacts of wind farms on land surface temperature. *Nature Clim Change* 2012;2:539–43.
- [52] Barthelmie R., Pryor S., Frandsen S., Larsen S. Analytical and empirical modeling of flow downwind of large wind farm clusters. The science of making torque from wind, EWEA special topic conference, Delft; 2004. p. 346–355.
- [53] Roy SB, Traitor JJ. Impacts of wind farms on surface air temperature. *Proceedings of the national academy of sciences of the United States of America* 2010;107(42):17899–904.
- [54] Keith DW, DeCarolis JF, Denkenberger DC, Lenschow DH, Malyshov SL, Pacala S, et al. The influence of large-scale wind power on global climate. *Proceedings of the national academy of sciences of the United States of America* 2004;101:16115–20.
- [55] Santa Maria MRV, Jacobson MZ. Investigating the effect of large wind farms on energy in the atmosphere. *Energies* 2009;2:816–38.
- [56] Ishihara T., Takamotob G., Sarwar M.W. Seismic load evaluation of wind turbine support structures with consideration of uncertainty in response spectrum and higher modes. Offshore wind energy conference. Amsterdam: The Netherlands; 2011.
- [57] Chou JS, Tu WT. Failure analysis and risk management of a collapsed large wind turbine tower. *Eng Failure Anal* 2011;18(1):295–313.
- [58] Chen X, Li C, Xu J. Failure investigation on a coastal wind farm damaged by super typhoon: a forensic engineering study. *J Wind Eng Indus Aerodyn* 2015;147:132–42.
- [59] Risø. Guidelines for design of wind turbines. Copenhagen, Denmark: Wind Energy Department, Risø National Laboratory and Det Norske Veritas; 2001.
- [60] GL. Guideline for the certification of wind turbines. Hamburg, Germany: Germanischer Lloyd; 2010.
- [61] IEC (2005). IEC 61400-1 Ed. 3: Wind turbines—Part 1: Design requirements. International Electrotechnical Commission, Geneva, Switzerland.
- [62] Murtagh PJ, Basu B, Broderick BM. Along-wind response of a wind turbine tower with blade coupling subjected to rotationally sampled wind loading. *Eng Struct* 2005;27:1209–19.
- [63] Lavassas I, Nikolaidis G, Zervas P, Efthimiou E, Doudoumi IN, Baniotopoulos CC. Analysis and design of the prototype of a steel 1-MW wind turbine tower. *Eng Struct* 2003;25:1097–106.
- [64] Bazeos N, Hatzigeorgiou GD, Hondros ID, et al. Static, seismic and stability analyses of a prototype wind turbine steel tower. *Eng Struct* 2002;24(8):1015–25.
- [65] Rohrmann RG, Thöns S, Rücker W. Integrated monitoring of offshore wind turbines—requirements, concepts and experiences. *Struct Infrastruct Eng* 2010;6(5):575–91.
- [66] Ritschel U., Warnke I., Kirchner J., et al. Wind turbines and earthquakes. World wind energy conference Cape Town, South Africa; 2003.
- [67] Prowell I., Elgamal A., Uang C., et al. Estimation of seismic load demand for a wind turbine in the time domain. European wind energy conference and exhibition. Warsaw, Poland; 2010.
- [68] Nuta E, Christopoulos C, Packer JA. Methodology for seismic risk assessment for tubular steel wind turbine towers: application to Canadian seismic environment. *Can J Civil Eng* 2011;38:293–304.
- [69] Katsanos EI, Sextos A,G, Manolis GD. Selection of earthquake ground motion records: a state-of-the-art review from a structural engineering perspective. *Soil Dyn Earthq Eng* 2010;30(4):157–69.

- [70] Stamatopoulos GN. Response of a wind turbine subjected to near-fault excitation and comparison with the Greek aseismic code provisions. *Soil Dyn Earthq Eng* 2013;46:77–84.
- [71] Díaz O, Suárez LE. Seismic analysis of wind turbines. *Earthq Spec* 2013;30(2):743–65.
- [72] Riziotis VA, Voutsinas SG, Politis ES, Chavaropolos PK. Aeroelastic stability of wind turbines: the problem, the methods and the issues. *Wind Energ* 2004;7(4):373–92.
- [73] Prowell I, Elgamal A, Uang CM, et al. Shake table testing and numerical simulation of a utility-scale wind turbine including operational effects. *Wind Energ* 2014;17(7):997–1016.
- [74] Molinari M, Pozzi M, Zonta D, et al. In-field testing of a steel wind turbine tower. *Struct Dyn Renew Energ* 2011;1:103–12.
- [75] Velazquez A, Swartz RA. Probabilistic analysis of mean-response along-wind induced vibrations on wind turbine towers using wireless network data sensors. San Diego, CA: SPIE Smart Structures and Materials + Nondestructive Evaluation and Health Monitoring; 2011.
- [76] Kusiak A, Zhang Z. Analysis of wind turbine vibrations based on SCADA data. *J Solar Energ Eng* 2010;132(3):031008.
- [77] Tcherniak D, Chauhan S, Hansen MH. Applicability limits of operational modal analysis to operational wind turbines. 1. Jacksonville, FL: IMAC-XXVIII; 2011. p. 317–27.
- [78] M. Ozbek Monitoring the dynamics of large wind turbines in operation using optical measurement techniques. We@Sea, IJmuiden, North Holland, Dutch, 2007.
- [79] Allen MS, Sracic MW, Chauhan S, et al. Output-only modal analysis of linear time-periodic systems with application to wind turbine simulation data. *Mechan Syst Signal Process* 2011;25(4):1174–91.
- [80] Malcolm DJ. Modal response of 3-bladed wind turbines. *J Solar Energ Eng* 2002;124(4):372–7.
- [81] Hartmann D., Smarsly K., Law K.H. Coupling sensor-based structural health monitoring with finite element model updating for probabilistic lifetime estimation of wind energy converter structures. The eighth international workshop on structural health monitoring, 2011: Stanford, CA.
- [82] Sohn H., Farrar C.R., Fugate M.L., et al. Structural health monitoring of welded connections. The first international conference on steel & composite structures, 2001: Pusan, Korea.
- [83] Lacalle R, Cicero S, Álvarez JA, et al. On the analysis of the causes of cracking in a wind tower. *Eng Failure Anal* 2011;18(7):1698–710.
- [84] Benedetti M, Fontanari V, Zonta D. Structural health monitoring of wind towers: remote damage detection using strain sensors. *Smart Mater Struct* 2011;20(5) 055009.
- [85] Bang HJ, Jang M, Shin H. Structural health monitoring of wind turbines using fiber Bragg grating based sensing system. San Diego, CA: Smart structures and materials + nondestructive evaluation and health monitoring; 2011.
- [86] Smarsly K, Hartman D, Law KH. An integrated monitoring system for life-cycle management of wind turbines. *Int J Smart Struct Syst* 2013;12(2):209–33.
- [87] Pavlov GK. Design of health monitoring system to detect tower oscillations. Denmark: Department of Mechanical Engineering, Technical University of Denmark; 2008.
- [88] Kim JT, Ryu YS, Cho HM, Stubbs N. Damage identification in beam-type structures: frequency-based method vs mode-shape-base method. *Eng Struct* 2003;25:57–67.
- [89] Lee YY, Liew KM. Detection of damage locations in a beam using the wavelet analysis. *Int J Struct Stab Dyn* 2001;1(03):455–65.

- [90] Yang JN, Lei Y, Pan S, et al. System identification of linear structures based on Hilbert–Huang spectral analysis. Part 1: Normal modes.. *Earthq Eng Struct Vib* 2003;32(9):1443–67.
- [91] Masri SF, Nakamura M, Chassiakos A, et al. Neural network approach to detection of changes in structural Parameters. *J Eng Mech* 1996;122(4):350–60.
- [92] Sohn H, Czarnecki JA, Farrar CR. Structural health monitoring using statistical process control. *J Struct Eng* 2000;126(11):1356–63.
- [93] Murtagh PJ, Ghosh A, Basu B, et al. Passive control of wind turbine vibrations including blade/tower interaction and rotationally sampled turbulence. *Wind Energ* 2008;11(4):305–17.
- [94] Karimi HR, Zapateiro M, Luo N. Semiactive vibration control of offshore wind turbine towers with tuned liquid column dampers using $H\infty$ output feedback control. Yokohama, Japan: International Conference on Control Applications (CCA); 2010.
- [95] Pirner M. Actual behaviour of a ball vibration absorber. *J Wind Eng Indus Aerodyn* 2002;90(8):987–1005.
- [96] Fischer O. Wind-excited vibrations—solution by passive dynamic vibration absorbers of different types. *J Wind Eng Indus Aerodyn* 2007;95(9):1028–39.
- [97] Carcangiu CE, Pineda I, Fischer T, et al. Wind turbine structural damping control for tower load reduction, in civil engineering topics, 4. New York, NY: Springer; 2011. p. 141–53.
- [98] Wang J, Dai K, Mao R, Xiang Z, Lu Z. A new passive damper for wind turbine vibration control. Hefei, China: The 13th international symposium on structural engineering; 2014.

This page intentionally left blank

Chapter 23

Wind Turbines and Landscape

Marc van Grieken and Beatrice Dower

MVGLA, Perthshire, United Kingdom

Email: marc@mvbla.com

23.1 A PASSION FOR LANDSCAPE

Most people are passionate about landscape, whether as a source of inspiration for paintings or poetry; as the backdrop of a favorite walk; providing the growing environment for food; to sustain animal livestock; as the setting of carefully crafted views; or simply as daily surroundings. Irrespective of whether the landscape has formal recognition as being of outstanding value or quality, with statutory protection, for example, as a National Scenic Area in Scotland, as an Area of Outstanding Natural Beauty in England or as a National Park (see Fig. 23.1), or whether it is fairly degraded land frequently found on the edge of our cities, changes in the landscape tend to invoke strong feelings and opinions in people.

In this chapter we will discuss how wind energy developments affect people's perception of landscape and how the number, composition, and size of turbines (which make up a wind farm) influence this perception. We will discuss the meaning of landscape and consider how the development of wind farms in the landscape may affect the qualities and values that people attach to the landscape.

23.2 WHAT IS LANDSCAPE?

Governments across the European Union have ratified the European Landscape Convention (ELC), which is designed to achieve improved approaches to the planning, management, and protection of landscapes throughout Europe. It has also put people at the heart of this process. The ELC defines landscape as: "*an area, as perceived by people, whose character is the result of the action and interaction of natural and/or human factors*" [1]. As quoted in the current UK Guidelines for Landscape and Visual Impact Assessment, "*landscape is about the relationship between people and place. It provides the setting for our day-to-day lives. The term*



FIGURE 23.1 Glaciers across the world are retreating due to global temperature increases, Abel Tasman Glacier, New Zealand. *Photo: M van Grieken. Copyright © 2017 Marc van Grieken. Published by Elsevier Inc. All rights reserved.*



FIGURE 23.2 A 360 degree panorama from the Comrie Standing Stones, Scotland (OS Grid ref: NN 754 224). *Photo: M van Grieken. Copyright © 2017 Marc van Grieken. Published by Elsevier Inc. All rights reserved.*

does not mean just special or designated landscapes and it does not only apply to the countryside” [2,3]. These descriptions confirm that landscape is important to people and therefore changes in the landscape may affect people in different ways.

Particularly in recent years, theories about the importance of landscape have evolved and the significance of the ELC definition is that it has moved thinking about landscape beyond the idea that landscape is only a matter of aesthetics and visual amenity. The ELC encourages a focus on landscape as a resource in its own right and not just on the setting for human activity (See Fig. 23.2). Understanding and evaluating landscape allows us to conceptualize our surroundings and consider the effects of introducing

developments into our landscapes, and it can contribute to providing a spatial framework for managing landscape change. This enables informed discussion and debate about a wide range of environmental, land use, and development issues including wind farms.

23.3 CHANGING LANDSCAPE

The description of landscape in the ELC fully encompasses the changes that a landscape undergoes when humans live in it, aptly captured by Susan and Geoffrey Jellicoe in their book *The Landscape of Man*: “*Throughout history men have moulded their environment to express or to symbolize ideas—power, order, comfort, harmony, pleasure, mystery*” [4].

Landscapes are constantly changing as a result of human intervention, such as intensification of agriculture, felling of rainforests for cultivation, or loss of agricultural countryside to urban development, and importantly it is widely accepted that landscapes will change further through climate change (see Fig. 23.3). Some of our land will be lost to the sea, some parts of the world will become more arid, and other areas may become wetter as a result of natural processes and these changes to our landscapes are among the consequences of climate change that people have limited control over. Notably, however, other significant changes in landscapes will be the result of the measures we take to address climate change.

Drastically cutting CO₂ emissions by reducing reliance on fossil fuels is one of the primary measures to address climate change. This has led to governments across the world setting renewable energy targets to reduce CO₂ emission levels in accordance with the Kyoto protocol [5]. In many countries, the development, construction, and operation of wind farms, both on- and offshore, are part of the mix of measures taken to address climate change. Introducing a wind farm in any landscape or in the sea (located ‘inshore,’ i.e., within sight of the land) has effects on the views of the landscape and may affect the perception of the landscape and seascape character and thus the wind farm itself contributes to landscape change.

23.3.1 People’s Opinions

One of the most common comments made by local people who are consulted on a wind energy proposal in their local area is: “*I am all in favour of renewable energy and wind farms but this is not the right place.*” Given that the primary concern of most people with respect to wind farms is their effect on landscape, views, and visual amenity, government support or otherwise for this type of development has therefore increasingly become a political issue. This is in itself not unique, as other forms of energy generation invoke

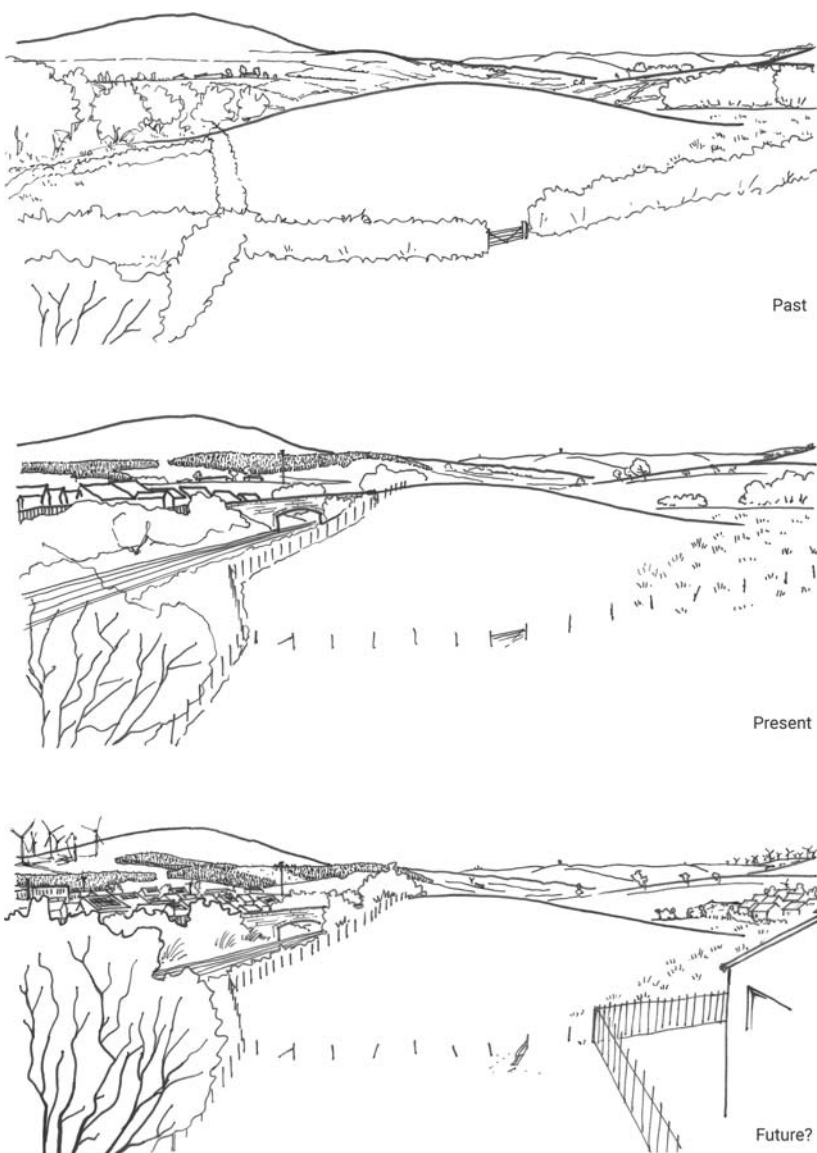


FIGURE 23.3 A changing landscape. MVGLA.

equally strong opinions, as may be illustrated by the prolonged debate about new nuclear power plants in the United Kingdom or about fracking.

Whilst wind turbines are seen by some people as sculptural objects in the landscape, others see them as industrial monstrosities. Irrespective of this, wind farms are not being constructed for artistic reasons, but are designed



FIGURE 23.4 The Angel of the North, near Gateshead, United Kingdom. *Photo: B Dower.*

and built to generate electricity, and the form of the turbines is driven by aerodynamic rather than sculptural considerations. They may therefore be comparable in scale, but not in function, to large sculptures such as the Angel of the North, near Gateshead, United Kingdom (see Fig. 23.4).

Landscape architects recognize that any type of development leads to changes in the landscape and on views and visual amenity. Some of these changes resulting from development are very subtle or barely perceptible but other types of development lead to more substantive change in the landscape and in the perception of the landscape. The tall nature of modern wind turbines, currently up to 200 m tall for the largest turbines, and the associated movement of the rotating blades, means that they are potentially visible from great distances, in some landscapes and visibility conditions up to 50–60 km.

Landscape architects describe the likely change in landscape by using readily recognizable terminology that will resonate with most people. In order to explain varying degrees of wind energy developments in the landscape, different levels of development may be described as ‘landscape without wind farms,’ ‘landscape with occasional wind farms,’ ‘landscape with wind farms,’ and for the most developed landscapes with the term ‘wind farm landscape’ (see Fig. 23.5). Such terminology is not unique to wind energy development and may equally apply to, for example, coniferous forestry: ‘landscape without forest,’ ‘landscape with occasional forest,’ and ‘forest landscape.’

It is clear that landscapes are constantly changing, as a consequence of urban development, changes in farming practices, land use planning policies,



FIGURE 23.5 Wind farms can be seen to be a defining feature of this landscape. *Photo: M van Grieken. Copyright © 2017 Marc van Grieken. Published by Elsevier Inc. All rights reserved.*

and indeed as a consequence of wind farm development. Rather than ‘standing on the side lines,’ and reactively responding to the effects of wind farms, we need to continue to study the effects of wind farm developments on landscape, and proactively debate and decide which landscapes are more suitable and capable of accommodating wind energy development and which landscapes are more vulnerable to losing their unique qualities. In our view it is necessary and possible to ‘take control’ with respect to which landscape can accommodate wind farm developments, and to design how these landscapes may change in the future as a result of wind energy development.

23.4 TECHNOLOGICAL ADVANCEMENT

It is thought that wind energy will make a substantial contribution to our energy supply in the (relatively) short term of the next 25–50 years. In this timescale it is possible that new technologies will come on stream that will replace on- and offshore wind, and ultimately lead to the removal of wind turbines from our landscape. There is plenty of evidence from history to demonstrate how the process of technological advancement led to the introduction and subsequent abandonment of power generation industries that have had a major effect on the landscape.

In the 20th century we have seen the effect of the transition of coal-fired power stations to gas-fired power stations. The introduction of a very large coal-fired power station near Didcot raised considerable landscape and visual



FIGURE 23.6 A wind-driven corn mill converted to a café, Boechout, Belgium. Photo: B Dower.

concerns in 1965. Sue and Geoffrey Jellicoe wrote: “*The cooling towers of Didcot Power Station, Berkshire, are symbolic of energy waste, destructive to the human scale and an intrusion into a famous rural vale that was almost universally resented*” [4].

Wind energy has been harnessed for centuries with wind-driven mills draining the land in the Netherlands or milling grain into flour across the world. Many of these windmills are now listed and are protected as valued historic structures (see Fig. 23.6).

Electricity generating turbines are more recent and have become increasingly commonplace since the 1990s. Early turbines were relatively small, noisy, and inefficient with low-energy yields. In recent years, however, driven by the pressing need for more efficient sources of renewable energy, technological advancement has accelerated. Modern machines are considerably more efficient, with greater energy yield per unit of swept area, but this has also led to ever increasing height and size of both on shore and offshore wind turbines.

One of the first commercially developed wind farms in Scotland, Hagshaw Hill in South Lanarkshire, uses turbines with a hub height of 35 m and a rotor diameter of 41 m (therefore 55.5 m to blade tip) generating 600 kW per turbine (see also Fig. 23.7).

The recently installed Westerwind turbines near Urk in the Netherlands have a 135 m hub height and blades of 63 m length resulting in a tip height of 198 m, and can generate potentially 7.54 MW each. Notably part of the



FIGURE 23.7 Small, first generation turbines in Flevoland, the Netherlands. *Photo: M van Grieken. Copyright © 2017 Marc van Grieken. Published by Elsevier Inc. All rights reserved.*

Westerwind development is what may be termed inshore with the turbines within the Zuiderzee, the large inland sea within the Netherlands. The inshore turbines of the Westerwind development are ‘only’ 165 m to tip high.

To date, the most commonly proposed commercial onshore wind turbine in the United Kingdom is in the order of 125–150 m to blade tip, with a generating potential of 2–3.5 MW.

Technological advancement, planning and ‘acceptability’ thresholds are key factors influencing the size of turbines as part of commercial developments, with, for example, 150 m being the United Kingdom threshold above which aviation lights are required on each turbine. Several consenting authorities have also undertaken or commissioned so-called ‘wind farm capacity studies’ trying to ascertain what size of turbine and size of wind farm can be accommodated without substantial landscape character change. These studies are informative with respect to ‘fitting’ development into the landscape but do not proactively plan for, or design and manage landscape change. Planning for, and accommodating more wholesome landscape change through developing wind farms, requires development of design strategies and policies which are expressly supportive of this type of development, and which actively embrace technology and size and scale advancement. However, most landscapes in the United Kingdom are subject to conservation strategies aimed at maintaining or restoring existing landscape character. Some would therefore consider that what could be described as a lag in technology in the United Kingdom is due to public objection to large structures in UK landscapes, and the reluctance of consenting authorities to support them.

Different foundation technologies have been used offshore enabling increasingly larger turbines to be used offshore. Phase 1 of Thorntonbank Wind Farm off the Belgian coast was constructed in 2012 using concrete gravity foundations, with 5 MW machines that are 157 m to the hub with 126 m rotor diameters giving 220 m tip heights. Later phases used steel



FIGURE 23.8 Split blade technology with one complete turbine and two awaiting blade sections. *Photo: M van Grieken. Copyright © 2017 Marc van Grieken. Published by Elsevier Inc. All rights reserved.*

jacket foundations and REPower 6.15 MW machines, the largest available in 2013, with rotor diameters of 152 m [6].

On land, the limitation to turbine size was initially the length of blade, with 46.5 m blades being the longest transportable on British roads, particularly on winding lanes through small villages, giving a maximum rotor diameter of 93 m. Split blade technology has dramatically changed this, with 60 m and longer blades now being available and deliverable (see Fig. 23.8). As with most types of development, a key factor influencing turbine design and overall development size of wind farm proposals, is economic and technical viability and optimization.

Some professionals are of the view that the landscapes of the United Kingdom are smaller in scale than landscapes elsewhere in Europe or the world, and that as a result, the UK landscape is less capable of absorbing large turbines. This does not necessarily mean that the scale of the landscape features is smaller, but that the extent of each landscape type is small, and variation across the country is diverse. This is the case in some places but certainly not across the United Kingdom as a whole. Different scale landscapes exist across the United Kingdom from the more densely populated parts of England to the less densely populated landscapes in the north and more rural parts of Wales and Scotland.

Similar differences in landscapes exist in France, Spain, Germany, the Netherlands, and Denmark. There are no European countries with landscapes similar to the vast plains of the United States or China, that can accommodate hundreds of turbines extending for miles. This leads to the question of

whether these European landscapes can only accommodate smaller technologies? The answer to this question depends to some extent on the level of fit required. Whilst when purely considering landscape scale and size an argument can be had in favor of relatively small turbines, in practice the economics of wind energy developments in the United Kingdom and the availability of commercially viable turbines pushes developments toward larger size machines. This is further driven by the fact that the windiest locations have mostly been developed, and new developments may require taller turbines with larger rotor diameters in order to be economically viable on lower wind yield sites.

Both of these trends, development on lower wind speed sites and the availability of turbines, drive developers toward increasing turbine size.

23.5 THE PERCEPTION OF WIND FARMS

There are three primary components of a wind farm that influence the perception of the development by people in the wider area around the wind farm.

Firstly, the height and size of the turbines as objects are important factors. Introducing objects of the height and size currently commonly proposed for commercial-scale wind energy development into any landscape represents a unique form of development which most people are not familiar with.

Secondly, the placement or composition of the individual turbines that collectively form the wind farm in different geometric formations (straight or curved line, square or triangular grid, loose group, etc.) greatly influences the perception of the wind farm with turbines in lines, grids, or groups creating strikingly different images.

The third unique aspect of wind energy development is the rotation of the blades, which introduces movement into the view, whilst most landscapes are generally ‘still’ above ground level. The relevance of movement is particularly evident when viewing two bladed turbines. When the lower blade passes the tower, either in front or behind, this appears to interrupt the flow of rotation, which some people may experience as an on/off effect (see [Fig. 23.9](#)).

23.5.1 Height and Size

People are accustomed to proposals for new developments into their local landscape and in general most proposed developments are designed to limit landscape change and to provide as good as possible a fit to the host environment. For example, housing developments in rural areas tend to follow the vernacular design and be of a size and scale similar to existing buildings. Likewise development of a city block in the center of New York may lead to the design of a skyscraper.



FIGURE 23.9 Two bladed turbines create varied visual effects. *Photo: M van Grieken.* Copyright © 2017 Marc van Grieken. Published by Elsevier Inc. All rights reserved.

Early onshore wind energy developments comprised turbines of 35–55 m tall and at this height there is still a clear visual relationship between the turbine and other objects in the landscape such as trees that may be in the order of 20–30 m tall. Arguably at this height, turbines fit into the landscape. With the increase in absolute height this ‘connection’ between the turbine and existing landscape features is broken: a 125 m turbine does not relate to the vertical dimension of common landscape features we humans are familiar with. Arguably this disparity increases with turbines of 150–198 m, but in fact many people are incapable of readily estimating the actual height of turbines in excess of 100 m, because we are not used to these dimensions. This introduces a further factor that may influence people’s response, namely the ‘sense of scale’ and a desire to relate the height of an object to something we know. Some people also feel overawed when they know that turbines of a wind farm are taller than, for example, the telecommunications tower in London, or the Eiffel Tower in Paris.

Objections to wind farms often include references to the height of the proposed turbines relative to other known features in order to illustrate at these turbines are out of scale and therefore out of place. However, the actual ability to estimate the height of an object in the landscape depends on the availability of scale objects and importantly on perspective. This is illustrated in Fig. 23.10.

Furthermore in our experience, rather than absolute height, the predisposition of the observer to seeing wind turbines in the landscape is also an important factor in how he or she will perceive height.



FIGURE 23.10 The height and size of these turbines is difficult to estimate despite the presence of clear scale indicators such as trees and farm buildings. *Photo: M van Grieken. Copyright © 2017 Marc van Grieken. Published by Elsevier Inc. All rights reserved.*

23.5.2 Composition

Wind farms comprise more than one turbine. In the United States and China there are some wind farms of several hundred turbines, but in Western Europe most wind farms comprise between 10 and 50 turbines. The placement of a number of towers in a group formation or in a grid or in a straight, curving, or random line leads to a composition of objects which can be observed by people from different angles (see Fig. 23.11). Geometric layouts create very formal compositions and effects of stacking and perspectives are predictable. Group or irregular layouts have less predictable compositional effects.

Turbines must be separated from each other for safety and to avoid turbulence that reduces yield and causes additional wear and tear. This means that the turbines making up a wind farm must be spaced out, with distance increasing with increasing rotor diameter. Typically turbines are spaced a minimum of 6 times rotor diameter (some developers require 7 rotor diameters) from each other in the prevailing wind direction and 4 or 5 times across the wind. This represents a unique design challenge: four turbines with 100 m rotor diameters would be at least 600 m (5 full length football pitches) by 500 m apart. Whilst the actual footprint of a turbine is quite small, the ‘land take’ per typical commercial sized turbine (90–110 m rotor diameter) is therefore in the order of 30 hectares! This is illustrated in Fig. 23.12.

23.5.3 Movement

The movement of the blades, especially when seen from greater distances, may be the primary factor for a wind turbine being noticed in the landscape.

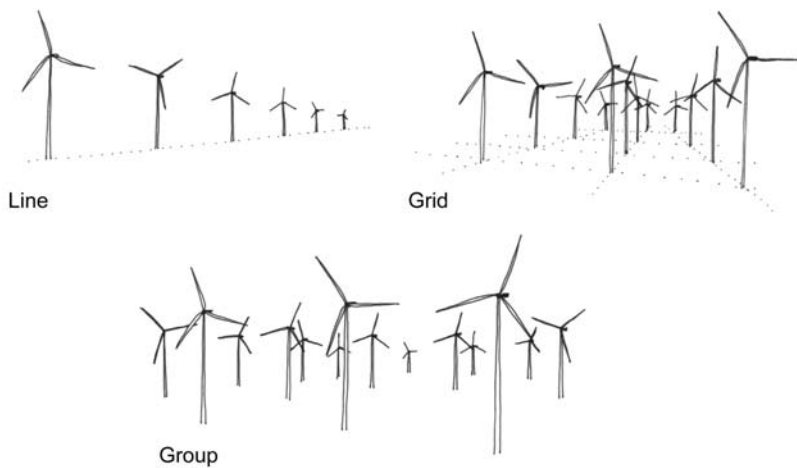


FIGURE 23.11 Lines, grids, and groups of turbines create different compositional effects. MVGLA.

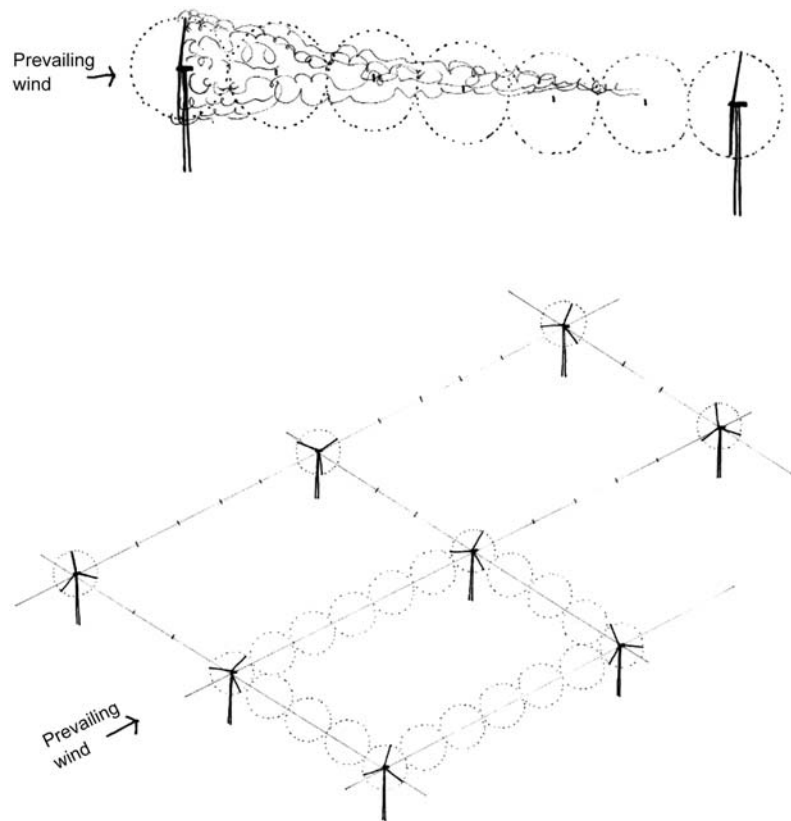


FIGURE 23.12 Turbine separation requirements take account of wake. MVGLA

what we see:



what the brain interprets:

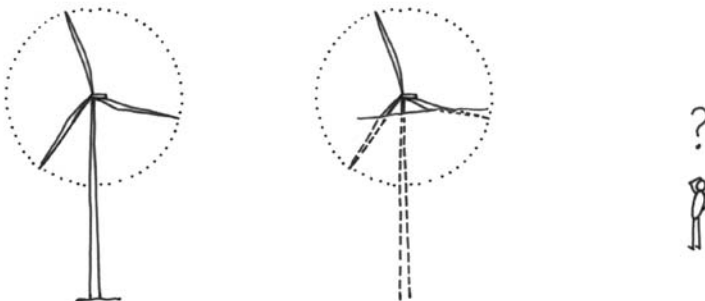


FIGURE 23.13 The proportion of a turbine visible affects our interpretation of it. MVGLA.

It is an instinctive defensive reaction to look at moving objects in our peripheral vision. There are different aspects to this movement: the movement of the blades themselves; the rotation of the turbine to follow the direction of the wind; and the extent of the turbine that is visible to the observer. The diagrams in Fig. 23.13 illustrate:

- a turbine which is visible in full;
- a turbine where the tower is largely hidden but the hub or nacelle is visible and therefore one or two of the blades are fully visible at any one time;
- a turbine that is largely hidden, with only part of a blade visible.

In the second scenario, people will perceive a full turbine even if they do not ‘see’ the full object because the brain completes the picture. In the latter scenario we do not ‘see’ the whole wind turbine and the movement of the blade can be disconcerting if it is perceived as a windscreens wiper effect (see Fig. 23.14).

23.6 LANDSCAPES WITH POWER GENERATION OBJECTS

As we said in the introduction of this chapter some landscape change causes strong feelings, particularly when change is man-made, and none so more



FIGURE 23.14 An isolated blade tip creates a windscreen wiper effect, South Ronaldsay, United Kingdom. Photo: B Dower.

than for power generation. Coal mining, quarrying, oil refineries, power stations, hydroelectric dams, wind farms, fracking, and solar panels on agricultural land are amongst the types of development that trigger strong responses. Some of those responses are influenced by the predisposition of the observer to the type of development proposed: people who are predisposed to supporting nuclear power and are of the view that wind farms are a waste of time may have strong negative responses to seeing wind turbines in the landscape, yet be more accepting of views of a nuclear power station. Opponents to nuclear power will not just ‘see’ the building housing the nuclear reactor but will also view this object as a facility they disagree with or are frightened of.

Current Scottish guidance on siting and designing wind farms points out that “*People’s responses to wind farms vary—to some a wind farm may seem to dominate its surroundings, while others may view it as an exciting, modern addition with symbolic associations with clean energy and sustainability*” [7]. Opinions on wind energy have evoked strong reactions: “*Any windmill will wreck the scenery, it’s what the Scots deserve if they want their countryside wrecked*” (Sir Bernard Ingham, former press officer for Margaret Thatcher [8]), though the younger generation are more imaginative: “*I can see a wind farm from my house, I think they look like angels*” (Jessica Dalgleish, age 9 [9]). Jessica has since had one of those “angels” named after her. Elsewhere, turbine have been given names: “*Gigha Wind Farm was the first community-owned project to be connected to the National Grid, and the turbines are locally known as the Three Dancing Ladies—Faith, Hope and Charity*” [10] (see Fig. 23.15).

It is important to be aware of these personal views and opinions with respect to seeing wind farms in the landscape. It is one of the most visible forms of renewable energy generation, as wind turbines are large, moving structures that have been put in prominent places seen by many people, while

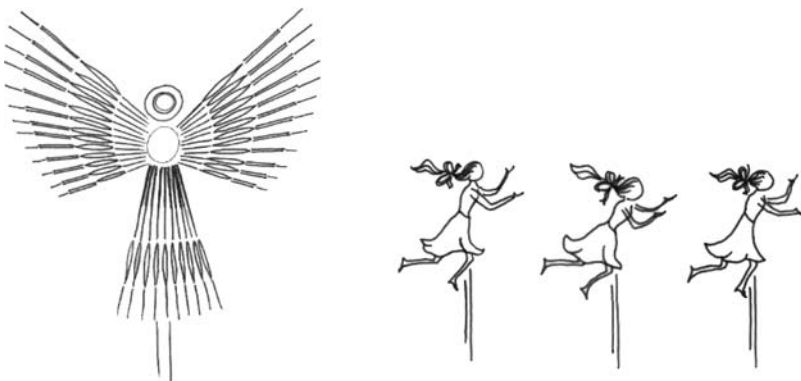


FIGURE 23.15 Turbines have been described as angels or dancing ladies. MVGLA.

other renewable energy technologies such as biomass plants, hydro schemes, and wave or tidal schemes are less visible and more infrequent. Wind farms can be seen from long distances, and are becoming sufficiently numerous that they are unavoidably noticeable in some parts of the world.

With the increase of the number of wind energy developments in our landscapes, people's views, especially of those opposed to this type of development, are increasingly vocal and planning decisions relating to wind power developments are increasingly adversarial. It is therefore important that landscape and visual impact assessments, which are undertaken as part of wind farm planning applications, remain professionally objective and neutral, and remain free from any potential personal opinion of the assessor. These assessments need to present an objective, well-reasoned and logical evaluation of the effects of the proposed wind farm in a particular landscape, and of the effects of the proposal on existing views and visual amenity.

If the proposal is granted consent, the introduction of wind turbines in any landscape will contribute to change in the character of the landscape. As said previously to some people this change is acceptable while others see wind farms as blight on the landscape. Assessments must recognize that opinions are varied and strong, and must present the facts and judgements in an unbiased way.

23.7 WHAT ARE THE EFFECTS OF WIND FARMS ON OUR LANDSCAPE?

Wind farms have a range of potential effects on our landscape, including direct effects on the site on which the turbines are built, effects on character and effects on views and visual amenity. It is common practice to evaluate the likely effect of wind energy proposals on our landscape by considering

effects on views and visual amenity distinct from effects on the landscape fabric and its character. These latter effects are called landscape effects.

23.7.1 Landscape Effects

Wind turbines alter the landscape by introducing large moving structures above ground level, as well as tracks and other infrastructure elements at ground level. Direct effects include the loss of existing land uses, such as arable or grazing land, forestry, etc. as a direct consequence of the construction of tracks, substation, and works compound turbine foundations and other physical components of the wind farm (see Figs. 23.16 and 23.17). The power from each turbine needs to be cabled to an on-site substation from where it is exported to the electricity transmission network, ground disturbance also occurs along buried grid connection routes. Track and cable route construction may involve the removal of features such as hedge or wall sections, and substations may need new screening planting. Wind farms on forested land commonly require complete or partial felling of plantations.

These changes directly affect features in the landscape at a local level, but can also affect landscape pattern. Landscapes with a simple pattern of rectilinear fields or open un-enclosed moorland can be greatly affected by meandering tracks that do not respond to field boundaries or other existing features. Other more complex landscapes may be able to accommodate the development better, but may also become overwhelmed by it.

While the ground level land take is small, and land uses can largely continue below the turbines (with the exception of forestry), the perception of the character of the landscape changes. An open, undisturbed moorland area would be altered to a wind energy generating site with areas of moorland between the tracks and turbines. The introduction of an industrial layer to the landscape is a greater change in some environments than in others. Lowland, settled landscapes where man-made features are more common, can potentially accommodate wind turbines with less perceived change to the character of the landscape compared with remote undisturbed landscapes. However, settled landscapes have more potential objectors living locally, and while remote landscapes often have better wind resources, they are also often more environmentally sensitive.

Commercial forest plantations are man-made land use areas, and are not as sensitive to development as open areas. However, forest trees causes turbulence above the canopy, which we understand adversely affects performance of the turbines. Because of this manufacturers recommend that there should be a significant clearance between the lowest point of the swept circle and the tops of the trees (see Fig. 23.18). This means that full grown forest trees are too tall to be allowed to grow below the turbines in most circumstances, and trees must be felled and the land left bare, or replanted trees must be felled early, before they grow too high. An alternative is to increase



FIGURE 23.16 Newly constructed tracks cause ground disturbance. *Photo: M van Grieken. Copyright © 2017 Marc van Grieken. Published by Elsevier Inc. All rights reserved.*



FIGURE 23.17 Tracks, transformers, and meteorological mast are visible infrastructure elements, Braes of Doune Wind farm, United Kingdom. *Photo: M van Grieken. Copyright © 2017 Marc van Grieken. Published by Elsevier Inc. All rights reserved.*

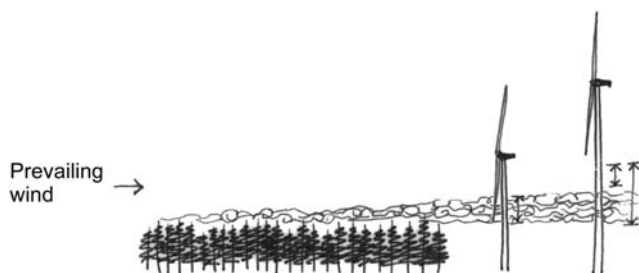


FIGURE 23.18 Trees cause turbulence that reduces yield. MVGLA.

tower heights to lift the rotors out of the affected zone, and to allow turbines to be constructed in small clearings called ‘key holes’ in retained forest plantations.

An important consideration when assessing effects on landscape is a perception of its character, and how the character of the landscape is affected or changed by introducing wind farms or turbines.

That turbines should ‘fit’ in the landscape has long been a recommendation with a view to minimizing landscape change. While turbines are in a similar height range to trees and buildings, it is possible to say that these can ‘fit’ in the landscape as features of similar scale to those existing. Turbines over 50–80 m to tip, however, can no longer be seen as fitting with other more human-scale elements. This is becoming more of an issue with turbines taller than 125 m and certainly with turbines up to 200 m. In many places turbines of this size will be perceived to be ‘out of character’ partly because we are unfamiliar with the size and height of these structures.

This poses unique challenges for the design of wind farms. It requires a different approach, recognizing that people find it hard to gauge the size of objects and may be overawed when they know the physical dimensions. Designing with structures of a height and size very much larger than trees or buildings requires an approach that recognizes that they should be designed to be viewed from afar as well as from nearby.

23.7.2 Visual Effects

Of interest to most people are the effects of wind farms on views and visual amenity. Visual effects of wind turbines relate to the appearance of the turbines, either as a single object or as a group of objects arranged as a wind farm, when seen from different places within the surrounding area. Key factors in the assessment of visual effects are number, size, scale and composition of the turbines in a view. The wind farm may be described with reference to the prominence of turbines in the view, and what role the wind farm would have within the view, perhaps as a new focal feature or as a peripheral element on the horizon. Description of the composition of a wind farm may include references to the group of turbines having a balanced appearance, and whether certain turbines appear separated off as ‘outliers’ from the main group when seen from certain angles. Visual effects are normally assessed from representative locations such as popular scenic viewpoints or places where people stop to admire the view, as well as from settlements and places where people congregate. The potentially eye-catching effect of a moving object such as the rotation of turbine blades means that turbines are more noticeable than still structures, and they may affect the sense of tranquility and stillness in remote landscapes. Conversely the movement of turbines close to urban areas or within industrial areas fits very well with the perception of busy urban landscapes.

23.7.3 Landscape and Visual Effects

Whilst landscape and visual effects tend to be assessed separately and considered as different aspects of introducing turbines in our landscape, there is a clear relationship between the two: visual influence of turbines in a certain landscape will have an effect on how people perceive its character, and the loss of landscape features, for example, the felling of woodland, clearly also has visual effects. This is also the case when considering potential effects on so-called ‘wild land.’ Wild land has been mapped in Scotland based on systematic evaluation of aspects and qualities such as remoteness, naturalness, absence of human influences (such as telecommunication masts, powerlines, commercial forest, etc.), and a sense of isolation. These areas of wild land are neither generally accessible nor accessed, so that few people would see a development, but they are wild because of the absence of human influence. The potential effects on wild land are therefore not only experienced by being there, but also by imagining the turbines in places where there are no other human artefacts or humans.

23.8 MITIGATION

It is not possible to avoid all adverse effects on landscape and visual amenity resulting from wind energy proposals, and all onshore and offshore wind energy developments visible from the land will have a number of adverse effects. In general wind farms are designed to try and minimize the extent and number of significant effects whilst optimizing the generation capacity.

The design of a wind farm is critical to the appearance of the wind farm and its relationship with the landscape it is in. Wind farms should be designed with heed to the overall appearance of the development and how it relates to the existing pattern of the landscape. Structures can be placed in a landscape in ways that either detract or enhance the landscape: referring again to the cooling towers of Didcot Power Station, Berkshire: “*The cooling towers were re-composed from the purely functional into the picturesque so agreeably that horror at their presence is mitigated by an appreciation of their grandeur – gigantic follies composed like gods in converse*” [4].

In large flat open and geometric landscapes, such as, for example, the Fens in England or the polders in the Netherlands, formal geometric compositions of turbines in lines or grid formation may be most appropriate in terms of ‘built-in’ mitigation (see Fig. 23.19). In a gently rolling uplands, a loose grouping may be more appropriate (see Fig. 23.20), whilst in a landscape comprising of ridges, it may be appropriate to follow the ridge lines.

It may be appropriate when designing a wind farm to ask the question as to what extent the proposed wind farm will induce landscape change, and whether this change will mean that the landscape crosses a threshold, perhaps from a ‘landscape with wind farms’ to a ‘wind farm landscape.’ If this



FIGURE 23.19 A geometric composition in a formal Dutch landscape. *Photo: M van Grieken.*
Copyright © 2017 Marc van Grieken. Published by Elsevier Inc. All rights reserved.



FIGURE 23.20 An informal layout in rolling upland, Clyde Wind farm, United Kingdom.
Photo: B Dower.

is the case the designer needs to decide whether or not the development should be contained to avoid crossing that threshold, or whether it could be enlarged in order to maximize energy yield, given that the landscape change is inevitable.

23.8.1 Strategic Approach

To date the approach to wind farm developments in the UK landscapes has been to minimize and limit landscape change, but this has led to subtle

erosion of landscape character in many landscapes, and a gradual, reluctant response to increases in turbine size. An alternative, more proactive approach might have been to allow more change in some areas, using larger turbines in larger scale landscapes and maximizing energy yield while minimizing the number of areas affected. With the existing, apparently haphazard, scattering of small groups of turbines with relatively small turbines across wide areas of the UK landscape, it is difficult to see a way forward toward a more coherent strategic approach. There may be opportunities in the medium term, however, when wind farms come to the end of their operational lives, to redesign new wind farms for the same sites, a process known as repowering. If repowering can be done with a proactive approach taking in the larger turbine sizes available at the time, and exchanging a number of smaller developments with fewer, larger, well-designed developments, the landscape and visual effects may be no more than before, and the energy yields will certainly be considerably higher.

It is interesting to note that in the municipality of Zuid Flevoland in the Netherlands, Westerwind Wind Park will comprise 100 new turbines with tip heights of up to 220 m, which will replace the current 220 turbines and generate 2.5 times the total amount of electricity [11].

In the longer term, it is possible that wind turbines are a temporary measure, and as technology develops, they might be phased out in favor of some other, more efficient form of renewable power generation. In 25–75 years it is possible that landscape architects will be designing new landscapes with new technologies, while taking out some of the wind farms. Perhaps the composition of these new structures could be the emphasis for design, rather than the avoidance of landscape and visual effects.

23.9 CONCLUSION

The landscape around us is a valued resource and changes to it evoke passionate responses. The only constant in a landscape is that it will change. Change is happening through natural processes, human processes, and as a result of our measures to combat climate change. Wind farms are renewable energy technologies that are changing our landscapes, affecting both views and the perceived character of the areas into which they are introduced. The number, size, and composition of turbines in wind farms are the key factors that influence the appearance of a wind farm in the landscape, and how it relates to its surroundings. The design of wind farms must take into account the nature of the receiving landscape and the potential effects that a proposal may have on the local area, as well as the technological requirements of the development as a power generating facility.

REFERENCES

- [1] Council of Europe. European landscape convention. Council of Europe; 2000.
- [2] Landscape Institute and the Institute of Environmental Management & Assessment. Guidelines for landscape and visual impact assessment. 3rd ed. London and New York: Routledge; 2013.
- [3] Swanwick C, Land Use Consultants. Landscape character assessment for England and Scotland. Cheltenham and Edinburgh: Countryside Agency and Scottish Natural Heritage; 2002.
- [4] Jellicoe G, Jellicoe S. The landscape of man, shaping the environment from prehistory to the present day. London: Thames and Hudson Ltd.; 1975.
- [5] United Nations. Kyoto Protocol to the United Nations framework convention on climate change; 1998.
- [6] RWE Innogy website. <<http://www.rwe.com/web/cms/en/248922/rwe-innogy/sites/wind-offshore/in-operation/thornton-bank/>>; 2016 [accessed 20.07.16].
- [7] Scottish Natural Heritage. Siting and designing wind farms in the landscape. Version 2; 2014.
- [8] Sir Bernard Ingham. Quoted in The Sunday Herald. April 7, 2002.
- [9] Jessica Dalgleish. Quoted in The Sunday Herald, April 7, 2002.
- [10] Sunday Herald. Gigha: God's island of growth. Published July 28, 2008 (accessed 08.06.16).
- [11] Zuid Flevoland Westerwind Wind Park website, <www.windparkzeewolde.nl>; 2016 [accessed 02.08.16].

This page intentionally left blank

Chapter 24

Global Rare Earth Supply, Life Cycle Assessment, and Wind Energy

Zhehan Weng^{1,2} and Gavin M. Mudd¹

¹*Monash University, Clayton, VIC, Australia*, ²*Ghent University, Ghent, Belgium*

Email: Zhehan.Weng@UGent.be

24.1 BACKGROUND OF RARE EARTH ELEMENTS

The rare earth elements (REE) are now considered as key elements for various emerging technologies. In the early stages of their discovery (by Arrhenius in 1787 at Ytterby in Sweden), the term “rare” originated from the belief that the only known source of these new elements was at Ytterby [1,2]. The term “earth” was an archaic reference to oxidic materials in the 19th century [3]—despite the fact they were metallic elements [4]. With scientific advancement in REE exploration and utilization, during the past two centuries, both the perceptions of REE’s geological scarcity and its chemical properties have proven to be obsolete. The International Union of Applied and Pure Chemistry (IUPAC) defines REEs as the group of 15 lanthanide elements plus scandium and yttrium (as shown in Fig. 24.1). In general Sc is not extracted, and so in this chapter we use the abbreviation of TREO+Y to highlight that our data is rare earth oxides plus yttrium only.

It is important to understand that, each REE has distinctive physical and chemical characteristics, and hence, different downstream uses. The term light rare earth elements (LREE; La to Gd) and heavy rare earth elements (HREE; Tb to Lu), defined by similar electron shell configurations, are commonly used to classify the lanthanide elements more accurately. Despite having a relatively small molecular weight, yttrium is typically classified as a HREE, and scandium is not formally classified as either a LREE or a HREE due to the lack of similarities to either group; yet, it is included with the REE as a whole.

Since the latter part of the 20th century the increasing demands for high-performance REE materials (see Fig. 24.2) in emerging technological

11-6206-1

FIGURE 24.1 Rare earth elements (REE) within the periodic table [5].**FIGURE 24.2** Rare earth elements (REE)-dependent technologies [6].

applications has altered the global REE demands. This is exemplified by the utilizations of REE “mischmetals” in the permanent magnet industry. Superior magnetic strength of the neodymium-iron-boron ($\text{Nd}_2\text{Fe}_{14}\text{B}$) magnet and the ability of the samarium cobalt (SmCo) magnet to retain the

magnetic characteristics even at elevated temperatures make them both essential components in precise weaponry systems, electric vehicles, and wind turbines [7,8].

However, the unique characteristics and the associated complexity of REE in the downstream applications often make them extremely difficult to recycle. Binnemans et al. [9] stated that, in 2011, less than 1% of REE were recycled. Finding substitutions for REE in most applications is also difficult, if not impossible [3,10–12]. For example, for NdFeB-based permanent magnets (generally regarded as the strongest permanent magnets yet discovered), the possible alternative for Nd is Pr, with a loss in magnetic strength. For Dy, there is no feasible alternative element to date [13,14]. As a result the continuous growth of REE-dependent technologies in conjunction with new discoveries of REE applications aimed at a low-carbon society will significantly increase the future global demands for REE [6,15,16].

24.2 GLOBAL REE SUPPLY

In global terms the REE are not “rare” from a geological abundance perspective—as some REE have a similar abundance to copper. Typical REE abundance in the Earth’s crust varies significantly. For example, Ce has an average crustal concentration of $63 \mu\text{mol mol}^{-1}$ (63 ppm), which is higher than several base metal elements such as copper (Cu, 28 ppm) and lead (Pb, 17 ppm), in the earth’s upper crust [17]. In comparison Tm and Lu have average upper crustal concentrations of 0.3 ppm and 0.31 ppm, respectively, which are much lower than the majority of other significant economic metals, but higher than gold (Au), silver (Ag), and the platinum (Pt) group elements [17]. Similar results of REE abundances have also been reported by Hoatson et al. [5].

From a production perspective, the REE are primarily produced as rare earth oxides, or more specifically, rare earth oxides plus yttrium (TREO+Y). Fig. 24.3 shows the historical TREO+Y production since 1950; the global production was dominated by monazite extraction until major weathered carbonatite projects came into production. The Mountain Pass Project ore body in California, United States was discovered in 1949 [21], and was the world’s largest REE supplier until the early 1990s. During the same period, REE-enriched bastnäsite extracted from Mountain Pass became the primary global source for TREO+Y [22–24]. Since the 1990s, largely due to the rapid rise of Bayan Obo in northern China, the global TREO+Y market has been dominated by Chinese production. In 2006 China’s annual production peaked at 133,000 t TREO+Y (where t refers to metric tonne), accounting for 97.1% of the global production that year. Since then the Chinese production has maintained its dominance. It also exemplifies the long-term supply risk inherent in having the global supply of the TREO+Y dependent on a single dominant supplier or country. As a result concern about the long-term

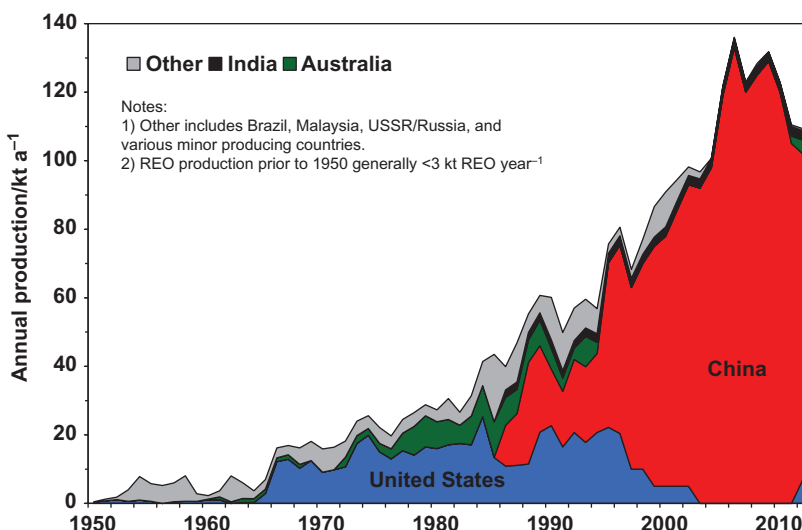


FIGURE 24.3 Global annual TREO+Y mine production. Data sources: USBoM. Mineral resources of the United States. Washington, DC: U.S. Bureau of Mines (USBoM); 1927–1934; USGS. Various minerals commodity summaries. Reston, VA: U.S. Geological Survey (USGS); 1997–2015 [18,19]; Australian TREO+Y based on monazite production data from BoMRGG. The Australian mineral industry review. ACT, Australia; Australia, Bureau of Mineral Resources, Geology and Geophysics (BoMRGG); 1960–1985 [20] and under the assumption of minimum 60% contained TREO+Y. Here “a” refers to annum.

TREO+Y supply has become a strategic issue for major consumers like the United States and the European Union (EU) [13,14,25–27].

Weng et al. [28] reported a minimum global TREO+Y mineral resource of 619.5×10^6 t (619.5 million tonnes) with average ore grade of 0.63%. In other words, there are abundant proven mineral resources hosted within a variety of different types of REE deposits, each of which has a diverse range of mineralogy. The study also suggests future global TREO+Y supply would shift from a few bastnäsite-based carbonatite mines toward a more diversified range of production from a range of differing geological types. Demands for certain essential REE (especially HREE)-dependent products or applications (e.g., wind turbine) should be fulfilled by targeting suitable deposits (e.g., HREE-enriched ionic clay deposits) with viable ore grades and implementing novel and site-specific mining, beneficiation and refining technologies, and plant configurations to optimize the production efficiency of the desired end products while minimizing environmental impacts.

24.3 REE PERMANENT MAGNETS

The NdFeB permanent magnet is the key functional component in modern wind turbine industry. It is used for making permanent magnet synchronous

generators (PMSG) and high temperature superconductors (HTS) [16,29,30]. The superior magnetic strength of NdFeB magnets, together with their special high induction and coercive force properties [31], has enabled the development and utilization of lighter and larger wind turbines with, greater aerodynamic efficiency, better reliability, and reduced maintenance requirements. As summarized by Wiser et al. [32], “the availability and cost of rare earth permanent magnets are expected to affect significantly the size and cost of future direct-drive generator designs” (pp. 580).

REE-dependent permanent magnets provide significantly better “maximum static energy product” capacity $BH_{(max)}$ compared to traditional aluminum-nickel-cobalt (Alnico) and ceramic (Ferrite) magnets (see Fig. 24.4). Given their superior magnetic strength (e.g., NdFeB magnet) and excellent resistance to demagnetization at elevated temperatures (SmCo magnet) REE permanent magnets have become essential components for various modern wind turbine designs and manufacturers [7,8].

Humphries [16] estimated the REE permanent magnet production is the single largest sector (approximately 20%) of global REE demands in 2010, and it was expected to grow by 10%–16% per year till 2015 (see Fig. 24.5). Lucas et al. [35] stated that wind turbine production uses about 10% of global annual permanent magnet supply.

Given the importance of REE in facilitating clean energy technologies to help with addressing climate change, it is clear that there is a need to examine the finer details underlying basis of the criticality of REE—especially potential supply rates to meet growing demands for a variety of specific technologies. As systematically summarized by numerous articles, governmental, and industrial reports: the design, generation capacity, and efficiency

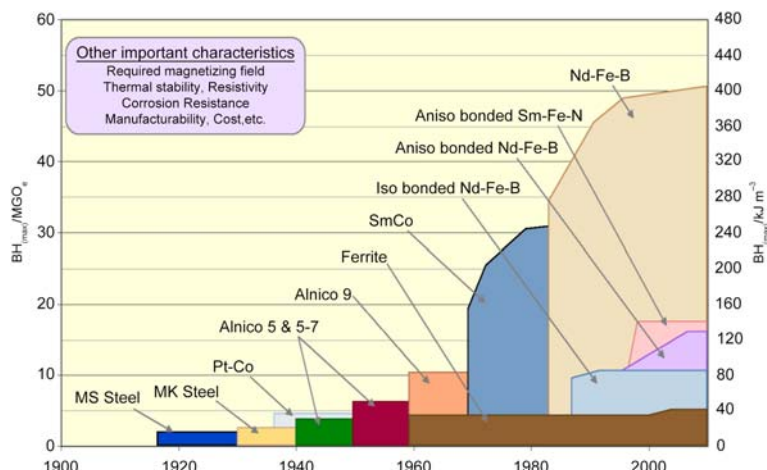


FIGURE 24.4 The development of permanent magnets [33,34].

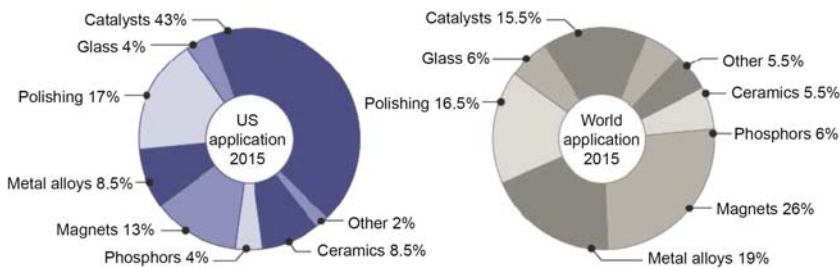


FIGURE 24.5 2015 REE demand estimate by application—United States and World [16].

of future wind energy plant will be dependent on the availability of REE permanent magnets, especially the neodymium-iron-boron (NdFeB) permanent magnet [29,32,35,36].

24.4 LIFE CYCLE ASSESSMENT OF THE USE OF REE MAGNETS IN WIND TURBINES

In this section we compare two life cycle assessments (LCA) between two onshore low–medium speed wind turbines; namely: Vestas V112 3~3.45 MW with a PMSG [37] and Vestas V126 3.3 MW with single-fed induction generator (SFIG) made of steel and copper [38], to demonstrate the importance of REE in wind turbine environmental footprints.

Table 24.1 summarizes the raw material breakdowns for each system. Compared to V126, the V112 turbine contains an additional 485 kg of NdFeB permanent magnet, 3 t of copper, and 6 t of polymer materials to achieve remarkable savings of 86 t of steel and iron materials (22%), 1 t aluminum (23%) and electronics (30%), 480 kg lubricants (27%), and 364 kg other unspecified material. However, the irreplaceability and complex recycling process of REE unavoidably impacts on the overall recyclability of PMSG wind turbines compared to other models which utilize more conventional (e.g., Alnico, Ferrite) magnets.

The overall life cycle impacts of a 100-MW wind plant (farm) (20 years life cycle) composed of 33 units of V112 or V126 are summarized in Table 24.2. Again comparing the V126 to V112, the V112 has much lower overall environmental profiles than the SFIG model in almost all impact categories, especially as related to human toxicity (54%), eutrophication (39%), and acidification (36%) potential. Moreover, a wind power plant is often considered as one of the crucial “clean energy” systems that reduce greenhouse gas (GHG) emissions. The global warming potential (GWP), measured in carbon dioxide emissions equivalent (CO₂e), is an essential indicator to demonstrate overall environmental polluting capacity. Under the same operating conditions (e.g., operating hours, wind speed, plant life cycle, etc.), a wind power plant involving Vestas V112 turbines has a 15% lower GHG

TABLE 24.1 Material Breakdowns for the Vestas V112 and V126 Wind Turbines [37,38]

Material Inputs Inventory	Units	V112	V126
Designed capacity	MW	3~3.45	3.3
Steel and iron materials	t	311	397
Aluminum and aluminum alloys	t	3.4	4.5
Copper	t	4.8	1.8
Copper alloys	kg	9.1	30
Polymer materials	t	21	15
Process polymers	kg	765	1 939
Other materials and material compounds	t	27	25
Electronics/electrics	t	2.4	3.4
Lubricants and liquids	t	1.3	1.8
Not specified	kg	N/A	364
REE permanent magnets	kg	485	N/A
Recyclability	%	81	89

Notes: Average material inputs for each wind turbine are adapted from total 33 units of each system installed in 100 MW wind plant. t, tonne

TABLE 24.2 Life Cycle Environmental Impacts for 100 MW Onshore Wind Power Plant [37,38]

Life Cycle Environmental Impacts	Units	V112	V126
Global warming potential (GWP)	gCO _{2e} (kW h) ⁻¹	7.0	8.2
Eutrophication potential (EP)	mg PO ₄ (kW h) ⁻¹	2.7	4.4
Human toxicity potential (HTP)	mg DCBe (kW h) ⁻¹	833	1 810
Acidification potential (AP)	mg SO _{2e} (kW h) ⁻¹	28	44

footprint than a plant involving V126 turbines kW h⁻¹ electricity generated. This comparison highlights the critical role that REE permanent magnets play in the wind turbine industry by significantly reducing the raw material requirements and improving the overall environmental performance.

The detailed Nd, Dy, and Tb mineral resources data and corresponding environmental impacts in the production stage have been adapted from Refs.

TABLE 24.3 Rare Earth Elements (REE) Composition of Medium-High and Low-Speed Permanent Magnet Synchronous Generators (PMSG) Wind Turbines

System	REE	Value/(kg MW ⁻¹)	Data Source
Medium-high speed PMSG (onshore wind turbine)	Nd	24	[14]
	Dy	2	[14]
	Tb	0.8	[41]
Low-speed PMSG (offshore wind turbine)	Nd	207	[14]
	Dy	18	[14]
	Tb	7	[41]

[28,39]; the NdFeB magnet production LCIA data adapted from Ref. [7]; and LCIA of onshore and offshore wind turbines are based on data from Ref. [40]. The REE composition inventory of medium-high and low-speed PMSG wind turbines is shown in Table 24.3.

Principal assumptions include:

- Typical life cycle period of a wind turbine is 25 years [42] with GWP as primary environmental impact indicator of this assessment.
- Medium-high speed PMSG is only utilized in onshore wind turbines.
- Low-speed PMSG is only utilized in offshore wind turbines.
- The average capacity factors (Ratio of wind turbine's actual power output and peak power output under 100% nameplate capacity for the same period of time) for both onshore and offshore PMSG wind turbine are estimated as 28% [43] while the maximum and the minimum capacity factor is calculated based on full load hours (FLH) for corresponding systems [42].
- Other metal demands of permanent magnet production (e.g., Fe, Cu, Ni, B, etc.) are assumed to be covered by existing LCA studies with environmental impacts and has been included as part of the wind turbine's overall environmental footprint.
- Environmental impacts of REE production and NdFeB magnet manufacturing characterizations and allocations are based on mass fractions of metal.

Table 24.4 shows the results of this LCA analysis. Regarding the GWP assessment, regardless of onshore or offshore wind turbine, the REE production, and magnet production only accounts for a negligible proportion of the total GWP footprint for a wind turbine. This is expected given that the impact characterizations are based on the mass fractions of each material, and the relatively small amount of REE material in each turbine (Table 24.3). Our

TABLE 24.4 Life Cycle Assessments (LCA) of Medium-High and Low-Speed Permanent Magnet Synchronous Generators (PMSG) Wind Turbines

System and Process		Maximum	Average	Minimum
		gCO _{2e} / (kWh) ⁻¹	gCO _{2e} / (kWh) ⁻¹	gCO _{2e} / (kWh) ⁻¹
Onshore PMSG medium-high	Nd production	2×10^{-3}	1×10^{-3}	1×10^{-3}
	Dy production	1×10^{-4}	9×10^{-5}	6×10^{-5}
	Tb production	1×10^{-5}	8×10^{-6}	6×10^{-6}
	Magnet production	0.040	0.037	0.040
	Entire system	45	15	3
Offshore PMSG low-speed	Nd production	1×10^{-2}	1×10^{-2}	9×10^{-3}
	Dy production	7×10^{-4}	7×10^{-4}	5×10^{-4}
	Tb production	7×10^{-5}	7×10^{-5}	4×10^{-5}
	Magnet production	0.23	0.29	0.29
	Entire system	23	12	7

assessment also suggests that the overall GWP footprint for electricity generated from both onshore and offshore wind farms are the lowest when compared to power plants based on other energy sources (Fig. 24.6).

Compared to medium-high speed PMSGs, which dominates the current wind turbine market, low-speed generators have a significant higher REE (i.e., Dy, Nd, Tb) amount per megawatt capacity, in exchange for lighter weight, better energy efficiency (or capacity factors), and lower GHG footprint. This is also seen in the lower average total GWP impact of low-speed PMSG as compared to the medium-high speed PMSG units. Broadly speaking, it is reasonable to believe that extrapolating GWP impacts from REE production and permanent magnet manufacturing processing, to future wind turbine production (especially for low-speed PMSG), the utilization of REE permanent magnets will not compromise but will enhance the systems overall GWP footprint. Hence REE permanent magnets will become even more important for future wind turbine designs and application, especially given that the market is shifting toward high capacity low-speed PMSG wind plants.

It is also worth mentioning that, due to lack of good quality data, current indicative LCA focus only on GWP impacts. The available data is insufficient to determine the overall environmental burden of global REE production. There is a broad range of other critical issues such as REE recovery

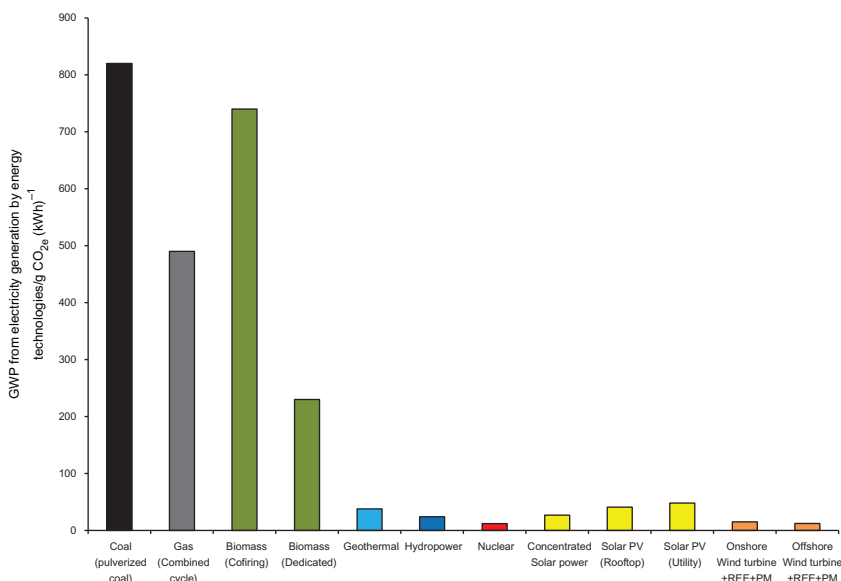


FIGURE 24.6 Emissions of selected electricity supply technologies. Notes: Average GWP impacts of other energy technologies are adapted from Schlömer S, Bruckner T, Fulton L, Hertwich E, McKinnon A, Perczyk D, et al. Annex III: technology-specific cost and performance parameters. In: Edenhofer O, Pichs-Madruga R, Sokona Y, Farahani E, Kadner S, Seyboth K, Adler A, Baum I, Brunner S, Eickemeier P, Kriemann B, Savolainen J, Schlömer S, von Stechow C, Zwickel T, Min JC, editors. Climate change 2014: mitigation of climate change. Contribution of working group III to the fifth assessment report of the intergovernmental panel on climate change. Cambridge, United Kingdom: Intergovernmental Panel on Climate Change (IPCC); 2014. p. 1331–1354.

efficiency, supply capacity, health concerns, acidification potential, and radiation exposure from hazardous by/coproducts (e.g., thorium and uranium, etc.), which should be addressed before making a conclusion on the overall impact of REEs with relevance to future sustainable energy systems.

Table 24.5 presents the environmental benefits related to Vestas V112 and V126 wind turbines. The obvious result suggests the applications of REE magnets in modern wind turbine systems provides greater environmental benefits for wind turbines compared to the associated environmental costs from REE mineral extraction and magnet production stages.

24.5 GLOBAL WIND ENERGY PROJECTIONS

The International Energy Agency (IEA) predicts the evolution of the global energy sector toward 2040 [44]. The projections are divided into three primary scenarios that assess key aspects: energy sources by regions and sectors; energy security and environmental protection; and economic

TABLE 24.5 Benefit Accounting Based on Vestas V112 and V126 Systems With Rare Earth Elements (REE) Production Stage Footprints [37–39,42]

System and Process	GWP Reduction/ mg CO _{2e} (kW h) ⁻¹
Nd production	-3.3
Dy production	-0.2
Tb production	-0.02
REE magnet production	-290
GWP benefit	+1200
Overall benefit	+906

development. The three core scenarios and their underlying assumptions about the evolution of energy-related government policies are summarized below:

- *The Current Policies Scenario (CPS)*: This scenario only considers existing energy policies for which implementing measures have been formally adopted as of mid-2015 and make the assumption that these policies persist unchanged until 2040.
- *The New Policies Scenario (NPS)*: In addition to incorporating the policies and measures that affect energy markets that have been adopted as of mid-2015, it also takes into account other relevant intentions that have been announced, even when the precise implementing measures have yet to be fully defined. This includes the energy-related components of the Intended Nationally Determined Contributions (INDCs), submitted by national governments by October 01, 2015 as pledges in the run-up to the United Nations Framework Convention on Climate Change Conference of the Parties (COP21). These policies include programmes to support renewable energy and improve energy efficiency, to promote alternative fuels and vehicles, carbon pricing, reform of energy subsidies, and the introduction, expansion or phase out of nuclear power. NPS is the moderate estimate of all three scenarios with considerations based on both existing and most likely developments for renewable energy growth.
- *The 450 Scenario (450S)*: The “450” scenario assumes a set of policies based on the trajectory of GHG emissions from the energy sector that is consistent with the international goal to limit the rise in the long-term average global temperature to 2°C, compared with preindustrial levels. The policies collectively ensure an emission trajectory consistent with stabilization of the GHG concentration after 2100 at around 450 ppm. Compared to the previous two scenarios, 450S provides the most optimistic projection for renewable energy growth.

All scenarios have predicted a rapid growth of the renewable energy sector toward 2040. For example, in the NPS scenario, with increasing policy support from governments, reducing production and implementation costs, and greater scale use of new technologies, the fraction of renewable energy in total global energy market is expected to rise from 14% in 2014 to 19% in 2040, with a total renewable power generation of $78,000 \times 10^{15}$ J (78,000 petajoules) in 2014 and 140,090 Mtoe (140,090 million tonnes of oil equivalent) in 2040 [44]. The electricity generations from renewable energy sources are projected to reach 13,429 TW h in 2040, with wind turbines expected to increase from 635 TW h in 2014 to 3568 TW h in 2040—an average 6.7% annual growth rate. The projected wind energy capacity requirements derived from all three scenarios are summarized in Fig. 24.7.

The substantial increase in global wind energy sector will require a corresponding growth in upstream REE-dependent component or material industries (e.g., NdFeB magnets) thus steering the economic drivers to increasing TREO+Y production over the coming decades along with other REE-dependent technologies.

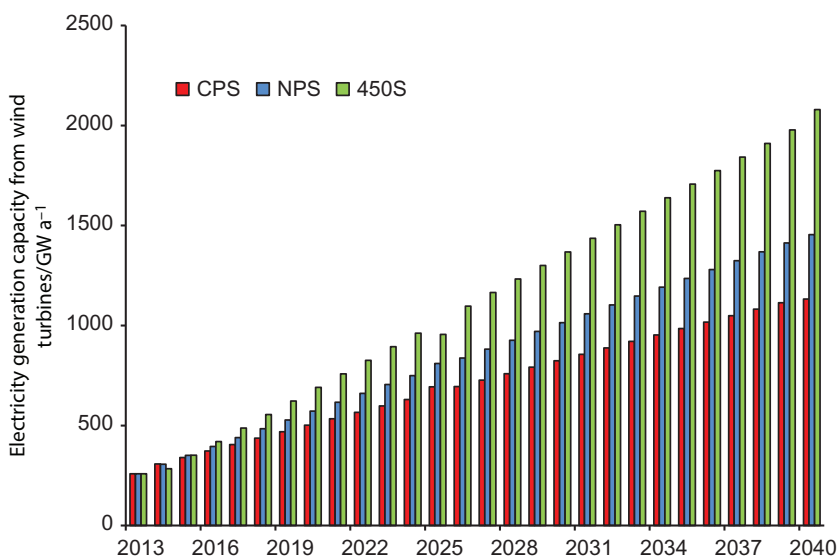


FIGURE 24.7 Projected wind energy capacity requirements to 2040. Notes: an Average capacity factor used in this assessment is 28% GWEC. Global wind energy outlook 2014. Brussel, Belgium: Global Wind Energy Council (GWEC); 2015a. p. 60 [43]; Annual electricity generation projection is adapted from IEA. IEA, World energy outlook 2015, International Energy Agency (IEA), Organisation for Economic Co-operation and Development (OCED), Paris, France, 2015; p. 718. © OECD/IEA 2015 World Energy Outlook, IEA Publishing.

24.6 IMPLICATIONS FOR FUTURE REE SUPPLY

The limited TREO+Y production capacity, China's monopoly position in REE processing, and commercial, geopolitical, and environmental supply risks, all contribute to the implication that insufficient long-term REE supply will be the most severe constraint for wind energy to meet projected demands. In order to provide a more reliable and robust assessment of wind energy growth and expected demand, this sector presents a quantitative analysis of intercorrelations between available mineral resources [28], TREO +Y production capacity [28,39], and projected REE demands from IEA's three wind energy scenarios (i.e., CPS, NPS, and 450S).

[Fig. 24.8](#) shows the expected growth of global wind-based electricity generation capacity and evolution toward PMSG wind turbines. As estimated by Moss et al. [14], electricity production from PMSG wind farms will account for 15% of European wind energy market and 20% global market in 2030. The European Wind Energy Association, EWEA, established an ambitious goal for global offshore wind energy of 4.3% of overall wind demand in 2020 [47]. This assessment uses the European wind energy targets based on the growth of various PMSG technologies (i.e., medium-high vs low-speed PMSG) as a benchmark for global wind energy evolution. The cumulative REE demands (2013–40) to meet these global energy targets are summarized in [Table 24.6](#).

Again as stated by Weng et al. [28], the geological scarcity of available mineral resources is not an immediate problem for wind energy development.

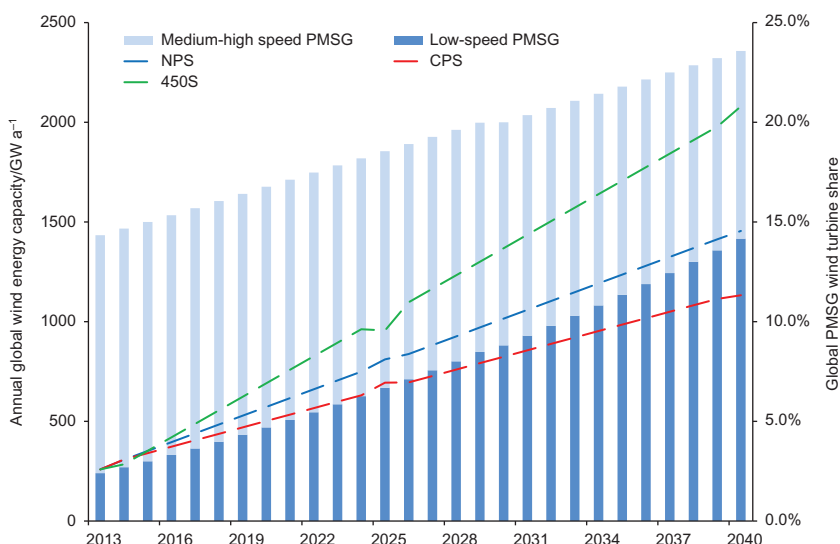


FIGURE 24.8 Projected global wind energy demands and permanent magnet synchronous generators (PMSG) share [13,44–46].

TABLE 24.6 Cumulative REE Demand (2013–40) Driven by Medium-High and Low-Speed Permanent Magnet Synchronous Generators (PMSC) Wind Turbines

REE	Wind Energy Scenario	Cumulative Demands/(kt)	Mineral Resources/(kt)
Dy	CPS	35	4 601
	NPS	44	
	450S	58.7	
Nd	CPS	419	72 821
	NPS	515	
	450S	692.6	
Tb	CPS	14	973
	NPS	17	
	450S	23.5	

This can be gauged by considering the most ‘rare’ REE in the group—Tb. The estimated quantity of Tb in the world is 973 kt, which is more than enough to satisfy the most optimistic Tb (23.5 kt) demands, even considering the 450S scenario. Nd is also widely considered as one of the most critically scarce REE, however, as given in Table 24.6, the total Nd demands (considering the 450S scenario) of 693 kt accounts for less than 0.1% of geologically available Nd. However, converting these geological resources into saleable commodities or functional materials will require complex mining, beneficiation, and refining processes. Hence, the real limitation is the annual REE production capacity instead of the REE geological scarcity.

Fig. 24.9 shows the projected annual TREO+Y production based on Tb demand in wind turbines. The projected Tb demand based on all three scenarios (CPS, NPS, and 450S) increases from 63 t in 2013 to 1208, 1552, and 2218 t in 2040, respectively. Corresponding annual production required to meet these demands have increased from 2.12×10^6 t (2.12 million tonnes) to 39×10^6 t, 50×10^6 t and 72×10^6 t TREO+Y, respectively, based on several key assumptions. These assumptions include: the average Tb proportion (0.11%) calculated from carbonatite REE deposits [28]; the average wind energy share (10%; [35]) of global REE permanent magnet market; and the permanent magnet share in global REE demand of 20% [16]. These assumptions were consistent throughout the modeling period (2013–14). According to Ref. [19], the reported annual global TREO+Y production is presently 110,000 t while the peak production occurred in 2006 with 137,000 t

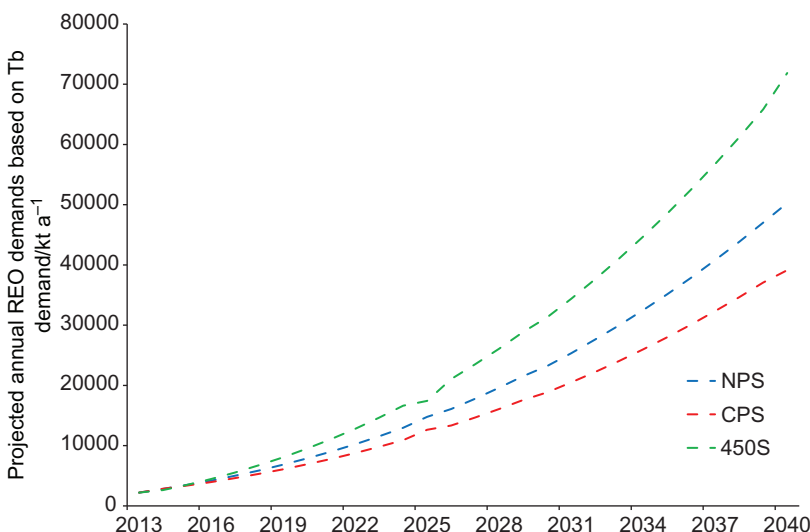


FIGURE 24.9 Projected annual REO production driven by estimated Tb demand.

produced; this being only 6% of the expected supply to meet Tb demands in 2013. The main explanation of such significant difference between expected and reported TREO+Y production is that current global HREE are derived mainly from southern China ionic clay projects instead of traditional carbonatite projects with a much higher average HREE concentrations.

24.7 CONCLUSION

The use of REE permanent magnets will not compromise but enhance the environmental footprint of wind turbines. Furthermore they lead to greater environmental benefits for the life cycle of wind turbines, which includes the associated environmental impacts from REE mineral production stages. Therefore REE permanent magnets as key functional components will become even more critical for future wind turbine design and applications, especially given the market shifting toward high capacity low-speed PMSG wind turbines.

However, as a global industry, the overall environmental impact from increasing REE production are still significant especially considering the exponentially increasing global REE demands driven by other emerging technological applications like electric vehicles (EV), photovoltaic (PV) thin films, and new sustainable system in future. Hence novel REE extraction, recovery, and diverse supply chain based on various REE mineralogy are needed to cope with expected demands. Also instead of the long-term availability of REE mineral resources, the short to medium term TREO+Y

production capacity and recovery efficiency are the main challenges for future REE supply.

Furthermore current global REE mineral resources are dominated by LREE instead of HREE (e.g. Dy, Tb, Er, etc.) with an average ratio of light rare earth element oxides (LREO) to heavy rare earth element oxides (HREO) of 13:1. The recent global REE supply has been dominated by the production of LREE-enriched bastnäsite-based carbonatite projects (e.g., Bayan Obo in China and the Mountain Pass in United States; the latter was shut down again in 2015). However, the predicted global REO consumption growth is mostly driven by increasing HREE (and particular LREE such as Eu, Nd) demands from the emerging and advanced technology sector. Therefore by simply increasing the production at the current carbonatite REE mines may result in an excess of LREE production while not being able to meet the demands for a particular HREE. As highlighted in Fig. 24.9, the expected Tb demands are simply too high based on traditional TREO+Y supply from bastnäsite-based carbonatite projects.

REFERENCES

- [1] Gschneider KA. 1787–1987 Two hundred years of rare earths, rare earth information center. IA: Iowa State University; 1987. p. 32.
- [2] Klinger JM. A historical geography of rare earth elements: from discovery to the atomic age. Extr Ind Soc 2015;2:572–80.
- [3] Zepf V. Chapter 1—an overview of the usefulness and strategic value of rare earth metals A2-Filho, Ismar Borges De LimaWalter Leal. Boston: Rare Earths Industry, Elsevier; 2016. p. 3–17.
- [4] IUPAC, Nomenclature of inorganic chemistry IUPAC recommendations 2005. International Union of Pure and Applied Chemistry (IUPAC). Zürich, Switzerland; 2005.
- [5] Hoatson DM, Jaireth S, Miezitis Y. The major rare earth element deposits of Australia: geological setting, exploration, and resources. , ACT, Australia: Geoscience Australia; 2011. p. 204.
- [6] USDoE. Critical mineral strategies. Washington, DC: U.S. Department of Energy; 2011. p. 189.
- [7] Sprecher B, Xiao Y, Walton A, Speight J, Harris R, Kleijn R, et al. Life cycle inventory of the production of rare earths and the subsequent production of NdFeB rare earth permanent magnets. Environ Sci Technol 2014;48:3951–8.
- [8] Zimmermann T, Gößling-Reisemann S. Critical materials and dissipative losses: a screening study. Sci Total Environ 2013;461–462:774–80.
- [9] Binnemans K, Jones PT. Perspectives for the recovery of rare earths from end-of-life fluorescent lamps. J Rare Earth 2014;32:195–200.
- [10] Graedel TE, Harper EM, Nassar NT, Nuss P, Reck BK. Criticality of metals and metalloids. Proc Natl Acad Sci U. S. A. 2015;112:4257–62.
- [11] Graedel TE, Harper EM, Nassar NT, Reck BK. On the materials basis of modern society. Proc Natl Acad Sci 2015;112:6295–300.
- [12] Habib K, Wenzel H. Exploring rare earths supply constraints for the emerging clean energy technologies and the role of recycling. J Cleaner Prod 2014;84:348–59.

- [13] Moss RL, Tzimas E, Kara H, Willis P, Kooroshy J. The potential risks from metals bottlenecks to the deployment of strategic energy technologies. *Energy Policy* 2013;55:556–64.
- [14] Moss RL, Tzimas E, Kara WP, Kooroshy J. Critical metals in strategic energy technologies. Luxembourg: European Commission Joint Research Centre; 2011. p. 161.
- [15] Hoenderdaal S, Espinoza LT, Marscheider-Weidemann F, Graus W. Can a dysprosium shortage threaten green energy technologies? *Energy* 2013;49:344–55.
- [16] Humphries M. Rare earth elements: the global supply chain. Washington, DC: U.S. Congressional Research Service; 2013. p. 27.
- [17] Rudnick RL, Gao S. Composition of the continental crust. In: Holland HD, Turekian KK, editors. *Treatise on geochemistry*, vol. 3. Oxford: Elsevier Pergamon; 2014. p. 1–64.
- [18] USBoM. Mineral resources of the United States. Washington, DC: U.S. Bureau of Mines (USBoM); 1927–34.
- [19] USGS. Various minerals commodity summaries. Reston, VA: U.S. Geological Survey (USGS); 1997–2015.
- [20] BoMRGG. The Australian mineral industry review. ACT, Australia: Australia, Bureau of Mineral Resources, Geology and Geophysics (BoMRGG); 1960–85.
- [21] Olson JC, Shawe DR, Pray LC, Sharp WN. Rare-earth mineral deposits of the mountain pass district, San Bernardino County, California. *Science* 1954;119:325–6.
- [22] Castor SB. The Mountain Pass rare earth carbonatite and associated ultrapotassic rocks, California. *Can Mineral* 2008;46:779–806.
- [23] Mariano AN, Mariano Jr A. Rare earth mining and exploration in North America. *Elements* 2012;8:369–76.
- [24] USEPA. Rare earth elements: a review of production, processing, recycling, and associated environmental issues. Washington, DC: U.S. Environmental Protection Agency (USEPA); 2012. p. 135.
- [25] Hayes-Labru L, Schillebeeckx SJD, Workman M, Shah N. Contrasting perspectives on China's rare earths policies: reframing the debate through a stakeholder lens. *Energy Policy* 2013;63:55–68.
- [26] Morrison WM, Tang R. China's rare earth industry and export regime: economic and trade implications for the United States. Washington, DC: U.S. Congressional Research Service; 2012. p. 17.
- [27] Wübbeke J. Rare earth elements in China: policies and narratives of reinventing an industry. *Res Policy* 2013;38:384–94.
- [28] Weng Z, Jowitt SM, Mudd GM, Nawshad H. A detailed assessment of global rare earth element resources: opportunities and challenges. *Econ Geol* 2015;110:1925–52.
- [29] Buchert M. Rare earths - a bottleneck for future wind turbine technologies? Berlin: Oeko-Institut e.V; 2011. p. 29.
- [30] Wang RJ, Gerber S. Magnetically geared wind generator technologies: Opportunities and challenges. *Appl Energy* 2014;136:817–26.
- [31] Dent PC. Rare earth elements and permanent magnets (invited). *J Appl Phys* 2012;111:7.
- [32] Wiser R, Yang Z, Hand M, Hohmeyer O, Infield D, Jensen PH, et al. Wind energy. In: Edenhofer O, Pichs-Madruga R, Sokona Y, Seyboth K, Matschoss P, Kadner S, Zwickel T, Eickemeier P, Hansen G, Schlömer S, von Stechow C, editors. *IPCC special report on renewable energy sources and climate change mitigation*. New York: Intergovernmental Panel on Climate Change (IPCC); 2011. p. 539–96.
- [33] Arnold. Market outlook for ferrite, rare earth and other permanent magnets. ARNOLD Magnetic Technologies (ARNOLD); 2016. p. 43. <http://www.magneticsmagazine.com/conferences/2016/Presentations/Arnold_Constantinides.pdf>.

- [34] Strnat KJ. Modern permanent magnets for applications in electro-technology. *Proc Inst Electr Electron Eng* 1990;78:923.
- [35] Lucas J, Lucas P, Le Mercier T, Rollat A, Davenport W. Chapter 14-Rare earth-based permanent magnets preparation and uses. Amsterdam, Netherland: Rare Earths, Elsevier; 2015. p. 231–49.
- [36] Tripathi SM, Tiwari AN, Singh D. Grid-integrated permanent magnet synchronous generator based wind energy conversion systems: a technology review. *Renewable Sustainable Energy Rev* 2015;51:1288–305.
- [37] D'Souza N, Gbegbaje-Das E, Shonfield P. Life cycle assessment of electricity production from a V112 Turbine Wind Park. Randers, Denmark: Vestas Wind Systems A/S (Vestas); 2011. p. 87.
- [38] Garrett P, Rønde K. Life cycle assessment of electricity production from an onshore V126-3.3 MW wind plant. Aarhus, Denmark: Vestas Wind System A/S; 2014. p. 116.
- [39] Weng Z, Nawshad H, Mudd GM, Jowitt SM. Assessing energy and global warming potentials of rare earth production. *J Cleaner Prod* 2016;139:1282–97.
- [40] Dolan S, Heath G. Life cycle greenhouse gas emissions of utility-scale wind power: systematic review and harmonization. *J Ind Ecol* 2012;16(S1):136–54.
- [41] Öhrlund I. Future metal demand from photovoltaic cells and wind turbines. Brussels, Belgium: European Parliament Science and Technology Options Assessment (EPSTOA); 2011. p. 72.
- [42] Schlämer S, Bruckner T, Fulton L, Hertwich E, McKinnon A, Perczyk D, et al. Annex III: technology-specific cost and performance parameters. In: Edenhofer O, Pichs-Madruga R, Sokona Y, Farahani E, Kadner S, Seyboth K, Adler A, Baum I, Brunner S, Eickemeier P, Kriemann B, Savolainen J, Schlämer S, von Stechow C, Zwickel T, Min JC, editors. Climate change 2014: mitigation of climate change. Contribution of working group III to the fifth assessment report of the intergovernmental panel on climate change. Cambridge, United Kingdom: Intergovernmental Panel on Climate Change (IPCC); 2014. p. 1331–54.
- [43] GWEC. Global wind energy outlook 2014. Brussel, Belgium: Global Wind Energy Council (GWEC); 2015. p. 60.
- [44] IEA, World energy outlook. International Energy Agency (IEA). Paris, France: Organisation for Economic Co-operation and Development (OCED); 2015. p. 718.
- [45] EWEA. The European offshore wind industry-key trends and statistics 2014. European Wind Energy Association (EWEA); 2015. p. 25.
- [46] GWEC. Global wind report annual market update 2014. Brussel, Belgium: Global Wind Energy Council (GWEC); 2015. p. 80.
- [47] EWEA. Pure power wind energy targets for 2020 and 2030-a report by the European Wind Energy Association-2009 update. Stockholm, Sweden: European Wind Energy Association (EWEA); 2009. p. 78.

Part VI

Financial Modeling/Wind Economics

This page intentionally left blank

Chapter 25

Economics of Wind Power Generation

Magdi Ragheb

University of Illinois at Urbana-Champaign, Urbana, IL, United States

Email: mragheb@illinois.edu

Everything on Earth belongs to princes, except the wind.

Victor Hugo, French author

25.1 INTRODUCTION

Wind energy capital costs have declined steadily. A typical cost for a typical onshore wind farm has reached around $\$1000 \text{ kW}^{-1}$ of installed rated capacity, and for offshore wind farms about $\$1600 \text{ kW}^{-1}$. The corresponding electricity costs vary due to wind speed variations, locations, and different institutional frameworks in different countries [1].

A symbiotic relationship is emerging between agricultural farming and electrical wind farming in the American Midwest. Landowners obtain attractive royalties from the installation of wind turbines on their land while continuing to farm around them; much like ranchers obtain royalties from oil and gas wells drilled on their cattle grazing properties. Each turbine uses an area of about 1–1.6 ha (2.5–4 acres) including the electrical cabling and access roads, while paying a royalty in the range of \$5000–10000 per year per installed turbine. Small businesses with wind turbines installations can extract energy from the electrical grid, overcoming the intermittence property of the wind, and its surplus production; if not stored, can be wheeled into the electrical grid (Fig. 25.1).

25.2 ECONOMIC CONSIDERATIONS

A driver behind the growth in wind energy investment is the falling cost of wind-produced electricity. The cost of generating electricity from



FIGURE 25.1 Single wind turbine providing power to a small business, despite the availability of an electrical grid supply at Rochester, New York: Harbeck Plastics, Inc. It can extract energy from the grid, overcoming the intermittence of the wind and its surplus production; if not stored, can be wheeled into the electrical grid. *Courtesy Chris Kabureck.*



FIGURE 25.2 Radio towers with two anemometers for wind measurements installed at highest point in Champaign County, IL, United States. *Courtesy Paul Lenz.*

utility-scale wind systems has dropped by more than 80%. When large-scale wind farms were first set up in the early 1980s, wind energy was costing as much as $\$0.30 \text{ (kW h)}^{-1}$ (30 cents per kilowatt-hour). New installations in the most favorable locations can produce electricity at less than $\$0.05 \text{ (kW h)}^{-1}$, which is competitive to other energy sources (Fig. 25.2).

Fossil fuels such as petroleum, coal, and natural gas prices are helping to make wind power generation competitive. Even where wind power is still not able to compete head-on with cheaper power sources in some locations, it is getting close.

Continued investment will depend on whether energy prices of other sources will stay high. Developers of wind power installations are looking at a 20-year investment span. If natural gas prices fall over that period, a project that is now profitable could become uncompetitive a few years into the future. The growth is driven by tax incentives, utility demand, falling costs, and improved technology, including taller towers and lighter rotor blades [2, 3].

25.3 WIND ENERGY COST ANALYSIS

In generation technologies, the cost of electricity is primarily affected by three main components:

1. Capital and investment cost
2. Operation and maintenance (O&M) cost
3. Fuel cost.

Wind power generation benefits from a fuel cost of zero. Studies of the cost of wind energy and other renewable energy sources could become unreliable because of a lack of understanding of both the technology and the economics involved. Misleading comparisons of costs of different energy technologies are common. The cost of electricity in wind power generation includes the following components:

1. Economic depreciation of the capital equipment
2. Interest paid on the borrowed capital
3. The operation and maintenance cost
4. Taxes paid to local and federal authorities
5. Government incentives and tax credits
6. Royalties paid to landowners
7. Payment for electricity used on a standby mode
8. Energy storage components, if used.

25.4 LEVELIZED COST OF ELECTRICITY

The levelized cost of electricity (LCOE) in electrical energy production can be defined as the present value of the price of the produced electrical energy (usually expressed in units of cents per kilowatt hour), considering the economic life of the plant and the costs incurred in the construction, operation and maintenance, and the fuel costs.

The fuel cost is zero in wind power generation, and the wind turbine is factory-assembled and directly delivered to the wind park site, resulting in a short construction time, t . This results in the following form for the LCOE for wind power generation, accounting for the intermittence factor IF, the production tax credit, PTC _{t} , the depreciation credit D_t , the tax levy T_t , and the royalties or land payments R_t :

$$\text{LCOE}_{\text{wind}} = \frac{\sum_{t=1}^n (I_t + O\&M_t - \text{PTC}_t - D_t + T_t + R_t) \frac{1}{(1+i)^t}}{\text{IF} \sum_{t=0}^{t=n-1} P_t} \quad (25.1)$$

where

$\text{LCOE}_{\text{wind}}$	= Generation [cost cents (kW h) ⁻¹]
I_t	= Investment made in year t [\$]
$O\&M_t$	= Operation and maintenance in year t [\$]
PTC_t	= Production tax credit [\$]
D_t	= Depreciation credit [\$]
T_t	= Tax levy [\$]
R_t	= Royalties or land rents [\$]
IF	= Intermittence factor
P_t	= Electrical generation capacity in year t [kW h]
G_t	= Electrical energy generation in year t [kW h], $G_t = \text{IF} \times P_t$
n	= Duration of the generation period [years]
i	= Discount rate

The present value factor (PVF) is:

$$\text{PVF} = \frac{1}{(1+i)^t} \quad (25.2)$$

The LCOE is estimated over the lifetime of the energy-generating technology, typically 20 years for wind generators. The discount rate (i) is chosen depending on the cost and the source of the available capital, considering a balance between equity and debt financing and an estimate of the financial risks entailed by the project.

25.5 NET PRESENT VALUE

It is advisable to consider the effect of inflation, and consequently using the real interest rate r instead of just i . The net present value of a project is the value of all payments, discounted back to the beginning of the investment.

For its estimation, the real rate of interest r defined as the sum of the discount rate i and the inflation rate s :

$$\begin{aligned}\text{Real rate of interest} &= \text{Discount rate} + \text{Inflation rate} \\ r &= i + s\end{aligned}\quad (25.3)$$

should be used to evaluate the future income and expenditures.

If the net present value is positive, the project has a real rate of return which is larger than the real rate of interest r . If the net present value is negative, the project has an unsustainable rate of return. The net present value is computed by taking the first yearly payment and dividing it by $(1 + r)$. The next payment is then divided by $(1 + r)^2$, the third payment by $(1 + r)^3$, and the n th payment by $(1 + r)^n$. Those terms are added together to the initial investment to estimate the net present value:

$$\text{Net present value} = \frac{P_1}{(1+r)^1} + \frac{P_2}{(1+r)^2} + \cdots + \frac{P_n}{(1+r)^n} \quad (25.4)$$

The electricity cost per kilowatt hour is calculated by first estimating the sum of the total investment and the discounted value of operation and maintenance costs in all years. The income from the electricity sales is subtracted from all nonzero amounts of payments at each year of the project period.

Depreciation is used in accounting, economics, and finance to spread the cost of an asset over the span of its productive life span. Depreciation is the reduction in the value of an asset or good due to usage, passage of time, wear and tear, technological outdated or obsolescence, depletion, inadequacy, rot, rust, decay, or other similar factors. Tax depreciation or accounting depreciation is sometimes confused with economic depreciation.

25.6 STRAIGHT LINE DEPRECIATION

Straight line depreciation is the simplest and most often used method in which we can estimate the real value of the asset at the end of the period during which it will be used to generate revenues, or its economic life. It will expense a portion of the original cost in equal increments over the period. The real value is an estimate of the value of the asset or good at the time it will be replaced, sold, or disposed of. It may be zero or even negative. Accordingly:

$$\text{Annual depreciation expense} = \frac{\text{Original cost} - \text{Real value}}{\text{Life span}} \left[\frac{\$}{a} \right] \quad (25.5)$$

where a refers to annum or year.

25.7 PRICE AND COST CONCEPTS

The words “cost” and “price” are sometimes mistakenly used as synonyms. The price of a product is determined by supply and demand for the product. Some people assume that the price of a product is somehow a result of adding a normal or reasonable profit to a cost, which is not necessarily the case unless it is applied to a government-managed monopoly. A factor that is a function of the scarcity of wind resources at a given location, as well as the taxes paid, could be accounted for; thus:

$$\begin{aligned} \text{Price} = & \text{Capital cost} + \text{Profit} + \text{Taxes} + \text{Installation cost} + \text{Fuel} + O\&M \\ & - \text{Government incentives and tax credits} \\ & + f(\text{scarcity}) \end{aligned} \quad (25.6)$$

25.8 WIND TURBINES PRICES

Wind turbine prices may vary due to the transportation costs, different tower heights, rotor diameters, generators capacities, and the grid connection costs. Some of the manufacturers’ deliveries are complete turnkey projects including planning, turbine nacelles, rotor blades, towers, foundations, transformers, switchgear, and other installation costs including road building and power lines. The manufacturer sales figures also include service and sales of spare parts.

The manufacturers’ sales include licensing income, but the corresponding rated power in units of megawatts is not registered in the company’s accounts. Sales may vary significantly between markets for high-wind resources turbines and low-wind resources turbines. The prices of different types of turbines are different. The patterns of sales, types of turbines, and types of contracts vary significantly from year to year and depend on the different locations and markets. A reasonable approach is to obtain the prices from the price lists and to consider the price in units of dollars per square meter of rotor swept area.

The operation and maintenance cost can be estimated as either a fixed amount per year or a percentage of the cost of the turbine. This could also include a service contract with the wind turbine manufacturer.

25.9 INTERMITTENCE FACTOR

The intermittence factor (IF), similar to the capacity factor (CF) for an energy-generating technology is equal to the ratio of the actual annual energy production to the rated maximum energy production, if the generator were running at its rated electrical power all year.

$$IF = \frac{\text{Actual annual energy production}}{\text{Rated maximum energy production}} \quad (25.7)$$

Depending on the wind statistics for a particular site, the practical intermittence factor for an onshore wind turbine is in the range of 25%–40%.

25.10 LAND RENTS, ROYALTIES, AND PROJECT PROFITABILITY

In wind energy production, the land rents or royalties depend on the profitability of a project and not vice versa.

$$\text{Royalties} = f(\text{Profitability}) \quad (25.8)$$

The compensation, land rents, or royalties paid to landowners where the turbines are located is sometimes treated as a cost of wind energy. In fact, it is only a minor share of the compensation which is a cost of the loss of crop on the area that can no longer be farmed; a possible nuisance compensation since the farmer has to make extra turns when plowing the fields underneath the wind turbines and he must be compensated for soil compaction and the damage to tiling from the heavy equipment access to the turbine site.

If the compensation exceeds what is paid to install a power line tower, the excess is an income transfer. It is not a cost to society, but is a transfer of income or profits from the wind turbine operator to the landowner. Such a profit transfer is called a land rent by economists. A rent payment does not transfer real resources from one use to another.

There is no standard compensation for placing a wind turbine on agricultural land. It depends on the quality of the site, the availability of the wind, and the grid access nearby. A landowner can bargain for a high compensation in a good location, since the turbine operator can afford to pay it due to the profitability of the site. If the site has low wind speed, and high installation costs, the compensation will be estimated closer to the nuisance value of the turbine.

25.11 PROJECT LIFETIME

The figure used for the design lifetime of a typical wind turbine is 20 years. It used to be a 30-year lifetime. With the low turbulence of offshore wind conditions leading to lower vibrations and fatigue stresses, it is likely that the turbines can last longer, from 25 to 30 years, provided that corrosion from salty conditions can be controlled. Offshore foundations for oil installations are designed to last 50 years, and it may be possible to consider two generations of turbines to be built on the same foundations, with an overhaul repair at the midlife point after 25 years.

25.12 BENCHMARK WIND TURBINE PRESENT VALUE COST ANALYSIS

An attempt is made at the estimation of a present value cost analysis for the cost of electricity over 20 years' turbine project duration. A benchmark problem is first presented that could be later modified to accommodate other factors, such as the PTC, depreciation, and taxes [8].

25.12.1 Investment

Expected lifetime = 20 a.

Turbine rated power: 600 kW.

Turbine cost: \$450 000

Installation costs: 30% of turbine price = $\$450\ 000 \times 0.30 = \$135\ 000$

Total turbine cost = Turbine cost + Installation cost

$$\begin{aligned} &= \$450\ 000 + \$135\ 000 \\ &= \$585\ 000 \end{aligned}$$

25.12.2 Payments

The payments, including the initial payment, are used to calculate the net present value and the real rate of return over 20 years' project lifetime since this is the main economic aspect of the analysis. The tax payments and credits and the depreciation credits are not considered for simplification but could be added for a more detailed analysis later. We consider that the capital is in the form of available invested funds: if the capital cost is all borrowed funds, then the interest payment on the loan or the bonds must be accounted for.

Operation and maintenance: 1.5% of turbine price = $0.015 \times 450\ 000 = 6750 [\$/a]$.

Total expenditure = Total turbine cost + Operation and maintenance cost over expected lifetime

$$\begin{aligned} &= \$585\ 000 + \$6\ 750/a \times 20/a \\ &= \$585\ 000 + \$135\ 000 \\ &= \$720\ 000 \end{aligned}$$

25.12.3 Current Income and Expenditures per Year

Intermittence factor: 28.54% = 0.2854.

Energy produced in a year: $600 \times 365 \times 24 \times 0.2854 = 1\ 500\ 000 \text{ kW h a}^{-1}$.

Price of electricity = \$0.05 kW h⁻¹.

Gross yearly income from electricity sale: $1\ 500\ 000 \text{ kW h a}^{-1}$ at $\$0.05 \text{ (kW h)}^{-1} = 1\ 500\ 000 \times 0.05 = \$75\ 000 \text{ a}^{-1}$.

Net income stream per year: $\$75\ 000 - \$6750 = \$68\ 250 \text{ a}^{-1}$.

One can construct Table 25.1 over the 20 years' useful lifetime of the turbine.

TABLE 25.1 Benchmark Present Value Calculation for a 0.6 MW Rated Power Wind Turbine

Number of Years	Expenditures/\$	Gross Income Stream/\$	Net Income Stream/\$	Present Value Factor $1/(1 + r)^n$ $r = 0.05$	Net Present Value of Income Stream/\$
0	− 585 000	—	—	—	—
1	− 6 750	75 000	68 250	0.9524	65 000
2	− 6 750	75 000	68 250	0.9070	61 903
3	− 6 750	75 000	68 250	0.8638	58 957
4	− 6 750	75 000	68 250	0.8227	56 149
5	− 6 750	75 000	68 250	0.7835	53 475
6	− 6 750	75 000	68 250	0.7462	50 929
7	− 6 750	75 000	68 250	0.7107	48 504
8	− 6 750	75 000	68 250	0.6768	46 194
9	− 6 750	75 000	68 250	0.6446	43 995
10	− 6 750	75 000	68 250	0.6139	41 899
11	− 6 750	75 000	68 250	0.5847	39 904
12	− 6 750	75 000	68 250	0.5568	38 004
13	− 6 750	75 000	68 250	0.5303	36 194
14	− 6 750	75 000	68 250	0.5051	34 471
15	− 6 750	75 000	68 250	0.4810	32 829
16	− 6 750	75 000	68 250	0.4581	31 266
17	− 6 750	75 000	68 250	0.4363	29 777
18	− 6 750	75 000	68 250	0.4155	28 359
19	− 6 750	75 000	68 250	0.3957	27 009
20	− 6 750	75 000	68 250	0.3769	25 723
Total	− 720 000	1 500 000	1 365 000	—	850 531.5

From the table the net present value of income stream at $r = 5\% \text{ a}^{-1}$ real rate of interest: \$850 531.5.

$$\begin{aligned}\text{Yearly net real rate of return} &= \frac{\text{Net present value of income stream}}{\text{Total turbine cost}} \cdot \frac{1}{\text{Project lifetime}} \\ &= (\$850\,531/\$585\,000)/20 \text{ a} \\ &= 0.072695 \\ &= 7.27\% \text{ a}^{-1}\end{aligned}$$

$$\begin{aligned}\text{Present value of electricity per kW h} &= \frac{\text{Net present value of income stream}}{\text{Yearly energy production} \cdot \text{Project lifetime}} \\ &= \$0.02835/\text{kW h} \\ &= 2.84 \text{ cents/kW h}\end{aligned}$$

25.13 INCENTIVES AND SUBSIDIES

25.13.1 Production Tax Credit (PTC)

In a measure taken by the US Congress a federal policy for promoting the development of renewable energy was initiated. The PTC provided initially a $\$0.015 \text{ kW h}^{-1}$ (1.5 cents per kilowatt-hour) benefit for the first 10 years of a renewable energy facility's operation. Originally enacted in 1992 the PTC has been renewed and expanded numerous times (Fig. 25.3). The USA FY16 Omnibus Appropriation Bill included a 5-year extension and phase-down of the PTC and the option to elect the Investment Tax Credit (ITC) for wind energy. The tax credits, extended through 2019, are phased-down by 20 percent each year beginning in 2017.

25.13.2 Investment Tax Credit (ITC)

Renewable energy facilities placed in service after 2008 and commencing construction prior to 2015 (or 2020 for wind facilities) may elect to make an irrevocable election to claim the investment tax credit (ITC) in lieu of the PTC. Projects that began construction in 2015 and 2016 are eligible for a full 30 percent ITC, for 2017 a 24 percent, for 2018 an 18 percent, and for 2019 a 12 percent ITC. Wind facilities making such an election will have the ITC amount reduced by the same phase-down specified above for facilities commencing construction in 2017, 2018, or 2019. The Consolidated Appropriations Act 2016 (H.R. 2029 Section 301) extended both the PTC and permission for PTC-eligible facilities to claim the ITC in lieu of the PTC through the end of 2016 (and the end of 2019 for wind facilities) (Fig. 25.3).

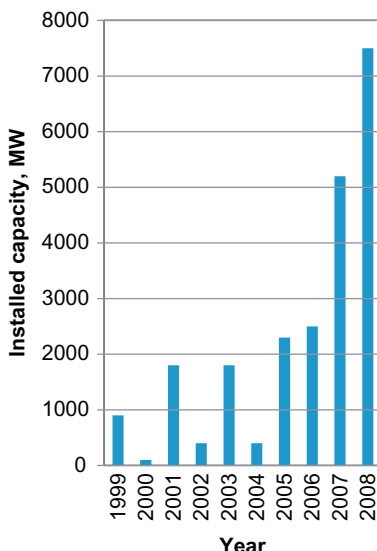


FIGURE 25.3 The effect of the PTC on the installed wind power capacity in the United States. A 93%, 73%, and 77% drops occurred in 2000, 2002, and 2004, respectively, upon temporary expiration then restarting of PTC. *Source: American Wind Energy Association (AWEA).*

25.13.3 Renewable Energy Production Incentive (REPI)

An incentive similar to the PTC is made available to public utilities, which do not pay taxes and therefore cannot benefit from a tax credit. The incentive is called the renewable energy production incentive (REPI) and it consists of a direct payment to a public utility installing a wind plant that is equal to the PTC at $\$0.015 \text{ kW h}^{-1}$ (1.5 cents per kilowatt-hour) adjusted for inflation. Since the REPI involves the actual spending of federal funds, money must be “appropriated” or voted for it annually by the US Congress. It is sometimes difficult to obtain full funding for REPI because of competing federal spending priorities.

The American Wind Energy Association (AWEA) estimates that the investment in renewable systems could fall by as much as 50% without the PTC in place. This would wreak havoc with the energy investment cycle and all but shut many projects down. Losing the PTC would strangle the vendor base disrupt the work force and curtail future output.

Combined with a growing number of states that have adopted renewable electricity standards, the PTC has been a major driver of wind power development over the last years. Unfortunately the “on-again/off-again” status that has historically been associated with the PTC contributes to a boom-bust cycle of development that plagues the wind industry. The cycle begins with the wind industry experiencing strong growth in development around the

country during the years leading up to the PTC's expiration. Lapses in the PTC then cause a dramatic slowdown in the implementation of planned wind projects. When the PTC is restored the wind power industry takes time to regain its footing and then experiences strong growth until the tax credits expire.

Extending the PTC allows the wind industry to continue building on previous years' momentum but it is insufficient for sustaining the long-term growth of renewable energy. The planning and permitting process for new wind facilities can take up to 2 years or longer to complete. As a result many renewable energy developers that depend on the PTC to improve a facility's cost effectiveness may hesitate to start a new project due to the uncertainty that the credit will still be available to them when the project is completed.

25.14 WIND TURBINE PRESENT VALUE COST ANALYSIS ACCOUNTING FOR THE PTC

We modify the calculation scheme for the benchmark problem to study the effect of the PTC on the present value of the produced electrical energy.

25.14.1 Payments

Installation costs: 30% of turbine price = $\$45\,000 \times 0.30 = \$135\,000$.

Total turbine cost = Turbine cost + Installation cost.

$$\begin{aligned} &= \$450\,000 + \$135\,000 \\ &= \$585\,000 \end{aligned}$$

Operation and maintenance: 1.5% of turbine price = $\$0.015 \times 450\,000 = \6750 a^{-1} .

Total expenditure = Total turbine cost + Operation and maintenance cost over expected lifetime.

$$\begin{aligned} &= \$585\,000 + \$6\,750\text{ a}^{-1} \times 20\text{ a} \\ &= \$585\,000 + \$135\,000 \\ &= \$720\,000 \end{aligned}$$

25.14.2 Current Income and Expenditures per Year

Intermittence factor (28.54%) = 0.2854.

Energy produced in a year: $600 \times 365 \times 24 \times 0.2854 = 1\,500\,000\text{ kW h a}^{-1}$.

Gross yearly income from electricity sale: $1\,500\,000\text{ kW h a}^{-1}$ at $\$0.05\text{ (kW h)}^{-1} = 1\,500\,000 \times 0.05 = \$75\,000\text{ a}^{-1}$.

Yearly income from PTC of 1.5 cents $(\text{kW h})^{-1} = 1\,500\,000 \times 0.015 = \$22\,500\text{ a}^{-1}$ (over first 10 years of project).

TABLE 25.2 Benchmark Present Value Calculation for a 0.6 MW Rated Power Wind Turbine Accounting for the PTC Incentive

Year n	Expenditures/\$	Gross Income Stream/\$	PTC/\$	Net Income Stream/\$	Present Value Factor $1/(1 + r)^n$ $r = 0.05$	Net Present Value of Income Stream/\$
0	− 585 000	−	−	−	−	−
1	− 6 750	75 000	22 500	90 750	0.9524	86 430
2	− 6 750	75 000	22 500	90 750	0.9070	82 310
3	− 6 750	75 000	22 500	90 750	0.8638	78 390
4	− 6 750	75 000	22 500	90 750	0.8227	74 660
5	− 6 750	75 000	22 500	90 750	0.7835	71 103
6	− 6 750	75 000	22 500	90 750	0.7462	67 718
7	− 6 750	75 000	22 500	90 750	0.7107	64 496
8	− 6 750	75 000	22 500	90 750	0.6768	61 420
9	− 6 750	75 000	22 500	90 750	0.6446	58 497
10	− 6 750	75 000	22 500	90 750	0.6139	55 711
11	− 6 750	75 000	−	68 250	0.5847	39 904
12	− 6 750	75 000	−	68 250	0.5568	38 004
13	− 6 750	75 000	−	68 250	0.5303	36 194
14	− 6 750	75 000	−	68 250	0.5051	34 471
15	− 6 750	75 000	−	68 250	0.4810	32 829
16	− 6 750	75 000	−	68 250	0.4581	31 266
17	− 6 750	75 000	−	68 250	0.4363	29 777
18	− 6 750	75 000	−	68 250	0.4155	28 359
19	− 6 750	75 000	−	68 250	0.3957	27 009
20	− 6 750	75 000	−	68 250	0.3769	25 723
Total	− 720 000	1 500 000	225 000	1 590 000	−	1 024 271

Net income stream per year (first 10 years): $\$75\ 000 - \$6750 + 22\ 500 = \$90\ 750\ a^{-1}$.

Net income stream per year (next 10 years): $\$75\ 000 - \$6750 = \$68\ 250\ a^{-1}$ ([Table 25.2](#)).

The PTC pays fully $225\ 000/585\ 000 = 0.3846$ or 38.46% of the initial cost of the turbine.

Net present value of income stream at $r = 5\% \text{ a}^{-1}$. Real rate of interest: \$1 24 271.

$$\begin{aligned}\text{Yearly net real rate of return} &= \frac{\text{Net present value of income stream}}{\text{Total turbine cost}} \\ &\cdot \frac{1}{\text{Project lifetime}} \\ &= (\$1\ 024\ 271/\$585\ 000)/20 \text{ a} \\ &= 0.087545 \\ &= 8.75\% \text{ a}^{-1}\end{aligned}$$

$$\begin{aligned}\text{Present value of electricity per kWh} &= \frac{\text{Net present value of income stream}}{\text{Yearly energy production} \cdot \text{Project lifetime}} \\ &= \frac{\$1\ 024\ 271}{1\ 500\ 000 \frac{\text{kWh}}{\text{year}} \times 20 \text{ years}} \\ &= \$0.03414(\text{kWh})^{-1} \\ &= 3.41 \text{ cents/kWh}\end{aligned}$$

Compared with the benchmark calculation, the PTC can be inferred to contribute a present value of:

$$(\$0.0341 - 0.0284) = 0.57 c(\text{kWh})^{-1}$$

to the income stream from the produced electricity.

25.15 ACCOUNTING FOR THE PTC AS WELL AS DEPRECIATION AND TAXES

The owner of a wind power farm has to pay taxes for the incomes he is obtaining from the electricity sales. Assuming a 25% tax rate ([Table 25.3](#)).

$$\text{Tax payment per year} = 0.25 \times (75\ 003.12 - 6750) = \$17\ 063.28.$$

However if we consider the effect of depreciation we can compute the net tax payment (net tax) as:

$$\text{Net tax} = \text{tax payment} - \text{depreciation credit} = 17\ 063.28 - 14\ 625 = \$2438.28.$$

Then the net income stream for the first 10 years is:

$$\text{Net income} = \text{Gross income} - \text{Expenditure} - \text{Net tax} + \text{PTC}.$$

$$\text{Net income} = 75\ 003.12 - 6750 - 2\ 438.28 + 22\ 500.93 = \$101\ 815.776.$$

TABLE 25.3 Benchmark Present Value Calculation for a 0.6 MW Rated Power Wind Turbine Accounting for the PTC Incentive as Well as Depreciation and Tax Payments

Year	Expenditure/\$	Gross Income From Electricity Sale/\$	Tax 25% Gross Expenditure/\$	Linear Depreciation at 2.5% a^{-1} /\$	PTC/\$	Net Taxes (Tax Depreciation)/\$	Net Income/\$	Present Value Factor	Net present value of income/\$
0	-585 000	—	—	—	—	—	—	—	—
1	-6 750	75 003.12	17 063.28	14 625	22 500.936	2 438.28	101 815.776	0.952380952	96 967.41
2	-6 750	75 003.12	17 063.28	14 625	22 500.936	2 438.28	101 815.776	0.907029478	92 349.91
3	-6 750	75 003.12	17 063.28	14 625	22 500.936	2 438.28	101 815.776	0.863837599	87 952.29
4	-6 750	75 003.12	17 063.28	14 625	22 500.936	2 438.28	101 815.776	0.822702475	83 764.09
5	-6 750	75 003.12	17 063.28	14 625	22 500.936	2 438.28	101 815.776	0.783526166	79 775.32
6	-6 750	75 003.12	17 063.28	14 625	22 500.936	2 438.28	101 815.776	0.746215397	75 976.50
7	-6 750	75 003.12	17 063.28	14 625	22 500.936	2 438.28	101 815.776	0.71068133	72 358.57
8	-6 750	75 003.12	17 063.28	14 625	22 500.936	2 438.28	101 815.776	0.676839362	68 912.92
9	-6 750	75 003.12	17 063.28	14 625	22 500.936	2 438.28	101 815.776	0.644608916	65 631.36
10	-6 750	75 003.12	17 063.28	14 625	22 500.936	2 438.28	101 815.776	0.613913254	62 506.05
11	-6 750	75 003.12	17 063.28	14 625	0	2 438.28	79 314.84	0.584679289	46 373.74
12	-6 750	75 003.12	17 063.28	14 625	0	2 438.28	79 314.84	0.556837418	44 165.47
13	-6 750	75 003.12	17 063.28	14 625	0	2 438.28	79 314.84	0.530321351	42 062.35

(Continued)

TABLE 25.3 (Continued)

Year	Expenditure/\$	Gross Income From Electricity Sale/\$	Tax 25% Gross Expenditure/\$	Linear Depreciation at 2.5% a^{-1} /\$	PTC/\$	Net Taxes (Tax Depreciation)/\$	Net Income/\$	Present Value Factor	Net present value of income/\$
14	-6 750	75 003.12	17 063.28	14 625	0	2 438.28	79 314.84	0.505067953	40 059.38
15	-6 750	75 003.12	17 063.28	14 625	0	2 438.28	79 314.84	0.481017098	38 151.79
16	-6 750	75 003.12	17 063.28	14 625	0	2 438.28	79 314.84	0.458111522	36 335.04
17	-6 750	75 003.12	17 063.28	14 625	0	2 438.28	79 314.84	0.436296688	34 604.80
18	-6 750	75 003.12	17 063.28	14 625	0	2 438.28	79 314.84	0.415520655	32 956.95
19	-6 750	75 003.12	17 063.28	14 625	0	2 438.28	79 314.84	0.395733957	31 387.57
20	-6 750	75 003.12	17 063.28	14 625	0	2 438.28	79 314.84	0.376889483	29 892.93
TOTAL	-720 000	1 500 062.4	341 265.6	292 500	225 009.36	48 765.6	1 811 306.16	—	1 162 184.48

Net present value of income stream at $r = 5\% \text{ a}^{-1}$ real rate of interest:
\$1 162 184.84.

$$\begin{aligned}\text{Yearly net real rate of return} &= \frac{\text{Net present value of income stream}}{\text{Total turbine cost}} \cdot \frac{1}{\text{Project lifetime}} \\ &= (\$1 162 184.84 / \$585 000) / 20 \text{ a} \\ &= 0.099332 \\ &= 9.93\% \text{ a}^{-1}\end{aligned}$$

$$\begin{aligned}\text{Present value of electricity per kWh} &= \frac{\text{Net present value of income stream}}{\text{Yearly energy production} \cdot \text{Project lifetime}} \\ &= \frac{1 162 184.84}{585 000} \times \frac{1}{20} = 3.87 \text{ cents/kWh}\end{aligned}$$

25.16 TRANSMISSION AND GRID ISSUES

Transmission costs are a major issue in wind energy development. Some of the best locations for generating wind energy are far distant from the consuming industrial and population centers. Some areas have a better more reliable source of wind power than others. Although half of the United States' installed wind power capacity is based in Texas and California, the greatest potential for wind generation can be found in areas where there is little demand for electrical power. For instance, there exists a significant amount of wind potential in North Dakota but there are just not a lot of people or industries in North Dakota to consume the electrical power. The highest wind speeds exist in the remote and inaccessible Aleutian Islands in Alaska and necessitate an energy storage and conveyance medium such as hydrogen from water as a transportation fuel in fuel cells. A massive upgrade of the transmission lines nationwide through the national electrical power grid using high-voltage DC instead of high-voltage AC is needed to tap those distant sources [4–7].

Where water supplies are abundant along seashores or internal lakes or rivers, the electricity produced could be used for extracting hydrogen from water through the electrolysis process. Hydrogen then can become the storage medium and energy carrier of wind energy. It would be conveyed or transmitted to the energy consumption sites possibly through the existing natural gas pipeline system which covers the United States.

Another alternative is to convert hydrogen with coal into methane gas (CH_4) that could be distributed through the existing natural gas distribution grid without significant modifications. Methane itself can be

converted into methanol or methyl alcohol (CH_3OH) as a liquid transportation fuel.

In the long term to reduce the electrical transmission losses, one can envision superconducting electrical transmission lines cooled with cryogenic hydrogen carrying simultaneously electricity and hydrogen from the wind energy production sites to the consumption sites. Such a visionary futuristic power transmission system could also provide the electrical power for a modern mass transit system using magnetically levitated (Maglev) high-speed trains transporting goods and people supplementing the current highway system in the United States.

25.17 DISCUSSION

Wind and other renewable sources of energy are creeping toward competitiveness and weaning out from subsidies compared with traditional electricity generated from conventional fossil and nuclear power plants. It must be admitted that the electricity from wind turbines is currently more expensive than traditional generation such as from coal or natural gas. However the future scarcity would bring cost increases as rising fuel costs wage hikes and environmental requirements will affect the costs of conventionally generated electricity but not of wind energy.

If one shares the view that the fossil fuel resources are finite and depletable and that the first signs of shortage are already appearing on the horizon; then one is compelled to recognize the threat of international vicious competition for the control of the remaining supplies of fossil fuels. This makes a compelling case for wind energy.

REFERENCES

- [1] Johnson GL. *Wind energy systems*. Englewood Cliffs, NJ: Prentice Hall; 1985.
- [2] Ragheb M. Ragheb A.M. Wind turbines theory—the Betz equation and optimal rotor tip speed ratio. Fundamental and advanced topics in wind power. In: Carriveau R, editor. ISBN: 978-953-307-508-2 InTech, <<http://www.intechopen.com/articles/show/title/wind-turbines-theory-the-betz-equation-and-optimal-rotor-tip-speed-ratio>>; 2011.
- [3] Adam M. Ragheb and Magdi Ragheb. Wind turbine gearbox technologies. Fundamental and advanced topics in wind power. In Carriveau R, editor. ISBN: 978-953-307-508-2 InTech, <<http://www.intechopen.com/articles/show/title/wind-turbine-gearbox-technologies>>; 2011.
- [4] Ragheb M. Coupling wind power as a renewable source to nuclear energy as a conventional energy option. Invited paper submitted for presentation at the Academy of Sciences for the Developing World—Arab Regional Office TWAS-ARO 7th annual meeting

seminar: Water nuclear and renewable energies: challenges versus opportunities. Conference Center for Special Studies and Programs CSSP Bibliotheca Alexandrina Alexandria Egypt, <<http://www.bibalex.org/CSSP/Presentations/Attachments/Coupling%20Wind%20Power%20as%20a%20Renewable%20Resource%20to%20Nuclear%20Energy%20as%20a%20Conv%20Ent%20Energy%20Option.pdf>>; 2011.

- [5] Rogers K, Ragheb M. Symbiotic coupling of wind power and nuclear power generation. Proceedings of the 1st international nuclear and renewable energy conference (INREC10). Amman, Jordan; 2010.
- [6] Weisensee P, Ragheb M. Integrated wind and solar Qattara depression project with pumped storage as part of Desertec. The role of engineering towards a better environment RETBE'12 9th international conference. Alexandria University Faculty of Engineering; 2012.
- [7] M. Ragheb. Wind power systems: NPREG 475. Lecture notes. <<http://www.mragheb.com/NPRE%20475%20Wind%20Power%20Systems/index.htm>>; 2016.
- [8] Danish Wind Association, <www.windpower.org>.
- [9] Beck R, Ragheb M. Production of carbon-neutral hydrocarbons from CO₂ and H₂ in lieu of carbon capture and storage (CCS). The 10th international conference on role of engineering towards a better environment RETBE14 Alexandria University Faculty of Engineering; 2014.

This page intentionally left blank

Part VII

Investment, Growth Trends, and the Future of Wind Energy

This page intentionally left blank

Chapter 26

Growth Trends and the Future of Wind Energy

Lauha Fried, Shruti Shukla, and Steve Sawyer

Global Wind Energy Council, Brussels, Belgium

Email: Lauha.fried@gwec.net

26.1 INTRODUCTION: GLOBAL STATUS OF WIND POWER (ON- AND OFFSHORE) IN 2015

Wind power is a mature technology with proven reliability and cost competitiveness across an ever-increasing number of markets today. The cost-stability of wind power makes it a very attractive option for utilities, independent power producers, and companies who are looking for a hedge against the wildly fluctuating prices of fossil fuels while reducing their carbon footprint.

Wind power remains the most competitive way of adding new power generation capacity to the grid in a large number of markets around the world, even when competing against heavily subsidized conventional generation technologies.

If we are to have any chance of safeguarding the world against serious climate change, global CO₂ emissions must be reduced before 2020, and a dramatic increase in renewable energy deployment is urgently required to help make this happen. In the short term the three key options available for mitigating greenhouse gas emissions include a rapid deployment of renewable energy, primarily wind power; escalation of efforts toward promoting energy efficiency and conservation; and fuel switching from coal to gas.

By 2020 the Global Wind Energy Council (GWEC) projections suggest that wind power alone could save 8.2×10^9 t (8.2 billion tonnes) of CO₂. On average each kilowatt hour of wind power generated avoids 600 g of CO₂ by displacing the need for the generation of the same unit of electricity from conventional energy sources (coal, oil, or gas).

2015 was an unprecedented year for the wind industry as annual installations crossed the 60 GW mark for the first time in history. More than 63 GW

of new wind power capacity was brought online. The last record was set in 2014 when over 51.7 GW of new capacity was installed globally.

In 2015 total investments in the clean energy sector reached a record US \$ 329×10^9 (US\$ 329 billion). The figures for 2015 were up 4% from 2014's investment of US\$ 316×10^9 and beating the previous record, set in 2011 by 3% [1]. The new global total at the end of 2015 was 432.9 GW, representing cumulative market growth of more than 17%. This growth was powered by an astonishing new installations figure of 30.8 GW in China; the global wind power industry installed 63.5 GW in 2015, representing annual market growth of 22%.

China the largest overall market for wind power since 2009, retained the top spot in 2015. Installations in Asia again led global markets, with Europe in the second spot, and North America in third place.

As a result of this, was that in 2015, the majority of wind installations globally were *outside* the Organization for Economic Co-operation and Development (OECD) once again. This has been the case since 2010, with the exception of 2012. This trend will continue for the foreseeable future.

By the end of last year the number of countries with more than 1000 MW installed capacity was 26: including 17 in Europe; 4 in Asia-Pacific (China, India, Japan, and Australia); 3 in North America (Canada, Mexico, United States), 1 in Latin America (Brazil), and 1 in Africa (South Africa).

By the end of 2015 eight countries had more than 10 000 MW of installed capacity including China (145 362 MW), the United States (74 471 MW), Germany (44 947 MW), India (25 088 MW), Spain (23 025 MW), United Kingdom (13 603 MW), Canada (11 205 MW), and France (10 358 MW).

China crossed the 100 000 MW mark in 2014, adding another milestone to its already exceptional history of renewable energy development since 2005. This year it made history again and strengthened its position on the leaderboard.

Europe and North America both had strong years in 2015, led by Germany and the United States, respectively. Guatemala and Jordan each added their first large commercial wind farms, and South Africa became the first African market to pass the 1 GW mark.

26.1.1 Asia: Remarkable Year for China

For the seventh year in a row, Asia was the world's largest regional market for new wind power development, with capacity additions totaling just over 33.9 GW.

In terms of annual installations China maintained its leadership position. China added 30.8 GW of new capacity in 2015, once again the highest annual number for any country ever.

In 2015 wind power generation in China reached 186.3 TW h, accounting for 3.3% of total electricity generation [2]. This follows a pattern of steady increase in wind-based electricity generation despite heavy curtailment. In 2012 wind-generated electricity in China was just over a 100 TW h, accounting for 2% of the country's total electricity output. Wind provided almost 135 TW h of electricity in 2013, contributing 2.6% of the country's total electricity generation [3]. Total wind power generation reached over 153 TW h in 2014, 2.78% of total electricity generation [4].

The Chinese wind market almost doubled its capacity from 75 GW in 2012 to reach 145 GW by the end of 2015, reinforcing China's lead in terms of cumulative installed wind power capacity.

All observers continue to be surprised by the astonishing track record for growth of the wind sector in China over the last decade. The current pace of growth in the Chinese wind power market may see a slowdown in 2017. However, we have often been positively surprised when time and again when China's latest installation figures are presented.

Curtailment on wind farms in China worsened in 2015, as plunging utilization rates kept almost 34 TW h from being delivered to the grid. According to the National Energy Administration (NEA), the country wasted 15% of wind power generated in 2015 [5].

Ongoing curtailment of electricity generation is a challenge for wind power projects. However, the NEA and State Grid are working to solve the transmission bottlenecks and other grid issues, and the situation is expected to improve.

India continues to be the second largest wind market in Asia, offering ample prospects for both international and domestic players. The Indian wind sector has struggled over the years to repeat the strong market performance of 2011 when over 3 GW was installed. 2015 seems to signal the onset of a recovery phase given the government desire to address some of the structural bottlenecks in the market.

India's new wind energy installations totaled 2.6 GW in 2015, for a total of 25 GW. This kept the Indian wind power market firmly in the top five rankings globally. The total grid-connected renewable energy installations in the country reached approximately 39.5 GW [6].

The Indian government has committed to a target of 175 GW of renewables by 2022. The target includes achieving 100 GW of solar capacity and 60 GW of cumulative wind power capacity by 2022. The government has also indicated its support for rapidly growing the power sector, renewables being a core part of this strategy.

While the rest of Asia did not make much progress in 2015, there are some favorable signs on the horizon. The Japanese market installed almost 245 MW in 2015 to reach a cumulative capacity of 3 GW. This represents around 0.5% of the total power supply in Japan. Japan is slowly moving toward a transformation of its energy system to allow for a more diverse

energy mix including more wind power and other renewables. However, removing existing barriers will take time. Offshore wind development, in particular floating turbines, is a promising prospect for the future.

Although South Korea still has “green growth” as one of its national development priorities, wind power is still a relatively small energy generation technology, with 225 MW of new installations in 2015, bringing total installed capacity to just over 835 MW.

Taiwan added 14 MW of new capacity, bringing its total installed capacity to 647 MW. As for the rest of Asia, we expect new projects to come online in Pakistan, Thailand, and Vietnam in 2016.

26.1.2 North America: Resurgence in the United States

The year 2015 ranks as the third highest year for wind installations for the United States, the single largest market in terms of total installed capacity after China. The US market added 4000 new turbines for a total of 8.6 GW last year, a 77% increase over 2014, and total installed capacity reached 74.5 GW.

Wind produced over 190 TW h in the United States in 2015, which was 4.7% of the total electricity generated in the United States.

Wind energy accounted for almost 31% of all new generating capacity installed between 2011 and 2016. Wind energy provided more than 25% of the electricity in Iowa and South Dakota, and 12% or more of the generation in a total of nine states [7].

In terms of annual capacity additions, Texas led the 2015 market with 3.6 GW, followed by Oklahoma (1.4 GW), Kansas (799 MW), Iowa (524 MW), and Colorado (399 MW).

At year-end wind developers reported more than 9.4 GW of construction activity across 72 projects in 22 states (plus Guam). This included over 1.8 GW of new construction announcements made toward the end of 2015.

The 5-year extension and phase out of production tax credit (PTC) provides the greatest degree of long-term policy stability the US wind industry has ever seen. This, combined with a broader range of customers, and an ongoing “wind rush” driven by technological improvements is setting the stage for more years like 2015 in the United States.

In Canada 1.5 GW of new wind capacity came online, making it the sixth largest market in 2015. Canada finished with over 11.2 GW of total installed capacity making it the seventh largest market globally in 2015. Canada’s new wind energy projects in 2015 represent over US\$ 3×10^9 (US\$ 3 billion) in investment. At the end of 2015 wind power was supplying approximately 5% of Canada’s electricity demand. The Canadian wind industry demonstrated a 5-year annual average growth rate of 23% per annum.

Canada added new wind capacity through the commissioning of 36 projects, 23 of which involved Aboriginal Peoples, municipal or local

ownership. For comparison in 2014 of the 37 new wind energy projects installed, 15 projects also included significant ownership stakes from Aboriginal Peoples, municipal or local ownership. This is a sign that local communities are taking a keen interest in wind energy.

Most of the growth was centered in the provinces of Ontario (871 MW), Quebec (397 MW), and Nova Scotia (186 MW). The Canadian industry expects to see another record year in 2016.

Mexico installed an impressive 713.6 MW of new capacity to reach a total of 3.0 GW by the end of 2015. Mexico's Energy Reform legislation was enacted in December 2013.

Mexico has set an ambitious annual target of 2.0 GW a^{-1} until 2023. The country is facing one of its biggest energy challenges in 20 years, with the current energy reform opening up the electricity market like never before. The market reforms for the electricity sector are expected to have a significant impact on the future of wind power in the country. 2016 will be another strong year for the Mexican wind power market.

26.1.3 Europe: Unparalleled Year for Germany

Across Europe 13.8 GW of wind power was installed in 2015. The European Union member states (EU) accounted for 12.8 GW of the total.

There are now almost 141.6 GW installed in the EU with a total cumulative capacity of 147.7 GW for all of Europe. Wind power installed more than any other form of power generation in 2015, accounting for 44.2% of total 2015 power capacity installations. Wind energy overtook hydropower as the third largest source of power generation in the EU with a 15.6% share of total power capacity by the end of 2015.

Renewables accounted for 77% of new power plant installations in 2015 (22.3 GW of a total of 29 GW) of which wind accounted for 44%.

The overall EU installation levels mask significant volatility across Europe. Germany alone accounted for almost 50% of total EU wind energy installations with 6.0 GW. Poland at 1.3 GW and France at 1.1 GW were the only two other markets to install over 1 GW during the year. Together these three countries account for over two-thirds of all installations. In a number of previously healthy markets such as Sweden and the United Kingdom, installations slowed down significantly.

At the end of 2015 the EU had 142 GW of installed wind power capacity of which 131 GW was onshore and 11 GW offshore. However, 47% of all new EU installations in 2015 took place in Germany and 73% occurred in the top four markets, a similar trend to the one seen in 2014. This is unlike previous years when installations were less concentrated and spread across many more healthy European markets.

In Europe wind energy development saw $\text{€}26.4 \times 10^9$ (€26.4 billion) invested in 2015, 40% higher than the total investment in 2014. While wind

power led 2015 installations, solar photovoltaics accounted for 29%, coal 16%, and gas 6.4%.

Germany remains the EU country with the largest installed capacity (44.9 GW), followed by Spain (23 GW), United Kingdom (13.6 GW), France (10 GW), and Italy (9 GW). Sweden, Denmark, Poland, and Portugal have more than 5 GW installed.

Annual installations of wind power in the EU have increased over the last 14 years, from 3.2 GW in 2000, to 12.8 GW in 2015 at a compound annual growth rate (CAGR) of 9%. Wind power accounts for one-third of all new power installations since 2000 in the EU.

In 2015 the annual onshore market in the EU decreased by 7.8%, but offshore installations more than doubled compared to 2014. Overall EU wind energy annual installations increased by 6.3% compared to 2014.

Offshore wind accounted for almost a quarter of total EU wind power installations in 2015, and investment in offshore wind in Europe doubled to $\text{€}13.3 \times 10^9$ (€13.3 billion). It was a record year for financing and grid-connected installations. Germany (2.3 GW), United Kingdom (572 MW), and the Netherlands (180 MW) were the three countries to grid-connect new offshore wind turbines in 2015 with 14 projects reaching completion.

The United Kingdom still has the largest offshore wind capacity in Europe at 5.1 GW, accounting for 46% of total European installations. Germany had a stellar year and rose to the second spot in 2015. Germany saw total installation rise to 3.3 GW (29.9%). With 1.3 GW (11.5%), Denmark is third, followed by Belgium at 712 MW (6.5%), the Netherlands at 427 MW (3.9%), and Sweden with 202 MW (1.8%). Other small markets include Finland with 26 MW, Ireland with 25 MW, Spain with 5 MW; Norway with 2 MW, and Portugal with 2 MW.

Weakened legislative frameworks, ongoing economic crisis and austerity measures implemented across Europe continue to hinder growth of the wind power industry. The year ahead is likely to be difficult but the broader investment shift away from fossil fuels could boost the European renewables sector.

Beyond the EU, Turkey is the largest market, with annual installations of 956 MW in 2015. The Turkish market reached a cumulative installed capacity of 4.7 GW last year. Looking ahead, the future of wind sector in Turkey looks promising.

26.1.4 Latin America and the Caribbean: Brazil Continues to Lead

Latin America and the Caribbean had a good year. The region saw 3.7 GW of new capacity come online, bringing total installed capacity to 12.2 GW. Latin America has begun developing a substantial wind power industry to complement its rich hydro and biomass (and potentially solar) resources.

Post the Paris Agreement at the Conference of Parties 21 (COP21) [8], the demand for clean energy bolstered by concerns for energy security and diversity of supply will promote the growth of wind power in Latin America and the Caribbean.

For the fourth year in a row the Latin American market installed over 1 GW of new capacity. In 2012 six markets in the region installed 1.2 GW of new wind capacity for a total installed capacity of just over 3.5 GW. In 2013 just five markets including Argentina, Brazil, Chile, Dominican Republic, and Uruguay accounted for 1.2 GW of new wind power capacity for a total installed capacity of 4.7 GW. In 2014 ten markets added new capacity. These included Argentina, Brazil, Chile, Costa Rica, Ecuador, Peru, Honduras, Nicaragua, Venezuela, and Uruguay. In 2015 eight markets added new capacity. These included Argentina, Brazil, Chile, Costa Rica, Guatemala, Honduras, Panama, and Uruguay.

Brazil led Latin America with installations of almost 2.8 GW; although the projects were fully commissioned not all of them could be given a grid connection before the end of the year. Brazil continues to be the most promising onshore market for wind energy in the region out to 2020.

Uruguay has a goal to generate as much as 38% of its power from wind by the end of 2017 and added almost 316 MW, bringing its total installed capacity to over 845 MW. With its neighbors Argentina and Brazil, Uruguay has traded electricity for years. In 2013 for the first time in more than a decade Uruguay did not import electricity from its neighbors selling US\$ 21×10^6 (US\$ 21 million) worth of electricity to Argentina in 2013. The National Utility—UTE and Brazil's Eletrobras are testing a 500 MW transmission line, which could enable Uruguay to add more wind power [9].

Chile added 169 MW of new capacity to reach a total installed capacity of almost 1 GW. Panama added record capacity of 235 MW to reach 270 MW, and Costa Rica added 70 MW of new capacity to reach a total of 268 MW. Honduras saw its total installed capacity reach 176 MW, when it added 50 MW of new capacity in 2015. Guatemala for the first time added wind power to its energy mix in 2015, with a 50 MW project.

Argentina added 8 MW of new capacity to bring its total installed capacity up to 279 MW last year. The Caribbean reached a total installed capacity of 250 MW across various island states by the end of 2015.

26.1.5 Pacific

The region saw its total installed capacity rise to just over 4.8 GW last year. The Australia added 380 MW in 2015, bringing its total installed capacity up to 4.2 GW.

The previous Australian Prime Minister did not support renewables and was causing significant difficulties for the renewable energy industry in Australia. In a strange move in the run up to COP21 last year, the Australian

parliament approved legislation cutting the Renewable Energy Target from 41 to 33 TW h [10]. However, the target is at least now fixed, and the new Prime Minister is more forward looking. In a positive development, the province of South Australia committed to a new target of zero net emissions by 2050 last year.

Samoa added 550 kW of new wind power capacity in 2015. This was the first wind project in the Pacific Island nation. The project site is located on the island of Upolu; Samoa's second largest island. United Arab Emirates-based energy firm Masdar developed the project with funds from the UAE's Pacific Partnership Fund.

New Zealand and the rest of the Pacific did not add any new wind power capacity in 2015, just like 2014.

26.1.6 Africa and the Middle East

The Africa and Middle East region saw 953 MW of new capacity additions last year, bringing cumulative capacity for the region up to 3.5 GW. Africa's wind resource is best around the coasts and in the eastern highlands, but until last year it was in North and East Africa that wind power has been developed at scale.

South Africa installed 483 MW of new capacity, for a cumulative capacity of 1.1 GW. This is just the beginning of a promising wind market in the region, which has surpassed 1 GW in just 2 years.

Egypt saw a new wind farm come online in 2015. It is one of the largest wind farms in Africa with 100 turbines with a total capacity of 200 MW. It was inaugurated in Egypt's Gulf of El-Zayt. This brought Egypt's total installed capacity up to 810 MW. Egypt wants to source 20% of its energy from renewable sources by 2030.

Ethiopia had a good year as well, as 153 MW of new capacity came online last year. This brought total installed capacity in Ethiopia to over 324 MW.

In 2015 Jordan added its first large wind farm (117 MW) to its generation mix for a total of 119 MW. The Tafila wind farm is the first utility scale wind power project in the Middle East. The wind farm accounts for almost 6.5% of Jordan's 1.8 GW renewable energy target for 2020 [11].

At the end of 2015 over 99% of the region's total wind installations were spread across 10 countries—South Africa (1053 MW), Morocco (787 MW), Egypt (810 MW), Tunisia (245 MW), Ethiopia (324 MW), Jordan (119 MW), Iran (91 MW), Cape Verde (24 MW), Kenya (19 MW), Israel (6.25 MW), and Algeria (10 MW). New projects are expected to come online in Egypt, Ethiopia, Kenya, Morocco, Tanzania, and South Africa in 2016.

26.1.7 2015: Extraordinary Year Fueled by China's FIT Reduction Plan

After a slowdown in 2013 the wind industry set a new record for annual installations in 2014 by installing 51.7 GW of new wind power. In 2015,

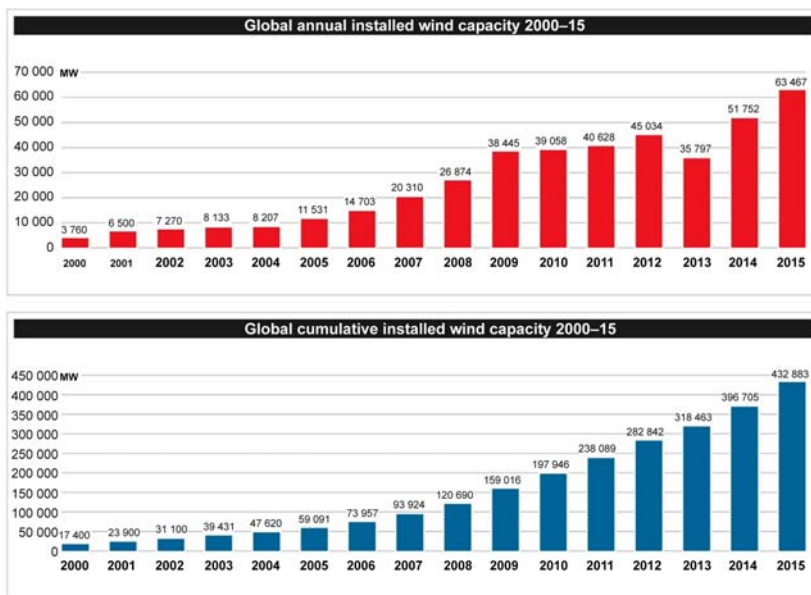


FIGURE 26.1 Global annual and cumulative installed wind capacity 2000–15. *From GWEC.*

however, the global wind industry smashed all previous records by installing over 63 GW of new capacity—see Figs. 26.1–26.3.

The record-setting figure represents a 22% increase in the annual market. Total cumulative installations stood at 432 GW at the end of 2015, representing cumulative growth of 17%. This record was led by China's annual capacity addition, which alone accounted for 48% of total global installations.

2015 was a big year for the big markets—China, the United States, Germany, and Brazil, all of which set new records. But there is a lot of activity in new markets around the world and in 2016 the installations are likely to see a broader distribution.

There is a still an acute need around the world for new power generation, which is clean, affordable, indigenous, reliable, and quick to install. Wind power is leading the charge in the transition away from fossil fuels; and is blowing away the competition on price, performance, and reliability.

26.2 OFFSHORE WIND ENERGY

2015 was a significant year for offshore wind installations. New capacity additions totaled more than 3.4 GW across five global markets. This brought the total offshore wind installed capacity to over 12 GW. See Fig. 26.4.

At the end of 2015 more than 91% (11.0 GW) of all offshore wind installations were located in waters off the coast of 11 European countries.

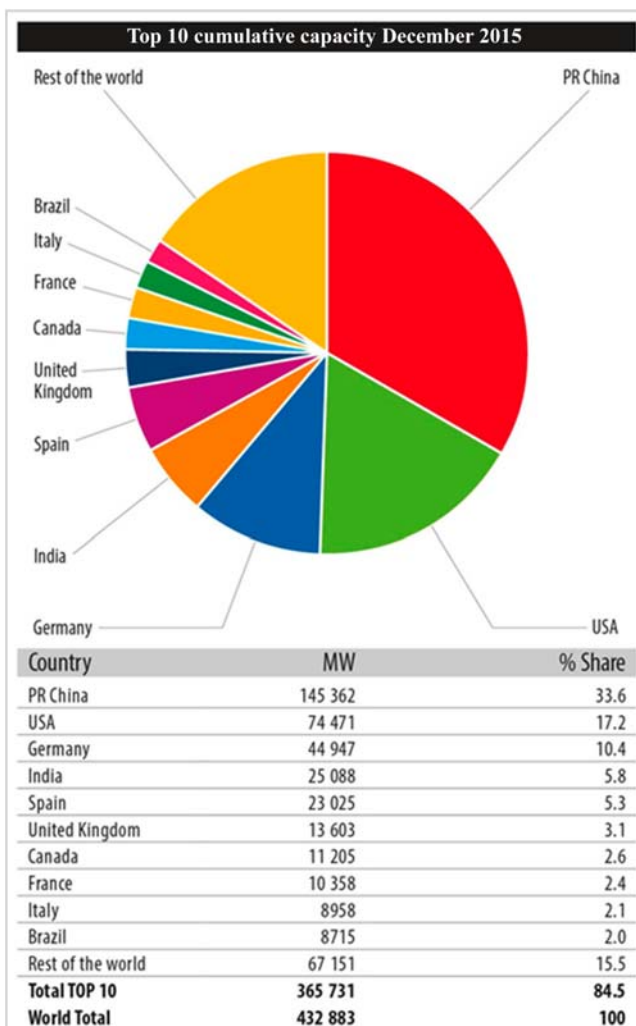


FIGURE 26.2 Top 10 cumulative capacity, December 2015. From GWEC.

The remaining 9% of the installed capacity is located largely in China, followed by Japan and South Korea.

Globally the United Kingdom is the largest offshore wind market today and accounts for over 40% of the installed capacity, followed by Germany in the second spot with 27%. Denmark accounts for 10.5%, Belgium for almost 6%, Netherlands for 3.5%, and Sweden for 1.6%. Other European markets including Finland, Ireland, Norway, Spain, and Portugal make up about 0.5% of the market. The largest market outside of the European waters is China, which accounts for approximately 8.4% of the global market in the sector.

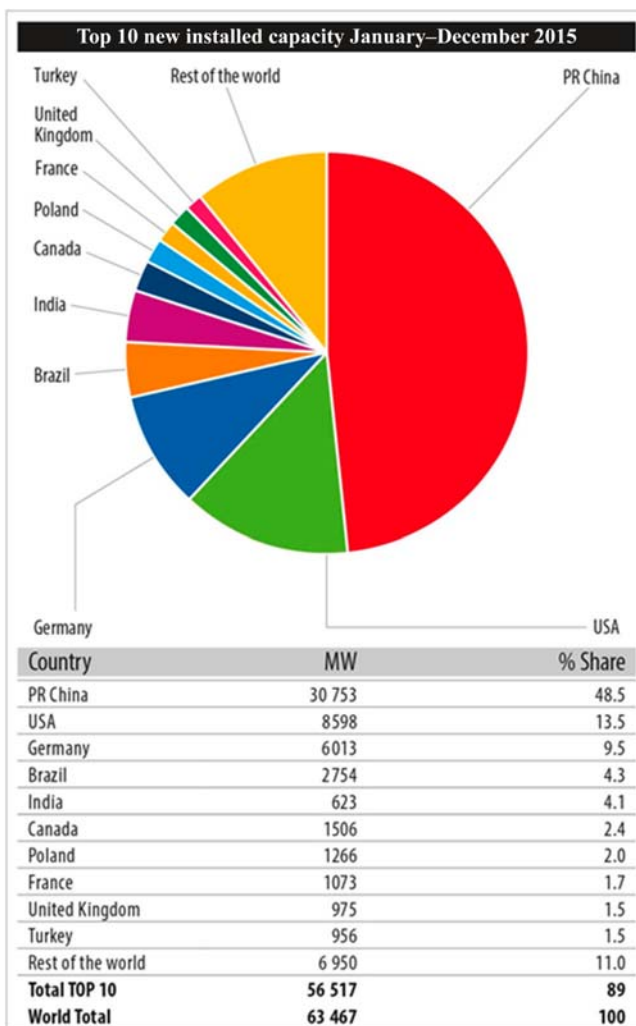


FIGURE 26.3 Top 10 newly installed cumulative capacity, January–December 2015. *From GWEC.*

Governments outside of Europe are now setting ambitious targets for offshore wind and development is starting to take off in some of these markets. Japan, South Korea, and Taiwan have put actual turbines in the water. The United States saw the first commercial project start construction in 2015. The GWEC led FOWIND consortium is developing an offshore wind roadmap for India.

Relatively higher costs and installation complexity compared to onshore wind are a big challenge for offshore wind development. However, according

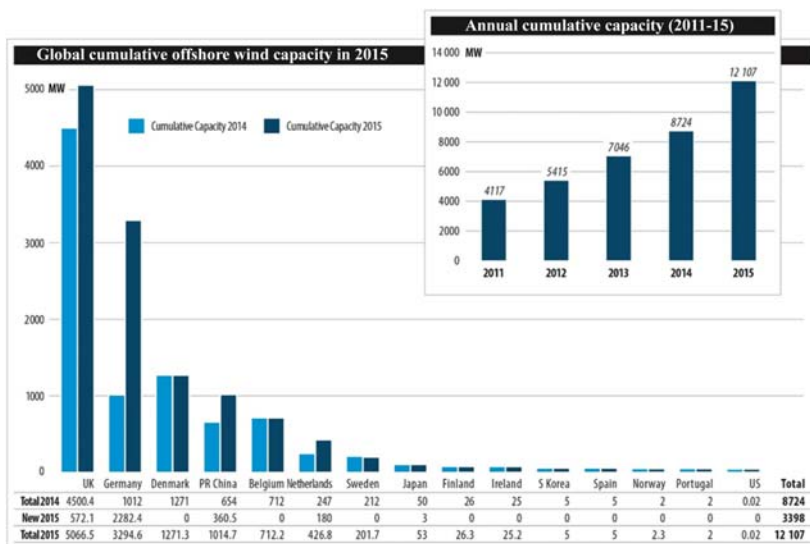


FIGURE 26.4 Global cumulative offshore wind capacity in 2015. Inset: Annual cumulative offshore wind capacity, 2011–15. From GWEC, 2016.

to a study [12] commissioned by E&Y in 2015, offshore wind cost could be reduced to €90 (MW h^{-1}) (€90 per megawatt hour) by 2030. The report says that the sector will have nearly reduced the LCOE to €100 (MW h^{-1}) by 2020, by which time cumulative installed capacity in European waters is expected to have reached 23.5 GW.

Key cost reduction steps include: deploying larger turbines to increase energy capture (a 9% saving); encouraging greater competition (7%); keeping the volumes up (7%); and tackling supply-chain challenges (3%). The offshore industry is on its way to meeting the goal of getting the leveled cost of electricity (LCOE) down to €100 (MW h^{-1}). At present the average offshore wind turbine size is 4.2 MW in European waters, average water depth 27.1 m and average distance from shore 43.3 km.

26.2.1 Europe Passes 11 GW Mark

In 2015 an astounding 3.0 GW of new offshore wind capacity came online in Europe, a 108% increase over the 2014 market. Offshore wind accounted for 24% of total EU wind power installations in 2015, up from 13% share of annual additions in 2014.

Three underlying factors enabled this growth: effective policy, the grid connectivity of large amounts of offshore capacity installed but not grid-connected in 2014, and the industry's rush to complete installations before the German market switches to market-based arrangements in 2017.

Overall 419 new turbines were erected in 2015. Also for the first time offshore turbines were decommissioned. A total of 7 turbines in the United Kingdom and Sweden were decommissioned, resulting in a net addition of 412 turbines. A total of 14 projects were completed in 2015.

Over 75% of all net capacity brought online was in Germany (2.3 GW), a fourfold increase in its grid-connected capacity compared to 2014. This was in large part due to the delay in grid connections finally coming online in 2015.

The remaining installations in the EU took place in just two markets. The second largest market was the United Kingdom with 572 MW, and an 18.7% share of total installations. The Netherlands follows with 180 MW, a 5.9% share of the market.

Overall 3230 turbines are now installed and grid-connected, bringing the cumulative total to just above 11 GW in Europe. The currently installed capacity is capable of producing 40.6 TW h in a normal wind year. See [Table 26.1](#).

The United Kingdom has the largest amount of installed offshore wind capacity in Europe at over 5 GW representing almost 46% of all installations. Germany follows with 3.2 GW with almost 30% share of all installations. Denmark stands third with 1.2 GW installed capacity accounting for 11.5% of total European installations. By the end of 2015 Belgium had 712 MW with 6.5% market share, the Netherlands had 427 MW with 3.9% market share, Sweden had 202 MW with 1.8% market share. Finland had 26 MW installed and Ireland had installed 25.2 MW. Spain, Norway, and Portugal each have one wind turbine operating offshore.

Siemens is the lead offshore wind turbine supplier in Europe with 63.5% of total installed capacity. MHI Vestas (18.5%) is the second biggest turbine supplier, followed by Senvion (7.4%), Adwen (5.7%), and BARD (3.6%).

In terms of the total number of wind turbines connected to the grid at the end of 2015, Siemens remains the top supplier with 2059 turbines, accounting for 63.6% of the market.

MHI Vestas has 750 grid-connected turbines representing 23.2% of the total, followed by Senvion (140 turbines, 4.3%), Adwen (127 turbines, 3.9%), BARD (80 turbines, 2.5%), WinWind (18 turbines, 0.6%), and GE Renewable Energy with 15 turbines (0.5%).

2015 also marked an important year for offshore wind financing. Ten projects worth $\text{€}13.3 \times 10^9$ (13.3 billion euros) in total reached final investment decision in 2015, compared to $\text{€}6.5 \times 10^9$ in 2014. In total 3 GW of new gross capacity were financed across four countries, 66% of which was in the United Kingdom.

Total investments in offshore wind in 2015 were more than $\text{€}18 \times 10^9$; this includes investments in construction of offshore wind projects, transmission assets, and refinancing. This makes 2015 a record year in terms of total committed funds.

TABLE 26.1 Number of Wind Farms, Turbines, and MW Fully Connected to the Grid in Europe (2015)

	Belgium	Germany	Denmark	Spain	Finland	Ireland	Netherlands	Norway	Portugal	Sweden	United Kingdom	Total
No. of farms	5	18	12	1	2	1	6	1	1	5	27	80
No. of turbines	182	792	513	1	9	7	184	1	1	86	1454	3230
Capacity installed by 2015/ MW	712.2	3294.6	1271.3	5	26.3	25.2	426.8	2.3	2	201.7	5066.5	11 034

Source: EWEA (2016); Rounding and decommissioning of 16 MW affect the sums.

An estimated financing of $\text{€}11 \times 10^9$ will be needed for just over 3 GW of new capacity in 2016. Several transactions are already under appraisal or expected to go through final investment decision in 2016.

Projects under appraisal include the Otary Rentel (294 MW) wind farm, Hornsea Phase 1 (1 200 MW), Hohe See (492 MW), Dudgeon (402 MW), Beatrice (664 MW), and the refinancing of Luchterduinen (129 MW).

Additionally reduced risk perception for offshore wind projects has led to the emergence of project bonds as a means of financing. For the first time in 2015 $\text{€}1.5 \times 10^9$ was raised through project bonds for the construction and refinancing of offshore wind farms.

26.2.2 UK Remains Largest Global Market

The United Kingdom has the highest share of consented offshore wind capacity today. It continued to lead the world's offshore industry in terms of cumulative installations in 2015.

Out of the 22 offshore wind farms where work was carried out in Europe last year, five were in the United Kingdom. At four offshore wind sites—Gwynt y Môr, Westernmost Rough, Humber Gateway, and Kentish Flats 2 Extension—153 turbines were connected in 2015, for a total annual market of 572 MW. At one offshore wind farm—Robin Rigg—two turbines of 3 MW each were decommissioned.

At the time of writing over 4 GW of projects are fully contracted and will be delivered over the next 4 years, with a further 1 GW anticipated to reach financial close within weeks.

In November 2015 Amber Rudd, UK's Minister for Climate and Energy stated that based on current plans the country expects to see 10 GW of offshore wind installed by 2020. However, this is linked to the industry meeting its obligation of bringing offshore costs to under $\text{£}100 (\text{MW h})^{-1}$ (GBP 100 per megawatt hour) by 2020. The UK industry is well on its way to meeting this goal. The Minister further said that the government will make funding available for three auctions and intends to hold the first of these auctions by the end of 2016 [13].

26.2.3 Germany Had an Exceptional Year

The offshore wind industry in Germany had a record year. A total of 546 offshore wind turbines came online bringing the offshore capacity in Germany up to 2.3 GW. Over 75% of all net capacity brought online in Europe was in Germany, a fourfold increase in its grid-connected capacity compared to 2014. Cumulatively Germany accounts for about 30% of the offshore capacity installed in Europe.

The German offshore wind market had surpassed the 1 GW mark in 2014, more than doubling both 2013s annual market and the country's

cumulative offshore capacity. At the end of 2015 Germany accounted for almost 26% of all consented projects in Europe. Sites in Germany are an average of 52.6 km from shore. The total number of turbines connected to the grid by December 31, 2015 up to 792, with a combined capacity of 3.3 GW.

In 2015 Germany saw 41 wind turbines with a total capacity of 246 MW fully erected, but not yet connected to the grid. One hundred twenty-two foundations were constructed offshore in 2015 for wind turbines to be installed in 2016.

According to the working group *AG Energiebilanzen*, offshore wind turbines produced over 8 TW h of electricity in 2015. This was enough to cover the power consumption of over 2 million households or around 1.4% of the gross electricity generation in Germany that year [14].

In 2016 the German government is expected to adopt a revision to the Renewable Energy Sources Act (EEG), which will lay the foundations for a stable domestic market. The German offshore sector under the EEG 2016 will see an intermediate expansion target of 11 GW by 2025. This will limit the annual market to approximately 700 MW over the next 10 years.

The industry considers reliable, continuous expansion more important in the long term than any one-off records. To achieve such continuity it is necessary that the Renewable Energy Sources Act (EEG) 2016 and the Offshore Grid Development Plan (O-NEP) 2025 are properly coordinated. The industry has asked for the annual market to be at least 900 MW so as to be able to achieve economies-of-scale and long-term certainty for investing in further cost reductions. It is expected that Germany will add approximately 700 MW of new offshore capacity in 2016.

26.2.4 Netherlands: Fourth Largest Market Globally

In 2015 Netherlands added 180 MW of offshore capacity, installing 60 turbines, which make it the world's sixth largest offshore market. Netherland's total installed capacity reached 427 MW by the end of last year.

The Netherlands has a 15% renewable energy goal out to 2020. It has a plan to expand the country's offshore wind power capacity by 3.5 GW through several tenders by 2023.

In March 2016 the Senate approved a law that will allow the Dutch government to move ahead with an offshore wind tender. This amendment to the Dutch Electricity Act allows transmission operator TenneT to start construction of grid infrastructure required for the new wind farms off the country's coast and at Borssele (Zeeland). This amendment also clarifies for wind farm developers the damage liability from delays and disruption to the grid.

A key challenge for the sector is to ensure a smooth running of the planned tenders for offshore wind energy. The first tender is expected to be

held during spring 2016, a second one before the end of the year, and a further 1400 MW are planned to be auctioned in the Borssele area.

The industry has also a goal to reduce costs by 40% over the next 5 years. Over the longer term, the Dutch North Sea has huge potential to further develop large-scale wind after the 2023 targets have been achieved; to start with the already designated area of IJmuiden Ver could accommodate 6.0 GW of offshore wind power.

26.2.5 France Gearing up to Deliver

Six offshore wind farms totaling 3 GW are currently under construction. The *Round 1 projects include*: Courseulles (500 MW), Fécamp (500 MW), Saint-Nazaire (500 MW), Saint-Brieuc (500 MW); and the *Round 2 projects include*: Dieppe-Le Tréport (500 MW) and Iles d'Yeu et de Noirmoutier (500 MW). The industry expects the third tender for offshore wind power to be launched by the end of 2016.

The key challenges faced by the sector are the need for cost reductions; integration of offshore farms within the maritime areas; and increased competition in the market. A public debate focusing on offshore wind power development in France is planned during the summer of 2016. The French wind industry has set ambitious goals to reach 12 GW of bottom-fixed and 6 GW of floating offshore wind capacity by 2030.

26.2.6 China Passes the 1 GW Milestone

By the end of 2015 China added 360.5 MW of new offshore capacity. This was a 57% increase over last year. At the end of 2015 cumulative installed capacity reached 1015 MW, making China the fourth largest market globally. See [Table 26.2](#).

The new offshore projects are spread across sites along the coasts of Guangdong, Fujian, and Jiangsu provinces. The majority of Chinese offshore projects are installed in the shallow waters close to the shore, called *inter-tidal* projects, where the sites dry out (or nearly so) at low tide. Most of the projects in deeper waters, such as those granted under the first round of tenders, are either still in development or have just started construction. See details of the newly added offshore projects in the [Table 26.2](#). Most of these projects are inter-tidal.

In China offshore development is accelerating slowly and is expected to pick up steam this year. An ever-increasing number of developers are “testing the waters” with inter-tidal offshore projects.

However, the major bottleneck for large-scale offshore development is the low FIT. This is currently set as RMB $0.85 (\text{kW h})^{-1}$ (€0.12 per kilowatt hour or/US\$ 0.13 per kilowatt hour) for “near-shore” offshore projects and RMB $0.75 (\text{kW h})^{-1}$ for inter-tidal projects. For projects to get this tariff

TABLE 26.2 China's Offshore Installations 2007–15

Year	New Installed Capacity/MW	Cumulative Installed Capacity/MW
2007	1.5	
2009	14.0	15.5
2010	135.5	151
2011	109.58	260.58
2012	127.0	387.58
2013	39.0	426.58
2014	227.6	654.18
2015	360.5	1014.68

there is a cut-off date of 2017. This is complicating matters and also making it difficult for some developers to make a decision given the uncertain course of the feed in tariff (FIT).

Another bottleneck is the difficulty in getting all the necessary licenses, as the offshore projects are controlled by multiple government agencies. In some cases the environmental impact assessment (EIA) has been particularly difficult to conduct and finish.

China's offshore wind progress will continue but at a much slower pace than the onshore growth. Local developers are seeking to gain experience and expertise in this sector. Major changes to this market are expected after 2017, when the existing tariff is set to expire and a new FIT for offshore will kick in.

26.2.7 Domestic Industry Moves Japan Forward

By the end of 2015 Japan had 53 MW of offshore wind power, including two 2 MW of floating wind turbines. A Siemens semioffshore 3 MW wind turbine was installed at the Eurus Akita port in 2015. The Japanese government fixed the FIT at $\text{JPY } 36 (\text{kW h})^{-1}$ ($\text{€}28$ or $\text{US\$ } 33$ per kilowatt hour) for offshore wind power in March 2014. The offshore FIT is 1.6 times higher than the onshore tariff ($\text{JPY } 22 (\text{kW h})^{-1}$), which improves investment confidence in the sector. See [Table 26.3](#).

12 MW of floating offshore turbines will start to operate in 2016. Several projects are expected to start construction within a couple of years; Kashima Port Project1-Phase1 shall be the earliest. Overall there are 1.4 GW of offshore wind power projects currently under planning.

Currently there is no law or regulation for offshore wind power development in Japan for undesignated areas. A marine area in Japan is categorized

TABLE 26.3 Offshore Wind Power in Japan at the End of 2015

Type	Location		Distance/km	Depth/m	Rated/MW	No. of WTG	Total/MW	Start Operation		
Fixed	Hokkaido	Setana Port	0.7	13	0.6	2	1.2	Dec. 2003		
	Akita	Akita Port	0.1	—	3.0	1	3.0	Feb. 2015		
	Yamagata	Sakata port	0.05	4	2.0	5	10.0	Jan. 2004		
	Ibaragi	Kamisu	0.04	4	2.0	7	14.0	Feb. 2010		
		Kamisu	~0.05	4	2.0	8	16.0	Feb. 2013		
	Chiba	Choshi ^a	3.1	12	2.4	1	2.4	Mar. 2013		
Floating	Nagasaki	Kabashima ^a	1.0	100	2.0	1	2.0	Oct. 2013		
	Fukushima	Iwaki city	20	120	2.0	1	2.0	Dec. 2013		
		Naraha ^a			7.0	(1)	(+12.0)	2016		
					5.0	(1)		2016		
Total						27	52.6			

^aNational projects: Under commissioning/construction.

into two kinds, either as a *Port associated area* or as a *General common sea area*. The former one is controlled by port authorities, therefore the entity from whom official permissions are needed is clear. Unfortunately there is no law or regulation for the latter area. Hence there is a significant business risk for projects planned under the *General common sea area* at present.

All of the four projects installed up until 2013 were government-led investments and were mainly developed for testing different technologies. 2014 saw commercial development begin and bring a positive change echoing the introduction of the offshore FIT.

Ten commercial projects with a total capacity of 800 MW are being considered for the *Port associated area* and three projects with 580 MW are being considered for the *General common sea area*. The former is more feasible to develop thanks to lower business risk.

As for national projects the Japanese Ministry of Environment (MOE) is conducting a Floating Offshore Wind Turbine Demonstration Project (GOTO FOWT) at Kabashima in the Goto islands in the Nagasaki prefecture. A Hitachi 2 MW downwind rotor wind turbine on the spar-type floater has been in operation since October 2013. The electricity produced by this wind turbine was used for producing hydrogen in 2015. This turbine will soon be moved from Kabashima to Fukue Island, which has a bigger population and electricity demand.

As for METI's Fukushima FORWARD project, the second floating offshore turbine (7 MW) was anchored in August 2015 and was commissioned thereafter. The third floating offshore turbine (5 MW) is being manufactured at Hitachi's factory. This will be installed on the JMU's advanced spar-type floater and will start operation in 2016. A total of three floating turbines with 12 MW capacity will start operation in 2016.

Japan's New Energy and Industrial Technology Development Organization (NEDO) started a feasibility study for a new advanced floating offshore wind power demonstration project in 2015. Two groups are nominated as potential candidates. Each group will try to develop two floating offshore wind turbines within the rated capacity of 7.5 MW in total with the intention to achieve cost reduction compared to the former projects. The long coast line and high cost for onshore development, makes offshore wind an attractive option for the Japanese wind industry.

26.2.8 Upcoming Markets

26.2.8.1 US Set to Deliver the First Commercial Project

No offshore wind capacity is installed in the United States with the exception of the University of Maine's 0.02 MW VolturnUS floating turbine project. The first wind farm will be commissioned 5 km (3 miles) off the coast of Block Island, Rhode Island.

Construction on the 30 MW, US\$ 290×10^6 (€255 million) project began in early 2015 and Deepwater Wind, the developer responsible for building the farm, says it is on track to be generating power by the fourth quarter of 2016. A construction milestone was celebrated in July 2015 when five steel foundation jackets and deck platforms were placed in the water.

According to the company's website, the five-turbine farm will connect Block Island to the mainland for the first time with an underground cable and is expected to supply power to 17 200 Rhode Island homes by generating approximately $125\,000 \text{ MW h a}^{-1}$ where a refers to annum [15]. Block Island will receive about 90% of its energy needs from this project. Whenever the wind farm is under maintenance or not producing enough power, the mainland grid will serve the island. Diesel power is the current source of the island's energy.

The National Renewable Energy Laboratory (NREL) estimates that the United States has 4200 GW of developable offshore wind potential, compared to its estimate of 11 000 GW of onshore wind potential. Wind resources are classified on a scale of 0–7 based on their power density, and more than 66% of offshore wind in the United States is in wind power class six or seven.

Developers have proposed building nearly 4.9 GW of offshore wind capacity off the coasts of nine different states mostly along the northeast coast. But some challenges remain even for projects that have progressed through key regulatory and market milestones.

The US Department of Energy supported demo projects—the Virginia Offshore Wind Technology Advancement (VOWTAP [16]) Project, Fisherman's Energy Wind [17] of New Jersey and WindFloat of Oregon—face development hurdles despite making significant progress in project development.

Each of these projects received US\$ 4×10^6 (€3.5 million) in design and planning support. Eventually these three projects were to get as much as US \$ 47×10^6 (€41 million) each to help fund construction. The goal was to have the projects up and running in 2017, but both Fishermen's Energy and WindFloat (semisubmersible)—are facing serious challenges [18].

Fishermen's Energy's proposal has a two-phase approach, the first phase a 25 MW project in New Jersey State Waters followed by a 330 MW utility scale project in Federal Waters, for the second phase.

In March 2016 the New Jersey legislature passed a second bill [19] that requires the Board of Utilities to re-open an application window for a 20–25 MW offshore wind project in state waters, a move aimed at providing Fishermen's Energy a final chance to win regulatory approval. The NJ Board of Utilities (BU) has twice rejected Fishermen's fully permitted 24 MW, US \$ 220×10^6 (€194 million) project on grounds that it fails to provide the state with sufficient economic and environmental benefits to qualify for Offshore Renewable Energy Certificates [20] (ORECs).

Further the BU disagreed with the developer's proposed OREC price of US\$ 199.17 (MW h)⁻¹, as this was contingent on Fishermen's Energy receiving about US\$ 100×10^6 (100 million dollars) in federal subsidies that it did not have fully in hand last year [21]. In a renewed effort to address these concerns, the project developer switched from XEMC to Siemens turbines, while pledging to utilize traditional project financing along with proven technology [22].

On the other end the US Department of Interior's Bureau of Ocean Energy Management (BOEM) is in charge of the permitting process for off-shore projects including planning, leasing, site assessment, construction and operations. It has executed individual lease sales in a number of states including Rhode Island and Massachusetts (2013), Virginia (2013), Maryland (2014), Massachusetts (2015), and New Jersey (2016) [23].

United States will see its first commercial offshore project come online in 2016. The path forward will be challenging, and will be linked to the outcome of the upcoming Presidential election results as well. The level of federal support for offshore wind could come under a scanner in case a Republican President is elected come November.

26.2.8.2 India Sets the Ball Rolling

The Indian Ministry of New and Renewable Energy (MNRE) has initiated discussions on promoting a demonstration project in India. In October 2015, it announced India's Offshore Wind Policy. The National Institute for Wind Energy (NIWE) is the nodal agency for implementing the policy and creating the necessary ecosystem for the sector.

Facilitating Offshore Wind in India [24] (FOWIND) is a European Union supported 4-year project. A GWEC led consortium is implementing this project in Gujarat and Tamil Nadu. NIWE is the knowledge partner for the project in India. FOWIND will undertake the first offshore wind resource measurement in the Gulf of Khambat, off the coast of Gujarat in 2016. FOWIND works in close consultation with the MNRE and state government agencies to establish a roadmap for offshore wind power development in India.

The Offshore Wind Policy outlines an international competitive bidding mechanism for the sector. The first tender is likely to be announced in late 2018.

26.3 THE FUTURE: MARKET FORECAST (ON- AND OFFSHORE) TO 2020

Looking ahead GWEC anticipates a period of steady growth, although not expecting the kind of spectacular growth we have seen in the last two years. Asia will continue to dominate the period from 2016–20, capturing at least 50% of the global market, although its dominance may be tempered slightly



FIGURE 26.5 Market forecast for 2016–20. From July 7, Global Wind Energy Council: Lauha Fried, Shruti Shukla, and Steve Sawyer.

toward the end of the decade. Europe will continue its steady pace towards its 2020 targets, although increasing policy uncertainty might mean some bumps in the road. With Mexico, Canada and the United States all on a strong policy footing, North America *should* continue its strong growth for the rest of the decade. See Fig. 26.5.

Latin America will continue to be driven largely by Brazil, although there will be increasing contributions from a variety of markets, including a large new potential market in Argentina. Africa and the Middle East continue to diversify, although in the short term it will be dominated by South Africa, Egypt, and Morocco, with Kenya and Ethiopia coming on strong. The Pacific region will return to substantial growth with a period of policy stability in Australia.

China surpassed the EU in cumulative installations in 2015, and will continue to drive Asian growth. Despite FIT cuts for wind as of this year and again in 2018, the new 5-Year Plan has upped the target for China's wind sector for 2020 once again, this time to 250 GW, which the market is likely to in fact exceed. Also the "take-off" of the Chinese offshore sector is likely to happen, with about 1 GW of projects in the construction phase, adding a new dimension to the world's largest market.

Despite the Indian government's commitment to renewables' development, the wind industry only experienced modest growth in 2015, and it is not yet clear how fast the industry can grow given infrastructure limitations and the overall parlous state of the electricity industry's finances. The government is working hard to overcome these, however, and modest growth is expected in India throughout 2020. Elsewhere in Asia, while not too much is expected from South Korea and Japan in the short term, but new markets will emerge every year, and the signing of PPAs in Indonesia are hopefully the beginnings of a large new potential market. Pakistan, Philippines, and

Mongolia continue to grow, and hopefully Vietnam can begin to exploit its excellent wind resources before the end of the decade. Overall the Asian market is likely to roughly double between now and 2020, adding 177 GW over the period.

In Europe Germany posted extraordinary numbers in 2015, bolstered by more than 2 GW of offshore installations, which is not likely to be repeated in the near future. Poland was Europe's number two market last year, at least partly due to a rush to install prior to the change in the support scheme, and the United Kingdom is facing a period of policy instability which may, ironically, lead to stronger installations in the short term but does not bode well for the medium term. Turkey's market remains strong and is looking to grow significantly in 2016, and some southern European markets are recovering from the aftereffects of the financial crisis. However, it seems likely that there will be a small downturn in 2016, with later recovery at least in part dependent upon the outcome of EU-wide deliberations on post-2020 targets and support schemes.

The United States *could* grow spectacularly, far above current predictions depending on a number of political and economic factors. Regardless a strong and increasingly stable market in the United States is expected over the next 5 years.

The big picture view of the Canadian market has also improved of late, with the recent election of a Liberal government in Ottawa led by Justin Trudeau, which is determined to resume Canada's leadership role in the international climate debate. Coupled with a very progressive provincial government in Alberta and increasing market diversity across the country, the world's seventh largest market (sixth in terms of annual market in 2015) looks set for a period of solid growth. Mexico's newly reformed market is just getting underway, so it is too soon to say whether it will reach its target of 2 GW year⁻¹ any time soon, but early results are encouraging. Overall the North American market is likely to add about 60 GW over the next 5 years.

Despite Brazil's political and economic woes, the wind sector continues to power ahead with another 10 GW already contracted by 2019, and two auctions scheduled for 2016. Elsewhere in the region Chile and Uruguay will add capacity in 2016, although Uruguay is likely to pause there for a while. Peru's recent successful and very low-priced tender results could mean that market is going to move in earnest, and there are some stirrings in Colombia.

But the big new story in Latin America is Argentina, with the advent of a new government and a new commitment to utilizing the country's vast renewable energy sources, sorting out the electricity sector's finances and re-establishing itself as a leader in the international climate debate. We could have a major new South American market relatively soon. Much could go wrong, of course, but the current government is working hard to put things in place as soon as possible. 30 GW of new wind power is expected across the region by 2020.

Jordan inaugurated its first wind farm in 2015, underlining the diversification of the uptake of wind power across the region, albeit most of them are small markets, at least for now. South Africa, despite Eskom's financial woes, which prevented the round four projects from reaching financial close in 2015, will continue to be the largest market in the region. Morocco will see a number of projects come online over the next 5 years, mostly from the famous tender won by the consortium of EGP, Nareva, and Siemens early this year. Egypt is still a sleeping giant, waiting for the pieces to fall into place with their new support systems, but they still maintain very aggressive targets for 2022.

Ethiopia is rapidly taking steps to allow independent power producers (IPPs) to take advantage of their tremendous wind resources, which augurs well for that market, and Kenya's Lake Turkana project finally started construction during 2015. Elsewhere in the region a number of smaller projects are at various stages of development, and we are very optimistic about the spread of wind power across Africa to meet the development needs of its growing economies, which will result in about 16 GW of new installations out to 2020.

After a relatively quiet year in the main market in the Pacific, Australia seems poised for another round of growth based on the clarification of the Renewable Energy Target, bringing some visibility to the market out to the end of the decade. Australia's new Prime Minister has shown a more positive attitude toward renewables than his predecessor, and the market for wind in Australia is expected to nearly double over the next 5 years. This combined with some activity in the Islands and New Zealand, leads us to anticipate that about 4.5 GW will be added in the region in the period from 2016–20.

Figs 26.6–26.11 of wind turbines around the world.



FIGURE 26.6 Wild Horse Renewable Energy Center. US © Puget Sound Energy.



FIGURE 26.7 A wind farm in Ceará on Brazil's northeast coast. *Bons Ventos wind farm, Ceará, Brazil* © Suzlon.



FIGURE 26.8 An offshore turbine access via RIB (rigid inflatable boat) on a calm day in the German North Sea. © Stiftung OFFSHORE-WINDENERGIE Jan Oelker.



FIGURE 26.9 Wild Horse Renewable Energy Center. US © Puget Sound Energy.



FIGURE 26.10 Gamesa turbines at Zafarana Wind Farm on the Gulf of Suez coast in Egypt.



FIGURE 26.11 Attaching blade of an Enercon turbine to the rotor hub.

REFERENCES

- [1] <<http://www.bloomberg.com/company/clean-energy-investment/#form>>.
- [2] <http://www.nea.gov.cn/2016-02/02/c_135066586.htm>.
- [3] <http://www.chinadaily.com.cn/bizchina/greenchina/2014-02/26/content_17306185.htm>.
- [4] <<http://www.reuters.com/article/2015/02/12/china-power-windpower-idUSL4N0VM3XJ20150212>>.
- [5] <http://www.nea.gov.cn/2016-02/02/c_135066586.htm>.
- [6] <<http://www.mnre.gov.in/mission-and-vision-2/achievements/>>.
- [7] <<http://www.ferc.gov/CalendarFiles/20150213081555-Gramlich,%20AWEA.pdf>>.
- [8] <http://unfccc.int/files/meetings/paris_nov_2015/application/pdf/paris_agreement_english_.pdf>.
- [9] <<http://www.bloomberg.com/news/articles/2015-06-17/uruguay-spends-2-6-billion-to-become-south-america-wind-leader>>.
- [10] <<http://www.windpowernightly.com/article/1352943/australia-approves-ret-cut-33tw h>>.
- [11] <http://www.masdar.ae/assets/downloads/content/4282/2016_jordan.pdf>.
- [12] Offshore Wind in Europe: Walking the tightrope to success. Ernst & Young, 2015.
- [13] <<https://www.gov.uk/government/speeches/amber-rudds-speech-on-a-new-direction-for-uk-energy-policy>>.
- [14] <<https://www.wind-energie.de/en/press/press-releases/2016/offshore-wind-energy-germany-figures-2015-record-achieved-due-catch>>.
- [15] <<http://dwwind.com/project/block-island-wind-farm/>>.
- [16] Dominion Power's VOWTAP project include the National Renewable Energy Laboratory; General Electric, which will supply the Alstom-designed turbines; KBR, a global engineering, construction and services firm; Keystone Engineering, the substructure designer; Newport News Shipbuilding, and the Virginia Tech Advanced Research Institute.
- [17] <<http://www.fishermensenergy.com/offshore-new-jersey.php>>.
- [18] <<http://breakingenergy.com/2015/06/25/oregon-offshore-wind-projects-troubles-leave-the-doe-0-for-3-so-far/>>.
- [19] The General Assembly voted 53–21 in favour of S988, which the state Senate passed last month. S988 calls for the new application window to be opened within 60 days following enactment of the bill into law. The bill will move to Governor Chris Christie, who allowed the first similar legislation to die earlier this year by declining to sign it. At the time of writing it remains to be seen if he will sign or veto S988. <<http://www.fishermensenergy.com/pdf/2016/03/letter-to-gov-christie.pdf>>.
- [20] Electric utilities would be required to purchase ORECs-a revenue guarantee mechanism that would allow developers to finance offshore wind projects. Their developers would obtain one OREC per MW h at a price set by the BU.
- [21] <<http://www.rechargenews.com/wind/1427269/nj-legislature-passes-new-bill-to-help-fishermens-wind-pilot>>.
- [22] <<http://www.njspotlight.com/stories/15/10/14/its-day-in-court-over-fishermen-s-energy-revamps-offshore-wind-proposal/>>.
- [23] <<http://www.boem.gov/Lease-and-Grant-Information/>>.
- [24] <<http://www.fowind.in>>.

Index

A

Above ground level (AGL), 395
Accommodation cyclic behavior, 292
“Accommodation”, 283–284
Active stall control, 153
“Adaptation”, 283–284
Adaptive linear element (ADALINE), 42
Advantages of wind energy, 8–10
compatibility with other land uses, 8
conservation of water, 9
cost effectiveness, 9
creation of jobs and local resources, 9–10
destructive mining, reduction of, 9
electricity cost, stability of, 10
international cooperation, 10
location, 8
national security, 8
power supply, diversification of, 10
provision for clean source of energy, 8
rapid instigation of power, 10
reduction of costly transport costs of
electricity, 8
short commissioning time, 9
source of income for farmers, ranchers and
foresters and grid operators, 10
sustainability, 8
Aegean and Mediterranean windmills,
133–135
Aerodynamic damping, 482–483
Aerodynamic rotor, 146
Aerodynamics and design of horizontal-axis
wind turbines, 161
aerodynamic blade design, 178–181
blade element momentum (BEM) method,
167–172
design process, brief description of, 183
1D momentum equations, 163–166

steady blade element momentum method,
use of, 172–178
unsteady loads and fatigue, 181–183
working of wind turbine, 162–163
Aeronautical Research Institute of Sweden
(FFA), 206
Agency for the Cooperation of Energy
Regulators (ACER), 107–108
Age-specific death rate, 315–317
Air temperature, 31
Aire Limitée Adaptation dynamique
Développement International
(ALADIN) model, 40–41
Airfoil properties, relative importance of, 179t
Al Damashqi, 131
Al Massoudi, Ali, 131
Ambient excitation method, 483
American Petroleum Institute (API), 355–357
American Petroleum Institute (API) code,
281–282, 341
limitations of, 282–283
American windmill, 138–139, 138f
AMOS (Aerodrome Meteorological
Observation System) wind data, 32
Ancillary services (ASs), 83–84, 110,
117–118
ANSYS software, 290–295
Artificial neural network (ANN), 41–43
Aspect ratio, 197
Asynchronous (induction) generator, 149–151
Auto Regressive Integrated Moving Average
(ARIMA) based methods, 41
Auto Regressive Moving Average (ARMA)
models, 41–43
Automatic Generation Control (AGC),
422–424
Auto-Regressive Conditional
Heteroskedasticity (ARCH), 42

B

- B&Q, 393–394
 Background, of wind energy, 5–7
 Balance of systems, 443
 Ballast stabilized spar buoy concept, 237
 Barotrauma-related internal hemorrhaging, 476–477
 Baseload generating plants, 377–378
 Bat mortality, wind-turbine-induced, 476
 Bayesian model, 34
 Benchmark wind turbine present value cost analysis, 544–546
 current income and expenditures per year, 544–546
 investment, 544
 payments, 544
 Betz Limit, 21–22, 166
 Biot–Savart law, 170
 Bird mortality, wind-turbine-induced, 476
 Blade element momentum (BEM) method, 167–178, 215–216
 Blades, 442
 Bohai Sea, 257, 261–264
 wave height and period in, 261t
 British Wind Energy Association (BWEA), 392–393, 393f
 Buoyancy stabilized semi-submersible, 237
 Burbo wind farm, 226–227

C

- Caisson flexibility, 370–371
 Cambered airfoil, 194
 Cantilever cross-coupling term, explanation of, 337f
 Capacitor bank, 151–152
 Capacity factors (CFs), 22, 58, 65–66, 440
 CAPEX (Capital expenditure), 239
 Capital energy cost (CEC), 439–440, 445–447, 447f, 451f, 457t
 Carbon dioxide emissions, 3–5, 13, 95, 495
 Carbon footprint of storing wind energy, 383–385
 Carbon-trading and carbon reduction target, 88
 Catastrophic failures, 314
 Central government, 79
 CfD (Contract for Difference), 227–228
 Challenges facing the wind turbine industry, 10–12
 aesthetics, 11
 frequency of light and shadows, 11–12

- good sites often in remote locations, 11
 initial cost, 12
 intermittency of wind, 11
 new and unfamiliar technology, 12
 noise pollution, 11
 safety, 11
 shortage of rare earth element, neodymium, 12
 turbine blades damaging wildlife, 11
 China, wind energy development in, 76–80
 barriers to, 81–86
 demand response and energy storage, lack of, 84
 differential priorities between central government and local governments, 85
 nonrenewable power plants, overcapacity in, 81
 poor grid connectivity, 83
 vested interests between coal companies and the government, 85–86
 well-functioned ancillary service market, lack of, 83–84
 wind curtailment, 81–82
 drivers of, 86–88
 carbon-trading and carbon reduction target, 88
 coal-fired power plants' retrofit and energy storage, 87
 emerging ancillary service market, 88
 energy coordination, 86–87
 smart DR, 87–88
 electricity market and wind energy market, 76–78
 future of, 89–91
 distributed generation deployment and proactive transmission planning, 89
 merit-order-based dispatch, 90–91
 offshore wind power planning, 89–90
 pricing improvement, 91
 smart grid, 90
 key players in wind energy market, 78–80
 central government, 79
 grid companies, 80
 local governments, 79–80
 wind energy developers, 78
 wind turbine manufacturers, 78–79
 wind curtailment rate 2010–16, 82f
 wind energy capacity development 2001–15, 76f
 China Seas, wind condition summary in, 245, 258t

- Chinese waters
 extreme wind and wave loading condition in, 257–260
 foundations supporting wind turbines used in, 254*f*
 ground conditions in, 260–265
 wave height and period in, 261*t*
- Circular tuning liquid column dampers (CTLCD), 484–485
- Civil engineering aspects of wind farm and wind turbine structures, 221
 choice of foundations for a site, 228
 energy challenge, 221
 foundation types, 228–238
 floating turbine system, 237–238
 gravity-based foundation system, 233
 pile foundations, 234–235
 seabed frame/jacket supporting supported on pile/caissons, 235–237
 suction buckets, 233–234
 general arrangement of wind farm, 228
 site layout, spacing of turbines, and geology of the site, 239–242
 economy of scales for foundation, 241–242
 Westermost Rough, 240
- wind farm and Fukushima nuclear disaster, 221–223
 performance of near shore wind farm during 2012 Tohoku earthquake, 221–223
- wind farm site selection, 224–228
 ASIDE on the economics, 227–228
 Burbo wind farm, 226–227
- Claessens, 195
- Climate change, 3–5, 480–481
- Closed-form solutions, for foundation stiffness, 332, 334–336
- Coal-fired power plants, 83, 85–86
 retrofit and energy storage, 87
- Coal-heavy electricity system, 67–68
- Coleman conversion method, 483
- Combined heat-and-power (CHP), 84
- Commercial forest plantations, 509–511
- Commercial operating date (COD), 313
- Competitive Renewable Energy Zone (CREZ), 433
- Computational fluid dynamics (CFD), 178–179, 196, 207–209
 -based approaches, 28, 36
- Computational simulations, 283
- Conditional reliability, 319–320
- Conference of the Parties (COP 21), 51
- Connection-related network codes, 109–110
- Consents and legislations, 226
- Contemporary wind turbine technologies, 155–159
 fixed-speed wind turbines (Type 1), 155–156, 155*f*
 limited variable-speed wind turbines (Type 2), 156–157, 156*f*
 variable-speed wind turbines
 with full-scale power converter (Type 4), 158–159, 158*f*
 with partial-scale power converter (Type 3), 157–158, 157*f*
- Continuous Reliability Enhancement for Wind (CREW), 309, 311
- Control system and wind turbine control capabilities, 152–155
- Corrective maintenances, 315
- Corrosion, 304
- Cost analysis, wind energy, 539
- Cost of energy (COE), 299–300
- Crane free solution, 233
- Crane-assisted solution, 233
- Cross-coupling stiffnesses, 338
- Cumulative energy demand (CED), 439–440, 444
- Current income and expenditures per year, 544–546, 548–550
- Current Policies Scenario (CPS), 527
- Curtailing renewable resources, 380
- Cut-in speed speed, 29–30
- Cut-out wind speed, 29–30
- Cyclic hardening, 284
- Cyclic loading, 283–284, 355–357, 367*f*
- Cyclic overturning moments, 279
- Cyclic softening, 284
- Cyclic stress ratio (CSR)
 in the soil in the shear zone, 363

D

- “Darrieus” wind turbine, 188–189
 “Darrieus-type” VAWTs, 190–191
- Demand response (DR), 84
 DR and energy storage, lack of, 84
- Det Norske Veritas (DNV) code, 354
- Det Norske Veritas-Keuring van Elektrotechnische Materialen te Arnhem (DNV KEMA), 309, 311
- Differential priorities between central government and local governments, 85
- Dimensional analysis, 360

- Discrete element method (DEM) analysis, 285
 monopile analysis using, 286–290
- Distributed generation deployment and
 proactive transmission planning, 89
- Donghai Bridge 100 MW Offshore Wind
 Power Demonstration Project, 243
- Double-slotted (MFFS) multielement wind
 turbine blade, 213*f*
- Doubly fed induction generator (DFIG),
 150–151
- Drag, 6–7
- DU 00-W-401 airfoil, 206–207, 207*f*,
 209–210
- DU 06-W-200 airfoil, 195, 195*f*
- DU 91-W2-250 airfoil, 214, 216
- Dutch and European windmills, 135–138
- Dynamic–structure–foundation–soil
 interaction, 256
- E**
- Earth Resources Observation and Science
 (EROS) Data Center, 56
- East China Sea, 257–258
 wave height and period in, 261*t*
- Economics of wind power generation, 535
 accounting for PTC as well as depreciation
 and taxes, 550–553
- benchmark wind turbine present value cost
 analysis, 544–546
- current income and expenditures per
 year, 544–546
- investment, 544
- payments, 544
- economic considerations, 537–539
- intermittence factor (IF), 542–543
- investment tax credit, 546
- land rents, royalties, and project
 profitability, 543
- levelized cost of electricity (LCOE),
 539–540
- net present value, 540–541
- price and cost concepts, 542
- production tax credit (PTC), 546
- project lifetime, 543
- renewable energy production incentive,
 547–548
- straight line depreciation, 541
- transmission and grid issues, 553–554
- wind energy cost analysis, 539
- wind turbine present value cost analysis
 accounting for PTC, 548–550
- current income and expenditures per
 year, 548–550
- payments, 548
- wind turbines prices, 542
- Economy of scales for foundation,
 241–242
- EERA-DTOC project, 121
- E-highway 2050 project, 121
- Eigen frequency, 247–248, 253, 277, 329
- Elastic–plastic model, 281, 341
- Electric Reliability Council of Texas
 (ERCOT), 62–63, 425–426
- Electrical energy storage (EES), 381–382
- Electricity market and wind energy market,
 76–78
- Emerging ancillary service market, 88
- Enercon E115 blade, 205
- Energy Capture Optimization by
 Revolutionary Onboard Turbine
 Reshape (ECO ROTR), 216
- Energy challenge, 221
- Energy coordination, 86–87
- Energy management system (EMS), 115
- Energy payback time (EPBT), 444–445, 457*t*
- Energy Sector Management Assistance
 Program (ESMAP), 26
- Energy storage, 378–379, 383, 385–386
- Energy-related carbon dioxide (CO₂)
 emissions, 3–4
- ENTSO-E Ten Year Network Development
 Plan (TYNDP), 105
- Environmental and structural safety issues
 related to wind energy, 475
- environmental issues and countermeasures,
 475–481
- birds and bats, effects on, 476–478
- climate change and considerations,
 480–481
- marine species, effects on, 478
- noise problems and possible solutions,
 478–479
- visual impacts and mitigation, 479–480
- wind turbine towers, 481–485
 health monitoring and vibration control
 of, 483–485
 structural performances under wind and
 seismic loads, 481–483
- Environmentally friendly generation
 dispatching (ESGD) model, 90–91
- EROI value, 382–383
- Estimation of wind energy potential and
 prediction of wind power, 25

- estimating wind power based on wind speed measurements, 33–34

further considerations for wind speed assessment, 38–39

main aspects of wind assessment program, 28–33

principles for successful development for wind assessment program, 26–28

wind resource estimation project, 34–38

wind speed and power forecasting, 39–44

European Landscape Convention (ELC), 493–495

European wind integration projects and studies, 119–121

European windmills, 135–138

EWIS project, 120

External loading conditions, complexity of, 353–355

F

FACTS, 108

Failure mode effect criticality analysis (FMEA), 300–301

Failure rate in reliability. *See* Hazard rate function

Farlie–Gumbel–Morgenstern (FGM) approach, 34

Fatigue limit state (FLS), 253, 277, 329

Federal Energy Regulatory Commission (FERC), 423–424

Feed-forward back-propagation (FFBP), 42

Feed-in-tariff (FIT), 77, 91

Finite element analysis (FEA), soil models used in, 283–285

Finite Element Models (FEM), 183

Fixed-speed wind turbines (Type 1), 153–156, 155f

FlexiSlip induction generators, 150

Floating system, 233

Floating turbine system, 237–238

“Float-out and sink” solution, 233

Flow angle, 168

Flux, 19–20

Forecasting, 319–320

Forecasting wind speed, 40

Fossil fuel, 4–5

Fossil-fuel-based resources, 430–431

Foundation, 443

and cover, 443

Foundation design, 269–271

challenges in monopile foundation design and installation, 270–271

jacket on flexible piles, 271

Foundation design, importance of, 252–253

Foundation stiffness for design of offshore wind turbines, estimating, 329

advanced methods, 334, 336

comparison with SAP 2000 analysis, 349–350

obtaining foundation stiffness from standard and advanced method, 337–344

example problem, 340–344

pile head deflections and rotations, 345

prediction of the natural frequency, 346–349

simplified method, 332, 334–336

standard method, 332–334, 336

Foundations

choice of, 228

definition, 228

for fixed (grounded) systems, 250f

technical review/appraisal of, 358

types, 228–238

floating turbine system, 237–238

gravity-based foundation system, 233

pile foundations, 234–235

seabed frame or jacket supporting supported on pile or caissons, 235–237

suction buckets, 233–234

Foundation–soil interaction

advanced analysis to study, 283–285

discrete element model analysis basics, 285

soil models in finite element analysis, 283–285

450 Scenario (450S), 527

Fractional reinvestment, 445

Free-flowing wind energy, 423–424

Frequency converter, 152

Fujian Sea, 262–263

Fukushima nuclear disaster

wind farm and, 221–223

G

Gamesa G128, 205

GBS from Thornton Bank Project, 234f

Gearbox spares planning, 320–321

Gearing and generator, 443

General Electric Company, 55

Generalized Auto-Regressive Conditional Heteroskedasticity (GARCH), 42

Generation technology lifecycle, 384t

- Generator, 147–151
 asynchronous (induction) generator, 149–151
 synchronous generator, 148
- Geographic Information System (GIS) data, 26
- German system, wind power in, 95
 energy policy goals, 96/
 European wind integration projects and studies, 119–121
 integration of renewables in Germany and Europe, 95–98
 network operation and grid development, 102–110
 connection-related network codes, 109–110
 innovative methods to plan and operate the power system, 105–108
 market-related network codes, 108–109
 system operation network codes, 108
- new control concepts for PE-dominated power systems, 111–112
- onshore and offshore wind development, 99–102
- sector coupling concepts, 118–119
- virtual power plants, 117–118
- wind farm clusters, 114–117
- wind power forecasts, 112–113
- Germanischer Lloyd (GL) Garrard Hassan, 309, 311
- “Giromill”, 190–191
- Glauert correction, 166–167
- Global Digital Elevation Model (GTOPO30), 56
- Global greenhouse gas (GHG) emissions, 3–4
- Global potential for wind-generated electricity, 51
 methodology, 54–58
 results, 58–68
 China perspective, 65–68
 global perspective, 58–60
 US perspective, 61–64
- Global storage capacity, 379/
 Global warming potential (GWP), 522–523
- Global wind industry, net energy trajectory of, 450–452
- Goddard Earth Observing System Data Assimilation System (GEOS-5 DAS), 35, 54–55
- Gravity-based foundation system, 233, 241
- Greenhouse gases (GHG), 75
 GHG emissions, 420, 445, 522–523
- Grid companies, 80
- Grid development, network operation and, 102–110
 connection-related network codes, 109–110
 innovative methods to plan and operate the power system, 105–108
 market-related network codes, 108–109
 system operation network codes, 108
- Grid Development Plan (GDP), 104–105
- Grid EROI, 382–383
- Grid flexibility, 377–378
- Ground conditions, in Chinese waters, 260–265
 Bohai Sea, 261–264
 seismic effects, 264–265
- Grounded system, 231–232
- H**
- Halladay design, 139
- Harmonization, 447–449
 of study boundaries and data, 446
- Harnessing wind power, history of, 125
 Aegean and Mediterranean windmills, 133–135
 American windmill, 138–139, 138/
 Dutch and European windmills, 135–138
 historical developments, 139–141
 Islamic civilization windmills, 130–132
 medieval European windmills, 132–133
 wind machines in antiquity, 129–130
 windmills applications, 141
- Hazard rate function, 315–317
- Heavy rare earth element oxides (HREO), 532
- Heavy rare earth elements (HREE), 517
- High Resolution Local Area Model (HIRLAM), 40–41
- High temperature superconductors (HTS), 520–521
- High-voltage direct current (HVDC)
 connections, 104–105, 109–110
- Horizontal Axis Wind Turbine (HAWT), 185–186
- Horizontal-axis machines, 135–137
- Horns Rev 1, monopile for, 340–344
- H-rotor, 190–191
- Hub, 442
- Hurricane Saomai, 258–259, 259/
 260/
 Hydroelectricity production, 4
- Hydrostatic ETA model, 40–41

I

- IEC, 481–483
- Infant failures, 304
- InnoBlade, 205
- Innovative methods to plan and operate power system, 105–108
- challenge for operation of transmission grid, 106
- dynamic line rating, 106
- impact of reduced inertia on power system frequency, 106–108
- Installation date, 313
- Institute of Electrical Engineers (IEC), 355–357
- Integration time step (ITS) method, 291
- Intended Nationally Determined Contributions (INDCs), 527
- Intermittence factor (IF), 542–543
- Internal energy (IE), 51–52
- International Energy Agency (IEA), 526–528
- International Geosphere-Biosphere Programme (IGBP), 55–56
- Investment, 544
- Investment tax credit (ITC), 546
- IRPWIND project, 121
- Islamic civilization windmills, 130–132
- Island of Grand Cayman, 188

J

- Jacket on flexible piles, 271
- Jackson–Hunt based approach, 36–37
- JONSWAP (Joint North Sea Wave Project) spectrum, 256

K

- Kaimal spectrum, 256
- Kaimal wind spectrum, 354
- Kalman filter based methods, 41–42
- Kamisu (Hasaki) wind farm, 222/*f*
- Kentish Flats and Thanet (UK), 275
- Kinematic hardening, 284–285
- Kinetic energy (KE), 51–52
- Kinetic energy flux, 19–21
- Kirke's prototype machine, 197

L

- Land rents, royalties, and project profitability, 543

Landscape, 493–495

- changing, 495–498, 496/*f*
- effects of wind farms on landscape, 508–512
- landscape and visual effects, 512
- landscape effects, 509–511
- visual effects, 511
- mitigation, 512–514
- strategic approach, 513–514
- passion for, 493
- perception of wind farms, 502–506
- composition, 504
- height and size, 502–503
- movement, 504–506
- power generation objects, landscapes with, 506–508
- technological advancement, 498–502

Landwirtschaftskammer Schleswig-Holstein (LWK), 309

- Last known operating date, 313
- Least-cost wind integration solution, 426
- Levelized cost of electricity (LCOE), 227–228, 329–330, 439, 539–540
- Levelized Cost of Energy (LCoE), 161, 183, 358
- Levelized cost of offshore wind, 226
- LIDAR (Light Detection and Ranging system), 30–31
- Life-cycle assessment (LCA), 382–383, 437
- cumulative energy demand (CED), 444
- energy payback time (EPBT), 444–445
- fractional reinvestment, 445
- metaanalysis, 445–446

harmonization of study boundaries and data, 446

literature screening, 446

literature search, 445–446

results and discussion, 446–452

capital energetic costs (CEC), 446–447, 451/*f*

components, 449

harmonization, 447–449

life-cycle energy costs (LCEC), 447, 448/*f*, 449/*f*

net energy trajectory of the global wind industry, 450–452

trends in parameters, 450

wind energy technologies, 440–443

balance of systems, 443

foundation, 443

nacelle, 442–443

rotor, 442

tower, 443

- Life-cycle energy cost (LCEC), 439–440, 445, 447, 448*f*, 449*f*, 457*t*
 Life-cycle impact assessment (LCIA), 444
 Life-cycle inventory (LCI), 444
 Lifetime distributions
 classification of, 317*t*
 reliability models for, 316*t*
 Lift, 6–7
 Lift coefficient, 203–204
 Lift versus drag-based VAWT, 189–192, 192*f*
 Light rare earth element oxides (LREO), 532
 Light rare earth elements (LREE), 517
 Limit State Design philosophy, 252–253
 Limited variable-speed wind turbines (Type 2), 156–157, 156*f*
 Line commutated converter technology (LCC-HVDC), 110
 LLC truck, 204
 Loads acting on foundations, 254–257
 extreme wind and wave loading condition
 in Chinese waters, 257–260
 types and nature of, 254–260
 Loads acting on OWT, 354*f*
 Local governments, 79–80
 Log-likelihood value, 318–319
 Long-term deformation, 253, 277, 329
 Long-term forecasting, 40
 Low Carbon Buildings Programme, 393–394, 399
 Low carbon energy (LCE), 221
 Low-frequency demand disconnection (LFDD), 110
 Low-voltage demand disconnection (LVDD), 110
- M**
- Marine aspects, 225
 Market-related network codes, 108–109
 Markov chain models, 42
 Markov Chain Monte Carlo sampling methods, 34
 Mass flux, 19–20
 Maximum Likelihood Estimation (MLE), 317–319
 Mean Absolute Error (MAE), 427–428
 Mean time between failures (MTBFs), 299
 Mean time to failure (MTTF), 303
 Measure-Correlate-Predict (MCP), 32–33, 38
 Medieval European windmills, 132–133
 Mediterranean windmills, 133–135
- Medium-term forecasting, 40
 Merit-order-based dispatch, 90–91
 Mesoscale numerical weather prediction (MNWP) models, 36–37
 Method of Independent Storms (MIS), 38
 Metrics, 302–303
 MFF-089 multielement geometry, 208–209, 208*f*, 214
 MFFS-018 airfoil, 209–210, 210*f*, 211*f*, 213*f*
 MFOIL graphical user interface, 209
 Microgeneration Installation Standard
 MIS3003 issue 2.0, 396–397
 Micrositing, 27, 36
 Micro-wind
 fundamental concern for, 395–401
 future for, 414–415
 Mid-Continent Independent System Operator (MISO), 427
 Mill's ratio, 315–317
 Modeling of capital costs, 226
 Moderate-Resolution Imaging
 Spectroradiometer (MODIS)
 instruments, 55–56
 Modern utility-scale wind turbines, 299
 Modified Gumbel, 38
 Mohr–Coulomb material model, 344
 Monopile, design process for, 330, 331*f*
 Monopile analysis
 using DEM, 286–290
 using FEM, 290–295
 Monopile foundation, 231*f*, 234–235, 241, 361
 design and installation, challenges in, 270–271
 Monopile system, 3D view of, 291*f*
 Mounted turbines, building, 401–414
 field trial observations, 411–414
 findings, 409–410
 rural building mounted turbine, 405–406
 suburban building mounted turbine, 407
 urban building mounted turbine, 408–409
 MS3DJH/3R models, 36
 MSES code, 209
 Multielement airfoils for wind turbines, 203
 aerodynamics, 203–204, 209–210, 216–217
 MFF arrangement, 207–208, 208*f*
 MFFS arrangement, 209–210, 212–214
 multielement wind turbine blades, 206–215
 multielement wind turbine research, 215–216
 segmented blades, 205

- structural benefits, 205–206
 transportation benefits, 204–205
- Multiple Architecture System (MAS), 43
- Multipod foundation wind turbines, 370*f*
 scaling laws for OWTs supported on,
 368–373
- Multipod foundations, 236*f*
- N**
- Nacelle, 442–443
 foundation and cover, 443
 gearing and generator, 443
- National Development and Reform Commission (NDRC), 77–79, 85, 88
- National grids, integration into, 419
 wind integration, 419–421
 current/standard measures for,
 421–429
 future of, 429–434
- National Renewable Energy Laboratory (NREL), 445
- Natural frequency, 253
 prediction of, 346–349
- Navigation risk assessment survey, 226
- NdFeB permanent magnet, 520–521
- Net present value, 540–541
- Network codes
 connection-related, 109–110
 market-related, 108–109
 system operation, 108
- New Policies Scenario (NPS), 527
- New York State Energy Research and Development Authority, 26–27
- Noise problems and possible solutions,
 478–479
- Nonlinear Winkler spring
 standard method based on beam on,
 281–283
- Nonrenewable power plants, overcapacity in,
 81
- North Hoyle project, 253
- North Seas Countries Offshore Grid Initiative (NSCOGI), 105
- Not-In-My-Backyard syndrome (NIMBY),
 479
- NSON project, 121
- Numerical Objective Analysis Boundary Layer (NOABL) wind speed modeling tool, 392, 395
- Numerical weather prediction (NWP)
 methods, 40–41, 43–44, 113
- O**
- Offshore Grid Development Plan (O-GDP),
 104–105
- Offshore substation, 230*f*
- Offshore wind farms around United Kingdom,
 224*f*
- Offshore wind farms in China Sea, 246
- Offshore wind potential in China, 243–245
- Offshore wind power planning, 89–90
- Offshore wind turbine (OWT), 243, 266–268,
 271–272, 353
 complexity of external loading conditions,
 353–355
 design challenges, 355–358
 dynamic sensitivity of OWT structures,
 245–247
- mechanical model, 247*f*
- physical modeling of, 359–361
 definition of scaling laws for
 investigating OWTs, 360–361
 dimensional analysis, 360
 reflective loop for, 359*f*
- prediction of prototype response, physical
 modeling for, 358–359
- resonance-type problem, 355–357
- scaling laws for OWTs supported on
 monopiles, 361–368
 bending strain in the monopile, 365
 CSR in the soil in the shear zone,
 363
- experimental investigation for studying
 long-term response of 1–100 scale
 OWT, 366–368
- fatigue in the monopile, 365–366
- monopile foundation, 361
- rate of soil loading, 364
- strain field in the soil around the laterally
 loaded pile, 361–363
- system dynamics, 364–365
- scaling laws for OWTs supported on
 multipod foundations, 368–373
 typical experimental setups and results,
 372–373
- soil–structure interaction, 355–359, 357*f*
- technical review/appraisal of new types of
 foundations, 358
- Oil age, 221
- 1 g testing, 358–359
- 1D momentum equations, 163–166
- 1P loading, 255–256, 275, 353–354
- Onshore and offshore wind development,
 99–102

Operation and maintenance (O&M) costs, 299–300
 OptiSlip/FlexiSlip induction generators, 150
 Overhead lines (OHLs), 106
 Overnight capital cost, 439

P

PaciCorp, 428–429
 Pattern-painted wind turbine blades, 477–478
 Payments, 544, 548
 Peaks-Over-Threshold (POT), 38
 PE-dominated power systems, new control concepts for, 111–112
 PEGASE project, 120–121
 Permanent magnet synchronous generator (PMSG), 148, 520–521, 529
 Permanent magnets, development of, 521f
 Photovoltaic (PV) technology, 429–430
 Pierson–Moskowitz wave spectrum, 354
 Pile foundations, 234–235
 Pitch bearing maintenance scheduling, 321–324
 Pitch control (active control), 153
 Plasticity, 284–285
 PLAXIS 3D, 344, 344f
 Plug-in electric vehicles, 62
 Pole mounted turbines, 411–414
 Poor grid connectivity, 83
 Potential energy (PE), 51–52
 Potential of wind energy worldwide, 13
 Potential wind-generated electricity, 62–63
 Power Coefficient, 21
 Power electronic interface, 151–152
 Power electronics (PE), 102
 Power export/grid connection, 226
 Power forecasting, wind speed and, 39–44
 Power generation objects, landscapes with, 506–508
 Power spectral densities (PSDs), 246–247
 Prandtl's tip loss correction, 171
 Premature failures, 304
 Preventive maintenances, 315
 Price and cost concepts, 542
 Probability of failure, 319–320
 Production tax credit (PTC), 546
 accounting for PTC as well as depreciation and taxes, 550–553
 wind turbine present value cost analysis accounting for, 548–550
 PROFOIL code, 209
 Project lifetime, 543

PROPID, 210–212, 214, 217
 Public Utility Regulatory Policies Act (PURPA), 419
 Pumped hydroelectric storage (PHS), 377–378, 380
 $p-y$ curve, 281–283, 282f, 336

R

Radial basis function (RBF), 42
 Random failures, 304–305
 Rank Regression, 317–318
 Raptor Nonlinear (Raptor NL) software, 36
 Rare earth elements (REE), 517
 background of, 517–519
 -dependent permanent magnets, 521
 -dependent technologies, 518f
 future REE supply, implications for, 529–531
 global REE supply, 519–520
 global wind energy projections, 526–528
 life cycle assessment of use of REE
 magnets in wind turbines, 522–526
 permanent magnets, 520–522, 521f
 within the periodic table, 518f
 “Ratcheting”, 283–284
 Rated power, 29–30
 Regional Atmospheric Modeling System (RAMS) model, 43–44
 Reliability, defined, 301–302
 Reliability engineering, 312–320
 data collection, 312–315
 forecasting, 319–320
 model development, 315–319
 Reliability of wind turbines, 299
 case studies, 320–324
 gearbox spares planning, 320–321
 pitch bearing maintenance scheduling, 321–324
 current status, 305–312
 terminology, 301–303
 failure types, 304–305
 metrics, 302–303
 taxonomy, 303
 ReliaWind, 309
 Renewable energies (REs), 75
 Renewable energy production incentive, 547–548
 Renewable energy sources (RESs), 95, 102, 117
 Renewables, integration of
 in Germany and Europe, 95–98

- Response spectrum analysis method, 482–483
 Reynolds number, 177–178, 198
 Risk-based inspection approach, 324
 Robustness and ease of installation, 253, 277,
 330
 Rotor, 442
 blades, 442
 hub, 442
 Rudong intertidal wind farm, 255*f*
 Rural building mounted turbine, 405–406
- S**
- Samarium cobalt (SmCo) magnet, 517–519
 Sandia National Laboratory, 194
 SAP 2000, 349–350
 SAVEWIND project, 121
 “Savonius” VAWT, 189–190
 SC(2)-0714 airfoil, 206
 SCADA system, 313
 Scaling laws
 for OWTs supported on monopiles,
 361–368
 bending strain in the monopile, 365
 CSR in the soil in the shear zone, 363
 experimental investigation for studying
 long-term response of 1–100 scale
 OWT, 366–368
 fatigue in the monopile, 365–366
 monopile foundation, 361
 rate of soil loading, 364
 strain field in the soil around the laterally
 loaded pile, 361–363
 system dynamics, 364–365
 for OWTs supported on multipod
 foundations, 368–373
 typical experimental setups and results,
 372–373
 SCOE (Society’s Cost of Energy), 227–228
 Seabed frame/jacket supporting supported on
 pile or caissons, 235–237
 Secant Young’s Modulus of soil, 287–288
 Sector coupling concepts, 118–119
 Segmented blades, 205
 Selig S1210 airfoil, 194–195, 195*f*
 Serviceability limit state (SLS), 253,
 277–278, 329
 design criteria, 265–266
 Short-term forecasting, 39
 Silsoe, 402–403
 Single-degree-of-freedom model, 482–483
 Single-fed induction generator (SFIG), 522
- Small-scale wind turbine model, 372*f*, 389
 micro-wind, fundamental concern for,
 395–401
 micro-wind, future for, 414–415
 mounted turbines, building, 401–414
 field trial observations, 411–414
 findings, 409–410
 rural building mounted turbine, 405–406
 suburban building mounted turbine, 407
 urban building mounted turbine,
 408–409
 Smart DR, 87–88
 Smart grid, 90
 SODAR (Sound Detection and Ranging
 system), 30
 Soft starter, 151
 Soft–soft structures, 251
 Soft–stiff design, 257
 Soft–stiff structures, 251
 Soil models in finite element analysis,
 283–285
 Soil–pile model, 291
 Soil–structure interaction (SSI) analysis of
 OWT foundations, numerical methods
 for, 275
 advanced analysis to study foundation–soil
 interaction, 283–285
 example application of, 285–295
 monopile analysis using DEM, 286–290
 monopile analysis using FEM, 290–295
 need for, 281
 standard method based on beam on
 nonlinear Winkler spring, 281–283
 Soil–structure interaction, challenges in
 analysis of, 266–269
 Solar and Wind Energy Resource Assessment
 (SWERA) project, 26
 Solar PV, 431–432
 and wind turbines, 377
 South China Sea, 258, 264*f*
 wave height and period in, 261*t*
 Southwest Power Pool, 427
 Space frame tower (SFT) turbine, 216
 Spacing of turbines, 239–240, 240*f*
 Split blade technology, 501, 501*f*
 Squirrel-cage induction generator (SCIG),
 149–150, 149*f*
 Stall control (passive control), 153
 Standard Gumbel, 38
 State Grid Corporation (SGC), 78
 State of the Art Wind Technologies (SAWT),
 199

- State-owned enterprises (SOEs), 77–78
 Steady blade element momentum method, use of, 172–178
 Stiff–stiff structures, 251
 Stored wind energy
 carbon footprint of storing wind energy, 383–385
 energy and carbon intensities of, 375
 key characteristics for storage, 378–380
 need for storage, 377–378
 net energy analysis of storing and curtailing wind resources, 380–383
 Straight line depreciation, 541
 Structural health monitoring of wind turbine towers, 483–485
 Structural vibration control technologies, 484–485
 Struts, 199–200
 Substructure, 231–233
 Suburban building mounted turbine, 407
 Suction buckets, 233–234
 Suction caissons, 233–234
 Support structure design, dynamic issues in, 247–253
 Support vector machines (SVMs), 41–43
 Suspensions, 313–314
 Symmetric airfoils, 194
 Synchronous generator, 148
 System operation network codes, 108
- T**
 Taiwan Strait, 258
 Tangential force coefficient, 203–204
 Target natural frequency, 277, 329
 Taxonomy, 303
 3P loading, 353–354
 Tjaereborg rotor, 174–177
 TLP (tension leg platform) concept, 237
 Tohoku earthquake (2012), 221–223
 Tower, 443
 TRADEWIND project, 120
 Transition piece (TP), 234–235
 Transmission system, 146–147
 Transmission system operators (TSOs), 102–104, 112
 TRL (Technology Readiness Level)
 numbering, 358, 358t
 Tuning liquid column dampers (TLCD), 484–485
 Tuning liquid dampers (TLD), 484–485
 Tuning mass dampers (TMD), 484–485
- Turbine blades, extraction of wind energy by, 6–7
 Turbine power capture, 21–22
 Turbulent Intensity (TI), 404–405
 2P/3P loading, 256, 275
 Typhoon related damage to wind turbines in China, 258–260
 Typhoons, 257
- U**
 UK's National Micro-wind Field Trial, 401
 Ultimate limit state (ULS), 252, 275–276, 329
 Ultrahigh voltage (UHV) transmission lines, 86–87
 Ultrasonic anemometer, 407f
 UN Framework Convention on Climate Change (UNFCCC), 51
 United Nations Framework Convention on Climate Change (UNFCCC), 3–4
 University of Southampton (UoS) building, 395
 Urban building mounted turbine, 408–409
 US Geological Survey (USGS), 56
- V**
 Variable-speed wind turbines, 154–155
 with full-scale power converter (Type 4), 158–159, 158f
 with partial-scale power converter (Type 3), 157–158, 157f
 Vertical axis wind turbines (VAWTs), 185, 389, 440
 counter-rotating VAWT, 187f, 188
 design guidelines, 188–200
 blade airfoil choice, 194–197
 blade Reynolds number, 198
 blade-tip vortices, 197
 lift versus drag-based VAWT, 189–192
 number of blades, 199
 power coefficient, 189
 starting, 193–194
 struts, 199–200
 turbine diameter, 198–199
 turbine mass, 198
 history, 185
 vertical axis wind farms, 186–188
 initial research on VAWT farms, 186–187
 power density, 187–188

- Vertical-axis windmills, 135, 140
 Very short-term forecasting, 39
 Vestas, 216
 Vested interests between coal companies and the government, 85–86
 Windstat, 309
 Virtual power plants (VPPs), 117–118
 Visual effects, 511
 landscape and, 512
 Visual impacts and mitigation, 479–480
 Voltage source converter technology (VSC-HVDC), 110
 Volume flux, 19–20
 Vortex system, 170, 171*f*
 VTT, 309
- W**
- Wake turbulence, 239*f*
 WarwickWindTrial study, 394, 399
 Water-driven mills, 128
 Weibull distributions, 33–34
 Well-functioned ancillary service market, lack of, 83–84
 Westermost Rough, 240
 Wind, 17
 generation of, 17
 types, 18–19
 Wind assessment program
 main aspects of, 28–33
 principles for successful development for, 26–28
 Wind Atlas Analysis and Application Program (WAsP), 36, 38
 Wind atlases, 27
 Wind cluster management system (WCMS), 115
 Wind curtailment, 81–82
 Wind energy developers, 78
 Wind energy flow rate, 20
 Wind energy-Information-Data-Pool (WInD-Pool), 309
 Wind farms
 clusters, 114–117
 in Europe, 225*f*
 on landscape, 508–512
 landscape and visual effects, 512
 landscape effects, 509–511
 visual effects, 511
 perception of, 502–506
 composition, 504
 height and size, 502–503
 movement, 504–506
- site selection, 224–228
 ASIDE on the economics, 227–228
 Burbo wind farm, 226–227
- Wind integration, 419–421
 current/standard measures
 for, 421–429
 future of, 429–434
- Wind machines in antiquity, 129–130
- Wind physics, 17
- Wind power, 20, 475
 assessment program, 34–35
 capture, 21–23
 efficiency in extracting, 21–23
 estimating, based on wind speed measurements, 33–34
 fundamental equation of, 19–21
 Wind power density (WPD), 19–21
 Wind power forecasts, 112–113
 Wind power fundamentals, 15
 fundamental equation of wind power, 19–21
 wind physics basics: what is wind and how wind is generated, 17
 wind power capture: efficiency in extracting wind power, 21–23
 wind types: brief overview of wind power meteorology, 18–19
 Wind power meteorology, 18–19
 Wind resource estimation project, 34–38
 Wind resources, 225
 Wind speed
 assessment, 38–39
 and power forecasting, 39–44
 Wind speed forecasting models, classification of, 40*f*
 Wind speed measurements, estimating wind power based on, 33–34
 Wind turbine, working of, 162–163
 Wind turbine generators (WTGs), 270–271
 Wind turbine manufacturers, 78–79
 Wind turbine technologies, 145
 aerodynamic rotor, 146
 contemporary wind turbine technologies, 155–159
 fixed-speed wind turbines (Type 1), 155–156, 155*f*
 limited variable-speed wind turbines (Type 2), 156–157, 156*f*
 variable-speed wind turbines with full-scale power converter (Type 4), 158–159, 158*f*

- Wind turbine technologies (*Continued*)
variable-speed wind turbines with partial-scale power converter (Type 3), 157–158, 157*f*
control system and wind turbine control capabilities, 152–155
generator, 147–151
 asynchronous (induction) generator, 149–151
 synchronous generator, 148
power electronic interface, 151–152
transmission system, 146–147
- Wind turbine towers, 481–485
 health monitoring and vibration control of, 483–485
 structural performances under wind and seismic loads, 481–483
- Wind turbines prices, 542
- Wind-energy-induced environmental issues
 and countermeasures, 475–481
 birds and bats, effects on, 476–478
 climate change and considerations, 480–481
 marine species, effects on, 478
 noise problems and possible solutions, 478–479
 visual impacts and mitigation, 479–480
- WindGrid project, 120
- Windmills, 128
 Aegean and Mediterranean windmills, 133–135
 American windmill, 138–139, 138*f*
- applications, 141
Dutch and European windmills, 135–138
Islamic civilization windmills, 130–132
medieval European windmills, 132–133
- Windsave WS1000 turbine, 397–399, 402, 407*f*, 408*f*
- Windspire VAWT, 195
- WindStats, 309
- Wissenschaftliches Mess- und Evaluierungsprogramm (WMEP), 309
- Wound rotor induction generator (WRIG), 150–151
- Wound rotor synchronous generator (WRSG), 148
- Wound rotor with slip rings, 150*f*
- X**
- Xcel Energy Colorado, 427–428
- XFOIL code, 178–179
- “XL” monopile, 270–271
- XL/XXL piles, 241
- Y**
- Yellow Sea, 257, 262–263
 wave height and period in, 261*t*
- Z**
- Zero-emission wind power, 88

Wind Energy Engineering

A Handbook for Onshore and Offshore Wind Turbines

Edited by Trevor M. Letcher

A core reference on developments in the expanding wind energy technology and application

Wind energy is pivotal in global electricity generation and for contributing to achieving future essential energy demands and targets. In this fast moving field, *Wind Energy Engineering: A Handbook for onshore and offshore Wind Turbines* is the most advanced, up to date, and research focused text on all aspects of wind energy engineering.

This must-have edition starts with an in-depth look at the fundamentals of wind power, the present state of wind power in the worldwide, integration into national grids, and continues with a high-level assessment of the advances in turbine technology and how the investment, planning, aesthetics, and economic infrastructure can support those innovations. It also includes chapters on storing wind energy, small-scale wind systems, life cycle assessments, investments, and growth trends.

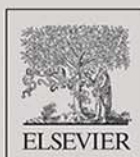
Each chapter includes a research overview with a detailed analysis and new case studies looking at how recent research developments can be applied. Written by some of the most forward thinking professionals in the field and giving a complete examination of one of the most promising and efficient sources of renewable energy, this book is an invaluable reference into this cross-disciplinary field for engineers.

- Each chapter contains analysis of the latest high-level research and explores real world application potential in relation to the developments.
- Uses system international (SI) units and imperial units throughout to appeal to global engineers.
- Each chapter offers measurable data written by a world expert in the field on the latest developments in this fast moving and vital subject.

Trevor M. Letcher is Emeritus Professor of Chemistry at the University of KwaZulu-Natal, Durban and a Fellow of the Royal Society of Chemistry. He is a past Director of the International Association of Chemical Thermodynamics and his research involves the thermodynamics of liquid mixtures and energy from landfill.

He has published over 280 papers in peer review journals and has edited, co-edited, and written 18 books in his research and related fields. His latest books include *Waste* (2011), *Unraveling Environmental Disasters* (2013), *Chemical Processes for a Sustainable Future* (2015), *Future Energy*, 2nd edition (2014), *Volume Properties* (2015), *Climate Change*, 2nd edition (2015), and *Storing Energy* (2016).

Cover image: Horns Rev 1 owned by Vattenfall.
Photographer Christian Steiness



ACADEMIC PRESS

An imprint of Elsevier
elsevier.com/books-and-journals

ISBN 978-0-12-809451-8

